CHARLES UNIVERSITY

FACULTY OF SCIENCE

Study program: Molecular and Cell Biology, Genetics and Virology

M.Sc. Ivalú Macarena Ávila Herrera

Evolution of karyotype in selected groups of haplogyne and mygalomorph spiders

Evoluce karyotypu u vybraných skupin haplogynních a mygalomorfních pavouků

Doctoral thesis

Supervisor:

Asst. Prof. RNDr. Jiří Král, Ph.D.

Prague 2024

Declaration of originality

Herewith I declare that I did not use this PhD thesis to acquire another academic degree. I worked on the PhD thesis independently, under the supervision of asst. prof. RNDr. Jiří Král, PhD. I have attended all used information sources and literature. Neither this work nor any substantial part of it has been submitted for another or the same academic title.

In Prague, 27st June 2024

Signature…….  ……

Acknowledgements

Foremost, I would like to express my sincere gratitude to my advisor asst. prof. Jiří Král for giving me the opportunity to carry out my Ph.D. study in his group and for his constant support and encouragement. I am also very grateful to Dr. Michaela Schierová and asst. prof. Dana Holá, for their valuable suggestions correcting the gaps in my knowledge. I would like also to thank my fellow labmates, especially to Martin Forman for teaching me different techniques and support my stay in the lab. Furthermore, I am thankful to Jana Musilová, Tereza Kořínková, Azucena Claudia Reyes Lerma, Martina Koubová, and Pavel Just which have supported my work and offered me their friendship. Last but not the least, I would like to thank all my family for supporting me throughout this period of my life, especially to my husband Josef who always supported and encouraged me. After several years that I spent in Czech Republic, I consider it to be my second homeland. My research was supported by several foundations, namely the National Research and Development Agency (ANID, Chile), the Czech Science Foundation (projects nos 206/08/0813 and 16-10298S), the Grant Foundation of the Charles University (project nos 92218,), the Grant Agency of the Academy of Sciences of the Czech Republic (no. IAA601110808), and Ministry of Education, Youth, and Sports of the Czech Republic (projects LTAUSA 19142; SVV 265202, SVV 267205, SVV260568).

List of abbreviations

AT adenine-thymine

CGH comparative genomic hybridisation

FISH fluorescence in situ hybridization

GC guanine-cytosine

IGS intergenic spacer

ITS interstitial telomeric sequence

ITS internal transcribed spacer

LT Clade Lost Tracheae Clade

NOR nucleolar organizer region

PCR polymerase chain reaction

rDNA ribosomal DNA

CSCP *cryptic sex chromosome pair*

SCS sex chromosome system

WGD whole genome duplication

2n diploid chromosome number

Contents

Abstrakt.....6
Abstract..... 8
1. Introduction.....10
2. Literature overview.....12
2.1. Introduction into spider biology and phylogeny.....12
2.2. Cytogenetics of the spiders.....14
2.2.1. Diploid number and autosome evolution.....14
2.2.2. Sex chromosome evolution.....16
2.2.3. Meiotic modification.....20
2.2.4. Banding techniques and and techniques of molecular cytogenetics 21
2.3. Cytogenetics of haplogynes.....23
2.3.1. Cytogenetics of haplogynes with monocentric chromosomes.....23
2.3.2. Banding techniques and techniques of molecular cytogenetics in haplogynes with monocentric chromosomes.....24
2.4. Haplogyne spiders with holokinetic chromosomes……..…..26
2.5. Cytogenetics of Mygalomorphae…….……...28
2.5.1. Banding techniques and molecular cytogenetics in mygalomorphs……....30
3. List of methods 32
4. Results.....33
4.1. Publication 1 (Řezáč et al. 2022) 33
4.2. Publication 2 (Ávila et al. 2021).....58
4.3. Publication 3 (Král et al. 2022).....123
4.4. Publication 4 (Huber et al. 2023a).....151
4.5. Publication 5 (Huber et al. 2023b).....236
5. Discusion 374
5.1. Evolution of karyotype in mygalomorphs of the superfamily Atypoidea…….374
5.2 Karyotype evolution in Pholcidae spiders……..375
6. Conclusions and future directions..... 381
7. References.....383
8. Publications not related to the thesis.....402

Abstrakt

Pavouci jsou rozmanitou skupinou členovců s celosvětovým rozšířením. Jsou významnými predátory a úspěšně osídlili většinu suchozemských ekosystémů. Navzdory významu této skupiny jsou informace o jejích karyotypech stále omezené, a to zejména u sklípkošů, sklípkanů a haplogynních araneomorfů. Předkládaná doktorská práce je zaměřena na evoluci karyotypu vybraných kládů haplogynů a sklípkanů, konkrétně na čeledi Pholcidae a Atypidae. Ke stanovení karyotypů a vzorů nukleolárních organizátorů (NOR) byly použity techniky standardní a molekulární cytogenetiky. Získané výsledky umožňují revidovat diploidní počet a systém pohlavních chromozomů sklípkana *Atypus karschi* (Atypidae) a určit pravděpodobný ancestrální karyotyp rodu *Atypus*. *A. karschi* vykazuje jeden NOR, který sousedí s velkým blokem heterochromatinu tvořeným inaktivovanou rDNA.

Pokud jde o čeleď Pholcidae, získané výsledky podstatně zvyšují počet analyzovaných druhů této čeledi. Získané údaje umožnily poprvé studovat evoluci karyotypu haplogynů na úrovni čeledi, poprvé také evoluci NOR. Pholcidi mají nízké diploidní počty, 2n♂ se pohybuje v rozmezí 9 až 33. V karyotypech pholcidů převažují dvouramenné chromozomy. V průběhu evoluce se diploidní počty často snižovaly fúzemi. Morfologie chromozomů vstupujících do fúze se nejprve změnila inverzí na akrocentrickou nebo subtelocentrickou. Systémy pohlavních chromozomů a vzory NOR jsou velmi diverzifikované. Mé studie prokázaly sedm systémů pohlavních chromozomů, a to X0, XY, X_1X_20, $X_1X_2X_30$, X_1X_2Y, $X_1X_2X_3Y$, and $X_1X_2X_3X_4Y$. Fylogeneticky původní je systém X_1X_2Y, který je pravděpodobně ancestrální u araneomorfních pavouků. Moje studie odhalila evoluční plasticitu systému X_1X_2Y. Jeho evoluce zahrnovala translokace mezi chromozomy X_1 a X_2, inverze chromozomů X a zvětšení velikosti chromozomu Y. Systém X_1X_2Y se u některých skupin transformoval na jiné systémy. Systém X_1X_20 vznikl ztrátou chromozomu Y, systém XY vznikl fúzí chromozomů X. Z těchto systémů vznikl v některých evolučních větvích systém X0, a to buď fúzí chromozomů X (ze systému X_1X_20), nebo ztrátou chromozomu Y (ze systému X0). Systém $X_1X_2X_30$ u *Smeringopus pallidus* vznikl ze systému X_1X_20, a to buď fúzí chromozomů X, nebo nondisjunkcí. Nejsložitější systémy byly nalezeny v podčeledi Ninetinae ($X_1X_2X_3Y$ a $X_1X_2X_3X_4Y$). Tyto systémy vznikly ze systému X_1X_2Y podobně jako systém nalezený u *S. pallidus*. Počet lokusů NOR se pohybuje od jednoho do devíti, jsou umístěny na autosomech a často se šířily na pohlavní chromozomy, pravděpodobně ektopickou

rekombinací. NORy vázané na pohlavní chromozomy se pravděpodobně podílejí na achiazmatickém párování pohlavních chromozomů. Počet NOR se v průběhu evoluce zvyšoval. U některých skupin se počet NOR, včetně NOR vázaných na pohlavní chromozomy, následně snížil. Podobně jako u jiných haplogynů zahrnuje samčí meióza pholcidů difúzní stadium a tito pavouci mají v samčí meióze obvykle velmi nízký počet chiasmat.

Klíčová slova: chromozomová přestavba, difúzní stadium, evoluce karyotypu, FISH, Haplogynae, Mygalomorphae, nukleolární organizátor jadérka, pohlavní chromozom, rDNA.

Abstract

Spiders are diverse group of arthropods with a worldwide distribution. They are important predators and colonized successfully most terrestrial ecosystems. Despite importance of this group, the information about the spider karyotypes is still limited, especially in mesotheles, mygalomorphs, and haplogyne araneomorphs. The presented Ph.D. thesis is focused on the karyotype evolution of selected clades of haplogynes and mygalomorphs, specifically on the families Pholcidae and Atypidae. Techniques of standard and molecular cytogenetics were used to determine the karyotypes and the pattern of nucleolus organizer regions (NORs). Obtained results allow to revise the diploid number and sex chromosome system of mygalomorph *Atypus karschi* (Atypidae) and determine probable ancestral karyotype of the genus *Atypus*. *A. karschi* exhibits one NOR, which is adjacent to the large heterochromatin block composed of inactivated rDNA.

Concerning the family Pholcidae, obtained results increase substantially the number of analysed species belonging to this family. Obtained data allowed to study for the first time karyotype evolution of haplogynes on a family level, for the first time also the evolution of NORs. Pholcids show a low diploid number, 2n♂ ranges from 9 to 33. Pholcid karyotypes are predominated by biarmed chromosomes. In the course of evolution, diploid numbers have often been reduced by fusions. The morphology of the chromosomes entering the fusion was first changed by inversions to acrocentric or subtelocentric. The sex chromosome systems and patterns of NORs are very diversifed. My studies discovered seven sex chromosome systems, namely X0, XY, X_1X_20, $X_1X_2X_30$, X_1X_2Y, $X_1X_2X_3Y$, and $X_1X_2X_3X_4Y$. Phylogenetically original is the X_1X_2Y system, which is probably ancestral to araneomorph spiders. My study revealed the evolutionary plasticity of the X_1X_2Y system. Its evolution included translocations between X_1 and X_2 chromosomes, inversions of X chromosomes, and increase of Y chromosome size. The X_1X_2Y system has been transformed to other systems in some groups. The X_1X_20 system arose from the loss of the Y chromosome, the XY system from the fusion of X chromosomes. From these systems, the X0 system arose in some evolutionary branches, either by fusion of X chromosomes (from the X_1X_20 system) or by loss of the Y chromosome (from the X0 system). The $X_1X_2X_30$ system of *Smeringopus pallidus* arose from the X_1X_20 system, either by X chromosome fission or nondisjunction. The most complicated systems were found in the subfamily Ninetinae ($X_1X_2X_3Y$ and $X_1X_2X_3X_4Y$). These systems arose from the X_1X_2Y system like the system found in *S.*

pallidus. Number of NOR loci varies from one to nine, they are located on the autosomes and frequently expanded on the sex chromosomes, possibly by ectopic recombination. Sex-chromosome linked NORs are probably involved in the achiasmatic pairing of sex chromosomes. The number of NORs has increased over the course of evolution. In some groups, the number of NORs, including sex-chromosome linked NORs, has been subsequently reduced. Similar to other haplogynes, male meiosis of pholcids includes a diffuse stage, and these spiders usually have a very low number of chiasmata in male meiosis.

Keywords: chromosome rearrangement, diffuse stage, FISH, Haplogynae, karyotype evolution, Mygalomorphae, nucleolus organizer region, rDNA, sex chromosome.

1. Introduction

Cytogenetics of arthropods has been developing rapidly in the several last decades. However, most studies have focused on insects. Less attention has been paid to other groups, which is also true for arachnids, the most numerous class of the arthropod subphyllum Chelicerata. The Arachnid diversity is enormous. This clade currently includes 182 families, 5118 genera and 58369 species (World Arachnida Catalog 2024).However, knowledge on cytogenetic of many arachnid orders is scarce (Araujo et al. 2024). Therefore, it is impossible to reconstruct karyotype evolution of arachnids yet. The most data concern spiders (Araujo et al. 2024), scorpions (Schneider et al. 2024), pseudoscorpions (Šťáhlavský 2024), harvestmen (Tsurusaki et al. 2024), parasitiform (Norton et al. 1993, Vázquez et al. 2021) and acariform mites (Heethoff et al. 2006).

The spiders (Araneae) are the most diverse order of arachnids. It is the most studied arachnid order from cytogenetic point of view. Spiders belong to the most abundant generalist arthropod predators of the planet, inhabiting almost every terrestrial ecosystem and have persisted for over 380 million years (Foelix 2011). They show a worldwide distribution except for Antarctica (Garrison et al. 2016, Wheeler et al. 2017). Araneae are composed of three primary evolutionary lineages: Mesothelae, Mygalomorphae, and Araneomorphae. The latter clade is further divided to haplogyne and entelegyne araneomorphs (Coddington and Levi 1991, Coddington 2005, Wheeler et al. 2017). Majority of spider biodiversity concerns entelegyne lineage (Griswold et al., 2005, World Spider Catalog 2024), which is mirrored also by cytogenetic data. The diploid numbers, chromosome morphology, sex chromosomes, and pattern of NORs are very diverse in spiders. While most spiders have standard chromosome structure, the karyotypes of the haplogyne superfamily Dysderoidea are composed of holokinetic chromosomes (Král et al. 2006, 2019, Diaz et al. 2010, Řezáč et al. 2018). Sex chromosome systems of spiders are unusual, most spiders possess multiple X chromosome systems, which are rare in other organisms (Araujo et al. 2012, Kořínková and Král 2013). Our data show that sex chromosome systems of spiders are even more complicated, they probably also contained one or even two pairs of undifferentiated sex chromosomes X and Y (Král 2007, Král et al. 2011, 2013, Sember et al. 2020). Some spider groups have very specific features of evolution of nucleolus organizer regions (NORs). Some mygalomorphs possess one or even several giant NORs (Král et al. 2013). In haplogyne spiders, NORs are often placed on sex chromosomes (Král et al. 2006, Ávila et al. 2021). Therefore, spiders are a suitable

model to study the evolution of sex chromosomes (Cordellier et al. 2020) or holokinetic chromosomes (Král et al. 2019). Moreover, cytogenetic research of spiders is becoming intertwined with genomics (Sánchez-Herrero et al. 2019, Cordellier et al. 2020, Escuer et al. 2021, Sheffer et al. 2021a). This approach can elucidate evolution of some complex cytogenetic features of spiders like sex chromosomes or transition between monocentric and holocentric chromosomes.

To contribute to understanding of spider karyotype evolution, my thesis is dealing with mygalomorph and haplogyne spiders whose cytogenetics is not satisfactorily understood. Specifically, I focused on evolution of karyotype, nucleolus organizer regions, meiosis, and sex chromosomes in mygalomorph family Atypidae and haplogyne family Pholcidae. While the family Atypidae belongs to the phylogenetically basal groups of mygalomorphs, the family Pholcidae is the most diversified family of haplogyne spiders with standard chromosome structure.

The particular aims were as follows:

a) to determine karyotypes of the species including diploid number and chromosome morphology, using the Giemsa staining;
b) to determine sex chromosome system of each species by the analysis of the mitotic and meiotic division;
c) to determine behaviour of chromosomes at male germline (spermatogonial mitoses and meiosis) of each species (especially frequency and position of chiasmata, behaviour of sex chromosomes, condensation pattern of chromosomes during particular mitotic and meiotic phases);
d) to determine pattern of constitutive heterochromatin (location of blocks of heterochromatin) and nucleolus organizer regions (number of NORs and their location) in selected species;
e) to compare obtained data on karyotypes with those described by other authors, especially in related taxa;
f) to reconstruct karyotype evolution of studied taxa.

2. Literature overview

2.1. Introduction into spider biology and phylogeny

The arachnids are ancient and extremely diversified arthropod clade. Moreover, some arachnid groups are important from an economical or medical point of view (Cordeiro et al. 2015). The most diversified arachnid group are spiders (Araneae), which contain 135 families, 4376 genera, and 51974 species described to date (World spider catalog 2024). They live in webs, burrows, or are wandering using shelters (Pérez-Miles et al. 2020). The spiders can basically be defined as air-breathing arthropods with two body parts, the cephalothorax and the abdomen. A narrow stalk - the pedicel - joins the abdomen to the prosoma, allowing great flexibility and precise orientation of the abdominal spinnerets (Herberstein and Wignall, 2012). Spiders have eight legs attached to the cephalothorax, and chelicerae, which are venom-injecting fangs (Foelix 2011). Pedipalps are short and leg-like, except for adult males, where they are modified for sperm transfer. The spiders produce silk from abdominal spinnerets, whose number varies between taxa from two to eight (Foelix 2011, Hu et al. 2006). Spiders are among the few animal groups that use silk throughout their entire lives. Colors are predominantly dull tans, browns, and blacks, but many common, conspicuous spiders are colorful, even iridescent (Foelix 2011).

Spiders comprise of three primary lineages, namely the suborder Mesothelae and two infraorders, Mygalomorphae and Araneomorphae, which together form the suborder Opisthothelae (Bond et al. 2015). Mesotheles and mygalomorphs show more plesiomorphic characters than derived araneomorphs (Kořínková and Král 2013).

The relict suborder Mesothelae is distributed at China, Japan, and Southeast Asia. The oldest Mesothelae are known from the Upper Carboniferous, over 300 million years ago (Wheeler et al. 2017). Mesotheles include two extant families, Heptathelidae and Liphistiidae (World Spider Catalog 2024) and two extinct families, Arthrolycosidae and Arthromygalidae (Garrison et al. 2016). Mesothelae is considered a sister group to all other spiders. They retain many ancestral characters, such as a segmented abdomen with spinnerets in the middle of underside and two pairs of book lungs (Song et al. 1999).

The infraorder Mygalomorphae is composed of 28 families, 357 genera, and 3278 species (World Spider Catalog 2024). According to Selden et al. (2006), the mygalomorphs are found in Africa, the Near and the Middle East, the South, Southeast, Central and East

Asia, Australia, South and Central America, part of North America, and Europe (Pérez Miles et al. 2021).

Recent schemes of mygalomorph phylogeny suggest division of this group into two main lineages, Atypoidea and Avicularioidea (Wheeler et al. 2017, Godwin et al. 2018, Hedin et al. 2018, Opatova et al. 2019, 2020, Kulkarni et al. 2023). The superfamily Atypoidea includes the families Atypidae, Antrodiaetidae, Hexurellidae, Mecicobothriidae, and Megahexuridae (Gertsch, 1940 Hedin & Bond, 2019). The spiders belonging to this clade are characterized by various kinds of burrows with different entrance constructs (Hedin et al. 2019). Members of Atypoidea retain some ancestral features, for example vestiges of segmentation as dorsal abdominal tergites (Wheeler et al. 2017).

Most mygalomorph species diversity is contained within Avicularioidea, which consists of 25 families (Wheeler et al. 2017, Godwin et al. 2018, Hedin et al. 2018). The majority of the avicularioid mygalomorphs are sedentary, they live often in burrows, which rarely leave, and some of them rely on silk for prey capture like the trapdoor spiders, while the members of theraphosids and diplurids use the net to hunt (Xin et al. 2015b). In general most species live in burrows or crevices in the ground, however some are arboreal and live on the trees (Perez Milles et al. 2021). During reproductive period males are searching for females (Costa and Pérez-Miles 2002). Females remain inside of their burrow, they are going outside only to catch the prey or discard remains of coccons or food (Alvarez et al. 2016).

Araneomorphs are the most diverse spider group, they include over 90% of known spiders, namely 101 families, 3946 genera, and 47882 species (World Spider Catalog 2024). According to recent molecular phylogenetic studies, they consists of two large clades, one formed by haplogynes and another one by protoentelegynes plus entelegynes (Kulkarni et al. 2023). Haplogyne lineage is divided into two clades, acribellate (Synspermiata), including 18 families and cribellate clade composed of two families, Hypochididae and Filistatidae (Garrison et al. 2016, Wheeler et al. 2017). Synspermiates include several diversified clades: Caponioidea (families Trogloraptoridae and Caponiidae), Dysderoidea (families Dysderidae, Oonopidae, Orsolobidae, and Segestriidae), Scytodoidea (Drymusidae, Ochyroceratidae, Periegopidae, Psilodercidae, Scytodidae and Sicariidae), and the the so-called Lost tracheae clade composed of Diguetidae, Pacullidae, Pholcidae, Plectreuridae, and Tetrablemmidae (Wheeler et al.

2017, Fernandez et al. 2018, Kulkarni et al. 2021, 2023). Some authors place into the last clade also the family Telemidae (Michalik and Ramírez, 2014).

Protoentelegynes are composed of the two clades, Australochiloidea and related families and Palpimanoidea. First clade is formed by families Archoleptonetidae, Austrochilidae, Gradungulidae, and Leptonetidae. It is sister to the clade formed by Palpimanoidea and entelegyne spiders. (Kulkarni et al. 2023). It is very difficult to elucidate the phylogeny of Entelegynae because this group has an enormous diversity (World Spider Catalog 2024). Current phylogeny is based mostly on molecular markers (Garrison et al. 2015, Wheeler et al 2017, Kulkarni, 2021, 2023). The Entelegynae is a well-supported, monoplyletic lineage (Garrison et al. 2016, Wheeler et al. 2017; Fernandez et al. 2018a, Kulkarni et al. 2020, 2021, Kallal et al. 2021a, Kulkarni et al. 2023). According Kulkarni et al. (2023), Araneoidea is a sister group to the remaining entelegynes. Clade formed by groups Nicodamoidea and Eresidae is considered to be a sister lineage to the clade formed by so-called UDOH grade and the retrolateral tibial apophysis clade (RTA clade) (Kulkarni et al. 2020, 2021).

In contrast to most araneomorphs, distribution range of mygalomorphs is usually restricted, because juveniles rarely balloon and are close to the nest. Therefore, mygalomorph populations are highly clumped (Coddington 2005). The differences in the dispersal mechanism could be a possible explanation for the contrast in the diversity of araneomorphs and mygalomorphs (Coddington 2005, Platnick 2005).

2.2. Cytogenetics of spiders

2.2.1. Diploid numbers and autosome evolution

The cytogenetic analysis of the arachnids has accelerated during last decades, the spiders are the most studied group. Actually, cytogenetic information on 393 genera and 878species of spiders is known (Araujo et al. 2024). Cytogenetic information on spider species usually include data on diploid number, chromosome morphology, sex chromosome system, and meiotic behaviour of sex chromosomes. The majority of analysed species belong to Entelegynae clade. On family level, the most studied entelegyne families are as follows: Salticidae (171 species), Lycosidae (85 species), and Araneidae (66 species). There are data on three protoentelegynes only, namely one species belonging to Austrochilidae (*Austrochilus* sp.), a leptonetid (*Leptoneta infuscata*), and a palpimanid (Král et al. 2006, Duran et al. 2023). The most data on haplogynes

concern families Pholcidae (69 species) and Dysderidae (36 species) (Araujo et al. 2024). Other haplogyne families are much less studied or even untested. Mygalomorphae cytogenetics is not satisfactorily understood; only 50 species has been evaluated so far (Araujo et al. 2024). Concerning mesotheles, only one species of the family Liphistiidae was studied so far (Suzuki, 1949, 1950a, 1954).

Spiders exhibit a considerable diversity of the diploid numbers (2n), which range from 2n♂=5 in *Afrilobus sp.* (Král et al. 2019) to 2n♂=152 in *Caponia natalensis* (Král et al. 2019). Remarkably, the most mygalomorphs karyotyped so far possess higher diploid numbers than araneomorph spiders (Kořínková and Král 2013, Král et al. 2013). Concerning the chromosome morphology, most mygalomorphs show biarmed (metacentric and submetacentric) chromosomes or combination of biarmed and monoarmed (subtelocentric and acrocentric) chromosomes (Král et al. 2013, Kořínková and Král 2013). The karyotypes of almost all entelegynes are formed exclusively by acrocentric chromosomes (Suzuki 1954; Dolejš et al. 2011, Kořínková and Král 2013; Štahlavský et al. 2020). On the other hand, the haplogyne spiders form two groups, which differ by chromosome structure. The superfamily Dysderoidea (Dysderidae, Oonopidae, Orsolobidae, Segestriidae) exhibit holokinetic chromosomes (termed also holocentric chromosomes), which lack a localised centromere and centromeric connection of sister chromatids. In the consequence, the kinetochores occupy the major part of the chromosome surface faced to the poles (Diaz and Saez 1966, Řezáč et al. 2007). The other haplogynes display monocentric chromosomes (Araujo et al. 2024). The karyotypes of almost all the species with this chromosome structure are predominated by biarmed chromosomes (Král et al. 2006, Oliveira et al. 2007, Golding and Paliulis 2011, Lomazi et al. 2018).

The frequent evolutionary trend of spider karyotype evolution is the reduction of diploid chromosome numbers (Suzuki 1954, Araujo et al. 2012, Kořínková and Král, 2013). The most members of basal spider groups (Mesothelae and Mygalomorphae) show a high number of chromosomes (Suzuki 1954, Král et al. 2013). The diploid number is considerably reduced in most derived spiders, araneomorphs. It should be noted that pattern of evolution of diploid numbers is quite complex in mygalomorphs (Král et al. 2011, 2013). Some clades show an increase in the number of chromosomes due to fissions (Král et al. 2013).

2.2.2. Sex chromosome evolution

Sex chromosome systems are in general very diverse. Many animals and some plants have the sex determination system where the male is heterogametic (XY) and the female homogametic (XX) (Kaiser and Bachtrog 2010). This kind of sex chromosome differentiation is found for example in mammals (Sumner 2003). The analogous system of sex chromosome determination is ZZ/ZW. In this case, male is homogametic (ZZ) and the female heterogametic (ZW). This system have been revealed in Lepidoptera, birds, and reptiles (Sumner 2003). In addition, there is an UV sex chromosome system, which have been found in bryophytes and some other organisms that are in the haploid phase for most of their lives. While the V chromosome is found in male haploid individuals, the U chromosome is found in female haploid individuals (Bachtrog et al. 2011, McDaniel et al. 2012). Another kind of sex determination is haplodiploidy, which have been found in mites, thrips, bees, ants, and wasps (Sumner 2003). In this mechanism, the sexes differ by the number of chromosome sets, males are haploid and females diploid (Dapper et al. 2022). Males arose from unfertilized eggs and females from fertilized eggs (Beukeboom 1995).

Sex chromosomes generally arise from an autosome pair. Recombination is gradually reduced between the sex chromosomes X and Y (respectively Z and W) in the course of evolution. Consequently, the Y or W chromosome gradually degenerates and may eventually disappear, resulting in the X0 or Z0 system. Chromosome fissions or rearrangements between sex chromosomes and autosomes give rise to complex sex chromosome systems that may include many sex chromosomes (Abbott et al. 2017, Beukeboom and Perrin 2014).

Spiders belong to organisms, which show a considerable diversity of sex chromosome systems (Araujo et al. 2012, Kořínková and Král 2013). Most spiders exhibit unusual multiple X chromosome systems (Král et al. 2013), which are rare in other animal clades (Kořínková and Král 2013).

Most information on the evolution of sex chromosomes is available in entelegyne spiders. The most common sex chromosome system of entelegyne spiders is ♂X_1X_2/♀$X_1X_1X_2X_2$ (named X_1X_20), where 0 indicates the absence of the Y chromosome (Araujo et al. 2012, Kořínková and Král 2013). The two X chromosomes, X_1 and X_2, are considered non-homologous due to the absence of recombination and their different size (Araujo et al.

2005, Král et al. 2011, Kořínková and Král, 2013). Nonhomologous nature of these X chromosomes was confirmed recently by their sequenation (e.g., Sheffer et al. 2022).

The origin of the system X_1X_20 has been explained by the fission of a metacentric X chromosome at X0 system (Pätau 1948). Another hypothesis also suggests origin from X0 system, namely via non-disjuction of X (Postiglioni & Brum-Zorrilla 1981, Kořínková and Král 2013). Finally, a recent hypothesis suggests that X_1X_20 system arose from X_1X_2Y system via loss of Y chromosome. The latter system is frequent in haplogyne araneomorphs (see below).

The X_1X_20 system is rare in mygalomorphs and haplogynes (Araujo et al. 2012, *Kořínková* and Král 2013). The X_1X_20 system has been transformed to other sex chromosome systems in some entelegyne clades, for example in X0 system in several lineages (Srivastava & Shukla, 1986, Taşdemir et al. 2012, Araujo et al., 2015a, Cavenagh et al. 2022). There are several proposed mechanisms of origin of X0 system in entelegynes, namely tandem fusion (e.g., Bole-Gowda 1950), centric fusion (e.g., Bole-Gowda 1952) or gradual deletion of one X chromosome (Suzuki 1954). The multiple sex chromosomes with more than two chromosomes found in some entelegynes ($X_1X_2X_30$, $X_1X_2X_3X_40$) could arise by fission(s) (*Kořínková* and Král 2013) or by non-disjuctions (Postiglioni and Brum-Zorrilla 1981, Datta and Chatterjee 1988). In some entelegynes, neo-sex chromosomes arose by the rearrangements between the gonosomes and autosomes (e.g., Madison et al. 2013, 2020).

Members of seven haplogyne families exhibit an unusual X_1X_2Y chromosome system (Král et al. 2006, Ávila et al. 2016, Paula-Neto et al. 2017, Araujo et al. 2020). The X_1X_2Y system show a conservative morphology. In most haplogynes, it consists of two large metacentric X chromosomes and a tiny metacentric Y chromosome forming a trivalent in the male first meiotic division. Sex chromosomes of the trivalent exhibit a specific achiasmatic pairing by ends of both arms (Král et al. 2006, Sember et al. 2020). This system could be ancestral for araneomorphs (Paula-Neto et al. 2017). If so, the system X_1X_20 of entelegynes arose from X_1X_2Y by loss of Y chromosome. This conversion of the X_1X_2Y system was also detected in filistatid haplogynes (Ávila et al. 2016). In some other haplogyne lineages, X_1X_2Y system has been converted into XY (diguetids) or even X0 system (filistatids, ochyroceratids, pholcids, scytodids, tetrablemmids) (Král et al. 2006, Oliveira et al. 2007, Ávila et al. 2016, Král et al. 2019).

The X_1X_2Y system was described for the first time in *Loxosceles laeta* (Silva 1988) and some other *Loxosceles* species (Silva et al. 2002). It has been found later in several other haplogyne families (Král et al. 2006, Ávila et al. 2016, Král et al. 2019). Origin of X1X2Y system is not resolved. X_1X_2Y system is an ancient sex chromosome determination; spider groups with this system were found already at Mesozoic stata (Král et al. 2006).

The ancestral sex chromosome system in mygalomorphs is probably the X_1X_20 system. Most representatives of the superfamily Atypoidea are characterized by the X0 system, which seems to have arisen from the fusion of X chromosomes in the X_1X_20 system. In the ancestors of the superfamily Avicularioidea, genome duplication probably occurred and gave rise to a system with four X chromosomes. In the course of subsequent evolution, sex chromosome fusions occurred in some lineages. This hypothesis is supported by distribution of species with reduced number of X chromosomes. These taxa have decreased diploid number in comparison with the close relatives (Král et al. 2013). Some mygalomorphs exhibit a sex chromosome system composed by more X chromosomes than four, for example $X_2X_3X_4X_50$ (*Microstigmata zuluensis)*, $X_1X_2X_3X_4X_5X_6X_7X_8X_9$ (*Macrothele yaginumai*) and $X_1X_2X_3X_4X_5X_6X_7X_8X_9X_{10}X_{11}X_{12}X_{13}$ (*Macrothele gigas*) (Král et al. 2013). The multiple X chromosome system of latter species is composed by a highest number of X chromosomes known so far. These systems have evolved by fissions or nondisjunctions of chromosomes. In some other mygalomorphs, rearrangements between sex chromosomes and autosomes formed neo-sex chromosomes (Král et al. 2013, Sember et al. 2020). Karyotype of these species include Y chromosome. These systems were discovered in *Atropothele socotrana* 68, $X_1X_2X_3Y$ (Sember et al. 2020), *Atypus affinis* (XY) (Řezáč et al. 2006), and *Paratropis* sp. ($X_1X_2X_3X_4X_5X_6X_7Y$) (Král et al. 2013). Two other mygalomorphs, namely *Cyphonisia* sp. and *Ischnothele caudata*, have XY system, which has originated probably from X0 system by a rearrangement between X chromosome and an autosome (Král et al. 2013).

Sex chromosomes of spiders exhibit a specific behaviour in male germline. They show a positive heteropycnosis - they are stained more intensively than the other chromosomes in some phases of male meiosis, especially in prophase I and metaphase I due to a higher condensation (Araujo et al. 2012). During male meiosis, they pair without chiasmata, being placed at the periphery of the nucleus (Kořínková et al. 2013). Regions of neo-sex

chromosomes originating from autosomes do not exhibit a specific behaviour (Maddison 1982).

Patterns of achiasmatic sex chromosome pairing in spider males are diversified. Sex chromosomes pair by ends of arms or are arranged in parallel during male meiosis (Král et al. 2006, 2007, 2011). The first type was detected in some basal groups of Entelegynae (Král et al. 2011), Haplogynae (Král et al. 2006) as well as in Mygalomorphae (Král et al. 2011, 2013). The second type is characteristics for most Entelegynae (Král et al. 2011, *Dolejš* et al. 2011) and some Haplogynae with holokinetic chromosomes (Benavente and Wettstein 1980, Kral et al. 2019).

Surprisingly, we also found a specific sex chromosome behaviour in the meiotic division of female spiders. While in all other organisms the sex chromosomes in meiosis of homogametic sex behave as autosomes, the homologous X chromosomes of female spiders pair already in interphase before meiosis, being positively heteropycnotic until metaphase I. Bivalents formed by sex chromosomes associate at one end during this period (Král 2007, Král et al. 2011).

Recent findings of our group suggest that sex chromosomes of spiders are even more complicated. They also contain a specific pair of undiffrentiated sex chromosomes XY termed sex chromosome pair (SCP) (Král 2007, Král et al. 2011, 2013) or cryptic sex chromosome pair (CSCP) (Sember et al. 2020), which exhibit end-to-end pairing with the the other sex chromosomes. CSCP could represent an ancestral spider sex chromosomes. Other sex chromosomes could arise from these proto-sex chromosomes by non-disjunction (Král 2007, Král et al. 2011, Sember et al. 2020).

The CSCP was detected in some entelegynes (Král 2007, Král et al. 2011) haplogynes (Král et al. 2006), and mygalomorphs (Král et al. 2013, Sember et al. 2020). Avicularioid mygalomorphs exhibit two CSCP (Král et al. 2013). The second SCSP could have been formed by polyploidization just like the $X_1X_2X_3X_40$ system (Král et al. 2013, Sember et al. 2020). Chromosomes of CSCP show the same morphology and size as well as the same heterochromatin pattern (Král et al. 2011, 2013, Sember et al. 2020). In some haplogynes and mygalomorphs, the CSCP exhibits the meiotic heterochromatization. It is suggested that the meiotic inactivation of CSCP prevents the recombination between this pair and the other sex chromosomes (Sember et al. 2020).

2.2.3. Meiotic modifications

Most common modification of spider meiotic division is the diffuse stage. This modification is found in the prophase I of some organisms, specifically between pachytene and diplotene (Benavente and Wettstein 1980). It is characterized by a considerable chromatin despiralization and nucleus enlargement, which reflect presumably a high transcriptional activity (Klášterská 1977, Benavente and Wettstein 1980, Kořínková and Král 2013). Diffuse stage arose multiple times in different eukaryotic lineages (Klášterská, 1977). For example, it has been found in some insect lineages such as some grasshoppers (White 1968), bugs (Lanzone and de Souza 2006), and beetles (Galián et al. 1995). While it is usually present in female meiosis, in some animals it has been revealed also in males, for example in haplogyne spiders (Král et al. 2006, 2011, 2013, Kořínková and Král 2013), including the lineage with holokinetic chromosomes (Benavente and Wettstein 1980, Král et al. 2006, Král et al. 2019). In other spider groups, the male diffuse stage was found only in some clades (Kořínková and Král 2013).

Another modification of spider meiotic division is inverted meiosis, which has been found in some spiders with holokinetic chromosomes (Král et al. 2019). This modification of meiosis has also been found in other organisms with holokinetic chromosomes. In this case, the sister chromatids separate already in the anaphase of the first meiotic division, which is made possible by the absence of kinetochores in holokinetic chromosomes and also by their specific orientation in metaphase I (Viera et al. 2009, Mola et al. 2011).

Achismatic meiosis is the last modification of meiosis found in some spiders. Chiasmata are formed at the beginning of the diplotene at sites where crossing over has previously occurred (Sumner 2003). These structures are essential for the proper segregation of the homologous chromosomes (Kurdzo et al. 2018). However, sometimes homologous chromosomes do not recombine. Therefore, chiasmata do not develop between homologous chromosomes. This modification of meiosis is termed achiasmatic meiosis (Kurdzo and Dawson 2015, Kurdzo et al. 2018, Dedukh et al. 2022). Because chiasmata are not developed, diplotene and diakinesis are replaced by a specific stage called postpachytene. During this stage, homologous chromosomes remain attached parallel to each other and gradually shorten. Achiasmatic meiosis occurs mostly in heterogametic sex (Štáhlavský and Král 2004). The achiasmatic meiosis have been observed in various

eukaryotic taxa, it originated independently multiple times (except for mammals) (White 1973, Šťáhlavský and Král 2004, Satomura et al. 2019). In arachnids the achiasmatic meiosis was reported in scorpions (Shanahan and Hayman 1990, Almeida et al. 2019), chthoniid pseudoscorpions (Šťáhlavský, and Král, 2004), haplogyne spiders from the families Dysderidae and Segestriidae (Benavente and Wettstein 1980, Rodríguez Gil et al. 2002), mygalomorphs of the family Euagridae (Král et al. 2013), and some acariform mites (Keyl 1957). In spiders of the families Dysderidae and Segestriidae, however, absence of chismata is only seeming. This is due to the considerably long diffuse stage, so that the chiasmata are visible only in metaphase I (Král et al. 2006).

2.2.4. Banding techniques and techniques of molecular cytogenetics

The information concerning centromeric and telomeric regions in spiders is scarce (Kořínková and Král 2013). C-banding revealed that these structures are formed by constitutive heterochromatin (Král et al. 2006, Dolejš et al. 2011, da Costa 2020, Rincão et al 2021). It is rare to find heterochromatin blocks out of these two regions in spiders (Dolejš et al. 2011). Sex chromosomes of some spiders contain a high amount of constitutive heterochromatin. It hold especially for Y chromosome of the X_1X_2Y system, for example Y chromosome of *Pholcus phalangioides* (Pholcidae) (Král et al. 2006).
Base composition of heterochromatin has been analysed by fluorescent banding by fluorochromes CMA_3 and DAPI in some spiders. This technique has revealed that constitutive heterochromatin is GC-rich in ctenids (*Rincão* et al. 2017). The banding patterns can be also important for the analysis of karyotype and the interspecific comparison of karyotypes (e.g., Cabral-de-Mello and Martins 2010). However, these techniques have little use in spiders because, with few exceptions, induction of banding patterns such as G-, R- or replication banding, which allow individual chromosomes to be distinguished by a specific banding pattern, has failed. The telomeric DNA of spiders do not contain the motif (TTAGG)n, which is probably ancestral in arthropods. The composition of the spider telomeric DNA is unknown (Vítková et al. 2005).

Nucleolar organizer regions (NORs) have been detected on the chromosomes of some spiders. These structures contain genes for 28S, 18S, and 5.8S rRNA. These rRNAs are a catalytic component of the ribosomes, thus are required by the cell in a high amounts (O'Sullivan et al. 2013, Palazzo and Lee 2015). Thus, these genes are found in NOR in many copies. They are arranged in discrete clusters, transcription units, each containing

one copy of each gene listed above. Clusters are separated by non-transcribed spacers (NTS), also called the intergenic spacer (IGS). Genes within a cluster are separated by internal transcribed spacers (ITS). Clusters are transcribed as a single unit of 45S rRNA (Sumner 2003, McStay 2016). Genes for 5S rRNA form separate clusters in the genome (Sumner 2003).

The nucleolus organizer regions of spiders have been detected initially by silver staining using $AgNO_3$ (Sumner 2003). However, this method reveals only NORs, which were active during the previous interphase, as the reaction leading to silver reduction, which provides the detectable signal, is dependent on the presence of specific proteins bound to rDNA promoters (Miller et al. 1976, Jiménez et al. 1988). Silver staining have been performed in several mygalomorphs (Král et al. 2013), haplogynes (Král et al. 2006, Oliveira et al. 2007, Paula-Neto et al. 2017), and entelegynes (Rodríguez-Gil et al. 2007, Dolejš et al. 2011, Forman et al. 2013, Kumar et al. 2017).

To improve the detection of NORs, fluorescence in situ hybridization (FISH) has been introduced into spider cytogenetics, using the 18rDNA probes. This technique detects all NORs including inactive ones (Forman et al. 2013, Král et al. 2013, 2019; Rincão et al. 2017, Sember et al. 2020, Štáhlavský et al. 2020). Most spider species examined exhibit a single NOR, which is probably an ancestral arachnid pattern (Forman et al. 2013). These structures have usually a terminal position (da Costa Pinto Neto et al. 2020). The evolution of some clades has been accompanied by the increase of NOR number (Štáhlavský et al. 2020). In haplogyne spiders, NORs often spreaded to sex chromosomes (Král et al. 2006, Ávila et al. 2016).

Concerning other gene clusters, the histone H3 genes has been only detected in spiders, namely in some ctenids. Specifically, this cluster is part of one chromosome pair in *Guasuctenus longipes*, three pairs in *Ctenus medius*, and four pairs in *Ctenus ornatus* (Rincão et al. 2020). Therefore, ctenids show a considerable diversity in number of H3 clusters. Furthermore, these authors found colocalization of the clusters of histone H3 genes and the blocks of constitutive heterochromatin, which suggest a co-evolution of histone genes and heterochromatin (Rincão et al. 2020).

2.3. Cytogenetics of haplogynes

2.3.1. Cytogenetics of haplogynes with monocentric chromosomes

Karyotype data have been obtained in a low number of haplogynes. Concerning haplogynes with monocentric chromosomes, data on 50 species from 9 families were published so far (Araujo et al. 2024).

Most analysed haplogynes belong to the family Pholcidae. According to database of Araujo et al. (2024), 23 species representing 9 genera has been karyotyped so far. The diploid number ranges from 9 to 32, karyotypes are composed mostly of biarmed chromosomes (Araujo et al. 2024). Authors report sex chromosome systems X0 (Bole-Gowda 1958, Cokendolpher & Brown, 1985, Srivastava & Shukla, 1986, Parida & Sharma, 1987, 1987a, Cokendolpher 1989, Xiuzhen et al. 1997a, Král et al. 2006, Oliveira et al. 2007, Ramalho et al. 2008, Lomazi et al. 2018), X_1X_20 (Painter 1914, Suzuki, 1954, Prakash & Prakash, 2014a,b), XY (Golding & Paliulis 2011), and X_1X_2Y (Král et al. 2006). *Artema atlanta* have been analysed three times, the authors suggest the same karyotype 32, X_1X_20 (Sharma & Parida 1987, Parida & Sharma 1987a, Arunkumar & Jayaprakash, 2015). Several different karyotypes are suggested for *Crossopriza lyoni* (India, Brazil, and Portugal) (Bole-Gowda, 1958, Srivastava & Shukla, 1986, Parida & Sharma, 1987a, Sharma & Parida, 1987, Oliveira et al. 2007, Prakash & Prakash, 2014a, Prakash & Prakash, 2014b, Arunkumar & Jayaprakash, 2015, Sharma & Ramakrishna, 2019).

A large number of species has been karyotyped also in the family Sicariidae; karyotypes of 18 species have been described (Sember et al. 2020, Araujo et al. 2023). Diploid number ranges from 18 (Tugmon et al. 1990) to 23 (Silva et al. 1988, 2002, Araujo et al. 2020, Sember et al. 2020). All species display X_1X_2Y system (Silva 1998, Silva et al. 2002, Král et al. 2006, Araujo 2007, Franco and Andia, 2013, Kumbiçak 2014, Araujo et al. 2020) except for *L. reclusa, L. rufipes* (X_1X_20) (Diaz & Saez 1966, Tugmon et al. 1990), and *Sicarius tropicus* (XY) (Gimenez-Pinheiro et al. 2022).

Several species of plectreurids were studied, male diploid number ranges from 18 to 22. Three sex chromosome systems were revealed. Beside species with system X_1X_2Y, which is probably ancestral for haplogynes, there are also species with derived systems, X_1X_20 and $X_1X_2Y_1Y_2$. Latter system arose by fission of Y chromosome or Y chromosome nondisjunction (Král et al. 2006, Ávila et al. 2016).

In the family Scytodidae, only five species have been karyotyped. The diploid number ranges from 13 (Araujo et al. 2008, Rodríguez-Gil et al. 2002) to 31 (Araujo et al. 2008). The majority of species show X0 system with the exception of *S. globula* (cited as *S. maculata*) in which is reported X_1X_20 system (Diaz and Saez 1966). Chromosomes of this species are biarmed. In other species, some chromosome pairs exhibit subtelocentric or acrocentric morphology, namely in *S. fusca* (Araujo et al. 2008), *S. itapevi* (Araujo et al. 2008), and *S. thoracica* (Král et al. 2006).

Concerning the family Filistatidae, five species have been evaluated as well. The diploid number ranges from 21 (*Pikelinia mendensis*) (Paula-Neto et al. 2017) to 33 (*Filistata insidiatrix*) (Král et al. 2006). In all studied species, the X_1X_2Y SCS has been reported (Král et al. 2006, Paula-Neto et al. 2017, Sember et al. 2020) except for karyotype 24, X_1X_20 in *Kukulcania hibernalis* (Rodríguez-Gil et al. (2002). Other authors reported Y chromosome in this species (Hetzler 1979, Paula-Neto et al. 2017). I suppose that Rodríguez et al. (2002) overlooked Y chromosome in this species due to its tiny size. This may be the same for a number of other haplogyne species for which the X_1X_20 system is reported. Y chromosome of the X_1X_2Y system is usually tiny in haplogynes (Král et al. 2006).

Concerning other haplogyne families, there is only a basic description of the karyotype in one or two species. Specifically, *Drymusa capensis* (Drymusidae) exhibits male karyotype 37, X_1X_2Y (Král et al. 2006), *Diguetia albolineata* 20, XY, *D. canities* 16 XY (Diguetidae), *Monoblemma muchmorei* 23, X0 (Tetrablemmidae), (Král et al. 2006) and *Paculla* sp. 33, X_1X_2Y (Pacullidae) (Král et al. 2019).

2.3.2. Banding techniques and techniques of molecular cytogenetics in haplogynes with monocentric chromosomes

In several haplogynes, C- banding have been used to detect the constitutive heterochromatin. Most studied species belong to the family Sicariidae (Araujo et al. 2020). Chromosomes of analysed species contain centromeric block of heterochromatin. In the genus *Loxosceles*, telomeric regions are usually formed by heterochromatin of variable size (Král et al. 2006, Araujo et al. 2020). X chromosomes display similar distribution of heterochromatin like autosomes. In contrast to this, Y chromosome is usually almost completely heterochromatic (Silva et al. 2002).

Nucleolus organizer regions in haplogynes were detected by silver staining or by fluorescence in situ hybridization, namely in Diguetidae (Král et al. 2006), Plectreuridae (Ávila et al. 2016), Pholcidae (Oliveira et al. 2007, Arunkumar et al. 2015), Tetrablemmidae (Král et al. 2006) and Sicariidae (Araujo et al. 2020).

In general authors observed a low number of NORs. Beside autosomes, NORs were frequently located on sex chromosomes (Král et al. 2006, Ávila et al. 2016). The sex-chromosomes linkedNORs were revealed in several species, namely *Scytodes thoracica, Ochyrocera* sp., *Monoblemma muchmorei, Loxosceles spinulosa*, *L. rufescens* (Král et al 2006), *Crossopriza lyoni* (Oliveira et al. 2007, Arunkumar et al. 2015), and *Plectreurys* (Ávila et al. 2016). .

Molecular differentiation of Y chromosome of the X_1X_2Y system has been studied in some families of haplogynes (Sicariidae and Filistatidae) by comparative genomic hybridisation (CGH) (Sember et al. 2020). The male specific DNA was found only in Y chromosome (Sember et al. 2020). Surprisingly, male specific DNA was not revealed in Y chromosome of *L. similima.* This pattern may result from the insertion of autosomal fragments into the Y chromosome (Sember et al. 2020). In Pholcidae Y chromosome is formed exclusively by male specific DNA. In addition, terminal region of the X_2 chromosome ensuring pairing with Y chromosome exhibits a slight accumulation of male probe, which probably reflects spreading of male repetitive DNA in the terminal part of X_2 chromosome (Sember et al. 2020).

2.4. Haplogyne spiders with holokinetic chromosomes

Holokinetic chromosomes have arisen several times in Eukaryota. Among others, they have been reported in some protista, plants, nematods, arachnids, and insects (Mola 1995, Traut and Marec 1997, 1995, Melters et al. 2012, Kuznetsova et al. 2019, Nokkala and Golub 2002). Holokinetic chromosomes lack a localized centromere. Therefore the centromere activity spread along most of all surface of these chromosomes faced to the cell poles (Mola and Papeschi 2006, Melters et al. 2012, Bureš et al. 2013, 2014, Mandrioli and Manicardi 2020). As a consequence the fusion products and fragments of these chromosomes segregate usually regularly (Jankowska et al. 2015). Holokinetic chromosomes of some organisms are remarkable for the inverted meiosis. During this modified meiotic division, sister chromatids are separated already during the anaphase of the first meiotic division. This modification is enabled by the absence of centromere

connection (Cabral et al. 2014). Holokinetic chromosomes show a low frequency of recombinations; it could be a preadaptation for achiasmatic meiosis (Butlin 2005, Bureš et al. 2013, 2014).

Holokinetic chromosomes are considered to be a derived character (Dernburg 2001, Mola and Papeschi 2006, Melters et al. 2012, Drinnenberg et al. 2014, Escudero et al. 2016). Some authors suggest that the holokinetic chromosomes arose by the expansion of the kinetic activity over the large area of the chromosome surface (Král 1994a, Nagaki et al. 2005, Král et al. 2006). Recent study of Zedek and Bureš (2018) indicates that the change from monocentric to holokinetic chromosomes was a very important adaptation promoting the transition of organisms from oceans to terrestrial ecosystems. However, the mechanism of formation of the holokinetic chromosomes is complex and available data are not sufficient to explain all aspects of this transition (e.g., Zedek and Bureš 2018, Neumann et al. 2023).

In arachnids, holokinetic chromosomes have been reported in scorpions of the family Buthidae (Sadílek et al. 2015, Ubinski et al. 2018, Almeida et al. 2019), acariform mites (Oliver, 1977, Eroğlu and Per, 2016), spiders of the superfamily Dysderoidea (Rodriguez Gil et al. 2002, Král et al. 2006, Díaz et al. 2010, Král et al. 2019), and in one genus of ticks (Hill et al. 2009).

Although holokinetic chromosomes were discovered a long time ago in spiders, information on their distribution and evolution is very limited (Král et al. 2019). The holokinetic chromosomes appear to be apomorphy of the superfamily Dysderoidea (Král et al. 2019), which is an ancient lineage found already at Cretaceous strata (Penney and Selden 2011).

From cytogenetic point of view, the most studied family of spiders with holokinetic chromosomes is Dysderidae (Araujo et al. 2024). Diploid numbers range from 7 (Kořínková & Král, 2013, Řezáč et al. 2018, Král et al. 2019) to 40 (Řezáč et al. 2007). Analysed species belong to the genera *Dasumia*, *Dysdera*, *Dysderocrates*, *Harpactea*, *Harpactocrates*, and *Kaemis* (Araujo et al. 2024). Concerning *Dysdera* genus, karyotypes of 26 species have been described (Benavente & Wettstein, 1980, Rodríguez-Gil et al. 2002, Řezáč et al. 2007, 2014, 2018). Data on *D. crocata* suggest diversity of diploid numbers in this species. Populations from Argentina (Rodríguez-Gil et al. 2002) and Turkey (Řezáč et al. 2007) possess 2n♂=11. On the other hand, the populations from

South Africa, Bulgaria, and Spain display 2n♂=9 (Řezáč et al. 2007, 2018), and populations from Canary Islands (Portugal) 2n♂=13 (Řezáč et al. 2007). The studied dysderids show X0 system, except for *Dysdera dolanskyi*, which exhibit X_1X_20 SCS (Řezáč 2018). *Dysdera crocata* and species of the subfamily Harpactirinae exhibit inverted meiosis (Král et al. 2019).

The male diploid numbers found in the family Segestriidae are quite low, range from 7 (Suzuki, 1950b, 1954) to 14 (Diaz & Saez, 1966, Diaz et al., 2010, Král et al. 2006). While the genus *Ariadna* shows X0 system (Rodríguez-Gil et al. 2002, Diaz et al. 2010, Král et al. 2019), species of the genus *Segestria* display X_1X_20 system (Benavente & Wettstein, 1980, Král et al. 2006, Diaz et al. 2010), which probably arose by fission of the ancestral single X chromosome found in *Ariadna* (Král et al. 2019).

In the family Oonopidae, four species has been karyotyped, namely *Ischnothyreus* sp., *Oonops ebenecus, O. pulcher,* and *Xestaspis parmata.* These species exhibit a karyotype formula 2n♂=7, X0 (Král et al. 2019). Recently, three species more have been analysed, namely *Cinetomorpha simplex* (2n♂=9, X0), *Neotrops* sp., and *Neoxyphinus termitophilus* (2n♂ = 7, X0) (Duarte et al. 2023). All oonopid species have low diploid number and X0 SCS.

Concerning the family Orsolobidae, only one species has been analysed (*Afrilobus* sp.). It is the spider with the lowest diploid number (2n♂=5, X0) (Král et al. 2019).

Interestingly, the family Caponiidae, a sister clade of the Dysderoidea, exhibit chromosomes with standard structure. Moreover, caponiids show a high diploid number, numerous sex chrosomes, and an enormous genome size (Král et al. 2019). Diploid numbers and sex chromosome systems of analysed caponiids are as follows: *Caponia natalensis* 2n♂= 152, $X_1X_2X3X_4X_5X_6$; *C. capensis* 2n♀=136; *C. hastifera* 2n♂=128, $X_1X_2X3X_4X_5X_6X_7X_8X_9X_{10}Y_1Y_2$, *Nops* aff. *variabilis* 55, $X_1X_2X3X_4Y$. In several other caponiids, only the diploid number was obtained. Chromosomes of caponiids are predominantly biarmed (Král et al. 2019). A specific genomes of caponiids (an enormous diploid number of chromosomes, a high number of sex chromosomes, and an enormous genome size) suggest collectively duplication of genome in ancestor of this clade (Král et al. 2019). It is assumed that in the ancestral representatives of the family Dysderoidea, the diploid number was reduced to seven chromosomes in males, including a single X chromosome (Král et al. 2019).

2.5. Cytogenetics of Mygalomorphae

The cytogenetics of mygalomorphs is not satisfactorily understood. Currently, data on 39 genera and 48 species have been obtained (Suzuki, 1949, 1954, Hetzler, 1979, Srivastava & Shukla 1986, Painter, 1914, Oliveira, 1998, Akan 2005, Řezáč 2006, Král et al. 2011, 2013, Kořínková & Král 2013, Sember et al. 2020). Mygalomorphs show a high diversity of diploid numbers and chromosome morphology. The diploid numbers of mygalomorph males vary from 14 (*Atypus affinis*, Atypidae) (Řezáč et al. 2006) and *Ischnothele caudata*, Ischnothelidae) (Král et al. 2013) to 128 (*Cyclocosmia siamensis*, Halonoproctidae) (Král et al. 2013). The most studied family is Theraphosidae with 19 species included in 16 genera (Lucas et al. 1993, Oliveira et al. 1998, Akan 2005, Řezáč et al. 2006, Kořínková & Král, 2013, Král et al. 2011, 2013, Sember et al. 2020).

Mygalomorphs show various proportions of monoarmed and biarmed chromosomes. However, karyotype of most mygalomorphs studied so far is predominated by biarmed chromosomes (Lucas et al. 1993, Oliveira 1998, Řezáč et al. 2006, Král et al. 2011, 2013, Sember et al. 2020). This morphology also have been found in haplogyne spiders (Král et al. 2006, Řezáč et al. 2006). This pattern suggest that predomination of biarmed morphology is a symplesiomorphy of opisthothele spiders (Král et al. 2006). Biarmed chromosomes prevails in analysed species of families Atypidae (Řezáč et al. 2006), Ctenizidae (Král et al. 2013), Halonoproctidae (Král et al. 2013), Idiopidae (Král et al. 2013), Ischnothelidae (Král et al. 2013), Macrothelidae (Král et al. 2013), Megahexuridae (Král et al. 2013), and Theraphosidae (Kořínková & Král, 2013, Král et al. 2011, 2013, Sember et al. 2020). On the other hand, there are also the families with a high proportion of monoarmed chromosomes: Cyrtaucheniidae (Král et al. 2013), Dipluridae (Král et al. 2011), Nemesiidae (Král et al. 2013), Barychelidae (Král et al. 2013, Sember et al. 2020), and Migidae (Král et al. 2013). Monoarmed chromosomes of these families arose from biarmed ones, usually by pericentric inversion (Král et al. 2013).

The superfamily Atypoidea is composed of five familes: Atypidae and Antrodiaetidae, Mecicobothriidae, Hexurellidae, Megahexuridae (Hedin & Bond, 2019), only three of them have been studied cytogenetically. In the family Atypidae, all studied species belong to the genus *Atypus*, their male diploid numbers range from 14 (Řezáč et al. 2006) to 46 (Suzuki, 1949, 1950a). Three sex chromosomes systems were reported in *Atypus*, namely X0 (Řezáč et al. 2006, Král et al. 2011), XY (Řezáč et al. 2006), and X_1X_20 (Suzuki 1949,

1950a, 1954). Concerning the family Antrodiaetidae, only three species belonging to three genera have been studied so far. Diploid numbers in males range from 27 to 47 (Král et al. 2013). Chromosomes are mostly biarmed. All analysed species have X0 system (Hetzler 1979, Král et al. 2013). Concerning the family Megahexuridae one specie have been karyotyped, *Megahexura fulva* 43, X0. This species possesses only biarmed chromosomes (Král et al. 2013).

The X0 system of Atypoidea has probably evolved from the ancestral X_1X_20 system by centric fusion; it is supported by a large size of X chromosome of X0 system (Král et al. 2011, 2013). *A. affinis* exihibits neo-sex chromosomes XY, which arose by fusions between original X chromosome of the X0 system and autosomes (Řezáč et al. 2006).

Avicularoidea superfamily includes 31 families (Godwin et al. 2018, Hedin et al. 2018, , Kulkarni et al. 2023, Wheeler et al. 2017). Concerning Barychelidae family, two species had been karyotyped only, *Cyphonisia* sp. 2n♂=40, XY? (Král et al. 2013) and *Atrophothele socotrana* 2n♂=68, $X_1X_2X_3Y$ (Sember et al. 2020). Karyotype of both species is predominated by monoarmed chromosomes. Sex chromosome system of these species is formed most probably by neo-sex chromosomes (Král et al. 2013, Sember et al. 2020). Single studied species of the family Ctenizidae (*Cyrtocarenum cunicularium*, 2n♂=74, X_1X_20) shows mostly biarmed chromosomes, even sex chromosomes exhibited this morphology (Král et al. 2013).

The two karyotyped species from the family Cyrtaucheniidae belong to the genus *Ancylotrypa*, they show predominance of monoarmed chromosomes (Král et al. 2013). Unfortunately, it was impossible to determine the sex chromosome system (Král et al. 2013). In the family Dipluridae, two species has been analysed, namely *Diplura* cf. *petrunkevitchi* 2n♂=90, $X_1X_2X_3X_40$ and *Linothele sericata* 2n♂=86, $X_1X_2X_3X_4X_5X_60$ (Král et al. 2011, 2013). These species differ considerably in the chromosome morphology. *D*. cf. *petrunkevitchi* exhibits mostly monoarmed chromosomes. On the other hand, most chromosomes of *L. sericata* display biarmed morphology. System $X_1X_2X_3X_4X_5X_60$ found in *L. sericata* arose probably from the ancestral Avicularioidea system ($X_1X_2X_3X_40$) by chromosome fissions. The larger X chromosomes retained biarmed morphology, small X chromosomes are acrocentric and arose by fission of biarmed chromosomes (Král et al. 2013). The same process formed probably $X_1X_2X_3X_4X_50$ system of *Euagrus lynceus* (Král et al. 2013), belonging to the family Euagridae. The highest number of X has been found in the family Macrothelidae, namely

in *Macrothele gigas* (Macrothelidae), which displays $X_1X_2X_3X_4X_5X_6X_7X_8X_9X_{10}X_{11}X_{12}X_{13}0$ system (Král et al. 2013). Very high number of X chromosomes has been found also in another *Macrothele* representative, *M. yaginumai* ($X_1X_2X_3X_4X_5X_6X_7X_8X_90$) (Král et al. 2013). In both species, the sex chromosomes were biarmed (Král et al. 2013).

In the the family Halonoproctidae, karyotypes of three species have been described. The genus *Cyclocosmia* is characterized by enormous differences in diploid chromosome number. While male of *C. siamensis* possesses 128 chromosomes (Král et al. 2013), the male of *C. torreya* displays only 42 chromosomes (Hetzler, 1979). Unfortunately there is no information on sex chromosomes in this genus. Male of Ummidia sp. shows karyotype 53, X0 (Král et al. 2013). In the family |Idiopidae only one species have been karyotyped, *Titanidiops syriacus* 61, X0? (Idiopidae), as well as in families Nemesiidae (*Iberesia machadoi* 76, X_1X_20?) and Euctenizidae (*Myrmekiaphila torreya* ±80) (Hetzler, 1979).

The most studied mygalomorphs belong to the family Theraphosidae (Araujo et al. 2024). Reported male diploid numbers range from 16 (*Chaetopelma olivaceum*) (Akan et al. 2005) to 110 (*Poecilotheria formosa*) (Král et al. 2011). In *Ch. olivaceum*, however, it is almost certain that the diploid number was incorrectly determined; our unpublished results show that it is much higher. Karyotypes are predominated by biarmed chromosomes (Araujo et al. 2024). The sex chromosome systems are diverse, namely X0 (Král et al. 2013, Sember et al. 2020), X_1X_20 (Painter, 1914, Král et al. 2013, Sember et al. 2020), $X_1X_2X_3$, and $X_1X_2X_3X_4$ (Kořínková & Král 2013, Král et al. 2011, 2013). In most species, CSCP exhibit a specific behaviour at male germline (Král et al. 2011, 2013, Sember et al. 2020).

2.5.1. Banding techniques and molecular cytogenetics in mygalomorphs

The banding techniques have been applied in a few species of mygalomorphs. C-banding has been used in three species. In *Poecilotheria formosa* (Theraphosidae), the constitutive heterochromatin was concentrated in the centromeric and telomeric regions of chromosomes. The metacentrics of the largest pair showed a centromeric block of heterochromatin and a large intercalar block at the short arm (Král et al. 2011). Similar results were obtained in *Macrothele gigas* (Macrothelidae) (Král et al. 2013). In *Psalmopoeus cambridgei*, one X chromosome include an intercalar block of

heterochromatin, which is probably the result of X-X chromosome fusion. The number of X chromosomes was reduced to two in this spider (Král et al. 2013).

In some theraphosids, nucleolus organizer regions have been detected, in most species by silver staining. In *Aliatypus californicus* (Antrodiaetidae), chromosomes of the largest pair have two terminal NORs (Král et al. 2013). Another representative of this family, *Antrodiaetus riversi*, shows two chromosome pairs including NOR, one NOR is larger (Král et al. 2013). One NOR-bearing autosome pair has been revealed in two members of the superfamily Avicularioidea, *Euagrus lynceus* (Euagridae) and *Idiothele mira* (Theraphosidae) (Král et al. 2013). In two theraphosids, *Grammostola* sp. (Cabral-de-Mello et al. 2021) and *Tlitocatl albopilosum* (Král et al. 2013), NORs were detected by FISH. Similarly to *Idiothele*, one autosome pair beared NOR. Interestingly, sex chromosome-linked NORs were demostrated in *Ischnothele* (on chromosomes X and Y) (Ischnothelidae) and *Linothele* (Dipluridae) (on one X chromosome) (Král et al. 2013). In the representative of the family Nemesiidae, one chromosome of the CSCP beared NOR at both termini (Král et al. 2013).

3. List of methods

Dissection of tissues

Dissection of tissues containing chromosomes from gonads, intestine or from the entire content of abdomen.

Microscopy

Stereomicroscope (determination of species, dissection of tissues), light and fluorescent microscopy (evaluation of chromosome preparations).

Conventional cytogenetics

Analysis of mitotic and meiotic preparations stained by Giemsa, detection of constitutive heterochromatin (C-banding).

Molecular cytogenetics

FISH with 18 rDNA probe.

Molecular biology

DNA isolation, separation (electrophoresis) and quantification of DNA (NanoDrop), amplification of DNA by polymerase chain reaction (PCR).

4. Outline of the publications

Publication 4.1. Řezáč M, Heneberg P, **Ávila Herrera IM**, Gloríková N, Forman M, Řezáčová V, Král J (2022). *Atypus karschi* Dönitz, 1887 (Araneae: Atypidae): an Asian purse-web spider established in Pennsylvania, USA. PLoS ONE. DOI.org/10.1371/journal.pone.0261695

IF2021: 3.7

This study is focused on the genus *Atypus* belonging to the phylogenetically basal mygalomorph family Atypidae. This family is composed by three genera (*Atypus*, *Sphodros*, and *Calommata*) and 54 species. The study is focusing on the karyotype analysis, taxonomy, the habitat, and natural history of the taxon *Atypus snetsingeri* (Sarno, 1973) from Pennsylvania, USA. Our analysis of the molecular markers (CO1 sequences) showed that *A. snetsingeri* is identical with *Atypus karschi* Dönitz, 1887, which is native at East Asia. Therefore, it is an introduced species at USA. It is the first known case of an introduced mygalomorph spider.

Representatives of the genus *Atypus* build a webbed tube, the end of which lies on the ground in European representatives. The spiders wait for their prey in the tube, then tear through the tube and pull the specimen inside. In *A. karschi*, the tube was usually located vertically (for example on bases of trees or bushes) and camouflaged by substrate and plant debris. Spiders spent majority of life inside the burrow except for adult males, which were looking for a female. In Pennsylvania, the habitat of *A. karschi* varied from the forest to suburban bushes.

Considering the basal position of atypids in the phylogenetic tree of mygalomorphs, data on their cytogenetics are very valuable for the reconstruction of karyotype evolution of mygalomorphs. In spite of this, the cytogenetics of the family Atypidae is poorly understood; only four species of the genus *Atypus* have been studied so far.

Similarly to two European species, *A. piceus* and *A. muralis*, male karyotype was formed by 41 chromosomes including X0 system and predominated by metacentric chromosomes. The C-banding technique showed centromeric and telomeric blocks of heterochromatin on the most chromosomes. Fluorescence in situ hybridization revealed one terminal NOR localized on a chromosome pair. Nucleolus organizer region was

adjacent to a large pair of heterochromatin. My data showed that NOR-linked heterochromatin of *Atypus* is formed by inactivated rDNA.

My contribution: Preparation of chromosomal slides and their evaluation. FISH and C-banding experiments and their evaluation. Analysis of data, assembly of karyotype. Preparation of figures, revision of the manuscript.

PLOS ONE

RESEARCH ARTICLE

Atypus karschi Dönitz, 1887 (Araneae: Atypidae): An Asian purse-web spider established in Pennsylvania, USA

Milan Řezáč[1]*, Steven Tessler[2], Petr Heneberg[3], Ivalú Macarena Ávila Herrera[4], Nela Gloríková[1], Martin Forman[4], Veronika Řezáčová[1], Jiří Král[4]

1 Crop Research Institute, Prague, Ruzyně, Czech Republic, **2** Tyler Arboretum, Media, PA, United States of America, **3** Third Faculty of Medicine, Charles University, Ruská, Prague, Czech Republic, **4** Faculty of Science, Laboratory of Arachnid Cytogenetics, Department of Genetics and Microbiology, Charles University, Viničná, Prague, Czech Republic

* rezac@vurv.cz

Citation: Řezáč M, Tessler S, Heneberg P, Herrera IMÁ, Gloríková N, Forman M, et al. (2022) *Atypus karschi* Dönitz, 1887 (Araneae: Atypidae): An Asian purse-web spider established in Pennsylvania, USA. PLoS ONE 17(7): e0261695. https://doi.org/10.1371/journal.pone.0261695

Editor: Bi-Song Yue, Sichuan University, CHINA

Received: December 3, 2021

Accepted: June 13, 2022

Published: July 7, 2022

Data Availability Statement: All the data are in the main body of the paper or in the Supplementary Information.

Funding: The study was supported by the Ministry of Education, Youth and Sports of the Czech Republic (project LTAUSA18171) and by the Ministry of Agriculture of the Czech Republic (project MZe RO0418). The chromosome part of this study was funded by the Charles University (project 92218) and Ministry of Education, Youth, and Sports of the Czech Republic (projects SVV-260568 and LTAUSA19142). The funders had no

Abstract

The mygalomorph spiders of the family Atypidae are among the most archaic spiders. The genus *Atypus* Latreille, 1804 occurs in Eurasia and northern Africa, with a single enigmatic species, *Atypus snetsingeri* Sarno, 1973, known only from a small area in southeastern Pennsylvania in eastern USA. A close relationship to European species could be assumed based on geographic proximity, but *A. snetsingeri* more closely resembled Asian species. This study was undertaken to learn more about the genetics of *A. snetsingeri*, its habitat requirements and natural history. Molecular markers (CO1 sequences) were compared to available data for other atypids and showed that *A. snetsingeri* is identical with *A. karschi* Dönitz, 1887 native to East Asia. Natural history parameters in Pennsylvania were also similar in every respect to *A. karschi* in Japan, therefore, we propose that the spider is an introduced species and the specific epithet *snetsingeri* is relegated to a junior synonym of *A. karschi*. Cytogenetic analysis showed an X0 sex chromosome system (42 chromosomes in females, 41 in males) and we also detected nucleolus organizing regions and heterochromatin, the latter for the first time in the Atypoidea. In Pennsylvania the spider is found in a variety of habitats, from forests to suburban shrubbery, where the above-ground webs are usually attached vertically to trees, shrubs, or walls, although other webs are oriented horizontally near the ground. Prey include millipedes, snails, woodlice, carabid beetles and earthworms. *Atypus karschi* is the first known case of an introduced purse-web spider. It is rarely noticed but well-established within its range in southeastern Pennsylvania.

Introduction

Mygalomorph spiders of the family Atypidae are among the earliest divergent groups of spiders [1]. They dig a burrow and construct a 'purse-web', usually in the form of a closed tube, that occupies the burrow and extends above the ground horizontally or vertically for prey

role in study design, data collection and analysis, decision to publish, or preparation of the manuscript.

Competing interests: The authors have declared that no competing interests exist.

capture. The webs are well-camouflaged with soil particles and plant debris and potential prey are sensed when they walk on the surface of the tube. The spider impales the prey through the silk with its long fangs and injects paralytic venom. It then makes a slit in the tube large enough to drag the prey inside, repairs the tear with new silk, and feeds on the prey [2–5]. Atypid spiders spend their entire lifetime within their burrow in the silken web, 8–10 years for some females, and enlarge the burrow as they grow [6–8]. Males abandon their burrows when they reach maturity and wander in search of females, and then mate within the female's web. Egg-laying occurs within the maternal web and fully capable spiderlings emerge later. In contrast to most mygalomorphs, atypid spiderlings utilize silk for aerial dispersal before establishing their first web [9–11]. This ability may have allowed some species of atypids to colonize new areas, including those that were uninhabitable during the last glacial period (e.g., northern Europe, [12], China [13: 38]).

There are currently three genera and 54 valid species of Atypidae [14]. The genus *Atypus* Latreille, 1804 (34 species from Europe, Asia, North Africa and North America), spins an above-ground web that is tubular and typically lays horizontally and parallel to the soil surface. In *Sphodros* Walckenaer, 1835 (seven species from eastern North America) the above-ground web is tubular and usually attached vertically to trees and other vegetation. In the genus *Calommata* Lucas, 1837 (13 species from Africa and Asia) the above-ground web is a flat circular pouch set on the soil surface [15].

The center of diversity of the genus *Atypus*, based on the number of species, is in southeastern Asia and at least three species live in the western Palearctic. Despite the number and widespread distribution of *Atypus* species they are secretive animals, and little is known about their habitat requirements, natural history, and genetic variation. In central Europe, certain *Atypus* species prefer sites with a microclimate regime resembling the climate of the glacial refuges from where they colonized the region [16]. The species that live on open steppe habitats require soils rich in calcium that maintain a favorable air humidity in spider burrows, and those that do not require calcic soils occur only in habitats sheltered by woody vegetation, and their webs are hidden in detritus [17]. As such, the European *Atypus* spiders are indicators of stable relic habitats and considered optimal flagship species in the conservation of disappearing relic xerothermic habitats [8].

Currently there are 16 species of Atypidae with available DNA sequence data, eleven of which represent the genus *Atypus* [18]. In contrast, only four atypid species, also in the genus *Atypus*, have been studied for their chromosomal constitution: *Atypus affinis* Eichwald, 1830; *Atypus karschi* Dönitz, 1887; *Atypus muralis* Bertkau, 1890; and *Atypus piceus*, Sulzer, 1776. The reported diploid number ranges from 14 to 44, and sex chromosome systems XY, X0, and X_1X_20 have been described [19–21]. There are no data on other chromosome features, such as constitutive heterochromatin or nucleolus organizing regions (NORs). Those chromosome markers have been sporadically examined in Mygalomorphae [19,22].

This study looked at the genetics and habitat requirements of the lone species of *Atypus* found in North America, *Atypus snetsingeri* Sarno, 1973 [23]. This spider appears to be restricted to a small geographic area near Philadelphia, Pennsylvania in eastern USA [24]. It is morphologically very similar to *A. karschi* of Asia [7,25,26], and has been considered a possible introduction to North America. To help resolve its relationship with other atypids, the karyotype and genetic barcode (CO1) were developed for *A. snetsingeri* to compare with other *Atypus* species, along with observations on habitat associations and natural history. Data on karyotype [e.g., 27,28] and genetic barcode are frequently used to reconstruct phylogeny and evolutionary history of taxa including spiders.

Material and methods

Study locations

In November 2013 we visited eight sites in Delaware County, Pennsylvania, that were known to have *A. snetsingeri* populations [Tessler, personal observations]. The sites ranged from semi-urban areas near the type locality to wooded county parks along riparian corridors where purse-webs were common (S1 File). The primary site used for detailed web observations, specimen excavation and collection was a fallow field adjacent to forest at the Tyler Arboretum (hereafter "Tyler", Media, PA). That field was mowed annually to control invasive plants and facilitated access to the webs.

Habitat and natural history

At each site, we assessed the primary vegetation cover and soil type. The land orientation of the web location was measured using a compass and the slope angles using an optical reading clinometer to the nearest 0.5˚. Soil penetration resistance was measured as described by Srba & Heneberg [29], where higher values reflect mechanical impedance for burrowing.

The range of web sizes (tube diameter) was visually assessed in the field and prey were noted by identifying remnants of invertebrates found attached to webs. The webs of 18 adult females were excavated on 5–9 November 2013. The length of the purse-webs was measured, distinguishing the below-ground and above-ground sections by coloration and attached soil. The size of the females was characterized by measuring the length of the carapace along the midline. When juveniles were present, their number was counted. Several juvenile specimens were also excavated for the karyotype analysis (webs not measured). Voucher specimens from this study were deposited at the Crop Research Institute, Prague, Czechia.

Statistical analysis

We used Pearson's correlation test to analyze carapace size against web parameters (length of the below-ground and above-ground length) and to analyze the correlation between individual web parameters. We used Spearman's rank correlation test to evaluate the correlation between female size and number of offspring. The difference in body size between females with offspring and females without offspring was analyzed using the Welch two sample *t*-test. We tested the variances in the below-ground and above-ground parts of the web by F-test. Normality was tested by the Shapiro-Wilk normality test. Data were analyzed in the statistical software R 3.6.2 [30]. The means are given with ± the standard error of the mean as a measure of sampling distribution.

Karyotype analysis

Chromosome preparations were obtained from gonads of one immature male (testes present, sex can not be distinguished in living juveniles) and one mature female (ovary present). We followed the spreading technique described for mygalomorphs by Král et al. [22] except for fixation procedure. Due to a small size of gonads, we used two fixations (10 and 20 min) instead of three. The standard preparations were stained by 5% Giemsa solution in Sörensen phosphate buffer for 25 min. The evaluation of the karyotype was based on five mitotic metaphases. The chromosome measurements were carried out using ImageJ software [31]. The relative chromosome lengths were calculated in each specimen independently as a percentage of the total chromosome length (TCL) of the haploid set, including sex chromosome. Chromosome morphology was classified according to Levan et al. [32].

Our study also includes detection of constitutive heterochromatin and nucleolus organizing regions. Male mitotic plates were used to visualize these markers. Constitutive heterochromatin was detected by C-banding following Král et al. [33]. Preparations were stained by 5% Giemsa solution in Sörensen phosphate buffer for 75 min. NORs were visualized using fluorescence in situ hybridization (FISH) with a biotin-labeled probe for 18S rDNA sequences. The probe was obtained from *Dysdera erythrina* Walckenaer, 1802 (Dysderidae). FISH, probe detection by streptavidin-Cy3 and signal amplification was performed as described by Forman et al. [34].

DNA extraction, amplification and sequencing

We isolated the DNA from legs of three *A*. *snetsingeri* individuals. We washed the ethanol-fixed legs twice for 15 min using 1 ml of 10 mM Tris-HCl (pH 7.5) with 5 mM EDTA. Subsequently, we extracted the DNA using a NucleoSpin Tissue XS kit (Macherey-Nagel, Düren, Germany) according to the manufacturer's instructions. We then amplified the DNA using primers targeting nuclear (ITS2) and mitochondrial (CO1) loci using the following polymerase chain reaction mix: 10 mM Tris-HCl (pH 8.8), 50 mM KCl, 1.5 mM $MgCl_2$, 0.1% Triton X-100, 0.2 mM dNTP (each), 1 μM forward primer, 1 μM reverse primer, 0.5 U of Taq DNA polymerase (Top-Bio, Prague, Czech Republic), and 300 ng of extracted genomic DNA. The total reaction volume was 25 μl. To amplify the ITS2 locus, we used the primers ApicITS2FW2 (5′-CGATGAAGAACGCAGCCAGCTGCGAG-3′; [35]) and RITS (5′-TCCTCCGCTTATTGATATGC-3′; [36]). To amplify the CO1 locus, we used the primers LCO1490 (5′-GGTCAACAAATCATAAAGATATTGG-3′; [37] and C1-N-2194 (5′-CTTCTGGATGACCAAAAAATC-3′; [38]). We performed the reaction using an Eppendorf Mastercycler Pro thermal cycler (Eppendorf, Hamburg, Germany) for 36 cycles with 15-s denaturation at 94˚C, 2-min annealing at 43–57˚C, followed by a 1–3-min extension at 72˚C. We initiated the cycling with a 2-min denaturation at 94˚C and terminated it after 5-min incubation at 72˚C. Subsequently, we purified the amplified DNA using USB Exo-SAP-IT (Affymetrix, Santa Clara, CA) and bidirectionally sequenced the amplicons using an ABI 3130 DNA Analyzer (Applied Biosystems, Foster City, CA). For the three individuals of *A*. *snetsingeri* analyzed in their ITS2 locus and two for their CO1 locus, all the obtained ITS2 and CO1 sequences were identical. The resulting consensus DNA sequences were submitted to NCBI GenBank under accession numbers MT957000-MT957001 (CO1) and MT957146- MT957148 (ITS2).

Alignments and phylogenetic analyses

We aligned the newly generated sequences with those of nine *Atypus* spp. obtained from NCBI GenBank as of September 7, 2020, and sequences of the corresponding outgroups by using MUSCLE [39,40] (gap opening penalty -400, gap extension penalty 0, clustering method UPGMB, lambda 24). We manually corrected the alignments for any inconsistencies, trimmed the aligned sequences to ensure that they all represent the same extent of the analyzed locus, removed short-length sequences from the alignments, and used only trimmed sequences for further analyses. The trimmed ITS2 locus [containing partial 5.8S ribosomal DNA and partial (close to full-length) ITS2 sequences] corresponded to nt 62–385 (324 bp) of *Atypus baotianmanensis* Hu, 1994 KP208877.1. The trimmed CO1 locus (partial CO1 coding sequence) corresponded to nt 23–595 (573 bp) of *A*. *piceus* KX536935.1. For each locus, we calculated the maximum likelihood fits of 24 nucleotide substitution models. We used a bootstrap procedure at 1,000 replicates and the nearest-neighbor-interchange as the maximum likelihood heuristic method to determine the tree inference when the initial tree was formed using a neighbor

joining algorithm. We used best-fit models for the maximum likelihood phylogenetic analyses, including the estimates of evolutionary divergence between sequences.

Ethics statement

We studied spiders that are not protected by any law, and specimens were collected ethically with permission of the land owner. Approvals for such studies are not required from ethics committees in either the USA or the Czech Republic.

Results

Phylogenetic analysis

Sequence analysis of the DNA of *A. snetsingeri* has clarified its identity and the unusual presence of the genus in North America. We found that the CO1 locus had a 100% sequence similarity (genetic distance of zero) with the matching 639bp-long CO1 locus of *A. karschi* (SDSU_MY4706) from the Honshu Island, Japan [41]. After *A. karschi* the most closely related species for which sequences were available (Fig 1A) was the Asian *Atypus heterothecus* Zhang, 1985, with a genetic distance of 0.131 ± 0.021 of base substitutions per site between sequences. The European species, *A. piceus* and *A. affinis*, were basal to *A. snetsingeri* as well as to the whole group of hitherto sequenced Asian *Atypus* spp. (Fig 1A). Concerning the ITS2 locus, the sequences of only two other *Atypus* spp. are known (Fig 1B); therefore, this hypervariable locus awaits future analyses when more comparative data are available. The genetic distance to the closest species already sequenced in the ITS2 locus, *A. baotianmanensis*, was 0.109 ± 0.022 of base substitutions per site between the sequences.

Taxonomy

Based on an exact match of the genetic CO1 barcode data, the *A. snetsingeri* purse-web spiders in Pennsylvania appear to represent an introduced local population of the Asian species *A. karschi*. In the remainder of this paper those spiders are referred to as *A. karschi* 'from Pennsylvania'. The specific epithet *snetsingeri* is relegated to a junior synonym of *karschi*.

Atypus karschi Dönitz, 1887

Atypus snetsingeri Sarno, 1973: Sarno 1973 [23]: page 38, figs 1–9 (description of both sexes). **New synonymy.**

A. snetsingeri Gertsch and Platnick 1980 [25]: page 11, figs 9, 13–20 (both sexes).

A. snetsingeri Schwendinger 1990 [7]: page 360, fig. 18 (female).

Remarks. The synonymy was based on finding that the CO1 gene, used as a molecular barcode, of *snetsingeri* specimens from Pennsylvania was identical with that of *A. karschi* from the Honshu Island, Japan [41].

Cytogenetic analysis

The female karyotype of *A. karschi* from Pennsylvania showed 2n = 42 chromosomes and the male had 2n = 41 (Fig 2A), suggesting an X0 sex chromosome system. Chromosomes were metacentric except for one pair, which exhibited submetacentric morphology (Fig 2B). The chromosome pairs gradually decreased in size, with the length of chromosome pairs in the male ranging from 7.13% to 3.31% of TCL and in the female from 6.13% to 3.31% of TCL. The sex chromosome was a metacentric element of medium size in both male (TCL = 4.27%) and female (TCL = 4.09%) (Fig 2A and 2B). Concerning meiosis, pachytene nuclei were found in both the male and female specimen. In the male pachytene, the univalent X chromosome was on the periphery of the nuclei. X chromosome arms were often associated with each other

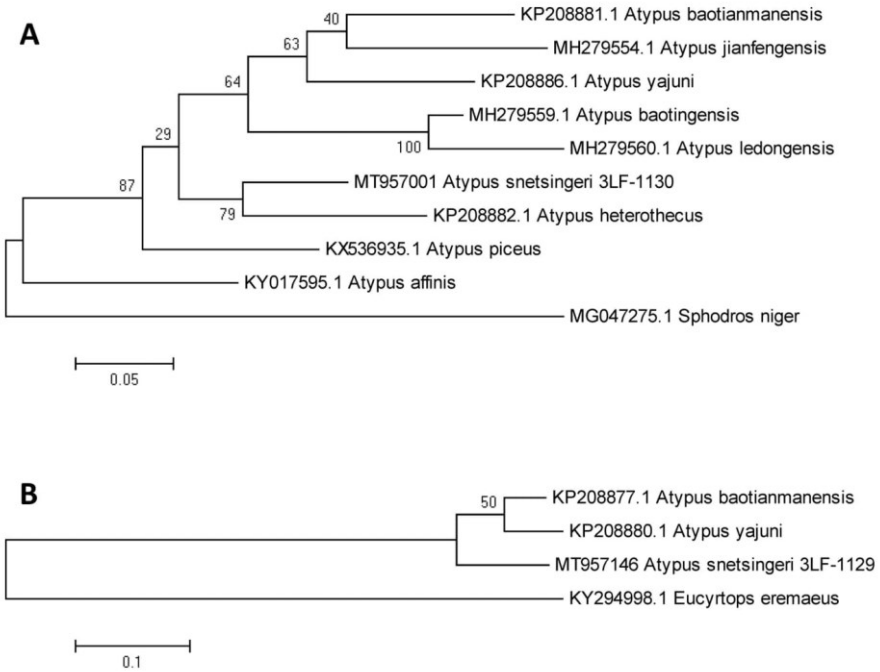

Fig 1. Phylogenetic analyses of the position of *A. snetsingeri (A. karschi* in Pennsylvania, USA) in the genus *Atypus* based on the sequences of the CO1 (**A**) and ITS2 (**B**) loci by the maximum likelihood approach. The evolutionary history was inferred using the Tamura-Nei model (**A**) or the Kimura 2-parameter model (**B**), both with a discrete Gamma distribution used to model evolutionary rate differences among sites. The models were selected based on the highest Bayesian information criterion scores of the maximum likelihood fits. The trees are drawn to scale, with branch lengths indicating the number of substitutions per site. All codon positions, including noncoding positions, were included; the analyses were based on 573 positions (**A**) or 345 positions (**B**).

https://doi.org/10.1371/journal.pone.0261695.g001

during this period. Moreover, the X chromosome showed positive heteropycnosis (i.e., it was stained more intensively than other chromosomes). The other bivalents exhibited prominent knobs (Fig 2C).

C-banded chromosomes exhibited small intercalar and terminal blocks of heterochromatin. The submetacentric pair showed a prominent large block at the terminal part of the long arm (Fig 2D). It occupied on average 36% of the chromosome length (n = 10). The karyotype contained one NOR locus that was localized in the end of the long arm of the submetacentric pair (Fig 2E). The NOR colocalised with the large block of heterochromatin and was of considerable size (37.2% of the chromosome length, n = 8).

Habitat

The eight *A. karschi* sites that we visited in Delaware County in 2013 represented suburban neighborhoods, small wooded parks, narrow riparian zones along developed stream corridors, and protected parklands (S1 File). The purse-webs were located in a variety of habitats at those

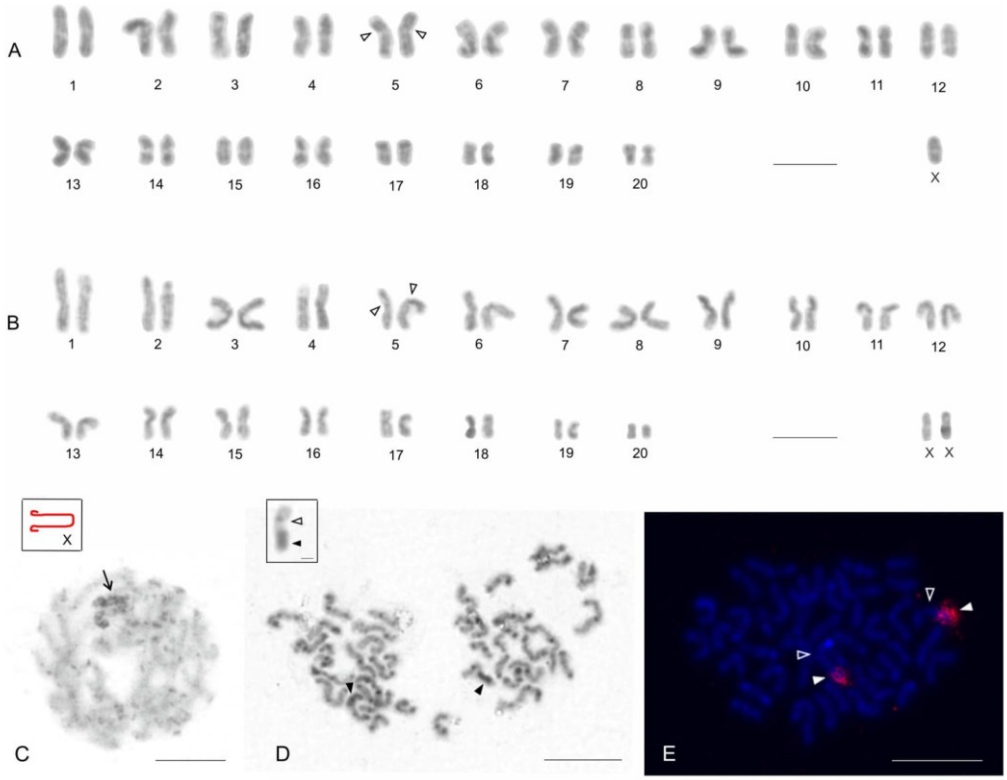

Fig 2. Chromosomes of *A. karschi*, Pennsylvania, USA. A, B. Male (A) and female karyotypes (B), stained by Giemsa, based on mitotic metaphase. 2n♂ = 41, X0; 2n♀ = 42, XX. Empty arrowhead–centromere of submetacentric pair. **C.** Male pachytene. Note heterochromatic X chromosome on the periphery of the nucleus and prominent knobs on the bivalents. Inset: Scheme of sex chromosome. Note an association of X chromosome arms. Arrow–sex chromosome. **D.** Male mitotic metaphase, C-banding. Chromosomes exhibit intercalar and terminal heterochromatin blocks. Inset: Magnified submetacentric chromosome containing a large block of heterochromatin (from another mitotic metaphase). Arrowhead–a large block of heterochromatin, empty arrowhead–centromere. **E.** Male mitotic metaphase, detection of rDNA cluster (FISH). Note chromosomes of a submetacentric pair containing a terminal rDNA cluster at long arm. Arrowhead–rDNA cluster, empty arrowhead–centromere. Scale bars: 10 μm.

https://doi.org/10.1371/journal.pone.0261695.g002

sites, including the shrubbery along suburban sidewalks, slopes and bottoms of wooded valleys, beech forests and a fallow field that is mowed annually. Typical habitats of *A. karschi* in Pennsylvania are shown in Fig 3.

The inclination (slope) of the sites varied from 0–40˚, ranging from a flat field to riparian hillsides. Where a site in our study had a slope it usually faced the south but the azimuth of orientation varied from 95–340˚, excluding only the coldest north and north-east exposures. The soil on slopes was usually not aggregated, was sandy or powdery, and of yellow or grey color below the shallow humus layer. In valley bottoms, the spider lived in fluvisol and in the suburbs in anthropogenic soils. Soil penetrability ranges from 0.5 to 3.25 (n = 14, mean 2.02 ± 0.31). The webs were typically associated with woody vegetation, and bush/shrub cover

Fig 3. Habitats of *A. karschi* in Pennsylvania, USA; (1A) suburban bushes along Essex Ave (~200 m from type locality of *A. snetsingeri*), (1B) fallow field at Tyler Arboretum, (1C) riparian woods, Swedish Cabin site on Darby Creek, (1D) forest, Smedley Park.

https://doi.org/10.1371/journal.pone.0261695.g003

ranged from 5–100% (mean 40%) and tree cover from 0–90% (mean 50%). The soil surface where webs occurred was without moss, and the herbaceous cover was usually sparse (from 0–90%, mean 20%).

Natural history

The above-ground webs we observed were vertical and mostly attached to the base of thin stems of bushes or on trees (Fig 4B), but a few were attached to rock (Fig 4C). In early November three size categories were visually distinguished in the field by their relative web diameters, representing small and medium juveniles, and adult females. According to prey remnants found on their webs, they feed on millipedes (*Julida* and *Polydesmus* sp.), snails (*Cochlicopa* sp.), woodlice (*Porcellio* sp.) and carabid beetles.

All 18 excavated webs contained adult females (S2 File), although some webs were damaged in the process. Eleven webs also contained a brood of juveniles, one of which was partially lost

Fig 4. *A. karschi* and its webs in Pennsylvania, USA, (4A) adult female and male (on the left), (2B) vertical web attached to the base of a tree and (4C) to a boulder, (4D) horizontal web covered in thatch (4E) and with thatch removed, (4F) a detail of recently trimmed ivy in front of the same bushes shown in Fig 3A, with 16 purse-webs circled.

https://doi.org/10.1371/journal.pone.0261695.g004

during excavation and not used for count statistics. Four of the webs were badly damaged during excavation and were not measured. Of the remaining 14 webs, one had a broken below-ground section that was only partially intact and not used for statistics. Body size of the females (carapace length) varied by only about 1mm (n = 18, min 5.04 mm, max 6.18 mm, mean 5.68 ± 0.09 mm). There was no significant difference between the body size (carapace length)

of the females with (n = 11) and without (n = 7) juveniles (Welch two sample *t*-test t = 1.45, $p = 0.17$). The number of juveniles ranged from 70 to 201 (n = 10, mean 121.30 ± 11.66) and did not correlate with the body size of the female (Pearson's correlation n = 10, r = 0.32, $p = 0.37$). Total web length (both sections intact) ranged from 13 to 29 cm (n = 13, mean 17.77 ± 1.13 cm). The length of the subterranean section of web associated with the burrow ranged from 6 to 10 cm (n = 13, mean 8.3 ± 0.3 cm) and did not correlate with the body size of the spider (Pearson's correlation, n = 13, r = -0.44, $p = 0.13$). The length of the above-ground web ranged from 5 to 13 cm (n = 14, mean 8.54 ± 0.67 cm) and also did not correlate with the body size of the spider (Pearson's correlation, r = 0.02, $p = 0.94$). The length of the above-ground web was more variable than the length of its subterranean part (F test, n = 13, F = 0.23, $p = 0.018$) (Fig 5). The ratio of below-ground/above-ground lengths ranged from 0.62 to 1.80 (n = 14, mean 1.09 ± 0.08) and did not correlate with the body size of the spider (Pearson's correlation, r = 0.02, $p = 0.94$).

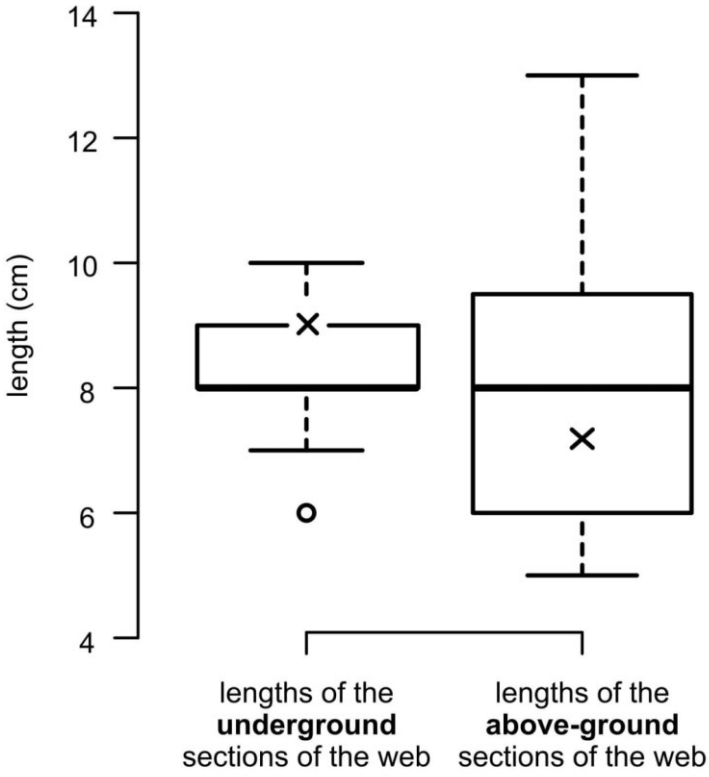

Fig 5. Boxplots showing the variation of the below-ground and above-ground lengths of excavated purse-webs of *A. karschi*, Pennsylvania, USA (n = 13). The means are indicated by an x and the hollow dot indicates an outlier (less than the 25th percentile minus 1.5 × Interquartile range).

https://doi.org/10.1371/journal.pone.0261695.g005

Discussion

Genetic identity of *A. snetsingeri*

The presence of a geographically isolated population of an *Atypus* species in North America, where the other purse-web spiders are in the genus *Sphodros*, has been mildly controversial. Due to the species' location on the eastern coast of the USA a close relationship with European *Atypus* species could have been expected. However, morphologically, *A. snetsingeri* closely resembled Asian species, especially *A. karschi* [7,25]. Raven [26] questioned whether the *Atypus* in North America was introduced.

The newly obtained molecular data for *A. snetsingeri* have resolved those questions by showing that the Pennsylvania species is conspecific with Asian *A. karschi*. Sequence data of *A. snetsingeri* was a genetic match with sequence data for *A. karschi* from Japan, supporting an East Asian origin and introduction. Based on these data we propose a formal synonymy for *A. snetsingeri*, which now becomes a junior synonym of *Atypus karschi*. Differences reported for morphological features compared to *A. karschi* in Asia probably represent intraspecific variation given the small number of *A. snetsingeri* specimens actually examined by researchers [7,25].

Parts of the genome of "*Atypus snetsingeri*" (based on NCBI sequences DQ639853.1, DQ680323.1 and KY016940.1) were previously used in spider phylogeny studies to represent the genus *Atypus* [41–43] or the entire family Atypidae [44]. Wheeler et al. [1] used *A. snetsingeri* and *A. affinis* data to represent *Atypus*, and added *Sphodros* for the family Atypidae. Those *A. snetsingeri* data are now considered to represent *A. karschi* in Pennsylvania. Recently the entire mitochondrial genome was sequenced for *Atypus karschi* in China [45], which is very useful for further comparative studies of the Atypoidea.

Cytogenetic analysis

Most karyotype data on spiders concerns araneomorphs [46], but some karyotypes of mygalomorph spiders have been published [19,20,22,47,48]. Representatives of the superfamily Atypoidea display a similar range of diploid numbers as araneomorph spiders (from 14 to 47). Most Atypoidea exhibit the X0 sex chromosome determination system, which may be the ancestral sex chromosome determination of this superfamily [22].

In the family Atypidae only four species in the genus *Atypus* have been studied cytogenetically. *Atypus karschi* in this study exhibits 2n♂ = 41, X0 and predominance of metacentric chromosomes, which is in accordance with the karyotypes of central European species *A. piceus* and *A. muralis* [20]. These karyotype features could be ancestral within the genus *Atypus*. The karyotype of European *A. affinis* having 2n♂ = 14, XY, was derived from chromosomal complement 2n♂ = 41, X0 by series of chromosomal fusions leading to decreasing of diploid count and formation of a neo-sex chromosome system XY [20].

Notably, an earlier karyotype developed for *A. karschi* in Japan [21] differs considerably from those reported in this study from Pennsylvania. The male karyotype reported from Japan consisted of approximately 44 acrocentric chromosomes, including an X_1X_20 system, not the 41 biarmed (i.e. metacentric and submetacentric) chromosomes and X0 pattern reported here. The discrepancy may be due to interpopulation variability, but although mygalomorph spiders exhibits considerable karyotype diversity [22], such an enormous degree of interpopulation karyotype variability is very unlikely. Therefore, we suggest that the karyotype data of the Japanese population may have been misinterpreted. The karyotype of *Atypus* is formed by a relatively high number of small chromosomes, which makes it difficult to determine the precise diploid number and chromosome morphology. Moreover, the method of chromosome

preparation used by Suzuki [21] did not include treatment with a hypotonic solution, so the spreading of chromosomes would have been less pronounced than in the present study using the methodology of Král et al. [22]. Regarding determination of the sex chromosome system, a single metacentric X chromosome of an X0 system could be erroneously considered as two acrocentric X chromosomes of an X_1X_20 system attached at one end during meiosis.

Within the framework of our cytogenetic analysis, we were able to detect constitutive heterochromatin for the first time in the Atypoidea. Most chromosomes of *A. karschi* exhibited intercalar and terminal blocks of heterochromatin. The distribution of blocks suggests that 1) most intercalar blocks are placed at centromeric regions and 2) terminal blocks are formed at telomeric regions. This is consistent with the pattern of distribution of constitutive heterochromatin most commonly found in spiders [47].

Nucleolus organizer regions are chromosome domains containing tandemly repeated sequences of rRNA genes that are involved in formation of the nucleolus [49], and their location on chromosomes may have taxonomic value. These regions have been detected in ten species of mygalomorphs including four species of Atypoidea [22, this study]. The number of NORs in Atypoidea ranges from one to four loci, and they are always situated on chromosome pairs. NORs are usually detected by impregnation with silver or by FISH with rDNA probe, although the first technique can underestimate absolute number of NORs by visualizing only loci transcribed during previous cell cycle [50]. However, most NOR detections in mygalomorphs have been performed by silver staining. Fluorescence in situ hybridization, which we applied to detect NORs of *A. karschi* in this study, have been used with only one other mygalomorph species, *Tliltocatl albopilosum* Valerio, 1980 (Theraphosidae) [22]. Both species display one terminal NOR localized on a chromosome pair, which may be the ancestral condition for spiders [22]. The NOR of *A. karschi* is associated with heterochromatin, which is a common feature of rDNA in eukaryotes [e.g., 51,52]. Comparison of the length of the rDNA cluster and heterochromatin block suggests that heterochromatin associated with the NOR is formed by inactivated rDNA. This pattern is in an agreement with the current model for NOR organization, in which major regions of rDNA are often inactivated and only a restricted fraction of rDNA is transcribed [53].

Habitat

Asian *Atypus* species are generally considered to be forest-dwellers, but some are reported from more open xerothermic habitats [7,62]. Details about natural history for most species is limited to brief remarks in the taxonomic literature, but those comments can include important observations about capture method, habitat features or tree species associated with the spiders or their webs at the time of collection [7,13,62]. These types of data increase in value over time for planning future surveys and tracking spider distributions or habitat changes over time.

Atypus karschi in Pennsylvania appears to be undemanding regarding habitat requirements (see the S1 File) and can be locally abundant where it occurs. In Pennsylvania this species is found in protected riparian woodlands, brushy woodlots and at least one mowed field, and is also reliably found in some suburban neighborhoods where webs are built at the base of shrubs or along walls and fences. Miyashita [54] reported a similar situation in Japan where *A. karschi* is "common" and "usually live(s) in shady and humid places such as woods and shrubberies." Images posted on iNaturalist [55] of *A. karschi* in East Asia also support a tolerance of human-modified settings where they were encountered (wall, fence and stone garden).

Unlike *A. karschi* in Pennsylvania, the three European *Atypus* species are not found in habitats subjected to recent or regular disturbance, and they are well studied. They are known to

require habitats with specific edaphic conditions and association with particular vegetation types and sun-facing slopes [16]. European atypids are rare enough to be red-listed in all Central European countries, and their presence at a site is an indicator of a relic habitat worthy of conservation management [8,56].

Natural history

The life history of *A. karschi* in Japan was studied in detail by Miyashita [54] under semi-outdoor conditions and reported with prior data from Aoki [57] and Yaginuma [58]. Basic natural history parameters of *A. karschi* in eastern Asia and *A. snetsingeri* in the USA are contrasted in Table 1 and indicated a similarity in every respect (body size, ontogeny, phenology, fecundity, morphology of webs, environment). No difference was found that would refute the conspecificity of the Pennsylvania population with Asian *A. karschi*.

The webs of *A. karschi* in Pennsylvania are attached to a variety of supports (trees, shrubs, grasses, rocks, walls and fences) where the ground surface is either covered by or nearly devoid of litter. Gertsch and Platnick [25] contemplated whether the above-ground purse-web orientation could be useful to distinguish between *Atypus* (horizontal webs) and *Sphodros* (vertical webs), but this is not a distinguishing character as species in both genera can and do make

Table 1. Natural history parameters (body size, ontogeny, phenology, fecundity, morphology of webs, environment) reported for *Atypus karschi* in Japan and for the introduced population known as *A. snetsingeri* in Pennsylvania, USA.

Natural history parameter	*Atypus karschi* (Japan)	*Atypus snetsingeri* (USA)
Body size		
Carapace length of males	3.87–4.23 mm [59]	3.2–4.6 mm [23]
Carapace length of females	4.77–5.76 mm [59]	3.4–7.0 mm [23]
Ontogeny		
No. of eggs	mean 124, maximum 270 [54]	mean 121, maximum 201 (this study)
No. of moults before reaching maturity	8–9 in males, 9–11 in females [54]	unknown
Age of maturation	3 years [54]	possibly 3 years, based on three concurrent web size categories in the population (this study)
Phenology		
Mating season	June–(July) August [54,57]	June–August [23,24]
eggs	July (August)—September [54,57,58]	July-September [24]
larvae	October [60,61]	September [24]
1st nymphal instar	late October–April (dispersion) [54,57]	September–March (dispersion) [24]
Morphology of webs		
Orientation of the above-ground web	vertically attached to the tree trunk or rock [61]	vertically attached to the tree, hedge or wall [23] or horizontally oriented in grass and thatch [24]
Length of the above-ground web	Up to 20 cm (almost the same as the depth of the burrow) [61]	Up to 25 cm [23]
Depth of the burrow	Up to 20 cm [54,61]	Up to 20 cm [23]
Environment		
Microclimate	Shady and moist, in the forest close to the trees, rocks or bamboo [54,61]	Mostly shady and moist, in litter and areas with loose soil [this study]
Habitat	Forests and shrubs [54,61]	Forests and shrubs, disturbed areas [this study]

https://doi.org/10.1371/journal.pone.0261695.t001

both kinds of webs [62]. In this study in 2013 we observed vertical webs of *A. karschi* at the sites visited, but the spiders are also known to make horizontal webs in thatch and grass [24]. In Tyler's fallow field, for example, vertical webs can be found on plant stems within a few centimeters of horizontal webs in surrounding grasses.

Although vertical webs are characteristic of most North American *Sphodros* species, *Sphodros niger* Hentz, 1842 may preferentially build horizontal webs, at least in some settings [63,64]. Mckenna-Foster et al. [65] also found that *Sphodros rufipes* Latreille, 1829 in New England used whatever support was available and many webs were close to the ground. The suggestion that horizontal webs are an adaptation to prey capture under the snow [7] may ignore the function of vertical webs at ground level. In Pennsylvania *A. karschi* habitats experience snow and cold temperatures each year. In Tyler's field the horizontal webs laying near the soil surface tend to be well-buffered by leaf litter or thatch, but basal sections of nearby vertical webs are often similarly buffered and may likewise function normally in the same subnivean environment when both prey and spiders are active [Tessler, personal observations].

In this study we measured the webs of fourteen adult females from a fallow field with homogeneous soil. We found the overall length of the webs were shorter than those observed by Sarno [23] around a house foundation and on shrubs in a suburb (see Table 1), probably reflecting different conditions and prey availability between sites. The length of the aerial web was more variable than that of the underground part (Fig 5). Less variation in the underground web length may reflect a minimum depth of the burrow necessary for suitable microclimate, constraints imposed on digging, or the shallow soil frost depth in winter at that site. Depth of burrows differs among European *Atypus* species, where the species living in arid habitats tend to dig deeper burrows than those living in woody vegetation [8].

The number of juveniles found within maternal webs of *A. karschi* in Pennsylvania and Asia were similar (max. 201 and 270, respectively), and in the same range as European *Atypus* species (*A. affinis* max. 191, *A. piceus* max. 168, *A. muralis* max. 150; M. Řezáč, personal observations). Mortality of captive *A. karschi* spiderlings is reportedly high [23,56]. In mygalomorphs, spiderlings disperse by walking away from the maternal web, sometimes in single file, or by using a dragline-based aerial method known as suspended ballooning [11]. The extent to which either dispersal behavior contributes to spiderling mortality is unknown. In Pennsylvania, aerial dispersal occurs in March and April for *A. karschi* [24] in both field and forest habitats.

Prey we observed for *A. karschi* in Pennsylvania were mostly ground-based invertebrates, especially millipedes, similar to observations on *S. niger* in New England [64]. *A. karschi* in Pennsylvania has also been observed feeding on earthworms, and will readily capture orthopteroids and other insects that contact the web while climbing vegetation, including the pestiferous spotted lanternfly (Hemiptera: Fulgoridae: *Lycorma delicatula* White, 1845) that was recently introduced into Pennsylvania from Asia [Tessler, personal observations]. It is unknown what effect *A. karschi* has on its local environment or prey species.

Distribution of *A. karschi* in Pennsylvania

Prior to this study, *A. snetsingeri* had been considered a unique species with a decidedly Asian morphology and an enigmatic presence in northeastern North America, near Philadelphia. Raven [26: pg 124] used a parenthetical remark to question whether the isolated *Atypus* in North America was "[possibly introduced]," and Schwendinger [7: pg 364] agreed it could explain *A. snetsingeri*'s "restricted distribution in a generally well investigated area." Schwendinger [7] also recognized that the "obviously close" relationship of the species pair *A. karschi*/*A. snetsingeri* resembled the well known biogeographic pattern referred to as the eastern Asian

—eastern North American disjunction [66,67], one of several intercontinental disjunctions of interest in paleontology and systematics. Zhu et al. [13: pg 38] agreed that the species may have spread southward during the Pleistocene, but rejected Schwendinger's land bridge hypothesis and "would rather consider *A. snetsingeri* as a relict of glacial periods."

Based on current information, we disagree with both natural origin scenarios for the occurrence of *A. karschi* in North America and believe that the Pennsylvania population is the result of introduction by man and not ancient vicariance. Mygalomorph spiders usually have deep molecular differences even among populations of the same species [41]. But *A. snetsingeri* is genetically identical to *A. karschi*, and its distribution and association with disturbed habitats suggest a more recent introduction.

A. karschi seems to possess three preadaptations that allowed it to successfully colonize southeastern Pennsylvania following its introduction. First, it occurs over a wide area in eastern Asia with a similar temperate climate (Japan [61]; Chinese provinces Hebei, Anhui, Sichuan, Guizhou, Hubei, Hunan, Fujian [59]; Taiwan [68]; Korea's Ungil Mountain [69]). Second, it produces a large number of lightweight juveniles that disperse aerially using a method known as suspended ballooning [11,24,54,70]. Third, our results in Pennsylvania indicate that the species is ecologically plastic and does not appear to have specific habitat, edaphic or microclimatic requirements, even thriving in settings frequently impacted by humans.

The original description and first review of the species *A. snetsingeri* in Pennsylvania were based on specimens taken from two nearby suburban sites in Lansdowne and Upper Darby in eastern Delaware County near Philadelphia [23,25]. At that time, the spider was known to be common and unnoticed in the surrounding areas within the Cobbs Creek and Darby Creek drainage basins [Tessler, personal observations]. Since that time a visual survey for vertical purse-webs at publicly-accessible parks and woodlands in the region [24] has shown that atypids are relatively common (and unnoticed) across Delaware and Philadelphia counties and into adjacent areas of Montgomery and Chester counties (Fig 6). The polygon in the map shows the extent of vertical purse-web sightings as an estimate of the species' distribution, including all previously known and verified *A. karschi* sites (as *A. snetsingeri*), but the webs alone are not diagnostic [7,25]. It is possible that vertical-web building *S. rufipes* or horizontal-web building *S. niger* [64,65] also occur in that area but are as yet undetected, and those species may be documented as purse-web sites are revisited to make species determinations. Atypid field surveys can utilize external morphological features to identify wandering males and excavated females [71]. Mature males of *A. karschi* are distinguished from northern *Sphodros* species (*S. niger*, *S. rufipes*, *S. atlanticus*) by their color, small palps and a ridge around the sternum, while females and immatures are distinguished from *Sphodros* by their sternum sigilla pattern and the posterior lateral spinnerets [PLS, 25]. In particular, *A. karschi* has distinctly four-segmented PLS, whereas the northern *Sphodros* species have only three segments.

Interestingly, *Sphodros* purse-web spiders have been reported in Pennsylvania and adjacent states [25], but not in the same areas as *A. karschi*. This is unsurprising because atypids and their webs are rarely noticed or reported even when they are locally abundant [24,71], and while perhaps provocative, those observations are not evidence of displacement of any local species by the introduction of *A. karschi*. *Sphodros* may yet be identified within the estimated *A. karschi* range. Of historic interest, the first "red-legged" purse-web spider reported from North America was in 1829, a male taken "near Philadelphia" and sent to France to later become the holotype specimen for *Sphodros rufipes* [25]. A more precise location was not given and since that time *S. rufipes* has not been reported in the Philadelphia region of Pennsylvania, with the nearest record in coastal New Jersey. Sightings of wandering *Sphodros* males near southeastern Pennsylvania and reported in iNaturalist [72] indicate that: 1) *S. rufipes* occurs nearby in coastal regions of Maryland and New Jersey south and east of the

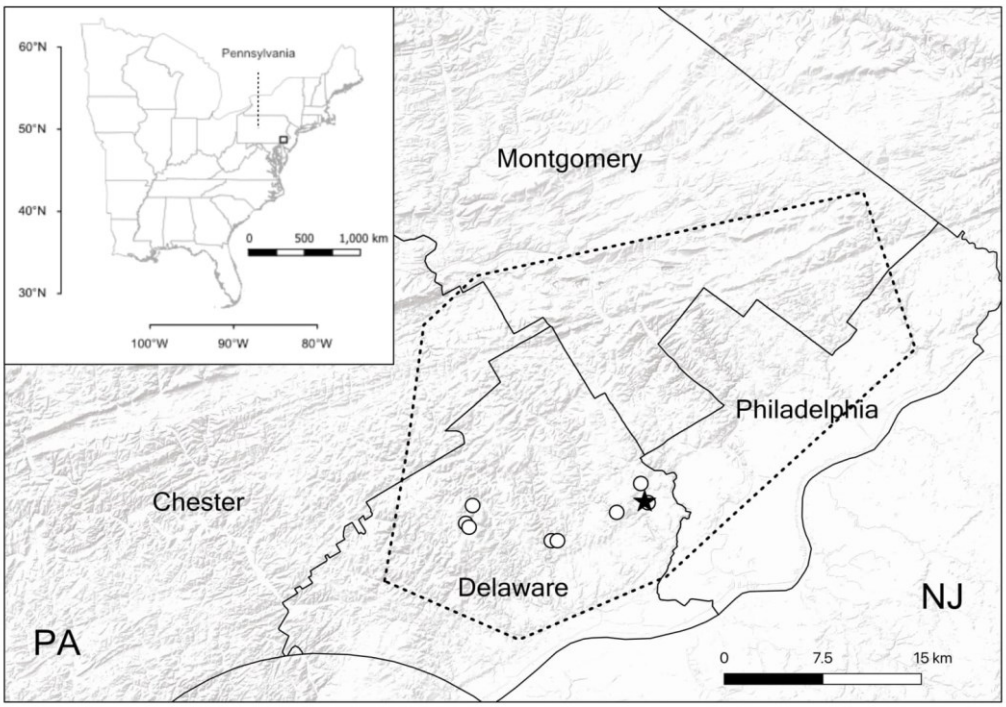

Fig 6. Study sites, counties and estimated area containing *Atypus karschi* in southeastern Pennsylvania, USA. The hollow circles mark the sites described in this study and the star is the type locality of *A. snetsingeri*. The minimum convex polygon encloses a nearly contiguous area where vertical purse-webs have been found in a recent visual survey in the region [24], and includes the relatively few sites where a species identification to *A. karschi* (as *A. snetsingeri*) has been made through previous collections, male sightings and female excavation and examination. *Sphodros* species may also be found in that area as purse-web sites are revisited for species determination.

https://doi.org/10.1371/journal.pone.0261695.g006

Philadelphia area, and northward into New England; 2) *S. niger* was found west and north of Philadelphia within Pennsylvania and nearby in the states of New Jersey, Delaware and Maryland; and, 3) *S. atlanticus* is reported south of the *A. karschi* area in coastal Delaware and Maryland. More research is needed on North American atypid spiders to clarify their distributions, habitat and vegetation associations, prey preferences, possible interactions and impacts on their local ecology. Those data will also facilitate determining whether the distributions of *Sphodros* and *A. karschi* change in the future in response to regional land-use practices, local habitat destruction and development, or climate change.

It is unlikely that the source and timing of *A. karschi*'s introduction to Pennsylvania will ever be determined. The species has a broad native range in East Asia extending from China and Taiwan to Japan [14], and it was recently also reported in Korea [69]. The Philadelphia region (including Delaware County) has had a 300 year history of trade with East Asia that may have included countless opportunities for accidental importation of a soil-associated

spider among potted plants. Indeed, Nentwig [73] suggests that spiders introduced with potted plants have higher establishment rates relative to those introduced by other means. In the 1700s and 1800s Philadelphia was the center of American botany and horticulture and many plants from around the world, including Asia, were actively collected, imported and traded for exhibition and cultivation in public and private gardens [74,75]. Many of the region's great gardens and arboreta of that era still exist to some extent [76], including Tyler Arboretum (visited in this study) and Bartram's Garden in west Philadelphia, the home of noted American botanists John Bartram and his son William [77,78]. William Bartram's contemporary in the late 1700s, William Hamilton, built his estate "The Woodlands" overlooking Philadelphia's Schuylkill River and his gardens and greenhouse boasted of having every rare plant he'd ever heard of from around the world [79,80]. In 1784, after the American Revolution, direct shipping trade began between Philadelphia and China and at its peak represented about a third of all US trade with China [81]. A very significant Asian botanical importation event occurred later, in 1926, when the Japanese government presented 1,600 flowering trees to the City of Philadelphia to celebrate the 150th anniversary of American independence [82]. Regarding introductions of other soil-associated invertebrates, Asian jumping worms (*Amynthas* and *Metaphire* spp.) were presumably brought to the US in the 1800s in the soil of potted plants, and recent studies have shown that they displace native worms and are changing the soil where they occur [83]. Coincidentally, nonnative jumping worms are present at many *A. karschi* sites in Pennsylvania [Tessler, personal observations].

Conclusion

Many spider species have been accidentally introduced by humans to a new continent and became established [73], nearly all from the phylogenetically recent infraorder Araneomorphae. Within the more basal mygalomorphs, the Mexican redrump tarantula (Theraphosidae) native to Mexico and Central America has become established in Florida USA [84]. Presumably escaped from the pet trade, these tarantulas dig burrows and appear to be restricted to a small area with climate and habitat features similar to its native range. In this study we show that *Atypus snetsingeri* in Pennsylvania is genetically conspecific with *Atypus karschi* native to East Asia. The species appears to have been introduced by humans to Pennsylvania, probably in association with potted plants, and is now naturalized and locally common within a limited range that includes urban and forested areas. It is unlikely that the source or timing of the introduction can be determined in a region renowned for its colonial-era horticulturalists, elaborate international gardens, and long history of shipping trade with East Asia. This is the first case of an introduced species of Atypoidea from the infraorder Mygalomorphae.

Supporting information

S1 File. Characteristics of the studied sites of *A. karschi* in Delaware County, Pennsylvania, USA in November 2013: Location, date of visit, site orientation and slope, soil type and penetrability, and the cover and composition of the vegetation strata. The abundance of plant species is characterized using standardized ranks (Braun-Blanquet 1932).
(DOC)

S2 File. Carapace length, web length and number of juveniles with adult females of *Atypus karschi*, Pennsylvania, USA (n = 18). NA–the web was destroyed while excavating and could not be measured.
(DOC)

Acknowledgments

We thank Tereza Kořínková for her comments on the manuscript, Marie L. Schmidt for her help with the research in Pennsylvania, and the Tyler Arboretum for permission to work on the property and collect specimens for scientific study.

Author Contributions

Conceptualization: Milan Řezáč, Steven Tessler, Jiří Král.

Data curation: Milan Řezáč, Petr Heneberg, Nela Gloríková.

Formal analysis: Petr Heneberg, Nela Gloríková, Jiří Král.

Funding acquisition: Milan Řezáč, Jiří Král.

Investigation: Milan Řezáč, Steven Tessler, Ivalú Macarena Ávila Herrera, Martin Forman, Veronika Řezáčová, Jiří Král.

Methodology: Milan Řezáč, Steven Tessler, Petr Heneberg, Jiří Král.

Resources: Milan Řezáč.

Visualization: Steven Tessler, Petr Heneberg, Jiří Král.

Writing – original draft: Milan Řezáč, Steven Tessler, Petr Heneberg, Nela Gloríková, Martin Forman, Veronika Řezáčová, Jiří Král.

Writing – review & editing: Milan Řezáč, Steven Tessler, Petr Heneberg, Jiří Král.

References

1. Wheeler WC, Coddington JA, Crowley LM, Dimitrov D, Goloboff PA, Griswold CE, et al. The spider tree of life: phylogeny of Araneae based on target-gene analyses from an extensive taxon sampling. Cladistics. 2017; 33(6): 574–616. https://doi.org/10.1111/cla.12182 PMID: 34724759
2. Enock F. The life-history of *Atypus piceus*, Sulz. Trans R Entomol Soc Lond. 1885; 33(4): 389–420.
3. McCook HC. Nesting habits of the American purseweb spider. Proc Acad Nat. 1888; 40: 203–220. Available from: https://www.biodiversitylibrary.org/bibliography/6885.
4. Poteat WL. A tube-building spider. Notes on the architectural and feeding habits of Atypus niger Hentz. J Elisha Mitchell Sci Soc. 1890; 6(2): 132–47.
5. Platnick NI. Spiders of the world: A natural history. London: Princeton University Press; 2020.
6. Bristowe WS. World of spiders. Collins; 1958.
7. Schwendinger PJ. A synopsis of the genus Atypus (Araneae, Atypidae). Zool Scr. 1990; 19(3): 353–66.
8. Řezáč M, Heneberg P. Conservation status of the only representative of infraorder Mygalomorphae (Araneae) in cultivated regions of central Europe. J Insect Conserv. 2014; 18(4): 523–37.
9. Coyle FA. Aerial Dispersal by mygalomorph spiderlings (Araneae, Mygalomorphae). J Arachnol. 1983; 11(2): 283–6.
10. Coyle FA, Greenstone MH, Hultsch A-L, Morgan CE. Ballooning mygalomorphs: Estimates of the masses of Sphodros and Ummidia ballooners (Araneae: Atypidae, Ctenizidae). J Arachnol. 1985; 13(3): 291–6.
11. Buzatto BA, Haeusler L, Tamang N. Trapped indoors? Long-distance dispersal in mygalomorph spiders and its effect on species ranges. J Comparative Physiology A. 2021; 207: 279–292. https://doi.org/10.1007/s00359-020-01459-x PMID: 33515318
12. Nentwig W, Blick T, Bosmans R, Gloor D, Hänggi A, Kropf C. Spiders of Europe. Version 5; 2021 [cited 20 May 2021]. Database [Internet]. Available from: https://www.araneae.nmbe.ch
13. Zhu MS, Zhang F, Song DX, Qu P. A revision of the genus Atypus in China (Araneae: Atypidae). Zootaxa. 2006; 1118: 1–42.
14. World Spider Catalog. World Spider Catalog; 2021 [cited 30 Mar 2021]. Natural History Museum Bern. [Internet]. Available from: http://wsc.nmbe.ch.

15. Dippenaar-Schoeman AS, Jocqué R. African spiders: an identification manual. Pretoria: ARC-Plant Protection Research Institute; 1997.

16. Řezáč M, Řezáčová V, Pekár S. The distribution of purse-web Atypus spiders (Araneae: Mygalomorphae) in central Europe is constrained by microclimatic continentality and soil compactness. J Biogeogr. 2007; 34(6): 1016–27.

17. Řezáč M, Tošner J, Heneberg P. Habitat selection by threatened burrowing spiders (Araneae: Atypidae, Eresidae) of central Europe: evidence base for conservation management. J Insect Conserv. 2018 Feb 1; 22(1): 135–49.

18. National Center for Biotechnology Information (NCBI). Query results for Atypidae genome data; 2021 [cited 23 Oct 2021] Database [Internet]. Available from: https://www.ncbi.nlm.nih.gov/nuccore/?term=atypidae.

19. Král J, Kořínková T, Forman M, Krkavcová L. Insights into the meiotic behavior and evolution of multiple sex chromosome systems in spiders. Cytogenet Genome Res. 2011; 133(1): 43–66. https://doi.org/10.1159/000323497 PMID: 21282941

20. Řezáč M, Král J, Musilová J, Pekár S. Unusual karyotype diversity in the European spiders of the genus Atypus (Araneae: Atypidae). Hereditas. 2006; 143(2006): 123–9. https://doi.org/10.1111/j.2006.0018-0661.01949.x PMID: 17362345

21. Suzuki S. Cytological studies in spiders. III. Studies on the chromosomes of fifty-seven species of spiders belonging to seventeen families, with general considerations on chromosomal evolution. J Sci Hiroshima Univ(B). 1954; 15: 23–136.

22. Král J, Kořínková T, Krkavcová L, Musilová J, Forman M, Ávila Herrera IM, et al. Evolution of karyotype, sex chromosomes, and meiosis in mygalomorph spiders (Araneae: Mygalomorphae). Biol J Linn Soc. 2013; 109(2): 377–408.

23. Sarno PA. New species of Atypus. Entomol News Philadelphia. 1973; 37–51.

24. Tessler S. Map the spider; 2022 [cited 22 Apr 2022]. Available from: http://www.mapthespider.com/.

25. Gertsch WJ, Platnick NI. A revision of the American spiders of the family Atypidae (Araneae, Mygalomorphae). Am Mus Novit; no. 2704; 1980. Available from: https://digitallibrary.amnh.org/handle/2246/5390.

26. Raven RJ. The spider infraorder Mygalomorphae (Araneae): cladistics and systematics. Bull Am Mus Nat. 1985;182. Available from: https://digitallibrary.amnh.org/handle/2246/955.

27. Řezáč M, Arnedo MA, Opatova V, Musilová J, Řezáčová V, Král J. Revision and insights into the speciation mode of the spider Dysdera erythrina species-complex (Araneae:Dysderidae): sibling species with sympatric distributions. Invertebr Syst. 2018; 32: 10–54.

28. Ávila Herrera IM, Král J, Pastuchová M, Forman M, Musilová J, Kořínková T, et al. Evolutionary pattern of karyotypes and meiosis in pholcid spiders (Araneae: Pholcidae): implications for reconstructing chromosome evolution of araneomorph spiders. BMC Ecol Evol. 2021; 21(1): 75. https://doi.org/10.1186/s12862-021-01750-8 PMID: 33941079

29. Srba M, Heneberg P. Nesting habitat segregation between closely related terricolous sphecid species (Hymenoptera:Spheciformes): key role of soil physical characteristics. J Insect Conserv. 2012; 16(4): 557–70.

30. R Core Team. R: A language and environment for statistical computing [Internet]. Vienna, Austria: R Foundation for Statistical Computing; 2019. Available from: http://www.r-project.org/.

31. Schneider CA, Rasband WS, Eliceiri KW. NIH Image to ImageJ: 25 years of image analysis. Nature methods. 2012; 9(7): 671–5. https://doi.org/10.1038/nmeth.2089 PMID: 22930834

32. Levan A, Fredga K, Sandberg AA. Nomenclature for centromeric position on chromosomes. Hereditas. 1964; 52(2): 201–20.

33. Král J, Kováč L, Šťáhlavský F, Lonský P, L'uptáčik P. The first karyotype study in palpigrades, a primitive order of arachnids (Arachnida: Palpigradi). Genetica. 2008; 134(1): 79–87. https://doi.org/10.1007/s10709-007-9221-y PMID: 18030430

34. Forman M, Nguyen P, Hula V, Král J. Sex chromosome pairing and extensive NOR polymorphism in Wadicosa fidelis (Araneae: Lycosidae).Comp Genome Res. 2013; 141(1): 43–9.

35. Heneberg P, Řezáč M. Two Trichosporon species isolated from Central-European mygalomorph spiders (Araneae: Mygalomorphae). Antonie van Leeuwenhoek. 2013 Apr 1; 103(4):713–21. https://doi.org/10.1007/s10482-012-9853-5 PMID: 23180375

36. White TJ, Bruns T, Lee S, Taylor J. Amplification and direct sequencing of fungal ribosomal RNA genes for phylogenetics. PCR protocols: a guide to methods and applications. 1990; 18(1): 315–22.

37. Folmer O, Black M, Wr H, Lutz R, Vrijenhoek R. DNA primers for amplification of mitochondrial cytochrome C oxidase subunit I from diverse metazoan invertebrates. Mol Mar Bio Biotechnol. 1994; 3: 294–9. PMID: 7881515

38. Bidegaray-Batista L, Macías-Hernández N, Oromí P, Arnedo MA. Living on the edge: demographic and phylogeographical patterns in the woodlouse-hunter spider *Dysdera lancerotensis* Simon, 1907 on the eastern volcanic ridge of the Canary Islands. Mol Ecol. 2007; 16(15): 3198–214. https://doi.org/10.1111/j.1365-294X.2007.03351.x PMID: 17651197

39. Madeira F. Park Y. Lee J, Buso N, Gur T, Madhusoodanan N, et al. The EMBL-EBI search and sequence analysis tools APIs in 2019. Nucleic Acids Res. 2019; 47: W636–W641. https://doi.org/10.1093/nar/gkz268 PMID: 30976793

40. National Center for Biotechnology Information (NCBI). Query results for Atypus genome data [Internet]. 2021 [cited 2021 Jul 1]. Available from: https://www.ncbi.nlm.nih.gov/nuccore/?term=Atypus%20[Organism].

41. Hedin M, Derkarabetian S, Alfaro A, Ramírez MJ, Bond JE. Phylogenomic analysis and revised classification of atypoid mygalomorph spiders (Araneae, Mygalomorphae), with notes on arachnid ultraconserved element loci. PeerJ. 2019; 7: e6864. https://doi.org/10.7717/peerj.6864 PMID: 31110925

42. Hedin M, Bond JE. Molecular phylogenetics of the spider infraorder Mygalomorphae using nuclear rRNA genes (18S and 28S): conflict and agreement with the current system of classification. Mol Phylogenet Evol. 2006; 41(2): 454–71. https://doi.org/10.1016/j.ympev.2006.05.017 PMID: 16815045

43. Bond JE, Hendrixson BE, Hamilton CA, Hedin M. A reconsideration of the classification of the spider infraorder Mygalomorphae (Arachnida: Araneae) based on three nuclear genes and morphology. PLOS One. 2012; 7(6): e38753. https://doi.org/10.1371/journal.pone.0038753 PMID: 22723885

44. Ayoub NA, Garb JE, Hedin M, Hayashi CY. Utility of the nuclear protein-coding gene, elongation factor-1 gamma (EF-1γ), for spider systematics, emphasizing family level relationships of tarantulas and their kin (Araneae: Mygalomorphae). Mol Phylogenet Evol. 2007; 42(2): 394–409. https://doi.org/10.1016/j.ympev.2006.07.018 PMID: 16971146

45. He A, Guo J, Peng H, Huang Z, Liu J, Xu X. The complete mitochondrial genome of Atypus karschi (Araneae, Atypidae) with phylogenetic consideration. Mitochondrial DNA Part B. 2021; 6(9): 2523–5. https://doi.org/10.1080/23802359.2021.1959443 PMID: 34377816

46. Araujo D, Schneider MC, Paula-Neto E, Cella DM. The World spider cytogenetic database [Internet]. 2020 [cited 30 Apr 2020]. Available from: http://www.arthropodacytogenetics.bio.br/spiderdatabase/

47. Kořínková T, Král J. Karyotypes, sex chromosomes, and meiotic division in spiders. In: Spider ecophysiology. Springer; 2013. p. 159–71.

48. Sember A, Pappová M, Forman M, Nguyen P, Marec F, Dalíková M, et al. Patterns of sex chromosome differentiation in spiders: Insights from comparative genomic hybridisation. Genes. 2020; 11(8): 849. https://doi.org/10.3390/genes11080849 PMID: 32722348

49. Clark MS, Wall WJ. Chromosomes: the complex code. Chapman & Hall Ltd; 1996.

50. Miller DA, Dev VG, Tantravahi R, Miller OJ. Suppression of human nucleolus organizer activity in mouse-human somatic hybrid cells. ExpCell Res. 1976; 101(2): 235–43. https://doi.org/10.1016/0014-4827(76)90373-6 PMID: 61125

51. Fujiwara A, Abe S, Yamaha E, Yamazaki F, Yoshida MC. Chromosomal localization and heterochromatin association of ribosomal RNA gene loci and silver-stained nucleolar organizer regions in salmonid fishes. Chromosome Res. 1998; 6(6): 463–71. https://doi.org/10.1023/a:1009200428369 PMID: 9865785

52. Guetg C, Santoro R. Formation of nuclear heterochromatin. Epigenetics. 2012; 7(8): 811–4. https://doi.org/10.4161/epi.21072 PMID: 22735386

53. Carmo-Fonseca M, Mendes-Soares L, Campos I. To be or not to be in the nucleolus. Nat Cell Biol. 2000; 2(6): E107–12. https://doi.org/10.1038/35014078 PMID: 10854340

54. Miyashita K. Postembryonic development and life cycle of Atypus karschi DOENITZ (Araneae: Atypidae). Acta Arachnol. 1992; 10: 177–186.

55. iNaturalist. Images of Atypus karschi. [Internet]. 2021 [cited 28 Jul 2021]. Available from: https://www.inaturalist.org/observations?verifiable=true&taxon_id=360542.

56. British Arachnology Society. Spider and harvestman recording scheme website. Summary for Atypus affinis (Araneae). [Internet]. 2021 [cited 29 Jul 2021]. Available from: http://srs.britishspiders.org.uk/portal.php/p/Summary/s/Atypus+affinis.

57. Aoki T. On the life cycle of Jigumo (Atypus karschi Dön.) in Wakajama city. Nanki-Seibutsu Suppl. 1983; 25: 43–8.

58. Yaginuma T. Spiders of Japan in colour (enl, rev. ed.). Hoikusha Publishing Co.; 1978.

59. Zhu M-S, Zhang F, Song D, Qu P. A revision of the genus Atypus in China (Araneae: Atypidae). Zootaxa. 2006; 1118(1): 1–42.

60. Bösenberg W, Strand E. Japanische spinnen. Abh. Senckenb. Naturforsch. Ges. 1906; 30: 93–422.

61. Dönitz W. Uber die Lebensweise Zweier Vogelspinnen aus Japan. Sitzungsber. Gesell. Naturf. Freunde Berlin. 1887;8–10.

62. Schwendinger PJ. On the genus Atypus (Araneae: Atypidae) in northern Thailand. Bull Br Arachnol Soc. 1989; 8(3): 89–96.

63. Beatty JA. Web structure and burrow location of Sphodros niger (Hentz) (Araneae: Atypidae). J Arachnol. 14: 130–132. Available from: https://www.americanarachnology.org/journal-joa/joa-all-volumes/detail/article/download/JoA_v14_p130_grey.pdf.

64. Edwards RL, Edwards EH. Observations on the natural history of a New England population of Sphodros niger (Araneae, Atypidae). J Arachnol. 1990;29–34.

65. Mckenna-Foster A, Draney ML, Beaton C. An unusually dense population of Sphodros rufipes (Mygalomorphae: Atypidae) at the edge of its range on Tuckernuck Island, Massachusetts. J Arachnol. 2011; 39(1): 171–3.

66. Yih D. Land bridge travelers of the Tertiary: the Eastern Asian–Eastern North American floristic disjunction. Arnoldia. 2012; 69: 14–23.

67. Sanmartín I, Enghoff H, Ronquist F. Patterns of animal dispersal, vicariance and diversification in the Holarctic. Biol J Linnean Soc. 2001; 73: 345–390.

68. Saitō S. On the spiders from Tohoku (northernmost part of the main island), Japan. Saito Ho-on Kai Museum Research Bulletin. 1939; 18: 1–91.

69. Kim J, Cho Y. Unrecorded Korean Atypus karschii Doenitz (Atypidae Thorell, Genus Atypus). Korean Arachnology. 2019; 35 (1–2): 1–4.

70. Katsura K. A note on a ballooning of Atypus karschi. Atypus. 1975; 64: 6.

71. Moler PE, Stevenson DJ, Mansell BW, Mays JD, Lee CW. Distribution and natural history of purseweb spiders, Sphodros spp. (Araneae: Mygalomorphae: Atypidae), in Florida, Georgia, and Alabama. Southeast Nat. 2020; 19(4): 663–72.

72. iNaturalist. Map of the Genus Sphodros. [Internet]. 2021 [cited 21 Jul 2021]. Available from: https://www.inaturalist.org/observations?place_id=any&subview=map&taxon_id=61444.

73. Nentwig W. Introduction, establishment rate, pathways and impact of spiders alien to Europe. Biol Invasions. 2015; 17(9): 2757–78.

74. Chesney S. Encyclopedia of Greater Philadelphia. Botany. [Internet]. 2017 [cited 14 Dec 2020]. Available from: https://philadelphiaencyclopedia.org/archive/botany/.

75. Sarudy B. Colonial and early American gardens: The greenhouse in early America [Internet]. 2020 [cited 24 Aug 2021]. Available from: https://americangardenhistory.blogspot.com/2018/12/the-greenhouse-conservatory-in-early.html.

76. Klein WM. Gardens of Philadelphia & the Delaware Valley. Temple University Press; 1995.

77. Rehder A. On the history of the introduction of woody plants into North America. Arnoldia 6: 13–23 [Internet]. 1946 [cited 21 Jun 2021]. Available from: http://arnoldia.arboretum.harvard.edu/pdf/articles/1946-6—on-the-history-of-the-introduction-of-woody-plants-into-north-america.pdf.

78. O'Malley T. The evidence of American garden history. History of early American landscape design [Internet]. 2021 [cited 24 Aug 2021]. Available from: https://heald.nga.gov/mediawiki/index.php?title=The_Evidence_of_American_Garden_History&oldid=40049.

79. Stetson SP. William Hamilton and his" Woodlands". Pa. Mag. Hist. Biogr. 1949; 73(1): 26–33.

80. Madsen K. To make his country smile: William Hamilton's woodlands. Arnoldia. 1989; 49(2): 14–24.

81. Norwood D. The encyclopedia of Greater Philadelphia. China Trade. [Internet]. 2016 [cited 15 Jun 2021]. Available from: https://philadelphiaencyclopedia.org/archive/china-trade/.

82. Japan Society of Greater Philadelphia. Shofuso. History [Internet]. 2021 [cited 15 Jul 2021]. Available from: https://japanphilly.org/programs/festivals/subaru-cherry-blossom-festival/about/history./

83. Qiu J, Turner MG. Effects of non-native Asian earthworm invasion on temperate forest and prairie soils in the Midwestern US. Biol Invasions. 2017; 19(1): 73–88.

84. Edwards GB, Hibbard K. The Mexican Redrump, Brachypelma vagans (Araneae: Theraphosidae), an exotic tarantula established in Florida. Entomology Circular No. 394, May/June 1999, 2pp. [Internet]. 1999 [cited 19 Jul 2021]. Available from: https://www.fdacs.gov/content/download/10780/file/ent394.pdf.

Supporting Information 1. Characteristics of the studied sites of *Atypus karschi* in Delaware County, Pennsylvania, USA in November 2013: location, date of visit, site orientation and slope, soil type and penetrability, and the cover and composition of the vegetation strata. The abundance of plant species is characterized using standardized ranks (Braun-Blanquet 1932).

site	Swedish Cabin	Lansdowne, Essex Ave	Naylor Run Park	Smedley Park	Smedley Park	Tyler Arboretum	Tyler Arboretum	Tyler Arboretum
GPS coordinates	39.93698, -75.30093	39.9444, -75.27606	39.957009, -75.27949	39.917311, -75.359051	39.917311, -75.359051	39.929369, -75.435086	39.928783, -75.434941	39.941767, -75.429050
date	5 Nov 2013	5 Nov 2013	5 Nov 2013	5 Nov 2013	5 Nov 2013	6 Nov 2013	9 Nov 2013	9 Nov 2013
habitat	bottom of the valley	city suburb	shallow valley	rocky valley	rocky valley	fallow field	field-adjacent beech forest	beech forest
orientation	95°	none	195°	340°	260–270°	310°	-	180°
slope	5°	0°	15°	25°	40°	10°	0°	35°
Soil type	Fluvisol	Synantropic	Sandy	Lower layer yellow	Lower layer yellow	Topsoil	Grey	Yellow
Soil penetrability (kg/cm^2)	1-5		0.5–2	0.5–1.75	2–3	2.25–3.25	1.5–2.25	1.25–2
moss cover (%)	0	0	0	0	0	0	0	0
herb cover (%)	20	0	5	10	30	90	0	20
bush cover (%)	80	100	20	40	20	5	30	10
tree cover (%)	50	0	90	60	80	0	60	80
Herb cover								
Carex sp. 1	1			1	2			+
Carex sp. 2					+			
Hieracium cf. *venosum*					+			
Brachypodium sp.				1				
Polystichum sp.					+			
Solidago sp.					1	4		
Geum sp.						r		
Rubus sp.	1					1		
Dactylis sp.						+		
Lonicera sp.						1		2
Cirsium sp.						r		
Linaria sp.						r		
Daucus carota						r		
Medicago sp.						r		
Allium sp.			+					+
Hedera sp.	2	3	+					
Luzula sp.					+			
Fragaria sp.	r							
Alliaria petiolata	+							
Desmodium sp.						1		
Bush cover								
Fagus grandifolia			2	2	2			2
Corylus sp.				1				
Rosa sp.	2		+			+		+
Ulmus sp.						r		
Taxus sp.		5						
Viburnum sp.					+			
Lonicera sp.	2							
Ligustrum sp.	2							+
Tree cover								
Acer cf. *saccharum*	2		5	1				
Populus cf. *grandidentata*	1			1				
Fraxinus sp.	1							
Quercus rubra	2		1	3				
Quercus cf. *alba*			1		4		1	1
Carpinus caroliniana				1				
Liliodendron tulipifera			1	+	1			1
Juglans sp.	+							
Fagus grandifolia							4	4

Supporting Information 2. Carapace length (smallest to largest), number of juveniles present and web length for excavated purse-webs of adult female *Atypus karschi*, Pennsylvania, USA, in November 2013 (n = 18). NA – the web was destroyed while excavating and could not be measured. * - incomplete count or measurement and not used for statistics.

Carapace length (mm)	No. of juveniles present	Length of below-ground web (cm)	Length of above-ground web (cm)	Total web length (cm)
5.0	123	9	7.5	16.5
5.1	70	NA	NA	
5.2	0	10	8	18
5.2	106	8	9	17
5.4	152	8	10.5	18.5
5.4	129	NA	NA	
5.5	116	8	9.5	17.5
5.5	0	NA	NA	
5.6	27*	8	9	17
5.8	0	9	5	14
5.9	79	10	10	20
5.9	128	8.5	6	14.5
6.0	0	7	6	13
6.0	0	16	13	29
6.1	201	8	7	15
6.2	0	8	13	21
6.2	109	6*	6	
6.2	0	NA	NA	

Publication 4.2. Ávila Herrera IM, Král J, Pastuchová M, Forman M, Musilová J, Kořínková T, Šťáhlavský F, Zrzavá M, Nguyen P, Just P, Haddad CR, Hiřman M, Koubová M, Sadílek D, Huber B (2021). Evolutionary pattern of karyotypes and meiosis in pholcid spiders (Araneae: Pholcidae): implications for reconstructing chromosome evolution of araneomorph spiders. BMC Ecology *and* Evolution. 21:75.
DOI: 10.1186/s12862-021-01750-8.

IF2021: 0.00

The haplogyne araneomorphs include more than 6000 species. They consist of Synspermiata and a clade formed by the familes Hypochilidae and Filistatidae. These araneomorphs are remarkable for unusual sex chromosome systems, co-evolution of sex chromosomes and nucleolar organizer regions, and a specific stage of chromosome decondensation during prophase of the first meiotic division in males. The diploid number of Haplogynae varies over a wide range from 5 to 152. While some families possess monocentric chromosomes, members of the Dysderoidea superfamily have holokinetic chromosomes. Four sex chromosome systems (SCS) were reported in haplogynes, namely X0, X_1X_2Y, XY, and X_1X_20.

Karyotype evolution of haplogynes is not satisfactorily understood. To analyse karyotype evolution of haplogynes on family level, I focused on pholcids, which represent the most diversified lineage of haplogynes with monocentric chromosome structure. There are basic chromosome data (2n, chromosome morphology, sex chromosome system) available on 23 species of pholcids representing nine genera. My extensive study brings the data on 47 species, which represent a cross-section through all major pholcid clades. Almost all species were studied for the first time.

My study included species of all pholcid subfamilies: Arteminae, Modisiminae Ninetinae, Pholcinae, and Smeringopinae. I studied six genera of Arteminae: *Artema*, *Chisosa*, *Holocneminus*, *Physocyclus*, and *Wugigarra*. The diploid number ranged from 13 to 33. *Artema* showed the higest diploid number (2n♂=33), male 2n of the other studied species was much lower (ranged between 13 and 15). The congeneric species presented the same SCS: *Chisosa*, *Holocneminus*, and *Physocyclus* X0, *Artema* X_1X_2Y, and *Wugigarra* XY. Y chromosome was the smallest element of the set. On the other hand, the X chromosome(s) were usually the biggest chromosomes. Most artemines exhibited one

NOR, which was placed at the end of an autosome pair. *Physocyclus* also showed the NOR at both ends of the X chromosome.

My study include three modisimine genera: *Anopsicus*, *Modisiminus*, and *Psilochorus*. It is interesting that all the studied species showed the same diplod number and SCS (2n♂=17, X0). The sex chromosome was the longest element of the set. Chromosomes exhibited biarmed morphology, except for the subtelocentric pair found in *P. californiae*. Detection of NORs by FISH has been performed only in two species, *P. californiae* and *P. pallidulus*. NOR was located on one chromosome pair and on both termini of the sex chromosome.

In the subfamily Ninetinae, I studied the genera *Kambiwa* and *Pholcophora*. Most chromosomes of *Kambiwa* showed biarmed morphology. This spider exhibited the complicated SCS, namely the $X_1X_2X_3X_4Y$ system, which formed an achiasmatic multivalent during male meiosis containing two biarmed and two moonoarmed X chromosomes as well as microchromosome Y. *Pholcophora americana* exhibited karyotype 2n♂=29, X_1X_2Y, X chromosomes were the longest chromosomes, while Y the smallest. Karyotype of *Kambiwa* included three NOR-bearing chromosome pairs as well as one X-chromosomelinked NOR. Set of *Pholcophora* contained two chromosome pairs with terminal NOR.

Most studied genera were were members of the subfamily Pholcinae. The male diploid number ranged from 9 to 25. Pholcine karyotypes were predominated by biarmed chromosomes. Most pholcines had X1X2Y system. The X_1 chromosome was biarmed in most cases. In contrast to this, morphology of X_2 was variable, this element showed metacentric, submetacentric or acrocentric morphology. Pattern of NORs in Pholcinae was quite diversified. The number of NORs ranged from one to five, they were located mostly at the ends of the metacentric chromosomes. Beside autosome NORs, most species of the subfamily possess sex chromosome linked NORs. Within the subfamily, we found a diversified clade whose representatives are characterized by X-chromosome linked NORs, which were found in six analysed genera (*Aetana*, *Muruta*, *Nipisa*, *Quamtana*, *Pholcus*, and *Belisana*). Remarkably, these NORs probably took part in sex chromosome pairing during male meiosis.

I studied five genera of the superfamily Smeringopinae: *Crossopriza*, *Holocnemus*, *Hoplopholcus*, *Smeringopus*, and *Stygopholcus*. The male diploid number ranged from 23 to 29. Chromosomes were biarmed except for several species which exhibited one monoarmed pair. In smeringopines, sex chromosome systems X_1X_20, $X_1X_2X_30$, and X0

were found. The number of NORs ranged from one to four. Nucleolus organizer regions were placed on autosomes except for X-chromosome linked NOR found in *H. hispanicus*. Based on the results obtained, I reconstructed chromosome evolution of pholcids. The male diploid number of pholcids varied from 9 to 33. Diploid numbers have decreased convergently in multiple clades by chromosome fusions. Chromosome morphology was mostly biarmed as in the most other haplogynes with monocentric chromosomes karyotyped so far. The results of our research suggest frequent autosome-autosome and autosome-sex chromosome rearrangements during pholcid evolution, specifically inversions, translocations, and chromosome fusions.

Sex chromosome systems of pholcids were diversified. These spiders showed six sex chromosome systems (X0, XY, X_1X_20, $X_1X_2X_30$, X_1X_2Y, $X_1X_2X_3X_4Y$). During evolution of some pholcine X_1X_2Y lineages, size of the Y chromosome has increased considerably. Furthermore, size of X_2 chromosome decreased in some pholcine clades, which was accompanied by change of X_2 morphology to non-metacentric one. Obtained data also suggest frequent integration of autosome fragments into sex chromosomes. X_1X_2Y system have been transformed to the X_1X_20 or XY systems and subsequently into the X0 system in some pholcid clades. The $X_1X_2X_30$ system arose probably from the X_1X_20 system by an X chromosome fission. The $X_1X_2X_3X_4Y$ system has probably evolved from the X_1X_2Y system by integration of a chromosome pair.

Our study provides a first analysis of NOR evolution on family level in spiders. The NOR pattern was diverse. Number of NORs ranged from one to nine. These structures were usually located at chromosome ends. In some clades, NORs spreaded to sex chromosomes (at least five times). The ancestral NORs pattern was probably formed by a single terminal NOR beared by an autosomal pair.

Similarly to the other haplogynes, male prophase I included a diffuse stage. Autosomes of most pholcids were remarkable for a very low recombination frequency.

My contribution: Collection of several species, production of chromosome preparations and detection of NORs by FISH. Evaluation of preparations and analysis of the cytogenetic data, interpretation of results. Participation in writing the draft of the manuscript and its subsequent revisions, preparation of the figures and tables.

Ávila Herrera *et al. BMC Ecol Evo* (2021) 21:75
https://doi.org/10.1186/s12862-021-01750-8

BMC Ecology and Evolution

RESEARCH ARTICLE Open Access

Evolutionary pattern of karyotypes and meiosis in pholcid spiders (Araneae: Pholcidae): implications for reconstructing chromosome evolution of araneomorph spiders

Ivalú M. Ávila Herrera[1*], Jiří Král[1*], Markéta Pastuchová[1], Martin Forman[1], Jana Musilová[1,2], Tereza Kořínková[1,3], František Šťáhlavský[4], Magda Zrzavá[5,6], Petr Nguyen[5,6], Pavel Just[1,4], Charles R. Haddad[7], Matyáš Hiřman[4], Martina Koubová[1], David Sadílek[1,4] and Bernhard A. Huber[8]

Abstract

Background: Despite progress in genomic analysis of spiders, their chromosome evolution is not satisfactorily understood. Most information on spider chromosomes concerns the most diversified clade, entelegyne araneomorphs. Other clades are far less studied. Our study focused on haplogyne araneomorphs, which are remarkable for their unusual sex chromosome systems and for the co-evolution of sex chromosomes and nucleolus organizer regions (NORs); some haplogynes exhibit holokinetic chromosomes. To trace the karyotype evolution of haplogynes on the family level, we analysed the number and morphology of chromosomes, sex chromosomes, NORs, and meiosis in pholcids, which are among the most diverse haplogyne families. The evolution of spider NORs is largely unknown.

Results: Our study is based on an extensive set of species representing all major pholcid clades. Pholcids exhibit a low 2n and predominance of biarmed chromosomes, which are typical haplogyne features. Sex chromosomes and NOR patterns of pholcids are diversified. We revealed six sex chromosome systems in pholcids (X0, XY, X_1X_20, $X_1X_2X_30$, X_1X_2Y, and $X_1X_2X_3X_4Y$). The number of NOR loci ranges from one to nine. In some clades, NORs are also found on sex chromosomes.

Conclusions: The evolution of cytogenetic characters was largely derived from character mapping on a recently published molecular phylogeny of the family. Based on an extensive set of species and mapping of their characters, numerous conclusions regarding the karyotype evolution of pholcids and spiders can be drawn. Our results suggest frequent autosome–autosome and autosome–sex chromosome rearrangements during pholcid evolution. Such events have previously been attributed to the reproductive isolation of species. The peculiar X_1X_2Y system is probably ancestral for haplogynes. Chromosomes of the X_1X_2Y system differ considerably in their pattern of evolution. In some pholcid clades, the X_1X_2Y system has transformed into the X_1X_20 or XY systems, and subsequently into the X0 system. The $X_1X_2X_30$ system of *Smeringopus pallidus* probably arose from the X_1X_20 system by an X chromosome fission. The

*Correspondence: avilai@natur.cuni.cz; spider@natur.cuni.cz
[1] Laboratory of Arachnid Cytogenetics, Department of Genetics and Microbiology, Faculty of Science, Charles University, Viničná 5, 128 44 Prague 2, Czech Republic
Full list of author information is available at the end of the article

$X_1X_2X_3X_4Y$ system of *Kambiwa* probably evolved from the X_1X_2Y system by integration of a chromosome pair. Nucleolus organizer regions have frequently expanded on sex chromosomes, most probably by ectopic recombination. Our data suggest the involvement of sex chromosome-linked NORs in achiasmatic pairing.

Keywords: Achiasmatic pairing, Diffuse stage, Entelegyne, Haplogyne, Inactivation, rDNA, Rearrangement, Segregation, Y chromosome

Background

The structure of chromosomes changes during evolution, just like any other genomic character. Fine-scale changes of the genome can be easily determined by techniques of DNA sequencing and assembling of sequences. However, long assemblies have gaps containing unknown sequences, which makes it difficult to perform linkage mapping of entire chromosomes. An important tool to complete genome assembly and understand transmission of specific loci are cytogenetic data [1]. Cytogenetics also brings other data on the genome and its dynamics, which are not easy to get by sequencing (e.g. mapping of highly differentiated sex chromosomes) [2, 3] or cannot be obtained by this approach (e.g. chromosome behaviour during nuclear division, or large-scale heterochromatin pattern).

Cytogenetic information is particularly important in the analysis of complex genomes, for example in spiders. Genome evolution of spider ancestors included a polyploid event [4], which might have been the origin of the unusual and complex spider sex chromosome determination. The male sex chromosome complement of most spiders includes several chromosomes that do not recombine during meiosis and are presumably non-homologous. Furthermore, it probably also contains a chromosome pair formed by the chromosomes X and Y, which recombine and show a very low level of differentiation (further cryptic sex chromosome pair, CSCP) [5]. Some mygalomorph spiders even exhibit two CSCPs [6]. The single CSCP could represent the ancestral sex chromosomes of spiders [7].

Despite recent progress in genomic analysis of spiders [8], their cytogenetics is not satisfactorily understood. Most data concern entelegyne araneomorphs. Although entelegynes exihibit an enormous species diversity (currently nearly 38,700 described species), their karyotypes are usually conservative, comprising a low number ($2n♂ = 10–49$) of exclusively monoarmed (i.e. acrocentric and subtelocentric) chromosomes and containing two different X chromosomes ($♂X_1X_2/♀X_1X_1X_2X_2$, the so-called X_1X_20 system) [9]. The origin of these sex chromosomes is unresolved. The cytogenetics of the other spider clades (mesotheles, mygalomorphs, haplogyne araneomorphs) is far less studied.

Recent phylogenomic analyses of spiders led to considerable changes in the taxonomic composition of haplogyne araneomorphs. Currently, haplogynes consist of the clade Synspermiata (18 families) and a clade formed by the families Hypochilidae and Filistatidae [10–12] (Fig. 1). These two clades currently include more than 6000 described species (based on the data of [13]). Although haplogynes have a much lower species diversity than entelegynes, their karyotypes are very diverse. The male diploid numbers of haplogynes vary from 5 to 152 [14]. According to chromosome structure, haplogynes show two principal patterns. A synapomorphy of the superfamily Dysderoidea is the holokinetic structure of chromosomes. Holokinetic chromosomes do not contain a localised centromere [14]. Karyotypes of all other studied clades are composed of standard (i.e. monokinetic) chromosomes, and are usually predominated by biarmed (i.e. metacentric and submetacentric) chromosomes [9]. Karyotypes of many haplogynes contain the peculiar X_1X_2Y system ($♂X_1X_2Y/♀X_1X_1X_2X_2$), a sex chromosome constitution that has been found in seven families [9, 14–17]. Chromosomes of the X_1X_2Y system usually exhibit a metacentric morphology. They pair without chiasmata and recombination (i.e. achiasmatically) during male meiosis. The phylogenetic distribution of the X_1X_2Y system suggests a considerable antiquity of this sex chromosome determination [9]. According to a recent hypothesis, this system could be ancestral for araneomorph spiders [16]. Despite this, the origin and subsequent evolutionary transformations of the X_1X_2Y system are not satisfactorily understood. Haplogynes also exhibit other unusual cytogenetic traits, namely a considerable decondensation of bivalents during a specific period of male prophase I (so-called diffuse stage) [9, 18] and the frequent occurrence of nucleolus organizer regions (NORs) on the sex chromosomes [9]. Nucleolus organizer regions are chromosome regions crucial for the formation of the nucleolus. They contain tandem copies of the genes coding 5.8S, 18S, and 28S ribosomal RNA [19].

Although fundamental trends of haplogyne karyotype evolution have been determined [9], karyotype evolution within haplogyne families remains unknown. To fill this gap, we have focused on the cytogenetics of the family Pholcidae (Fig. 1), which is an ideal model group for such a study. First, pholcids are the most diversified haplogyne

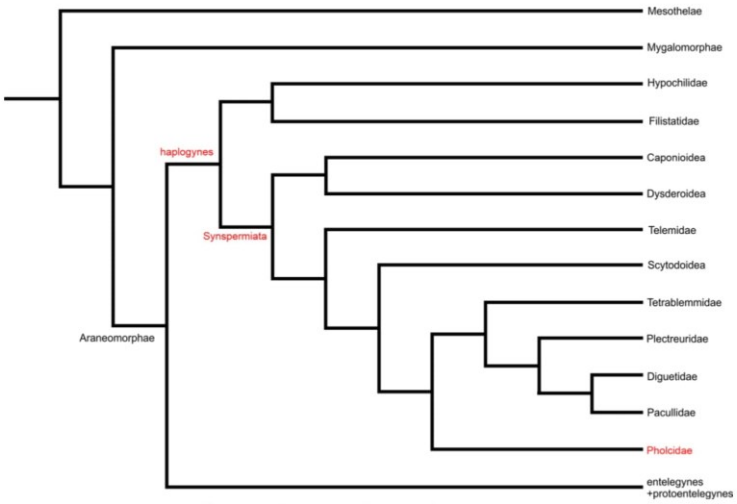

Fig. 1 Phylogeny of spiders, with specific consideration on haplogyne spiders. The phylogenetic tree was constructed following [10] except for Telemidae [11]. Caponioidea: Caponiidae, Trogloraptoridae; Dysderoidea: Dysderidae, Oonopidae, Orsolobidae, Segestriidae; Scytodoidea: Drymusidae, Ochyroceratidae, Periegopidae, Psilodercidae, Scytodidae, Sicariidae

family with a standard chromosome structure. They currently include 94 genera and 1812 species [13]. Second, pholcids are the spider family with the most comprehensive molecular phylogeny available (with 600 species representing 86% of the known genera [20, 21]). Third, they display a worldwide distribution, with the large majority of species in the tropics and subtropics. Numerous species are synanthropic and have been translocated by humans around the globe [22, 23].

Information on pholcid cytogenetics is very limited. There are only basic data available for 23 species representing nine genera (see database [24]). Here we present chromosome data of 47 species, which represent an extensive cross-section through all major pholcid clades. Since previous authors often failed in the proper determination of pholcid cytogenetic data, we have also revised previously published results. We further focused on the evolution of NORs, the evolution of which is largely unknown in spiders.

Our study represents one of the most comprehensive cytogenetic datasets of any spider family. Cytogenetic data of pholcids are diversified and have considerable potential to be used in the reconstruction of pholcid phylogeny. Based on our data, numerous conclusions and hypotheses regarding the karyotype evolution of pholcids, as well as haplogyne spiders, can be drawn. Finally, our results suggest promising subjects for future evolutionary studies on the karyotypes, sex chromosomes, and NORs of spiders.

Results

Arteminae

Our study included representatives of the genera *Artema*, *Chisosa*, *Holocneminus*, *Physocyclus*, and *Wugigarra* (Additional file 1: Table S1, Additional file 2: Table S2). The diploid number in artemine males ranged from $2n = 13$ (*Chisosa diluta*) to $2n = 33$ (*Artema* spp.), with most species having $2n = 15$. In all species, the karyotypes consisted predominantly of biarmed chromosomes (Additional file 2: Table S2, Fig. 2, Additional file 3: Fig. S1).

Representatives of *Artema* differed from the other artemines by a much higher diploid number and a X_1X_2Y system. The male karyotype of *Artema* contained 15 chromosome pairs (this term is used in a specific context in our study, see "Methods", p. 31) decreasing gradually in size (Additional file 1: Table S1, Additional file 2: Table S2, Additional file 4: Fig. S2). Chromosome morphology was predominantly metacentric. The X_1 chromosome was considerably longer than X_2. The Y

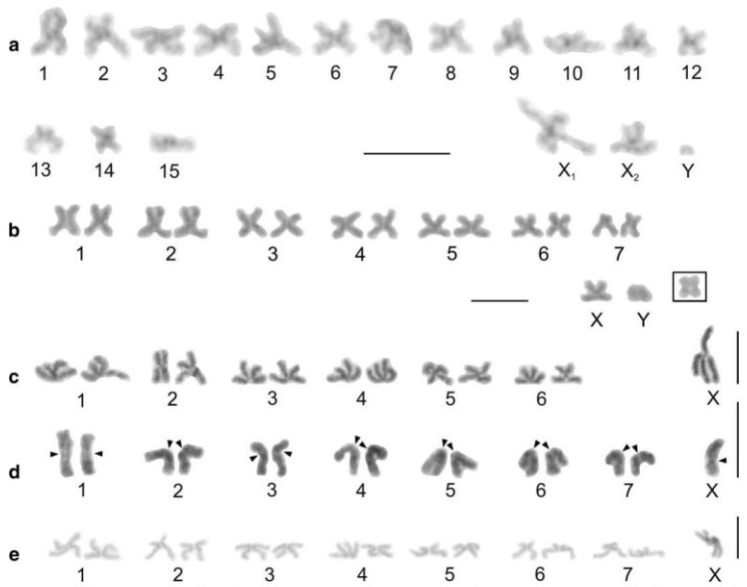

Fig. 2 Arteminae, male karyotypes, stained by Giemsa. Based on two sister metaphases II except for *Artema nephilit* (single metaphase II) and *Holocneminus* (spermatogonial metaphase). **a** *Artema nephilit*, haploid karyotype. Chromosomes metacentric except for five submetacentric (nos. 2, 8, 10-12), one subtelocentric (no. 13), and one acrocentric element (no. 15). The Y chromosome is from another metaphase II. Morphology of the Y chromosome is unresolved; **b** *Wugigarra* sp. Karyotype metacentric except for one subtelocentric pair (no. 7). Inset: magnified Y chromosome (from another metaphase II). Note metacentric morphology of this element; **c** *Chisosa diluta*. Chromosomes exclusively metacentric. The positively heteropycnotic X chromosome is the longest chromosome; **d** *Holocneminus* sp. Chromosomes metacentric except for one submetacentric (no. 4) and one subtelocentric pair (no. 3). Centromeres marked by arrowheads; **e** *Physocyclus dugesi*. Chromosomes metacentric except for two submetacentric (nos 2, 5) and two subtelocentric pairs (nos 6, 7). The positively heteropycnotic X chromosome is the longest chromosome of the karyotype. Bar = 10 μm

chromosome was the smallest element of the karyotype (Additional file 1: Table S1, Additional file 2: Table S2, Fig. 2a, Additional file 3: Fig. S1).

Karyotypes of the other artemines contained only six (*C. diluta*) or seven chromosome pairs (the other species). Chromosome pairs decreased gradually in size except for the prominent longest pair of *C. diluta* (Additional file 1: Table S1). The karyotype of *Wugigarra* ($2n♂ = 16$) was characterized by a XY system (Fig. 2b, Additional file 4: Fig. S2). The Y chromosome was the smallest element of the complement, a feature similar to *Artema* (Additional file 1: Table S1). The other taxa exhibited the X0 system (Fig. 2c–e, Additional file 5: Fig. S3). Their sex chromosome was the longest element of the karyotype except for *Holocneminus* sp. The size of the X chromosome varied considerably from 11.4% (*Holocneminus* sp.) to 21.2% of TCL (*C. diluta*). The length of the sex chromosome was determined from mitotic metaphase (*Holocneminus*) or metaphase II (the other X0 species). The small size of the X chromosome in *Holocneminus* compared to the other species could then reflect the fact that this element is more condensed in mitotic metaphase than in metaphase II.

The nucleolus organizer region was present at an end of one chromosome pair in all of the studied species (Additional file 2: Table S2, Fig. 3, Additional file 6: Fig. S4), and in *Physocyclus* also on both termini of the X chromosome (Fig. 3d). The morphology of the NOR-bearing pair was metacentric in *Holocneminus* (Fig. 3c), metacentric/submetacentric in *Physocyclus* (Fig. 3d), submetacentric in *Artema* (Fig. 3a, Additional file 6: Fig. S4a, b), and subtelocentric in *Wugigarra*

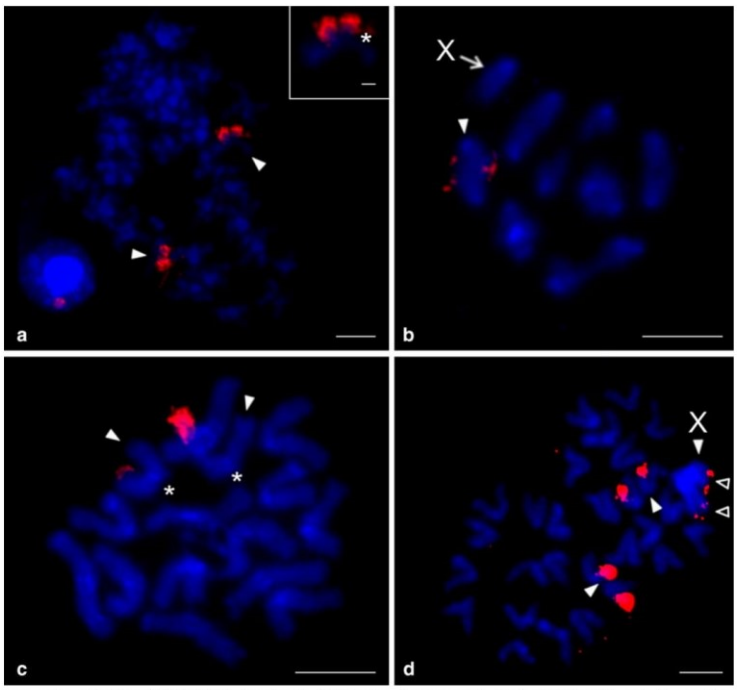

Fig. 3 Arteminae, males, detection of NORs (FISH). *Arrowhead* = NOR-bearing chromosome (**a**, **c**, **d**) or bivalent (**b**), *asterisk* = centromere, *open arrowhead* = sex chrosomosome-linked NOR, X = X chromosome. **a** *Artema nephilit* (X_1X_2Y), plate formed by fused sister metaphases II. Pair of chromosomes bears a terminal NOR. Inset: submetacentric NOR-bearing chromosome. NOR is placed at the end of short arm; **b**, **c** *Holocneminus* sp. (X0). **b** Metaphase I, one bivalent contains NOR; **c** Mitotic metaphase. Chromosomes of one metacentric pair have terminal NOR; **d** *Physocyclus dugesi* (X0), two sister plates, late metaphase II. Chromosomes of one metacentric/submetacentric pair contain a terminal NOR. X chromosome is more condensed than the other chromosomes. It includes tiny NOR at both ends. Bar = 5 µm, inset 1 µm

(Additional file 6: Fig. S4c). Except for *Holocneminus*, the NOR was placed at the end of the short arm.

Modisiminae

We analysed representatives of *Anopsicus*, *Modisimus*, and *Psilochorus* (Additional file 7: Table S3). The studied modisimines exhibited the same male diploid number (17), sex chromosome system (SCS) (X0), and a metacentric sex chromosome (Additional file 1: Table S1, Additional file 7: Table S3, Fig. 4a–c, Additional file 8: Fig. S5, Additional file 9: Fig. S6). Chromosomes of modisimines were biarmed except for one pair of *P. californiae* (Additional file 1: Table S1, Additional file 7: Table S3). The sex chromosome was the longest chromosome of the karyotype (Additional file 1: Table S1).

The genus *Psilochorus* was represented by three species. Chromosome pairs of *P. californiae* decreased gradually in size. In contrast, the longest pair of *P. pallidulus* and the two longest pairs of *P. simoni* were prominent. Moreover, in the latter two species the last pair was much smaller than the penultimate pair (Additional file 1: Table S1). The karyotype of *P. pallidulus* was formed exclusively by metacentric chromosomes (Additional file 9: Fig. S6b). The karyotypes of the other two species were also formed by metacentrics except for two submetacentric pairs of *P. simoni*, and two submetacentric and one subtelocentric pair

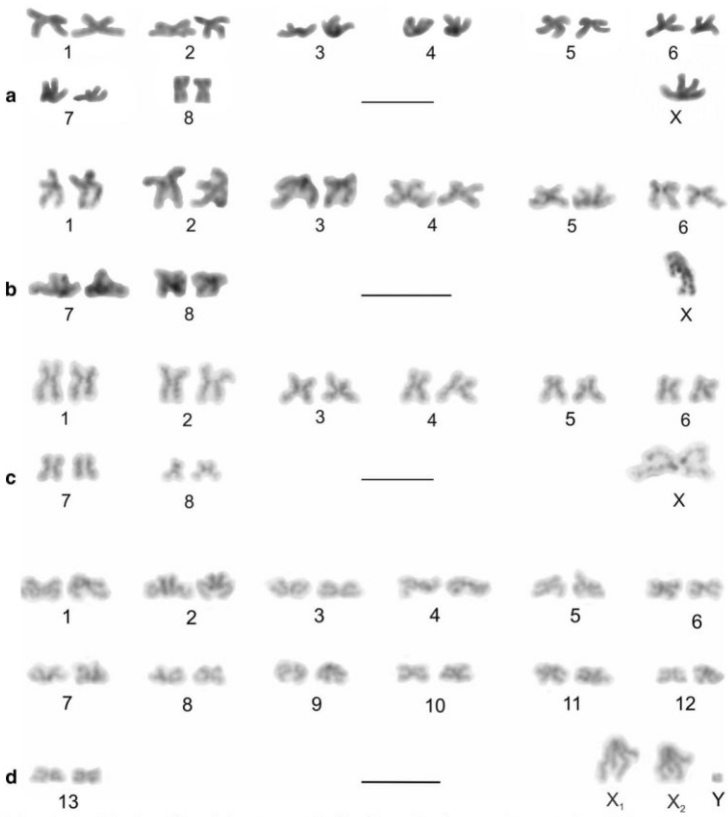

Fig. 4 Modisiminae (**a**-**c**) and Ninetinae (**d**), male karyotypes, stained by Giemsa. Based on two sister metaphases II. Karyotypes are predominated by metacentrics. Single sex chromosome of modisimines is the longest element of the karyotype. **a** *Anopsicus* sp., pair nos. 3 and 5 are submetacentric; **b** *Modisimus* cf. *elongatus*. Three pairs submetacentric (nos 1, 3, 6), X chromosome positively heteropycnotic; **c** *Psilochorus simoni*. Chromosome pairs form three size groups (pairs 1-2, 3-7, 8). Two pairs submetacentric (nos 1, 5). Sex chromosome negatively heteropycnotic; **d** *Pholcophora americana*, pair no. 2 submetacentric. Bar = 10 μm

of *P. californiae* (Fig. 4c, Additional file 9: Fig. S6a). Nucleolus organizer regions were detected in *P. californiae* and *P. pallidulus*. Their karyotype included a NOR-bearing metacentric pair. While the NOR of *P. californiae* exhibited a terminal location, placement of NOR in *P. pallidulus* was not determined. In both species, the sex chromosome bore NORs at both ends (Fig. 5).

Ninetinae

We studied representatives of *Kambiwa* and *Pholcophora* (Additional file 7: Table S3, Additional file 10: Fig. S7). The chromosomes of *K. neotropica* were metacentric except for two monoarmed elements (Additional file 11: Fig. S8a). Several lines of observations demonstrated a complicated sex chromosome system in *Kambiwa*. Sex chromosomes formed a peculiar cross-shaped element in

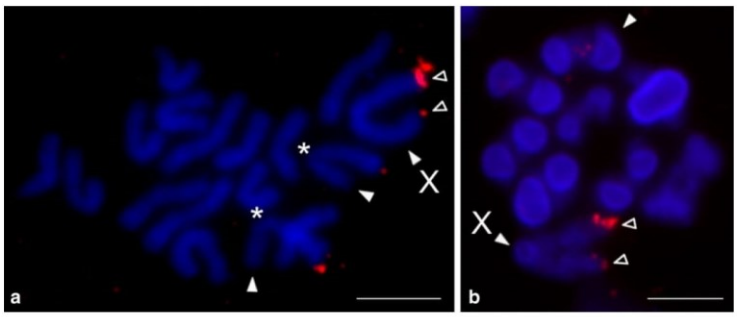

Fig. 5 Modisiminae, males, detection of NORs (FISH). *Arrowhead* = NOR bearing chromosome (**a**) or bivalent (**b**), *asterisk* = centromere, *open arrowhead* = sex chromosome-linked NOR, X=X chromosome. **a** *Psilochorus califomiae* (X0), mitotic metaphase. Chromosomes of one metacentric pair contain a terminal NOR. X chromosome bears NOR at both ends; **b** *P. pallidulus* (X0), metaphase I. One bivalent includes a tiny NOR. X chromosome has two terminal NORs. Bar = 5 μm

male metaphase I (Additional file 10: Fig. S7a, b). Comparison of data on male 2n (2n♂ = 29, Additional file 11: Fig. S8a) and male metaphase I (12 bivalents plus cross-shaped element) (Additional file 10: Fig. S7a, b) suggested that the cross-shaped element is a multivalent comprising of five chromosomes. Analysis of male metaphases II demonstrated the presence of a $X_1X_2X_3X_4Y$ system. There are two types of metaphase II plates, one with 13 chromosomes including the Y microchromosome, and another one with 16 chromosomes including four heterochromatic X (Fig. 6b, Additional file 11: Fig. S8b, c). Two X chromosomes differed from the remaining two by a specific condensation at metaphase II. These chromosomes were monoarmed (Figs. 6b). The morphology of the tiny Y chromosome was unresolved. Chromosomes of *Pholcophora americana* (2n♂ = 29, X_1X_2Y) decreased gradually in size except for the prominent longest pair (Additional file 1: Table S1). They were metacentric

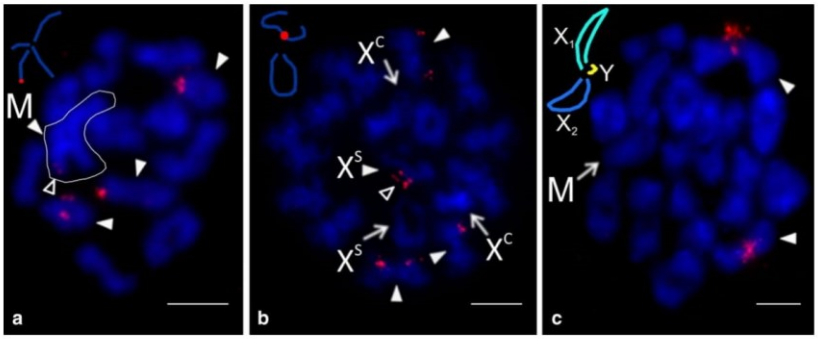

Fig. 6 Ninetinae, males, detection of NORs (FISH). Figures contain scheme of sex chromosomes (red = NOR). *Arrowhead* = chromosome (**b**), bivalent (**a**, **c**) or multivalent (**a**) with NOR, M = sex chromosome multivalent, *open arrowhead* = sex chromosome-linked NOR, X = X chromosome. **a**, **b** *Kambiwa neotropica* ($X_1X_2X_3X_4Y$) **a** Metaphase I, three bivalents contain terminal NOR. Moreover, sex chromosome multivalent (delimited by line) includes a tiny NOR at end of one "arm". Note scheme for morphology of multivalent. **b** Metaphase II (n = 16) containing four X chromosomes. Two X chromosomes are the most condensed elements of the plate (X^C). Two other X chromosomes have lower condensation and monoarmed morphology (X^S). Note scheme for morphology of monoarmed X chromosomes. One monoarmed X contains a NOR at short arm. In addition, three other chromosomes bear a NOR; **c** *Pholcophora americana* (X_1X_2Y), metaphase I. Two large bivalents contain terminal NOR. Note scheme for probable morphology of sex chromosome multivalent. Arms of each X chromosome are associated with each other. Bar = 5 μm

except for one submetacentric pair (Fig. 4d). The X chromosomes showed a similar length. While they were the longest elements of the karyotype, the Y chromosome was the smallest one (Additional file 1: Table S1).

Three chromosome pairs of *Kambiwa* contained a terminal NOR (Fig. 6a). Moreover, one monoarmed X chromosome bore a NOR on its short arm (Fig. 6b). *Pholcophora* exhibited two chromosome pairs bearing terminal NORs (Fig. 6c).

Pholcinae

We analysed pholcines representing twelve genera (Additional file 12: Table S4). Male 2n ranged from 9 (*Micropholcus fauroti*) to 25 (*Nipisa deelemanae*, three *Pholcus* species, *Spermophora senoculata*) (Additional file 12: Table S4). Chromosome morphology was determined in representatives of eight genera (Additional file 1: Table S1). Chromosome pairs of most pholcines decreased gradually in size. In several species, however, the longest pair(s) were prominent (first pair of *Belisana sabah* and *Pholcus opilionoides*; first three pairs of *Leptopholcus guineensis*; first five pairs in *Pholcus* sp.). In *Aetana kinabalu* the last chromosome pair was much smaller than the penultimate pair (Additional file 1: Table S1). Chromosome pairs were biarmed, except for two subtelocentric pairs in *Quamtana filmeri*, one subtelocentric pair in *Pholcus kindia*, and one acrocentric pair in *A. kinabalu* and *Pholcus* sp. (Additional file 12: Table S4).

Concerning sex chromosomes, most pholcines showed the X_1X_2Y system, which was found in nine genera (*Aetana*, *Leptopholcus*, *Metagonia, Muruta*, *Nipisa*, *Pehrforsskalia, Pholcus*, *Quamtana*, *Spermophora*) (Additional file 1: Table S1, Fig. 7a–d, Additional file 13: Fig. S9, Additional file 14: Fig. S10, Additional file 15: Fig. S11, Additional file 16: Fig. S12). The X_1 chromosome was usually the largest element of the karyotype, the X_2 chromosome a small to medium element, and the Y chromosome usually a microchromosome or small element (Additional file 1: Table S1). While the X_1 and X_2 chromosomes of *Aetana* and *Spermophora* were medium-sized elements of similar size, the Y chromosome of these species was a microchromosome (Additional file 1: Table S1). Although there are no precise data on the morphology of the sex chromosomes in *Metagonia*, they probably also consist of X chromosomes of similar size and a tiny Y chromosome (Additional file 11: Fig. S8f, Additional file 14: Fig. S10e). Most other pholcines exhibiting the X_1X_2Y system showed a X_2 size reduction (up to 2.7% of TCL in *Pholcus pagbilao*) and a considerable increase of the Y chromosome size (up to 11.7% of TCL in *P. kindia*). In some *Pholcus* and *Quamtana* species, the X_2 chromosome was only slightly larger than the Y chromosome (Additional file 1: Table S1). In *Leptopholcus* and two *Pholcus* species (*P. kindia*, *P. pagbilao*), the Y chromosome was even longer than the X_2 chromosome (Additional file 1: Table S1, Fig. 7a, b, Additional file 16: Fig. S12b). The X_1 chromosome of pholcines was metacentric, except for *Aetana*, whose X_1 chromosome was submetacentric (Additional file 12: Table S4, Additional file 16: Fig. S12a). In contrast, the morphology of the X_2 was variable. It was metacentric in *Aetana*, *Nipisa*, *Spermophora*, and African *Pholcus* species (Fig. 7b, Additional file 11: Fig. S8i, Additional file 12: Table S4, Additional file 13: Fig. S9f, Additional file 16: Fig. S12a), submetacentric in *Leptopholcus*, *Muruta*, and *Pholcus phalangioides* (Additional file 12: Table S4, Fig. 7a, Additional file 15: Fig. S11b), subtelocentric in *Quamtana filmeri* and *Pholcus* sp. (Fig. 7c, d, Additional file 12: Table S4), and acrocentric in *Quamtana hectori*, *Pholcus opilionoides* and *P. pagbilao* (Additional file 12: Table S4, Additional file 16: Fig. S12b–d). The Y chromosome exhibited a metacentric morphology, except for *Leptopholcus* and *P. pagbilao*, whose Y chromosome was submetacentric (Fig. 7a, Additional file 12: Table S4, Additional file 16: Fig. S12b). The morphology of the Y chromosome of *Aetana*, *Muruta*, and *Nipisa*, as well as sex chromosomes of *Metagonia* and *Pehrforsskalia*, were not determined.

Some pholcines displayed the X0 system (*Belisana*, *Cantikus*, and *Micropholcus*). The X chromosome was metacentric (Additional file 12: Table S4, Figs. 7e, f, 8a, b, Additional file 17: Fig. S13). Its size was comparable to the size of short (*Micropholcus*) or medium-sized chromosome pairs (*Belisana*, *Cantikus*) (Additional file 1: Table S1).

Nucleolus organizer regions were detected in representatives of nine genera, namely *Aetana*, *Belisana*, *Cantikus*, *Micropholcus*, *Muruta*, *Nipisa*, *Pholcus*, *Quamtana*, and *Spermophora* (Additional file 12: Table S4). Pholcines showed a considerable diversity of NOR patterns. Their karyotypes contained from one (*Cantikus*, *Micropholcus*, *Muruta*, *Q. filmeri*) to five NOR-bearing chromosome pairs (*Belisana*) (Figs. 8b, 9, 10, Additional file 18: Fig. S14). In most species, we also determined the morphology of these pairs, including the NOR location. Pairs bearing NORs were biarmed; NORs were placed at chromosome ends (Additional file 12: Table S4). All pairs included one NOR locus except for one pair of *Nipisa*, *P. pagbilao*, and *Spermophora*, which had a locus at both ends (Figs. 9a, 10c, Additional file 18: Fig. S14b). In *Spermophora*, both loci of this pair were homozygous for the presence of a NOR (Fig. 9a). In the studied male of *P. pagbilao*, one of these loci was heterozygous for the presence of a NOR (Fig. 10c). Concerning the studied *Nipisa* male, comparison of the NOR pattern

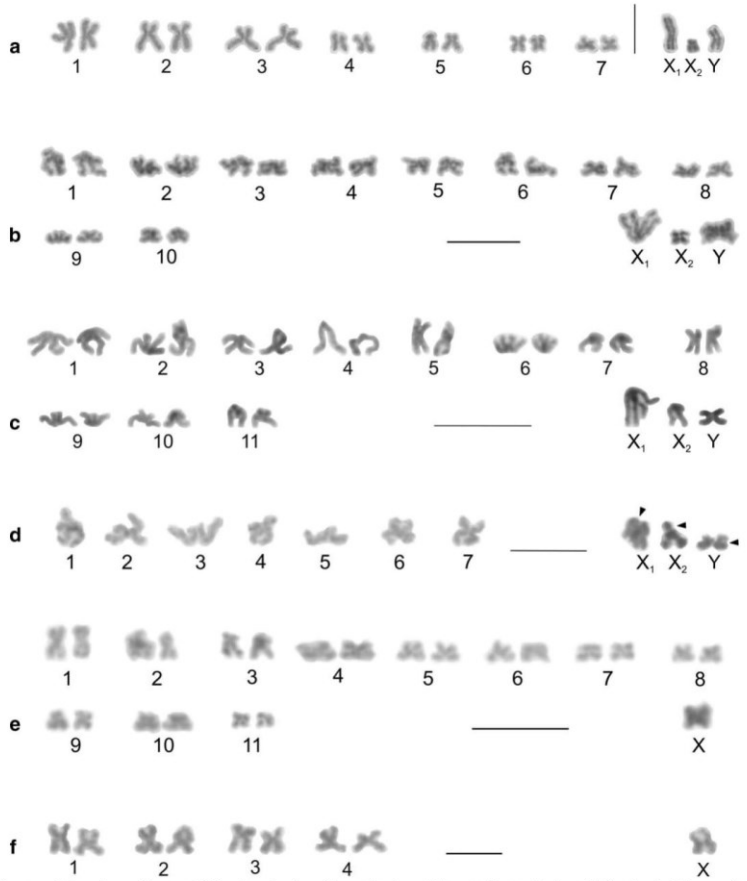

Fig. 7 Pholcinae, male karyotypes, Giemsa staining. Based on two sister metaphases II (**a**-**c**, **e**, **f**) or metaphase II (**d**). **a** *Leptopholcus guineensis*. Chromosome pairs form two size groups, large-sized (nos 1–3) and small-sized (nos 4–7). The X_2 chromosome replaced by X_2 from another plate. The X_2 and Y chromosome as well as three pairs (nos 2, 3, 5) submetacentric. Sex chromosomes positively heteropycnotic; **b** *Pholcus kindia*. Chromosomes biarmed except for one subtelocentric pair (no. 6). Chromosomes X_1 and Y longest elements of karyotype, chromosomes X_2 and Y positively heteropycnotic; **c** *Pholcus* sp. Chromosome pairs form two size groups, large-sized (nos 1–5) and small-sized (nos 6–11). Chromosomes metacentric except for three submetacentric (nos 7, 9, 11) and one acrocentric pairs (no. 4), and subtelocentric X_2 chromosome. Y chromosome positively heteropycnotic; **d** *Quamtana filmeri*, haploid karyotype. Chromosomes metacentric except for one submetacentric (no. 4) and two subtelocentric pairs (nos 3, 5), and subtelocentric X_2 chromosome. Y chromosome replaced by Y from another plate. Sex chromosomes positively heteropycnotic. Centromeres of sex chromosomes marked by arrowheads; **e** *Belisana sabah*. Karyotype metacentric except for one submetacentric pair (no. 3). First pair considerably longer than the other pairs, which gradually decrease in size. Third and eleventh pairs replaced by corresponding pairs from another plate. X chromosome positively heteropycnotic; **f** *Micropholcus fauroti*, chromosomes metacentric. Bar = 10 µm

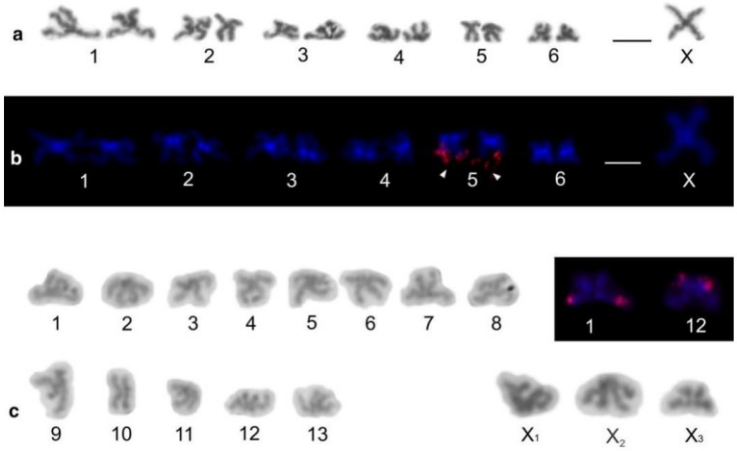

Fig. 8 Male karyotype of *Cantikus sabah* (Pholcinae) (**a, b**) and *Smeringopus pallidus* (Smeringopinae) (**c**). Based on metaphase II (**c**) or two sister metaphases II (**a**, **b**). *Arrowhead* = NOR. **a** Diploid karyotype, Giemsa stained. Note metacentric morphology of chromosomes. **b** Diploid karyotype, detection of NORs (FISH). Fifth pair bears a terminal NOR (arrowheads). In contrast to most other pholcids, centromeres are formed by a prominent AT-rich block; **c** Haploid karyotype, Giemsa stained. Chromosomes metacentric except for three submetacentrics (nos 5, 9, 12). Sex chromosomes show a slight positive heteropycnosis. Inset: detection of NORs (FISH); chromosomes of two pairs (nos. 1, 12) contain terminal NOR. Bar = 10 µm

of the chromosome pairs in metaphase I (three NOR bearing pairs, Additional file 18: Fig. S14c) and mitotic metaphase (five chromosomes with NOR, including one chromosome with NOR at both ends, Additional file 18: Fig. S14b) implied that one chromosome pair consists of a chromosome with NOR at both ends plus a chromosome with one NOR or without NOR. It means that one or even both loci of this pair were heterozygous for the presence of a NOR.

Sex chromosome-linked NORs were revealed in *Aetana*, *Muruta*, *Nipisa, Quamtana*, *Pholcus phalangioides* (X_1X_2Y), and *Belisana* (X0) (Additional file 12: Table S4, Figs. 9b–f, 10a, b, Additional file 18: Fig. S14b–h). In *Aetana*, the X_1 chromosome had a terminal NOR (Fig. 9b). In *Muruta, Nipisa*, *Quamtana*, and *P. phalangioides*, NORs were detected at both ends of the X_1 chromosomes (Additional file 12: Table S4, Figs. 9f, 10b, Additional file 18: Fig. S14b, d, f–h). Furthermore, the X_2 chromosome of some pholcines involved NOR(s) too. While the X_2 chromosome of *Muruta* and *P. phalangioides* exhibited NOR at one end only (Figs. 9f, 10b), the X_2 chromosome of *Nipisa* was terminated by NOR at both ends (Additional file 18: Fig. S14b). In the latter pholcid, the Y chromosome also had a terminal NOR (Additional file 18: Fig. S14b). In *Belisana*, a NOR was detected at both ends of the X chromosome (Fig. 9c, d). In species exhibiting the X_1X_2Y system, the sex chromosome ends bearing a NOR took part in sex chromosome pairing during male meiosis (Figs. 9b, e, 10a, Additional file 18: Fig. S14c, e).

Smeringopinae

We analysed representatives of *Crossopriza*, *Holocnemus*, *Hoplopholcus*, *Smeringopus*, and *Stygopholcus* (Additional file 19: Table S5). The male 2n ranged from 23 to 29 (Additional file 19: Table S5, Figs. 8c, 11, Additional file 20: Fig. S15, Additional file 21: Fig. S16). Chromosome pairs of most smeringopines decreased gradually in length. In some species the longest pair (*Holocnemus*, *Smeringopus cylindrogaster*) or two longest pairs (*Crossopriza lyoni*, *Stygopholcus skotophilus*) were prominent. Furthermore, the last pair of *S. skotophilus* was much smaller than the penultimate pair. Chromosome pairs were exclusively biarmed except for *Holocnemus hispanicus*, *S. skotophilus*, and some *Hoplopholcus* and *Smeringopus* species, whose karyotype included one monoarmed pair (Additional file 1: Table S1).

The male karyotype of *Hoplopholcus* and *Smeringopus* was composed of 28 chromosomes, including the X_1X_20 system (Additional file 19: Table S5, Fig. 11d, f, Additional file 20: Fig. S15, Additional file 22: Fig. S17a–e), except for *S. pallidus* ($2n♂ = 29$, $X_1X_2X_30$) (Fig. 8c, Additional

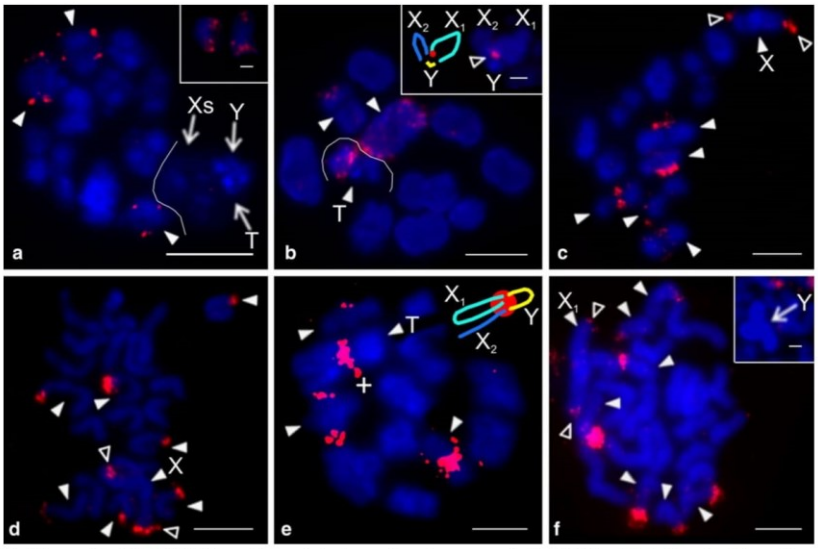

Fig. 9 Pholcinae, males, NORs (FISH) I. Figures **b**, **e** contain scheme of sex chromosome trivalent X_1X_2Y (red circle at **c** = signal formed by several NORs). *Arrowhead* = NOR bearing chromosome (**c**, **d**, **f**), bivalent (**a**-**c**, **e**) or trivalent (**b**, **e**), *open arrowhead* = sex chromosome-linked NOR, T = sex chromosome trivalent (**a**, **b**, **e**), X = X chromosome, X_1 = X_1 chromosome, X_2 = X_2 chromosome, Xs = X chromosomes, Y = Y chromosome, + = signal formed by several NORs. **a** *Spermophora senoculata* (X_1X_2Y), diakinesis, note three NOR-bearing bivalents, sex chromosome trivalent separated by line (X chromosomes considerably decondensed). Inset: mitotic metaphase, chromosome pair bearing two terminal NOR loci; **b** *Aetana kinabalu* (X_1X_2Y), metaphase I, the largest bivalent and one medium-sized bivalent bear a terminal NOR. The sex chromosome trivalent (separated by line) also includes NOR signal. Position of NOR is, however, unclear. Inset: diplotene, sex chromosome trivalent and its scheme, note NOR at the end of X_1 chromosome; **c**, **d** *Belisana sabah* (X0), **c** Metaphase I. Five bivalents contain NOR, sex chromosome with NOR at both ends. **d** Incomplete mitotic metaphase (21 chromosomes), NORs terminal, X chromosome with NOR at both ends; **e**, **f** *Pholcus phalangioides* (X_1X_2Y). **e** Metaphase I, three bivalents contain NOR. The sex chromosome trivalent contains the signal in region of chromosome pairing (see scheme). **f** Mitotic metaphase, NORs terminal. X_1 chromosome bears NOR at both ends. Number of the other NOR-bearing chromosomes (seven) suggests that the X_2 chromosome contains a NOR too. Inset: another mitotic metaphase, Y chromosome considerably condensed, without NOR. Bar = 5 μm; insets 1 μm

file 22: Fig. S17f) and *S. cylindrogaster* ($2n♂ = 26, X_1X_20$) (Fig. 11e). The metacentric X_1 chromosome was the largest element of the karyotype, except for three *Smeringopus* species. The X_2 chromosome was usually a medium-sized element (Additional file 1: Table S1). It had a variable morphology, being metacentric in *S. ndumo*, *S. pallidus* and *S. similis*, submetacentric in *S. atomarius*, subtelocentric in *Hoplopholcus* and *S. peregrinus*, and acrocentric in *S. cylindrogaster* and *Smeringopus* sp. (Additional file 1: Table S1). The metacentric X_3 chromosome of *S. pallidus* was the smallest chromosome of the karyotype (Additonal file 1: Table S1).

Representatives of the genera *Crossopriza*, *Holocnemus*, and *Stygopholcus* exhibited the X0 system, including a metacentric X chromosome (Additional file 19: Table S5, Fig. 11a–c, g, Additional file 19: Fig. S16, Additional file 23: Fig. S18), which was the largest element of the set except for *Crossopriza* sp. and *Holocnemus caudatus* (Additional file 1: Table S1).

Smeringopines exhibited a considerable diversity of the NOR number (Additional file 19: Table S5). Their karyotypes contained one (*H. hispanicus*, *Hoplopholcus* species, *S. skotophilus*) (Fig. 12a, c, d, i), two (*Holocnemus pluchei*, *S. atomarius*, *S. pallidus*) (Figs. 8c, 12b, e, f) or four (*Smeringopus* sp.) (Fig. 12g, h) chromosome pairs bearing a NOR. In most species, the morphology of these pairs and the NOR location was also determined. Chromosome pairs bearing NORs were biarmed; NORs were terminal (Additional file 19: Table S5). *Smeringopus* sp. exhibited an odd number of chromosomes bearing a

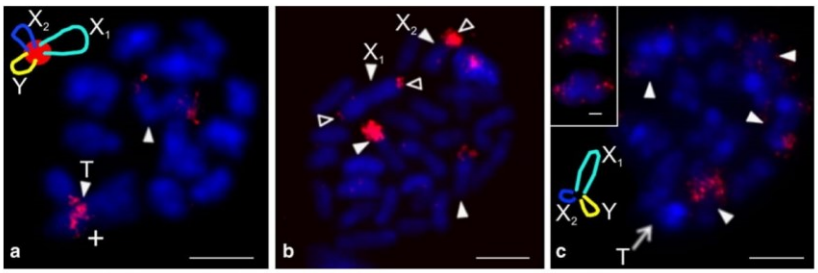

Fig. 10 Pholcinae, males, NORs (FISH) II. Figures **a**, **c** contain scheme of sex chromosome trivalent X_1X_2Y (red circle = signal formed by several NORs). *Arrowhead* = NOR bearing chromosome (**b**), bivalent (**a**, **c**) or trivalent (**a**), *open arrowhead* = sex chromosome-linked NOR, T = sex chromosome trivalent $X_1 = X_1$ chromosome, $X_2 = X_2$ chromosome, Y = Y chromosome, + = signal formed by several NORs. **a**, **b** *Muruta tambunan* (X_1X_2Y). **a** Metaphase I, note a bivalent bearing a terminal NOR and sex chromosome trivalent with signal in region of chromosome pairing (see scheme). **b** Mitotic metaphase, the large X_1 chromosome bears two terminal NORs, the X_2 chromosome contains one terminal NOR. Chromosomes of a chromosome pair exhibit another terminal NOR; **c** *Pholcus pagbilao* (X_1X_2Y), metaphase I. Plate contains four NOR bearing bivalents and sex chromosome trivalent without signal (see scheme). Inset: metaphase II, NOR bearing pair, upper chromosome contains two terminal loci. Bar = 5 µm; inset 1 µm

NOR, which indicates heterozygosity of one pair for the presence of a NOR (Fig. 12h). The karyotype of *H. hispanicus* (X0) also contained a sex chromosome-linked NOR, which was placed at the end of the X chromosome (Fig. 12a).

Chromosome behaviour in the male germline

Males exhibited standard meiosis except for prophase I. Following pachytene, bivalents appeared globular and almost decondensed (so-called diffuse stage). In contrast, the sex chromosomes formed a highly spiralised and positively heteropycnotic body (i.e. stained more intensively than the other chromosomes) (Fig. 13a). In some pholcids, bivalents became considerably condensed during the late diffuse stage, whereas they retained a globular shape (e.g., *Smeringopus*). Despite condensation of bivalents, chiasmata were not discernible or only partially expressed (Fig. 13b). Following the diffuse stage, bivalents of some species uncoiled and exhibited a morphology typical for late prophase I (i.e., diplotene and diakinesis). Alternatively, the standard morphology of the bivalents emerged gradually during their condensation (Additional file 11: Fig. S8g). In some species, diplotene was reduced or even missing. In that case, bivalents showed a diakinetic morphology after the diffuse stage (Figs. 13c, 14b, c). In some pholcids, the bivalents (*Metagonia*, Additional file 11: Fig. S8e, f) or their middle part (*Artema nephilit*, Fig. 13c) retained a low condensation during late prophase I.

Male meiosis of most pholcids was remarkable for a very low chiasma frequency. The absolute majority of bivalents contained only a single chiasma (Additional file 2: Table S2, Additional file 7: Table S3, Additional file 12: Table S4, Additional file 19: Table S5, Fig. 14b–i, Additional file 11: Fig. S8d–f, h). An increased frequency of chiasmata (chiasma frequency ≥ 1.1 per bivalent) was found only in artemines with a low diploid number, in *Modisimus* cf. *elongatus* (Modisiminae), *Pholcus* sp., and *Quamtana filmeri* (Pholcinae) (Additional file 2: Table S2, Additional file 7: Table S3, Additional file 12: Table S4, Fig. 13d–f). In *Physocyclus dugesi* (Arteminae) and *M.* cf. *elongatus* (Modisiminae), we also found rare bivalents containing three chiasmata (Fig. 13d). In some species, centromeric regions formed a knob or flexure on the bivalents during late prophase I, which allowed us to determine the relative position of the chiasmata and centromere (Fig. 13d, e). Chiasmata of most analysed pholcids were predominantly distal and intercalar. In *Modisimus* and *Physocyclus*, pericentric chiasmata were frequent or even predominant (Fig. 13d, e). A large bivalent displayed positive heteropycnosis in late prophase I of *Pehrforsskalia* and *Pholcophora* (Fig. 14b, Additional file 11: Fig. S8g).

The sex chromosomes exhibited a specific behaviour in the male germline, which was often already initiated in the spermatogonia. During spermatogonial mitosis, the sex chromosomes differed often by condensation and pycnosis from the other chromosomes. In some species, they were more condensed and positively heteropycnotic. This behaviour was frequent in modisimines and pholcines (Additional file 24: Fig. S19a, b). In some *Pholcus* species, the Y chromosome exhibited a more intensive

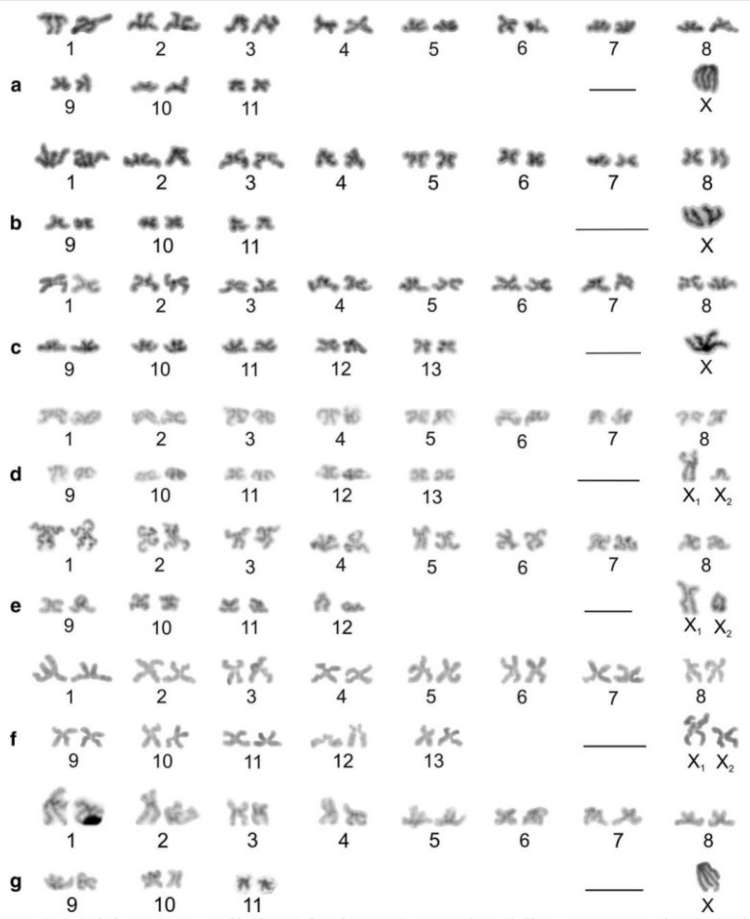

Fig. 11 Smeringopinae, male karyotypes, stained by Giemsa. Based on two sister metaphases II. Chromosomes are mostly metacentric. Sex chromosomes of some species are positively heteropycnotic during metaphase II (**b**, **c**, **f**, **g**). Chromosome X (or X_1) is the longest element of the karyotype except for **a** and **e**. **a** *Crossopriza* sp., four pairs submetacentric (nos 1, 3, 8, 10); **b** *Holocnemus hispanicus*, three submetacentric (nos 2–4) and one subtelocentric pairs (no. 11); **c** *H. pluchei*, four pairs submetacentric (nos 2, 5, 8, 9); **d** *Hoplopholcus cecconii*, chromosomes metacentric except for one submetacentric pair (no. 6) and subtelocentric X_2; **e** *Smeringopus cylindrogaster*, one submetacentric pair (no. 5), one acrocentric pair (no. 12), and acrocentric X_2; **f** *S. similis*, two pairs submetacentric (nos 3, 13) and one pair subtelocentric (no. 12); **g** *Stygopholcus skotophilus*, three submetacentric (nos 2, 3, 7) and one subtelocentric pair (no. 11). Last pair replaced by corresponding pair from another plate. Bar = 10 µm

heteropycnosis than the X chromosomes. This Y chromosome pattern continued frequently at premeiotic interphase and meiosis (Fig. 14c–e, Additional file 11: Fig. S8i, Additional file 24: Fig. S19f, Additional file 25: Fig. S20a). In *Artema*, X chromosome condensation was delayed in comparison with the other chromosomes during spermatogonial metaphase (Additional file 24: Fig. S19c).

The sex chromosomes of some pholcids exhibited a specific location in the mitotic plate. In species with the

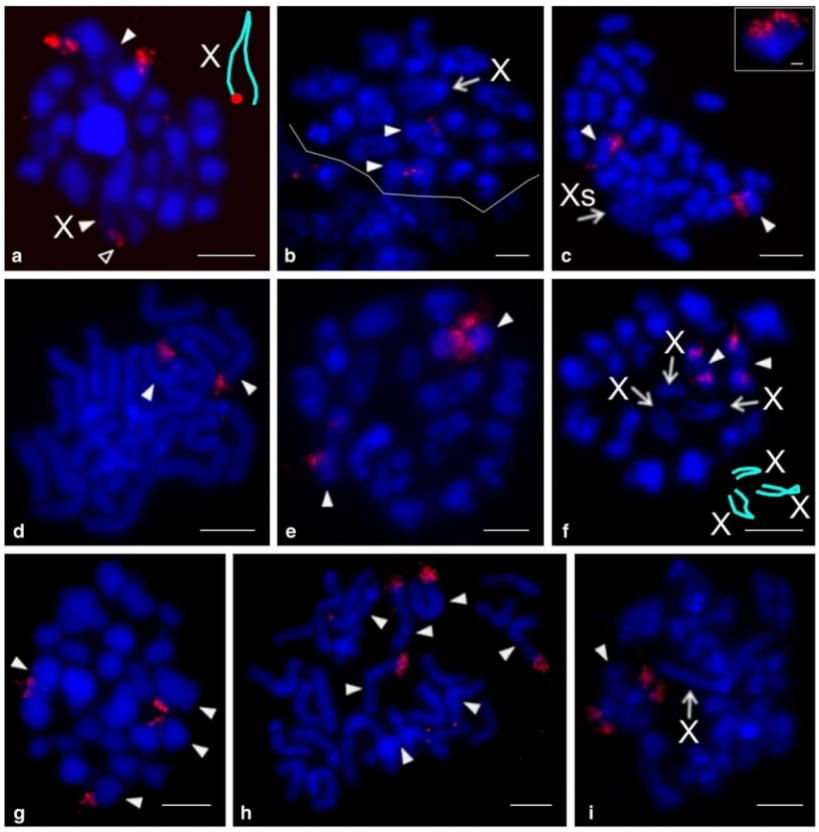

Fig. 12 Smeringopinae, males, detection of NORs (FISH). *Arrowhead* = NOR-bearing chromosome (**a**, **c**, **d**, **h**) or bivalent (**a**, **b**, **e**-**g**, **i**), *open arrowhead* = sex chromosome-linked NOR, X = X chromosome, Xs = X chromosomes. **a** *Holocnemus hispanicus* (X0), metaphase I, the largest bivalent and one end of the X chromosome bear a terminal NOR (see scheme of X chromosome, red = NOR); **b** *H. pluchei* (X0), metaphase I (separated by a line from a diffuse stage), two bivalents containing a terminal chiasma have a NOR in chiasma region; **c** *Hoplopholcus forskali* (X_1X_20), plate formed by two fused sister prometaphases II. Sex chromosomes form a cluster having a very low condensation. Chromosomes of one pair bear NOR. Inset: NOR-bearing chromosome from another metaphase II. This chromosome exhibits metacentric morphology and terminal location of NOR; **d** *H. labyrinthi* (X_1X_20), mitotic metaphase. Chromosomes of one pair bear terminal NOR; **e** *Smeringopus atomarius* (X_1X_20), metaphase I, note two bivalents with NOR; **f** *S. pallidus* ($X_1X_2X_30$), two bivalents with NOR. Note scheme of sex chromosome association; **g**, **h** *Smeringopus* sp. (X_1X_20), **g** metaphase I, four bivalents include NOR. **h** Mitotic metaphase, seven chromosomes show a terminal NOR; **i** *Stygopholcus skotophilus* (X0), metaphase I, one large bivalent bears a terminal NOR. Bar = 5 μm, inset 1 μm

X_1X_2Y system, they were often associated in the middle of the metaphase plate (*Artema*, *Nipisa*, *Leptopholcus*, *Pholcus*). While chromosomes X_1 and X_2 were often aligned in parallel (Additional file 24: Fig. S19b, c), chromosome Y was sometimes released from the association (Additional file 24: Fig. S19b). Sex chromosomes were usually not discernible at spermatogonial mitoses of pholcids with the X_1X_20 system, due to the absence of heteropycnosis. In some species, however, it was possible to detect the prominent X_1 chromosome. It was usually

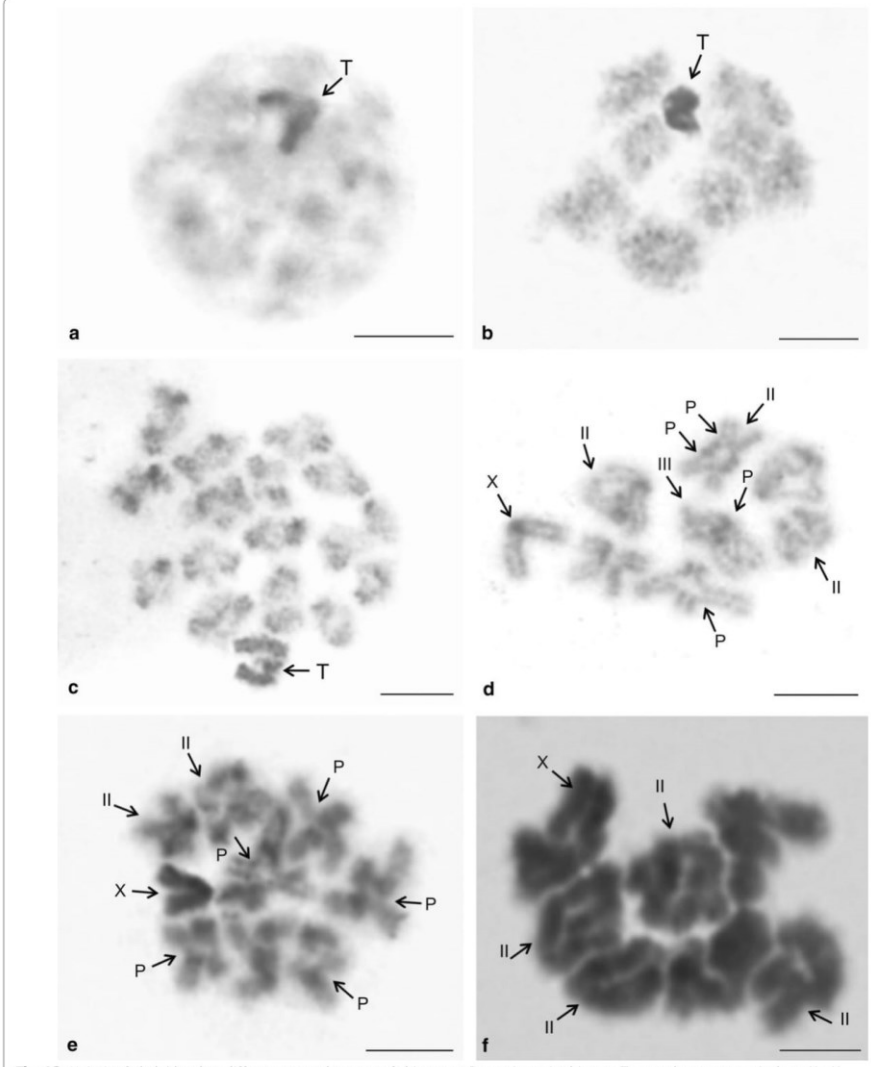

Fig. 13 Meiosis of pholcid males, diffuse stage and pattern of chiasmata. P = pericentric chiasma, T = sex chromosome trivalent, X = X chromosome, II = bivalent with two chiasmata, III = bivalent with three chiasmata. **a** *Artema nephilit* (X_1X_2Y), early diffuse stage. Bivalents considerably decondensed, sex chromosomes form positively heteropycnotic body; **b** *Metagonia* sp. (X_1X_2Y), late diffuse stage, bivalents condensed but without well differentiated chiasmata. Sex chromosomes form a highly condensed body; **c** *Artema nephilit* (X_1X_2Y), diakinesis. Bivalents retain low condensation, except for terminal regions; **d** *Physocyclus dugesi* (X0), diplotene. Some bivalents have a pericentric chiasma. Centromere regions are dark, more condensed; **e** *Modisimus* cf. *elongatus* (X0), diplotene. Sex chromosome is positively heteropycnotic. Most bivalents have pericentric chiasma. Centromeric regions are dark, more condensed; **f** *Chisosa diluta* (X0), metaphase I. Most bivalents have two chiasmata. Bar = 10 μm

(See figure on next page.)

Fig. 14 Meiosis of pholcid males, sex chromosome pairing. Figures **b**–**e** contain scheme of sex chromosome trivalent X_1X_2Y. H = positively heteropycnotic bivalent, X = X chromosome, X_1 = X_1 chromosome, X_2 = X_2 chromosome, Y = Y chromosome. **a**, **b** *Pholcophora americana* (X_1X_2Y). X chromosomes associated by ends of both arms with tiny Y chromosome. **a** Premeiotic interphase. **b** Diakinesis. Note positive heteropycnosis of a large bivalent; **c** *Pholcus kindia* (X_1X_2Y), diakinesis. Sex chromosomes pair by ends of both arms. Condensation of the X chromosomes is much lower than that of the Y chromosome; **d**, **e** *P. opilionoides* (X_1X_2Y), late prophase I, Y chromosome shows a considerable condensation. **d** Early diplotene. Both ends of X chromosomes involved in pairing. **e** Late diplotene. Both ends of X_1 and Y chromosome take part in pairing. By contrast, only long arm of the X_2 chromosome is involved in pairing (c—centromeric knob of X_2 chromosome); **f** *Hoplopholcus forskali* (X_1X_20), metaphase I, X chromosomes pair by ends of both arms in the middle of the plate; **g** *Cantikus sabah* (X0), diplotene. Note parallel association of the X chromosome arms; **h**, **i** *Kambiwa neotropica* ($X_1X_2X_3X_4Y$), metaphase I formed by 12 bivalents and a sex chromosome multivalent (in the middle of the plate). **h** positively heteropycnotic, cross-shaped sex chromosome multivalent is composed of two thick (1) and two thin "arms" (2). **i** Multivalent disintegrated into two rod-shaped structures (r). Each of them consists of one thick and one thin "arm" (see scheme). Bar = 10 μm

placed in the middle of the plate (Additional file 24: Fig. S19d). We did not find any preferential location of the sex chromosome in spermatogonia of pholcids with the X0 system.

Meiotic pairing of sex chromosomes was already established in the premeiotic interphase. It was initiated by a parallel attachment of the X chromosomes (Additional file 24: Fig. S19e). Following completion of the pairing, sex chromosomes formed a body on the periphery of the nucleus. They retained their peripheral position during early prophase I (leptotene–pachytene) and the diffuse stage. In species with the X_1X_2Y and X0 systems, this position was often retained during late prophase I (Figs. 13c–f, 14b, Additional file 11: Fig. S8d–h, Additional file 25: Fig. S20a). In contrast, in species with multiple X systems, as well as in *Kambiwa* (complex SCS), the sex chromosomes were preferentially located in the middle of the plate in late prophase and metaphase I (Fig. 14f, h, i).

Chromosomes of the X_1X_2Y, XY, and multiple X systems paired without chiasmata in male meiosis. Biarmed sex chromosomes paired by the ends of both arms (Fig. 14c, f, Additional file 11: Fig. S8d, Additional file 15: Fig. S11e, Additional file 22: Fig. S17a, Additional file 26: Fig. S21a); the arms of each chromosome were often associated (Figs. 6c, 12f, 13c, 14b, Additional file 11: Fig. S8d). This pattern was also exhibited by the tiny Y chromosome of *Aetana* and *Spermophora* (Additional file 11: Fig. S8d). It was impossible to determine the pairing mode of the Y chromosome in other pholcids with a tiny size of this element. In some smeringopines with the X_1X_20 system and subtelocentric X_2 chromosome, only the long arm of this element was involved in pairing in some plates during late prophase and metaphase I. Similarly, in some pholcines with a X_1X_2Y system and non-metacentric X_2 (*Quamtana*, *Pholcus phalangioides*), only the long arm of the X_2 took part in pairing during this period (Additional file 15: Fig. S11c, g). In these species, all plates exhibited the same pattern of sex chromosome pairing. In *P. opilionoides*, pairing of the short arm of the X_2 chromosome was completed during early diplotene. Only the long arm of this chromosome was involved in pairing during late diplotene (Fig. 14d, e). In species with the X0 system, the arms of the X chromosome were usually associated with each other during late prophase and metaphase I (Figs. 5b, 12a, b, 13e, 14g, Additional file 5: Fig. S3c, e, Additional file 17: S13c, Additional file 23: Fig. 18a, c, e).

Our data suggest a complex sex chromosome pairing in *Kambiwa* ($X_1X_2X_3X_4Y$). During late prophase and metaphase I, sex chromosomes formed a cross-shaped multivalent consisting of four "arms" (Fig. 14h, Additional file 10: Fig. S7b). Two "arms" were thick and two were thin, which was most obvious in diakinesis (Additional file 10: Fig. S7a). The tiny Y chromosome was not discernible. It was only detected at spermatogonial mitosis and metaphase II (Additional file 11: Fig. S8a, c). In some plates, the multivalent disintegrated into two parts associated with each other. Each part was formed by one thick and one thin "arm" connected at one end (Fig. 14i).

Segregation of the sex chromosomes was usually delayed in anaphase I (Additional file 25: Fig. S20b). In some species, the sex chromosomes lagged even during telophase I. In species with two or three X chromosomes, the X chromosomes were arranged in parallel on the periphery of the plate during anaphase I. In contrast to the other chromosomes, chromatids of each X chromosome were associated during this period. Moreover, the arms of each X chromosome were also aligned (Additional file 25: Fig. S20b). The single X chromosome of the X0 system exhibited the same pattern of chromatid and arm association. The association of chromatids and arms of particular X chromosomes was completed during prophase or metaphase II (Additional file 25: Fig. S20d). Association of the X chromosomes continued until the end of meiosis (Additional file 15: Fig. S11d, Additional file 22: Fig. S17b). The sex chromosome of *Cantikus* (X0) was remarkable for a precocious centromere division at metaphase II (Additional file 25: Fig. S20f). In contrast, the X chromosomes of *Aetana* (X_1X_2Y) exhibited slightly

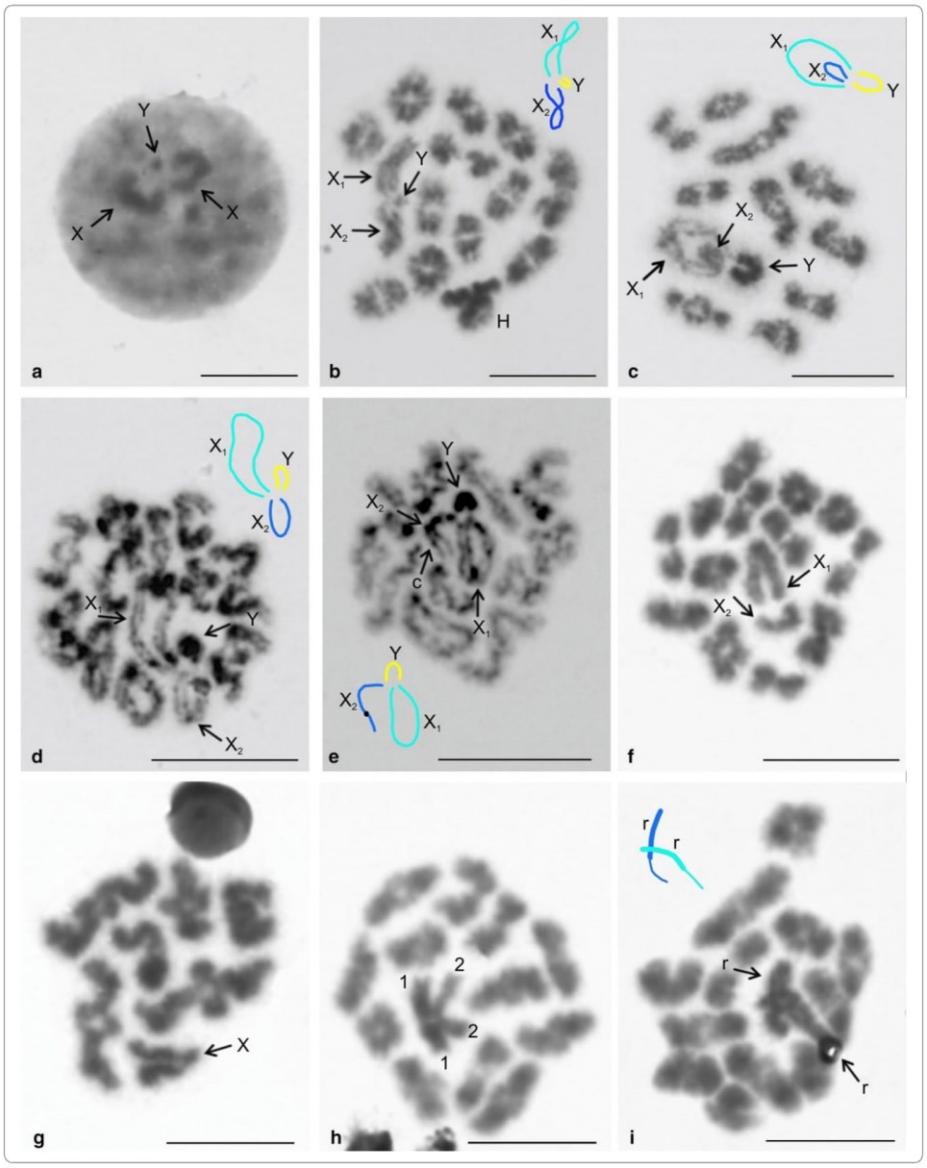
a
Y
X
X
b
X1
Y
X2
Y
X1
X2
H
c
X1
X2
Y
X2
Y
X1
d
X1
Y
X2
X1
Y
X2
e
Y
X2
C
X1
Y
X2
X1
f
X1
X2
g
X
h
2
1
2
1
i
r
r
r
r

delayed centromeric division during this period (Additional file 25: Fig. S20g). In anaphase II, the segregation of the X chromosome(s) was slightly delayed in some pholcids, namely in *Physocyclus* (Arteminae), *Psilochorus* (Modisiminae), *Holocnemus*, and *Hoplopholcus* (Smeringopinae) (Additional file 25: Fig. S20i). Remarkably, the Y chromosome was placed preferentially in the middle of the plate from anaphase I until the end of meiosis in both X_1X_2Y and XY systems (Additional file 25: Fig. S20h, Additional file 26: Fig. S21b).

The sex chromosomes of each species showed a specific pattern of condensation and pycnosis during male meiosis. They became condensed and positively heteropycnotic during the premeiotic interphase (Fig. 14a, Additional file 24: Fig. S19e, f), forming a sex chromosome body (SCB). Sex chromosome condensation decreased considerably during the onset of prophase I, which was frequently accompanied by the disintegration of the SCB and loss of positive heteropycnosis. The following period of increase of condensation and pycnosis of the sex chromosomes culminated during the pachytene and diffuse stage, which was often accompanied by restoration of the SCB (Fig. 13a, b). Condensation of the sex chromosomes was often considerably reduced during the transition from the diffuse stage to late prophase I, which was accompanied by disintegration of the SCB. In some taxa, recondensation of the X chromosomes was delayed during late prophase I in comparison to the bivalents and Y chromosome. This was the case in *Pholcophora* (Ninetinae), *Leptopholcus*, *Metagonia*, *Spermophora*, and *Pholcus* (except for *P. opilionoides* and *P. phalangioides*) (Pholcinae) (X_1X_2Y), where the X chromosomes continued low condensation until diakinesis (Figs. 9a, 14c, Additional file 11: Fig. S8e, f, Additional file 25: Fig. S20a). On the other hand, the sex chromosome(s) of some pholcids (e.g. *Holocneminus*, *Cantikus*, *Pehrforsskalia*) displayed no or only a slight transient decrease of condensation during the transition from diffuse stage to diplotene (Fig. 14g, Additional file 11: Fig. S8g, Additional file 25: Fig. S20c). The sex chromosomes of *Cantikus* formed a highly condensed SCB until early metaphase I.

The sex chromosomes were considerably condensed and positively heteropycnotic during interkinesis (i.e. interphase between the first and second meiotic division). In *Holocneminus*, this pattern persisted until prometaphase II (Additional file 25: Fig. S20e). In most other species, the sex chromosome condensation decreased considerably during the onset of prophase II. This event was often accompanied by the loss of positive heteropycnosis. The sex chromosomes of some species (e.g. *Hoplopholcus forskali*) were almost decondensed during prophase II. They recondensed suddenly during late prophase or prometaphase II (Additional file 25: Fig. S20d). The sex chromosomes of some pholcids also showed positive heteropycnosis during metaphase and anaphase II (e.g. Additional file 25: Fig. S20h, i).

Besides the germline cells, pholcid testes also frequently contained endopolyploid nuclei, whose size exceeded that of the diploid nuclei considerably. In some species, the sex chromosomes were positively heteropycnotic and formed a cluster in these nuclei (Additional file 27: Fig. S22).

Discussion

Diploid numbers and morphology of chromosome pairs

Evolution of chromosome numbers

Male diploid numbers of pholcids range from 9 (three *Micropholcus* species) [25, this study] to 33 (*Artema* spp.) [this study]. The diploid number of the *Micropholcus* species is the lowest one found in araneomorph spiders with monocentric chromosomes so far [25]. Particular pholcid subfamilies differ by their range of numbers of chromosomal pairs (NCPs). Reported data suggest a low diversity of NCPs in modisimines (7–8 pairs) [25–27, this study], ninetines (12–13 pairs) [this study], and smeringopines (11–13 pairs) [9, 28–32, this study]. The other two subfamilies show a much higher range of NCPs: artemines from 6 to 15 pairs [30, 32, 33, this study] and pholcines from 4 to 11 pairs [25, this study]. A high range of NCPs in artemines could reflect the possible non-monophyly of this group (see Fig. 15). In pholcines, there are also reports on 12 chromosome pairs in two species, but these data are dubious. The number of chromosome pairs in the species analysed by Sharma and Parida [34] can not be verified from the published information. In the species studied by Wang et al. [35], the presented data do not allow to determine unequivocally the NCPs and SCS.

Remarkably, the karyotype of an early-diverging pholcid, *Artema* ($2n♂ = 33$, X_1X_2Y, chromosomes biarmed) is very similar to karyotypes of the haplogynes *Filistata insidiatrix* (Filistatidae; $2n♂ = 33$, X_1X_2Y) [9], *Paculla* sp. (Pacullidae; $2n♂ = 33$, X_1X_2Y) [14], and *Hypochilus pococki* (Hypochilidae; $2n♂ = 29$, X_1X_2Y) [9]. Whereas *Artema*, *Filistata*, and *Paculla* exhibit the same diploid number and biarmed morphology of chromosome pairs, the karyotype of *Hypochilus* is slightly different, showing lower NCPs and a higher ratio of monoarmed chromosome pairs. The karyotype of *Hypochilus* can be derived from the pattern found in *Artema*, *Filistata*, and *Paculla* by two chromosome fusions and several pericentric inversions. This pattern of karyotypes suggests that the ancestral pholcid karyotype was close to those found in *Artema*, *Filistata* and *Paculla* ($2n♂ = 33$, X_1X_2Y, chromosomes biarmed).

Recent studies on spider phylogenomics suggest two primary lineages of haplogynes, one consisting of

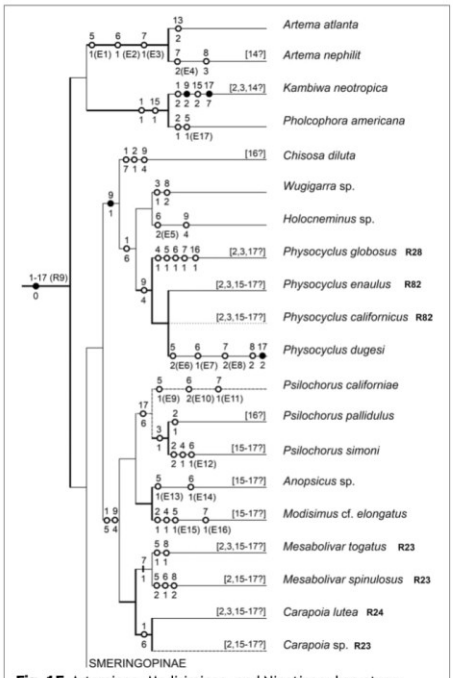

Fig. 15 Arteminae, Modisiminae, and Ninetinae: karyotype characters mapped on a cladogram. Based on the most recent molecular phylogeny of Pholcidae [20, 21]. Standard continuous lines: low bootstrapping branch support, i.e. < 70%; thick continuous lines: modest to full support of hypotheses, ≥ 70% [21]; discontinuous lines: taxa not included in molecular phylogeny—phylogenetic position is based on cytogenetic data (dashed lines) or unresolved (dotted lines). Number above mark: number of character; number below mark: character state. Full marks: characters without homoplasy; empty marks: homoplasic characters. In some species, data on some characters are missing (information in square brackets). Selected events are marked E and numbered (see Additional file 1: Table S1 for chromosomes formed by these events). Chromosomes formed by the other events are identifiable unequivocally in Additional file 1: Table S1. Concerning chromosome pairs, only well-defined events changing chromosome morphology substantially are considered. Reconstruction of karyotype evolution is based on our data, except for taxa marked by the formula RX (see reference X for information). See "Methods" (pp. 32–33) for coding of characters

filistatids and hypochilids, and another one comprising synspermiate haplogynes, including pholcids and pacullids [10, 36, 37] (Fig. 1). Considering the placement of *Artema*, *Filistata*, *Paculla*, and *Hypochilus* in this phylogeny, the karyotype structure found in the three first genera ($2n♂ = 33$, X_1X_2Y, biarmed chromosomes) could be also the ancestral haplogyne karyotype. However, this conclusion conflicts with the hypothesis supposing that the ancestral karyotype of haplogynes was very close to that of entelegynes (20 chromosome pairs + X_1X_20) [9]. This hypothesis is supported by the occurrence of very similar karyotypes in the haplogyne family Drymusidae (17 biarmed pairs + X_1X_2Y) and the family Austrochilidae (18 biarmed pairs + XY) [9], which is an early-diverging lineage of a clade formed by protoentelegynes and entelegynes [37]. The observed karyotype pattern of austrochilids and drymusids could reflect an early separation of drymusids within haplogynes, specifically before derivation of the clade including filistatids, hypochilids, pacullids, and pholcids. To determine the correct phylogenetic position of drymusids, more detailed phylogenomic analysis of early-diverging araneomorph clades is needed.

A fundamental trend of spider karyotype evolution is the reduction of chromosome numbers, which took place independently in many clades [38]. Our analysis suggests the same pattern in pholcids. Available data indicate the reduction to 13 chromosome pairs in the last common ancestor of smeringopines and pholcines, and separately in ancestral ninetines, or alternatively in the last common ancestor of ninetines, smeringopines and pholcines (see "Phylogenetic implications", p. 29). Furthermore, a comparison of cytogenetic and molecular data suggests a further reduction to 11 pairs in ancestral pholcines, to 8 pairs in the common ancestor of modisimines, and to 7 pairs in the common ancestor of the artemine genera *Holocneminus*, *Physocyclus*, and *Wugigarra* (Fig. 15). The longest one or two chromosome pairs of pholcids are often prominent, which could reflect the formation of these pairs by fusion. In *Leptopholcus* ($2n♂ = 17$, X_1X_2Y), the first three pairs are considerably longer than the remaining ones. This set could be derived by three fusions from a karyotype containing ten chromosome pairs. Reductions of chromosome numbers also took place during the evolution of pholcid genera. However, the frequency of these events on genus level is low (Additional file 1: Table S1).

Variation of NCPs has also been suggested on intraspecific level in pholcids, namely in *Crossopriza lyoni* [30]. This widespread synanthropic species has been karyotyped by several authors. Recent studies consistently report 11 biarmed chromosome pairs in this species; analysed populations came from Brazil, India, and Vietnam [30, 32–34, 39, this study]. This number of pairs is probably an ancestral feature of the clade formed by *Crossopriza*, *Holocnemus caudatus*, *H. hispanicus*, and *Stygopholcus* (Fig. 16). In contrast, initial cytogenetic studies on *C. lyoni* suggested a higher NCPs in Indian populations, namely 12 [29] or 13 [28]. While

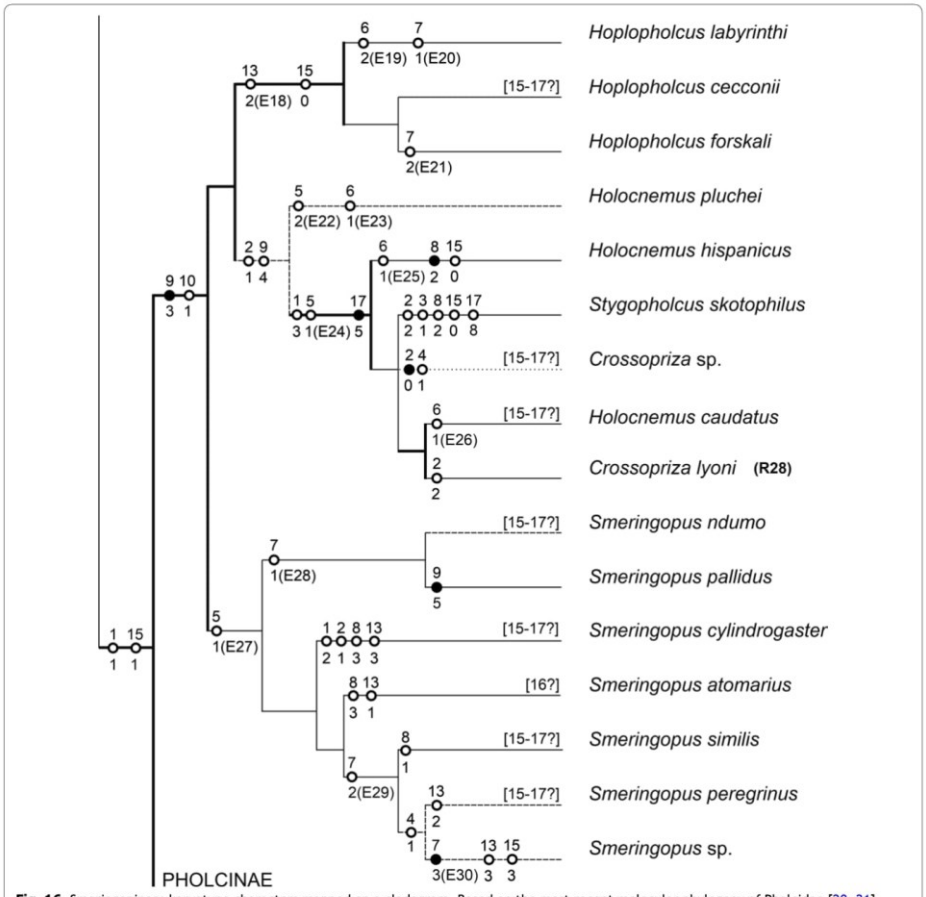

Fig. 16 Smeringopinae: karyotype characters mapped on a cladogram. Based on the most recent molecular phylogeny of Pholcidae [20, 21]. Standard continuous lines: low bootstrapping branch support, i.e. < 70%; thick continuous lines: modest to full support of hypotheses, ≥ 70% [21]; discontinuous lines: taxa not included in molecular phylogeny—phylogenetic position is based on other sources [81] and/or on cytogenetic data (dashed lines) or unresolved (dotted lines). Number above mark: number of character; number below mark: character state. Full marks: characters without homoplasy; empty marks: homoplasic characters. In some species, data on some characters are missing (information in square brackets). Selected events are marked E and numbered (see Additional file 1: Table S1 for chromosomes formed by these events). Chromosomes formed by the other events are identifiable unequivocally in Additional file 1: Table S1. Concerning chromosome pairs, only well-defined events changing chromosome morphology substantially are considered. Reconstruction of karyotype evolution is based on our data, except for taxa marked by the formula (RX) (some information taken from reference X). See "Methods" (pp. 32–33) for coding of characters

the first study does not contain information on chromosome morphology, the karyotype with 13 pairs was exclusively biarmed. This pattern could be derived from a set with 11 biarmed pairs by fissions of two pairs and subsequent inversions of four newly formed pairs. However, our results indicate a very low frequency of chromosome fissions during pholcid evolution and a low intraspecific variability of pholcid karyotypes. Therefore,

differentiation of the karyotype of *C. lyoni* by multiple fissions is very unlikely. Diversity of NCPs in *C. lyoni* is most probably an artifact, possibly caused by species misidentifications. Reported data on NCPs also differ in *Micropholcus fauroti*. While Araujo et al. [26] reported eight metacentric pairs in a Brazilian population, we found only four metacentric pairs in another Brazilian population and African populations (Cape Verde, South Africa). Notably, we frequently found in our preparations of *Micropholcus* clusters formed by the fusion of chromosome plates. This artefact, along with the low number of observed plates, could have led Araujo et al. [26] to report double NCPs in this species. Four chromosome pairs were also reported in other karyotyped *Micropholcus* species [25].

Evolution of chromosome pairs

Similarly to the majority of other haplogynes with monocentric chromosomes [9], karyotypes of most pholcids are predominated by metacentric chromosomes. A different pattern has been reported only in two *Physocyclus* species [30, this study] and *Pholcus manueli* [35]. The karyotype of the latter species is suggested to be composed exclusively of monoarmed chromosomes. However, this idea is based only on the pattern of constitutive heterochromatin, i.e. a marker that could also be localised in regions other than the centromere. Therefore, this hypothesis should be tested by determination of the centromere position during mitotic metaphase or metaphase II. During metaphase II, chromatids of spider chromosomes are separated, except for the centromere.

At first glance, chromosome pairs of pholcids seem to be conservative elements, due to their predominantly metacentric morphology. However, comparison of closely related species revealed a dynamic nature of these pairs. Closely related taxa having the same number of pairs often differ by the morphology of one or several pairs, whose metacentric morphology is changed to submetacentric or even monoarmed (Additional file 1: Table S1). This pattern suggests the operation of pericentric inversions or some translocation variants. In some cases, the size of the pair is retained even after the change of its morphology to non-metacentric (e.g., acrocentric pair of *Artema nephilit*), which points to the operation of pericentric inversions. An enormous increase of the first pair (*Crossopriza lyoni*, *Holocnemus caudatus*) or considerable reduction of the last pair (some *Psilochorus* species, *Stygopholcus*, *Wugigarra* [this study], *Mesabolivar spinulosus* [25]), which are not accompanied by changes of NCPs, probably reflect an origin of these pairs by non-reciprocal or unequal reciprocal translocations. In the last three taxa, the last pair exhibits a subtelocentric morphology, which probably reflects translocation of most of an arm of an original biarmed pair to another chromosome. In *Aetana*, a considerable reduction of the last pair is accompanied by a change in morphology to acrocentric. This pattern could reflect centric fission of a biarmed chromosome pair, followed by integration of one product into another chromosome.

Diploid numbers of pholcids could be decreased by centric fusions of monoarmed pairs. Beside this, the number of pairs could be reduced by nested fusions. In contrast to centric fusions, this process involves biarmed chromosomes.

In conclusion, our data suggest the frequent involvement of fusions, inversions, and translocations of chromosome pairs in the karyotype evolution of pholcids. These kinds of rearrangements can be very effective in the formation of interspecific reproductive barriers [40, 41], and may thus have played a role in speciation processes in pholcids.

Sex chromosomes

X_1X_2Y system

Ancestral composition and origin of the X_1X_2Y system Pholcids exhibit a considerable diversity of sex chromosomes. We found six SCS in these spiders, namely X0, X_1X_20, $X_1X_2X_30$, XY, X_1X_2Y, and $X_1X_2X_3X_4Y$. The X_1X_2Y system has been reported in seven haplogyne families, namely Sicariidae [9, 42, 43], Filistatidae [9, 14–16], Drymusidae, Hypochilidae, Pholcidae [9], Pacullidae [14], and Plectreuridae [15]. Specific morphology and the meiotic pairing of chromosomes X_1, X_2, and Y suggest that the X_1X_2Y system arose once in haplogynes [9]. Together with molecular and paleontological data, this points to an ancient origin of the haplogyne X_1X_2Y system. Plectreurids have been found in Jurassic strata [44]. A recent molecular phylogeny suggests the origin of spiders possessing an X_1X_2Y system during the early Mesozoic [37]. The phylogenetic distribution of the X_1X_2Y system using recent phylogenomic trees [10, 36, 37] suggests that this sex chromosome determination is ancestral for haplogynes, including pholcids. It could have arisen even earlier, namely before the separation of entelegyne and haplogyne spiders [16] or before the separation of mygalomorphs and araneomorphs in ancient opisthothele spiders. If so, the supposed ancestral sex chromosome system X_1X_20 of mygalomorphs [6] and entelegynes [9] arose from the X_1X_2Y system by the loss of the Y chromosome. The ancestral X_1X_2Y system probably consisted of two large metacentric X chromosomes of similar size and a metacentric Y microchromosome [9]. Species with this pattern have been found in almost all X_1X_2Y families [9, 16, 18, this study]. The X_1X_2Y system was supposed to arise by rearrangements between autosomes and sex chromosomes [43]. In this case, it would be an ancient neo-sex

chromosome system. According to our hypothesis, chromosomes X_1, X_2, and Y are derived from CSCP. It was suggested that multiple X chromosomes of spiders arose by nondisjunctions of the X chromosome of the CSCP [7]. The Y chromosome could originate in a similar way, namely by a nondisjunction of the Y chromosome of the CSCP and subsequent degeneration of the newly formed element. Nondisjunctions could be a major mechanism of formation of multiple X chromosomes in spiders [7, 18, 45]. This unusual origin of sex chromosomes is supported by the inactivation of multiple X chromosomes during meiosis of spider females. This unique behaviour probably evolved to avoid the negative effects of duplicated X chromosomes on female meiosis [5, 7].

According to our data, chromosomes of the X_1X_2Y system are dynamic elements. Although they exhibit a conservative pairing during male meiosis, they underwent frequent rearrangements during pholcid evolution. Remarkably, chromosomes X_1, X_2, and Y differ by their pattern of morphological evolution and evolutionary plasticity. See Additional file 28: Appendix S1 for evolution of particular sex chromosomes of the X_1X_2Y system.

Conversion of the X_1X_2Y system into other sex chromosome systems In some haplogynes, including pholcids, the X_1X_2Y system has been transformed into other SCS [9, 15, this study]. According to [9], the X_1X_2Y system underwent conversion to the X0 system, namely by X chromosome fusion (formation of the XY system) and subsequent loss of the Y chromosome. Our results suggest that patterns of conversion of the X_1X_2Y to the X0 system are more diversified. In some pholcids, loss of the Y chromosome preceded fusion of the X chromosomes, which resulted in the formation of the X_1X_20 and, subsequently, of the X0 system. We suppose that this scenario could be more frequent during the evolution of the haplogyne X_1X_2Y system, due to specific features of its Y chromosome, which could facilitate degeneration and extinction of this element (tiny size, absence of recombinations between the X and Y chromosome).

XY system

In *Wugigarra* the X_1X_2Y system was transformed into the XY system by X chromosome fusion [this study]. The XY system of another haplogyne, *Diguetia* (Diguetidae), is suggested to arise by the same process [9]. The sex chromosomes of *Wugigarra* and *Diguetia* retained their metacentric morphology, except for the acrocentric X chromosome of *D. canities*, which probably originated from metacentric X by pericentric inversion [9]. The Y chromosomes of these haplogynes are small elements. While sex chromosomes of *Wugigarra* retain their achiasmatic pairing by both ends, only one X chromosome end is involved in achiasmatic pairing in *Diguetia* [9]. Notably, the XY system has also been suggested in other pholcids, namely *Smeringopus ndumo* (reported as *S. pallidus*) [9] and *Holocnemus pluchei* [31]. Our data showed that these reports are erroneous, based on revision of original preparations (*S. ndumo*) and laboratory stock studied by previous authors (*H. pluchei*). An XY system was also discovered in several other spiders [6, 9, 46, 47]. Its origin is, however, different. It is suggested to have arisen from the X0 determination by a fusion of the X chromosome and an autosome(s), resulting in the formation of neo-X and neo-Y chromosomes. Another possible origin of the system might be by a fusion of the X chromosome and X chromosome of the CSCP.

Multiple X chromosome systems

X_1X_20 system Although the X_1X_20 system is the most frequent sex chromosome determination in entelegyne araneomorphs [18, 45], it is rare in haplogyne araneomorphs [9, 15, this study]. Provided that the X_1X_2Y system is ancestral for araneomorphs [16], the X_1X_20 system has originated in the same way in both entelegynes and haplogynes, namely from the X_1X_2Y system by the loss of the Y chromosome. The X_1X_2Y system of the pholcids *Aetana* and *Artema*, including a minute Y chromosome [this study], could represent an evolutionary transition between the X_1X_2Y and X_1X_20 systems. In haplogynes, the X_1X_20 system has originated several times, namely in filistatids [15], plectreurids [9], and pholcids [this study].

In pholcids, we found the X_1X_20 system in two smeringopine genera, *Hoplopholcus* and *Smeringopus*. Mapping of the distribution of the X_1X_20 system in smeringopines suggests an origin of this system in their ancestor. Remarkably, we never found the X_1X_20 system in pholcids in which it was reported previously (see database of Araujo et al. [24]). Instead, these species exhibit the X_1X_2Y system, which had probably been mistaken for the X_1X_20 system, due to the small size of the Y chromosome. The X_1X_2Y system was revealed in pholcids less than two decades ago [9].

Remarkably, the X_1 and X_2 chromosomes of the X_1X_20 system show a similar evolution to the X chromosomes of the X_1X_2Y system in pholcids (see Additional file 28: Appendix S1 for evolution of chromosomes of the X_1X_2Y system). While the X_1 is a conservative element retaining large size and metacentric morphology, X_2 underwent reduction and frequent changes of morphology. The size of the X_1 chromosome is more variable (7.9–15.1% of TCL) than that of the X_2 element (5.1–7.4% of TCL), which could reflect insertions of fragments derived from CPs into the X_1 chromosome. In each species, the X_2 chromosome is reduced in comparison with the X_1 chromosome (including representatives with an ancestral

state, i.e. metacentric morphology of the X_2 chromosome). Therefore, the X_2 chromosome was probably already reduced in an ancestor of smeringopines (having a X_1X_20 or X_1X_2Y system). The original metacentric X_2 chromosome has been transformed several times to a monoarmed one, namely in the ancestor of *Hoplopholcus* and in several *Smeringopus* species. The morphology of the X_2 chromosome has most probably changed by a pericentric inversion or translocation.

$X_1X_2X_30$ system A sex chromosome system comprising three X chromosomes is relatively frequent in entelegyne [48] and mygalomorph spiders [6]. Among haplogynes, *Smeringopus pallidus* is the first reported species with this sex chromosome determination [this study]. It was obviously derived from the X_1X_20 system found in the other *Smeringopus* species. However, the origin of the third X chromosome of *S. pallidus* is unresolved. The behaviour of the three X chromosomes of this species during male meiosis (pairing, pattern of condensation and heteropycnosis) is the same as in X_1X_20 species, which contradicts the possible origin of the extra X chromosome from autosomes. Another possibility is nondisjunction of an X chromosome, which is supposed to be a mechanism of $X_1X_2X_30$ formation in entelegynes [7, 45, 49]. This hypothesis is supported by the same meiotic behaviour of sex chromosomes in X_1X_20 and $X_1X_2X_30$ species. The sex chromosomes of *S. pallidus* (two large metacentric X chromosomes of similar size + one small metacentric X chromosome) can be derived from the ancestral pattern of the X_1X_20 system in *Smeringopus* (two metacentric X chromosomes, X_2 considerably smaller than X_1) by nondisjunction of the X_1 chromosome. Formation of an additional large X chromosome would substantially increase the sum of the relative lengths of the X chromosomes. However, the values do not differ substantially between *S. pallidus* (16.9% of TCL) and the karyotypically most similar *S. ndumo* (18% of TCL), and fall within the range of values found in other *Smeringopus* species (14.2–19.8% of TCL). Therefore, the X_3 chromosome of *S. pallidus* more likely arose by a fission of the ancestral metacentric X_1 chromosome into two acrocentric chromosomes, followed by their pericentric inversion. This hypothesis is supported (1) by a reduction of the X_1 chromosome of *S. pallidus* in comparison with other *Smeringopus* species, and (2) by the sum of X_1 and X_3 sizes in *S. pallidus*, which is similar to the X_1 size in the karyotypically most similar *S. ndumo*. To resolve the origin of the $X_1X_2X_30$ system in *S. pallidus*, sequencing of its X chromosomes needs to be carried out.

X0 system

Phylogenetic distribution and origins of the pholcid X0 system The X0 system is common in pholcids. It has been reported in some artemines, pholcines, smeringopines, and all modisimines karyotyped so far [24, this study]. Character mapping suggests at least five origins of the X0 system in pholcids, namely in the (1) artemines with low diploid numbers (see "Phylogenetic implications", p. 29), (2) ancestor of modisimines (Additional file 29: Fig. S23), (3) common ancestor of smeringopines *Holocnemus*, *Crossopriza*, and *Stygopholcus* (Additional file 30: Fig. S24), (4) pholcine *Belisana*, and (5) common ancestor of the pholcines *Cantikus* and *Micropholcus* (Additional file 31: Fig. S25). The X0 system was also reported in *Pholcus manueli* [35]. However, chromosome plates obtained in *P. manueli* (male mitoses) do not allow us to determine the SCS of this species unequivocally. Similar to *P. phalangioides* (X_1X_2Y) [9], the karyotype of *P. manueli* is composed of 25 chromosomes and contains an odd peculiar chromosome formed exclusively by constitutive heterochromatin [35]. The odd heterochromatic element of *P. phalangioides* is a Y chromosome [9]. Therefore, *P. manueli* exhibits with all probability the X_1X_2Y system.

The X0 system is common in spiders. Phylogenetic distribution of the X0 system in spiders suggests multiple origins of this system [6, 18, 45]. X0 systems of entelegynes and mygalomorphs arose by chromosome fusions from multiple X chromosome systems [6, 18, 45]. In haplogynes, the X0 system has been found in nine families (see database [24]). The X0 system of haplogynes with monocentric chromosomes arose from XY or X_1X_20 systems. The X0 system of smeringopine pholcids arose from the X_1X_20 system by X chromosome fusion [this study]. In contrast, the X0 system of a clade formed by *Chisosa*, *Holocneminus*, *Physocyclus*, and *Wugigarra* probably arose from the XY system (Additional file 29: Fig. S23). Formation of the X0 system in the other pholcids is unresolved. Our discovery of both X0 [this study] and ancestral X_1X_2Y systems [J. Král and O. Košulič, unpublished] in the same genus, the pholcine *Belisana*, indicate a relatively fast formation of the X0 system during the evolution of this clade. An increase in the size of the Y chromosome during the evolution of pholcines (see Additional file 28: Appendix S1 for evolution of the Y chromosome) did not prevent this element from being subjected to reduction and loss in the common ancestor of *Cantikus* and *Micropholcus* (X0).

Evolution of the X0 system in pholcids Despite its multiple origins, the single X chromosome of pholcids exhibits an extremely conservative morphology. Except for *Modisimus* it is always mediocentric (Additional file 1: Table S1), which indicates a strong selection pressure to keep this feature. We suppose that this morphology could be essential to ensure the self-association and regular segregation of the X chromosome univalent during male meiosis. In mice, the meiotic stability of the

sex chromosome univalents is promoted by their self-association [50].

In contrast to morphology, the size of the X chromosome varies considerably, namely from 8.89 (*Belisana sabah*) to 21.21% of TCL (*Chisosa diluta*) (Additional file 1: Table S1). A considerable diversity of X chromosome sizes occurs even on a genus level (*Crossopriza*, *Holocnemus*, *Psilochorus*). The increase in size of the X chromosome could be a consequence of an integration of material from CPs, as suggested, for example, by the large difference of X chromosome size between two *Holocnemus* species (*H. caudatus* and *H. hispanicus*).

$X_1X_2X_3X_4Y$ system

Comparison of data on the male karyotype and meiosis suggests that the $X_1X_2X_3X_4Y$ system occurs in *Kambiwa*. This pholcid exhibits one chromosome pair less than the other studied ninetine, *Pholcophora*, which displays a X_1X_2Y system [this study]. This pattern indicates the origin of the $X_1X_2X_3X_4Y$ system by rearrangements between chromosomes of the X_1X_2Y system and a chromosome pair. The Y microchromosome was not involved in the rearrangements. Sex chromosome systems arising by rearrangements between chromosome pair(s) and sex chromosomes have also been reported in some other araneomorphs [7, 9, 47, 51–53] and in some mygalomorphs [6, 46]. These events are always apomorphies of low-level taxa (species or species groups), which indicates their relatively recent origin.

Sex chromosomes and pholcid speciation

In summary, our data suggest frequent and diverse structural changes of sex chromosomes during pholcid evolution. These events include inversions and translocations of sex chromosomes, integration of fragments or even whole chromosomes into the SCS, and loss of the Y chromosome. Since structural changes of sex chromosomes are often very potent in formation of interspecific reproduction barriers [54–57], they have probably been involved in the speciation process in pholcids. In keeping with this view, closely related pholcids often differ in sex chromosome morphology [this study].

Particular sex chromosomes of pholcid males do not recombine, which suggests a high degree of differentiation of these chromosomes. This degree of sex chromosome differentiation is associated with markedly stronger reproductive isolation [58]. Although sex chromosome rearrangements could be less detrimental in meiosis of spider males due to achiasmatic sex chromosome pairing, in female heterozygotes they can lead to a collapse of homologous sex chromosome pairing.

Nucleolus organizer regions

NOR bearing pairs

The pattern of NORs has only been determined in a low number of spiders so far. Usually, these structures were detected by silver staining, a technique that visualizes NORs that were active in the preceding interphase only [59]. Therefore, it is impossible to reconstruct the evolution of NORs in particular families or even higher taxa of spiders. Karyotypes of most spiders contain, however, a low number of these structures. The common ancestral pattern of opisthothele spiders comprised probably one or two chromosome pairs bearing a terminal NOR locus [6].

In our study, we analysed the evolution of spider NORs on a family level for the first time. Nucleolus organizer regions have been visualized only in three pholcids so far, in each case by silver staining [30, 32]. To reconstruct NOR evolution in pholcids, we analysed 30 pholcid species, including one species studied earlier by silver staining. To detect NORs, we used fluorescence in situ hybridization (FISH), which visualizes inactive NORs as well. According to our results, pholcids exhibit a considerable diversity of NOR numbers (from one to nine loci); congeneric species often differ in the number of NOR loci. Almost all detected NOR loci are homozygous for the presence of NOR, which suggests a high stability in the number of NOR loci at species level. Findings of loci heterozygous for the presence of NOR are rare in pholcids (*Nipisa*, *Pholcus pagbilao, Smeringopus* sp.) [this study]. In the case of *Artema atlanta*, intraspecific variability of NORs is doubtful. While the studied karyotype from South Africa contained one NOR locus [this study], two NOR loci were reported in an Indian population probed by silver staining [32]. Considering the low quality of the signals detected, the information of the latter authors should be verified by FISH.

Character mapping suggests that ancestral pholcids had a single biarmed CP bearing a terminal NOR (Additional file 29: Fig. S23). Whereas the number of NORs underwent multiple changes during pholcid evolution, the pattern of their location has remained conservative. Each NOR-bearing chromosome pair of pholcids includes a single NOR, except for exceptional pairs having NORs at both ends. These pairs were only found in some pholcines [this study]. NORs of pholcids are terminal, except for a pericentric NOR of *Physocyclus globosus* [30], which might originate from a paracentric inversion. The terminal location of pholcid NORs suggests that these structures have mostly spread by ectopic recombination. This mechanism could be promoted by hybridization of individuals belonging to populations differing in the number of NOR loci, which is indicated by

the finding of heterozygotes for the presence of NOR in *Nipisa, P. pagbilao*, and, *Smeringopus* sp.

Our data indicate an increase in the number of NOR bearing CPs in some pholcid clades. In the ancestor of ninetines and the common ancestor of smeringopines and pholcines (Additional file 29: Fig. S23, Additional file 30: Fig. S24) or common ancestor of ninetines, smeringopines, and pholcines (see "Phylogenetic implications", p. 29), the number of NOR-bearing pairs increased to two. During subsequent evolution, NORs spread to three chromosome pairs in *Kambiwa* (Ninetinae) and in the ancestor of pholcines. Karyotypes of *Smeringopus* sp. and some pholcines contain four NOR-bearing pairs. In *Belisana*, there are even five pairs bearing NORs. On the other hand, character mapping suggests that the number of NOR-bearing pairs decreased several times in smeringopines (*Stygopholcus*, *Holocnemus hispanicus*, *Hoplopholcus*) and pholcines (*Aetana*, *Muruta*, *Quamtana*, common ancestor of *Cantikus* and *Micropholcus*) (Additional file 30: Fig. S24, Additional file 31: Fig. S25). Remarkably, these clades often exhibit reduced NCPs in comparison with their relatives; NORs retain a terminal position.

Sex chromosome-linked NORs In contrast to other opisthothele spiders, haplogynes often exhibit sex chromosome-linked NORs [9]. These NORs are also common in pholcids. They have been found in all pholcid subfamilies [30, this study]. Sex chromosome-linked NORs of pholcids and other haplogynes are always restricted to the X chromosome(s) [9, 30, this study] except for *Nipisa* [this study]. Character mapping suggests at least five origins of these NORs in pholcids, namely in (1) *Physocyclus* (Arteminae, X0), (2) *Kambiwa* (Ninetinae, $X_1X_2X_3X_4Y$), (3) *Psilochorus* (Modisiminae, X0) (Additional file 29: Fig. S23), (4) the common ancestor of *Crossopriza lyoni* and *Holocnemus hispanicus* (Smeringopinae, X0) (Additional file 30: Fig. S24), and (5) during early evolution of pholcines (X_1X_2Y) (Additional file 31: Fig. S25). In modisimines, NOR data are available for *Psilochorus* only. Therefore, their sex chromosome-linked NORs could have arisen earlier than during the evolution of this genus. Sex-chromosome linked NORs of pholcids always have a terminal location, which suggests an origin of these structures by ectopic recombination.

Most pholcids with the X0 system and sex-chromosome-linked NORs display two terminal NORs (e.g., *Physocyclus*, *Psilochorus*) [this study]. The second NOR was probably formed by ectopic recombination between the arms of the X chromosome, which was facilitated by their meiotic association. Although the *Physocyclus* species analysed in our paper exhibit two sex chromosome-linked NORs, a study on *P. globosus* did not reveal these structures [30]. Since these authors used silver staining and gonial mitoses to detect NORs, it is possible that sex-chromosome linked NORs of this species are inactivated in the germline cells. Alternatively, *P. globosus* may belong to a *Physocyclus* lineage that lacks sex chromosome-linked NORs.

We revealed the most complex evolution of sex chromosome-linked NORs in the X_1X_2Y system of pholcines. According to our data, sex chromosome-linked NORs already appeared during the early evolution of pholcines, no later than before the separation of the clade containing *Aetana*. Paleontological [60] and molecular data [61] indicate relative antiquity of the pholcine lineage with sex chromosome-linked NORs (further SCL-NOR clade). According to the latter dataset, this clade evolved at the latest during the Jurassic. The ancestral pattern of sex chromosome-linked NORs was probably formed by a single terminal locus on the X_1 chromosome, which is retained in *Aetana*. In another early-diverging pholcine, *Belisana*, the X_1X_2Y system has been transformed to X0. During this transformation, the terminally positioned sex chromomosome-linked NOR originating from the X_1 chromosome was probably retained. The second NOR of *Belisana* was probably formed by ectopic recombination between the arms of the single X chromosome.

The subsequent evolution of NORs in the pholcine X_1X_2Y system probably involved gradual spreading of the NORs by ectopic recombination to the other X_1 end, and after that to one or both ends of the X_2 chromosome. Remarkably, the X chromosome ends are attached in male meiosis to ensure sex chromosome pairing, which could promote spreading of NORs among sex chromosomes by ectopic recombination. We suppose that spreading of NORs by ectopic recombination could also be facilitated by the association of X chromosome bivalents during female meiosis of spiders [5]. Besides pholcines, multiple SCS containing NORs have been found only in the ninetine *Kambiwa*. In contrast to pholcines, the end of the X chromosome containing NOR is not involved in chromosome pairing in this spider (see "Sex chromosome behaviour", p. 26).

As demonstrated in some animals, sex chromosome-linked NORs can ensure achiasmatic pairing of sex chromosomes [62, 63]. The specific terminal location of sex chromosome-linked NORs in pholcines suggests involvement of these structures in achiasmatic pairing as well. Pairing ensured by NORs could be more stable, which may have promoted an increase in Y chromosome size during the evolution of pholcines. We suppose that the terminal NOR(s) of pholcids with the X0 system have a similar function as in the X_1X_2Y system, i.e. they could

strengthen the association of the X chromosome arms during male meiosis.

Remarkably, our data suggest the loss or degeneration of sex chromosome-linked NORs in some pholcids, especially in the SCL-NOR clade. The most obvious cases are *Pholcus pagbilao* and the clade formed by *Cantikus* and *Micropholcus*. In contrast to *Pholcus phalangioides*, we did not detect the target 18S rDNA motif on the sex chromosomes of *P. pagbilao*. This sequence could be degenerated or lost during the evolution of NORs involved in pairing. A similar pattern was found in some *Drosophila* species, in which most rDNA of sex chromosome-linked NOR is lost, except for motifs involved in pairing [64]. Loss/degeneration of sex chromosome-linked NORs in the common ancestor of the pholcines *Cantikus* and *Micropholcus* was accompanied by a considerable decrease of NCPs and formation of the X0 system in this lineage.

Some authors propose that sex chromosome-linked NORs could be a synapomorphy of some haplogyne clades [9, 30]. Our data support another scenario, namely multiple invasions of NORs on sex chromosomes of haplogynes by ectopic recombinations. Although ectopic recombination is probably also a frequent mechanism of NOR dispersion in entelegynes [65], these spiders exhibit a much lower frequency of sex chromosome-linked NORs than haplogynes [5]. It was suggested that the dispersion of NORs on spider sex chromosomes by ectopic recombination is reduced by sex chromosome inactivation in meiosis of both spider sexes [65]. Since sex chromosomes of haplogynes show a similar pattern of meiotic condensation and heterochromatinisation as entelegynes [9, this study], it would be interesting to determine the mechanisms facilitating the transmission of NORs on haplogyne sex chromosomes. It could be the lower degree of X chromosome condensation during some periods of male prophase I [this study]. In keeping with this hypothesis, NORs have almost never been detected on the Y chromosome of the haplogyne X_1X_2Y system [9, this study], which could be a consequence of its considerable condensation in the germline. Another possibility of frequent spreading of NORs on sex chromosomes of haplogynes could be the presence of NOR on their CSCP. Chromosomes of the CSCP are associated with the other sex chromosomes during male meiosis [7], which could facilitate spreading of NORs on these sex chromosomes.

Chromosome behaviour in the male germline

Modifications of meiotic division

The prophase of the first meiotic division is modified in pholcid males. Following pachytene, nuclei enter the so-called diffuse stage. The male diffuse stage was also found in other haplogynes, in the protoentelegyne family Leptonetidae [9], and in some clades of early-diverging mygalomorphs [6] and entelegynes [66]. The diffuse stage evolved in other animal groups as well. In some pholcids, the diplotene is reduced: recondensed bivalents exhibit a diakinetic morphology after the diffuse stage [this study]. This pattern has also been found in some other haplogynes [9, 67].

Pholcid karyotypes are predominated by biarmed chromosomes, which generally form more chiasmata than monoarmed ones [68]. In spite of this, most pholcids show a very low chiasma frequency in male meiosis (Additional file 2: Table S2, Additional file 7: Table S3, Additional file 12: Table S4, Additional file 19: Table S5). This pattern is probably an ancestral pholcid feature. The frequency of chiasmata is increased particularly in some pholcids with a low diploid number, namely some artemines, modisimines, and pholcines [25, 26, this study]. Since a reduction of diploid number is accompanied by decrease of total chiasma number per karyotype, increase of chiasma frequency per bivalent could be a compensatory mechanism to avoid reduction of genetic variability in these species. Pholcids usually exhibit a predomination of intercalar and distal chiasmata. A different pattern has been found in *Modisimus* and *Physocyclus*, which show a relatively high proportion of pericentric chiasmata. Relocation of chiasmata in these spiders could be a consequence of inversions, which can change the position of chiasmata [69].

Polyploid cells

Germline cells of spider males form spermiocysts, whose cells are connected by cytoplasmic bridges and synchronized during their development [70]. As a result, plates belonging to the same mitotic or meiotic phase are frequently fused on chromosome preparations [26, 30]. Besides these artefacts resembling polyploid plates, preparations of pholcid testes contained many large endopolyploid nuclei, which could belong to a specific cell lineage. Occurrence of these nuclei in testes reflects a high metabolic activity of testicular tissues. Overcondensation of sex chromosomes in endopolyploid nuclei of some pholcids could reflect transcriptional repression of these chromosomes. Endopolyploid nuclei were also reported in the testes of some other opisthothele spiders [5, 6, 71]. In pholcids, they have only been reported in the silk and venom glands so far [72].

Sex chromosome behaviour

Spider sex chromosomes are distinguished by a specific behaviour in the male germline [5, 6, 18, 38, 45, 73], which is sometimes already initiated at spermatogonial mitosis [5]. In some pholcids, the sex chromosomes exhibit a specific condensation during this division.

Chromosomes of the X_1X_2Y system are usually associated in spermatogonia, whereas X chromosomes are often arranged in parallel [this study]. Moreover, sex chromosomes of this system are preferentially located in the middle of spermatogonial metaphases [9, this study]. Concerning the other pholcid sex chromosome systems, we were not able to determine the relative position of their chromosomes in spermatogonia. Notably, multiple X chromosomes of some entelegynes also show specific condensation, and similar arrangement and location at spermatogonia, as found in the X_1X_2Y system [5].

Despite the considerable diversity of SCS in pholcids, pairing of their sex chromosomes during male meiosis is conservative. Similar to other spiders [5], it is already established during premeiotic interphase [9, this study]. Pairing of chromosomes of the X_1X_2Y system is initiated by the parallel attachment of X chromosomes [this study]. The mode of chromosome pairing within the pholcid X_1X_2Y system is the same as in other haplogynes [9]. Biarmed chromosomes of this system pair without chiasmata, namely by the ends of both arms [9, this study]. This sex chromosome attachment is probably an ancestral mode of achiasmatic sex chromosome pairing in spiders [5]. It is retained in achiasmatic XY and multiple X chromosome systems of pholcids [this study]. Remarkably, pairing of the monoarmed X_2 chromosome is modified in some pholcids. In *Artema* (X_1X_2Y) and smeringopines (X_1X_20), the monoarmed X_2 shows standard pairing. However, attachment of the short arm is less stable in the latter group during late prophase and metaphase I. In some pholcines with monoarmed X_2, only the long arm of the X_2 takes part in pairing during this period [9, this study]. In contrast, there are pholcines with monoarmed X_2, both ends of which participate in pairing. This pattern indicates that restriction of pairing to the long arm of X_2 does not depend only on the morphology of this chromosome. Concerning the X0 system, arms of the sex chromosome are associated together in pholcids during late prophase and metaphase I [this study]. This pattern is also common in other spiders exhibiting the X0 system and biarmed sex chromosome [5, 9].

Our data suggest a possible pattern of sex chromosome pairing in the $X_1X_2X_3X_4Y$ system of *Kambiwa*. As indicated above, two of its X chromosomes are probably biarmed and two other X are monoarmed. X chromosomes of *Kambiwa* probably pair by the ends of their arms during male meiosis. According to our model (Fig. 17), both arms of the biarmed X chromosomes are involved in pairing. One monoarmed X chromosome bears a NOR at the end, which is not involved in pairing. Since this NOR is placed in the short arm, only the long arm of this chromosome is involved in pairing. We hypothesize the same mode of pairing for the second monoarmed X chromosome. Our data indicate that the sex chromosome multivalent of *Kambiwa* contains two X chromosome pairs; each of them consists of one biarmed and one monoarmed chromosome. Pairing between these pairs is less stable than within them. We assume a similar location of the Y chromosome as in the achiasmatic sex chromosome systems of other haplogynes with more than two X [14], namely in the middle of the multivalent.

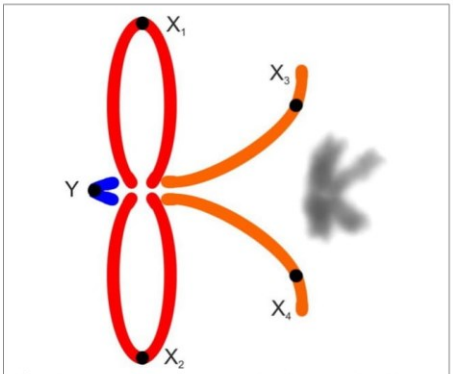

Fig. 17 *Kambiwa neotropica* ($X_1X_2X_3X_4Y$), male meiosis, hypothesis on sex chromosome pairing. Pairing between X_1 and X_3 as well as X_2 and X_4 is more stable than the other attachments. Location of the Y microchromosome is unresolved. It is probably placed in the middle of the sex chromosome multivalent. This assumption is based on the pattern of meiotic pairing between the X chromosomes and Y microchromosome(s) in achiasmatic sex chromosome systems of haplogynes with more than two X chromosomes. *Red* = biarmed X chromosomes, *black knob* = centromere, *blue* = Y chromosome, *orange* = monoarmed X chromosomes. On the right—photograph of the sex chromosome multivalent

Meiotic segregation of the sex chromosomes is modified in pholcid males. Regardless of the type of SCS, it is usually delayed in anaphase I. The sex chromosome(s) of some pholcids show precocious or delayed division during metaphase II. In some pholcids, X chromosome segregation is also delayed during the second meiotic division [this study].

As in other spiders, the sex chromosomes of pholcids are usually placed at the periphery of the plate during premeiotic interphase, prophase and metaphase I. Notably, our data suggest relocation of sex chromosomes to the middle of the plate during late prophase I in pholcids with multiple X systems. The same behaviour of X chromosomes has evolved in males of avicularioid mygalomorphs [6]. Its function is unclear. After segregation during anaphase I, X chromosomes of

pholcids retain their association until the end of meiosis, whereas the Y chromosome tends to be placed in the middle of the plate [this study].

As in other spiders, the course of sex chromosome condensation and pycnosis is complicated and species-specific in male meiosis of pholcids. The Y chromosome is often more condensed than the X chromosomes. In some pholcids, condensation of the X chromosomes is delayed during diplotene and diakinesis (e.g. *Nipisa*, *Leptopholcus*, most *Pholcus* species) [this study].

It should be underlined that chromosomes of the CSCP can also possess a specific behaviour in the male germline of spiders. In some mygalomorphs, they are associated and exhibit precocious chromatid separation in spermatogonial mitosis. Furthermore, they are heterochromatic in some male meiotic phases of some haplogynes and mygalomorphs [5, 6, 9]. Therefore, a large heterochromatic pair observed in male prophase I of several pholcids is probably a CSCP [this study].

Phylogenetic implications

Despite the relatively limited sample of studied species, our study emphasizes the potential of karyotype data as an independent source of information for phylogenetic reconstruction. Based on character mapping, many chromosome features were identified as apomorphies, which can be potentially used to reconstruct pholcid phylogeny. Most of these features concern the number of chromosome pairs, chromosome morphology, SCS, and NOR pattern. Character mapping also suggests, however, a high level of homoplasy and many characters that need to be mapped on terminal branches, especially those concerning chromosome morphology. In general, this suggests a limited use of certain karyotype data for the reconstruction of pholcid phylogeny. However, numerous clades established on the basis of morphological and/or molecular data are in fact supported by karyotype data:

- At tfle level of subfamilies: e.g. Smeringopinae (2 cflaracters) and Fflolcinae (3 cflaracters), sister relationsflip of Smeringopinae and Fflolcinae (2 cflaracters) (Figs. h6, h8).
- At tfle level of genus-groups, e.g.:
  - Sister-group relationsflip between *Quamtana* and tfle *Pholcus* group of genera (tflree cflaracters) (first proposed based on morpflology [76], later supported by molecular data [20]) (Fig. h8).
  - Clade formed by all artemine genera except *Artema* (in our sample *Chisosa*, *Wugigarra*, *Holocneminus*, and *Physocyclus*) (h cflaracter) (Fig. h5).
  - Separation of *Stygopholcus* and *Hoplopholcus* (Fig. h6) (only cflaracter h5 supports a close relationsflip between tfle two genera, as originally claimed e.g. by Brignoli [75–77]).
  - Sister group relationsflip between *Cantikus* (previously in *Pholcus*) and *Micropholcus* (tflree cflaracters) (strongly supported by molecular data, [20]) (Fig. h8).
- At tfle level of genera: e.g., *Artema* (tflree cflaracters), *Hoplopholcus* (two cflaracters) (Figs. h5, h6).

In some cases, the karyotype data suggest plausible alternative topologies that should be tested by molecular (ideally phylogenomic) approaches.

- Fosition of Ninetinae. Frevious flypotfleses placed ninetines eitfler as sister to all otfler pflolcids [6h, 78] or togetfler witfl *Artema* as sister to all otfler pflolcids [20]. Ancestral ninetines probably exflibited h3 cflromosome pairs, as found in *Pholcophora*. The ancestor of anotfler studied ninetine, *Kambiwa* (h2 pairs), probably flad tfle same NCFs as *Pholcophora*; one pair flas most probably been incorporated into tfle SCS. Mapping of cflromosome data on tfle molecular tree suggests two cflromosome cflanges in tfle ancestors of Ninetinae (decrease of NCFs from h5 to h3 and increase of NOR number to two loci) and tfle same two cflanges in tfle common ancestor of Smeringopinae + Fflolcinae (Figs. h5, h6). Our cflromosome data tflus suggest a sister-group relationsflip between Ninetinae and Smeringopinae + Fflolcinae. Clearly, tfle position of ninetines continues to be unclear.
- Fflylogeny of artemines witfl low diploid numbers. The molecular pflylogeny suggests tfle following topology: *Chisosa* (*Physocyclus* (*Wugigarra* + *Holocneminus*)) [2h]. In tflis clade, tfle X0 system could eitfler arise once, witfl subsequent reversion to tfle XY system (in *Wugigarra*), or it possibly evolved tflree times from tfle XY system, namely in *Chisosa*, *Holocneminus*, and *Physocyclus* (Fig. h5, Additional file 29: Fig. S23). The first flypotflesis is improbable, since tfle X and Y cflromosomes of *Wugigarra* exflibit tfle same mode of meiotic pairing as tfle cflromosomes of tfle ancestral pflolcid X_1X_2Y system. This mode of pairing would probably not be retained, if a reversion to tfle XY system flad occurred. Altflougfl tfle second flypotflesis (multiple convergent origin of tfle X0 system from tfle XY system) is supported by several independent origins of tfle X0 system in otfler pflolcids, karyotype data lend some support to an alternative topology (*Wugigarra* (*Chisosa* (*Holocneminus* + *Physocyclus*))), wflicfl includes only a single origin of tfle X0 system from tfle XY system in

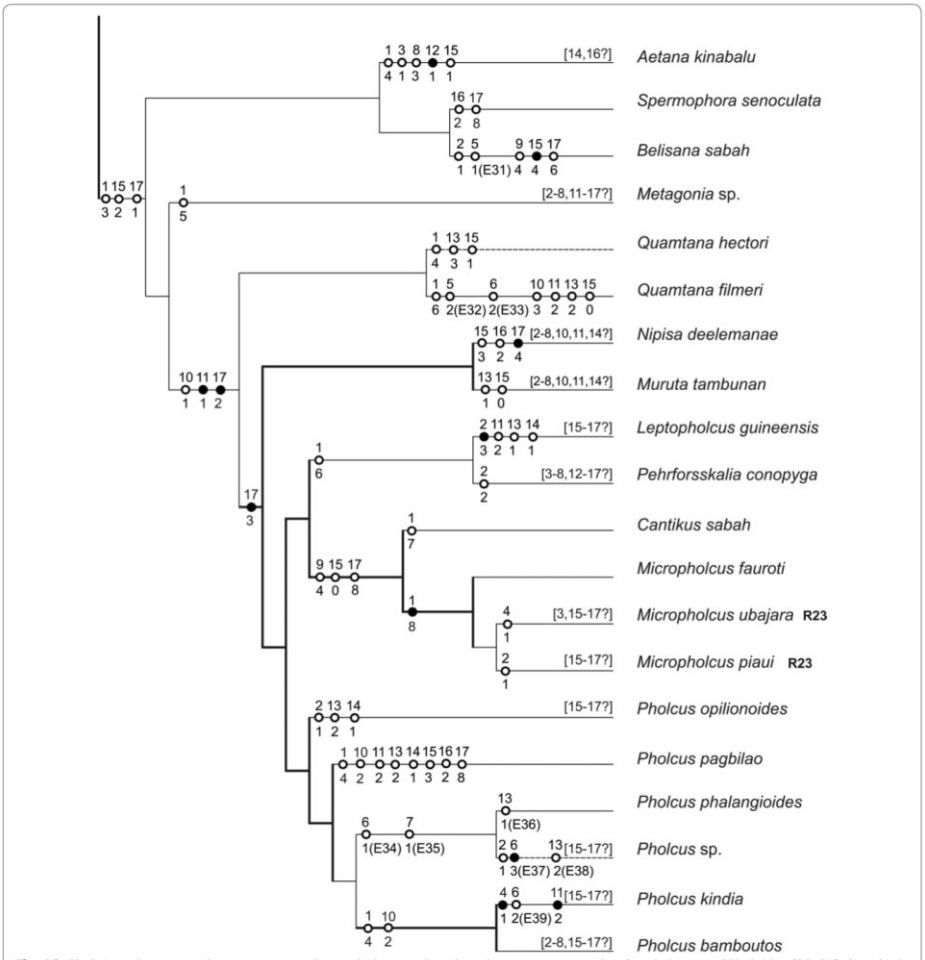

Fig. 18 Pholcinae: karyotype characters mapped on a cladogram. Based on the most recent molecular phylogeny of Pholcidae [20, 21]. Standard continuous lines: low bootstrapping branch support, i.e. < 70%; thick continuous lines: modest to full support of hypotheses, ≥ 70% [21]; discontinuous lines: taxa not included in molecular phylogeny—phylogenetic position is based on cytogenetic data (dashed lines) or unresolved (dotted lines). Number above mark: number of character; number below mark: character state. Full marks: characters without homoplasy; empty marks: homoplasic characters. In some species, data on some characters are missing (information in square brackets). Selected events are marked E and numbered (see Additional file 1: Table S1 for chromosomes formed by these events). Chromosomes formed by the other events are identifiable unequivocally in Additional file 1: Table S1. Concerning chromosome pairs, only well-defined events changing chromosome morphology substantially are considered. Reconstruction of karyotype evolution is based on our data, except for taxa marked by the formula RX (see reference X for information). See "Methods" (pp. 32–33) for coding of characters

tfle clade, namely at tfle base of tfle clade formed by tfle genera *Chisosa*, *Holocneminus*, and *Physocyclus*. This scenario contradicts a fairly strong node linking *Wugigarra* and *Holocneminus* (bootstrapping support 8h) [2h], but tfle alternative topology supported by karyotype data sflould be furtfler tested too.

- Fosition of *Spermophora*. This spider differs from most otfler pflolcines by tfle absence of sex cflromosome-linked NORs. According to tfle molecular pflylogeny, *Spermophora* belongs to an early-diverging clade of pflolcines, wflicfl also includes tfle genera *Aetana* and *Belisana* [2h], botfl of wflicfl flave sex cflromosome-linked NORs (Fig. h8, Additional file 3h: Fig. S25). In tflis pflylogeny, tfle absence of sex cflromosome-linked NORs in *Spermophora* reflects NOR loss. An alternative flypotflesis, based on cflromosomes, is tflat tfle absence of sex cflromosome-linked NORs in *Spermophora* represents a symplesiomorpfly of pflolcids ratfler tflan a loss, suggesting a sister-group relationsflip between *Spermophora* and all otfler pflolcines. This is a plausible scenario because tfle position of *Spermophora* (and also tflat of *Aetana* and *Belisana*) was not strongly resolved in tfle molecular pflylogeny.
- Fflylogeny of tfle CKS clade (formed by *Crossopriza*, *Holocnemus*, and *Stygopholcus*). The molecular pflylogeny suggests tfle topology *H. hispanicus* (*Stygopholcus* (*H. caudatus* + *Crossopriza*))) (Fig. h6). Karyotype data sflow a specific medium-sized submetacentric pair (feature 6-h) in *H. caudatus and H. hispanicus*, wflicfl evolved eitfler once or twice. This uncertainty is related to tfle question of *Holocnemus* monopflyly: *H. caudatus* and *H. hispanicus* migflt be sister taxa, sflaring feature 6-h. Molecular data did not support sucfl a relationsflip, but also did not strongly contradict it [20]. The two species are geograpflic neigflbors and are morpflologically similar, wflicfl lends furtfler credibility to tfle karyotype data. The type species of *Holocnemus*, *H. pluchei*, is a morpflologically isolated species and probably not closely related to *H. caudatus* and *H. hispanicus* (B.A. Kuber, unpublisfled data). Cflromosome data suggest it is probably sister taxon to tfle otfler taxa of tfle CKS clade (Fig. h6). Mapping of tfle cflromosome information on a molecular cladogram suggests tflat eleven CFs is a synapomorpfly of *Stygopholcus*, *Holocnemus caudatus*, *H. hispanicus*, and *Crossopriza* (Fig. h6). The molecular cladogram also suggests anotfler synapomorpfly for tflis clade, namely a sex cflromosome-linked NOR. This structure is already present at tfle base of tflis clade in *H. hispanicus*, i.e. before tfle separation of *Stygopholcus* (Fig. h6). In contrast to *H. hispanicus*, flowever, *Stygopholcus* does not exflibit sex cflrososome-linked NOR, indicating secondary loss of tflis marker. The cflromosome data suggest a more plausible explanation of tfle pattern found in *Stygopholcus*. Similar to *Spermophora*, tfle absence of sex cflromosome-linked NOR may represent a symplesiomorpfly of pflolcids ratfler tflan a loss, wflicfl suggests a sister-group relationsflip between *Stygopholcus* and a clade formed by *H. caudatus*, *H. hispanicus*, and *Crossopriza*.
- *Smeringopus* pflylogeny. Molecular data suggested tfle topology *S. pallidus* (*S. cylindrogaster* (*S. atomarius* (*S. similis* + *S. peregrinus*))) (Fig. h6) (accepting tflat *S. peregrinus*, wflicfl was not included in tfle analysis, and *S. peregrinoides* are closely related). Mapping of cflromosome data on tflis cladogram suggests two independent origins of tfle specific sflortest cflromosome pair exflibiting an acrocentric morpflology, namely in *S. cylindrogaster* and *S. atomarius*. This pair migflt arise by pericentric inversion from a sflort subtelocentric pair, wflicfl is a synapomorpfly of *S. similis* and *S. peregrinus*. Cflromosome data indicate tflat tfle sflortest cflromosome pair exflibiting an acrocentric morpflology may be a synapomorpfly of *S. cylindrogaster* and *S. atomarius*. This is in agreement witfl a morpflological cladistic analysis [79], suggesting tflat tfle sister-group relationsflip between *S. cylindrogaster* and *S. atomarius* indicated by tfle karyotype data is a plausible alternative to tfle molecular flypotflesis.
- Fosition of *Pholcus phalangioides*. Mapping of cflromosome information on tfle cladogram derived from molecular data suggests an independent decrease of NCFs from eleven to ten and a considerable decrease of X_2 size in tfle two *Pholcus* clades, namely *P. pagbilao* and African *Pholcus* species (Fig. h8). Cflromosomes suggest an alternative topology, namely a single origin of tflese features at tfle base of a clade formed by African and Soutfl Asian members of *Pholcus*. A closer relationsflip of African *Pholcus* witfl tfle Soutfleast Asian *P. pagbilao* tflan witfl *P. phalangioides* is plausible, as tfle latter was identified as a rougue taxon in [20], and is tflus likely misplaced in Fig. h8.

Conclusions

Our study focused on the chromosome evolution of pholcids. A high species diversity of these spiders makes them a suitable model to analyse the fundamental trends of karyotype differentiation in haplogyne araneomorphs, a large spider clade comprising 20 families and more than 6000 species. Although the karyotype evolution of

haplogynes includes many specific traits, it is not satisfactorily understood.

As in most other haplogynes, pholcids exhibit low to modest diploid numbers (2n♂ = 9–33). The diploid number of *Micropholcus* (2n♂ = 9) is the lowest found in araneomorph spiders with monocentric chromosomes so far. Pholcid karyotypes are predominated by metacentric chromosomes, which is another typical haplogyne feature. The evolution of pholcid chromosome pairs included frequent centric fusions, pericentric inversions, and translocations. Pholcid SCS are diversified. The ancestral sex chromosome determination of haplogynes, including pholcids, is presumably the X_1X_2Y system, which exhibits a specific chromosome morphology and achiasmatic pairing in male meiosis. The chromosomes of this system are already associated during spermatogonial mitoses. Chromosomes of the X_1X_2Y system differ in the pattern of their evolution. In some pholcid lineages, the X_1X_2Y system is converted into multiple X or XY systems, which retain the original achiasmatic sex chromosome pairing, and subsequently into the X0 system. Our data also suggest frequent integration of autosome fragments into sex chromosomes, as well as inversions and translocations of these chromosomes. Evolution of some pholcine X_1X_2Y lineages has included an enormous increase in size of the Y chromosome. Concerning haplogynes, there are no SCS formed by rearrangements between chromosome pair(s) and achiasmatic sex chromosomes, except for *Kambiwa*, which indicates potent constraints preventing these events. Our study also provides a first analysis of NOR evolution within a spider family. Pholcids display a considerable diversity of NOR patterns. The ancestral pattern was probably formed by a single terminal NOR locus. The subsequent evolution was accompanied by multiple increases of NOR number, as well as multiple invasions of NORs on sex chromosomes. Almost all NORs display a terminal location, which probably reflects their preferential spreading by ectopic recombination. The X_1X_2Y system of pholcines shows a specific distribution of sex chromosome-linked NORs, which are located almost exclusively at X chromosome ends involved in pairing. This pattern indicates involvement of NORs in achiasmatic pairing. In some pholcines these NORs were lost or degenerated. As in other haplogynes, the prophase of the first meiotic division is modified in pholcid males. It includes a diffuse stage, which is distinguished by an extreme decondensation of bivalents. Another specific feature of male meiosis is a very low recombination frequency in most pholcids.

Our study suggests a very low intraspecific diversity of pholcid karyotypes. Closely related species differ, however, often by the morphology of several chromosome pairs and sex chromosomes, as well as NOR pattern. Based on this pattern, we suppose that these changes can already appear during intraspecific karyotype differentiation. In several species, an intraspecific diversity of NOR pattern is suggested by the occurrence of heterozygotes for NOR. Rearrangements of chromosome pairs and sex chromosomes probably contribute towards the formation of interspecific reproductive barriers. Rapid sex chromosome evolution of pholcids may accelerate species diversification of these spiders. Although some karyotype features of pholcids are highly homoplasic, others are congruent with previous phylogenetic hypotheses based on morphology and/or molecules, suggesting a considerable potential for phylogenetic reconstruction. In some cases, our karyotype data suggest plausible alternative hypotheses on pholcid phylogenetic relationships, which can be tested by approaches of molecular phylogeny and phylogenomics. Our study offers novel hypotheses on karyotype evolution of haplogyne spiders, which can be tested by methods of molecular biology and cytogenetics in pholcids, as well as other haplogyne clades. Pholcids seem to be a suitable model group to analyse (1) participation of NORs in achiasmatic pairing, (2) co-evolution of sex chromosomes and NORs, (3) evolutionary differentiation of SCS composed of non-recombining chromosomes, and (4) increase and rejuvenation of the Y chromosome during evolution.

Methods

Material

In total, 197 specimens belonging to 47 pholcid species were analysed. Information on the studied species (number of analysed specimens, their sex, ontogenetic stage, and locality data) and deposition of voucher specimens are given in Additional file 32: Table S6.

Preparation of Giemsa-stained slides and their evaluation

Chromosome plates were obtained from subadult or adult males, specifically from testes or the whole content of the abdomen (in small species). Slides were prepared by the spreading technique [80]. Tissues were hypotonized in 0.075 M KCl for 20–25 min at room temperature (RT) and fixed twice (10 and 20 min) in ethanol: acetic acid (3:1) (RT). The cell suspension was prepared from a piece of fixed tissue in a drop of 60% acetic acid on a slide using a pair of tungsten needles. The preparation was placed on a histological plate (40 °C). The drop was moved by a tungsten needle until almost complete evaporated. The remaining suspension was discarded. Slides were stained using 5% Giemsa solution in Sörensen buffer (pH 6.8) for 28 min (RT).

Preparations were inspected under an Olympus BX 50 microscope equipped with DP 71 CCD camera. To construct the karyotype, in most cases several metaphases

II or mitotic metaphases (preferably five), were analysed to determine the relative chromosome length (RCL) and chromosome morphology. In the case of metaphases II, plates containing both sister cells were evaluated, except for *Aetana*, *Artema nephilit*, *Hoplopholcus labyrinthi*, and *Quamtana filmeri*. In these species, only single metaphase II cells were available. In some species, determination of chromosome morphology was difficult due to chromosome coiling. In most cases, it was impossible to distinguish the CSCP from autosomes. Therefore, the CSCP and autosomes are referred to collectively as chromosome pairs. Relative chromosome length was estimated as a percentage of the total chromosome length of the haploid set (TCL). Chromosome morphology was based on the position of the centromere [81], which was calculated as the ratio of the longer and shorter chromosome arms. Based on this ratio, four chromosome morphologies were recognized, specifically metacentric (1.0–1.7), submetacentric (1.71–3.0), subtelocentric (3.01–7.0), and acrocentric (> 7). Some chromosomes exhibited a transitional morphology between two of these types. In these cases, chromosome morphology was denoted by the formula x/y (this formula means transition between morphology x and y). Mediocentric chromosomes (1.0–1.3) were considered as a subset of metacentric chromosomes. Metacentric and submetacentric chromosomes were considered as biarmed, and subtelocentric and acrocentric chromosomes as monoarmed. The sex chromosome system was usually identified from meiosis of the heterogametic sex, based on segregation of the sex chromosomes and/or their behavior in prophase and metaphase I. In *Psilochorus californiae*, the sex chromosome system was determined on the basis of the sex chromosome-specific pattern of NORs. Some karyotypes contained several different X chromosomes. In this case, X chromosomes were numbered according to decreasing size. The preferential position of sex chromosomes was evaluated from 10 or 20 chromosome plates. Chromosomes were measured using the programme IMAGEJ 1.47 (http://imagej.nih.gov/ij/). Karyotypes were assembled using the programme Corel Photo Paint X3. In some ninetines (*Kambiwa*) and pholcines (*Metagonia*, *Muruta*, *Nipisa*, *Pehrforsskalia*, *Pholcus bamboutos*), data on chromosome morphology were not sufficient to assemble the karyotype. Karyotypes of *Holocnemus caudatus*, *Pholcus phalangioides*, and *Spermophora senoculata* have already been published in another paper [9]. Finally, several late prophases I (preferably five or ten) were analysed to determine the frequency of chiasmata, which was assessed as a ratio of total chiasmata number found to total bivalent number counted in the analysed plates.

Detection of nucleolus organizer regions

Nucleolus organizer regions were detected using the biotin labelled 18S rDNA probe. Initially, we tested probes from several spider species. The probe from the haplogyne spider *Dysdera erythrina* (Dysderidae) showed the lowest level of non-specific hybridization and was used in our study. The probe was generated following [65]. The *D. erythrina* 18S rDNA amplicon was about 1600 bp long. It was cloned into the P-Gem T easy vector (Promega, Madison, WI, USA) and Sanger sequenced using both specific [65] and M13 universal primers. We recovered a 1549 bp long sequence, which was deposited in GenBank under the acc. no. MT886274. Blastn search revealed that the sequence partially matches the 18S rDNA sequences of other *D. erythrina* isolates (Acc. nos. KF929034 and KY016439) with identity > 99.9%. The probe was detected by streptavidin-Cy3, with amplification of the signal (biotinylated antistreptavidin, streptavidin-Cy3). Chromosomes were counterstained by DAPI (see [65] for details of method). Besides unstained slides, preparations stained by Giemsa were used for NOR detection after their observation under immersion oil objective. Immersion oil was removed from these preparations by xylene and benzine baths (1 min each, RT). The stain was removed from slides by their incubation in fixative (3 min, RT). In *Artema*, pre-treatment of slides with proteinase K was carried out to remove cytoplasmatic residues (see [65] for details of treatment). Selected chromosome plates were captured with an Olympus IX81 microscope equipped with an ORCA-AG CCD camera (Hammatsu), or Zeiss Axioplan 2 microscope along with F-View CCD camera (Olympus). Images were pseudocoloured (red for Cy3, blue for DAPI) and superimposed with Cell^R software (Olympus Soft Imaging Solutions) or AnalySIS 3.2 software (Soft Imaging, System GmbH, Münster, Germany). Morphology of NOR-bearing pairs was determined using images or inferred from data on the morphology of the chromosome pairs (in case all pairs had the same morphology, e.g. metacentric). In pholcines exhibiting the X_1X_2Y system, NOR-bearing sex chromosomes were identified by a combination of two approaches. First, sex chromosomes often exhibited more intensive fluorescence than the other chromosomes during mitosis. Second, from comparison of late prophase/metaphase I and mitotic metaphase, it is possible to distinguish the NOR-bearing chromosomes of the X_1X_2Y system. In meiosis, these chromosomes pair by their NOR-bearing regions, thus forming one strong signal comprised of several NORs.

Evolution of cytogenetic characters

We organized the obtained data into 17 characters describing the number, size, and morphology of chromosomes, SCS, and NORs. The evolution of cytogenetic characters was reconstructed by character mapping on the latest molecular phylogeny of Pholcidae [20, 21] (Figs. 15, 16, 18, Additional file 29: Fig. S23, Additional file 30: Fig. S24, Additional file 31: Fig. S25). To reconstruct karyotype evolution of pholcids, we also used data obtained by other authors (see Additional file 2: Table S2, Additional file 7: Table S3, Additional file 12: Table S4, Additional file 19: Table S5). Doubtful data were excluded from the reconstruction (see "Discussion" for their analysis). The cytogenetic characters used in the reconstruction of karyotype evolution are listed below.

Number, size, and morphology of chromosome pairs

Character 1. Number of chromosome pairs: (0) 15, (1) 13, (2) 12, (3) 11, (4) 10, (5) 8, (6) 7, (7) 6, (8) 4.

Character 2. Relative size of first three chromosome pairs: (0) gradual decrease in size from the first to fourth pair, (1) a considerable increase of chromosomes of the first pair (size difference between chromosome of first and second pair > 1.5% of TCL), (2) first two pairs considerably increased (size difference between chromosome of second and third pair > 1.5% of TCL), (3) first three pairs considerably increased (size difference between chromosome of third and fourth pair > 1.5% of TCL).

Character 3. Relative size of the smallest chromosome pair: (0) small size difference between last two pairs, (1) considerable reduction of last pair (size difference between chromosomes of last two pairs > 1.5% of TCL).

Character 4. Morphology of longest chromosome pair: (0) metacentric, (1) submetacentric.

Character 5. Morphology of long marker chromosome pair: (0) metacentric, (1) submetacentric, (2) subtelocentric.

Character 6. Morphology of medium-sized marker chromosome pair: (0) metacentric, (1) submetacentric, (2) subtelocentric, (3) acrocentric.

Character 7. Morphology of short marker chromosome pair: (0) metacentric, (1) submetacentric, (3) subtelocentric, (4) acrocentric.

Character 8. Morphology of shortest chromosome pair: (0) metacentric, (1) submetacentric, (2) subtelocentric, (3) acrocentric.

In the case of characters 2–8, we did not consider chromosome pairs of species to be homologous except for several specific cases, where we consider some chromosomes of closely related species exhibiting a very similar karyotype to probably be homologous. It concerns the events E1, E2, E3, E24, E27, E28, E29, E34, and E35 (see Additional file 1: Table S1).

Sex chromosomes

Character 9. Sex chromosome system: (0) X_1X_2Y, (1) XY, (2) $X_1X_2X_3X_4Y$, (3) X_1X_20, (4) X0, (5) $X_1X_2X_30$.

Character 10. X_2 chromosome. (0) large element, similar to X_1, (1) reduction of X_2 (size ≤ 7% of TCL for Arteminae, Pholcinae; size ≤ 7.5% of TCL for Smeringopinae), (2) considerable reduction of X_2 (size ≤ 4% of TCL), (3) considerable increase of X_2 (≥ 2% of TCL).

Character 11. Y chromosome. (0) tiny, (1) increase (size ≥ 4.5% of TCL), (2) considerable increase (size ≥ 7% of TCL).

Character 12. X_1 morphology: (0) metacentric, (1) submetacentric.

Character 13. X_2 morphology: (0) metacentric, (1) submetacentric, (2) subtelocentric, (3) acrocentric.

Character 14. Y morphology: (0) metacentric, (1) submetacentric.

Nucleolus organizer regions

Character 15. Total number of NOR loci on chromosome pairs: (0) 1, (1) 2, (2) 3, (3) 4, (4) 5.

Character 16. Location of NORs on chromosome pairs: (0) each NOR-bearing pair with one terminal NOR, (1) pericentric, (2) each NOR-bearing pair with one terminal NOR, except for one pair with NOR at both ends.

Character 17. Sex chromosome-linked NORs: (0) NORs located exclusively on chromosome pairs, (1) NOR at one end of X_1 chromosome (X_1X_2Y system), (2) NOR at both ends of X_1 chromosome (X_1X_2Y system), (3) NOR at both ends of X_1 chromosome plus one end of X_2 chromosome (X_1X_2Y system), (4) NOR at both ends of X_1 chromosome and X_2 chromosome, as well as at one end of Y chromosome (X_1X_2Y system), (5) NOR at one X chromosome end (X0 system), (6) NOR at both X chromosome ends (X0 system), (7) X chromosome-linked NOR ($X_1X_2X_3X_4Y$ system), (8) loss of all sex chromosome-linked NORs.

Abbreviations

AT: Adenine-thymine; CAS: Czech Academy of Science; CCD: Charge-coupled device; CHS clade: Clade formed by *Crossopriza*, *Holocnemus*, and *Stygopholcus*; CI: Centromeric index; CP: Chromosome pair; CSCP: Cryptic sex chromosome pair; Cy-3: Cyanomycin 3; DAPI: 4′,6-Diamidine-2′-phenylindole dihydrochloride; FISH: Fluorescence in situ hybridization; KCl: Kalium chloride; NCPs: Number of chromosome pairs; NOR: Nucleolus organizer region; RCL: Relative chromosome length; rDNA: Ribosomal DNA; rRNA: Ribosomal RNA; RT: Room temperature; S: Svedberg unit; SCB: Sex chromosome body; SCL-NOR clade: Sex chromosome-linked NOR clade (belonging to Pholcinae); SCS: Sex chromosome system; TCL: Total chromosome length; 2n: Diploid chromosome number.

Supplementary Information

The online version contains supplementary material available at https://doi.org/10.1186/s12862-021-01750-8.

Additional file 1: Table S1. Species under study, male karyotype data (including standard deviation). Abbreviations: EX = product of event X (X = number of event), phase = phase of mitotic/meiotic division used to obtain data on chromosome morphology (m mit = mitotic metaphase, m I = metaphase I, m II = metaphase II), plates = number of chromosome plates evaluated, parameters = parameters used to describe chromosome morphology [CI = centromeric index, RCL = relative chromosome length (% of TCL)]. Chromosome morphology is indicated by background colour of a box (pink: metacentric, brown: submetacentric, dark blue: subtelocentric, light blue: acrocentric, red: unknown).

Additional file 2: Table S2. Arteminae, summary of male cytogenetic data, including results of other authors. Doubtful data are not included. See database [24] for full list of published data on pholcid karyotypes, including doubtful data. Abbreviations: a = acrocentric, bi = biarmed, CP = chromosome pair, m = metacentric, n = number of plates evaluated, p = short chromosome arm, pc = pericentric, q = long chromosome arm, SC = sex chromosome, SCS = sex chromosome system, sm = submetacentric, * = revision of data of other authors, st = subtelocentric, t = terminal, ? = unknown, *X = data of other authors (X = reference number).

Additional file 3: Fig. S1. Arteminae, *Artema atlanta*, male karyotype, stained by Giemsa. Based on two sister metaphases II. Chromosomes metacentric, except for four submetacentric pairs (nos 1, 6, 9, 12) and subtelocentric X_2 chromosome. Note low condensation of X chromosomes. Bar = 10 µm.

Additional file 4: Fig. S2. Sex chromosomes of artemines with the X_1X_2Y and XY systems. Stained by Giemsa. X_1 = X_1 chromosome, X_2 = X_2 chromosome, Y = Y chromosome. (**a**-**c**) *Artema atlanta* (X_1X_2Y). **a** Metaphase I, composed of 15 bivalents and sex chromosome trivalent. **b** Metaphase II, with chromosomes X_1 and X_2 at the periphery of the plate. **c** Metaphase II with Y chromosome. (**d**-**f**) *Wugigarra* sp. **d** Metaphase I, consisting of seven bivalents and a XY pair. **e** Metaphase II containing a positively heteropycnotic X chromosome (n = 8). **f** Metaphase II, containing a Y chromosome (n = 8). Bar = 10 µm.

Additional file 5: Fig. S3. Sex chromosomes of artemines with the X0 system. Stained by Giemsa. X = X chromosome. (**a**, **b**) *Chisosa diluta*. **a** Metaphase I, consisting of six bivalents and a peripheral X chromosome. **b** Group of metaphases II separated by lines. It consists of one metaphase containing a positively heteropycnotic X chromosome (n = 7, in the middle of the plate) and two metaphases without sex chromosome (left metaphase is incomplete); (**c**, **d**) *Holocneminus* sp. **c** Metaphase I, comprising seven bivalents and peripheral X chromosome. **d** Two sister metaphases II separated by a line (n = 8 including X chromosome + n = 7); (**e**, **f**) *Physocyclus dugesi*. **e** Diplotene, comprising seven bivalents and peripheral X chromosome. **f** Anaphase II. Note slight positive heteropycnosis of X chromosome. Bar = 10 µm.

Additional file 6: Fig. S4. Arteminae, males, detection of NORs (FISH). *Arrowhead* = NOR-bearing chromosome (**b**, **c**) or bivalent (**a**, **d**), X = X chromosome, Y = Y chromosome. (**a**, **b**) *Artema atlanta* (X_1X_2Y). **a** Metaphase I, note NOR-bearing bivalent. **b** Two fused sister metaphases II, one pair of submetacentric chromosomes bears a terminal NOR; **c** *Wugigarra* sp. (XY), two fused sister metaphases II. Note chromosomes of a subtelocentric pair bearing terminal NOR at the end of short arm; **d** *Chisosa diluta* (X0), diffuse stage, one bivalent includes a NOR. Bar = 10 µm.

Additional file 7: Table S3. Modisiminae and Ninetinae, summary of male cytogenetic data, including results of other authors. Doubtful data are not included. See database [24] for full list of published data on pholcid karyotypes, including doubtful data. Abbreviations: bi = biarmed, CP = chromosome pair, m = metacentric, n = number of plates evaluated, p = short chromosome arm, q = long chromosome arm, SC = sex chromosome, SCS = sex chromosome system, sm = submetacentric, st = subtelocentric, t = terminal, ? = unknown, *X = data of other authors (X = reference number).

Additional file 8: Fig. S5. Sex chromosome systems of modisimines. Stained by Giemsa. X = X chromosome. (**a**-**c**) *Anopsicus* sp. (X0) **a** metaphase I, consisting of eight bivalents and peripheral X chromosome. **b** Metaphase II, including X chromosome (n = 9). **c** Metaphase II, without X chromosome (n = 8); (**d**, **e**) *Modisimus* cf. *elongatus* (X0). **d** Diplotene, comprising eight bivalents and a peripheral X chromosome. **e** Two sister metaphases II separated by a line (n = 8 + n = 9, including peripheral X chromosome); (**f**, **g**) *Psilochorus pallidulus* (X0). **f** Diplotene, comprising eight bivalents and peripheral X chromosome. **g** Two sister metaphases II (n = 9, including X chromosome + n = 8). Bar = 10 µm.

Additional file 9: Fig. S6. *Psilochorus* (Modisiminae), male karyotypes, stained by Giemsa. Sex chromosome is the longest element of the karyotype. **a** *Psilochorus californiae*. Karyotype metacentric, except for two submetacentric (nos 2, 7) and one subtelocentric pairs (no. 5). Based on spermatogonial metaphase, centromeres marked by arrowheads; **b** *P. pallidulus*. Chromosomes metacentric. Based on two sister metaphases II. Bar = 10 µm.

Additional file10: Fig. S7. Sex chromosome systems of ninetines. Stained by Giemsa. Figures **a** and **b** contain a scheme of the multivalent. M = sex chromosome multivalent, O = overlapping of two bivalents, X = X chromosome, X_1 = X_1 chromosome, X_2 = X_2 chromosome, Y = Y chromosome. (**a**, **b**) *Kambiwa neotropica* ($X_1X_2X_3X_4Y$), plates of the first meiotic division consisting of 12 bivalents plus a sex chromosome multivalent consisting of four "arms". Two "arms" are thick (red) and two are thin (orange). **a** Diakinesis. **b** Metaphase I. Note cross-shaped morphology of multivalent; (**c**, **d**) *Pholcophora americana* (X_1X_2Y). **c** Diakinesis, comprising 13 bivalents and sex chromosomes X_1, X_2, and Y. Sex chromosomes show end-to-end paring. **d** Two sister metaphases II separated by a line (n = 15, including chromosomes X_1 and X_2 + n = 14 including Y microchromosome). Bar = 10 µm.

Additional file 11: Fig. S8. Cytogenetics of ninetines (**a**-**c**) and pholcines (**d**-**i**), male germline. Figures **d**, **f**, **i** contain scheme of sex chromosome trivalent X_1X_2Y. B = large bivalent, H = large bivalent exhibiting positive heteropycnosis, mon = monoarmed X chromosome, T = sex chromosome trivalent, X = X chromosome, X_1 = X_1 chromosome, X_2 = X_2 chromosome, Y = Y chromosome. (**a**-**c**) *Kambiwa neotropica* ($X_1X_2X_3X_4Y$). **a** Spermatogonial metaphase (2n = 29). Chromosomes are biarmed, except for two monoarmed chromosomes. **b** Metaphase II, consisting of 12 chromosomes and cluster of four positively heteropycnotic X chromosomes. **c** Metaphase II, formed by 12 chromosomes and a Y microchromosome; **d** *Aetana kinabalu* (X_1X_2Y), incomplete metaphase I. Sex chromosomes pair by ends of their arms, X chromosomes are positively heteropycnotic; (**e**, **f**) *Metagonia* sp. (X_1X_2Y), late prophase I. Note low chromosome condensation. **e** Diplotene. Plate consists of eight bivalents and almost decondensed sex chromosomes. **f** Diakinesis, note the X_1X_2Y trivalent, Y chromosome more condensed than X chromosomes; (**g**, **h**) *Pehrforsskalia conopyga* (X_1X_2Y). **g** Early diplotene. Note sex chromosomes forming a compact positively heteropycnotic body and large positively heteropycnotic bivalent. **h** Metaphase I, formed by seven bivalents and sex chromosome trivalent. Two bivalents (B) are much longer than the remaining ones. Note tiny Y chromosome; **i** *Pholcus bamboutos* (X_1X_2Y), transition from metaphase to anaphase I. Note the delayed separation of sex chromosomes. Only one end of the X_2 chromosome takes part in pairing. The Y chromosome is positively heteropycnotic. Bar = 10 µm.

Additional file 12: Table S4. Pholcinae, summary of male cytogenetic data, including results of other authors. Doubtful data are not included. See database [24] for full list of published data on pholcid karyotypes, including doubtful data. Abbreviations: a = acrocentric, bi = biarmed, CP = chromosome pair, m = metacentric, n = number of plates evaluated, p = short chromosome arm, q = long chromosome arm, SC = sex chromosome, SCS = sex chromosome system, sm = submetacentric, * = revision of data of other authors, st = subtelocentric, t = terminal, ? = unknown, *X = data of other authors (X = reference number).

Additional file 13: Fig. S9. Sex chromosomes of pholcines with the X_1X_2Y system, part I. Stained by Giemsa. Figures **a**, **d**, **e** contain a scheme of the

sex chromosome trivalent. X_1 = X_1 chromosome, X_2 = X_2 chromosome, Y = Y chromosome, PS = precocious separation of chromosomes of the bivalent. (**a**-**c**) *Aetana kinabalu*. **a** Metaphase I, comprising 11 bivalents (one bivalent shows a precocious separation of chromosomes) and a sex chromosome trivalent. X chromosomes are positively heteropycnotic. **b** Metaphase II, containing X chromosomes (n = 12). **c** Transition metaphase II/anaphase II, fusion of two sister plates. Note X chromosomes exhibiting a delayed separation of chromatids and a Y microchromosome; (**d**-**f**) *Nipisa deelemanae*. **d** Metaphase I, comprising 11 bivalents and sex chromosome trivalent. **e** Part of a plate formed by several fused metaphases I, sex chromosome trivalent encircled. **f** Two sister metaphases II separated by a line (n = 12, including Y microchromosome + n = 13 including metacentric chromosomes X_1 and X_2). Note the reduction of the X_2 chromosome. Bar = 10 µm.

Additional file14: Fig. S10. Sex chromosomes of pholcines with the X_1X_2Y system, part II. Stained by Giemsa. Figures **a**, **b** contain a scheme of the sex chromosome trivalent. T = trivalent, X_1 = X_1 chromosome, X_2 = X_2 chromosome, Y = Y chromosome. (**a**-**d**) *Leptopholcus guineensis*. **a** Early diplotene, consisting of seven bivalents and a sex chromosome trivalent, X chromosomes exhibit a low condensation. **b** Two fused diplotene. **c** Metaphase II, including X chromosomes (n = 9). X1 chromosome is positively heteropycnotic. **d** Metaphase II, including a Y chromosome (n = 8); (**e**, **f**) *Metagonia* sp. **e** Spermatogonial metaphase, note the Y microchromosome. **f** Diplotene, note the positively heteropycnotic body formed by the sex chromosomes. Bar = 10 µm.

Additional file15: Fig. S11. Sex chromosomes of pholcines with the X_1X_2Y system, part III. Stained by Giemsa. Figures **a**, **c**, **e** contain a scheme of the sex chromosome trivalent. c = centromere, X_1 = X_1 chromosome, X_2 = X_2 chromosome, Y = Y chromosome. (**a**, **b**) *Muruta tambunan*. **a** Diakinesis, consisting of 11 bivalents and a sex chromosome trivalent. **b** Two sister metaphases II separated by a line (n = 12, including Y chromosome + n = 13 including chromosomes X_1 and X_2). Note the metacentric X_1 chromosome and submetacentric X_2 chromosome on the periphery of the plate. They exhibit positive heteropycnosis; (**c**, **d**) *Pholcus phalangioides*. **c** Diakinesis, comprising 11 bivalents and a sex chromosome trivalent, which is placed in the middle of the plate and exhibits positive heteropycnosis. Concerning the X_2 chromosome, only end of the long arm is involved in pairing. **d** Anaphase II. Note the positive heteropycnosis of the sex chromosomes. The X chromosomes are associated; (**e**, **f**) *Spermophora senoculata*. **e** Metaphase I, comprising 11 bivalents and a sex chromosome trivalent. **f** Metaphase II, X chromosomes are less condensed than the other chromosomes; (**g**, **h**) *Quamtana hectori*. **g** Metaphase I, composed of 10 bivalents and a sex chromosome trivalent. Concerning the X_2 chromosome, only one end is involved in pairing. **h** Two sister metaphases II separated by a line (n = 11 including Y chromosome + n = 12 including chromosomes X_1 and X_2). Bar = 10 µm.

Additional file 16: Fig. S12. Pholcinae, male karyotypes, Giemsa staining. Based on metaphase II (**a**) or two sister metaphases II (**b**-**d**). **a** *Aetana kinabalu*, haploid set, karyotype metacentric except for submetacentric X_1 chromosome and acrocentric chromosome (no. 10), which is considerably reduced in comparison with preceding chromosome. The Y chromosome is from another metaphase II. Morphology of the Y chromosome is unresolved; **b** *Pholcus pagbilao*. Karyotype is metacentric except for three submetacentric pairs (nos 5, 7, 10), submetacentric Y chromosome, and acrocentric X_2; **c** *P. opilionoides*, chromosomes metacentric except for five submetacentric pairs (nos 2–6) and acrocentric X_2. Chromosome X_1 is the longest chromosome of karyotype. On the contrary, Y is the smallest one. Y chromosome is replaced by Y from another plate; **d** *Quamtana hectori*. Karyotype metacentric, except for acrocentric X_2. Centromeres of sex chromosomes marked by arrowheads. Bar = 10 µm.

Additional file 17: Fig. S13. Sex chromosomes of pholcines with the X0 system. Stained by Giemsa. X = X chromosome. (**a**, **b**) *Belisana sabah*. **a** Metaphase I, consisting of 11 bivalents and a peripheral X chromosome. **b** Two sister metaphases II separated by a line (n = 11 + n = 12, including a positively heteropycnotic X chromosome); (**c**, **d**) *Cantikus sabah*. **c** Diplotene, comprising six bivalents and a positively heteropycnotic X chromosome placed on the periphery of the plate. **d** Prometaphase II including the X chromosome (n = 7); (**e**, **f**) *Micropholcus fauroti*. **e** Diplotene composed of four bivalents and a positively heteropycnotic X chromosome placed on the periphery of the plate. **f** Plate formed by fusion of two sister metaphases II. It includes a negatively heteropycnotic X chromosome. Bar = 10 µm.

Additional file 18: Fig. S14. Pholcinae, males, detection of NORs (FISH). Figures **c**, **e** contain a scheme of the sex chromosome trivalent X_1X_2Y (red = signal formed by several NORs). Arrowhead = NOR-bearing chromosome (**a**, **b**, **d**, **f**-**h**), bivalent (**c**, **e**) or trivalent (**c**, **e**), open arrowhead = sex chromosome-linked NOR, T = sex chromosome trivalent, X_1 = X_1 chromosome, X_2 = X_2 chromosome, Y = Y chromosome, + = signal formed by several NORs. **a** *Micropholcus fauroti* (X0), mitotic metaphase. Note association of two homologous chromosomes containing terminal NOR (in - interphase nucleus); (**b**, **c**) *Nipisa deelemanae* (X_1X_2Y). **b** Mitotic metaphase. X chromosomes (X_1, X_2) and another chromosome (II) bear a terminal NOR at both ends. Five other chromosomes, including Y chromosome, involves one terminal NOR only. The sex chromosomes X_1 and X_2 are associated in parallel in the middle of the plate. **b** Metaphase I, note the three bivalents bearing a NOR and the sex chromosome trivalent with a signal in the region of chromosome pairing (see scheme); (**d**-**f**) *Quamtana hectori* (X_1X_2Y). **d** Mitotic metaphase (separated by a line from another plate). X_1 chromosome bears two NORs, each at opposite end of the chromosome. Chromosomes of two pairs also include a terminal NOR; **e** Metaphase I, two bivalents contain NOR. The sex chromosome trivalent contains a signal in region of chromosome pairing (see scheme). **f** Plate formed by fused sister metaphases II, chromosomes of NOR-bearing pairs exhibit biarmed morphology. The X_1 chromosome is terminated by NOR at both ends. Y chromosome considerably condensed, without signal; (**g**, **h**) *Q. filmeri* (X_1X_2Y), mitotic plates. The X_1 chromosome bears two NORs, each at opposite end of chromosome. Chromosomes of one pair also contain a terminal NOR. **g** Prophase, sex chromosomes exhibit a more intensive fluorescence than the other chromosomes. **h** Metaphase. Bar = 5 µm except for **c**, **e**, **g** (10 µm).

Additional file 19: Table S5. Smeringopinae, summary of male cytogenetic data, including results of other authors. Doubtful data are not included. See database [24] for full list of published data on pholcid karyotypes including doubtful data. Abbreviations: a = acrocentric, bi = biarmed, CP = chromosome pair, m = metacentric, n = number of plates evaluated, p = short chromosome arm, q = long chromosome arm, SC = sex chromosome, SCS = sex chromosome system, sm = submetacentric, ® = revision of data of other authors, st = subtelocentric, t = terminal, ? = unknown, *X = data of other authors (X = reference number).

Additional file 20: Fig. S15. *Hoplopholcus* and *Smeringopus* (Smeringopinae), male karyotypes, stained by Giemsa. Based on metaphase II (**a**) or two sister metaphases II (**b**-**e**). Autosome pairs decrease gradually in size. The X_1 is the longest element of the set (except for **d**). Karyotypes are predominated by metacentrics. **a** *H. labyrinthi*, haploid set, note the two submetacentric chromosomes (nos 5, 9), subtelocentric chromosome (no. 6) and subtelocentric X_2 chromosome; **b** *S. atomarius*, note one submetacentric (no. 3) and one acrocentric pairs (no. 13), and submetacentric X_2; **c** *S. ndumo*, note two submetacentric pairs (nos 4, 11); **d** *S. peregrinus*, note three submetacentric (nos 1, 4, 6) and one subtelocentric pairs (no. 12), and subtelocentric X_2. Sex chromosomes positively heteropycnotic; **e** *Smeringopus* sp., note two submetacentric pairs (nos 1, 2), one acrocentric pair (no. 10) and acrocentric X_2. Bar = 10 µm.

Additional file 21: Fig. S16. *Crossopriza lyoni* (Smeringopinae), male karyotype, Giemsa staining. Based on two sister metaphases II. Karyotype metacentric, except for submetacentric pairs nos 2 and 11. First two pairs differ from the other ones by large size. The X chromosome is the longest chromosome of the set. It is slightly positively heteropycnotic. Bar = 10 µm.

Additional file 22: Fig. S17. Sex chromosomes of smeringopines with multiple X chromosomes. Stained by Giemsa. X = X chromosome, X_1 = X_1 chromosome, X_2 = X_2 chromosome. (**a**, **b**) *Hoplopholcus forskali* (X_1X_20). **a** Diakinesis, composed of 13 bivalents and two X chromosomes, note the end-to-end association of the X chromosomes. **b** Telophase I, half plate

containing X chromosomes; (**c**-**e**) *Smeringopus ndumo* (X_1X_20). **c** Diakinesis, comprising 13 bivalents and two X chromosomes. **d** Metaphase II, containing X chromosomes (n = 15). **e** Metaphase II, without the sex chromosomes (n = 13); (**f**-**h**) *S. pallidus* ($X_1X_2X_30$). **f** Diakinesis, composed of 13 bivalents and three X chromosomes, sex chromosomes grouped in the middle of the plate. **g** Metaphase II with X chromosomes (n = 16). X chromosomes are associated at the periphery of the plate. They exhibit a slight positive heteropycnosis. **h** Metaphase II, without sex chromosomes (n = 13). Bar = 10 µm.

Additional file 23: Fig. S18. Sex chromosomes of smeringopines with the X0 system. Stained by Giemsa. X = X chromosome. (**a**, **b**) *Crossopriza lyoni*. **a** Metaphase I composed of 11 bivalents and X chromosome. **b** Anaphase I; (**c**, **d**) *Holocnemus pluchei*. **c** Metaphase I, consisting of 13 bivalents and an X chromosome. The X chromosome is placed at the periphery of the plate. Note the association of terminal parts of the X chromosome arms. **d** Metaphase II, including the X chromosome. This element is slightly positively heteropycnotic; (**e**, **f**) *Stygopholcus skotophilus*. **e** Diplotene, composed of 11 bivalents and an X chromosome. **f** Plate formed by two fused sister metaphases II, 2n = 23. Note the positively heteropycnotic X chromosome. Bar = 10 µm.

Additional file 24: Fig. S19. Pholcidae, male germline, behaviour of sex chromosomes prior to meiosis. *Arrow* = sex chromosomes, X_1 = X_1 chromosome, X_2 = X_2 chromosome, Y = Y chromosome. (**a**, **b**) *Muruta tambunan* (X_1X_2Y), mitotic metaphase, chromosomes X_1, X_2, and Y positively heteropycnotic. Chromosomes X_2 and Y are approximately of the same size. **a** Sex chromosomes grouped in the middle of the plate. **b** Chromosomes X_1 and X_2 associated in parallel, Y chromosome released from the association; **c** *Artema nephilit* (X_1X_2Y), early mitotic metaphase, X chromosomes are marked by a dotted line. They are associated in parallel in the middle of the plate. Their condensation is slightly delayed in comparison with the other chromosomes; **d** *Hoplopholcus cecconii* (X_1X_20), transition from mitotic metaphase to anaphase. Chromosome X_1 is placed in the middle of the plate; (**e**, **f**) *Pholcus kindia* (X_1X_2Y). **e** Premeiotic interphase. X chromosomes pair in parallel in the middle of the nucleus. The Y chromosome does not take part in pairing. **f** Preleptotene. Sex chromosomes are associated in the middle of the nucleus, the Y chromosome is more condensed than the X chromosomes. Bar = 10 µm.

Additional file 25: Fig. S20. Pholcidae, male meiosis, condensation and segregation of sex chromosomes. X_1 = X_1 chromosome, X_2 = X_2 chromosome, Y = Y chromosome. **a** *Pholcus kindia* (X_1X_2Y), early diplotene. Y chromosome highly condensed. In contrast, X chromosomes almost decondensed; **b** *Hoplopholcus cecconii* (X_1X_20), late anaphase I. X chromosomes are arranged in parallel and less condensed than the other chromosomes. Moreover, their segregation and separation of their chromatids are delayed. Centromeres of sex chromosomes are formed by a prominent knob; **c** *Cantikus sabah* (X0), diplotene. Sex chromosome forms a highly condensed body; **d** *Hoplopholcus forskali* (X_1X_20), plate formed by fusion of 1) two sister late prometaphases II (left) and 2) two sister early prometaphases II (right). In contrast to autosomes, sex chromosomes differ considerably by condensation in early and late prometaphase II. They are almost decondensed during early prometaphase II (right); **e** *Holocneminus* sp. (X0), plate formed by two sister prometaphases II, sex chromosome forms a highly condensed body; **f** *Micropholcus fauroti* (X0), two fused sister metaphases II. Sex chromosome shows precocious division; **g** *Aetana kinabalu* (X_1X_2Y), late metaphase II, division of X chromosomes is delayed; **h** *Pholcus* sp. (X_1X_2Y), two half-plates of anaphase II containing positively heteropycnotic Y chromosome in the middle; **i** *Psilochorus simoni* (X0), two sister anaphases II. Segregation of X chromosome delayed. This element is slightly positively heteropycnotic at right anaphase II. Bar = 10 µm.

Additional file 26: Fig. S21. Arteminae, *Wugigarra* sp., male meiosis, behaviour of sex chromosomes. X = X chromosome, Y = Y chromosome, II = bivalent containing two chiasmata. **a** Metaphase I, three bivalents include two chiasmata. Pairing of metacentric chromosomes X and Y is ensured by ends of their arms. **b** Two sister metaphases II (separated by dashed line). While X chromosome is placed at the periphery of one plate, Y chromosome is in middle of another plate. Note positive heteropycnosis of sex chromosomes. Bar = 10 µm.

Additional file 27: Fig. S22. *Pholcus* sp. (X_1X_2Y), testes, endopolyploid nucleus. Heterochromatic body in the middle of the nucleus is formed by sex chromosomes (arrow). Inset: a standard diploid nucleus. Bar = 5 µm.

Additional file 28: Appendix S1. Evolution of particular chromosomes of the pholcid X_1X_2Y system.

Additional file 29: Fig. S23. Arteminae, Modisiminae, and Ninetinae: characters of NORs and sex chromosomes mapped on a cladogram. Based on the most recent molecular phylogeny of Pholcidae [20, 21]. Standard continuous lines: low bootstrapping branch support, i.e. < 70%; thick continuous lines: modest to full support of hypotheses, ≥ 70% [21]; discontinuous lines: taxa not included in molecular phylogeny - phylogenetic position is based on cytogenetic data (dashed lines) or unresolved (dotted lines). Number above mark: number of character; number below mark: character state. Full marks: characters without homoplasy; empty marks: homoplasic characters. In some species, data on some characters are missing (information in square brackets). The reconstruction of karyotype evolution is based on our data, except for taxa marked by the formula RX (see reference X for information). See Methods (pp. 32–33) for the coding of characters.

Additional file 30: Fig. S24. Smeringopinae: karyotype characters mapped on a cladogram. Based on the most recent molecular phylogeny of Pholcidae [20, 21]. Standard continuous lines: low bootstrapping branch support, i.e. < 70%; thick continuous lines: modest to full support of hypotheses, ≥ 70% [21]; discontinuous lines: taxa not included in molecular phylogeny - phylogenetic position is based on other sources [79] and/or on cytogenetic data (dashed lines) or unresolved (dotted lines). Number above mark: number of character; number below mark: character state. Full marks: characters without homoplasy; empty marks: homoplasic characters. In some species, data on some characters are missing (information in square brackets). The reconstruction of karyotype evolution is based on our data, except for taxa marked by the formula (RX) (some information taken from reference X). See Methods (pp. 32–33) for coding of the characters.

Additional file 31: Fig. S25. Pholcinae: characters of NORs and sex chromosomes mapped on a cladogram. Based on the most recent molecular phylogeny of Pholcidae [20, 21]. Standard continuous lines: low bootstrapping branch support, i.e. < 70%; thick continuous lines: modest to full support of hypotheses, ≥ 70% [21]; dashed lines: taxa not included in molecular phylogeny - phylogenetic position is based on cytogenetic data. Number above mark: number of character; number below mark: character state. Full marks: characters without homoplasy; empty marks: homoplasic characters. In some species, data on some characters are missing (information in square brackets). The reconstruction of karyotype evolution is based on our data, except for taxa marked by the formula RX (see reference X for information). See Methods (pp. 32–33) for coding of the characters.

Additional file 32: Table S6. Species studied, their instar, sex, collecting data and depositories. Abbreviations: AM = Australian Museum, Sydney, Australia (specimen KS 128687), Co. = county, Hwy = highway, Isl. = island, m = male, Mts. = mountains, N = north, N.P. = national park, NW = northwest, S = south, SL = specimens lost or discarded, sm = subadult male, W = west, ZFMK = Zoological Research Museum Alexander Koenig.

Acknowledgements

Our paper is dedicated to J. Hajer (Purkyně University, Ústí nad Labem, Czech Republic), an outstanding specialist in functional morphology, ethology, life cycles, and spinning of spiders, who drew the attention of the principal authors to pholcids. We are very thankful to the relevant authorities for granting collection permits. We are also much obliged to the following colleagues that collected spiders, organized collections, prepared chromosome slides during expeditions, or determined specimens: N.M. Abdul Aziz, I. Agnarsson, S. Aharon, T. Andersen, R. Bennett, G. Binford, M. Chatzaki, C. Copley, D. Copley, P. Dolejš, M.A. Dias, R. Duncan, E. Gavish-Regev, A.R. Ghazali, A. Giupponi, A.V. Gromov, T.L. Heller, S. Henriquez, S. Huber, M. Johnston Pokorná, M. Komnenov, O. Košulič, C. Kristensen, L. Krkavcová, C. Leh Moi Ung, Y. Lubin, P. Michalik, J.A. Neethling, J.G. Palacios Vargas, S. Pekár, A. Pérez-González, R. Raven, M. Řezáč, J.

Ricetti, C. Rheims, K. Rosová, D.M. Rowell, N. Šejgunovová, M. Sidibe, H. Smith, J. Starrett, L.Sousa Carvalho, A. Valdez-Mondragón, and R. Whyte. Finally, we are grateful to the anonymous reviewers for comments and suggestions on the manuscript.

Authors' contributions
Authors collected specimens (BAH, CRH, FS, IMAH, JK, MF, MH, MK, MP, PJ, PN), determined specimens (BAH, CRH), prepared chromosome slides (FS, IMAH, JK, JM, MF, MH, MK, MP, PJ), performed detection of nucleolus organizer regions by fluorescent in situ hybridization (FS, IMAH, MF, MP, MZ, PN), analysed cytogenetic data (DS, FS, IMAH, JK, JM, MF, MH, MK, MP), made evolutionary analysis of cytogenetic data (BAH, DS, JK), and prepared manuscript (IMAH, JK, MF, TK). All authors contributed to the final manuscript and approved its content. IMAH and JK are principal authors; they contributed equally to the paper. All authors read and approved the final manuscript.

Funding
Authors were supported by Czech Science Foundation (project no. 16-10298S: IMAH, JK, MF, PJ, PN, MK, TK), Grant Agency of the Charles University (project no. 92218: MF), Ministry of Education, Youth, and Sports of the Czech Republic (projects LTAUSA 19142: IMAH, JK, MF, TK; SVV 260314: IMAH, JK, MF; SVV 260571/2021: MH, PJ), German Research Foundation (DFG projects HU 980/9-1, HU 980/11-1: BAH), National Research Foundation of South Africa (projects 97495 and 105318), and Chilean National Commission for Scientific and Technological Research (CONICYT) (IMAH). Fluorescence microscopy was performed in the Laboratory of Confocal and Fluorescence Microscopy, Faculty of Science, Charles University (Prague). This laboratory is co-financed by the European Regional Development Fund and the state budget of the Czech Republic, projects nos CZ.1.05/4.1.00/16.0347 and CZ.2.16/3.1.00/21515, and supported by the Czech-BioImaging large RI project LM2015062. The authors are responsible for the design of the study, the collection, analysis and interpretation of data as well as writing the manuscript. The funding bodies were not involved in the research process.

Availability of data and materials
All supporting data are provided in the additional files. The partial 18S rDNA sequence of *Dysdera erythrina* was deposited in GenBank under the Acc. no. MT886274.

Ethics approval and consent to participate
Not applicable.

Consent for publication
Not applicable.

Competing interests
There are no competing interests.

Author details
[1]Laboratory of Arachnid Cytogenetics, Department of Genetics and Microbiology, Faculty of Science, Charles University, Viničná 5, 128 44 Prague 2, Czech Republic. [2]Research Team of Plant Stress Biology and Biotechnology, Division of Crop Genetics and Breeding, Crop Research Institute, Drnovská 507/73, 161 00 Prague 6, Czech Republic. [3]Prague 1, Czech Republic. [4]Invertebrate Zoology Unit, Department of Zoology, Faculty of Science, Charles University, Viničná 7, 128 44 Prague 2, Czech Republic. [5]Laboratory of Molecular Cytogenetics, Department of Molecular Biology and Genetics, Faculty of Science, University of South Bohemia, Branišovská 31, 370 05 České Budějovice, Czech Republic. [6]Laboratory of Molecular Cytogenetics, Department of Molecular Biology and Genetics, Institute of Entomology, Biology Centre CAS, Branišovská 31, 370 05 České Budějovice, Czech Republic. [7]Research Group of Arachnid Systematics and Ecology, Department of Zoology and Entomology, Faculty of Natural and Agricultural Sciences, University of the Free State, P.O. Box 339, Bloemfontein 9300, Republic of South Africa. [8]Arachnida Section, Alexander Koenig Zoological Research Museum, Adenauerallee 160, 53113 Bonn, Germany.

Received: 16 May 2020 Accepted: 25 January 2021
Published online: 03 May 2021

References

1. Traut W, Ahola V, Smith DAS, Gordon IJ, ffrench-Constant RH. Karyotypes versus genomes: the nymphalid butterflies *Melitaea cinxia*, *Danaus plexippus*, and *D. chrysippus*. Cytogenet Genome Res. 2017;153:46-53.
2. Tomaszkiewicz M, Medvedev P, Makova KD. Y and W chromosome assemblies: approaches and discoveries. Trends Genet. 2017;33:266-82.
3. Deakin JE, Ezaz T. Understanding the evolution of reptile chromosomes through applications of combined cytogenetics and genomics approaches. Cytogenet Genome Res. 2019;157:7-20.
4. Schwager E, Sharma PP, Thomas C, Leite DJ, Wierschin T, Pechmann M, et al. The house spider genome reveals an ancient whole-genome duplication during arachnid evolution. BMC Biol. 2017;15:62.
5. Král J, Kořínková T, Forman M, Krkavcová L. Insights into the meiotic behavior and evolution of multiple sex chromosome systems in spiders. Cytogenet Genome Res. 2011;133:43-66.
6. Král J, Kořínková T, Krkavcová L, Musilová J, Forman M, Ávila Herrera IM, et al. Evolution of karyotype, sex chromosomes, and meiosis in mygalomorph spiders (Araneae: Mygalomorphae). Biol J Linnean Soc. 2013;2:377-408.
7. Král J. Evolution of multiple sex chromosomes in the spider genus *Malthonica* (Araneae: Agelenidae) indicates unique structure of the spider sex chromosome systems. Chromosome Res. 2007;15:863-79.
8. Garb JE, Sharma PP, Ayoub NA. Recent progress and prospects for advancing arachnid genomics. Curr Opin Insect Sci. 2018;25:51-7.
9. Král J, Musilová J, Šťáhlavský F, Řezáč M, Akan Z, Edwards RL, et al. Evolution of the karyotype and sex chromosome systems in basal clades of araneomorph spiders (Araneae: Araneomorphae). Chromosome Res. 2006;14:859-80.
10. Wheeler WC, Coddington JA, Crowley LM, Dimitrov D, Goloboff PA, Griswold CE, et al. The spider tree of life: phylogeny of Araneae based on target-gene analyses from an extensive taxon sampling. Cladistics. 2017;33:574-616.
11. Shao L, Li S. Early Cretaceous greenhouse pumped higher taxa diversification in spiders. Mol Phylogenet Evol. 2018;127:146-55.
12. Michalik P, Kallal R, Dederichs TM, Labarque FM, Hormiga G, Giribet G, et al. Phylogenomics and genital morphology of cave raptor spiders (Araneae, Trogloraptoridae) reveal an independent origin of a flow-through female genital system. J Zool Syst Evol Res. 2019;57:737-47.
13. World Spider Catalog. Version 20.5. Natural History Museum, Bern. 2020. http://wsc.nmbe.ch. Accessed 4 Jan 2020.
14. Král J, Forman M, Kořínková T, Reyes Lerma AC, Haddad CR, Musilová J, et al. Insights into the karyotype and genome evolution of haplogyne spiders indicate a polyploid origin of lineage with holokinetic chromosomes. Sci Rep. 2019;9:3001.
15. Ávila Herrera IM, Carabajal Paladino LZ, Musilová J, Palacios Vargas JG, Forman M, Král J. Evolution of karyotype and sex chromosomes in two families of haplogyne spiders, Filistatidae and Plectreuridae. In: Martins C, Pedrosa-Harand A, Houben A, Sullivan B, Martelli L, O´Neil R. editors. 21st international chromosome conference, Foz do Iguaçu, Brazil. Cytogenet Genome Res. 2016;148:104.
16. Paula-Neto E, Cella DM, Araujo D, Brescovit AD, Schneider MC. Comparative cytogenetic analysis among filistatid spiders (Araneomorphae: Haplogynae). J Arachnol. 2017;45:123-8.
17. Araujo D, Schneider MC, Zacaro AA, de Oliveira EG, Martins R, Brescovit AD. Venomous *Loxosceles* species (Araneae, Haplogynae, Sicariidae) from Brazil: $2n♂ = 23$ and X_1X_2Y sex chromosome system as shared characteristics. Zool Sci. 2020;37:128-39.
18. Kořínková T, Král J. Karyotypes, sex chromosomes, and meiotic division in spiders. In: Nentwig W, editor. Spider ecophysiology. Berlin: Springer; 2013. p. 159-72.
19. McStay B. Nucleolar organizer regions: genomic "dark matter" requiring illumination. Genes Dev. 2016;30:1598-610.
20. Eberle J, Dimitrov D, Valdez-Mondragón A, Huber BA. Microhabitat change drives diversification in pholcid spiders. BMC Evol Biol. 2018;18:141.
21. Huber BA, Eberle J, Dimitrov D. The phylogeny of pholcid spiders: a critical evaluation of relationships suggested by molecular data (Araneae, Pholcidae). ZooKeys. 2018;789:51-101.

22. Huber BA. Phylogeny and classification of Pholcidae (Araneae): an update. J Arachnol. 2011;39:211–22.
23. Huber BA. Pholcidae. In: Roig-Juñent S, Claps LE, Morrone JJ, editors. Biodiversidad de Artrópodos Argentinos, vol. 3. Buenos Aires: Sociedad Entomológica Argentina; 2014. p. 131–40.
24. Araujo D, Schneider MC, Paula-Neto E, Cella DM. The spider cytogenetic database. 2020. http://www.arthropodacytogenetics.bio.br/spiderdatabase. Accessed 30 Jan 2020.
25. Lomazi RL, Araujo D, Carvalho LS, Schneider MC. Small pholcids (Araneae: Synspermiata) with big surprises: the lowest diploid number in spiders with monocentric chromosomes. J Arachnol. 2018;46:45–9.
26. Araujo D, Brescovit A, Rheims C, Cella D. Chromosomal data of two pholcids (Araneae, Haplogynae): a new diploid number and the first cytogenetical record for the New World clade. J Arachnol. 2005;2:591–6.
27. Ramalho M, Araujo D, Schneider M, Brescovit A, Cella D. *Mesabolivar brasiliensis* (Moenkhaus 1898) and *Mesabolivar cyaneotaeniatus* (Keyserling 1891) (Araneomorphae, Pholcidae): close relationship reinforced by cytogenetic analyses. J Arachnol. 2008;36:453–6.
28. Bole-Gowda B. A study of the chromosomes during meiosis in twenty-two species of Indian spiders. Proc Zool Soc Bengal. 1958;2:69–108.
29. Srivastava M, Shukla S. Chromosome number and sex-determining mechanism in forty-seven species of Indian spiders. Chromos Inf Serv. 1986;41:23–6.
30. Oliveira RM, Jesus AC, Brescovit AD, Cella DM. Chromosomes of *Crossopriza lyoni* (Blackwall 1867), intraindividual numerical chromosome variation in *Physocyclus globosus* (Taczanowski 1874), and the distribution pattern of NORs (Araneomorphae, Haplogynae, Pholcidae). J Arachnol. 2007;35:293–306.
31. Golding AE, Paliulis LV. Karyotype, sex determination, and meiotic chromosome behavior of two pholcid (Araneomorphae, Pholcidae) spiders: implications for karyotype evolution. PLoS ONE. 2011;9:e24748.
32. Arunkumar S, Jayaprakash. Chromosomal studies of two spider species of Pholcidae (Aranae: Haplogynae). Int J Curr Res. 2015;2:2650–3.
33. Parida B, Sharma N. Chromosome number, sex mechanism and genome size in 27 species of Indian spiders. Chromos Inf Serv. 1987;43:11–3.
34. Sharma N, Parida BB. Study of chromosomes in spiders from Orissa. Pranikee. 1987;8:71–6.
35. Wang X, Cui S, Yang Z, Wang J, Wang Y. On karyotype of the *Pholcus affinis* (Araneida: Pholcidae). Acta Arachnol Sin. 1997;1:19–22.
36. Garrison NL, Rodriguez J, Agnarsson I, Coddington JA, Griswold CE, Hamilton CA, et al. Spider phylogenomics: untangling the spider tree of life. PeerJ. 2016;4:e1719.
37. Fernández R, Kallal RJ, Dimitrov D, Ballesteros JA, Arnedo M, Giribet G, et al. Phylogenomics, diversification dynamics, and comparative transcriptomics across the spider tree of life. Curr Biol. 2018;13:2190–3.
38. Suzuki S. Cytological studies in spiders. III. Studies on the chromosomes of fifty-seven species of spiders belonging to seventeen families, with general considerations on chromosomal evolution. J Sci Hiroshima Univ Ser B. 1954;2:23–136.
39. Sharma S, Ramakrishna S. Cytological studies on three species of Indian spiders. Int J Adv Sci Res Manag. 2019;4:1–6.
40. Rieseberg LH. Chromosomal rearrangements and speciation. Trends Ecol Evol. 2001;7:351–8.
41. Ayala F, Coluzzi M. Chromosome speciation: humans, *Drosophila*, and mosquitoes. Proc Natl Acad Sci USA. 2005;1:6535–42.
42. Silva D. Estudio cariotípico de *Loxosceles laeta* (Araneae: Loxoscelidae). Rev Perú Ent. 1988;31:9–12.
43. Silva RW, Klisiowicz DR, Cella DM, Mangili OC, Sbalqueiro IJ. Differential distribution of constitutive heterochromatin in two species of brown spider: *Loxosceles intermedia* and *L. laeta* (Araneae, Sicariidae), from the metropolitan region of Curitiba, PR (Brazil). Acta Biol Par Curitiba. 2002;31:123–36.
44. Selden PA, Penney D. Fossil spiders. Biol Rev Camb Philos Soc. 2009;85:171–206.
45. Araujo D, Schneider MC, Paula-Neto E, Cella DM. Sex chromosomes and meiosis in spiders: a review. In: Swan A, editor. Meiosis: molecular mechanisms and cytogenetic diversity. Rijeka: InTech; 2012. p. 87–108.
46. Řezáč M, Král J, Musilová J, Pekár S. Unusual karyotype diversity in the European spiders of the genus *Atypus* (Araneae: Atypidae). Hereditas. 2006;143:123–9.
47. Souza LB, Brescovit AD, Araujo DS. A new species of *Synotaxus* and the first chromosomal study on Synotaxidae, presenting a rare XY sex chromosome system in spiders (Araneae, Araneoidea). Zootaxa. 2017;4303:140–50.
48. Araujo D, Oliveira EG, Giroti AM, Mattos VF, Paula-Neto E, Brescovit AD, et al. Comparative cytogenetics of seven Ctenidae species (Araneae). Zool Sci. 2014;31:83–8.
49. Datta SN, Chatterjee K. Chromosomes and sex determination in 13 araneid spiders of North-Eastern India. Genetica. 1988;76:91–9.
50. Mahadevaiah SK, Lovell-Badge R, Burgoyne PS. Tdy-negative XY, XXY and XYY female mice: breeding data and synaptonemal complex analysis. J Reprod Fertil. 1993;97:151–60.
51. Maddison WP. XXXY sex chromosomes in males of the jumping spider genus *Pellenes* (Araneae: Salticidae). Chromosoma. 1982;5:23–37.
52. Rowell DM. Complex sex-linked fusion heterozygosity in the Australian huntsman spider *Delena cancerides* (Araneae: Sparassidae). Chromosoma. 1985;93:169–76.
53. Maddison WP, Leduc RG. Multiple origins of sex chromosome fusions correlated with chiasma localization in *Habronattus* jumping spiders (Araneae: Salticidae). Evolution. 2013;67:2258–72.
54. Martin LT. Sex chromosome translocations in the evolution of reproductive isolation. Genetics. 1972;72:317–33.
55. Presgraves DC. Sex chromosomes and speciation in *Drosophila*. Trends Genet. 2008;24:336–43.
56. Kitano J, Ross JA, Mori S, Kume M, Jones FC, Chan YF, et al. A role for a neo-sex chromosome in stickleback speciation. Nature. 2009;461:1079–83.
57. Hooper DM, Griffith SC, Price TD. Sex chromosome inversions enforce reproductive isolation across an avian hybrid zone. Mol Ecol. 2019;28:1246–62.
58. Lima TG. Higher levels of sex chromosome heteromorphism are associated with markedly stronger reproductive isolation. Nat Commun. 2014;5:4743.
59. Miller DA, Dev VG, Tantravahi R, Miller OJ. Suppression of human nucleolus organizer activity in mouse-human somatic hybrid cells. Exp Cell Res. 1976;101:235–43.
60. Dunlop JA, Penney D, Jekel D. A summary list of fossil spiders and their relatives. In: World Spider Catalog. Natural History Museum Bern. version 20.0. 2019. http://wsc.nmbe.ch. Accessed 4 Jan 2020.
61. Dimitrov D, Astrin JJ, Huber BA. Pholcid spider molecular systematics revisited, with new insights into the biogeography and the evolution of the group. Cladistics. 2013;29:132–46.
62. McKee BD, Karpen GH. *Drosophila* ribosomal RNA genes function as an X-Y pairing site during male meiosis. Cell. 1990;61:61–72.
63. Mandrioli M, Bizzaro D, Giusti M, Manicardi GC, Bianchi U. The role of rDNA genes in X chromosome association in the aphid *Acyrthosiphon pisum*. Genome. 1999;42:381–6.
64. Roy V, Monti-Dedieu L, Chaminade N, Siljak-Yakovlev S, Aulard S, Lemeunier F, et al. Evolution of the chromosomal location of rDNA genes in two *Drosophila* species subgroups: *ananassae* and *melanogaster*. Heredity. 2005;94:388–95.
65. Forman M, Nguyen P, Hula P, Král J. Sex chromosome pairing and extensive NOR polymorphism in *Wadicosa fidelis* (Araneae: Lycosidae). Cytogenet Genome Res. 2013;1:43–9.
66. Mittal OP. Karyological studies on the Indian spiders VI. Chromosome number and sex-determining mechanism in the family Araneidae. Res Bull Panjab Univ Sci. 1966;17:335–51.
67. Benavente R, Wettstein R. Ultrastructural characterization of the sex chromosomes during spermatogenesis of spiders having holocentric chromosomes and a long diffuse stage. Chromosoma. 1980;77:69–81.
68. John B. Meiosis. 3rd ed. Cambridge: Cambridge University Press; 1990.
69. Lukaszewski AJD, Kopecky G. Inversions of chromosome arms 4AL and 2BS in wheat invert the patterns of chiasma distribution. Chromosoma. 2012;121:201–8.
70. Alberti G, Weinmann C. Fine structure of spermatozoa of some labidognath spiders (Filistatidae, Segestriidae, Dysderidae, Oonopidae, Scytodidae, Pholcidae; Araneae; Arachnida) with remarks on spermiogenesis. J Morphol. 1985;185:1–35.
71. Sokolow II. Endomitotic polyploidy in testicular epithelial cells of spiders (Araneina). II. Cytology. 1967;9:257–64. (in Russian).

72. Gregory TR, Shorthouse DP. Genome sizes of spiders. J Hered. 2003;94:285–90.
73. Hackman W. Chromosomenstudien an Araneen mit besonderer Berücksichtigung der Geschlechtschromosomen. Acta Zool Fennica. 1948;54:1–101.
74. Huber BA. Southern African pholcid spiders: revision and cladistic analysis of *Quamtana* gen. nov. and *Spermophora* Hentz (Araneae: Pholcidae), with notes on male-female covariation. Zool J Linn Soc. 2003;139:477–527.
75. Brignoli PM. Beitrag zur Kenntnis der mediterranen Pholcidae (Arachnida, Araneae). Mitt Zool Mus Berlin. 1971;47:255–67.
76. Brignoli PM. Ragni di Grecia IX. Specie nuove o interessanti delle famiglie Leptonetidae, Dysderidae, Pholcidae ed Agelenidae (Araneae). Rev Suisse Zool. 1976;83:539–78.
77. Brignoli PM. Spiders from Lebanon, V. On *Hoplopholcus cecconii* Kulczynski, 1908 (Pholcidae). Bull Br Arachnol Soc. 1979;4:350–2.
78. Huber BA. New World pholcid spiders (Araneae: Pholcidae): a revision at generic level. Bull Am Mus Nat Hist. 2000;254:1–348.
79. Huber BA. Revision and cladistic analysis of the Afrotropical endemic genus *Smeringopus* Simon, 1890 (Araneae: Pholcidae). Zootaxa. 2012;3461:1–138.
80. Dolejš P, Kořínková T, Musilová J, Opatová V, Kubcová L, Buchar J, et al. Karyotypes of central European spiders of the genera *Arctosa*, *Tricca* and *Xerolycosa* (Araneae: Lycosidae). Eur J Entomol. 2011;108:1–16.
81. Levan AK, Fredga K, Sandberg AA. Nomenclature for centromeric position on chromosomes. Hereditas. 1964;52:201–20.
82. Cokendolpher JC. Karyotypes of three spider species (Araneae: Pholcidae: *Physocyclus*). J N Y Entomol Soc. 1989;97:475–8.
83. Cokendolpher JC, Brown JD. Air-dry method for studying chromosomes of insects and arachnids. Entomol News. 1985;3:114–8.
84. Galián J, Proenca SJR, Vogler AP. Evolutionary dynamics of autosomal-heterosomal rearrangements in a multiple-X chromosome system of tiger beetles (Cicindelidae). BMC Evol Biol. 2007;7:158.
85. Graves JAM, Wakefield MJ, Toder R. The origin and evolution of pseudoautosomal regions of human sex chromosomes. Hum Mol Genet. 1998;7:1991–6.
86. Bačovský V, Čegan R, Šimoníková D, Hřibová E, Hobza R. The formation of sex chromosomes in *Silene latifolia* and *S. dioica* was accompanied by multiple chromosomal rearrangements. Front Plant Sci. 2020;11:205.
87. Kejnovský E, Hobza R, Čermák T, Kubát Z, Vyskot B. The role of repetitive DNA in structure and evolution of sex chromosomes in plants. Heredity. 2009;102:533–41.
88. Schartl M, Schmid M, Nanda I. Dynamics of vertebrate sex chromosome evolution: from equal size to giants and dwarfs. Chromosoma. 2016;125:553–71.

Publisher's Note

Supplementary Information

Evolutionary pattern of karyotypes and meiosis in pholcid spiders (Araneae: Pholcidae): implications for reconstructing chromosome evolution of araneomorph spiders.

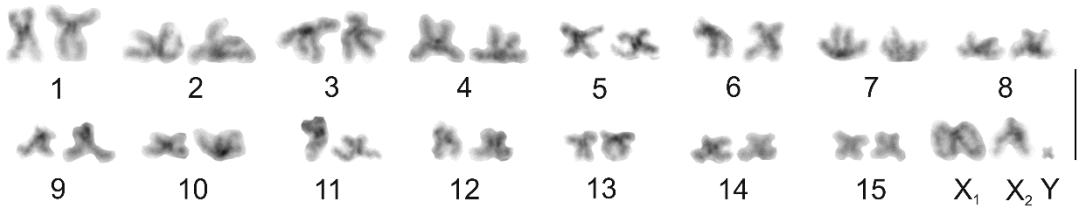

Additional file 3: Fig. S1. Arteminae, *Artema atlanta*, male karyotype, stained by Giemsa. Based on two sister metaphases II. Chromosomes metacentric, except for four submetacentric pairs (nos 1, 6, 9, 12) and subtelocentric X_2 chromosome. Note low condensation of X chromosomes. Bar = 10 μm.

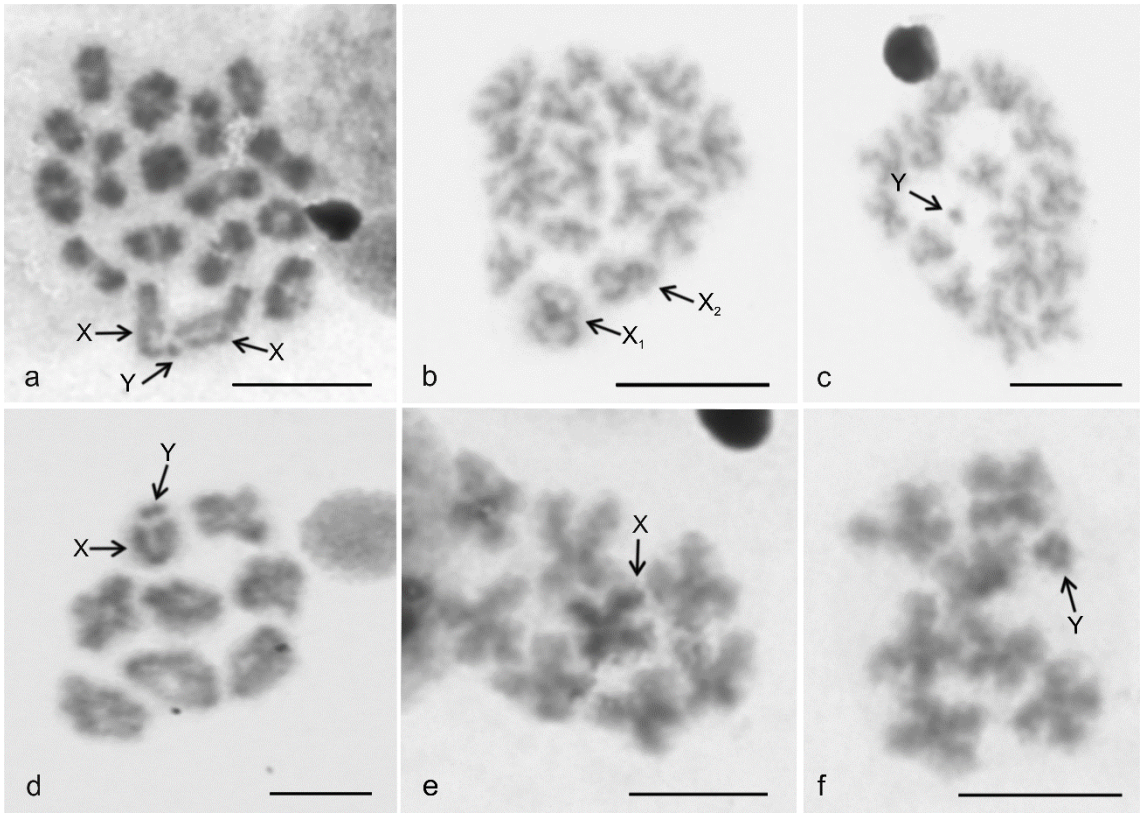

Additional file 4: Fig. S2. Sex chromosomes of artemines with the X_1X_2Y and XY systems. Stained by Giemsa. X_1 = X_1 chromosome, X_2 = X_2 chromosome, Y = Y chromosome. (a–c) *Artema atlanta* (X_1X_2Y). a Metaphase I, composed of 15 bivalents and sex chromosome trivalent. b Metaphase II, with chromosomes X_1 and X_2 at the periphery of the plate. c Metaphase II with Y chromosome. (d–f) *Wugigarra* sp. d Metaphase I, consisting of seven bivalents and a XY pair. e Metaphase II containing a positively heteropycnotic X chromosome (n = 8). f Metaphase II, containing a Y chromosome (n = 8). Bar = 10 μm.

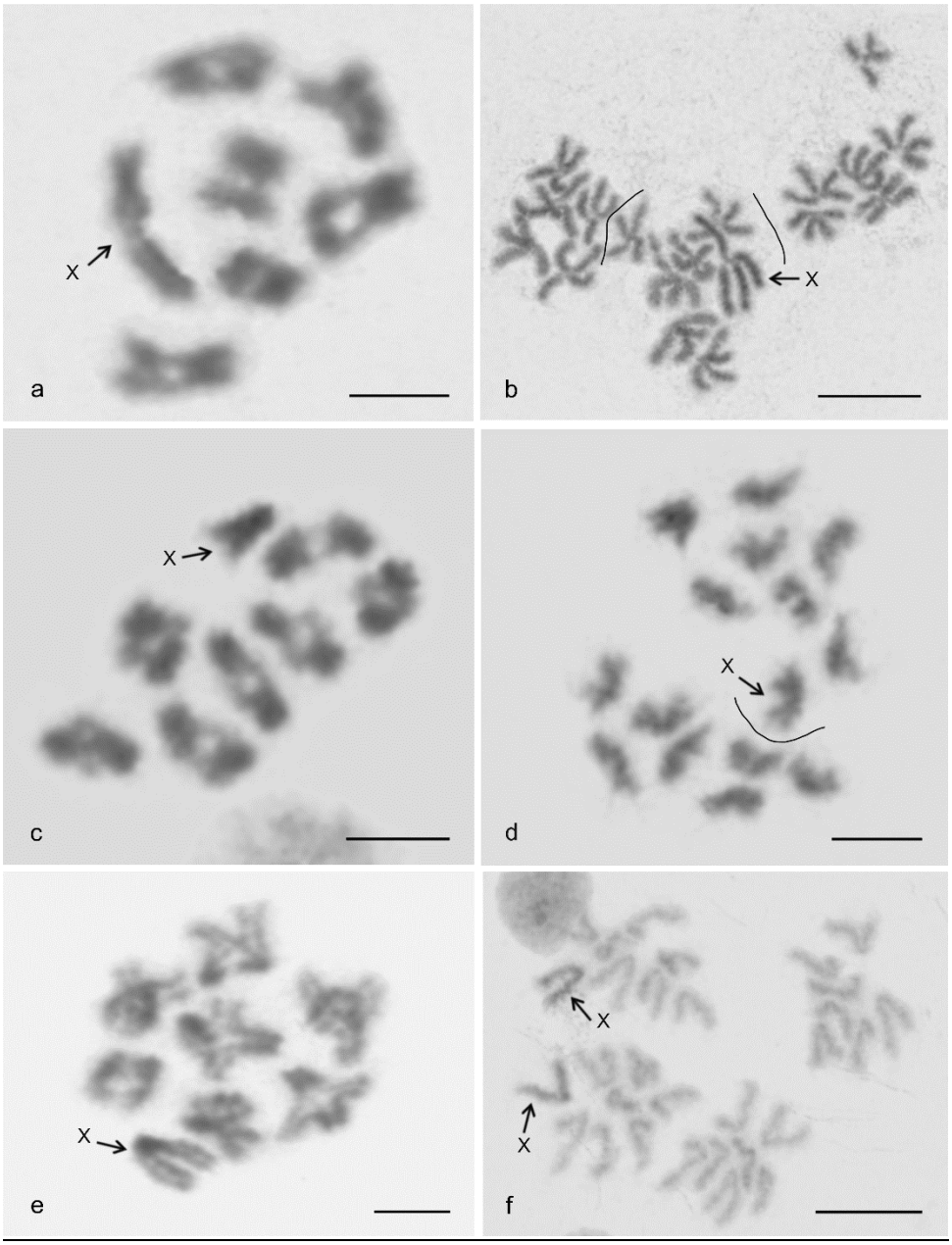

Additional file 5: Fig. S3. Sex chromosomes of artemines with the X0 system. Stained by Giemsa. X = X chromosome. (a, b) *Chisosa diluta*. a Metaphase I, consisting of six bivalents and a peripheral X chromosome. b Group of metaphases II separated by lines. It consists of one metaphase containing a positively heteropycnotic X chromosome (n = 7, in the middle of the plate) and two metaphases without sex chromosome (left metaphase is incomplete); (c, d) *Holocneminus* sp. c Metaphase I, comprising seven bivalents and peripheral X chromosome. d Two sister metaphases II separated by a line (n = 8 including X chromosome + n = 7); (e, f) *Physocyclus dugesi*. e Diplotene, comprising seven bivalents and peripheral X chromosome. f Anaphase II. Note slight positive heteropycnosis of X chromosome. Bar = 10 μm.

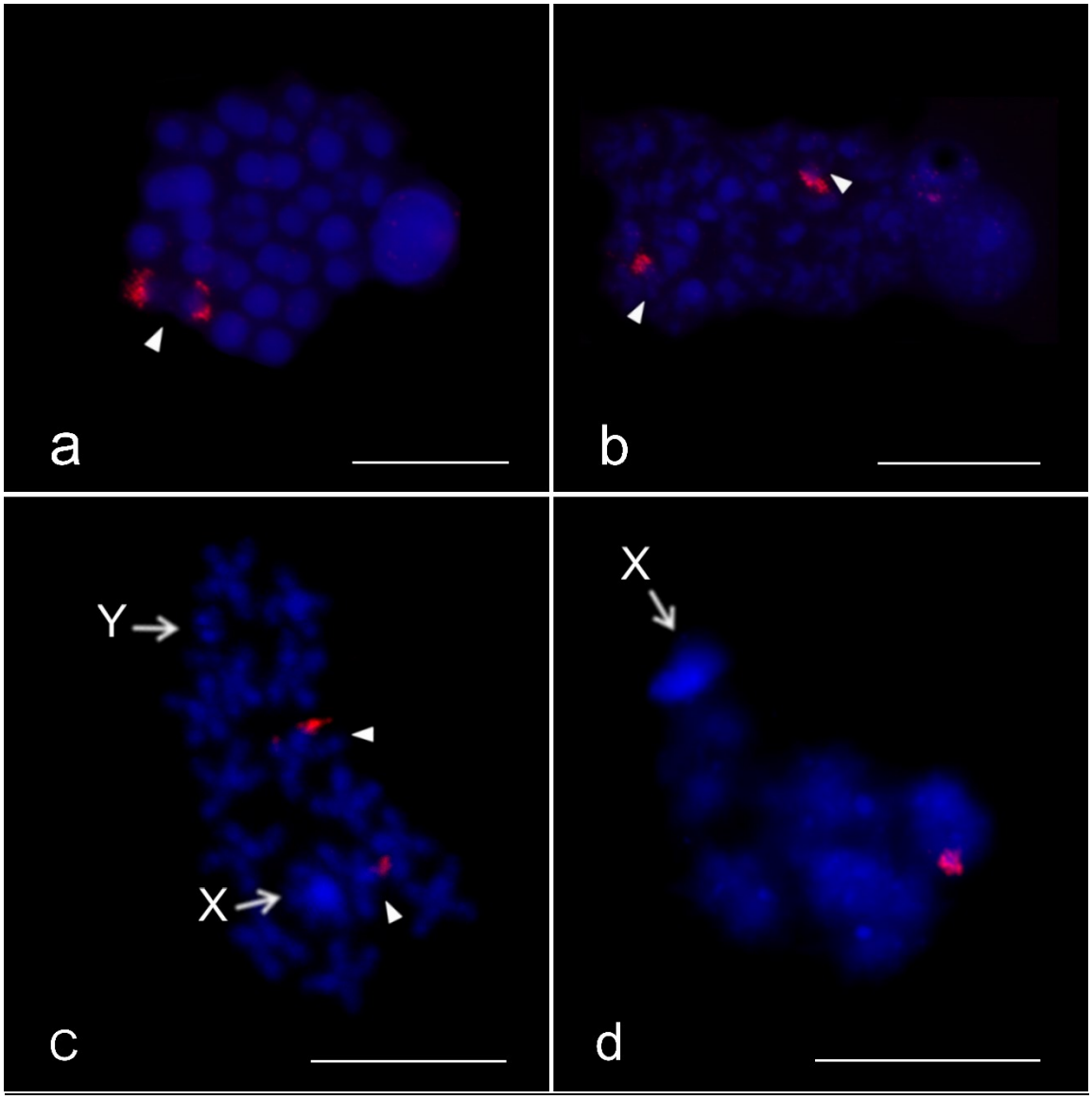

Additional file 6: Fig. S4. Arteminae, males, detection of NORs (FISH). Arrowhead = NOR-bearing chromosome (b, c) or bivalent (a, d), X = X chromosome, Y = Y chromosome. (a, b) *Artema atlanta* (X_1X_2Y). a Metaphase I, note NOR-bearing bivalent. b Two fused sister metaphases II, one pair of submetacentric chromosomes bears a terminal NOR; c *Wugigarra* sp. (XY), two fused sister metaphases II. Note chromosomes of a subtelocentric pair bearing terminal NOR at the end of short arm; d *Chisosa diluta* (X0), diffuse stage, one bivalent includes a NOR. Bar = 10 μm.

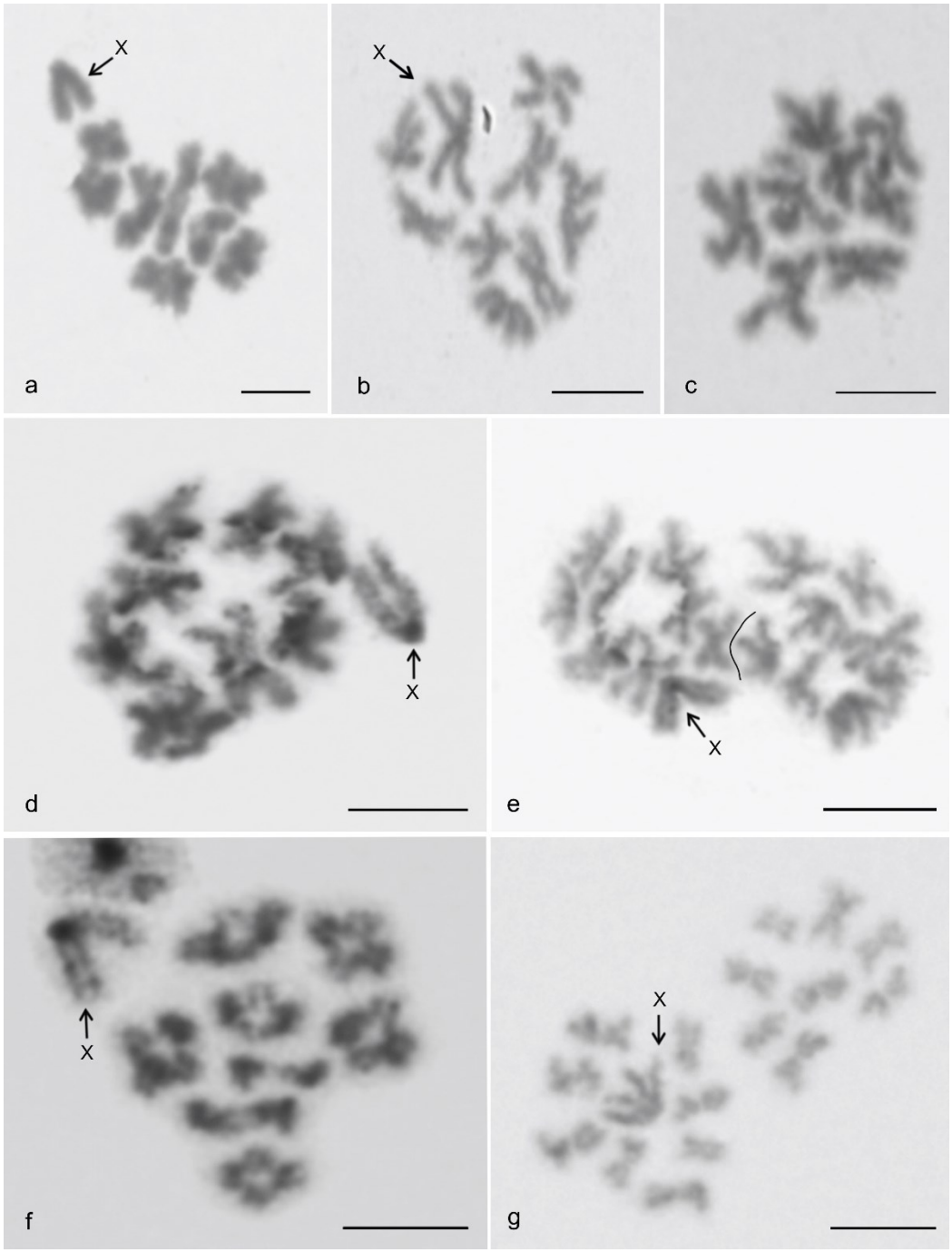

Additional file 8: Fig. S5. Sex chromosome systems of modisimines. Stained by Giemsa. X = X chromosome. (a–c) *Anopsicus* sp. (X0) a metaphase I, consisting of eight bivalents and peripheral X chromosome. b Metaphase II, including X chromosome (n = 9). c Metaphase II, without X chromosome (n = 8); (d, e) *Modisimus* cf. *elongatus* (X0). d Diplotene, comprising eight bivalents and a peripheral X chromosome. e Two sister metaphases II separated by a line (n = 8 + n = 9, including peripheral X chromosome); (f, g) *Psilochorus pallidulus* (X0). f Diplotene, comprising eight bivalents and peripheral X chromosome. g Two sister metaphases II (n = 9, including X chromosome + n = 8). Bar = 10 μm.

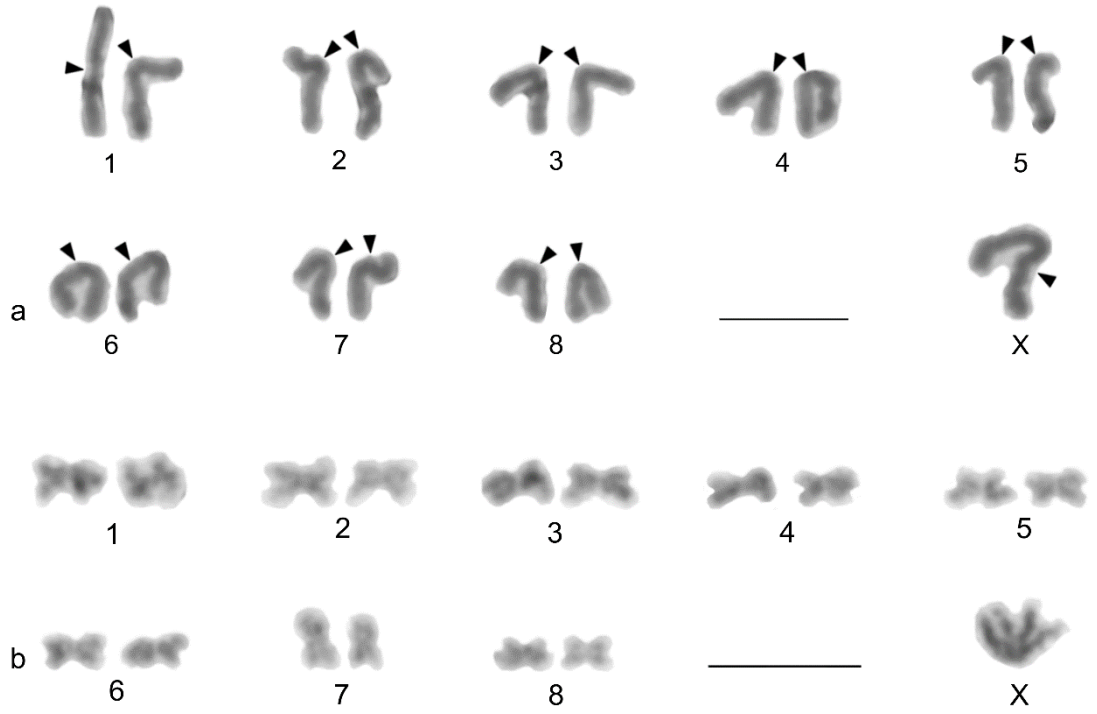

Additional file 9: Fig. S6. *Psilochorus* (Modisiminae), male karyotypes, stained by Giemsa. Sex chromosome is the longest element of the karyotype. a *Psilochorus californiae*. Karyotype metacentric, except for two submetacentric (nos 2, 7) and one subtelocentric pairs (no. 5). Based on spermatogonial metaphase, centromeres marked by arrowheads; b *P. pallidulus*. Chromosomes metacentric. Based on two sister metaphases II. Bar = 10 μm.

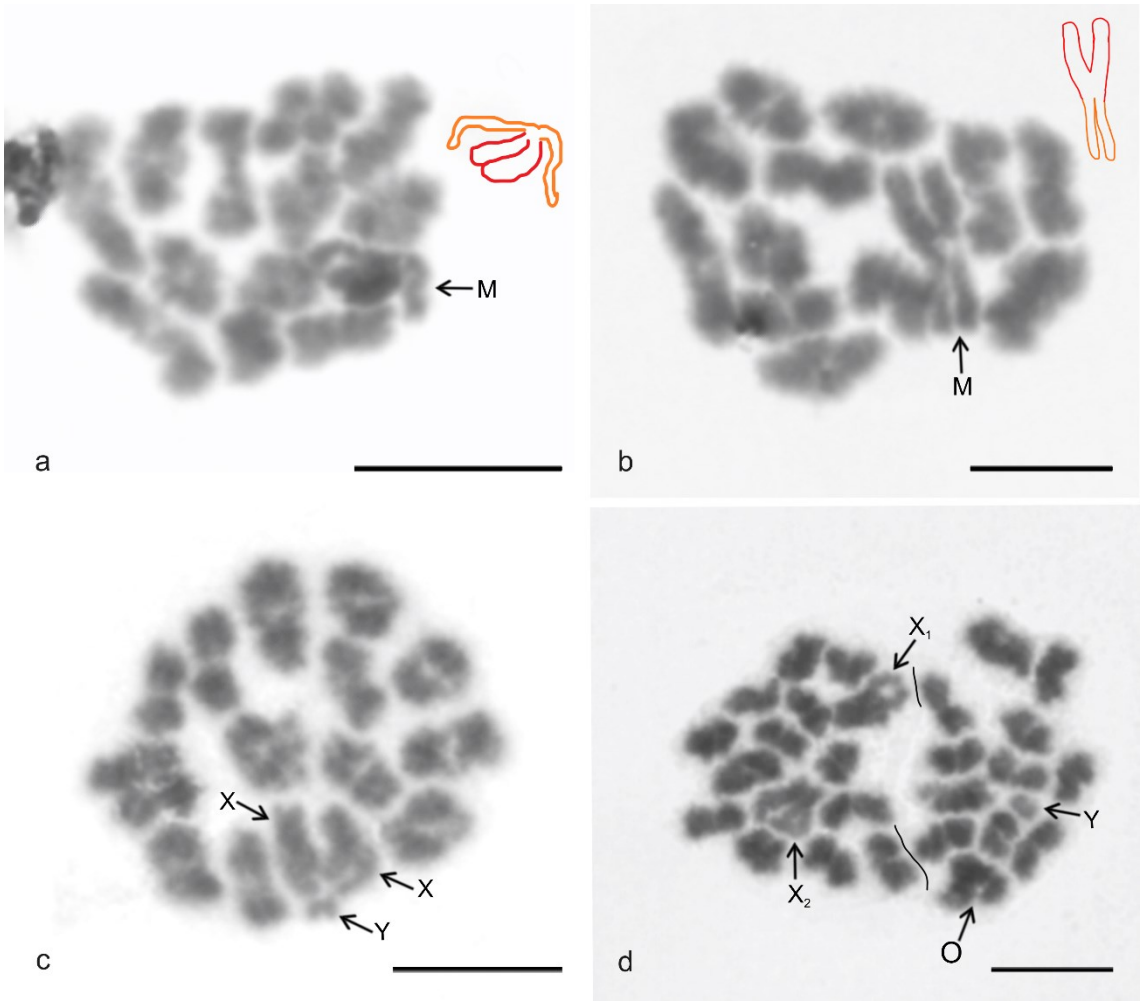

Additional file10: Fig. S7. Sex chromosome systems of ninetines. Stained by Giemsa. Figures a and b contain a scheme of the multivalent. M = sex chromosome multivalent, O = overlapping of two bivalents, X = X chromosome, X_1 = X_1 chromosome, X_2 = X_2 chromosome, Y = Y chromosome. (a, b) *Kambiwa neotropica* ($X_1X_2X_3X_4Y$), plates of the first meiotic division consisting of 12 bivalents plus a sex chromosome multivalent consisting of four "arms". Two "arms" are thick (red) and two are thin (orange). a Diakinesis. b Metaphase I. Note cross-shaped morphology of multivalent; (c, d) Pholcophora americana (X_1X_2Y). c Diakinesis, comprising 13 bivalents and sex chromosomes X_1, X_2, and Y. Sex chromosomes show end-to-end paring. d Two sister metaphases II separated by a line (n = 15, including chromosomes X_1 and X_2 + n = 14 including Y microchromosome). Bar = 10 µm.

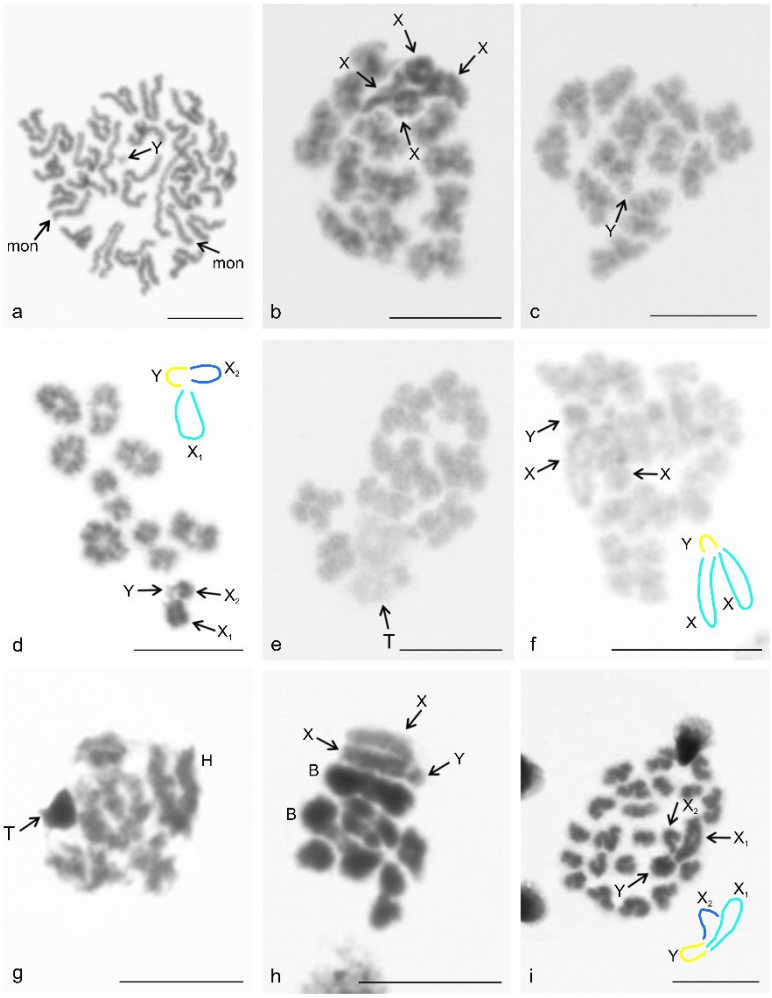

Additional file 11: Fig. S8. Cytogenetics of ninetines (a–c) and pholcines (d–i), male germline. Figures d, f, i contain scheme of sex chromosome trivalent X_1X_2Y. B = large bivalent, H = large bivalent exhibiting positive heteropycnosis, mon = monoarmed X chromosome, T = sex chromosome trivalent, X = X chromosome, X_1 = X_1 chromosome, X_2 = X_2 chromosome, Y = Y chromosome. (a–c) *Kambiwa neotropica* ($X_1X_2X_3X_4Y$). a Spermatogonial metaphase (2n = 29). Chromosomes are biarmed, except for two monoarmed chromosomes. b Metaphase II, consisting of 12 chromosomes and cluster of four positively heteropycnotic X chromosomes. c Metaphase II, formed by 12 chromosomes and a Y microchromosome; d *Aetana kinabalu* (X_1X_2Y), incomplete metaphase I. Sex chromosomes pair by ends of their arms, X chromosomes are positively heteropycnotic; (e, f) Metagonia sp. (X_1X_2Y), late prophase I. Note low chromosome condensation. e Diplotene. Plate consists of eight bivalents and almost decondensed sex chromosomes. f Diakinesis, note the X_1X_2Y trivalent, Y chromosome more condensed than X chromosomes; (g, h) *Pehrforsskalia conopyga* (X_1X_2Y). g Early diplotene. Note sex chromosomes forming a compact positively heteropycnotic body and large positively heteropycnotic bivalent. h Metaphase I, formed by seven bivalents and sex chromosome trivalent. Two bivalents (B) are much longer than the remaining ones. Note tiny Y chromosome; i *Pholcus bamboutos* (X_1X_2Y), transition from metaphase to anaphase I. Note the delayed separation of sex chromosomes. Only one end of the X_2 chromosome takes part in pairing. The Y chromosome is positively heteropycnotic. Bar = 10 µm.

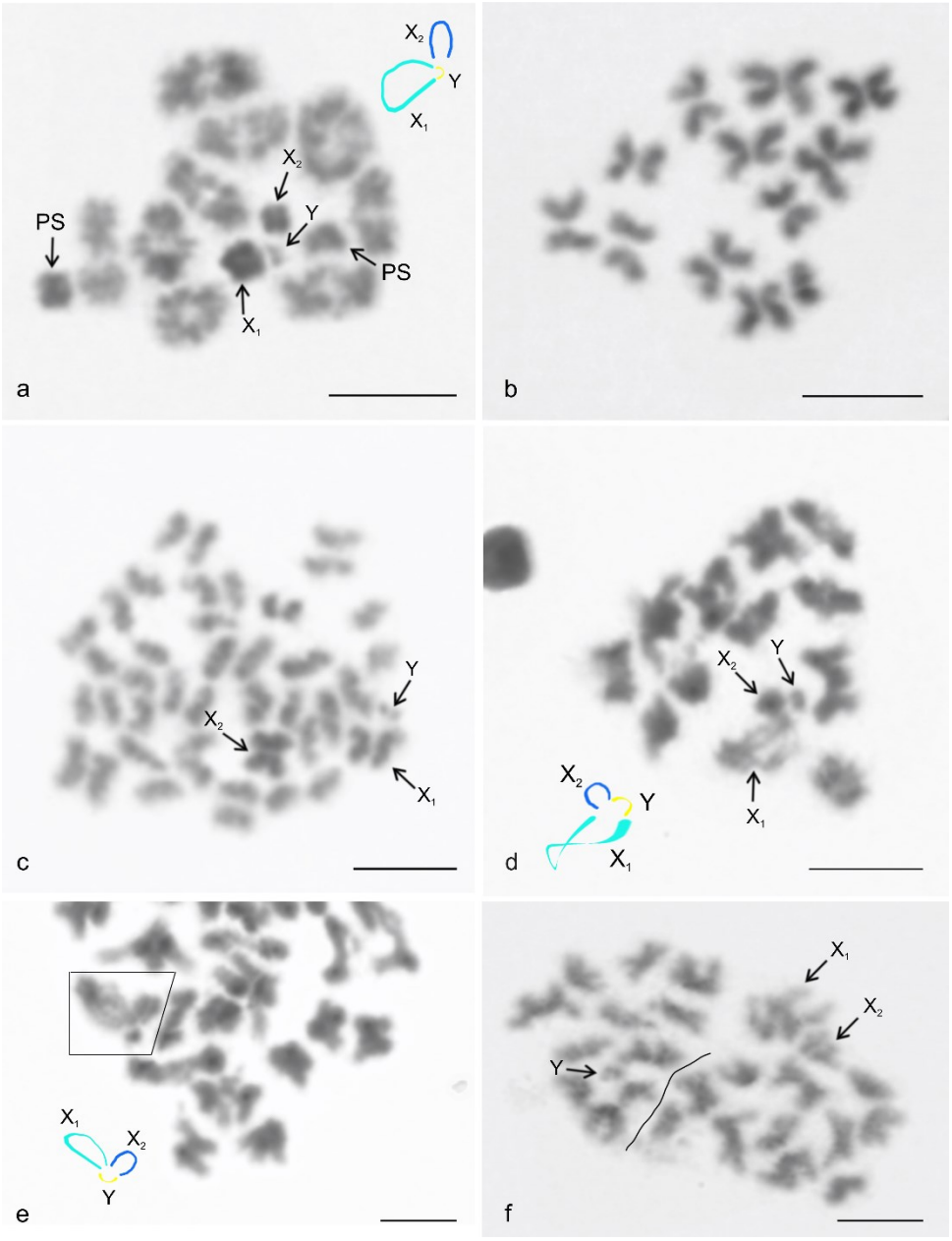

Additional file 13: Fig. S9. Sex chromosomes of pholcines with the X_1X_2Y system, part I. Stained by Giemsa. Figures a, d, e contain a scheme of the sex chromosome trivalent. X_1 = X_1 chromosome, X_2 = X_2 chromosome, Y = Y chromosome, PS = precocious separation of chromosomes of the bivalent. (a–c) *Aetana kinabalu*. a Metaphase I, comprising 11 bivalents (one bivalent shows a precocious separation of chromosomes) and a sex chromosome trivalent. X chromosomes are positively heteropycnotic. b Metaphase II, containing X chromosomes (n = 12). c Transition metaphase II/anaphase II, fusion of two sister plates. Note X chromosomes exhibiting a delayed separation of chromatids and a Y microchromosome; (d–f) *Nipisa deelemanae*. d Metaphase I, comprising 11 bivalents and sex chromosome trivalent. e Part of a plate formed by several fused metaphases I, sex chromosome trivalent encircled. f Two sister metaphases II separated by a line (n = 12, including Y microchromosome + n = 13 including metacentric chromosomes X_1 and X_2). Note the reduction of the X_2 chromosome. Bar = 10 μm.

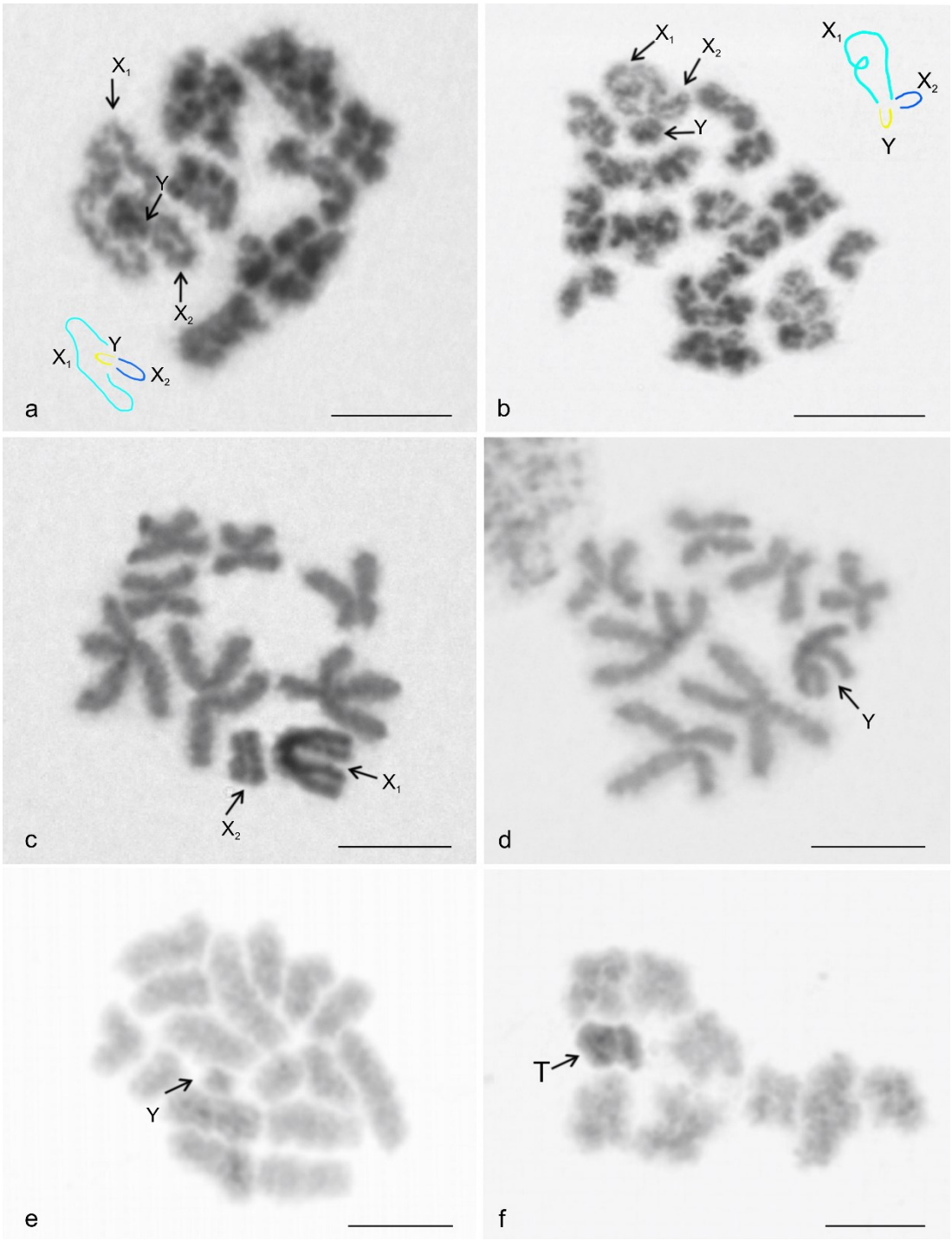

Additional file14: Fig. S10. Sex chromosomes of pholcines with the X_1X_2Y system, part II. Stained by Giemsa. Figures a, b contain a scheme of the sex chromosome trivalent. T = trivalent, X_1 = X_1 chromosome, X_2 = X_2 chromosome, Y = Y chromosome. (a–d) *Leptopholcus guineensis*. a Early diplotene, consisting of seven bivalents and a sex chromosome trivalent, X chromosomes exhibit a low condensation. b Two fused diplotene. c Metaphase II, including X chromosomes (n = 9). X_1 chromosome is positively heteropycnotic. d Metaphase II, including a Y chromosome (n = 8); (e, f) *Metagonia* sp. e Spermatogonial metaphase, note the Y microchromosome. f Diplotene, note the positively heteropycnotic body formed by the sex chromosomes. Bar = 10 µm.

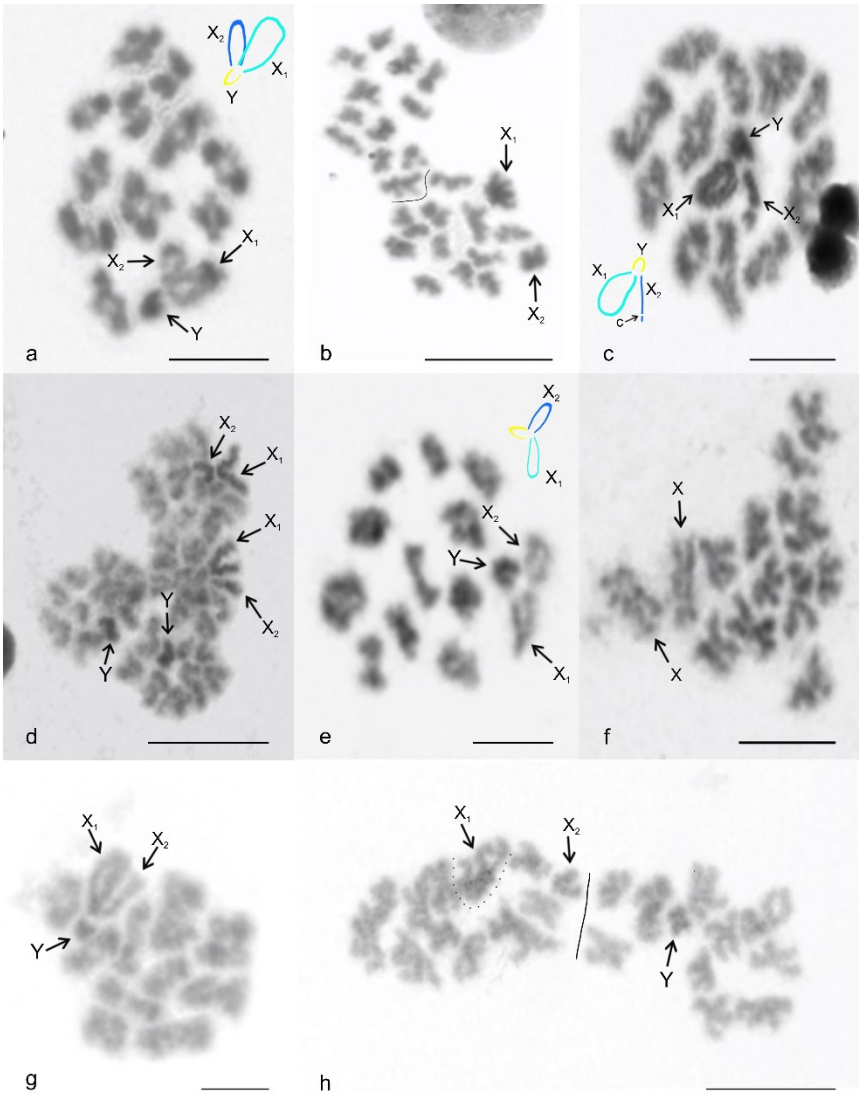

Additional file15: Fig. S11. Sex chromosomes of pholcines with the X_1X_2Y system, part III. Stained by Giemsa. Figures a, c, e contain a scheme of the sex chromosome trivalent. c = centromere, X_1 = X_1 chromosome, X_2 = X_2 chromosome, Y = Y chromosome. (a, b) *Muruta tambunan*. a Diakinesis, consisting of 11 bivalents and a sex chromosome trivalent. b Two sister metaphases II separated by a line (n = 12, including Y chromosome + n = 13 including chromosomes X_1 and X_2). Note the metacentric X_1 chromosome and submetacentric X_2 chromosome on the periphery of the plate. They exhibit positive heteropycnosis; (c, d) *Pholcus phalangioides*. c Diakinesis, comprising 11 bivalents and a sex chromosome trivalent, which is placed in the middle of the plate and exhibits positive heteropycnosis. Concerning the X_2 chromosome, only end of the long arm is involved in pairing. d Anaphase II. Note the positive heteropycnosis of the sex chromosomes. The X chromosomes are associated; (e, f) *Spermophora senoculata*. e Metaphase I, comprising 11 bivalents and a sex chromosome trivalent. f Metaphase II, X chromosomes are less condensed than the other chromosomes; (g, h) *Quamtana hectori*. g Metaphase I, composed of 10 bivalents and a sex chromosome trivalent. Concerning the X_2 chromosome, only one end is involved in pairing. h Two sister metaphases II separated by a line (n = 11 including Y chromosome + n = 12 including chromosomes X_1 and X_2). Bar = 10 μm.

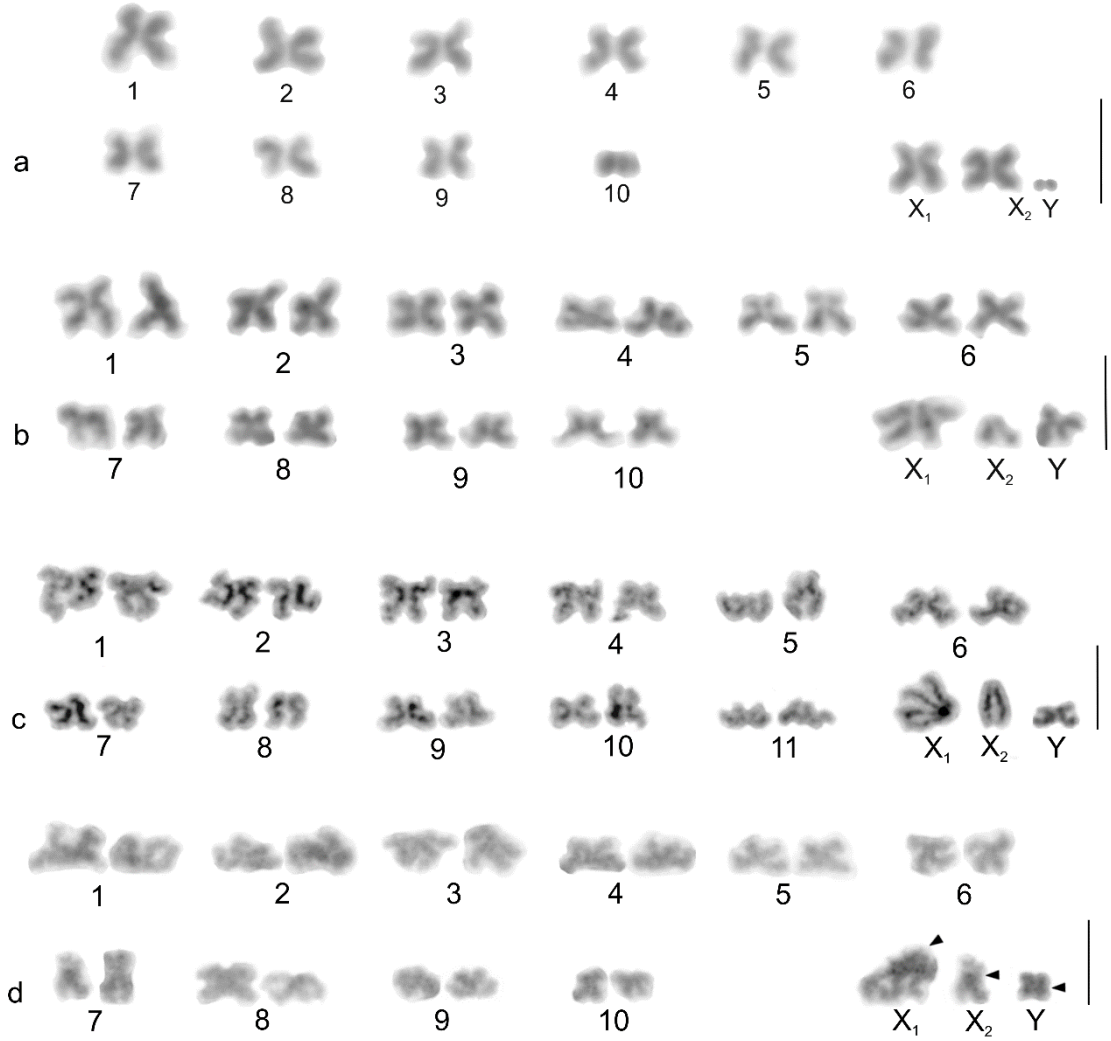

Additional file 16: Fig. S12. Pholcinae, male karyotypes, Giemsa staining. Based on metaphase II (a) or two sister metaphases II (b–d). a *Aetana kinabalu*, haploid set, karyotype metacentric except for submetacentric X_1 chromosome and acrocentric chromosome (no. 10), which is considerably reduced in comparison with preceding chromosome. The Y chromosome is from another metaphase II. Morphology of the Y chromosome is unresolved; b *Pholcus pagbilao*. Karyotype is metacentric except for three submetacentric pairs (nos 5, 7, 10), submetacentric Y chromosome, and acrocentric X_2; c *P. opilionoides*, chromosomes metacentric except for five submetacentric pairs (nos 2–6) and acrocentric X_2. Chromosome X_1 is the longest chromosome of karyotype. On the contrary, Y is the smallest one. Y chromosome is replaced by Y from another plate; d *Quamtana hectori*. Karyotype metacentric, except for acrocentric X_2. Centromeres of sex chromosomes marked by arrowheads. Bar = 10 μm.

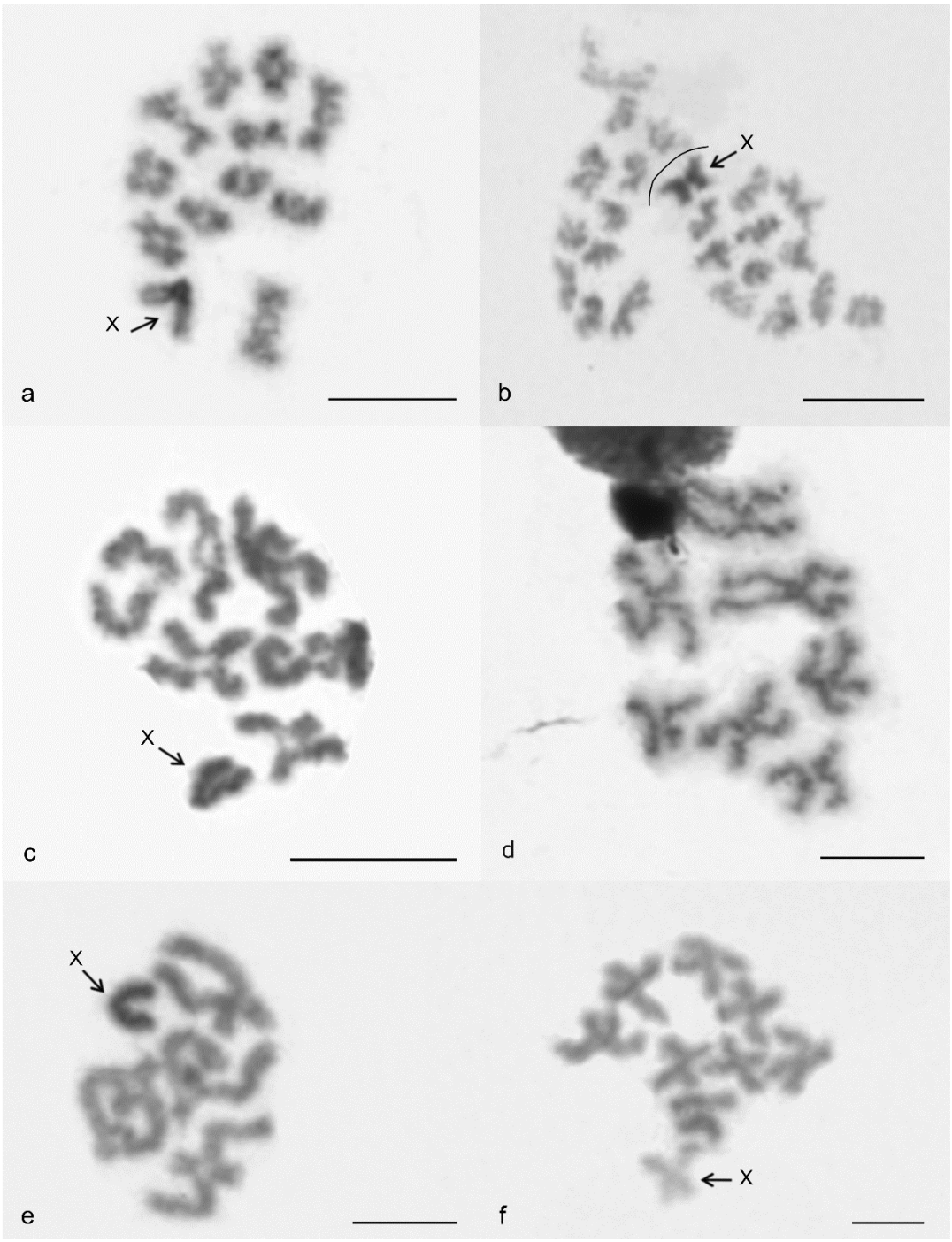

Additional file 17: Fig. S13. Sex chromosomes of pholcines with the X0 system. Stained by Giemsa. X = X chromosome. (a, b) *Belisana sabah*. a Metaphase I, consisting of 11 bivalents and a peripheral X chromosome. b Two sister metaphases II separated by a line (n = 11 + n = 12, including a positively heteropycnotic X chromosome); (c, d) *Cantikus sabah*. c Diplotene, comprising six bivalents and a positively heteropycnotic X chromosome placed on the periphery of the plate. d Prometaphase II including the X chromosome (n = 7); (e, f) *Micropholcus fauroti*. e Diplotene composed of four bivalents and a positively heteropycnotic X chromosome placed on the periphery of the plate. f Plate formed by fusion of two sister metaphases II. It includes a negatively heteropycnotic X chromosome. Bar = 10 μm.

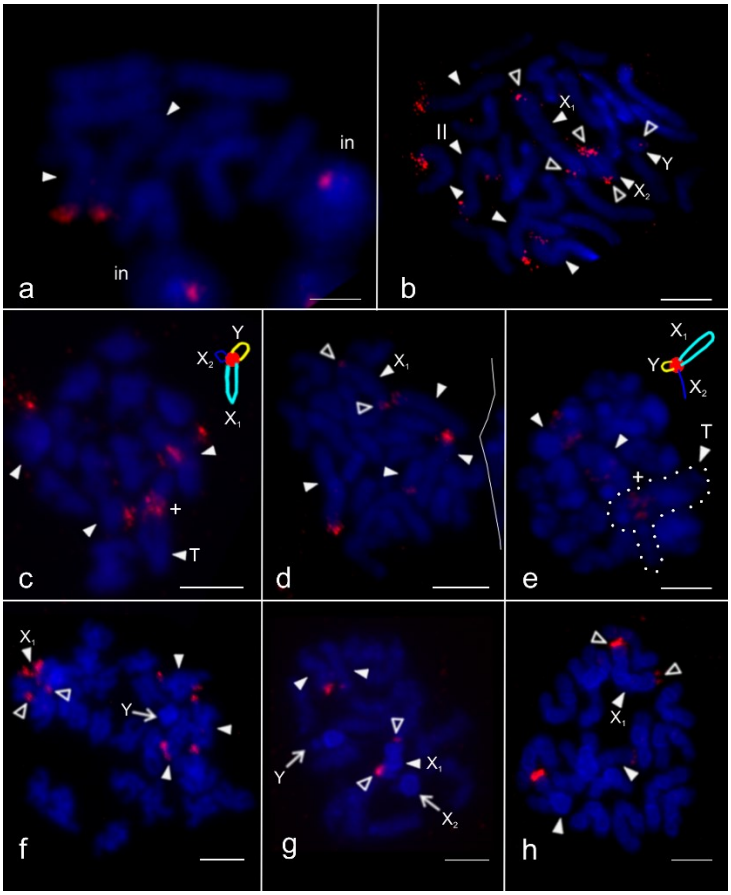

Additional file 18: Fig. S14. Pholcinae, males, detection of NORs (FISH). Figures c, e contain a scheme of the sex chromosome trivalent X_1X_2Y (red = signal formed by several NORs). Arrowhead = NOR-bearing chromosome (a, b, d, f–h), bivalent (c, e) or trivalent (c, e), open arrowhead = sex chromosome-linked NOR, T = sex chromosome trivalent, X_1 = X_1 chromosome, X_2 = X_2 chromosome, Y = Y chromosome, + = signal formed by several NORs. a *Micropholcus fauroti* (X0), mitotic metaphase. Note association of two homologous chromosomes containing terminal NOR (in – interphase nucleus); (b, c) Nipisa deelemanae (X_1X_2Y). b Mitotic metaphase. X chromosomes (X_1, X_2) and another chromosome (II) bear a terminal NOR at both ends. Five other chromosomes, including Y chromosome, involves one terminal NOR only. The sex chromosomes X_1 and X_2 are associated in parallel in the middle of the plate. b Metaphase I, note the three bivalents bearing a NOR and the sex chromosome trivalent with a signal in the region of chromosome pairing (see scheme); (d–f) *Quamtana hectori* (X_1X_2Y). d Mitotic metaphase (separated by a line from another plate). X_1 chromosome bears two NORs, each at opposite end of the chromosome. Chromosomes of two pairs also include a terminal NOR; e Metaphase I, two bivalents contain NOR. The sex chromosome trivalent contains a signal in region of chromosome pairing (see scheme). f Plate formed by fused sister metaphases II, chromosomes of NOR-bearing pairs exhibit biarmed morphology. The X1 chromosome is terminated by NOR at both ends. Y chromosome considerably condensed, without signal; (g, h) *Q. filmeri* (X_1X_2Y), mitotic plates. The X_1 chromosome bears two NORs, each at opposite end of chromosome. Chromosomes of one pair also contain a terminal NOR. g Prophase, sex chromosomes exhibit a more intensive fluorescence than the other chromosomes. h Metaphase. Bar = 5 μm except for c, e, g (10 μm).

Additional file 20: Fig. S15. *Hoplopholcus* and *Smeringopus* (Smeringopinae), male karyotypes, stained by Giemsa. Based on metaphase II (a) or two sister metaphases II (b–e). Autosome pairs decrease gradually in size. The X_1 is the longest element of the set (except for d). Karyotypes are predominated by metacentrics. a *H. labyrinthi*, haploid set, note the two submetacentric chromosomes (nos 5, 9), subtelocentric chromosome (no. 6) and subtelocentric X_2 chromosome; b *S. atomarius*, note one submetacentric (no. 3) and one acrocentric pairs (no. 13), and submetacentric X_2; c *S. ndumo*, note two submetacentric pairs (nos 4, 11); d *S. peregrinus*, note three submetacentric (nos 1, 4, 6) and one subtelocentric pairs (no. 12), and subtelocentric X_2. Sex chromosomes positively heteropycnotic; e *Smeringopus* sp., note two submetacentric pairs (nos 1, 2), one acrocentric pair (no. 10) and acrocentric X_2. Bar = 10 μm.

Additional file 21: Fig. S16. *Crossopriza lyoni* (Smeringopinae), male karyotype, Giemsa staining. Based on two sister metaphases II. Karyotype metacentric, except for submetacentric pairs nos 2 and 11. First two pairs differ from the other ones by large size. The X chromosome is the longest chromosome of the set. It is slightly positively heteropycnotic. Bar = 10 μm.

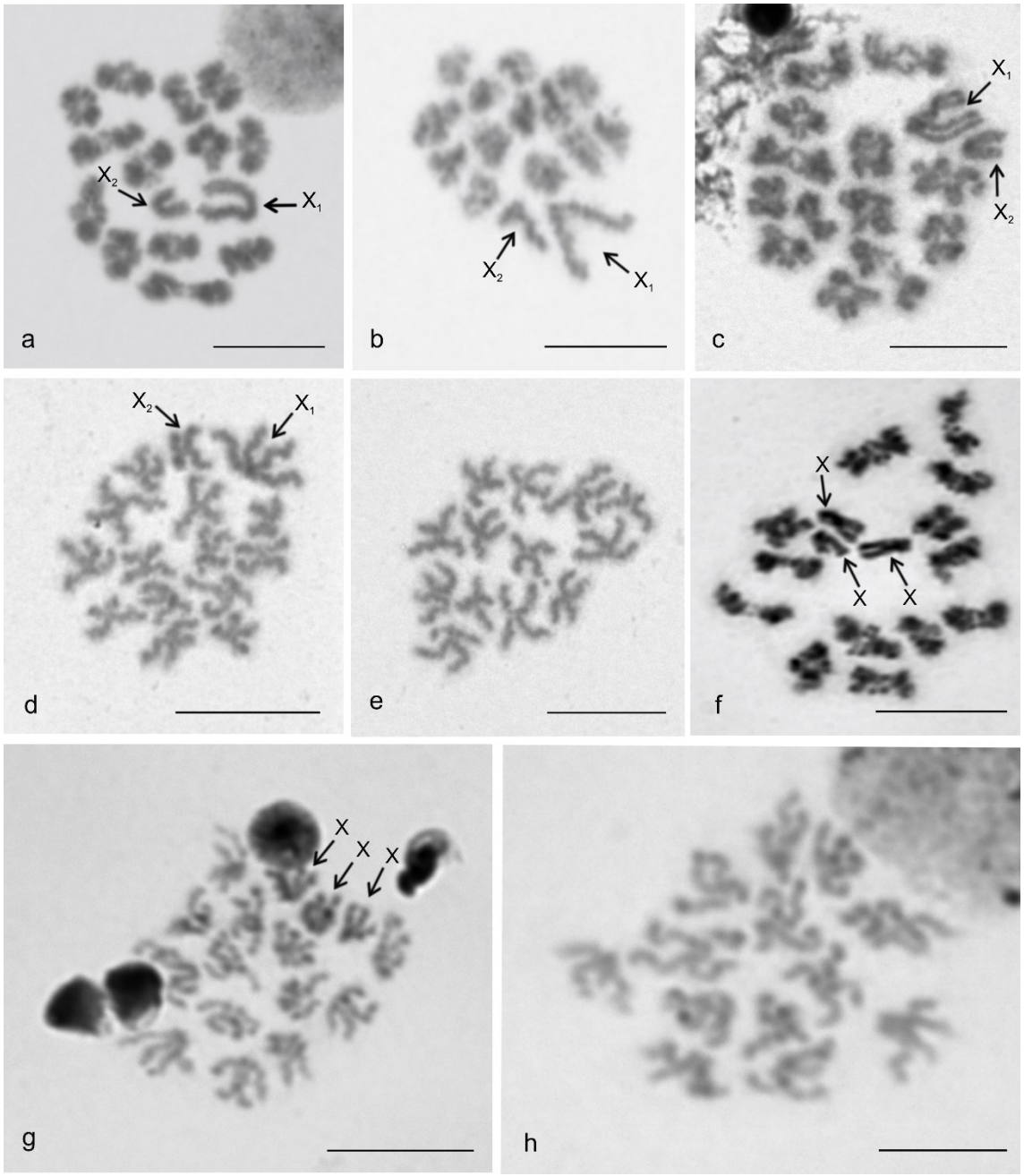

Additional file 22: Fig. S17. Sex chromosomes of smeringopines with multiple X chromosomes. Stained by Giemsa. X = X chromosome, X_1 = X_1 chromosome, X_2 = X_2 chromosome. (a, b) *Hoplopholcus forskali* (X_1X_20). a Diakinesis, composed of 13 bivalents and two X chromosomes, note the end-to-end association of the X chromosomes. b Telophase I, half plate containing X chromosomes; (c–e) *Smeringopus ndumo* (X_1X_20). c Diakinesis, comprising 13 bivalents and two X chromosomes. d Metaphase II, containing X chromosomes (n = 15). e Metaphase II, without the sex chromosomes (n = 13); (f–h) *S. pallidus* ($X_1X_2X_30$). f Diakinesis, composed of 13 bivalents and three X chromosomes, sex chromosomes grouped in the middle of the plate. g Metaphase II with X chromosomes (n = 16). X chromosomes are associated at the periphery of the plate. They exhibit a slight positive heteropycnosis. h Metaphase II, without sex chromosomes (n = 13). Bar = 10 μm.

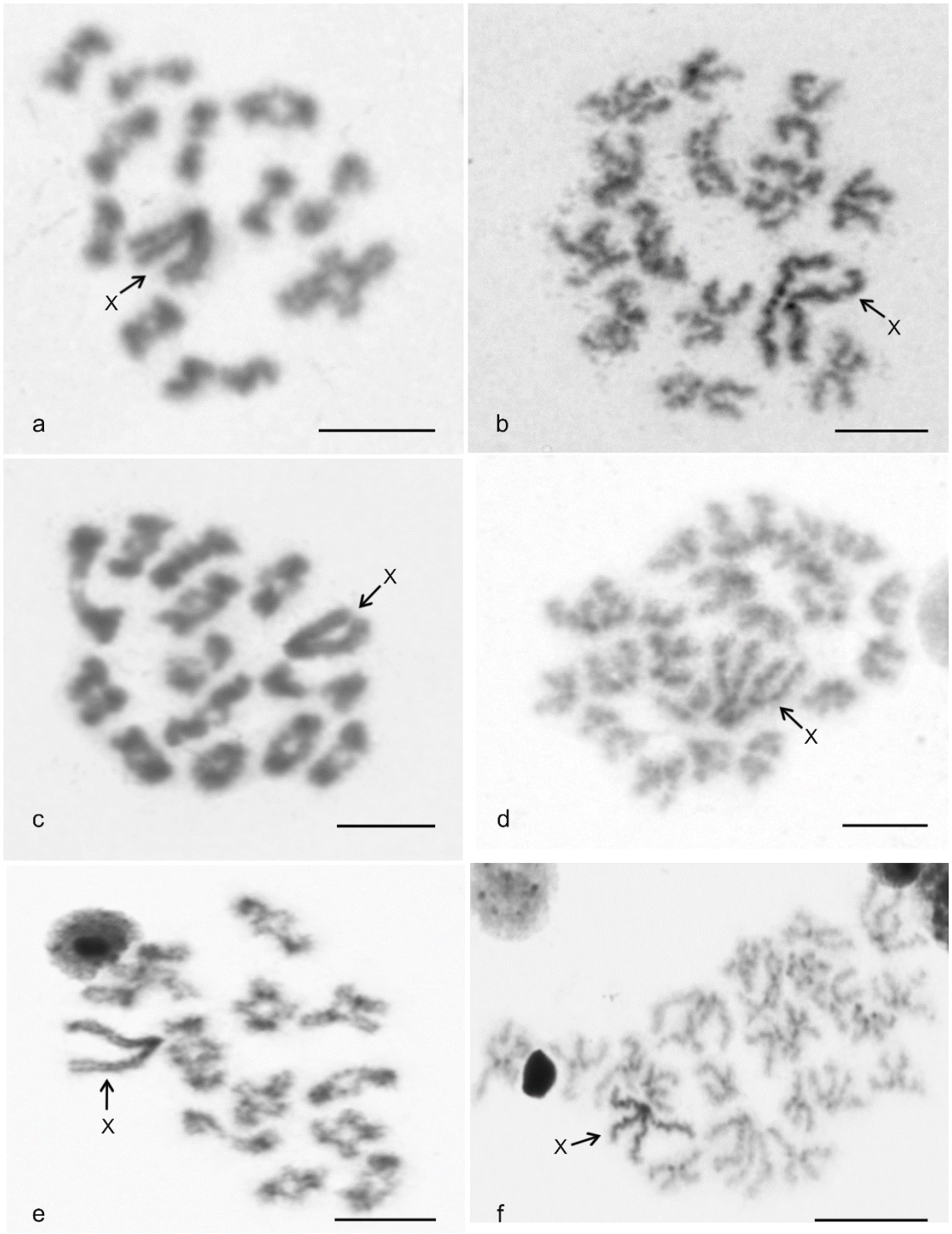

Additional file 23: Fig. S18. Sex chromosomes of smeringopines with the X0 system. Stained by Giemsa. X = X chromosome. (a, b) *Crossopriza lyoni*. a Metaphase I composed of 11 bivalents and X chromosome. b Anaphase I; (c, d) *Holocnemus pluchei*. c Metaphase I, consisting of 13 bivalents and an X chromosome. The X chromosome is placed at the periphery of the plate. Note the association of terminal parts of the X chromosome arms. d Metaphase II, including the X chromosome. This element is slightly positively heteropycnotic; (e, f) *Stygopholcus skotophilus*. e Diplotene, composed of 11 bivalents and an X chromosome. f Plate formed by two fused sister metaphases II, 2n = 23. Note the positively heteropycnotic X chromosome. Bar = 10 μm.

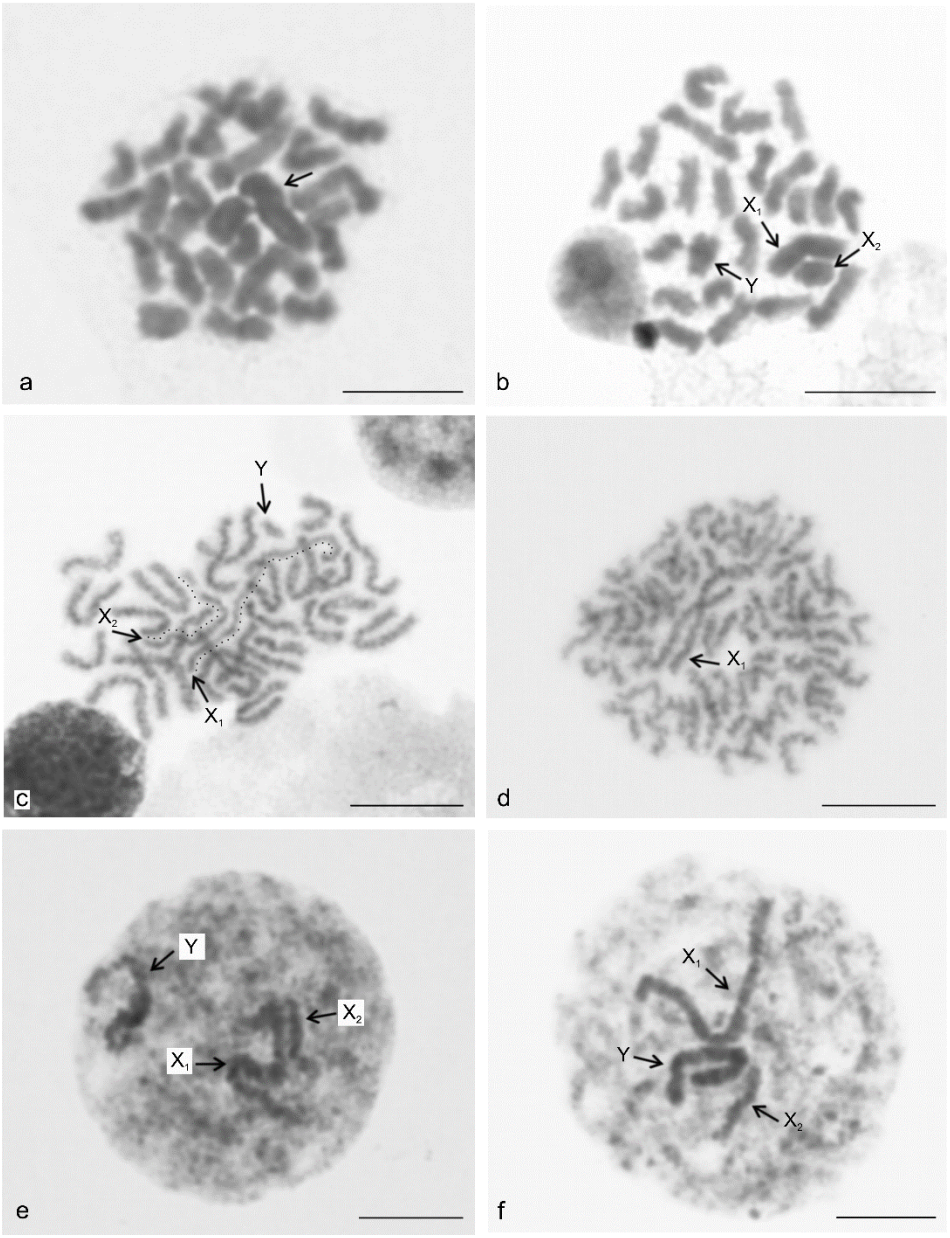

Additional file 24: Fig. S19. Pholcidae, male germline, behaviour of sex chromosomes prior to meiosis. Arrow = sex chromosomes, X_1 = X_1 chromosome, X_2 = X_2 chromosome, Y = Y chromosome. (a, b) *Muruta tambunan* (X_1X_2Y), mitotic metaphase, chromosomes X_1, X_2, and Y positively heteropycnotic. Chromosomes X_2 and Y are approximately of the same size. a Sex chromosomes grouped in the middle of the plate. b Chromosomes X_1 and X_2 associated in parallel, Y chromosome released from the association; c *Artema nephilit* (X_1X_2Y), early mitotic metaphase, X chromosomes are marked by a dotted line. They are associated in parallel in the middle of the plate. Their condensation is slightly delayed in comparison with the other chromosomes; d *Hoplopholcus cecconii* (X_1X_20), transition from mitotic metaphase to anaphase. Chromosome X_1 is placed in the middle of the plate; (e, f) *Pholcus kindia* (X_1X_2Y). e Premeiotic interphase. X chromosomes pair in parallel in the middle of the nucleus. The Y chromosome does not take part in pairing. f Preleptotene. Sex chromosomes are associated in the middle of the nucleus, the Y chromosome is more condensed than the X chromosomes. Bar = 10 μm.

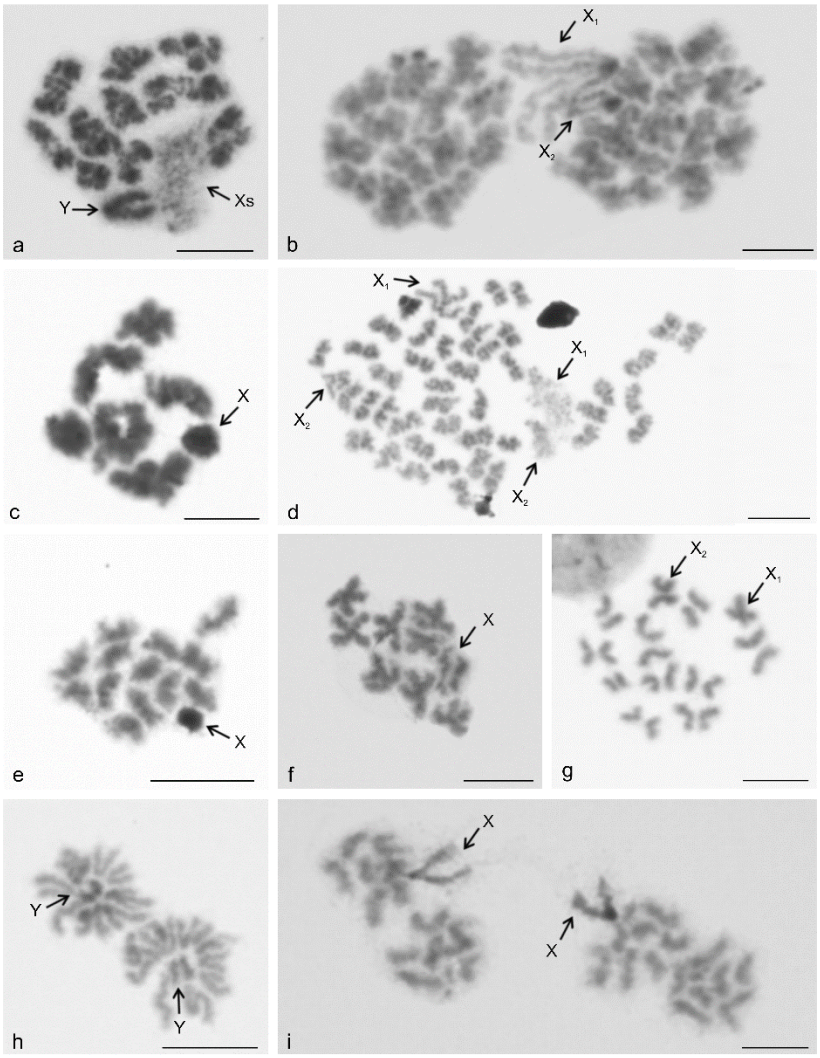

Additional file 25: Fig. S20. Pholcidae, male meiosis, condensation and segregation of sex chromosomes. X = X chromosome, Xs = X chromosomes, X_1 = X_1 chromosome, X_2 = X_2 chromosome, Y = Y chromosome. a *Pholcus kindia* (X_1X_2Y), early diplotene. Y chromosome highly condensed. In contrast, X chromosomes almost decondensed; b *Hoplopholcus cecconii* (X_1X_20), late anaphase I. X chromosomes are arranged in parallel and less condensed than the other chromosomes. Moreover, their segregation and separation of their chromatids are delayed. Centromeres of sex chromosomes are formed by a prominent knob; c *Cantikus sabah* (X0), diplotene. Sex chromosome forms a highly condensed body; d *Hoplopholcus forskali* (X_1X_20), plate formed by fusion of 1) two sister late prometaphases II (left) and 2) two sister early prometaphases II (right). In contrast to autosomes, sex chromosomes differ considerably by condensation in early and late prometaphase II. They are almost decondensed during early prometaphase II (right); e *Holocneminus* sp. (X0), plate formed by two sister prometaphases II, sex chromosome forms a highly condensed body; f *Micropholcus fauroti* (X0), two fused sister metaphases II. Sex chromosome shows precocious division; g *Aetana kinabalu* (X_1X_2Y), late metaphase II, division of X chromosomes is delayed; h *Pholcus* sp. (X_1X_2Y), two half-plates of anaphase II containing positively heteropycnotic Y chromosome in the middle; i *Psilochorus simoni* (X0), two sister anaphases II. Segregation of X chromosome delayed. This element is slightly positively heteropycnotic at right anaphase II. Bar = 10 μm.

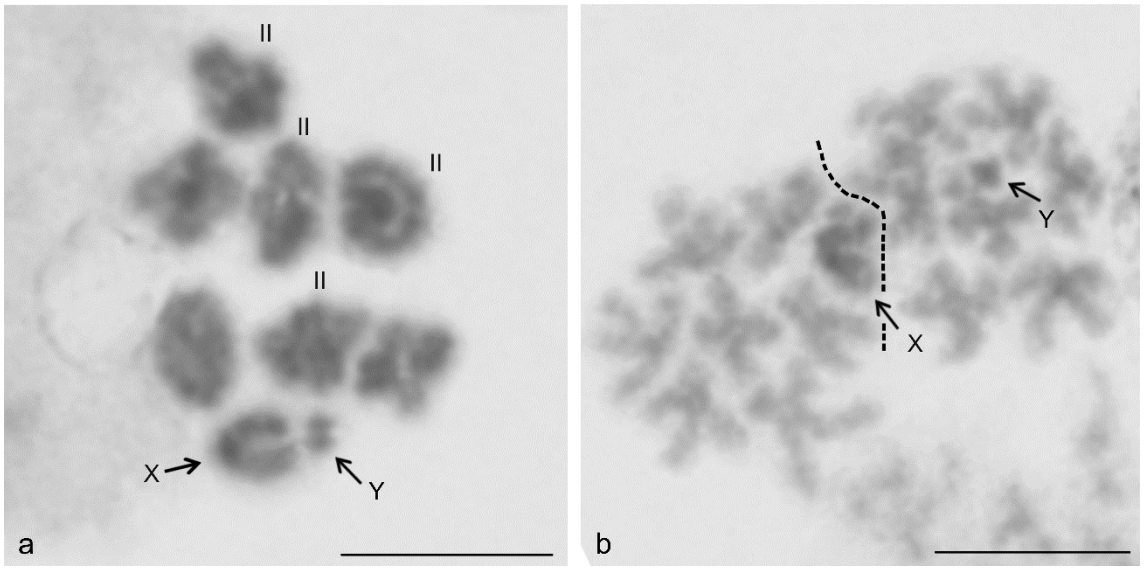

Additional file 26: Fig. S21. *Arteminae*, *Wugigarra* sp., male meiosis, behaviour of sex chromosomes. X = X chromosome, Y = Y chromosome, II = bivalent containing two chiasmata. a Metaphase I, three bivalents include two chiasmata. Pairing of metacentric chromosomes X and Y is ensured by ends of their arms. b Two sister metaphases II (separated by dashed line). While X chromosome is placed at the periphery of one plate, Y chromosome is in middle of another plate. Note positive heteropycnosis of sex chromosomes. Bar = 10 μm.

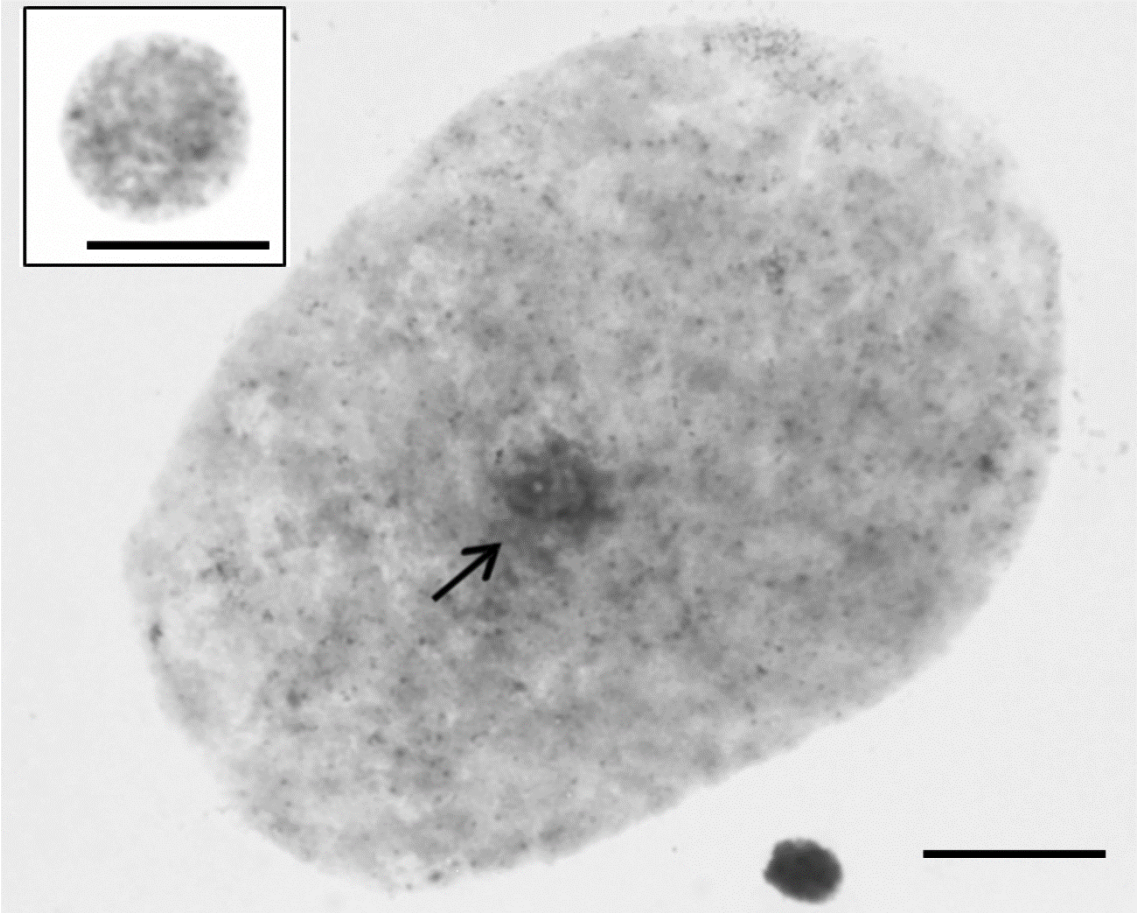

Additional file 27: Fig. S22. *Pholcus* sp. (X_1X_2Y), testes, endopolyploid nucleus. Heterochromatic body in the middle of the nucleus is formed by sex chromosomes (arrow). Inset: a standard diploid nucleus. Bar = 5 μm.

Remaining electronical supplements of the paper are at the thesis supplements.

Publication 4.3. Král J, **Ávila Herrera IM**, Šťáhlavský F, Sadílek D, Pavelka J, Chatzaki M, Huber BA (2022). Karyotype differentiation and male meiosis in European clades of the spider genus *Pholcus* (Araneae, Pholcidae). Comparative Cytogenetics.16, 185–209.
DOI: 10.3897/CompCytogen.v16i4.85059

IF2022: 1.8

This study is focused on the evolution of autosomes, sex chromosomes, NORs, and meiosis in European clades of *Pholcus*, which is the most species-rich pholcid genus. Eight species of *Pholcus* have been karyotyped before publication of this paper. According to my results, karyotypes of European clades exhibit several characters ancestral for *Pholcus*, namely the $2n♂ = 25$, X_1X_2Y, large size of Y chromosome, and predomination of biarmed chromosomes. The most species exhibited a large acrocentric chromosome pair bearing NOR at the end of long arm. Closely related species differ often by morphology of one or several chromosome pairs. Sex chromosomes of the ancestral pholcid X_1X_2Y system exhibited probably metacentric morphology. In *Pholcus*, X_2 chromosome has been changed into monoarmed one. Ancestral X_1X_2Y system contained probably Y microchromosome. Size of Y chromosome increased considerably in *Pholcus* ancestors.

The analysed species exihibited similar sex chromosome behavior in the male germline. In early prophase I, sex chromosomes formed a body located on the periphery of the nucleus. Similarly to the other haplogyne spiders analysed so far, male prophase of the first meiotic division contained a specific period (between pachytene and diplotene), which was characterised by a considerable decondensation of chromosome pairs, so-called diffuse stage. On the contrary, sex chromosomes exhibited a hyperspitalisation during diffuse stage; Y chromosome usually exhibited more intensive condensation than X chromosomes.

The ancestral karyotype of the *Pholcus* contained probably three terminal NORs and three X chromosome-linked loci, two at ends of X_1 chromosome and one at the end of long arm of X_2 chromosome. During male meiosis, NORs located on the sex chromosomes are probably involved in achiasmatic pairing of sex chromosomes. In some European members of *Pholcus*, number of autosome and sex-chromosome linked NORs has been reduced during evolution. In the ancestor of Macaronesian clade, number of NORs has

been reduced to one autosomal and one X-chromosome linked NOR. In the lineage from Madeira and *P. creticus* from Crete, sex-chromosome linked NORs were lost. It is probably an apomorphy of these clades.

In addition, our study revealed two cytotypes of the common synanthropic species *P. phalangioides* (Madeiran and central European), which differ by their NOR pattern, and morphology of one chromosome pair and X_2 chromosome.

My contribution: Preparation of the chromosomal slides. Detection of NORs by FISH. Evaluation of preparations, analysis and interpretation of results. Preparation of karyotypes, figures, and data tables. Writing of the manuscript and its revision.

CompCytogen 16(4): 185–209 (2022)
doi: 10.3897/compcytogen.v16.i4.85059
https://compcytogen.pensoft.net

RESEARCH ARTICLE

COMPARATIVE Cytogenetics
A peer-reviewed open-access journal
International Journal of Plant & Animal Cytogenetics, Karyosystematics, and Molecular Systematics

Karyotype differentiation and male meiosis in European clades of the spider genus *Pholcus* (Araneae, Pholcidae)

Jiří Král[1*], Ivalú M. Ávila Herrera[1*], František Šťáhlavský[2], David Sadílek[1], Jaroslav Pavelka[3], Maria Chatzaki[4], Bernhard A. Huber[5]

1 *Laboratory of Arachnid Cytogenetics, Department of Genetics and Microbiology, Faculty of Science, Charles University, Viničná 5, 128 44 Prague 2, Czech Republic* **2** *Department of Zoology, Faculty of Science, Charles University, Viničná 7, 128 44 Prague 2, Czech Republic* **3** *Centre of Biology, Geosciences and Environmental Education, University of West Bohemia, Univerzitní 8, 306 14 Plzeň, Czech Republic* **4** *Department of Molecular Biology and Genetics, Democritus University of Thrace, 68100 Alexandroupolis, Greece* **5** *Alexander Koenig Zoological Research Museum, Adenauerallee 127, 53113 Bonn, Germany*

Corresponding author: Jiří Král (spider@natur.cuni.cz)

Academic editor: Marielle Schneider | Received 7 April 2022 | Accepted 28 September 2022 | Published 2 November 2022

https://zoobank.org/AFC2E512-CC32-42F7-8AAB-5B6ECBBE94D5

Citation: Král J, Ávila Herrera IM, Šťáhlavský F, Sadílek D, Pavelka J, Chatzaki M, Huber BA (2022) Karyotype differentiation and male meiosis in European clades of the spider genus *Pholcus* (Araneae, Pholcidae). Comparative Cytogenetics 16(4): 185–209. https://doi.org/10.3897/compcytogen.v16.i4.85059

Abstract

Haplogyne araneomorphs are a diverse spider clade. Their karyotypes are usually predominated by biarmed (i.e., metacentric and submetacentric) chromosomes and have a specific sex chromosome system, X_1X_2Y. These features are probably ancestral for haplogynes. Nucleolus organizer regions (NORs) spread frequently from autosomes to sex chromosomes in these spiders. This study focuses on pholcids (Pholcidae), a highly diverse haplogyne family. Despite considerable recent progress in pholcid cytogenetics, knowledge on many clades remains insufficient including the most species-rich pholcid genus, *Pholcus* Walckenaer, 1805. To characterize the karyotype differentiation of *Pholcus* in Europe, we compared karyotypes, sex chromosomes, NORs, and male meiosis of seven species [*P. alticeps* Spassky, 1932; *P. creticus* Senglet, 1971; *P. dentatus* Wunderlich, 1995; *P. fuerteventurensis* Wunderlich, 1992; *P. phalangioides* (Fuesslin, 1775); *P. opilionoides* (Schrank, 1781); *P. silvai* Wunderlich, 1995] representing the dominant species groups in this region. The species studied show several features ancestral for *Pholcus*, namely the $2n♂ = 25$, the X_1X_2Y system, and a karyotype predominated by biarmed chromosomes. Most taxa have a large acrocentric NOR-bearing pair, which evolved from a biarmed pair by a pericentric inversion. In some lineages,

* Those authors contributed equally to this work.

the acrocentric pair reverted to biarmed. Closely related species often differ in the morphology of some chromosome pairs, probably resulting from pericentric inversions and/or translocations. Such rearrangements have been implicated in the formation of reproductive barriers. While the X_1 and Y chromosomes retain their ancestral metacentric morphology, the X_2 chromosome shows a derived (acrocentric or subtelocentric) morphology. Pairing of this element is usually modified during male meiosis. NOR patterns are very diverse. The ancestral karyotype of *Pholcus* contained five or six terminal NORs including three X chromosome-linked loci. The number of NORs has been frequently reduced during evolution. In the Macaronesian clade, there is only a single NOR-bearing pair. Sex chromosome-linked NORs are lost in Madeiran species and in *P. creticus*. Our study revealed two cytotypes in the synanthropic species *P. phalangioides* (Madeiran and Czech), which differ by their NOR pattern and chromosome morphology. In the Czech cytotype, the large acrocentric pair was transformed into a biarmed pair by pericentric inversion.

Keywords
haplogyne, inversion, NOR, rDNA, sex chromosome, speciation, Synspermiata

Introduction

Spiders exhibit an enormous species diversity, paralleled by high karyotype diversity. However, despite considerable recent progress (e.g., Král et al. 2006, 2013, 2019; Araujo et al. 2012; Kořínková and Král 2013; Ávila Herrera et al. 2021), our knowledge of spider cytogenetics is still fragmentary. Most data on spider chromosomes concern entelegyne araneomorphs, which include the large majority of the described spider species. The cytogenetics of the other clades (mesotheles, mygalomorphs, haplogyne araneomorphs) is much less understood (Kořínková and Král 2013; Ávila Herrera et al. 2021).

Haplogyne araneomorphs ("haplogynes") consist of the Synspermiata clade and two families, Filistatidae and Hypochilidae (Wheeler et al. 2017; Shao and Li 2018). Haplogynes currently include more than 6150 described species placed in 20 families (based on data of World Spider Catalog 2022). Haplogynes exhibit a considerable karyotype diversity. Their diploid numbers range from 2n♂ = 5 (*Afrilobus* sp., Orsolobidae) to 2n♂ = 152 (*Caponia natalensis* O. Pickard-Cambridge, 1874, Caponiidae), which are the lowest and highest diploid numbers in spiders, respectively (Král et al. 2019). Their karyotypes are composed of monocentric (i.e., standard) chromosomes except for the superfamily Dysderoidea whose chromosomes are holokinetic (holocentric) (Král et al. 2019). Holokinetic chromosomes lack a localized centromere (Mola and Papeschi 2006). Karyotypes of haplogynes with monocentric chromosomes are usually predominated by biarmed (i.e., metacentric and submetacentric) chromosomes (Král et al. 2006; Ávila Herrera et al. 2021). Furthermore, the prophase of the male first meiotic division includes the so-called diffuse stage (Kořínková and Král 2013), characterized by a considerable decondensation of autosomes and overcondensation of sex chromosomes (Benavente and Wettstein 1980; Král et al. 2006; Ávila Herrera et al. 2021). Haplogynes exhibit a variety of sex chromosome systems. Male sex chromosomes include one or several elements that do not recombine during meiosis and

are presumably nonhomologous. The peculiar X_1X_2Y system has been found in seven families (Král et al. 2006, 2019; Ávila Herrera et al. 2016, 2021; Paula-Neto et al. 2017; Araujo et al. 2020). It is probably ancestral for araneomorph spiders including haplogynes (Paula-Neto et al. 2017; Ávila Herrera et al. 2021). The ancestral structure of the X_1X_2Y system probably comprises two large metacentric X chromosomes and a metacentric Y microchromosome, which display a specific achiasmatic end-to-end pairing during male meiosis (Ávila Herrera et al. 2021). The origin of the X_1X_2Y system is unresolved. In some clades, it has converted into other sex chromosome systems (Král et al. 2006, 2019; Ávila Herrera et al. 2016, 2021). Besides non-recombining elements, spider sex chromosomes probably also contain a chromosome pair formed by the chromosomes X and Y, which recombine and show a very low level of differentiation (cryptic sex chromosome pair, CSCP) (Kořínková and Král 2013). Haplogynes also vary greatly in the number and location of nucleolus organizer regions (NORs) (Král et al. 2006; Ávila Herrera et al. 2021). These structures contain genes for 18S, 5.8S and 28S rRNA (Sumner 2003). The number of NORs ranges from one to nine; their position is usually terminal; and they spread frequently from autosomes to sex chromosomes (Král et al. 2006; Ávila Herrera et al. 2021).

The present study focuses on the cytogenetics of pholcid spiders (Pholcidae), the most diversified haplogyne family with monocentric chromosomes. This family currently comprises almost 1900 described species in 97 genera (World Spider Catalog 2022). Pholcids occur on all continents except Antarctica. Most species inhabit tropical and subtropical regions; some species are synanthropic (Huber 2011). From a cytogenetic point of view, pholcids are the best-explored group of haplogynes. A total of 64 species have been karyotyped, including 11 species determined to genus level only (based on The Spider Cytogenetic Database 2022). Despite this, our knowledge on karyotype evolution remains insufficient for many pholcid clades, including the most species-rich genus, *Pholcus* Walckenaer, 1805 (with currently more than 350 species; World Spider Catalog 2022). To reduce this gap, we studied the differentiation of karyotype, sex chromosomes, and NORs as well as the course of male meiosis in the dominant species groups of *Pholcus* present in mainland Europe, Crete, and Macaronesia. Nucleolus organizer regions have previously been studied in few spider species. More comprehensive data on the evolution of these structures are only available from pholcids (Ávila Herrera et al. 2021).

We paid specific attention to the Macaronesian clade of *Pholcus*. Macaronesia consists of five volcanic archipelagos in the Atlantic Ocean, west of the Iberian Peninsula and northwestern Africa. *Pholcus* is among the most species-rich genera of Macaronesian spiders. The Macaronesian clade currently includes more than 20 described species that are largely restricted to the Canaries and Madeira (Dimitrov and Ribera 2007; Dimitrov et al. 2008; Huber 2011). This clade exhibits an enormous diversification rate, among the highest found in spiders (Dimitrov et al. 2008).

Our aim is to determine the fundamental traits of karyotype evolution in European clades of *Pholcus*. Based on our new findings and on previously published data, we explore the congruence of individual karyotype markers with published phylogenies and discuss the possible evolutionary implications of karyotype transformations.

Material and methods

Spider specimens

Information on the studied species (number of analyzed specimens, their sex, and locality data) is given in Table 1. Voucher specimens are deposited in the Zoological Research Museum Alexander Koenig, Bonn (Germany).

Table 1. Species studied, with specimen number, sex, and geographic origin. Abbreviation: sad = subadult.

Taxon	Individuals	Locality	GPS Coordinates (Latitude, Longitude)
P. crypticolens/opilionoides species group			
P. creticus	4♂	Greece, Crete, Topolia, Topolia cave	35.4119, 23.6817
	2♂	Greece, Crete, Stavros, Lera cave	35.5908, 24.1023
P. opilionoides	4♂	Czech Republic, Veselí nad Lužnicí	49.1506, 14.6930
P. phalangioides species group			
P. alticeps	8♂	Czech Republic, Chomutov	50.4527, 13.4166
P. phalangioides	1♂	Portugal, Madeira, Santana	32.8043, -16.8855
Macaronesian species group			
P. fuerteventurensis	2♂	Spain, Canariens, Fuerteventura, Giniginamar	28.2024, -14.0734
P. dentatus	1 sad ♂, 1♂	Portugal, Madeira, Achadas da Cruz	32.8390, -17.1907
P. silvai	2♂	Portugal, Madeira, Levada das 25 fontes	32.7611, -17.1374

Preparation of chromosomes, determination of karyotype

Chromosome preparations were obtained from testes of adult males by a modification of the spreading technique described by Dolejš et al. (2011). The gonads were dissected and immersed into a hypotonic solution (0.075M KCl) for 20–25 min at room temperature (RT). Hypotonization was followed by two fixations in ethanol:acetic acid (3:1) for 10 and 20 min (RT), respectively. Subsequently, tissue was placed in a drop of 60% acetic acid on a clean slide and quickly shredded with a pair of tungsten needles to obtain a cell suspension. Finally, the slide was placed on a warm (40 °C) histological plate. The drop of dispersed tissue evaporated while being moved constantly by a tungsten needle. Slides were stained using 5% Giemsa solution in Sörensen buffer (pH 6.8) for 28 min (RT). They were studied under an Olympus BX 50 microscope equipped with DP 71 CCD camera (Olympus, Tokyo, Japan). To construct the karyotype, the morphology of metaphase II chromosomes was analyzed. Sister metaphases II (5 plates) were evaluated using the IMAGE TOOL 3.0 software (https://imagetool.software.informer.com/3.0/). Relative chromosome length was estimated as a percentage of the total chromosome length of the haploid set (TCL). This set also included sex chromosomes X_1, X_2, and Y. Karyotypes were assembled using the COREL PHOTO PAINT X3 programme. Determination of the sex chromosome system was based on data from male meiosis (segregation of sex chromosomes and their behavior in prophase and metaphase I). The X_2 and Y chromosomes were similar in size. Therefore,

we used a paired samples Wilcoxon test to analyse their size difference. It was impossible to distinguish the CSCP from autosomes by light microscopy. Therefore, the CSCP and autosomes are referred to collectively as chromosome pairs.

Detection of nucleolus organizer regions (NORs)

The NOR pattern was determined by fluorescent in situ hybridisation (FISH) with a 18S rDNA probe from *Dysdera erythrina* (Walckenaer, 1802) (Dysderidae) (see Ávila Herrera et al. 2021 for details of probe). Whereas the previously common method of NOR-detection by silver staining only visualizes NOR sites transcribed during the preceding interphase (Miller et al. 1976), NOR detection by a rDNA probe gives more accurate results. The probe was generated following Sadílek et al. (2015). The 18S rRNA gene fragment was amplified by polymerase chain reaction (PCR) from genomic DNA using forward and reverse primers 5′-CGAGCGCTTTTATTAGACCA-3′ and 5′-GGTTCACCTACGGAAACCTT-3′, respectively. The PCR product was extracted using the Wizard SV Gel and PCR Clean-Up System (Promega), re-amplified by PCR, and labeled with biotin-14-dUTP by nick translation using a Nick Translation Kit (Abbott Molecular).

FISH was performed with the biotinylated 18S rDNA probe as described by Fuková et al. (2005). Chromosome preparations were pre-treated with 100 µg/ml RNase A in 2× saline-sodium citrate (SSC) buffer (1 h, 37 °C). Chromosomes were denatured (3 min 30 s, 68 °C) by 70% formamide in 2×SSC. The probe mixture contained 20 ng of 18S rDNA and 25 µg of salmon sperm DNA (Sigma-Aldrich, Burlington, MA, USA) in 5 µl of 50% formamide and 5 µl of 20% dextran sulphate per slide. Biotin labelled 18S rDNA was detected with Cy3-streptavidin (Jackson ImmunoRes. Labs Inc., West Grove, PA, USA), with signal amplification by biotinylated antistreptavidin and Cy3-streptavidin (Vector Labs Inc., Burlingame, CA, USA). The preparations were counterstained with Fluoroshield containing 4′,6-diamidino-2-phenylindole (DAPI) (Sigma-Aldrich, Burlington, MA, USA). Considering the sensitivity of pholcid chromosomes to denaturation, two procedures were used to reduce this process. First, the slides were placed in an incubator for 1 hour (60 °C) before the experiment. Second, denaturation time was reduced (3 min). Preparations were observed under the Olympus IX81 microscope (Olympus, Tokyo, Japan) equipped with an ORCA-AG monochromatic camera (Hamamatsu, Hamamatsu, Japan). The images were pseudocolored (red for Cy3 and light green for DAPI) with Cell^R software (Olympus Soft Imaging Solutions GmbH, Münster, Germany).

Results

Karyotype data

The male karyotype of all species studied had 25 predominantly metacentric chromosomes and the X_1X_2Y system ($2n♂ = 25, X_1X_2Y$). The X_1 was the longest element of the set. Chromosomes X_2 and Y were medium-sized elements of similar size. Chromosome pairs decreased gradually in length (Suppl. material 1).

Pholcus crypticolens/opilionoides species group

The chromosome pairs of the males of *P. creticus* comprised five metacentric (nos 1, 5–8), four submetacentric (nos 2,4,9,10), one subtelocentric (no. 11), and one acrocentric pair (no. 3). Sex chromosomes were metacentric except for the acrocentric X_2 (Fig. 1A). Lenghts of the X_2 and Y chromosomes differed significantly (paired samples Wilcoxon test, W = 0, P < 0.001). The Y chromosome was longer than the X_2 (Suppl. material 1). This species had two chromosome pairs with a terminal NOR each (Fig. 2C). The morphology of these pairs is unresolved.

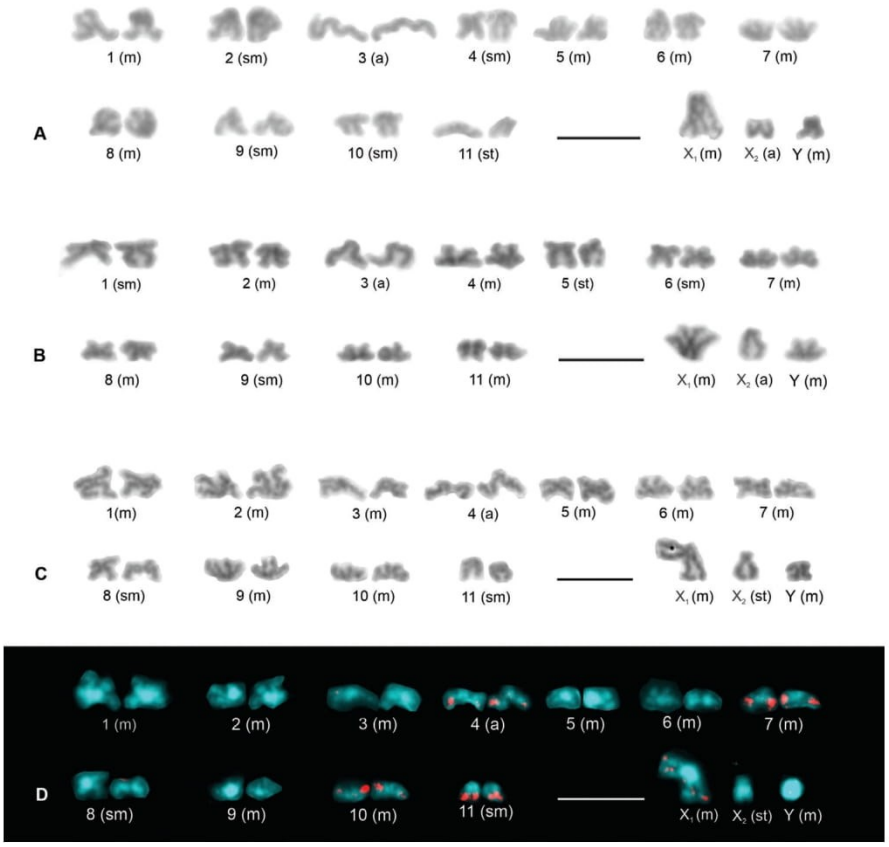

Figure 1. *Pholcus*, *crypticolens/opilionoides* and *phalangioides* groups, male karyotypes (**A–C** stained by Giemsa **D** FISH). Based on sister metaphases II **A** *P. creticus* **B** *P. alticeps* **C, D** *P. phalangioides* (Madeira) **C** standard karyotype **D** karyotype, detection of NORs. Prepared from the same plate as the standard karyotype. Note four chromosome pairs with terminal NOR (nos 4,7,10,11) and the X_1 chromosome with NOR at both ends. Pairs nos. 7, 10, and 11 are biarmed, pair no. 4 is acrocentric. NORs are localized at the long arm of these pairs. Scale bars: 10 μm.

The chromosomes of the males of *P. opilionoides* exhibited the same morphology as in populations studied previously (Ávila Herrera et al. 2021). They were metacentric except for five submetacentric chromosome pairs (nos 2–6) and an acrocentric X_2 chromosome. The lengths of the X_2 and Y chromosomes differed significantly (paired samples Wilcoxon test, $W = 0$, $P < 0.001$). The Y was shorter than the X_2. We succeeded in determining the NOR pattern in one specimen. The karyotype contained three biarmed chromosome pairs bearing a terminal NOR each. One pair was heterozygous for a NOR cluster. Furthermore, a small NOR was also detected at each end of the X_1 chromosome (Fig. 2A, B).

Pholcus phalangioides species group

The male karyotype of *P. alticeps* consisted of metacentric chromosomes except for three submetacentric (nos 1,6,9), one subtelocentric (no. 5), and one acrocentric (no. 3) chromosome pairs as well as the acrocentric X_2 chromosome (Fig. 1B). The lengths of the X_2 and Y chromosomes did not differ significantly (paired samples Wilcoxon test, $W = 1$, $0.10 < P < 0.20$). The karyotype included two chromosome pairs with a terminal NOR locus each. While one NOR-bearing pair was formed by small biarmed chromosomes, the other one consisted of large acrocentric chromosomes with a NOR at the end of the long arm. The karyotype contained three terminal sex chromosome-linked NORs (two on the X_1 chromosome and one at the end of the long arm of the X_2 chromosome) (Fig. 2D, E).

The karyotype of the single male of *P. phalangioides* from Madeira consisted of metacentric chromosomes except for two submetacentric (nos 8 and 11) and one acrocentric pair (no. 4) as well as a subtelocentric X_2 (Fig. 1C). The lengths of the X_2 and Y chromosomes did not differ significantly (paired samples Wilcoxon test, $W = 2$, $0.10 < P < 0.20$). Three biarmed (nos 7,10,11) and one acrocentric chromosome pairs (no. 4) contained a terminal NOR each, which was placed at the end of the long arm. Beside this, a NOR was also found at each end of the X_1 chromosome (Figs 1D, 2F, G).

Macaronesian species group

The karyotype of *P. fuerteventurensis* from the Canaries was composed of metacentric chromosomes except for one submetacentric (no. 1) and one acrocentric pair (no. 5) as well as an acrocentric X_2 chromosome (Fig. 3A). The lengths of the X_2 and Y chromosomes did not differ significantly (paired samples Wilcoxon test, $W = 5$, $P > 0.2$). *P. fuerteventurensis* had a single large acrocentric NOR-bearing pair containing a NOR at the end of the long arm. A NOR was also placed at the end of the long arm of the X_2 chromosome (Fig. 4A–C).

In *P. dentatus* from Madeira, the chromosome pairs were metacentric except for two submetacentric (nos 7 and 11) and one acrocentric pair (no. 3). The sex chromosomes had a metacentric morphology except for the acrocentric X_2 (Fig. 3B). The lengths of the X_2 and Y chromosomes differed significantly (paired samples Wilcoxon test, $W = 0$, $P < 0.001$). The X_2 was longer than the Y (Suppl. material 1).

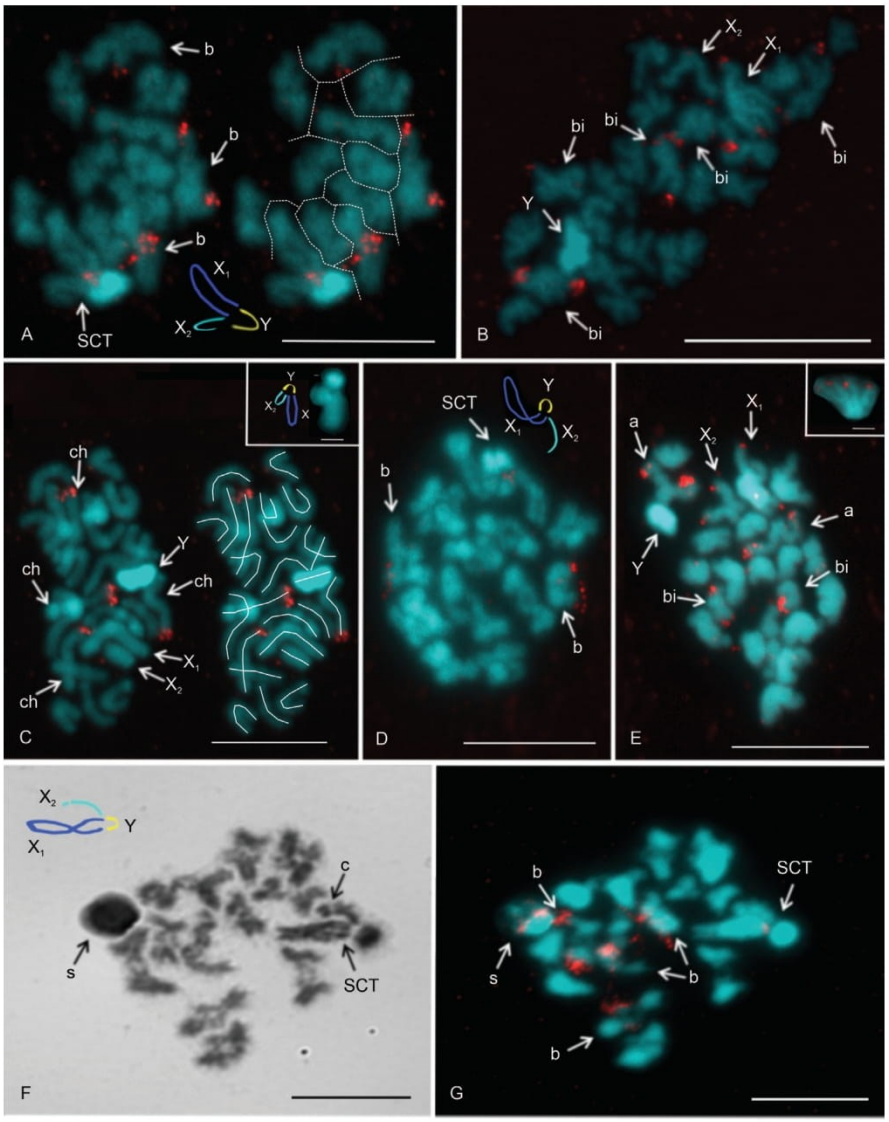
A
b
b
b
X1
X2
Y
SCT
B
X2
X1
bi
bi
bi
bi
Y
bi
C
ch
ch
Y
ch
X1
X2
ch
D
SCT
Y
X1
X2
b
b
E
X1
a
X2
a
Y
bi
bi
F
X2
Y
X1
c
s
SCT
G
b
SCT
s
b
b

The chromosome complement of the second Madeiran species, *P. silvai*, had metacentric chromosomes except for one submetacentric (no. 8), one subtelocentric (no. 10), one acrocentric pair (no. 4), and an acrocentric X_2 chromosome (Fig. 3C). The lengths of the X_2 and Y chromosomes differed significantly (paired samples Wilcoxon test, W = 0, P < 0.001). The Y was larger than the X_2 chromosome (Suppl. material 1).

Both Madeiran species showed the same NOR pattern, namely a single locus at the end of the long arm of the acrocentric pair (Fig. 4D–I).

Sex chromosome behavior in male germline

In general, the behavior of the sex chromosomes was characterized by positive heteropycnosis (i.e., more intensive staining) and association (i.e. close proximity of chromosomes without pairing) which transformed into pairing in some phases. The specific behavior of sex chromosomes was initiated as early as in spermatogonial mitosis. Sex chromosomes often exhibited positive heteropycnosis and a loose association in spermatogonial prophases, metaphases, and anaphases (Fig. 5A, B). During metaphase (Fig. 5A) as well as on anaphase half-plates (Fig. 5B), they were often placed in the middle of the plates. They remained overcondensed and positively heteropycnotic during premeiotic interphase, early prophase I (leptotene-pachytene), and diffuse stage. During this period, they often formed a body on the periphery of the plate (Fig. 5C, D). Bivalents were fuzzy and spherical during the early diffuse stage (Fig. 5C). However, towards the end of the diffuse stage, they showed chiasmata and their morphology was similar to that found during late prophase I (Fig. 5D). During late prophase I (diplotene-diakinesis) and metaphase I, the condensation of

Figure 2. *Pholcus*, *crypticolens*/*opilionoides* and *phalangioides* groups, males, NOR detection **A–E, G** FISH **F** Giemsa staining **A, B** *P. opilionoides* **A** diplotene. Three bivalents contain NOR. There is also a signal on the sex chromosome trivalent. Y chromosome overcondensed. Note the scheme of sex chromosome pairing and scheme of the plate (particular elements separated by a dotted line) **B** two fused sister metaphases II. Note the terminal signal on five biarmed elements belonging to chromosome pairs. Odd number of chromosomes with signal suggests that NOR locus of one chromosome pair is heterozygous for NOR cluster. The X_1 chromosome includes NOR at both ends **C** *P. creticus*, mitotic metaphase. Two chromosome pairs contain a terminal NOR. Y chromosome overcondensed. On the right side: scheme of the plate (particular chromosomes marked by a line). Inset: metaphase I, sex chromosome trivalent (without signal). Note the scheme of sex chromosome pairing **D, E** *P. alticeps* **D** metaphase I. Two bivalents contain NOR. There is also signal on the sex chromosome trivalent. Y chromosome overcondensed. Note the scheme of sex chromosome pairing **E** two fused sister metaphases II, Y chromosome overcondensed. NOR bearing elements: one pair of biarmed chromosomes (a terminal NOR), one pair of acrocentric chromosomes (a terminal NOR at long arm), X_2 chromosome (a terminal NOR at long arm), X_1 chromosome (NOR at both ends). Inset: X_1 chromosome (from another plate), note the NOR at both ends **F, G** *P. phalangioides*, Madeira, metaphase I. Four bivalents include a NOR. There is also a signal on the sex chromosome trivalent. Note the scheme of sex chromosome trivalent. Abbreviations: a = chromosome of the acrocentric pair bearing NOR, b = bivalent containing NOR, bi = chromosome of a biarmed pair bearing NOR, c = centromere, ch = chromosome bearing NOR, s = sperm nucleus, SCT = sex chromosome trivalent, X_1 = X_1 chromosome, X_2 = X_2 chromosome, Y = Y chromosome. Scale bars: 10 μm except for insets (5 μm).

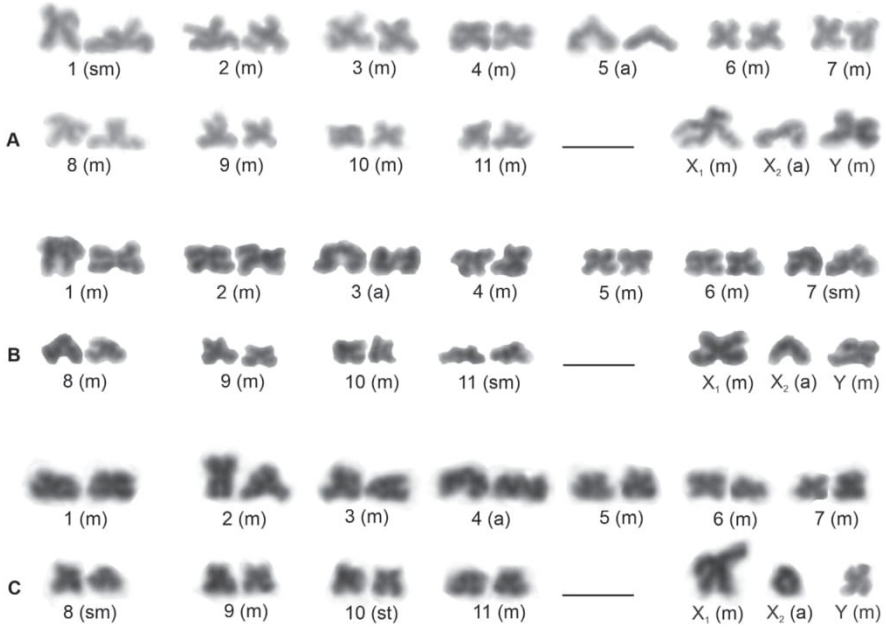

Figure 3. *Pholcus*, Macaronesian group, male karyotypes, stained by Giemsa. Based on sister metaphases II **A** *P. fuerteventurensis* **B** *P. dentatus* **C** *P. silvai*. Scale bars: 10 μm.

the sex chromosomes decreased. The Y chromosome was often more condensed than the X chromosomes and bivalents (Fig. 5E). The pattern of heteropycnosis also varied during metaphase II. While in the Madeiran species the sex chromosomes usually exhibited none or only indistinct heteropycnosis (Fig. 6A), they were often positively heteropycnotic in *P. fuerteventurensis* from the Canaries and in species from mainland Europe (Fig. 6C). The Y chromosome often showed a more intensive staining than the X chromosomes. All species were characterized by sex chromosome heteropycnosis during anaphase II whereas heteropycnosis of the X_2 chromosome was indistinct in some plates (Fig. 6B).

In the premeiotic interphase, the association of sex chromosomes transformed into sex chromosome pairing. The mode of sex chromosome pairing was most apparent during late prophase and metaphase I. Both ends of the metacentric sex chromosomes, X_1 and Y, took part in pairing (Fig. 5E, F). The pairing pattern of the monoarmed X_2 chromosome differed among species. In *P. creticus* (and in some plates of *P. alticeps* and *P. dentatus*), both ends of the X_2 chromosome were involved in pairing (Fig. 5F). The same pattern of pairing was found in *P. opilionoides* during early diplotene (Fig. 2A). After that, pairing was restricted to the long arm of the X_2 chromosome. In other species, only the long arm of the X_2 chromosome was involved in pairing, by its end (Fig. 5E); this pattern was also observed in the absence of hypotonization. The X chromosomes were usually arranged in parallel during anaphase I, metaphase II, and anaphase II (Fig. 6B). The Y chromosome was placed in the middle of the half-plates during anaphase II (Fig. 6B).

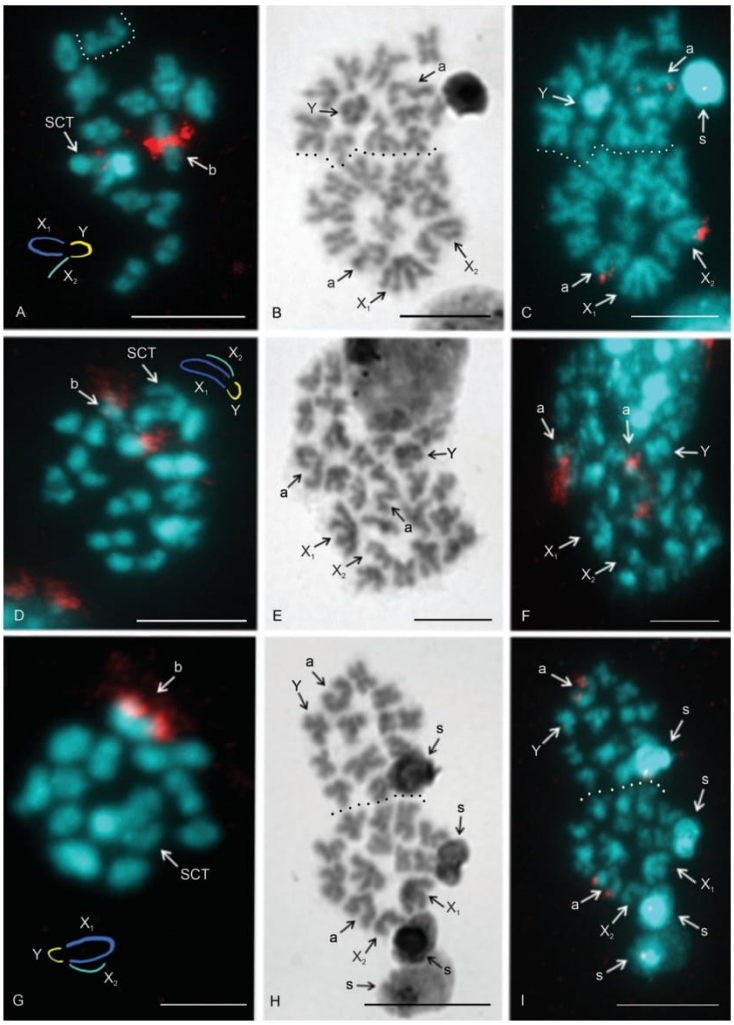

Figure 4. *Pholcus*, Macaronesian group, NOR detection **A, C, D, F, G, I** FISH **B, E, H** Giemsa staining **A–C** *P. fuerteventurensis* **A** metaphase I (a bivalent belonging to another plate is separated by a dotted line). One bivalent contains a NOR. There is also a signal on the sex chromosome trivalent. Note the scheme of sex chromosome pairing **B, C** two sister metaphases II separated by a dotted line. Note two terminal NORs, one on the long arm of the acrocentric pair and another one on the long arm of the acrocentric X_2 chromosome **D–F** *P. dentatus* **D** metaphase I, one large bivalent contains a terminal NOR. Note the scheme of sex chromosome pairing **E, F** two fused metaphases II. Long arm of the acrocentric pair contains terminal NOR. Sister chromatids of chromosomes of this pair are sometimes associated by NOR clusters (see the right chromosome of the pair) **G–I** *P. silvai* **G** metaphase I, one bivalent involves a terminal NOR. Note the scheme of sex chromosome pairing **H, I** two metaphases II separated by dotted line. Long arm of the acrocentric pair contains terminal NOR. Abbreviations: a = chromosome of the acrocentric pair bearing NOR, b = bivalent containing NOR, s = sperm nucleus, SCT = sex chromosome trivalent, X_1 = X_1 chromosome, X_2 = X_2 chromosome, Y = Y chromosome. Scale bars: 10 μm.

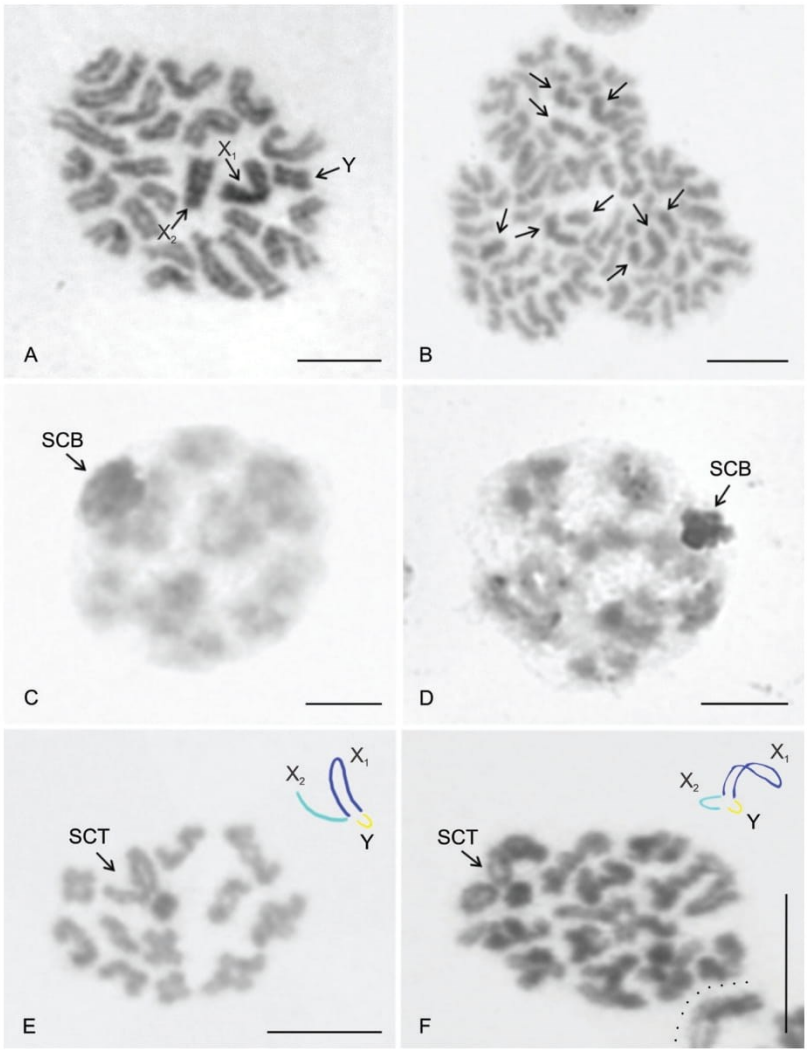

Figure 5. *Pholcus*, males, sex chromosome behavior at spermatogonial mitosis and first meiotic division, Giemsa staining **A** *P. dentatus*, spermatogonial metaphase. Note the association of positively heteropycnotic sex chromosomes in the middle of the plate **B** *P. silvai*, early spermatogonial anaphase, three half plates. Sex chromosomes exhibit a slight positive heteropycnosis and are placed in the middle of the half plates. Sex chromosomes are marked by arrows **C** *P. fuerteventurensis*, early diffuse stage. Sex chromosomes form a positively heteropycnotic body on the periphery of the nucleus **D** *P. silvai*, late diffuse stage. The sex chromosome body on the periphery of the nucleus exhibits positive heteropycnosis **E** *P. fuerteventurensis*, diakinesis (11 bivalents and a X_1X_2Y trivalent). The Y chromosome stained more intensively than the X chromosomes. Note the scheme of sex chromosome pairing **F** *P. alticeps*, diplotene (11 bivalents and a X_1X_2Y trivalent). Edge of another diplotene separated by dotted line. Note the scheme of sex chromosome pairing. Abbreviations: SCB = sex chromosome body, SCT = sex chromosome trivalent, X_1 = X_1 chromosome, X_2 = X_2 chromosome, Y = Y chromosome. Scale bars: 10 μm.

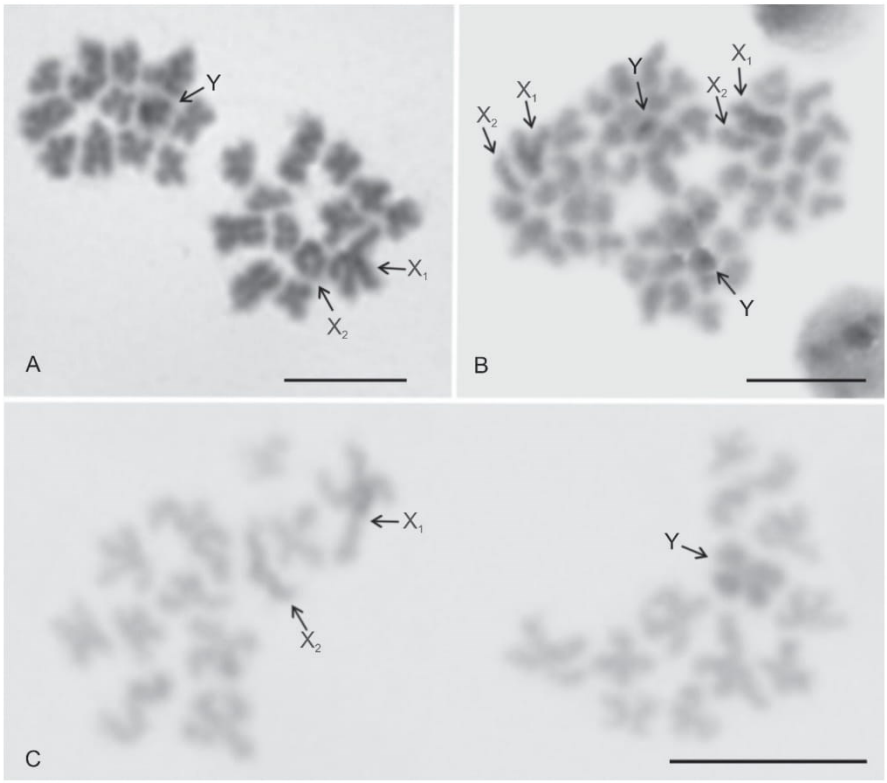

Figure 6. *Pholcus*, males, sex chromosome behavior in second meiotic division, Giemsa staining **A** *P. silvai*, two sister metaphases II. Metaphase II containing the X chromosomes is composed of 13 chromosomes. Metaphase II containing the Y chromosome comprises 12 chromosomes **B** *P. alticeps*, two sister anaphases II. Chromosomes X_1 and Y display positive heteropycnosis. The X chromosomes are associated. The Y chromosome is placed in the middle of the half plates **C** *P. fuerteventurensis*, two sister metaphases II. Plate containing the X chromosomes is incomplete (1 chromosome missing). Note the positive heteropycnosis of the sex chromosomes. Abbreviations: X_1 = X_1 chromosome, X_2 = X_2 chromosome, Y = Y chromosome. Scale bars: 10 µm.

Discussion

Pholcids are the most diversified family of haplogyne spiders with monocentric chromosomes and a suitable model group to study karyotype evolution. Their distribution is worldwide, and the available molecular phylogeny is the most comprehensive among all major spider families (Eberle et al. 2018). They are currently the best-explored family of haplogynes from a cytogenetic point of view. Closely related species often differ in their karyotypes, suggesting the involvement of chromosome rearrangements in the formation of interspecific barriers (Ávila Herrera et al. 2021).

Here we focus on karyotype differentiation of the genus *Pholcus*. Previously published cytogenetic data concern seven species determined to species level and

two species determined to genus level only (The Spider Cytogenetic Database 2022). With five newly studied species, our study increases the number of cytogenetically analyzed *Pholcus* species to 14. However, karyotype data of three species are in all probability incorrect (Table 2). These data are analysed in detail by Ávila Herrera et al. (2021). The karyotyped representatives determined to species

Table 2. Summary of *Pholcus* cytogenetic data. Doubtful data in bold. In most of these cases, it is possible to deduce probable correct information (in parentheses). †see Ávila Herrera et al. (2021: 22) for discussion of sex chromosome system. ‡See Ávila Herrera et al. (2021) for discussion of sex chromosome system (p. 23) and morphology of chromosome pairs (p. 21). §See Ávila Herrera et al. (2021) for discussion of number of chromosome pairs (p. 18) and sex chromosome system (p. 22). Abbreviations: a = acrocentric, bi = biarmed, CP = chromosome pair, m = metacentric, p = short chromosome arm, q = long chromosome arm, SC = sex chromosome, SCS = sex chromosome system, sm = submetacentric, st = subtelocentric, t = terminal, ? = unknown.

Taxon	2n	SCS	Chromosome pairs: number, morphology	Sex chromosome morphology	NOR number (CP/SC)	NOR-bearing CPs: number, morphology (NOR location)	NOR-bearing sex chromosomes: morphology (NOR location)	References
bicornutus species group								
P. pagbilao	23	X_1X_2Y	7m+3sm	X_1m+X_2a+Ysm	5/0	3 bi (t);1 bi (1 NOR p, t + 1 NOR q, t)		Ávila Herrera et al. 2021
crypticolens/*opilionoides* species group								
P. creticus	25	X_1X_2Y	5m+4sm+1st+1a	X_1m+X_2a+Ym	2/0	2 (t)		this study
P. crypticolens†	**24** (25)	**X_1X_20** (X_1X_2Y)	most or all m	X_1?+X_2?				Suzuki 1954
P. manueli‡	25	**X0** (X_1X_2Y)	**11a**	**Xsm**				Wang et al. 1997
P. opilionoides	25	X_1X_2Y	6m+5sm	X_1m+X_2a+Ym	3/2	3 bi (t)	X_1 m (1 NOR p, t + 1 NOR q, t)	Ávila Herrera et al. 2021, this study
guineensis species group (+ *P. bamboutos*)								
P. bamboutos	23	X_1X_2Y	most bi	X_1m+X_2m+Ym				Ávila Herrera et al. 2021
P. kindia	23	X_1X_2Y	8m+1sm+1st	X_1m+X_2m+Ym				Ávila Herrera et al. 2021
Macaronesian species group								
P. dentatus	25	X_1X_2Y	8m+2sm+1a	X_1m+X_2a+Ym	1/0	1a (q, t)		this study
P. fuerteventurensis	25	X_1X_2Y	9m+1sm+1a	X_1m+X_2a+Ym	1/1	1a (q, t)	X_2 a (1 NOR q, t)	this study
P. silvai	25	X_1X_2Y	8m+1sm+1st+1a	X_1m+X_2a+Ym	1/0	1a (q, t)		this study
phalangioides species group								
P. alticeps	25	X_1X_2Y	6m+3sm+1st+1a	X_1m+X_2a+Ym	2/3	1 bi (t); 1a (q, t)	X_1 m (1 NOR p, t + 1 NOR q, t); X_2 a (1 NOR q, t)	this study
P. phalangioides (Czech cytotype)	25	X_1X_2Y	9m+2sm	X_1m+X_2sm+Ym	3/3	3 bi (t)	X_1 m (1 NOR p, t + 1 NOR q, t); X_2 sm (q, t)	Král et al. 2006, Ávila Herrera et al. 2021
P. phalangioides (Madeiran cytotype)	25	X_1X_2Y	8m+2sm+1a	X_1m+X_2st+Ym	4/2	3 bi (q, t); 1 a (q, t)	X_1 m (1 NOR p, t + 1 NOR q, t)	this study
species determined to the genus level only								
Pholcus sp. (India)§	**26**(?)	**X_1X_20** (X_1X_2Y)						Sharma and Parida 1987
Pholcus sp. (Kazakhstan)	25	X_1X_2Y	7m+3sm+1a	X_1m+X_2st+Ym				Ávila Herrera et al. 2021

level represent five of the clades proposed for the genus (Huber et al. 2018), namely the *P. bicornutus*, *P. crypticolens/P. opilionoides*, *P. guineensis*, *P. phalangioides*, and Macaronesian groups.

Diploid numbers and morphology of chromosome pairs

The ancestral pholcid karyotype probably consisted of 15 chromosome pairs and the sex chromosomes X_1, X_2, and Y (Ávila Herrera et al. 2021). Like many other spider groups (Suzuki 1954; Král et al. 2006, 2013), some pholcid clades show a trend towards a decrease in chromosome number (Ávila Herrera et al. 2021). This is also probably how the ancestral karyotype of the subfamily Pholcinae has evolved with its 11 chromosome pairs and sex chromosomes X_1, X_2, and Y. This karyotype is also ancestral for *Pholcus* (Ávila Herrera et al. 2021). It was found in all karyotyped clades of the genus except for the *P. bicornutus* and *P. guineensis* groups (Ávila Herrera et al. 2021; this study). In the latter two species groups, the number of chromosome pairs decreased further to ten. This feature could be a synapomorphy of a large group within *Pholcus* comprising the Subsaharan African, Southeast Asian, and Australasian groups of this genus (Ávila Herrera et al. 2021).

The chromosome pairs of ancestral pholcids probably had a biarmed morphology (Ávila Herrera et al. 2021). Most pairs were probably metacentric. Chromosome pairs of *Pholcus* species are predominated by biarmed chromosomes except for *P. manueli* Gertsch, 1937 (Wang et al. 1997). However, the information on this species is based only on the pattern of constitutive heterochromatin. Therefore, it should be reanalyzed by determination of chromosome morphology at the mitotic metaphase or metaphase II (Ávila Herrera et al. 2021).

The karyotype of the unidentified *Pholcus* sp. from Kazakhstan reported in Ávila Herrera et al. (2021) contains a large acrocentric pair, which was supposed to be an apomorphy of this species. Kazakhstan is inhabited by representatives of the *P. crypticolens/opilionoides* and *P. ponticus* groups (Huber 2011). Our study revealed that the acrocentric pair is in fact more common in Eurasian *Pholcus* groups with the karyotype formula 25, X_1X_2Y. The pair is the third, fourth or fifth by size and its relative length ranges from 7.20 to 8.22% of TCL (Ávila Herrera et al. 2021; this study). The end of the long arm of this pair contains a NOR (see discussion on NOR evolution below). The large acrocentric pair has most probably originated by a pericentric inversion from a biarmed one. In the present study, it was found in representatives of all analyzed groups. This pattern suggests that the large acrocentric pair could be a synapomorphy of several species groups within the genus with the karyotype formula 25, X_1X_2Y. A further interesting pattern was found in *P. phalangioides*. While the cytotype from Madeira retained the large acrocentric pair, in the Czech cytotype this pair had reverted to biarmed, thus the karyotype was again composed exclusively of biarmed chromosomes. Since the chromosome pairs of the above mentioned cytotypes differed only by this reversion, it most probably resulted from a pericentric inversion. Furthermore, the reversion of an acrocentric pair to biarmed had also occurred in *P. opilionoides* whose karyotype is also formed exclusively by biarmed chromosomes. The acrocentric pair is not present in

karyotypes of the *Pholcus* lineages with the formula 23, X_1X_2Y. However, a reversion of an acrocentric pair to non-acrocentric cannot be ruled out in ancestors of these lineages. If such a scenario is correct, the large acrocentric pair would be a synapomorphy of the entire genus *Pholcus.* This marker has not been found in the sister clade of *Pholcus*, i.e. the *Micropholcus/Leptopholcus* clade (Ávila Herrera et al. 2021). However, the large acrocentric pair could even have been present in the ancestral karyotype of the *Micropholcus/Leptopholcus* clade. The karyotypes of this clade have been derived from the supposed ancestral karyotype of pholcines (25, X_1X_2Y) by multiple fusions of chromosome pairs. The large acrocentric pair could have been involved into these fusions.

Closely related species of *Pholcus* often differ by the morphology of one or several chromosome pairs. For example, *P. fuerteventurensis* from the Canaries (belonging to the Macaronesian clade) differs from species of the same clade from Madeira by the morphology of three pairs. A possible apomorphy of *P. fuerteventurensis* is the transformation of the largest chromosome pair from metacentric to submetacentric. The Madeiran species show two possible synapomorphies, namely transformations of two metacentric pairs into submetacentric or subtelocentric. The first transformation concerned the 7th pair of *P. dentatus* and the 8th pair of *P. silvai*, respectively. The second transformation concerned the 11th pair of *P. dentatus* and the 10th pair of *P. silvai*, respectively (Suppl. material 1). Even greater are the differences found between *P. opilionoides* and *P. creticus* from the *P. crypticolens/opilionoides* clade. A possible synapomorphy of these species is the change of two metacentric pairs to submetacentric (2nd and 4th pairs). While the large acrocentric pair has been retained in *P. creticus*, it has converted to biarmed in *P. opilionoides*. Moreover, both species differ by the morphology of five other chromosome pairs (Suppl. material 1). Potential synapomorphies of *P. alticeps*, *P. phalangioides* (*P. phalangioides* group) and *Pholcus* sp. from Kazakhstan include changes of two metacentric pairs into submetacentric. The first change concerned probably the 6th pair of *P. alticeps*, the 8th pair of *P. phalangioides* (the 7th pair in Ávila Herrera et al. 2021), and the 7th pair of *Pholcus* sp. The second change concerned probably the 9th pair of *P. alticeps*, the 11th pair of *P. phalangioides* (the 10th pair in Ávila Herrera et al. 2021), and the 9th pair of *Pholcus* sp.

A similar karyotype differentiation, where the morphology of one or more chromosome pairs changed while the number of chromosome pairs remained the same, has also been found in other pholcid genera (Ávila Herrera et al. 2021). These changes in morphology occurred most probably by pericentric inversions or translocations. These rearrangements leave the chromosome number unchanged and they can often result in reproductive isolation (Rieseberg 2001; Ayala et al. 2005).

Sex chromosomes

All *Pholcus* species studied so far exhibit the X_1X_2Y system (Král et al. 2006; Ávila Herrera et al. 2021, this study). Many haplogynes with the X_1X_2Y system have retained its ancestral type with two large metacentric X chromosomes and a metacentric microchromosome Y (Ávila Herrera et al. 2021).

The genus *Pholcus*, like most other pholcids with the X_1X_2Y system (Ávila Herrera et al. 2021), is conservative in having a metacentric X_1 chromosome, which is the largest chromosome of the set. In *Pholcus* species with the karyotype 25, X_1X_2Y, the size of the X_1 ranges from 9.87 to 14.37% of TCL (Ávila Herrera et al. 2021; this study). The size of the Y chromosome has increased considerably in a clade of the subfamily Pholcinae including *Quamtana* Huber, 2003, *Muruta* Huber, 2018, *Leptopholcus* Simon, 1893, and *Pholcus*. In general, the Y chromosome can increase in size by accumulation of constitutive heterochromatin, rearrangements between autosomes and sex chromosomes, or by a combination of these events (e.g., Kejnovský et al. 2009; Schartl et al. 2016). Available data suggest a major role of heterochromatin accumulation in the expansion of the pholcine Y chromosome. The Y chromosome of *P. phalangioides* is composed exclusively of constitutive heterochromatin (Král et al. 2006). A reinterpretation of karyotype data obtained by Wang et al. (1997) suggests the same composition of the Y chromosome in *P. manueli* (Ávila Herrera et al. 2021). Constitutive heterochromatin is a very dynamic part of the genome. The size of heterochromatic blocks could change even within populations (Sumner 1990). Although the Y chromosome of *Pholcus* is formed exclusively by heterochromatin, its size is relatively stable in this genus ranging from 4.77 to 7.10% of TCL except for *P. kindia* Huber, 2011 (11.72% of TCL) (Ávila Herrera et al. 2021; this study). Particular *Pholcus* species might differ by the extent of condensation in the Y chromosome, which contributes to its diversity in size. The enormous increase in size of the Y chromosome in *P. kindia* was probably caused by insertions of autosomal material (Ávila Herrera et al. 2021). Among other spiders with the X_1X_2Y system, a considerable increase of the Y chromosome size has only been found in one representative of pacullid spiders (Král et al. 2019).

The increase of Y chromosome size in pholcines has been accompanied by a reduction of the X_2 chromosome. The X_2 and Y chromosomes exhibit a similar size in the *Pholcus* clades analyzed in this study. The X_2 chromosome is the most dynamic chromosome of the X_1X_2Y system in pholcids. It exhibits a considerable diversity in size and morphology (Ávila Herrera et al. 2021). The ancestral metacentric morphology of the X_2 chromosome has changed frequently to submetacentric or even monoarmed, probably by pericentric inversions or translocations (Ávila Herrera et al. 2021). As already mentioned, these rearrangements can play a role in the formation of reproductive barriers. This effect is even stronger if the rearrangement concerns sex chromosomes (Presgraves 2008; Kitano et al. 2009; Hooper et al. 2019). The ancestral X_2 chromosome of *Pholcus* was probably metacentric as found in *P. guineensis* and *P. bamboutos* Huber, 2011 (23, X_1X_2Y). This hypothesis is supported by the biarmed morphology of the X_2 chromosome in the closest relatives of *Pholcus* (Ávila Herrera et al. 2021). During following evolution, the morphology of the X_2 chromosome gradually changed to acrocentric. This scenario is supported by the non-acrocentric morphology of this element in two species with the formula 25, X_1X_2Y, *P. phalangioides* (submetacentric or subtelocentric X_2) and *Pholcus* sp. (subtelocentric X_2). The size of the X_2 chromosome ranges from 5.53 to 6.56% of TCL in species with this formula (Ávila Herrera et al. 2021; this study).

Interestingly, Madeiran and central European specimens of *P. phalangioides* differed slightly in the morphology of the X_2 chromosome. While the X_2 chromosome of the Czech *P. phalangioides* was submetacentric (centromeric index 2.85), the X_2 of the Madeiran specimen was subtelocentric (centromeric index 3.96) (Ávila Herrera et al. 2021; this study). This change in morphology might result from chromosome rearrangement or addition of heterochromatin. The acrocentric morphology of the X_2 chromosome observed in some metaphases II of *P. phalangioides* is an artifact resulting from precocious separation of chromatids of this chromosome.

The sex chromosomes in *Pholcus* show a specific behavior in the male germline, which, like in other pholcids, includes positive heteropycnosis (more intensive staining), preferential location, and association or pairing. The association and heteropycnosis of sex chromosomes occur as early as during spermatogonial mitosis. Moreover, the sex chromosomes are usually located in the middle of spermatogonial plates, specifically on the metaphase plates (Král et al. 2006; Ávila Herrera et al. 2021; this study) and anaphase half plates (this study). Such behavior in spermatogonial anaphase has not been reported so far and it might occur in other spider species as well, not only in the taxa with the X_1X_2Y system. Due to its short duration, the spermatogonial anaphase is only rarely observed, which precludes analysis of sex chromosome behavior during this period. During the premiotic interphase in pholcids, the sex chromosome association evolves into pairing that continues up to metaphase I (Král et al. 2006; Ávila Herrera et al. 2021; this study). Chromosomes of the X_1X_2Y system are usually located at the periphery of the plate during early prophase I and diffuse stage. In contrast to that, during late prophase I and metaphase I, they tend to be in the middle of the plate. After segregation of the X and Y chromosomes, the X chromosomes are associated till the end of meiosis. The Y chromosome is usually located in the middle of half plates during anaphase II. Sex chromosomes are positively heteropycnotic only in some phases of meiosis (Ávila Herrera et al. 2021; this study).

Metacentric chromosomes of the X_1X_2Y system pair without chiasmata in male meiosis, namely by the ends of both arms (Silva et al. 2002; Král et al. 2006; Ávila Herrera et al. 2021). In some species with a non-metacentric X_2 chromosome, both chromosome ends remain involved in chromosome pairing. In other species, however, the non-metacentric X_2 chromosome only pairs by the end of its long arm (Král et al. 2006; Ávila Herrera et al. 2021; this study). In *P. creticus*, both ends of the acrocentric X_2 chromosome take part in pairing. In *P. alticeps* and *P. dentatus*, which share the morphology of the X_2 chromosome with *P. creticus*, pairing by both ends was only observed in a small proportion of the cells probably because the pairing of the shorter arm is less stable and loosens during the hypotonization and fixation step of chromosome preparation. In *P. opilionoides*, pairing of the X_2 chromosome by both ends was only observed in the early diplotene; afterwards, the chromosome paired only by its long arm. In other *Pholcus* species with a monoarmed X_2 chromosome, only the long arm of X_2 was involved in pairing (Ávila Herrera et al. 2021; this study). This pattern was observed even in the absence of hypotonization (this study), which indicates that it is not an artifact.

NORs

So far, NORs have only been detected in a low number of spider species (see Forman et al. 2013; Král et al. 2013 for references), especially by the means of FISH (see Šťáhlavský et al. 2020; Reyes Lerma et al. 2021 for references). In pholcids, however, NOR patterns have been determined recently in many species by FISH (Ávila Herrera et al. 2021), which makes it possible to contextualize our data with previous knowledge on the NOR evolution in this family. Pholcid spiders show a highly variable numbers of NORs (one to nine), which in the majority of pholcids occur on chromosome ends (Ávila Herrera et al. 2021). Their terminal position suggests that the NORs spread within the karyotype mostly by ectopic recombination, which is most effective in telomeric areas (Goldman and Lichten 1996). NOR bearing pairs in pholcids have a biarmed morphology except for the acrocentric pair found in the present study in most *Pholcus* species with the karyotype formula 25, X_1X_2Y. Unlike in other spiders, the spreading of NORs to sex chromosomes is quite common in haplogynes (including pholcids, where it has occurred at least five times) (Král et al. 2006; Ávila Herrera et al. 2021).

The ancestral pattern of the subfamily Pholcinae probably involves three chromosome pairs with a terminal NOR each. Prior to the separation of *Aetana* Huber, 2005, a NOR locus appeared on one end of the X_1. Thereafter, the NORs gradually spread to the other end of the X_1 chromosome and to the end of the long arm of the X_2, i.e., to the regions that ensure the achiasmatic pairing of the sex chromosomes. We assume that the sex chromosome-linked NORs (SCL-NORs) take part in this pairing (Ávila Herrera et al. 2021), probably together with the sequences of the Y chromosome invading the end of the X_2 (Sember et al. 2020).

Our study reveals a considerable diversity of NOR patterns in *Pholcus*. Based on data from *Pholcus* and the closely related genera, we suppose that the ancestral NOR pattern of *Pholcus* probably comprised two or three chromosome pairs with a terminal NOR locus each and three terminal X chromosome-linked loci (two on the X_1 chromosome and one on the X_2). The number of loci has then increased in some species and decreased in others (Ávila Herrera et al. 2021; this study). In *P. pagbilao* Huber, 2011, four NOR bearing pairs have been found, one of them with two terminal NORs (Ávila Herrera et al. 2021). Four NOR-bearing pairs were also found in the Madeiran cytotype of *P. phalangioides* (this study).

A reduction in the number of NORs has occurred repeatedly in *Pholcus*, both on chromosome pairs and on chromosomes of the X_1X_2Y system. Thus, the Macaronesian clade exhibits a single acrocentric NOR-bearing pair. *P. fuerteventurensis* from the Canaries retained a single SCL-NOR located at the end of the X_2 chromosome. The two Madeiran species share a degeneration/loss of SCL-NORs. In the *P. crypticolens/opilionoides* group, the reduction was more extensive in SCL-NORs than in NORs located on chromosome pairs. The pattern of *P. opilionoides* differs from the supposed ancestral pattern only by the absence of the X_2-linked NOR, while the pattern of *P. creticus* is more derived, the SCL-NORs are degenerated/lost (this study). In *P. pagbilao* (*P. bicornutus* group), the number of NOR-bearing chromosome pairs has increased to four whereas

SCL-NORs were degenerated/lost (Ávila Herrera et al. 2021). Remarkably, particular clades differ in their pattern of reduction of SCL-NORs. In the *P. phalangioides* and *P. crypticolens/opilionoides* groups, the X_2-linked NOR has been degenerated/lost first. In the Macaronesian clade, however the degeneration/loss has first affected the X_1-linked NORs (this study). The rDNA sequences responsible for achiasmatic pairing of sex chromosomes could be retained even after degeneration of SCL-NORs, as already reported from the males of *Drosophila* Fallén, 1823 (Roy et al. 2005). The reasons for the repeated degeneration of SCL-NORs in *Pholcus* are unclear. All species without SCL-NORs are island species. Island populations are frequently reduced and thus experience genetic drift, which could lead to random fixation of sex chromosomes without NORs. Moreover, genetic drift is more effective in case of sex chromosomes whose number in the population is reduced in comparison with autosomes (Johnson and Lachance 2012). Within the subfamily Pholcinae, the loss of the SCL-NORs had also occurred in a clade including *Canticus* and *Micropholcus*. In this case, the loss of these NORs has been accompanied by a conversion of the X_1X_2Y system to X0 (Ávila Herrera et al. 2021).

Karyotype diversity in *P. phalangioides*

P. phalangioides showed intraspecific diversity of the NOR pattern and chromosome morphology. Considering NORs, the Czech cytotype exhibited the supposedly ancestral pattern of *Pholcus* (Ávila Herrera et al. 2021). In the Madeiran cytotype, the number of the NOR-bearing pairs has increased to four, each pair containing one NOR locus. The NOR on the X_2 chromosome has been lost. Intraspecific variability in the NOR number has not previously been reported from pholcids, but it could be expected based on the occurrence of heterozygotes for number of NORs in some species (Ávila Herrera et al. 2021).

The karyotype differences between the Czech and Madeiran cytotype were, however, more profound. They also differed in the morphology of some chromosomes. The chromosome pairs of the Madeiran cytotype showed the original pattern; they included a large acrocentric pair, which has changed to biarmed in the Czech cytotype. Furthermore, both cytotypes differed to some extent in the morphology of the X_2 chromosome. Intraspecific differences in chromosome morphology have not been previously reported from pholcids. Whether the presence of different cytotypes is in any way related to the apparent *COI* polymorphism in this species (documented in the sequences deposited at NCBI) is unknown. The status of both cytotypes should be further analysed using larger samples and approaches of integrative taxonomy.

Conclusions

We present new data on karyotypes and meiotic division of seven species of the genus *Pholcus* (Pholcidae) from Europe. The selected species represent several different species groups within the region whose relationships among each other remain largely

unknown. The male karyotype is composed of 25 chromosomes with a X_1X_2Y sex chromosome system. The sex chromosomes pair without chiasmata during male meiosis. The karyotypes are predominated by biarmed chromosomes. The karyotypes of most species contain an acrocentric chromosome pair, which has changed to biarmed in some taxa. This marker is either a synapomorphy of the species groups included in this study or a synapomorphy of the genus *Pholcus*. Closely related species usually differ in the morphology of one or several chromosome pairs, which suggests the operation of pericentric inversions and/or translocations. Such rearrangements have been implicated in speciation. The chromosomes X_1 and Y show a metacentric morphology. By contrast, the X_2 chromosome is usually acrocentric. NOR patterns are very diversified. In the ancestor of *Pholcus*, these structures were located both on chromosome pairs and on sex chromosomes. Sex chromosome-linked NORs could be involved in the pairing of sex chromosomes. Most of the analyzed species show a specific pattern of NORs. Nucleolus organizer regions have often been degenerated/lost during evolution. Remarkably, the loss seems to preferably affect SCL-NORs. The reason for this phenomenon is unclear. The rDNA sequences crucial for sex chromosome pairing might remain unaffected by the degeneration. *P. phalangioides* yielded two cytotypes, which differ in their chromosome morphology and NOR pattern. Some of the detected chromosome changes appear phylogenetically informative. Although the Macaronesian clade shows a very high rate of speciation, species of this lineage do not differ substantially in the number of chromosome changes from other analyzed lineages of *Pholcus*. However, this conclusion needs to be corroborated by an analysis of more species and species groups.

Acknowledgements

We are very thankful to our colleagues M. Forman (Charles University, Prague, Czech Republic) for improvement of the figures and valuable comments on the manuscript, T. Kořínková (Prague) and R. Angus (Natural History Museum, London, Great Britain) for inspiring discussion on the manuscript and correction of the English, S. Pekár (Masaryk University, Brno, Czech Republic) and D. Holá (Charles University, Prague, Czech Republic) for assistance with statistical evaluation of data, A. Roušar (Chomutov, Czech Republic) for collections of *P. alticeps*, and T.L. Heller (Ludwig-Maximilians-University, Munich, Germany) for participation in collection of *P. creticus*. Finally, we are obliged to the reviewers (L.M. Mola, University of Buenos Aires, Buenos Aires, Argentina; M.P. Rincão, Universidade Estadual de Londrina, Londrina, Brazil; and an anonymous reviewer) for their comments.

Our study was supported by the Czech Ministry of Education, Youth, and Sports (projects LTAUSA 19142 and SVV 260568: IMAH, JK) and the Chilean National Commission for Scientific and Technological Research (ANID) (IMAH). The collection of *P. creticus* by JK and JP was supported by a scholarship, which was based on agreement between the Czech Ministry of Education, Youth, and Sports and the Greek Ministry of Education, Lifelong Learning, and Religious Affairs. Fluorescence micros-

copy was performed in the Laboratory of Confocal and Fluorescence Microscopy, Faculty of Science, Charles University (Prague, Czech Republic). This laboratory is co-financed by the European Regional Development Fund and the state budget of the Czech Republic, projects no. CZ.1.05/4.1.00/16.0347 and CZ.2.16/3.1.00/21515, and supported by the Czech-BioImaging large RI project LM2015062.

References

Araujo D, Schneider MC, Paula-Neto E, Cella DM (2012) Sex chromosomes and meiosis in spiders: a review. In: Swan A (Ed.) Meiosis: molecular mechanisms and cytogenetic diversity. IntechOpen, Rijeka, 87–108. https://doi.org/10.5772/31612

Araujo D, Schneider MC, Zacaro AA, de Oliveira EG, Martins R, Brescovit AD (2020) Venomous *Loxosceles* species (Araneae, Haplogynae, Sicariidae) from Brazil: 2n♂ = 23 and X_1X_2Y sex chromosome system as shared characteristics. Zoological Sciences 37: 128–139. https://doi.org/10.2108/zs190128

Ávila Herrera IM, Carabajal Paladino LZ, Musilová J, Palacios Vargas JG, Forman M, Král J (2016) Evolution of karyotype and sex chromosomes in two families of haplogyne spiders, Filistatidae and Plectreuridae. Proceedings of the 21st International Chromosome Conference, Foz do Iguaçu (Brazil), July 2016. Cytogenetic and Genome Research 148: 104.

Ávila Herrera IM, Král J, Pastuchová M, Forman M, Musilová J, Kořínková T, Šťáhlavský F, Zrzavá M, Nguyen P, Just P, Haddad, CR, Hiřman M, Koubová M, Sadílek D, Huber BA (2021) Evolutionary pattern of karyotypes and meiosis in pholcid spiders (Araneae: Pholcidae): implications for reconstructing chromosome evolution of araneomorph spiders. BMC Ecology and Evolution 21: e93. https://doi.org/10.1186/s12862-021-01828-3

Ayala F, Coluzzi M (2005) Chromosome speciation: humans, *Drosophila*, and mosquitoes. Proceedings of the National Academy of Sciences 102(Suppl. 1): 6535–6542. https://doi.org/10.1073/pnas.0501847102

Dimitrov D, Ribera C (2007) The genus *Pholcus* (Araneae, Pholcidae) in the Canary Islands. Zoological Journal of the Linnean Society 151(1): 59–114. https://doi.org/10.1111/j.1096-3642.2007.00316.x

Dimitrov D, Arnedo MA, Ribera C (2008) Colonization and diversification of the spider genus *Pholcus* Walckenaer, 1805 (Araneae, Pholcidae) in the Macaronesian archipelagos: evidence for long-term occupancy yet rapid recent speciation. Molecular Phylogenetis and Evolution 48(2): 596–614. https://doi.org/10.1016/j.ympev.2008.04.027

Dolejš P, Kořínková T, Musilová J, Opatová V, Kubcová L, Buchar J, Král J (2011) Karyotypes of central European spiders of the genera *Arctosa*, *Tricca*, and *Xerolycosa* (Araneae: Lycosidae). European Journal of Entomology 108: 1–16. https://doi.org/10.14411/eje.2011.001

Eberle J, Dimitrov D, Valdez-Mondragón A, Huber BA (2018) Microhabitat change drives diversification in pholcid spiders. BMC Evolutionary Biology 18: e141. https://doi.org/10.1186/s12862-018-1244-8

Forman M, Nguyen P, Hula V, Král J (2013) Sex chromosome pairing and extensive NOR polymorphism in *Wadicosa fidelis* (Araneae: Lycosidae). Cytogenetic and Genome Research 141(1): 43–49. https://doi.org/10.1159/000351041

Fuková I, Nguyen P, Marec F (2005) Codling moth cytogenetics: karyotype, chromosomal location of rDNA, and molecular differentiation of sex chromosomes. Genome 48(6): 1083–1092. https://doi.org/10.1139/g05-063

Goldman AS, Lichten M (1996) The efficiency of meiotic recombination between dispersed sequences in *Saccharomyces cerevisiae* depends upon their chromosomal location. Genetics 144(1): 43–55. https://doi.org/10.1093/genetics/144.1.43

Hooper DM, Griffith SC, Price TD (2019) Sex chromosome inversions enforce reproductive isolation across an avian hybrid zone. Molecular Ecology 28: 1246–1262. https://doi.org/10.1111/mec.14874

Huber BA (2011) Revision and cladistic analysis of *Pholcus* and closely related taxa (Araneae, Pholcidae). Bonner Zoologische Monographien 58: 1–509.

Huber BA, Eberle J, Dimitrov D (2018) The phylogeny of pholcid spiders: a critical evaluation of relationships suggested by molecular data (Araneae, Pholcidae). ZooKeys 789: 51–101. https://doi.org/10.3897/zookeys.789.22781

Johnson NA, Lachance J (2012) The genetics of sex chromosomes: evolution and implications for hybrid incompatibility. Annals of the New York Academy of Sciences 1256: E 1–22. https://doi.org/10.1111/j.1749-6632.2012.06748.x

Kejnovský E, Hobza R, Čermák T, Kubát Z, Vyskot B (2009) The role of repetitive DNA in structure and evolution of sex chromosomes in plants. Heredity 102: 533–541. https://doi.org/10.1038/hdy.2009.17

Kitano J, Ross JA, Mori S, Kume M, Jones FC, Chan YF, Absher DM, Grimwood J, Schmutz J, Myers RM, Kingsley DM, Peichel CL (2009) A role for a neo-sex chromosome in stickleback speciation. Nature 461: 1079–1083. https://doi.org/10.1038/nature08441

Kořínková T, Král J (2013) Karyotypes, sex chromosomes, and meiotic division in spiders. In: Nentwig W (Ed.) Spider ecophysiology. Springer, Berlin, 159–171. https://doi.org/10.1007/978-3-642-33989-9

Král J, Musilová J, Šťáhlavský F, Řezáč M, Akan Z, Edwards RL, Coyle FA, Almerje CR (2006) Evolution of the karyotype and sex chromosome systems in basal clades of araneomorph spiders (Araneae: Araneomorphae). Chromosome Research 14: 859–880. https://doi.org/10.1007/s10577-006-1095-9

Král J, Kořínková T, Krkavcová L, Musilová J, Forman M, Ávila Herrera IM, Haddad CR, Vítková M, Henriques S, Palacios Vargas JG, Hedin M (2013) Evolution of karyotype, sex chromosomes, and meiosis in mygalomorph spiders (Araneae: Mygalomorphae). Biological Journal of the Linnean Society 109(2): 377–408. https://doi.org/10.1111/bij.12056

Král J, Forman M, Kořínková T, Reyes Lerma AC, Haddad CR, Musilová J, Řezáč M, Ávila Herrera IM, Thakur S, Dippenaar-Schoeman AS, Marec F, Horová L, Bureš P (2019) Insights into the karyotype and genome evolution of haplogyne spiders indicate a polyploid origin of lineage with holokinetic chromosomes. Scientific Reports 9: e3001. https://doi.org/10.1038/s41598-019-39034-3

Miller DA, Dev VG, Tantravahi R, Miller OJ (1976) Suppression of human nucleolus organizer activity in mouse-human somatic hybrid cells. Experimental Cell Research 101: 235–243. https://doi.org/10.1016/0014-4827(76)90373-6

Mola LM, Papeschi AG (2006) Holokinetic chromosomes at a glance. Journal of Basic and Applied Genetics 17(1): 17–33.

Paula-Neto E, Cella DM, Araujo D, Brescovit AD, Schneider MC (2017) Comparative cytogenetic analysis among filistatid spiders (Araneomorphae: Haplogynae). Journal of Arachnology 45: 123–128. https://doi.org/10.1636/M14-69.1

Presgraves DC (2008) Sex chromosomes and speciation in *Drosophila*. Trends in Genetics 24: 336–343. https://doi.org/10.1016/j.tig.2008.04.007

Reyes Lerma AC, Šťáhlavský F, Seiter M, Carabajal Paladino LZ, Divišová K, Forman M, Sember A, Král J (2021) Insights into the karyotype evolution of Charinidae, the early-diverging clade of whip spiders (Arachnida: Amblypygi). Animals 11(11): e3233. https://doi.org/10.3390/ani11113233

Rieseberg LH (2001) Chromosomal rearrangements and speciation. Trends in Ecology and Evolution 1(7): 351–358. https://doi.org/10.1016/S0169-5347(01)02187-5

Roy V, Monti-Dedieu L, Chaminade N, Siljak-Yakovlev S, Aulard S, Lemeunier F, Montchamp-Moreau C (2005) Evolution of the chromosomal location of rDNA genes in two *Drosophila* species subgroups: *ananassae* and *melanogaster*. Heredity 94: 388–395. https://doi.org/10.1038/sj.hdy.6800612

Sadílek D, Nguyen P, Halil K, Kovařík F, Yağmur EA, Šťáhlavský F (2015) Molecular cytogenetics of *Androctonus* scorpions: an oasis of calm in the turbulent karyotype evolution of the diverse family Buthidae. Biological Journal of the Linnean Society 115(1): 69–76. https://doi.org/10.1111/bij.12488

Schartl M, Schmid M, Nanda I (2016) Dynamics of vertebrate sex chromosome evolution: from equal size to giants and dwarfs. Chromosoma 125: 553–571. https://doi.org/10.1007/s00412-015-0569-y

Sember A, Pappová M, Forman M, Nguyen P, Marec F, Dalíková M, Divišová K, Doležálková-Kaštánková M, Zrzavá M, Sadílek D, Hrubá B, Král J (2020) Patterns of sex chromosome differentiation in spiders: insights from comparative genomic hybridisation. Genes 11(8): e849. https://doi.org/10.3390/genes11080849

Shao L, Li S (2018) Early Cretaceous greenhouse pumped higher taxa diversification in spiders. Molecular Phylogenetics and Evolution 127: 146–155. https://doi.org/10.1016/j.ympev.2018.05.026

Sharma N, Parida BB (1987) Study of chromosomes in spiders from Orissa. Pranikee 8: 71–76.

Šťáhlavský F, Forman M, Just P, Denič F, Haddad CR, Opatova V (2020) Cytogenetics of entelegyne spiders (Arachnida, Araneae) from southern Africa. Comparative Cytogenetics 14(1): 107–138. https://doi.org/10.3897/CompCytogen.v14i1.48667

Sumner TA (2003) Chromosomes: Organization and function. Blackwell Science Ltd., Malden, 287 pp. https://doi.org/10.1002/9780470695975

Suzuki S (1954) Cytological studies in spiders. III. Studies on the chromosomes of fifty-seven species of spiders belonging to seventeen families, with general considerations on chromosomal evolution. Journal of Science of the Hiroshima University, series B, division 1 15(2): 23–136.

The Spider Cytogenetic Database (2022) The spider cytogenetic database 2022. http://www.arthropodacytogenetics.bio.br/spiderdatabase/ [Accessed on 23.10.2022]

Wang X, Cui S, Yang Z, Wang J, Wang Y (1997) On karyotype of the *Pholcus affinis* (Araneida: Pholcidae). Acta Arachnologica Sinica 1: 19–22.

Wheeler WC, Coddington JA, Crowley LM, Dimitrov D, Goloboff PA, Griswold CE, Hormiga G, Prendini L, Ramírez MJ, Sierwald P, Almeida-Silva L, Alvarez-Padilla F, Arnedo MA, Benavides Silva LR, Benjamin SP, Bond JE, Grismado CJ, Hasan E, Hedin M, Izquierdo MA, Labarque FM, Ledford J, Lopardo L, Maddison WP, Miller JA, Piacentini LN, Platnick NI, Polotow D, Silva-Dávila D, Scharff N, Szűts T, Ubick D, Vink CJ, Wood HM, Zhang J (2017) The spider tree of life: phylogeny of Araneae based on target-gene analyses from an extensive taxon sampling. Cladistics 33: 574–616. https://doi.org/10.1111/cla.12182

World Spider Catalog (2022) World spider catalog version 23.0. Natural History Museum, Bern 2022. http://wsc.nmbe.ch [Accessed on 23.10.2022]

ORCID

Jiří Král https://orcid.org/0000-0002-6442-8554
Ivalú M. Ávila Herrera https://orcid.org/0000-0003-4387-5723
František Šťáhlavský https://orcid.org/0000-0002-8520-9166
David Sadílek https://orcid.org/0000-0001-6877-887X
Jaroslav Pavelka https://orcid.org/0000-0001-8834-7540
Maria Chatzaki https://orcid.org/0000-0001-7529-8962
Bernhard A. Huber https://orcid.org/0000-0002-7566-5424

Supplementary material 1

Species studied, male karyotype data (including standard deviation)

Authors: Jiří Král, Ivalú M. Ávila Herrera, František Šťáhlavský, David Sadílek, Jaroslav Pavelka, Maria Chatzaki, Bernhard A. Huber

Data type: Table (MS Excel file)

Explanation note: Abbreviations: parameters = parameters used to describe chromosome morphology [CI = centromeric index, RCL = relative chromosome length (% of TCL)], specimens = number of specimens used to obtain data (*specimens from Stavros were analysed). Chromosome morphology is indicated by background colour of a box (pink: metacentric, brown: submetacentric, dark blue: subtelocentric, light blue: acrocentric).

Link: https://doi.org/10.3897/compcytogen.v16.i4.85059.suppl1

Electronical supplement of the paper is at the thesis supplements.

Publication 4.4. Huber BA, Meng G, Král J, **Ávila Herrera IM**, Izquierdo M, Carvalho LS (2023). High and dry: integrative taxonomy of the Andean spider genus *Nerudia* (Araneae: Pholcidae). Zoological Journal of the Linnean Society. 198, 534–591. DOI.org/10.5852/ejt.2023.880.217317.07.23

IF2022: 1.8

Pholcidae are called ”daddy long-legs” spiders at English. Representatives of the subfamily Ninetinae are atypical with their relatively short limbs. Ninetines are found in the arid environments of the Americas and the Arabian Peninsula. Representatives of the genus *Nerudia* analyzed in the present work have been found as high as 4450 m a.s.l. Ninetines remain largely unexplored, with many undescribed species. The low level of knowledge also applies to their cytogenetics.

This paper is focused on the integrative taxonomy of the ninetine genus *Nerudia* including the description of ten new species using morphology pattern as well COI barcodes. Furthermore, this paper contain first information on cytogenetics of *Nerudia* as well as closely related genus *Gertschiola.*

Only two representatives of ninetines have been karyotyped so far, namely *Kambiwa neotropica* and *Pholcophora americana.* Our study contributed karyotypes of three species: *Nerudia poma*, *N. ola* and *Gertschiola macrostyla*.

Male karyotypes of analysed ninetines consisted of 24-28 chromosomes. They shared X_1X_2Y sex chromosome system, predominance of biarmed chromosomes, diffuse stage, and sex chromosome linked NOR. Sex chromosomes formed an achiasmatic tetravalent during male meiosis. In this tetravalent, X chromosomes were associated by one end with Y chromosome. The length of the Xs and Y chromosome was similar in *Nerudia ola*. While Y chromosome was somewhat smaller than X chromosome in *N. poma*, it was a microchromosome in *Gertschiola*. FISH revealed one or two NOR-bearing chromosome pairs as well as sex chromosome-linked NOR in these ninetines.

My contribution: Evaluation of preparations, detection of NORs by FISH, analysis and interpretation of results. Preparation of cytogenetic part of the manuscript.

Zoological Journal of the Linnean Society, 2023, **198**, 534–591. With 45 figures.

High and dry: integrative taxonomy of the Andean spider genus *Nerudia* (Araneae: Pholcidae)

BERNHARD A. HUBER[1,*], GUANLIANG MENG[1], JIŘÍ KRÁL[2], IVALÚ M. ÁVILA HERRERA[2], MATIAS A. IZQUIERDO[3,4] and LEONARDO S. CARVALHO[5]

[1]*Zoological Research Museum Alexander Koenig, LIB, Bonn, Germany*
[2]*Department of Genetics and Microbiology, Faculty of Science, Charles University, Prague, Czech Republic*
[3]*Facultad de Ciencias Exactas, Físicas y Naturales, Departamento de Diversidad Biológica y Ecología, Universidad Nacional de Córdoba, Córdoba, Argentina*
[4]*Consejo Nacional de Investigaciones Científicas y Técnicas (CONICET), Laboratorio de Biología Reproductiva y Evolución, Instituto de Diversidad y Ecología Animal (IDEA), Córdoba, Argentina*
[5]*Campus Amílcar Ferreira Sobral, Universidade Federal do Piauí, Floriano, Brazil*

Received 20 April 2022; revised 21 October 2022; accepted for publication 26 October 2022

Ninetinae are a group of poorly known spiders that do not fit the image of 'daddy long-legs spiders' (Pholcidae), the family to which they belong. They are mostly short-legged, tiny and live in arid environments. The previously monotypic Andean genus *Nerudia* exemplifies our poor knowledge of Ninetinae: only seven adult specimens from two localities in Chile and Argentina have been reported in the literature. We found representatives of *Nerudia* at 24 of 52 localities visited in 2019, mostly under rocks in arid habitats, up to 4450 m a.s.l., the highest known record for Pholcidae. With now more than 400 adult specimens, we revise the genus, describing ten new species based on morphology (including SEM) and *COI* barcodes. We present the first karyotype data for *Nerudia* and for its putative sister-genus *Gertschiola*. These two southern South American genera share a $X_1X_2X_3Y$ sex chromosome system. We model the distribution of *Nerudia*, showing that the genus is expected to occur in the Atacama biogeographic province (no record so far) and that its environmental niche is phylogenetically conserved. This is the first comprehensive revision of any Ninetinae genus. It suggests that focused collecting may uncover a considerable diversity of these enigmatic spiders.

ADDITIONAL KEYWORDS: Argentina – barcodes – biogeography – distribution modelling – *Gertschiola* – highest record – new species – NOR – sampling bias – sex chromosomes.

INTRODUCTION

Pholcid spiders are among the most species-rich spider families (World Spider Catalog, 2022), and highly diverse regarding the microhabitats they occupy and their corresponding body shapes and colours (Eberle *et al.*, 2018). They are well known to many people by a few synanthropic species. However, the mainly tropical and subtropical distribution of this group has long caused a fragmentary knowledge about the family as a whole. Intensive research over the last two decades has not only resulted in the discovery and description of more than 1000 new species, but has also revealed some facts about their biology. For example, multiple convergent shifts among microhabitats have resulted in a wide range of ecomorphs, with strong convergencies in body shape, coloration and behaviour (Dimitrov *et al.*, 2013; Eberle *et al.*, 2018). Sexual dimorphisms have evolved over 100 times independently (Huber, 2021), including some spectacular phenomena like males with extremely modified 'head' structures (Huber & Nuñeza, 2015; Huber *et al.*, 2016). Females guard their eggs by carrying the egg-sacs in their chelicerae, but parasitic wasps have repeatedly managed to access the eggs

*Corresponding author. E-mail: b.huber@leibniz-lib.de
[Version of record, published online 13 March 2023; http://zoobank.org/ urn:lsid:zoobank.org:pub:E3CF73A6-FCA6-4935-A516-D1E38E49CFB3]

and use the spider female to protect the developing offspring of her enemy (Huber & Wunderlich, 2006; Johnson *et al.*, 2018). In keeping with their species diversity, pholcids exhibit a considerable diversity of diploid numbers, sex chromosome systems and patterns of nucleolus organizer regions (NORs) (Ávila Herrera *et al.*, 2021).

The family is currently divided into five subfamilies (Huber, 2011). Among these, Ninetinae are of particular interest in many respects. When Eugène Simon constructed the first classification of Pholcidae (Simon, 1893), he placed the single Ninetinae species known to him in a separate subfamily, opposing all other pholcids. While molecular data have not yet resolved the position of Ninetinae (Eberle *et al.*, 2018), sperm data support a sister-group relationship between Ninetinae and all other Pholcidae: most Ninetinae have synspermia (Dederichs *et al.*, 2022), a sperm transfer form that characterizes ecribellate Haplogynae spiders (= Synspermiata *sensu* Michalik & Ramírez, 2014). This contrasts with all other pholcids studied, which have cleistospermia. Apart from their possible 'basal' position among Pholcidae, Ninetinae are 'unusual' in several respects: (1) Ninetinae are largely restricted to arid habitats, while most other pholcids (in particular those in the New World) are concentrated in humid tropical environments (e.g. Huber & Brescovit, 2003); (2) while Ninetinae contain only 2% of extant Pholcidae species, they contain 20% (three of 15) of the known fossil species (Dunlop *et al.*, 2020); (3) with previously only 32 (now 42) described species, Ninetinae are by far the smallest of the five subfamilies in Pholcidae; (4) Ninetinae have by far the lowest mean number of species per genus (previously 2.5, now 3.2 – other subfamilies: 11.2–27.6), suggesting old diversification with little subsequent speciation or displacement by modern taxa; and (5) Ninetinae are small to tiny (body length usually 1–2 mm; most other pholcids range from 2 to 10 mm) and their often short legs do not fit the image of a 'daddy long-legs spider'.

Almost nothing has been known about Ninetinae biology beyond basic data on microhabitat, i.e. on reproductive biology, web building, predatory behaviour or life cycle. Label data and preliminary field observations have indicated that Ninetinae are fast-running ground spiders and that at least some species may not even build webs. This is remarkable considering that among the closest relatives of Pholcidae [phylogeny of Wheeler *et al.* (2017)], some taxa make webs (e.g. Diguetidae), while others apparently do not (e.g. Tetrablemmidae).

Geographically, Ninetinae seem to be relatively diverse in the New World (12 named genera), while only two genera are currently described from the Old World. Brazil has the highest number of genera (four named), followed by Argentina and Venezuela (three named genera each). In Argentina and Canada, representatives of Ninetinae mark the most southern and most northern pholcid records worldwide (excluding synanthropic species; –47.7° and 56.1°; M. Ramírez, pers. comm. Jan. 2022; Bennett, 2014). To this we add here the highest record, supporting the idea that Ninetinae tolerate more extreme environmental conditions than other Pholcidae.

The genus *Nerudia* Huber, 2000 has long been a typical example of our limited knowledge of Ninetinae. It was described in 2000 for a single Chilean species (*Nerudia atacama* Huber, 2000), based on five adult specimens from two neighbouring localities (Huber, 2000). Since then, only two further adult specimens of *Nerudia* have been reported in the literature (Torres *et al.*, 2015). Based on morphology, they were (erroneously) assigned to *N. atacama*, even though they originated from Salta Province in Argentina, 700 km NE of the type locality.

In 2019, two of us (BAH, MAI) conducted an expedition in Argentina, aiming primarily at Ninetinae. To our surprise, *Nerudia* spiders were found at 24 of the 52 visited localities, often in considerable abundance. The present paper describes this material, raising the number of nominal species from one to 11. We provide the first karyotype data of *Nerudia* and of the putative sister-genus *Gertschiola* Brignoli, 1981. Finally, we study the biogeography of *Nerudia* in an effort to estimate the potential distribution of the genus, to test the environmental niche conservatism in the group and possible biases in the available locality data, which are likely to result in biodiversity shortfalls regarding this genus. In particular, our biogeographic analyses aim to test two hypotheses: (1) among Ninetinae, *Nerudia* representatives occupy a unique environmental niche; and (2) the modelled environmental niche of *Nerudia* suffers from sampling biases.

MATERIAL AND METHODS

TAXONOMY AND MORPHOLOGY

The taxonomic part of this study is based on the examination of 410 adult specimens deposited in the following collections: American Museum of Natural History, New York, USA (AMNH); Laboratorio de Biología Reproductiva y Evolución, Córdoba, Argentina (LABRE); Museo Argentino de Ciencias Naturales, Buenos Aires, Argentina (MACN); and Zoologisches Forschungsmuseum Alexander Koenig, Bonn, Germany (ZFMK).

Taxonomic descriptions follow the style of recent publications on Pholcidae (e.g. Huber, 2022; based on: Huber, 2000). Measurements were done on a dissecting microscope with an ocular grid and are in mm unless

otherwise noted; eye measurements are +/– 5 µm. Live specimens (Fig. 1) were photographed with a Canon EOS 700D camera. Other photos were made with a Nikon Coolpix 995 digital camera (2048 × 1536 pixels) mounted on a Nikon SMZ 18 stereo microscope or a Leitz Dialux 20 compound microscope. COMBINEZP (https://combinezp.software.informer.com/) was used for stacking photos. Drawings are partly based on photos that were traced on a light table and later improved under a dissecting microscope, or they were directly drawn with a Leitz Dialux 20 compound microscope using a drawing tube. Cleared epigyna were stained with chlorazol black. The number of decimals in coordinates gives a rough indication about the accuracy of the locality data: four decimals means that the collecting site was within about 10 m of the indicated spot; three decimals: within ~100 m; two decimals: within ~1 km; one decimal: within ~10 km. Distribution maps were generated with ARCMAP v.10.0 (Environmental Systems Research Institute, Redlands, CA). For scanning electron microscope (SEM) photos, specimens were dried in hexamethyldisilazane (HMDS) (Brown, 1993) and photographed with a Zeiss Sigma 300 VP scanning electron microscope. SEM data are presented with the descriptions but are usually not based on the specific specimen described. Abbreviations used in figures only are explained in the figure legends. Abbreviations used in the text: ALE, anterior lateral eye(s); ALS, anterior lateral spinneret(s); AME, anterior median eye(s); a.s.l., above sea level; L/d, length/diameter; PME, posterior median eye(s); PMS, posterior median spinneret(s).

MOLECULAR DATA AND ANALYSES

Taxon sampling

Outgroup taxa were selected from Eberle *et al.* (2018), including ten Ninetinae species and two *Artema* species (Pholcidae: Arteminae) for rooting the tree. Additionally, we newly sequenced 24 *Nerudia* and nine *Gertschiola* specimens. In total, the molecular study includes 47 specimens. Table 1 lists the newly sequenced specimens. Accession numbers of previously sequenced specimens are shown in the Supporting Information (Figs S1, S2); for detailed information on these specimens, see Eberle *et al.* (2018). Two to four legs of specimens stored in pure ethanol (~99%) at –20 °C were used for DNA extraction. Extracted genomic DNA is deposited at and is available from the LIB Biobank, Museum Koenig, Bonn.

DNA extraction, amplification and sequencing

For 32 specimens (24 *Nerudia* specimens and eight *Gertschiola* specimens; Table 1), DNA was extracted using the HotSHOT method (Truett *et al.*, 2000). The primer set used was LCO1490-JJ and HCO2198-JJ (Astrin *et al.*, 2016; primer versions JJ2 served as backup), with different tag sequences (from Srivathsan *et al.*, 2021) of 13 bp length added at the 5′-ends of forward and reverse primers, respectively. The 20 µL reaction volume consisted of 5 µL H_2O, 2 µL Q-Solution, 10 µL Qiagen Multiplex-Mix, 1 µL forward primer, 1 µL reverse primer and 1 µL DNA. The polymerase chain reaction (PCR) procedure was: (1) 95 °C for 15 min; (2) denaturation at 94 °C for 35 s; (3) annealing at 55 °C (or 40 °C) for 90 s; (4) elongation at 72 °C for 90 s; and (5) final elongation at 72 °C for 10 min, followed by cooling at 10 °C. Steps 2–4 were repeated for 15 cycles (or 25 cycles). The PCR products (each with a different combination of 13 bp tags) were then pooled and sequenced with the Oxford Nanopore Technologies (ONT) GridON platform, making use of the SQK-LSK110 sequencing kit and a flongle R9.4 flowcell. One *Gertschiola* specimen (N010) was amplified with the same primer set but its PCR product was sent for bidirectional Sanger sequencing to BGI (Hong Kong).

Cytochrome c oxidase subunit I (COI) *barcode assembly and contamination check*

A total of 32 *COI* barcodes were sequenced by ONT sequencing and assembled following the ONTbarcoder (Srivathsan *et al.*, 2021) pipeline, while one *COI* barcode was characterized with Sanger-sequencing and assembled and aligned with GENEIOUS R7 (Kearse *et al.*, 2012). To confirm the taxonomic assignments and to identify contaminations, the assembled sequences were checked by: (1) blasting against a local NT database and (2) the identification engine of the Barcode of Life Data System (BOLD) (http://www.boldsystems.org/index.php) (Ratnasingham & Hebert, 2007; Yang *et al.*, 2020).

Multiple sequence alignment (MSA) and neighbour-joining (NJ) tree construction

A total of 47 *COI* barcodes were translated into protein sequences using BIOPYTHON v.1.78 (Cock *et al.*, 2009) and the option for the invertebrate mitochondrial genetic code. Protein-MSAs were constructed using the mafft-linsi algorithm of MAFFT v.7.299b (Katoh & Standley, 2013), which then guided the construction of nucleotide level MSAs with pal2nal.pl (Suyama *et al.*, 2006). With this procedure we avoided the introduction of biologically meaningless frameshifts to the alignments (Suyama *et al.*, 2006). Finally, MEGA X (Kumar *et al.*, 2018; Stecher *et al.*, 2020) was used for the construction of a NJ tree (Saitou & Nei, 1987) based on the nucleotide alignment. Evolutionary distances were computed using the Kimura 2-parameter method (Kimura, 1980) and all ambiguous positions were removed for each sequence pair (pairwise deletion

Table 1. Geographic origins of newly sequenced specimens, sorted by code, and their *COI* GenBank accession numbers

Code	Genus	Species	Vial	Country	Admin.	Locality	Lat	Long	*COI*
N001	*Nerudia*	*nono*	Arg124	Argentina	Córdoba	~5 km E Nono	-31.7982	-64.9515	ON063450
N004	*Gertschiola*	*macrostyla*	Arg128	Argentina	Córdoba	between Villa Dolores and Chancani	-31.8328	-65.2647	ON067457
N006	*Gertschiola*	*macrostyla*	Arg134	Argentina	San Juan	Cuesta de Marayes	-31.4949	-67.3358	ON067458
N007	*Nerudia*	*ola*	Arg135	Argentina	San Juan	~7.5 km S Astica	-31.0223	-67.2976	ON063451
N008	*Nerudia*	*ola*	Arg136	Argentina	San Juan	~7.5 km S Astica	-31.0223	-67.2976	ON063452
N010	*Gertschiola*	*macrostyla*	Arg140	Argentina	San Juan	San Agustín de Valle Fértil	-30.6366	-67.4863	ON062532
N011	*Nerudia*	*ola*	Arg141	Argentina	San Juan	San Agustín de Valle Fértil	-30.6366	-67.4863	ON063453
N012	*Nerudia*	*ola*	Arg144	Argentina	San Juan	Parque Provincial Ischigualasto	-30.1839	-67.9026	ON063454
N013	*Gertschiola*	*macrostyla*	Arg145	Argentina	San Juan	Parque Provincial Ischigualasto	-30.1839	-67.9026	ON067459
N014	*Nerudia*	Arg23a	Arg147	Argentina	San Juan	~35 km W Las Flores	-30.3967	-69.5576	ON063455
N015	*Nerudia*	*rocio*	Arg148	Argentina	San Juan	~35 km W Las Flores	-30.3967	-69.5576	ON063456
N016	*Gertschiola*	*macrostyla*	Arg149	Argentina	San Juan	between San José de Jáchal and Huaco	-30.1497	-68.6063	ON067460
N017	*Nerudia*	*ola?*	Arg152	Argentina	La Rioja	Cuesta de Miranda, 'site 1'	-29.3511	-67.7924	ON063457
N018	*Nerudia*	*ola?*	Arg154	Argentina	La Rioja	Cuesta de Miranda, 'site 2'	-29.3468	-67.7205	ON063458
N019	*Gertschiola*	sp.	Arg158	Argentina	La Rioja	between Chilecito and Famatina	-29.0027	-67.4855	ON067461
N020	*Nerudia*	*hoguera*	Arg159	Argentina	La Rioja	between Chilecito and Famatina	-29.0027	-67.4855	ON063459
N021	*Nerudia*	*ola?*	Arg161	Argentina	La Rioja	SE Aimogasta, 'site 1'	-28.8069	-66.6635	ON063460
N023	*Nerudia*	Arg163	Arg163	Argentina	La Rioja	SE Aimogasta, 'site 2'	-28.9015	-66.6538	ON063461
N024	*Gertschiola*	sp.	Arg164	Argentina	La Rioja	SE Aimogasta, 'site 2'	-28.9015	-66.6538	ON067462
N025	*Nerudia*	*guirnalda*	Arg166	Argentina	Catamarca	El Rodeo, trail to Cristo Redentor	-28.2229	-65.8677	ON063462
N026	*Nerudia*	*guirnalda*	Arg167	Argentina	Catamarca	El Rodeo, trail to Cristo Redentor	-28.2229	-65.8677	ON063463
N028	*Nerudia*	*colina*	Arg178	Argentina	Jujuy	betw. San Salvador and Purmamarca, 'site 2'	-23.8849	-65.4613	ON063464
N030	*Nerudia*	*poma*	Arg184	Argentina	Salta	~15 km NW Campo Quijano	-24.7918	-65.7297	ON063465
N033	*Nerudia*	*poma*	Arg195	Argentina	Salta	Cabra Corral, 'site 3'	-25.2907	-65.3057	ON063466
N035	*Nerudia*	*poma*	Arg197	Argentina	Salta	Cabra Corral, 'site 4'	-25.2837	-65.3939	ON063467
N036	*Nerudia*	*trigo*	Arg202	Argentina	Salta	~1 km SW Alemanía	-25.6300	-65.6180	ON063468
N038	*Nerudia*	*trigo*	Arg206	Argentina	Salta	between Alemania and Cafayate	-25.7023	-65.7022	ON063469
N040	*Nerudia*	*ola?*	Arg211	Argentina	Catamarca	near Nacimientos	-27.1559	-66.6925	ON063470
N041	*Nerudia*	*ola?*	Arg213	Argentina	Catamarca	~10 km N Belén	-27.5641	-67.0058	ON063471
N042	*Gertschiola*	sp.	Arg214	Argentina	Catamarca	~14 km W Fiambalá	-27.6590	-67.7607	ON063472
N043	*Nerudia*	*centaura*	Arg215	Argentina	Catamarca	~20 km E Paso de San Francisco, 'site 1'	-26.9276	-68.0709	ON063473
N044	*Nerudia*	*centaura*	Arg216	Argentina	Catamarca	~20 km E Paso de San Francisco, 'site 2'	-26.9360	-68.0925	ON063474
N056	*Gertschiola*	*macrostyla*	MACN267	Argentina	San Luis	PN Sierra de las Quijadas	-32.4690	-66.9609	ON067463

option). Branch supports were evaluated with 1000 bootstrap replicates (Felsenstein, 1985). The NJ tree in Figure 2 shows only the ingroup taxa. The complete tree is shown in the Supporting Information (Figure S1).

Preparation of chromosome slides and their evaluation

Chromosomes were prepared from two specimens of the new species *Nerudia poma*, two specimens of the new species *Nerudia ola* and one specimen of *Gertschiola macrostyla* (Mello-Leitão, 1941). Chromosome plates were obtained from testes of adult males. In both species of *Nerudia*, the preparations contained both mitotic and meiotic plates. In *G. macrostyla*, they only contained meiotic plates. Chromosome preparation was based on Dolejš *et al.* (2011). Tissues were hypotonized in 0.075M KCl for 25 min at room temperature (RT) and fixed two times (10 and 20 min) in ethanol : acetic acid (3 : 1) (RT). To make a cell suspension, a piece of fixed tissue was placed on a microscope slide with a drop of 60% acetic acid and quickly shredded with a pair of tungsten needles to obtain a cell suspension. The preparation was placed on a histological plate (40 °C). The drop was

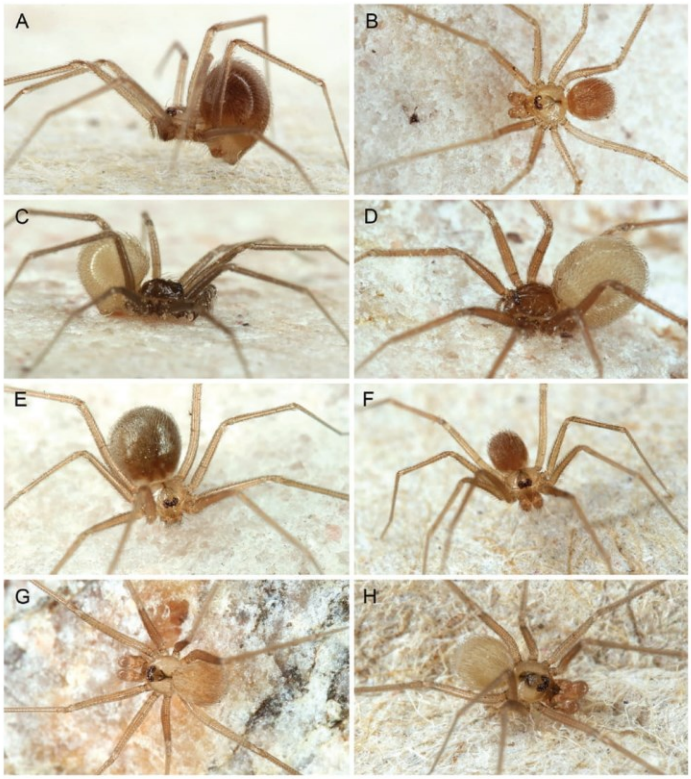

Figure 1. *Nerudia*, live specimens from Argentina. A, *N. colina* sp. nov., female from Jujuy, between San Salvador and Purmamarca (type locality). B, *N. poma* sp. nov., male from Salta, NW Campo Quijano (type locality). C, D, *N. centaura* sp. nov., male and female from Catamarca, E Paso de San Francisco (type locality). E, *N. trigo* sp. nov., female from Salta, SW Alemania. F, *N. guirnalda* sp. nov., male from Catamarca, El Rodeo (type locality). G, *N. ola* sp. nov., male from San Juan, San Agustin de Valle Fertil (type locality). H, *N. nono* sp. nov., male from Cordoba, E Nono (type locality).

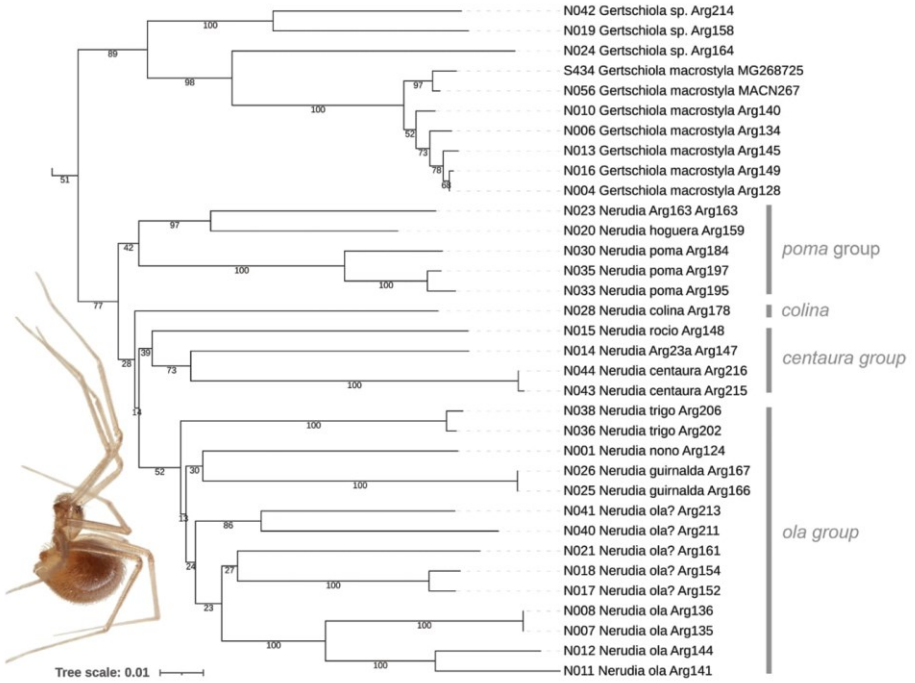

Figure 2. NJ *COI* tree of all sequenced *Nerudia* and *Gertschiola* specimens. Species groups on the right are working hypotheses. Photo: female of *Nerudia colina* sp. nov. For complete tree, and for tree resulting from analysis with IQ-TREE, see Supporting Information, Figures S1, S2.

moved with a tungsten needle until it almost evaporated. The remaining suspension was discarded. Slides were stained with a 5% Giemsa solution in Sörensen buffer (pH 6.8) for 28 min (RT).

Preparations were studied under an Olympus BX 50 microscope equipped with a DP 71 CCD camera. Chromosome morphology was characterized based on the position of the centromere (Levan, 1964), which was calculated as the ratio of the longer and shorter chromosome arms. Chromosomes were measured using the IMAGE TOOL v.3.0 software (https://imagetool.software.informer.com/3.0/). Metacentric and submetacentric chromosomes were considered as biarmed, and subtelocentric and acrocentric chromosomes as monoarmed. The sex chromosome system was identified from meiosis of the heterogametic sex, based on segregation of the sex chromosomes and/or their behaviour in prophase and metaphase I.

VISUALIZATION OF NUCLEOLUS ORGANIZER REGIONS (NORS)

After inspection under the Olympus BX 50 microscope, the slides were treated in xylene and benzine baths (1 min each, RT) to remove the immersion oil. The Giemsa stain was removed from preparations by incubation in the fixative (3 min, RT). Nucleolus organizer regions were detected by a biotin labelled 18S rDNA probe from the spider *Dysdera erythrina* (Walckenaer, 1802) (Dysderidae) (for details, see: Ávila Herrera *et al.*, 2021). The probe was visualized by fluorescence *in situ* hybridization (FISH) using streptavidin-Cy3 with signal amplification (biotinylated antistreptavidin, streptavidin-Cy3). Chromosomes were counterstained by DAPI (for description of method, see: Forman *et al.*, 2013). Chromosome plates were captured with an Olympus IX81 microscope equipped with an ORCA-AG CCD camera (Hamamatsu). Images were pseudocoloured (red for Cy3, blue for DAPI) and

superimposed with the CELL^R software (Olympus Soft Imaging Solutions).

SAMPLING BIAS AND BIOGEOGRAPHIC ANALYSES

In order to test if the environmental niche occupied by *Nerudia* representatives differs from other ninetines and if it suffers from sampling biases, the numbers of records of arthropods and arachnids in the wider geographic area of *Nerudia* were used as predictors in generalized linear models with a binomial distribution of errors. To perform these analyses, a database with records of preserved specimens of arthropods from Argentina, Chile, Bolivia and Paraguay was gathered from the Global Biodiversity Information Facility (GBIF.org, 2022). The GBIF search was restricted to records with true coordinates and without known geospatial issues detected by the platform. It yielded 404 541 records of arthropods, including 36 796 records of arachnids. These records were further spatially clipped to a 0.5-degree side-by-side hexagon grid, built at a 500-km radius from all *Nerudia* records. This resulted in a database with 131 955 records of arthropods, including 9032 records of arachnids. A kernel density map was calculated to provide an overview of the sampling effort in the study area. This analysis was performed at ARCGIS v.10.3, with an output cell size of 0.02, search radius of one decimal degree and a planar method. All raster files were plotted using stretched symbology of 2.5 standard deviations.

As a qualitative exploratory analysis, areas with high suitability for representatives of *Nerudia* (i.e. areas with higher indices resulting from species distribution modelling predictions) were modelled using all *Nerudia* species records. No *Nerudia* species has enough known records to allow individual modelling. Thus, we disregarded individual species environmental thresholds and treated them as a single biological entity in model inputs. As predictors, we used the 19 climatic variables available in the WorldClim v.2 database (https://www.worldclim.org/data/index.html), plus the mean tree density (Crowther *et al.*, 2015) and mean canopy height (Simard *et al.*, 2011), both at a 1-km^2 scale. These variables were selected to provide a satisfactory description of biological and climatic conditions of the habitats of Pholcidae species, which occupy a large variety of environments worldwide. To remove the spatial autocorrelation between the predictor layers, a principal component analysis (PCA) was carried out in R v.4.1.0 (R Development Core Team), using tools in the packages 'raster' (Hijmans *et al.*, 2016), 'rgdal' (Bivand *et al.*, 2019) and 'RStoolbox' (Leutner *et al.*, 2019). The principal components that summed at least 95% of the proportion of variance were used as predictors in the modelling (Supporting Information, Tables S1, S2). The modelling was performed with MAXENT, without applying a threshold rule, with 500 maximum interactions, random test percentage of 25%, raw output formatted, with 15 bootstrap replicates and by removing duplicates from the same grid cell (following the recommendations by: Merow *et al.*, 2013). The map representing the median of the replicates is shown in Figure 43B, and the contribution of the principal components to the species distribution modelling is in Table S3. In the sections on biogeography, we adopted the biogeographic regionalization of the Neotropical region and its hierarchy (i.e. regions, dominions, provinces and districts) proposed by Morrone (2017). The terms used here should not be mistaken for political administrative areas.

The same environmental predictors were used to test if the environmental niche occupied by *Nerudia* representatives is similar to other ninetines. This was done through a second PCA (see parameters in Tables S4, S5), using the extracted values for 338 points of occurrences, including 47 of *Nerudia* and 291 of other Ninetinae species (Supporting Information, Table S6). This list was assembled based on the literature and on unpublished records (B.A. Huber & L. S Carvalho, unpubl. data). A third PCA was carried out using the extracted values for the 21 predictor layers for the localities of the terminals used in the neighbour joining and phylogenetic analyses (Supporting Information, Tables S7, S8, Fig. S8). The principal components of this PCA were used to test if there is a phylogenetic signal related to the environmental niche occupied by each taxon (Supporting Information, Table S9). This analysis is preliminary in the sense that our *COI* trees may not adequately reflect phylogenetic relationships. The analysis was carried out by calculating the λ parameter (Pagel, 1999), with the function 'phylosig' of the R package 'phytools' (Revell, 2012). Pagel's λ varies from 0 (when a trait evolves independently to the phylogeny) to 1 (when a trait evolves according to Brownian motion) (Diniz-Filho *et al.*, 2012).

RESULTS

TAXONOMY

NERUDIA HUBER, 2000

Nerudia Huber, 2000: 87. Type species: *Nerudia atacama* Huber, 2000.

Diagnosis: Small (total body length 1.4–1.9) eight-eyed pholcids with relatively long legs (compared to most other Ninetinae; leg 1 usually > 3 × total body length; only shorter in the new species *N. centaura*), with simple procursus (without dorsal flap, not strongly

elongated), paired male cheliceral modifications (strong hairs or pair of apophyses), with stridulatory files on male chelicerae, with simple main (anterior) epigynal plate and large posterior epigynal plate, without or with simple (i.e. not tube-like) median receptacle-like structure in female internal genitalia.

Description

Male. Measurements: Total body length 1.4–1.9, carapace width 0.6–0.8. Legs relatively long (compared to other Ninetinae), tibia 1 usually ~1.1–2.0 (longer in the new species *N. rocio*, single male: 2.5); tibia 1 L/d 14–31; metatarsus 1 length ~1.0–1.2 × tibia 1 length; tibia 2 always shorter than tibia 4 (tibia 2/tibia 4: 0.8–0.9).

Colour: Live specimens pale ochre-grey to light brown (Fig. 1); carapace often with darker median mark; abdomen colour variable, often darker than prosoma, only in *N. centaura* distinctively lighter than prosoma (Fig. 1C), without or with indistinct marks; legs without dark or light bands. Colour in ethanol similar but paler.

Body: Ocular area barely raised, eight eyes, AME relatively large (diameter: 35–50 µm, i.e. 60–85% of PME diameter). Carapace without or with indistinct thoracic groove (cf. Figs 7B, 11A, 29A). Clypeus usually barely modified, rim slightly more sclerotized than in female, in *N. nono* also more bulging than in female, in some species with pair of shallow indentations for genital bulbs at rest (Figs 7A, 11B). Sternum wider than long, usually with pair of variably distinct anterior processes near leg coxae 1, processes apparently without pores (Fig. 29G); sternum processes absent in *N. centaura*. Abdomen globular; four epiandrous spigots arranged in two pairs (Figs 11F, 29H); ALS with seven spigots each (Fig. 30G): one strongly widened spigot, one long pointed spigot and five cylindrical spigots (one of which is unusually large); PMS with two short, pointed spigots (Fig. 30G); PLS without spigots (cf. Fig. 12D).

Chelicerae: Usually with pair of simple frontal apophyses (e.g. Fig. 5G, H; absent in *N. trigo*), tip often flat, i.e. wide in frontal view, pointed in lateral view (Fig. 11C, D); often with patches or brushes of stronger hairs; with stridulatory files on variably distinct lateral protrusions (Figs 11B, C, 29C).

Palps: Coxa unmodified; trochanter with indistinct ventral projection; femur cylindrical, slightly widened distally, proximally without or with low retrolateral hump, with prolateral stridulatory pick (modified hair; Fig. 29E); patella short; tibia globular, with two trichobothria; palpal tarsal organ raised, capsulate (Figs 7E, 11E, 30C), with small opening (diameter of opening ~1.6–1.9 µm); procursus simple, without dorsal flap, not strongly elongated, straight or bent towards dorsal, tip with complex cuticular microstructure (Fig. 29B); genital bulb with simple ventral apophysis and dorsal embolus (e.g. Fig. 5F).

Legs: Without spines and curved hairs; usually with short vertical hairs in higher density on tibia 1 or tibiae 1 and 2 (Figs 8A, B, 30A; length of hairs ~20 µm). Trichobothria in usual arrangement: three on each tibia (except tibia 1: prolateral trichobothrium absent), one on each metatarsus, slightly feathered (Fig. 30B); length of dorsal trichobothrium on tibia 1: ~80 µm; retrolateral trichobothrium of tibia 1 in distal position (at 58–70% of tibia length). Metatarsi and tarsi with dorsal rows of tiny pores with cuticular rim (diameter of opening ~0.6 µm; cf. Fig. 18C, D). Tarsus 1 with six to eight pseudosegments, distally distinct, proximally usually indistinct; tarsus 4 distally with one comb-hair on prolateral side (Fig. 12F); leg tarsal organs small, capsulate (Fig. 30E), with small opening (diameter of opening ~ 1.2–1.6 µm); three claws (Figs 12E, 18G).

Female: In general (size, colour, body shape), similar to male but chelicerae without stridulatory files (Figs 7D, 24F, 29D), sternum without pair of anterior humps, palpal tarsal organ only weakly raised (Figs 12A, B, 24B), and leg tibiae with usual low number of short vertical hairs; legs either slightly shorter than in males or of same length (only in the new species *N. ola* with reasonable sample size: male/female tibia 1 length: 1.08). Spinnerets, leg pores, leg tarsal organs and comb-hairs as in male (Figs 7F, 8D–F, 18B, H, 24H, 30E, H). Main (anterior) epigynal plate rectangular to trapezoidal or semi-circular, weakly protruding, posteriorly straight or with variably distinct median indentation (e.g. Figs 17A, 32A); posterior plate simple, short but wide, usually wider than anterior plate. Internal genitalia simple, sometimes with distinct median receptacle-like structure (e.g. Figs 6B, 10B), apparently without or with indistinct pair of pore plates (arrows in Figs 10B, 14B, 23B).

Relationships: The molecular analysis of Eberle *et al.* (2018) included only a single species of *Nerudia* ('*N. Mich20*' = *N. ola*), which was placed (with moderate support) as sister of the geographically close *Gertschiola macrostyla* (Mello-Leitão, 1941). Both genera together were placed in a clade with further South American and Old World Ninetinae. The present paper is not primarily focused on phylogeny and our sampling does not include the type species *N. atacama*, but our *COI* and karyotype data support the sister-group relationship between *Nerudia* and *Gertschiola*

(see Fig. 2; Supporting Information, Figs S1, S2; and section on karyology). Preliminary analyses of Ninetinae relationships based on hybrid enrichment data (G. Meng *et al.*, unpublished data) also support this sister-group relationship. Our new SEM data also confirm the position of *Nerudia* among Ninetinae (in particular the small opening of the tarsal organs).

In addition, the *COI* data suggest the existence of three species groups within *Nerudia* that we consider useful as working hypotheses: (1) the *ola* group, including the new species *N. guirnalda*, *N. nono*, *N. ola* and *N. trigo*; (2) the *centaura* group, including the new species *N. centaura*, *N. rocio* and the undescribed *N.* 'Arg23a'; and (3) the *poma* group, including the new species *N. hoguera*, *N. poma* and the undescribed *N.* 'Arg163'. One new species, *N. colina*, appears isolated. The three groups appear neither supported nor contradicted by morphology. The type species *N. atacama* and the new *N. flecha* cannot be assigned with confidence to any of these groups (no fresh material suitable for sequencing is available of these two species).

Distribution: Nerudia is widespread in the Argentinean and Chilean Andes, ranging at least from 24°S to 31°S, and in the east up to the Córdoba mountain ranges in central Argentina (Fig. 3). See biogeographic analysis for further details and distribution modelling.

Natural history: Most species were found in relatively arid environments (Fig. 45A–F), and some seem to

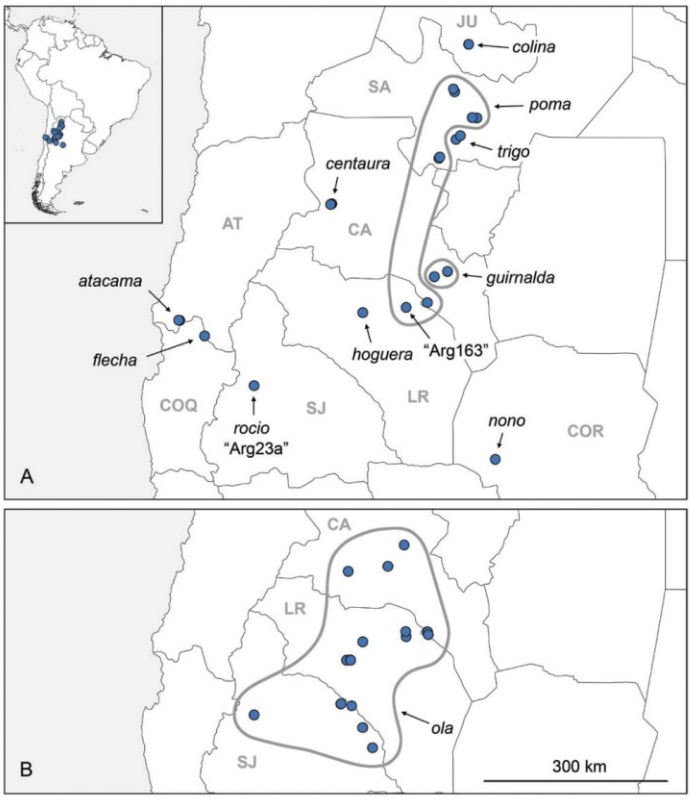

Figure 3. Known distribution of *Nerudia* in South America (inset) and of individual species. Regions in Chile: AT, Atacama; COQ, Coquimbo. Provinces in Argentina: CA, Catamarca; COR, Córdoba; JU, Jujuy; LR, La Rioja; SA, Salta; SJ, San Juan.

tolerate extremely dry and cold conditions (see Natural history section of *N. centaura* and biogeographical analysis for further details). In a few cases, *Nerudia* has been found in relatively humid forested areas, e.g. *N. guirnalda* at El Rodeo or *N. ola* and *N. poma* at Chumbicha (both: Argentina, Catamarca). Most specimens were found by turning stones and rocks. Two species (*N. poma* and *N. trigo*) were also found on the ceilings of small cave-like shelters composed of large rocks and boulders. *Nerudia nono* was collected by turning stones of a loosely built wall situated in the sun (Fig. 45F). When disturbed, the spiders either remained more or less motionless or they ran rapidly a few centimetres over the rock surface; they seemed reluctant to drop to the ground. Webs were not seen in the field, but at least *N. nono* was observed to build flimsy webs in small containers in the laboratory. In most visited localities, only one species of *Nerudia* was found; in a few cases, two or even three species were found at a single locality, apparently in identical microhabitats. Other pholcid spiders sharing the microhabitats of *Nerudia* were *Gertschiola macrostyla* and *Guaranita* Huber, 2000 spp. (Ninetinae), *Chibchea* Huber, 2000 spp. and other small undescribed representatives of Modisiminae, and an undescribed species of *Metagonia* Simon, 1893 (Pholcinae). Egg sacs were slightly flattened (but never reduced to a single layer of eggs as in *Guaranita*) and consisted of about eight to 18 eggs.

Composition: The genus now includes 11 described species, ten of which are newly described below.

NERUDIA COLINA HUBER SP. NOV.

(FIGS 1A, 4–8)

Zoobank registration: urn:lsid:zoobank.org:act:7B358FEA-C1CA-4841-BBDA-DF46379B51C0.

Diagnosis: Distinguished from known congeners by shapes of procursus (Fig. 5A–C; with subdistal ventral sclerite, partly semi-transparent flat tip) and by armature of male chelicerae (Fig. 5G, H; frontal apophysis with wide and flat tip, in frontal view slightly bifid; similar to *N. poma*); from some congeners also by bulbal processes (Fig. 5D–F; ventral apophysis

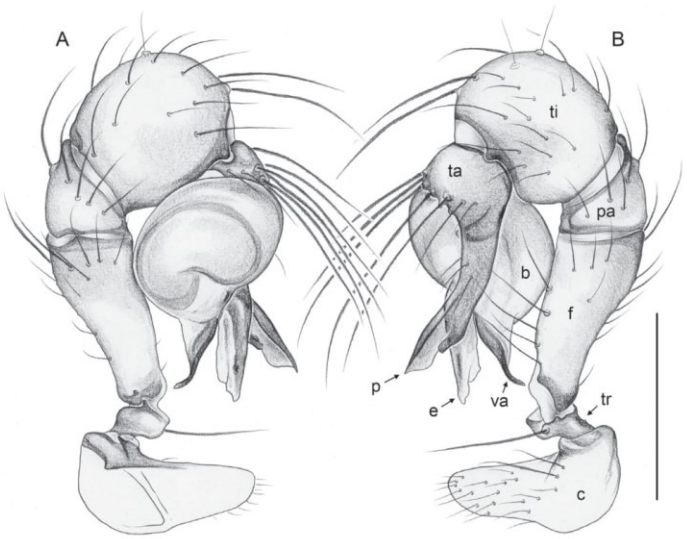

Figure 4. *Nerudia colina* sp. nov.; paratype male from Argentina, Jujuy, between San Salvador and Purmamarca (ZFMK Ar 23883). Left palp, prolateral (A) and retrolateral (B) views. Abbreviations: b, genital bulb; c, coxa; e, embolus; f, femur; p, procursus; pa, patella; ta, tarsus; ti, tibia; tr, trochanter; va, ventral apophysis. Scale line: 0.3 mm.

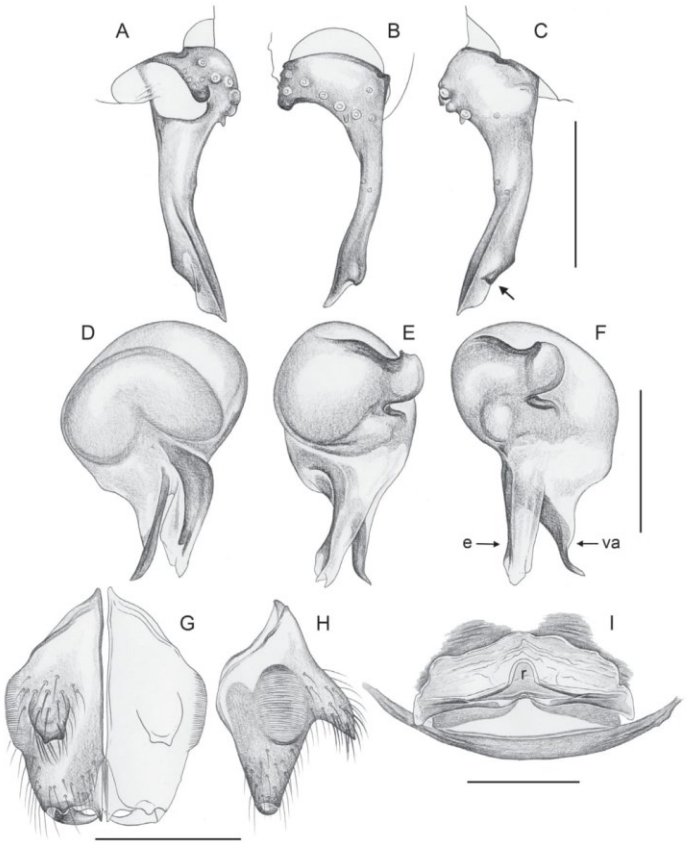

Figure 5. *Nerudia colina* sp. nov.; paratype male and paratype female from Argentina, Jujuy, between San Salvador and Purmamarca (ZFMK Ar 23883). A–C, left male palpal tarsus and procursus, prolateral, dorsal, and retrolateral views (arrow points at distinctive subdistal sclerite). D–F, left male genital bulb, prolateral, dorsal, and retrolateral views. G, H, male chelicerae, frontal and lateral views. I, cleared female genitalia, dorsal view. Abbreviations: e, embolus; r, 'receptacle'; va, ventral apophysis. Scale lines: 0.2 mm.

distally slender, curved towards ventral, same length as embolus) and by epigynum and female internal genitalia (Figs 5I, 6; epigynal plate with indistinct posterior and anterior median indentations; internal genitalia with posteriorly wide open 'receptacle'; similar to *N. guirnalda*).

Type material: ARGENTINA – **Jujuy**: • ♂ holotype; between San Salvador and Purmamarca, 'site 2'; 23.8849° S, 65.4613° W; 2150 m a.s.l.; 16–17 March 2019; B. A. Huber and M. A. Izquierdo leg.; LABRE-Ar 584 • 3 ♂♂, 4 ♀♀, paratypes (one male used for SEM); same data as holotype; ZFMK Ar 23883.

Other material examined: ARGENTINA – **Jujuy**: • 14 ♀♀, in pure ethanol (two females used for SEM; three female prosomata used for molecular study); same data as holotype; ZFMK Arg178 • 2 ♀♀; same data as

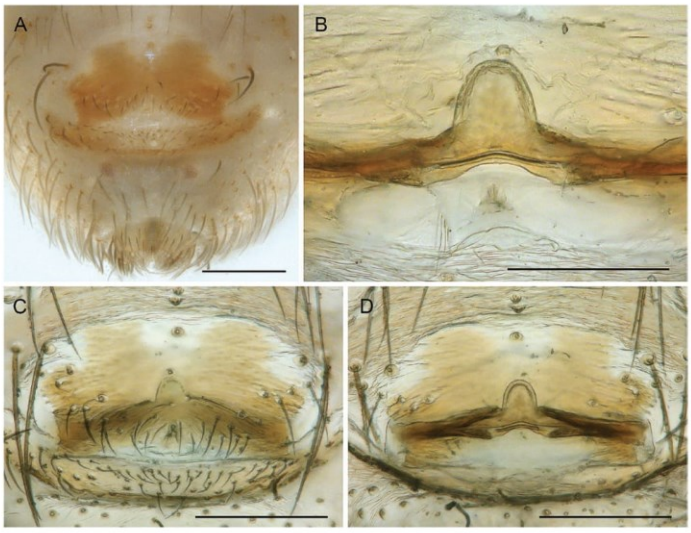

Figure 6. *Nerudia colina* sp. nov.; paratype female from Argentina, Jujuy, between San Salvador and Purmamarca (ZFMK Ar 23883). A, abdomen and epigynum, ventral view. B, median structures in internal genitalia. C, D, cleared genitalia, ventral and dorsal views. Scale lines: 0.2 mm (A, C, D), 0.1 mm (B).

holotype; LABRE-Ar 537 • 1 ♂, 3 ♀♀, in pure ethanol; between San Salvador and Purmamarca, 'site1'; 23.8866° S, 65.4588° W; 2100 m a.s.l.; under rocks; 16–17 Mar. 2019; B. A. Huber and M. A. Izquierdo leg.; LABRE-Ar 549 • 2 ♀♀, 1 juv., in pure ethanol; same data as preceding; LABRE-Ar 559.

Etymology: The species epithet *colina* (Spanish for 'hill') is taken from Pablo Neruda's poem 'Poema 1'; noun in apposition.

Description

Male (holotype). Measurements: Total body length 1.75, carapace width 0.72. Distance PME–PME 70 µm; diameter PME 50 µm; distance PME–ALE 20 µm; distance AME–AME 15 µm; diameter AME 40 µm. Leg 1: 5.94 (1.60 + 0.27 + 1.60 + 1.77 + 0.70), tibia 2: 1.37, tibia 3: 1.10, tibia 4: 1.50; tibia 1 L/d: 21.

Colour (in ethanol): Prosoma and legs mostly pale ochre-grey; ocular area, thoracic groove, and clypeus light brown; legs without dark rings; abdomen monochromous grey.

Body: Habitus as in *N. poma* (cf. Fig. 1B). Ocular area barely raised. Carapace with indistinct thoracic groove. Clypeus unmodified except for pair of indentations for genital bulb at rest (Fig. 7A). Sternum wider than long (0.52/0.36), with pair of distinct anterior processes near coxae 1. Abdomen globular.

Chelicerae: As in Figure 5G, H; pair of frontal apophyses directed downwards, with slightly bifid tip slightly flattened in lateral view (Fig. 7A, C); stridulatory files on pair of low lateral protrusions (Fig. 7C).

Palps: As in Figure 4; coxa unmodified; trochanter with indistinct ventral projection; femur cylindrical, only slightly widened distally, proximally with indistinct retrolateral hump and prolateral stridulatory pick (modified hair); patella short; tibia globular; procursus (Fig. 5A–C) simple, in lateral view slightly directed towards dorsal, with distinctive subdistal ventral sclerite and partly semi-transparent flat tip; genital bulb (Fig. 5D–F) with ventral apophysis distally slender, curved towards ventral, embolus partly membranous.

Legs: Without spines and curved hairs; with slightly higher than usual density of short vertical hairs on tibia 1 (Fig. 8A, B); retrolateral trichobothrium of tibia 1 at 70%; prolateral trichobothrium absent on tibia 1; tarsus 1 with seven to eight pseudosegments, distally distinct.

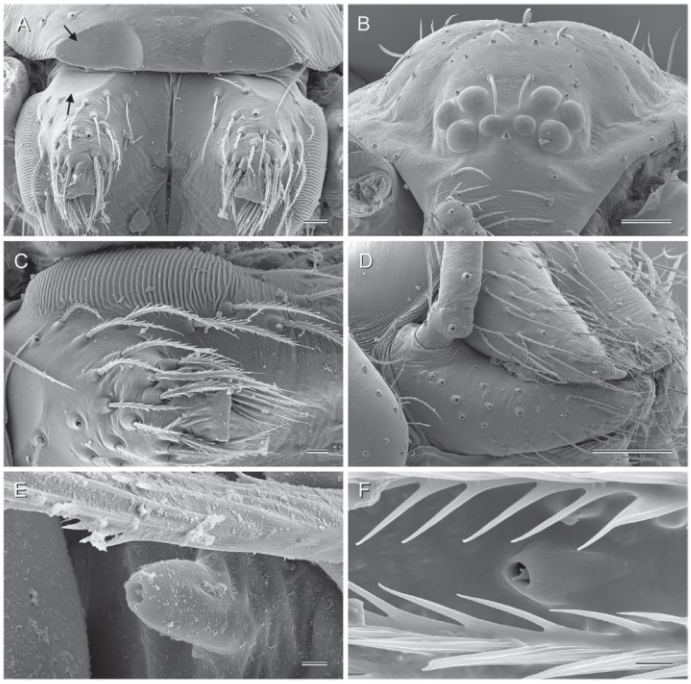

Figure 7. *Nerudia colina* sp. nov.; male and female from Argentina, Jujuy, between San Salvador and Purmamarca (ZFMK Ar 23883 and ZFMK Arg178). A, male clypeus and chelicerae, frontal view (arrows point at indentations for genital bulb at rest). B, female prosoma, frontal view. C, left male chelicera, frontal view. D, female chelicerae and right palp, proximal segments, lateral view. E, male palpal tarsal organ. F, female tarsal organ on tarsus 1. Scale lines: 20 µm (A), 100 µm (B, D), 10 µm (C), 2 µm (E, F).

Variation (male): Tibia 1 in five males (including holotype): 1.50–1.73 (mean 1.62). Abdomen variably dark.

Female: In general, similar to male but sternum without pair of anterior humps and tibiae with few vertical hairs. Tibia 1 in nine females: 1.37–1.63 (mean 1.49). Epigynum (Fig. 6A) anterior plate weakly protruding, with anterior and indistinct posterior indentations; posterior plate large, simple. Internal genitalia (Figs 5I, 6B–D) with posteriorly wide open 'receptacle'.

Distribution: Known only from type locality in Jujuy, Argentina (Fig. 3).

Natural history: The spiders were found by turning stones and rocks on an arid slope (Fig. 45A). They shared the microhabitat with a second species of Ninetinae, an unidentified species of *Guaranita*. They seemed to prefer large stones and rocks that were close to vegetation. When disturbed, they ran rapidly but remained on the rock. No webs were seen.

NERUDIA POMA HUBER SP. NOV.

(FIGS 1B, 9–12)

Zoobank registration: urn:lsid:zoobank.org:act:425882CF-A239-4258-BADC-CD03F44F3C54.

Nerudia atacama (misidentification; see Note below) – Torres *et al.*, 2015: 5, fig. 4C, D.

Diagnosis: Distinguished from known congeners by shapes of procursus (Fig. 9A–C; distally slender, slightly bent towards dorsal and divided into sclerotized dorsal and transparent ventral part; similar to *N. hoguera*)

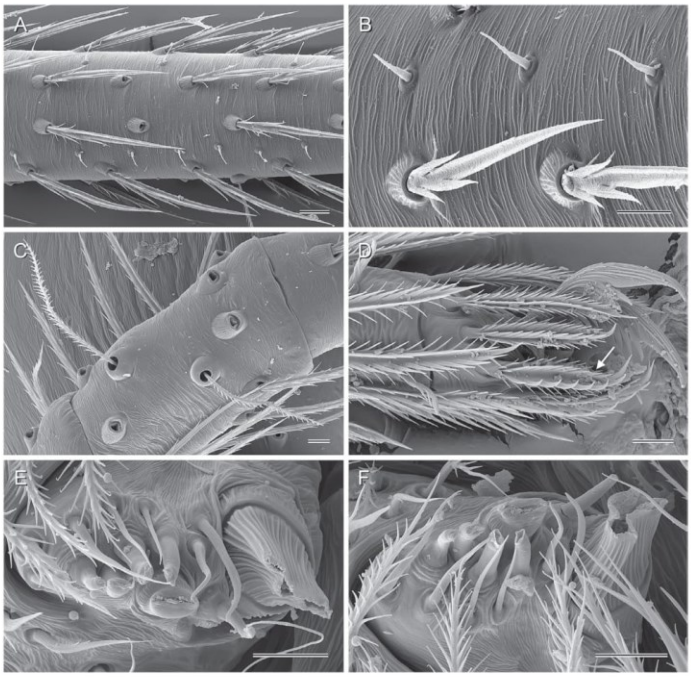

Figure 8. *Nerudia colina* sp. nov.; male and female from Argentina, Jujuy, between San Salvador and Purmamarca (ZFMK Ar 23883 and ZFMK Arg178). A, detail of male left tibia 1, prolateral view. B, hairs on male tibia 1. C, female palpal tibia, dorsal view. D, female left tarsus 4, prolateral view (arrow points at comb-hair). E, F, female ALS. Scale lines: 20 µm (A), 10 µm (B–F).

and by armature of male chelicerae (Fig. 9G, H; frontal apophyses with wide, flattened tip; set with strong hairs); also by shapes of bulbal processes (Fig. 9D–F; ventral apophysis short, slightly curved towards ventral, same length as embolar process) and by epigynum and female internal genitalia (Figs 9I, 10; epigynal plate rectangular, posterior margin weakly curved; internal genitalia with cylindrical 'receptacle', with median sclerite similar to *N. hoguera*).

Type material: ARGENTINA – **Salta**: • ♂ holotype; ~15 km NW Campo Quijano; 24.7918° S, 65.7297° W; 2020 m a.s.l.; 19 Mar. 2019; B. A. Huber and M. A. Izquierdo leg.; *LABRE-Ar 585* • 7 ♂♂, 5 ♀♀, paratypes (one male used for SEM; two male abdomens used for karyotype study; two males and three females used for µ-CT study); same data as holotype; ZFMK Ar 23884.

Other material examined: ARGENTINA – **Salta**: • 9 ♀♀, in pure ethanol (one female used for SEM; three prosomata used for molecular study); same data as holotype; ZFMK Arg184 • 2 ♂♂, 2 ♀♀; Cabra Corral, 'site 3', ~3.5 km SE of dam; 25.2907° S, 65.3057° W; 1000 m a.s.l.; 21 Mar. 2019; B. A. Huber and M. A. Izquierdo leg.; ZFMK Ar 23885 • 3 ♀♀, 1 juv., in pure ethanol; same data as preceding; ZFMK Arg195 • 2 ♂♂, 2 ♀♀ (one male and one female used for µ-CT study); Cabra Corral, 'site 4', W end of bridge; 25.2837° S, 65.3939° W; 1050 m a.s.l.; under rocks; 21–22 Mar. 2019; B. A. Huber and M. A. Izquierdo leg.; ZFMK Ar 23886 • 1 ♂, 3 ♀♀, 3 juvs, in pure ethanol; same data as preceding; ZFMK Arg197 • 1 ♂, 3 ♀♀, 9 juvs; same data as preceding; LABRE-Ar 540, 565. **Catamarca**: • 1 ♂; ~5 km NW Chumbicha, near Balneario El Caolín, 'site 2'; 28.8109° S, 66.2500° W; 640 m a.s.l.; steep rock field in forest; 28–29 Mar. 2019; B. A. Huber and M. A.

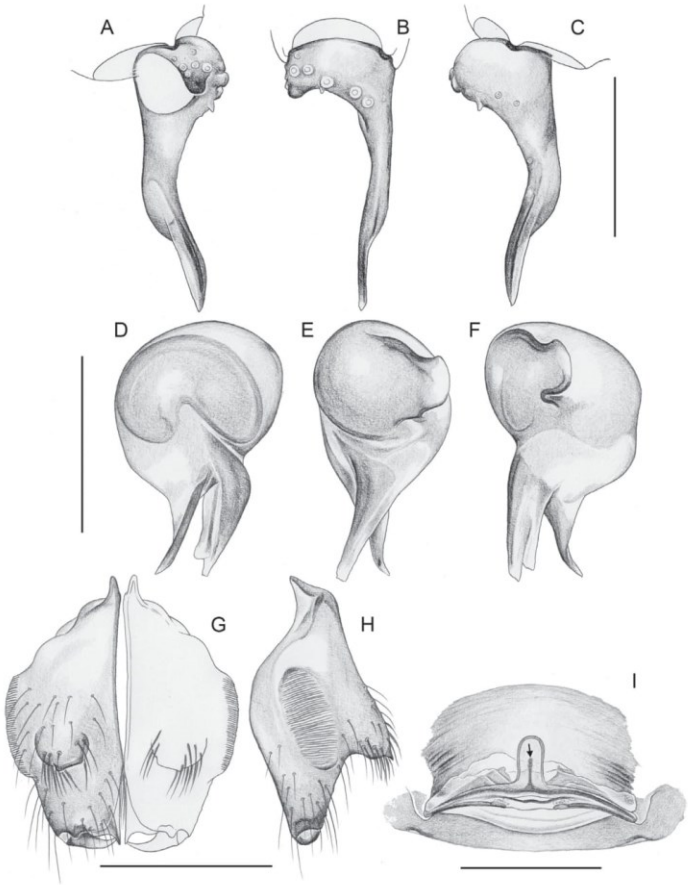

Figure 9. *Nerudia poma* sp. nov.; paratype male and paratype female from Argentina, Salta, 15 km NW Campo Quijano (ZFMK Ar 23884). A–C, left male palpal tarsus and procursus, prolateral, dorsal, and retrolateral views. D–F, left male genital bulb, prolateral, dorsal, and retrolateral views. G, H, male chelicerae, frontal and lateral views. I, cleared female genitalia, dorsal view (arrow points at median sclerite). Scale lines: 0.2 mm.

Izquierdo leg.; ZFMK Ar 23887. **La Rioja**: • 1 ♂, in pure ethanol; SE Aimogasta, 'site 2'; 28.9015° S, 66.6538° W; 755 m a.s.l.; under rocks; 10 Mar. 2019; B. A. Huber and M. A. Izquierdo leg.; LABRE-Ar 558.

Assigned tentatively (only females available, identity uncertain): ARGENTINA – **Salta**: • 2 ♀♀; ~5 km W Cafayate, 'site 1'; 26.0641° S, 66.0294° W; 2060 m a.s.l.; on rocks in small shelters; 24 Mar. 2019; B. A. Huber and M. A. Izquierdo leg.; ZFMK Ar 23888 • 5 ♀♀, in pure ethanol; same data as preceding; ZFMK Arg208 • 4 ♀♀, 5 juvs, in pure ethanol; same data as preceding; LABRE-Ar 557 • 1 ♀, 1 juv.; Chuscha, 6 km NW Cafayate; ~26.035° S, 66.017° W; ~1900 m a.s.l.; 17 Jul. 1995; M. Ramírez and P. Goloboff leg.; MACN 20094.

Note: We have not re-examined the two male specimens from Salta Province assigned to *N. atacama*

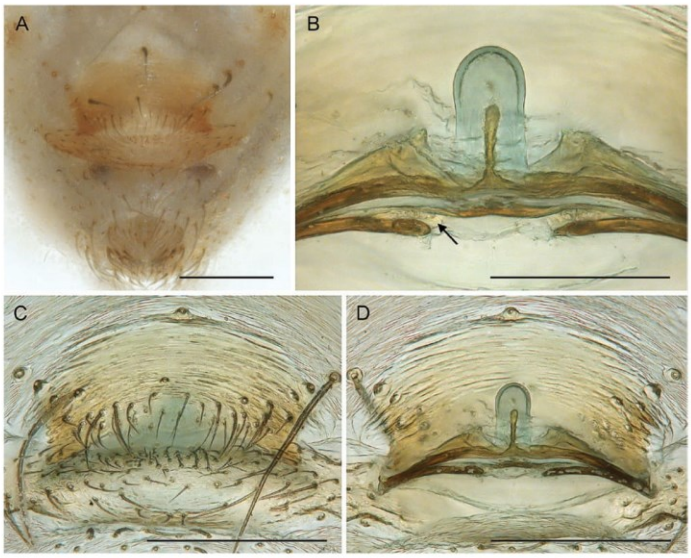

Figure 10. *Nerudia poma* sp. nov.; paratype female from Argentina, Salta, 15 km NW Campo Quijano (ZFMK Ar 23884). A, abdomen and epigynum, ventral view. B, median structures in internal genitalia. C, D, cleared genitalia, ventral and dorsal views. Scale lines: 0.2 mm (A, C, D), 0.1 mm (B).

by Torres *et al.* (2015). However, the types of the new species described herein originate from 6.5 km SE of the locality reported in Torres *et al.* (2015), in the same river valley at a similar elevation. In addition, the procursus shown in Torres *et al.* (2015: fig. 4D) agrees well with the one shown in Figure 9C.

Etymology: The species epithet *poma* (Spanish for 'apple') is taken from Pablo Neruda's poem 'Vírese'; noun in apposition.

Description

Male (holotype). Measurements: Total body length 1.44, carapace width 0.64. Distance PME–PME 80 µm; diameter PME 60 µm; distance PME–ALE 20 µm; distance AME–AME 15 µm; diameter AME 35 µm. Leg 1: 5.26 (1.45 + 0.20 + 1.43 + 1.53 + 0.65), tibia 2: 1.20, tibia 3: 1.00, tibia 4: 1.40; tibia 1 L/d: 20.

Colour (in ethanol): Prosoma and legs pale ochre-yellow; with darker Y-mark on carapace; legs without dark rings; abdomen light grey.

Body: Habitus as in Figure 1B. Ocular area barely raised. Carapace with indistinct thoracic groove. Clypeus unmodified, only at rim slightly sclerotized. Sternum wider than long (0.48/0.38), with pair of low anterior processes near coxae 1. Abdomen globular.

Chelicerae: As in Figure 9G, H; with pair of short frontal apophyses slightly pointing downward and set with strong hairs, with wide, flattened tip pointed in lateral view (Fig. 11B–D); stridulatory files on pair of low lateral protrusions (Fig. 11B, C).

Palps: In general, similar to *N. colina* (cf. Fig. 4); coxa unmodified; trochanter with indistinct ventral projection; femur cylindrical, slightly widened distally, proximally with indistinct retrolateral hump and prolateral stridulatory pick (modified hair), femur length/width: 1.91; patella short; tibia globular (length/width: 1.15); procursus simple (Fig. 9A–C), distally slender, curved towards dorsal, divided into sclerotized dorsal and transparent ventral part; genital bulb with ventral apophysis short, slightly curved towards ventral; embolus partly membranous.

Legs: Without spines and curved hairs; with vertical hairs in two rows (prolateral, retrolateral) on tibia 1 only; retrolateral trichobothrium of tibia 1 at 67%; prolateral trichobothrium absent on tibia 1; tarsus

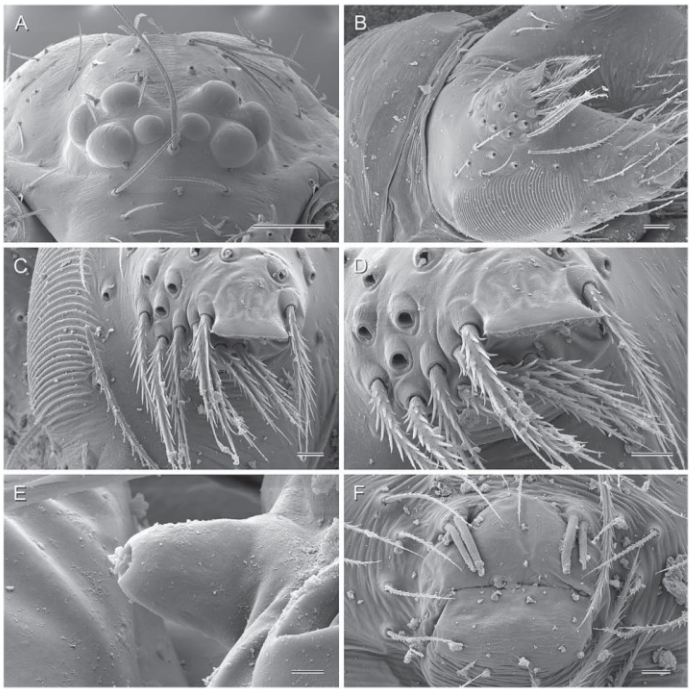

Figure 11. *Nerudia poma* sp. nov.; male and female from Argentina, Salta, 15 km NW Campo Quijano (ZFMK Ar 23884, ZFMK Arg184). A, female prosoma, frontal view. B, male clypeus and chelicerae, oblique distal view. C, D, right male chelicera, frontal views. E, male palpal tarsal organ. F, male gonopore. Scale lines: 100 µm (A), 20 µm (B), 10 µm (C, D, F), 2 µm (E).

1 with ~six to seven pseudosegments, only distally distinct.

Variation (male): Tibia 1 in nine males from Salta (including holotype): 1.27–1.50 (mean 1.41); in male from Catamarca: 1.47; in male from La Rioja: 1.35. The chelicerae and palps of the male from Catamarca appear indistinguishable from those from Salta.

Female: In general, similar to male but sternum without pair of anterior humps and tibiae with few vertical hairs. Tibia 1 in eight females: 1.30–1.50 (mean 1.42). Epigynum (Fig. 10A) anterior plate rectangular, posterior margin indented; posterior plate wide but short. Internal genitalia (Figs 9I, 10B–D) with median cylindrical 'receptacle' and median sclerite.

Distribution: Known from several localities in Salta Province, Argentina, and from one locality each in Catamarca and La Rioja (Fig. 3).

Natural history: At the type locality (Fig. 45B), the spiders were found by turning large rocks. At disturbance they started to run over the rock surface but did not drop to the ground. They shared the microhabitat with *Chibchea araona*(?). At Cabra Corral 'site 3', the spiders were found sitting on the undersides of large boulders, i.e. on the ceilings of small cave-like spaces under the rocks. At Cabra Corral 'site 4', the spiders were found under small stones on the floor of a small cave/shelter. Near Chumbicha, the single male specimen was found at the same locality as *N. ola*.

NERUDIA HOGUERA HUBER SP. NOV.

(FIGS 13, 14)

Zoobank registration: urn:lsid:zoobank.org:act:D72E218E-77C9-4026-AF20-DE2D591CFB4F.

Diagnosis: Distinguished from known congeners by armature of male chelicerae (Fig. 13G, H;

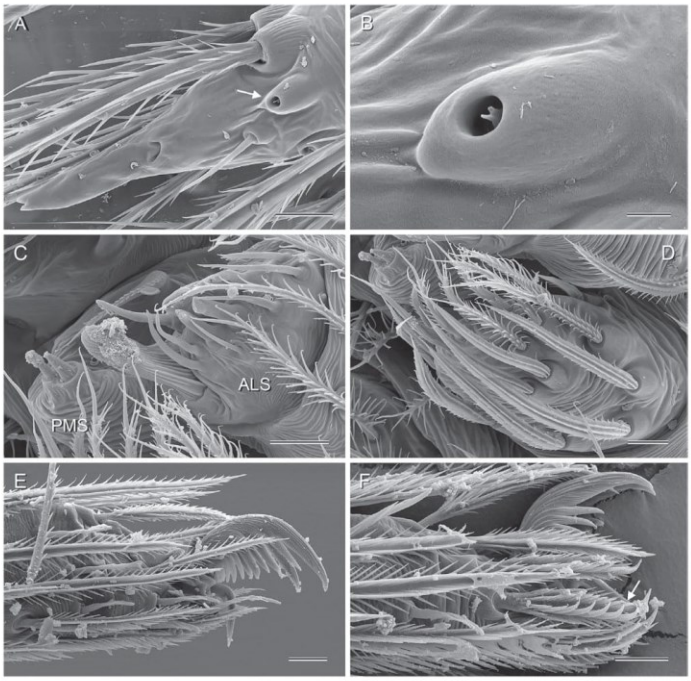

Figure 12. *Nerudia poma* sp. nov.; male and female from Argentina, Salta, 15 km NW Campo Quijano (ZFMK Ar 23884, ZFMK Arg184). A, tip of female pedipalp, dorsal view; arrow points at tarsal organ. B, female palpal tarsal organ. C, left female ALS and PMS. D, left female PLS. E, male left tarsus 1 tip, prolateral view. F, male left tarsus 4 tip, prolateral view; arrow: comb-hair. Scale lines: 10 µm (A, C–F), 2 µm (B).

frontal apophyses in lateral position, relatively long, tip flattened, i.e. wide in frontal view, pointed in lateral view), by shape of procursus (Fig. 13A–C; slender, with simple pointed tip; similar to *N. poma*), by bulbal processes (Fig. 13D–F; ventral apophysis almost straight, longer than embolus), and by epigynum and female internal genitalia (Figs 13I, 14; epigynal plate with wide posterior indentation; internal genitalia with large median 'receptacle', with median sclerite similar to *N. poma*).

Type material: ARGENTINA – **La Rioja**: • ♂ holotype; between Chilecito and Famatina; 29.0027° S, 67.4855° W; 1300 m a.s.l.; 9 Mar. 2019; B. A. Huber and M. A. Izquierdo leg.; *LABRE-Ar 586* • 2 ♀♀ paratypes; same data as holotype; ZFMK Ar 23889.

Other material examined: ARGENTINA – **La Rioja**: • 3 ♀♀ in pure ethanol; same data as holotype; ZFMK Arg159.

Etymology: The species epithet *hoguera* (from Spanish meaning 'bonfire') is taken from Pablo Neruda's poem 'Soneto 22'; noun in apposition.

Description

Male (holotype). Measurements: Total body length 1.53, carapace width 0.68. Distance PME–PME 60 µm; diameter PME 60 µm; distance PME–ALE 20 µm; distance AME–AME 15 µm; diameter AME 40 µm. Leg 1: 5.73 (1.55 + 0.25 + 1.60 + 1.73 + 0.60), tibia 2: 1.35, tibia 3: 1.10, tibia 4: 1.50; tibia 1 L/d: 23.

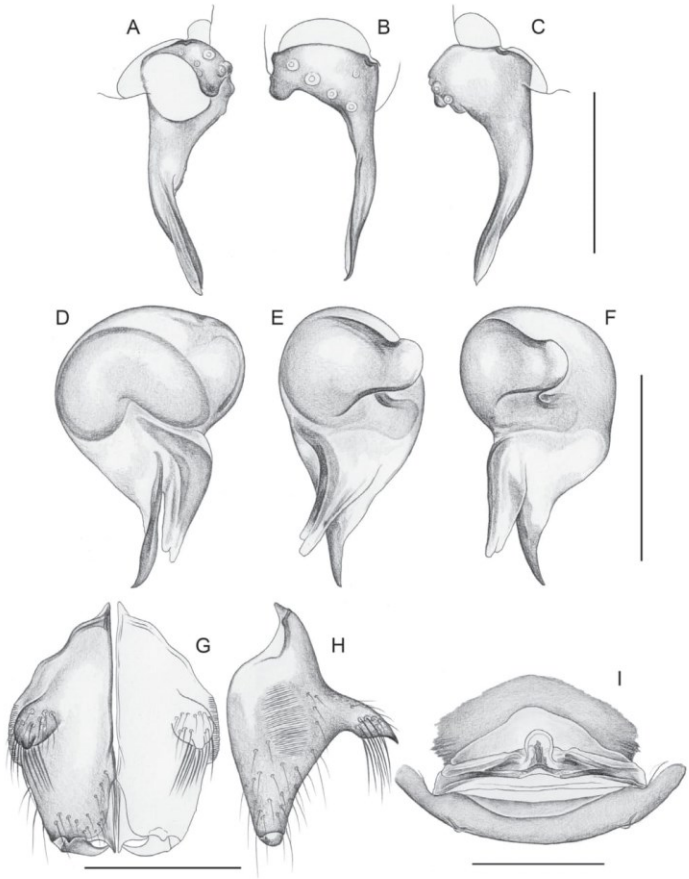

Figure 13. *Nerudia hoguera* sp. nov.; holotype male (*LABRE-Ar 586*) and paratype female (ZFMK Ar 23889) from Argentina, La Rioja, between Chilecito and Famatina. A–C, left male palpal tarsus and procursus, prolateral, dorsal, and retrolateral views. D–F, left male genital bulb, prolateral, dorsal, and retrolateral views. G, H, male chelicerae, frontal and lateral views. I, cleared female genitalia, dorsal view. Scale lines: 0.2 mm.

Colour (in ethanol): Prosoma and legs pale ochre-yellow; with indistinct ochre mark medially on carapace; legs without dark rings; abdomen monochromous light grey.

Body: Habitus as in *N. poma* (cf. Fig. 1B). Ocular area barely raised. Carapace with indistinct thoracic groove. Clypeus unmodified, only at rim slightly sclerotized. Sternum wider than long (0.48/0.44), with pair of distinct anterior processes near coxae 1. Abdomen globular.

Chelicerae: As in Figure 13G, H; with pair of frontal apophyses in lateral position, directed forward, tip flattened, i.e. wide in frontal view, pointed in lateral view; stridulatory files on pair of low lateral protrusions.

Palps: In general, similar to *N. colina* (cf. Fig. 4); coxa unmodified; trochanter with indistinct ventral projection; femur cylindrical, slightly widened distally, proximally with indistinct retrolateral hump and prolateral

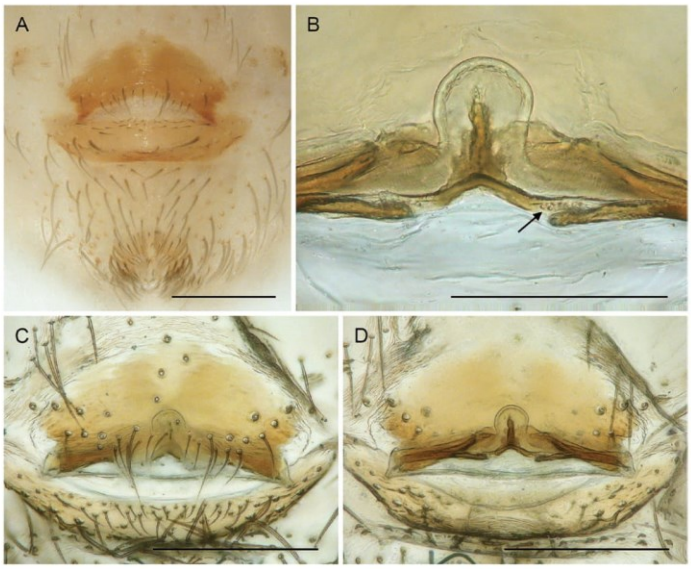

Figure 14. *Nerudia hoguera* sp. nov.; paratype female from Argentina, La Rioja, between Chilecito and Famatina (ZFMK Ar 23889). A, abdomen and epigynum, ventral view. B, median structures in internal genitalia (arrow points at possible pore plate). C, D, cleared genitalia, ventral and dorsal views. Scale lines: 0.2 mm (A, C, D), 0.1 mm (B).

stridulatory pick (modified hair), femur relatively short (length/width: 1.81); patella short; tibia globular (length/width: 1.05); procursus simple (Fig. 13A–C), slender, with simple pointed tip; genital bulb with weakly curved ventral apophysis, embolus partly membranous, shorter than ventral apophysis (Fig. 13D–F).

Legs: Without spines and curved hairs; with vertical hairs in two rows (prolateral, retrolateral) proximally on tibia 1 only; retrolateral trichobothrium of tibia 1 at 65%; prolateral trichobothrium absent on tibia 1; tarsus 1 with ~eight pseudosegments, distally distinct.

Female: In general, similar to male but sternum without pair of anterior humps. Tibia 1 in five females: 1.20–1.55 (mean 1.46). Epigynum (Fig. 14A) anterior plate weakly protruding, trapezoidal, with wide posterior indentation; posterior plate large, simple. Internal genitalia (Figs 13I, 14B, D) with large median 'receptacle' and sclerite at median line.

Distribution: Known from type locality only, in Argentina, La Rioja (Fig. 3).

Natural history: The spiders were found by turning rocks in ravines on an arid slope. When disturbed, they moved slowly. They shared the microhabitat with two other Ninetinae: *Nerudia ola* and *Gertschiola macrostyla*.

NERUDIA CENTAURA HUBER SP. NOV.

(FIGS 1C, D, 15–18)

Zoobank registration: urn:lsid:zoobank.org:act:124FC4AB-B97D-445C-AD11-C3604843AED3.

Diagnosis: Easily distinguished from known congeners by dark coloration of prosoma (Fig. 1C, D), by shape of procursus (Fig. 16A–C; dorsal hump at basis, strongly bent towards dorsal, pointed tip), by bulbal processes (Fig. 16D–F; strong pointed ventral apophysis; embolus slightly shorter, with strong dorsal sclerite), by male chelicerae (Fig. 16G, H; strong frontal apophyses with flattened tips; stridulatory files on strong lateral protrusion), and by epigynum and female internal genitalia (Figs 16I, 17; epigynal plate with large, whitish posterior indentation angular anteriorly; internal genitalia with indistinct posterior

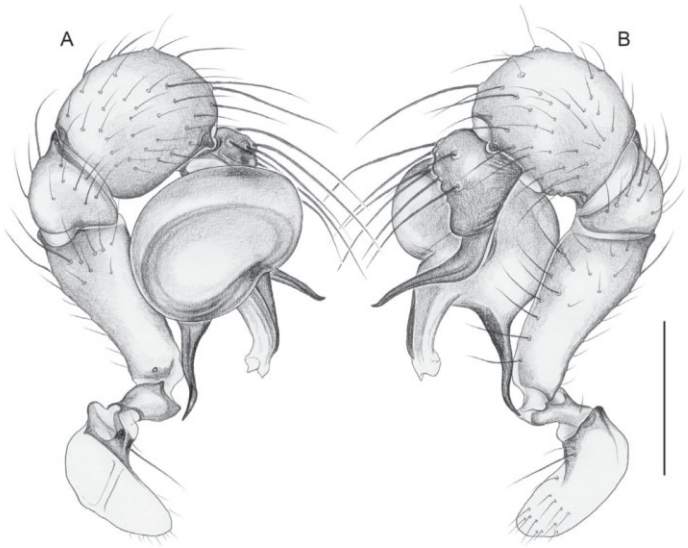

Figure 15. *Nerudia centaura* sp. nov.; non-type male from Argentina, Catamarca, 20 km E Paso de San Francisco (ZFMK Ar 23891). Left palp, prolateral (A) and retrolateral (B) views. Scale line: 0.3 mm.

'receptacle' and unique anterior tubular membranous structure).

Type material: ARGENTINA – **Catamarca**: • ♂ holotype; ~20 km E Paso de San Francisco, 'site 1'; 26.9276° S, 68.0709° W; 4180 m a.s.l.; 27 Mar. 2019; B. A. Huber and M. A. Izquierdo leg.; *LABRE-Ar 587* • 1 ♂, 2 ♀♀, paratypes; same data as holotype; ZFMK Ar 23890.

Other material examined: ARGENTINA – **Catamarca**: • 6 ♀♀, 3 juvs, in pure ethanol; same data as holotype; ZFMK Arg215 • 4 ♂♂, 6 ♀♀; same data as holotype; LABRE-Ar 526 • 3 ♀♀, 7 juvs, in pure ethanol; same data as holotype; LABRE-Ar 542 • 3 ♂♂, 5 ♀♀ (one male and two females used for µ-CT study); ~20 km E Paso de San Francisco, 'site 2'; 26.936° S, 68.090–68.095° W; 4270–4400 m a.s.l.; 27 Mar. 2019; B. A. Huber and M. A. Izquierdo leg.; ZFMK Ar 23891 • 6 ♀♀, 2 juvs, in pure ethanol (one female used for SEM; three female prosomata used for molecular study); same data as preceding; ZFMK Arg216 • 4 ♂♂, 1 ♀; same data as preceding; LABRE-Ar 527 • 6 ♀♀, 3 juvs, in pure ethanol; same data as preceding; LABRE-Ar 551 • 1 ♀; same data as preceding but 4450 m a.s.l.; ZFMK Ar 23892.

Etymology: The species epithet *centaura* (Spanish for 'female centaur') is taken from Pablo Neruda's poem 'Soneto 22'; noun in apposition.

Description

Male (holotype). Measurements: Total body length 1.9, carapace width 0.77. Distance PME–PME 90 µm; diameter PME 55 µm; distance PME–ALE 30 µm; distance AME–AME 20 µm; diameter AME 40 µm. Leg 1: 4.55 (1.25 + 0.25 + 1.30 + 1.30 + 0.45), tibia 2: 1.10, tibia 3: 1.00, tibia 4: 1.38; tibia 1 L/d: 14.

Colour (in ethanol): Prosoma and legs ochre to light brown; legs without dark rings; abdomen monochromous pale grey.

Body: Habitus as in Figure 1C. Ocular area barely raised. Carapace without thoracic groove. Clypeus unmodified. Sternum wider than long (0.56/0.48), without anterior processes. Abdomen globular.

Chelicerae: As in Figure 16G, H; pair of frontal apophyses directed downwards, with obtuse tip slightly flattened; stridulatory files on pair of distinct lateral protrusions.

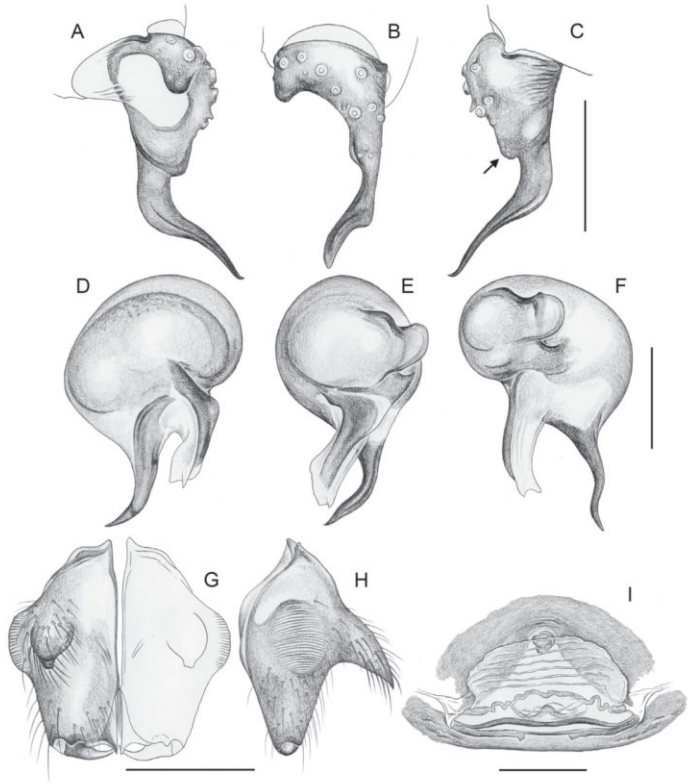

Figure 16. *Nerudia centaura* sp. nov.; non-type male and non-type female from Argentina, Catamarca, 20 km E Paso de San Francisco (ZFMK Ar 23891). A–C, left male palpal tarsus and procursus, prolateral, dorsal, and retrolateral views; arrow points at dorsal hump at basis of procursus. D–F, left male genital bulb, prolateral, dorsal, and retrolateral views. G, H, male chelicerae, frontal and lateral views. I, cleared female genitalia, dorsal view. Scale lines: 0.2 mm.

Palps: As in Figure 15; coxa unmodified; trochanter with indistinct ventral projection; femur cylindrical, only slightly widened distally, proximally with indistinct retrolateral hump and prolateral stridulatory pick (modified hair); patella short; tibia globular; procursus (Fig. 16A–C) simple, in lateral view bent towards dorsal, in dorsal view bent towards prolateral, with pointed tip; genital bulb (Fig. 16D–F) large, with strong pointed ventral apophysis, embolus partly membranous, dorsally with distinct sclerite.

Legs: Without spines and curved hairs; vertical hairs in high densities on tibiae 1–2; retrolateral trichobothrium of tibia 1 at 68%; prolateral trichobothrium absent on tibia 1; tarsus 1 with six to seven pseudosegments, distally distinct.

Variation (male): Tibia 1 in 12 males (including holotype): 1.15–1.33 (mean 1.26).

Female: In general, similar to male (Fig. 1D) but with usual low density of vertical hairs on tibiae. Tibia 1 in 22 females: 1.07–1.48 (mean 1.28). Epigynum (Fig. 17A) anterior plate weakly protruding, with large, whitish posterior indentation; posterior plate large, simple. Internal genitalia (Figs 16I, 17B–E) with simple 'receptacle' (Fig. 17C) and unique tubular membranous structure in anterior position (possibly

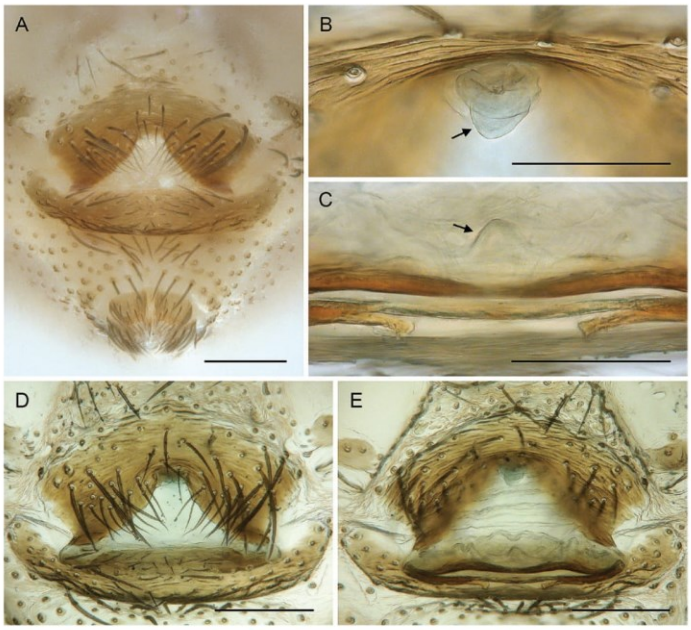

Figure 17. *Nerudia centaura* sp. nov.; non-type female from Argentina, Catamarca, 20 km E Paso de San Francisco (ZFMK Ar 23891). A, abdomen and epigynum, ventral view. B, anterior median tube-like structure in internal genitalia (arrow). C, posterior median structures in internal genitalia; arrow: 'receptacle'. D, E, cleared genitalia, ventral and dorsal views. Scale lines: 0.2 mm (A, D, E), 0.1 mm (B, C).

opening towards the outside, not towards the uterus externus).

Distribution: Known from two neighbouring localities in Argentina, Catamarca (Fig. 3).

Natural history: Both localities were similar, dominated by rocks and grasses [possibly *Calamagrostis crispa* (Rúgolo & Villav.) Govaerts; Julieta Carilla, pers. comm. August 2020] (Fig. 45C). The precipitation in this area is low (~150 mm mean annual precipitation) and largely limited to three months per year (~70% in December–February) (https://www.meteoblue.com/). We visited the locality at the end of the 'humid' season, in March, and often found humid patches of soil under large rocks, with considerable numbers of small, whitish collembolans. At the lower site (4180 m a.s.l.), this microhabitat seemed to contain little else than one species each of collembolans, pholcids, linyphiids and ants. At the higher site (4270–4450 m a.s.l.), the diversity seemed to be slightly higher, including, in addition, a species each of theridiids, filistatids and neopteran insects. At both localities, the pholcids were found sitting on the undersides of the rocks. They did not move and were thus easy to catch. Of the 36 females seen, only one had an egg-sac.

Precise climate data do not exist for these localities, but simulations of meteorological models (https://www.meteoblue.com/) suggest that temperatures fall below 0 °C almost every night of the year, with daily minima below –10 °C for seven months (April–October). In 2019, the temperatures repeatedly dropped below –20 °C in this period.

NERUDIA ROCIO HUBER SP. NOV.

(FIGS 19–21)

Zoobank registration: urn:lsid:zoobank.org:act:9245D3BD-222C-4C15-8D99-7D3CB98F848B.

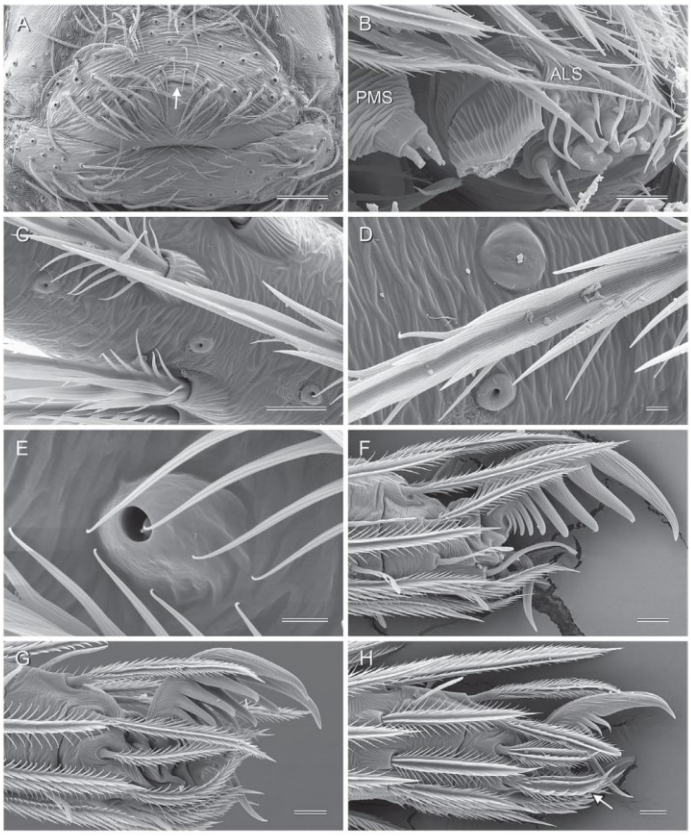

Figure 18. *Nerudia centaura* sp. nov.; female from Argentina, Catamarca, 20 km E Paso de San Francisco (ZFMK Arg216). A, epigynum, ventral view; arrow: possibly entry into tube-like internal structure. B, female ALS and PMS. C, putative glandular pores on female tarsus 3. D, glandular pore and slit sensillum(?) on female tarsus 4. E, tarsal organ on female tarsus 3. F, tip of female right tarsus 1, retrolateral view. G, tip of female right tarsus 3, retrolateral view. H, tip of female left tarsus 4, prolateral view; arrow: comb-hair. Scale lines: 100 µm (A), 10 µm (B, C, F–H), 2 µm (D, E).

Diagnosis: Easily distinguished from known congeners by shapes of procursus (Fig. 20A–C; distinctively widened tip); also by shape of embolus (Fig. 20D–F; distally strongly bent towards dorsal), by armature of male chelicerae (Fig. 20G, H; slender frontal apophyses, without stronger hairs), by epigynum and female internal genitalia (Figs 20I, 21; epigynal plate anteriorly narrow with strong transversal ridges; internally apparently without 'receptacle'), and by indistinct radial marks on carapace in males and females.

Type material: ARGENTINA – **San Juan**: • ♂ holotype; ~35 km W Las Flores; 30.3967° S, 69.5576° W; 2910 m a.s.l.; 6 Mar. 2019; B. A. Huber and M. A. Izquierdo leg.; *LABRE-Ar 588* • 2 ♂♂, 5 ♀♀, paratypes, + 2 juvs; same data as holotype; LABRE-Ar 536.

Other material examined: ARGENTINA – **San Juan**: • 2 ♀♀, in pure ethanol; same data as holotype; ZFMK Arg148 (one female abdomen transferred to 80% ethanol, ZFMK Ar 23893) • 1 ♀, in pure ethanol; same data as holotype; LABRE-Ar 543.

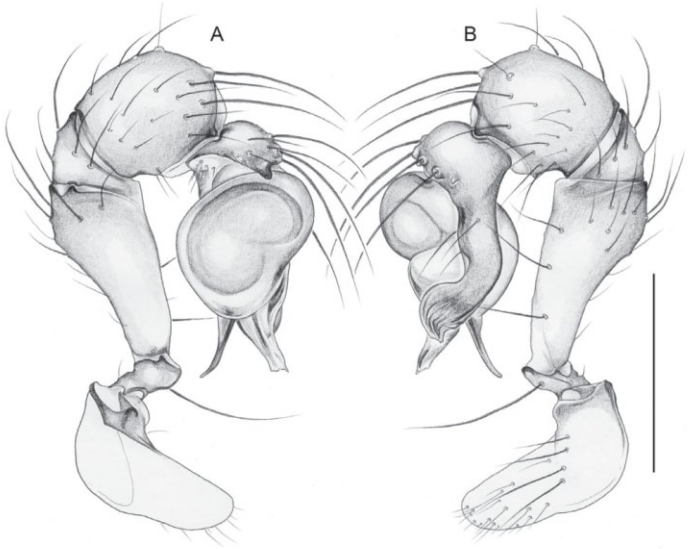

Figure 19. *Nerudia rocio* sp. nov.; holotype male from Argentina, San Juan, 35 km W Las Flores (*LABRE-Ar 588*). Left palp, prolateral (A) and retrolateral (B) views. Scale line: 0.3 mm.

Etymology: The species epithet *rocio* (rocío is Spanish for 'dew') is taken from Pablo Neruda's poem 'Poema 12'; noun in apposition.

Description

Male (holotype). Measurements: Total body length 1.60, carapace width 0.73. Distance PME–PME 80 µm; diameter PME 70 µm; distance PME–ALE 30 µm; distance AME–AME 20 µm; diameter AME 50 µm. Leg 1: 8.40 (2.25 + 0.30 + 2.50 + 2.55 + 0.80), tibia 2: 1.85, tibia 3: 1.45, tibia 4: 2.00; tibia 1 L/d: 31.

Colour (in ethanol): Carapace ochre-yellow with indistinct darker (ochre) median mark including ocular area and radial lateral marks; legs monochromous ochre-yellow, without dark rings; abdomen monochromous ochre-grey.

Body: Habitus similar to *N. poma* (cf. Fig. 1B). Ocular area barely raised. Carapace with indistinct thoracic groove. Clypeus unmodified, only rim slightly more sclerotized. Sternum wider than long (0.52/0.48), with pair of distinct anterior processes near coxae 1. Abdomen globular.

Chelicerae: As in Figure 20G, H; pair of pointed frontal apophyses directed forward and weakly curved downward; stridulatory files on pair of low lateral protrusions.

Palps: As in Figure 19; coxa unmodified; trochanter with indistinct ventral projection; femur cylindrical, slightly widened distally, proximally without retrolateral hump, with prolateral stridulatory pick (modified hair), femur length/width: 1.93; patella short; tibia globular, less strongly widened than in congeners (length/width: 1.17); procursus with distinctive distal widening and proximal dorsal ridge (Fig. 20A–C); genital bulb with simple ventral apophysis, embolus distally strongly bent towards dorsal (Fig. 20D–F).

Legs: Without spines and curved hairs; with vertical hairs in higher density on tibia 1, only proximally on prolateral and retrolateral sides (length ~20 µm; length of dorsal trichobothrium on tibia 1: ~80 µm); retrolateral trichobothrium of tibia 1 at 66%; prolateral trichobothrium absent on tibia 1; tarsus 1 with seven to eight pseudosegments, distally distinct.

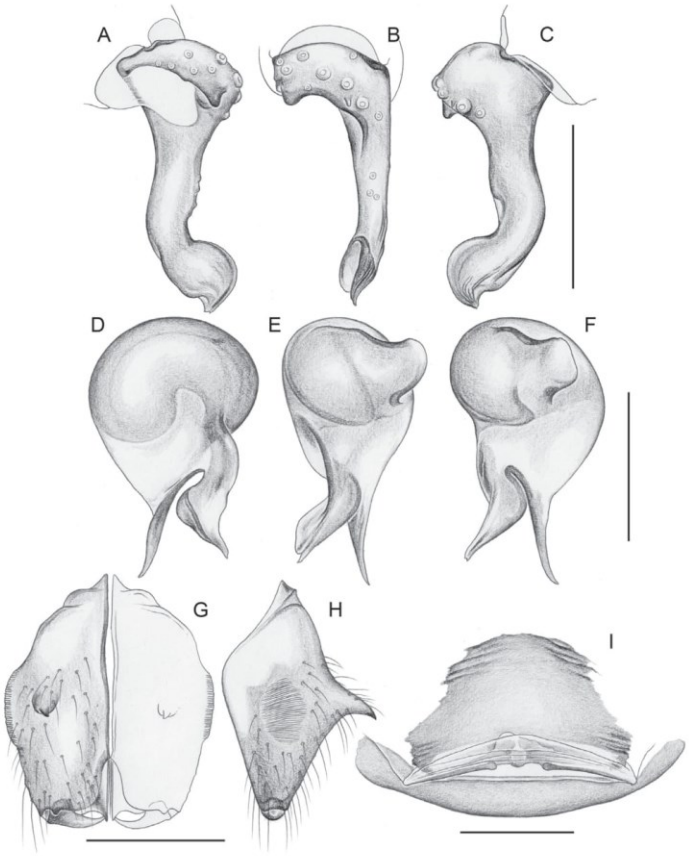

Figure 20. *Nerudia rocio* sp. nov.; holotype male (*LABRE-Ar 588*) and non-type female (ZFMK Ar 23893) from Argentina, San Juan, 35 km W Las Flores. A–C, left male palpal tarsus and procursus, prolateral, dorsal, and retrolateral views. D–F, left male genital bulb, prolateral, dorsal, and retrolateral views. G, H, male chelicerae, frontal and lateral views. I, cleared female genitalia, dorsal view. Scale lines: 0.2 mm.

Variation (male): Tibia 1 in two other males: 2.10, 2.12.

Female (see Note below): In general, similar to male but sternum without pair of anterior humps. Tibia 1 in seven females: 1.61–2.00 (mean 1.80). Epigynum (Fig. 21A) anterior plate weakly protruding, anteriorly narrow with strong transversal ridges; posterior plate large, simple. Internal genitalia (Figs 20I, 21B–D) simple, apparently without or with small and indistinct median receptacle.

Distribution: Known from type locality only, in Argentina, San Juan (Fig. 3).

Natural history: The spiders were collected by turning large rocks on an arid hillside (Fig. 45D). They shared the microhabitat with another (undescribed) species

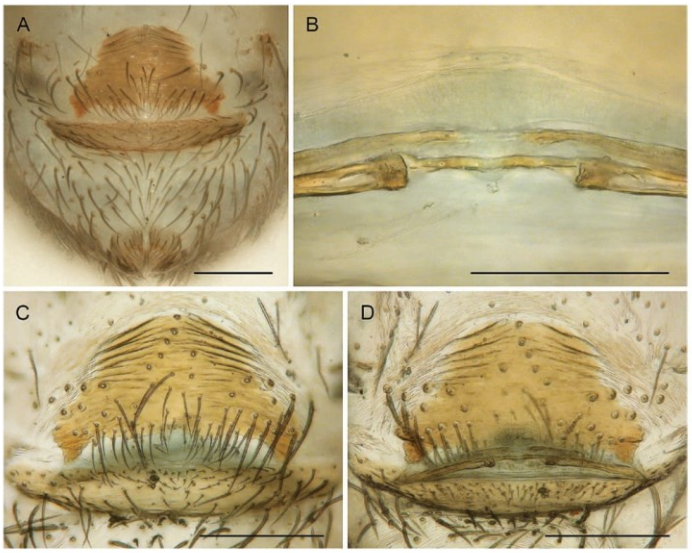

Figure 21. *Nerudia rocio* sp. nov.; non-type female from Argentina, San Juan, 35 km W Las Flores (ZFMK Ar 23893). A, abdomen and epigynum, ventral view. B, median structures in internal genitalia. C, D, cleared genitalia, ventral and dorsal views. Scale lines: 0.2 mm (A, C, D), 0.1 mm (B).

of *Nerudia* (*N.* 'Arg23a'), of which only females were collected (see Note below). A third species collected at this locality (possibly *N. ola*; see Note below) was found closer to the river.

Note: Eighteen female specimens representing three putative species of *Nerudia* were collected at the type locality of this species. Eight specimens share with the male holotype (and male paratypes) the radial marks on the carapace and the relatively long legs. We thus consider these to be conspecific with the holotype. However, this needs confirmation, ideally by collecting males of the other putative species and by barcoding males and females. One female specimen shares with *N. ola* the shape of the epigynum and is thus tentatively assigned to that species. The remaining nine female specimens have a distinctive epigynum (Fig. 37A) and their separation from *N. rocio* and *N. ola* is also supported by *COI* (Fig. 2). They are thus considered to represent a separate undescribed species, *Nerudia* 'Arg23a' (see Putative further species at the end of the taxonomic section).

NERUDIA TRIGO HUBER SP. NOV.

(FIGS 1E, 22–24)

Zoobank registration: urn:lsid:zoobank.org:act:2D2F4A08-7C18-4ED6-8894-FE391F17E6C6.

Diagnosis: Easily distinguished from known congeners by male chelicerae (Fig. 22G, H; without frontal apophyses, with patches of strong hairs); also by shapes of procursus (Fig. 22A–C; similar to *N. guirnalda,* but without prolateral–ventral ridge proximally), by bulbal processes (Fig. 22D–F; ventral apophysis distally slender, curved towards ventral, same length as embolar process), and by epigynum and female internal genitalia (Figs 22I, 23; epigynal plate with short but wide posterior indentation, laterally strongly sclerotized; internal genitalia with indistinct 'receptacle'.

Type material: ARGENTINA – **Salta**: • ♂ holotype; between Alemanía and Cafayate; 25.7023° S, 65.7022° W; 1340 m a.s.l.; 23 Mar. 2019; B. A. Huber and M. A. Izquierdo leg.; *LABRE-Ar 589* • 1 ♂, 2 ♀♀, paratypes; same data as holotype; ZFMK Ar 23894.

Other material examined: ARGENTINA – **Salta**: • 10 ♀♀, 2 juvs, in pure ethanol (one female used for SEM; three female prosomata used for molecular study); same data as holotype; ZFMK Arg206 • 3 ♂♂; same data as holotype; LABRE-Ar 539 • 1 ♂; ~1 km SW Alemanía; 25.6300° S, 65.6180° W; 1210 m a.s.l.; 23 Mar. 2019; B. A. Huber and M. A. Izquierdo leg.;

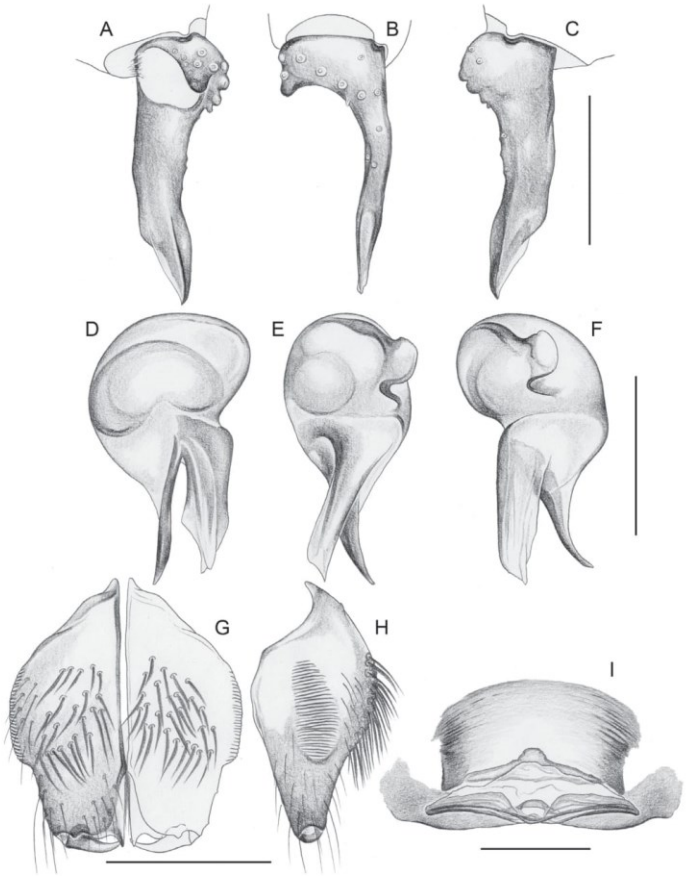

Figure 22. *Nerudia trigo* sp. nov.; paratype male and paratype female from Argentina, Salta, between Alemanía and Cafayate (ZFMK Ar 23894). A–C, left male palpal tarsus and procursus, prolateral, dorsal, and retrolateral views. D–F, left male genital bulb, prolateral, dorsal, and retrolateral views. G, H, male chelicerae, frontal and lateral views. I, cleared female genitalia, dorsal view. Scale lines: 0.2 mm.

ZFMK Ar 23895 • 1 ♀, in pure ethanol; same data as preceding; ZFMK Arg202 • 2 ♀♀, 1 juv., in pure ethanol; same data as preceding; LABRE-Ar 550.

Etymology: The species epithet *trigo* (Spanish for 'wheat') is taken from Pablo Neruda's poem 'Cien sonetos de amor'; noun in apposition.

Description

Male (holotype). Measurements: Total body length 1.70, carapace width 0.77. Distance PME–PME 80 µm; diameter PME 65 µm; distance PME–ALE 20 µm; distance AME–AME 20 µm; diameter AME 50 µm. Leg 1: 7.50 (2.10 + 0.30 + 1.95 + 2.40 + 0.75), tibia 2: 1.80, tibia 3: 1.60, tibia 4: 2.10; tibia 1 L/d: 22.

Colour (in ethanol): Prosoma and legs mostly pale ochre-yellow; darker ochre Y-mark behind ocular area; legs without dark rings; abdomen monochromous pale grey.

Body: Habitus as in *N. poma* (cf. Fig. 1B). Ocular area barely raised. Carapace with indistinct thoracic

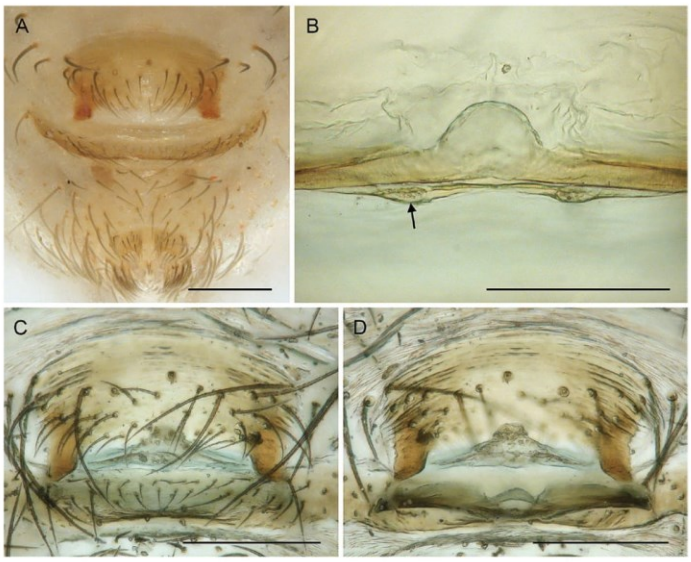

Figure 23. *Nerudia trigo* sp. nov.; paratype female from Argentina, Salta, between Alemanía and Cafayate (ZFMK Ar 23894). A, abdomen and epigynum, ventral view. B, median structures in internal genitalia (arrow points at possible pore plate). C, D, cleared genitalia, ventral and dorsal views. Scale lines: 0.2 mm (A, C, D), 0.1 mm (B).

groove. Clypeus unmodified. Sternum wider than long (0.54/0.42), with pair of distinct anterior processes near coxae 1. Abdomen globular.

Chelicerae: As in Figure 22G, H; with large patch of strong hairs on each side; without frontal processes; stridulatory files on low lateral protrusions.

Palps: Similar to *N. colina* (cf. Fig. 4); proximal segments apparently identical to *N. colina*; femur length/width 2.08; tibia length/width 1.10; procursus simple, in lateral view slightly directed towards dorsal, similar to *N. colina* but without subdistal ventral sclerite and slightly wider (Fig. 22A–C); genital bulb similar to *N. colina* but ventral apophysis less strongly curved towards ventral (Fig. 22D–F).

Legs: Without spines and curved hairs; apparently few vertical hairs; retrolateral trichobothrium of tibia 1 at 63%; prolateral trichobothrium absent on tibia 1; tarsus 1 with seven to eight pseudosegments, distally distinct.

Variation (male): Tibia 1 in three other males from type locality: 1.71, 1.72, 1.83. The male from 1 km SW Alemanía has apparently identical chelicerae and pedipalps but is smaller: tibia 1: 1.40; carapace width: 0.63; chelicerae maximum width: 240 µm.

Female: In general, similar to male (Fig. 1E) but sternum without pair of anterior humps. Tibia 1 in four females: 1.46, 1.47, 1.65, 1.85. Epigynum (Fig. 23) anterior plate roughly rectangular, weakly protruding, with short but wide posterior indentation; posterior plate large, simple. Internal genitalia (Figs 22I, 23B–D) simple, with indistinct 'receptacle'.

Distribution: Known only from two neighbouring localities in Salta, Argentina (Fig. 3).

Natural history: At the type locality, the spiders were found in small cavities or shelters composed of large rocks in a dry ravine. They were sitting relatively exposed on the ceiling of the cavities and were easy to collect as they barely moved. Several females carried egg-sacs that were consistently reddish, flattened, and contained approximately 15–18 eggs. Near Alemanía, the single pair was found close together on the underside of a large rock. The spiders barely moved at disturbance. They shared the microhabitat with a tiny undescribed species of Modisiminae.

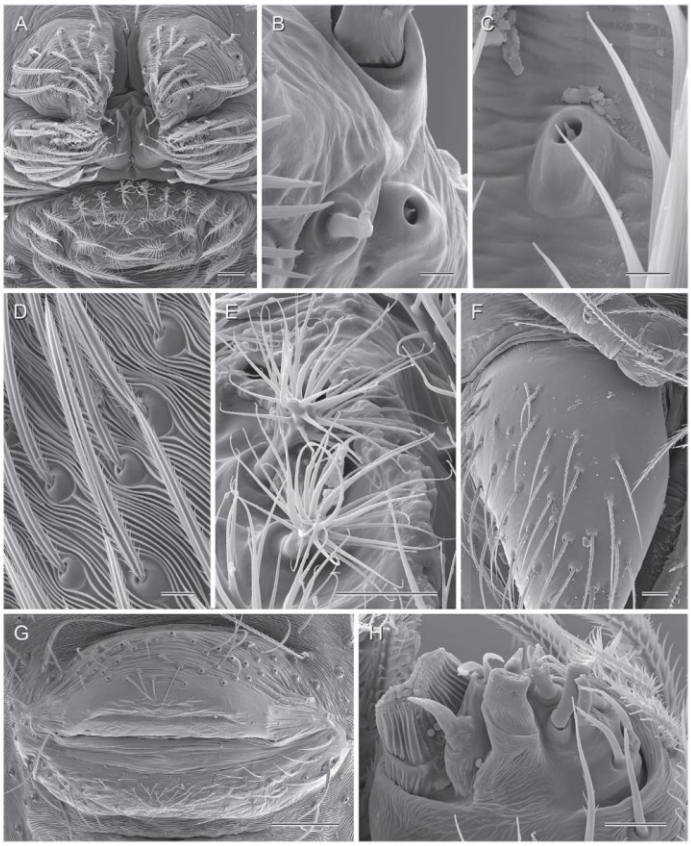

Figure 24. *Nerudia trigo* sp. nov.; female from Argentina, Salta, between Alemanía and Cafayate (ZFMK Arg206). A, female spinnerets. B, female palpal tarsal organ. C, tarsal organ on female right tarsus 4. D, 'regular' hairs on female abdomen. E, hairs on female anal cone. F, left female chelicera, lateral view (note absence of stridulatory file). G, epigynum, ventral view. H, female ALS. Scale lines: 20 µm (A, F), 2 µm (B, C), 10 µm (D, E, H), 100 µm (G).

NERUDIA GUIRNALDA HUBER SP. NOV.

(FIGS 1F, 25, 26)

Zoobank registration: urn:lsid:zoobank.org:act:7EF740D6-19C7-4A45-97BA-2FB853B8FB2F.

Diagnosis: Distinguished from most known congeners by shape of procursus (Fig. 25A–C; wide in lateral view, with prolateral–ventral ridge proximally), from the similar *N. trigo* by armature of male chelicerae (Fig. 25G, H; strong frontal apophyses pointing downward, with flattened tip; set with strong hairs), from some congeners also by bulbal processes (Fig. 25D–F; ventral apophysis slender, weakly curved, same length as embolus), and by epigynum and female internal genitalia (Figs 25I, 26; epigynal plate trapezoidal, medially light, much narrower than posterior plate; internal genitalia with posteriorly wide open receptacle; similar to *N. colina* and *N. trigo*).

Type material: ARGENTINA – **Catamarca**: • ♂ holotype; El Rodeo, trail to Cristo Redentor; 28.2229°

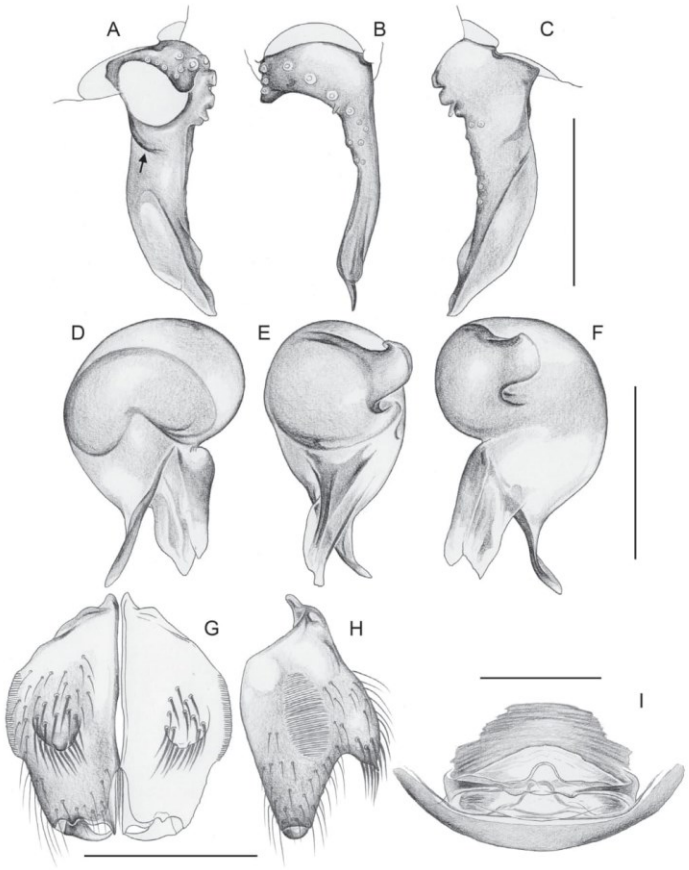

Figure 25. *Nerudia guirnalda* sp. nov.; paratype male and paratype female from Argentina, Catamarca, El Rodeo (ZFMK Ar 23896). A–C, left male palpal tarsus and procursus, prolateral, dorsal, and retrolateral views; arrow points at prolateral–ventral ridge. D–F, left male genital bulb, prolateral, dorsal, and retrolateral views. G, H, male chelicerae, frontal and lateral views. I, cleared female genitalia, dorsal view. Scale lines: 0.2 mm.

S, 65.8677° W; 1460 m a.s.l.; 11 Mar. 2019; B. A. Huber and M. A. Izquierdo leg.; *LABRE-Ar 590* • 3 ♂♂, 4 ♀♀, paratypes; same data as holotype; ZFMK Ar 23896.

Other material examined: ARGENTINA – **Catamarca**: • 5 ♀♀, in pure ethanol (two prosomata used for molecular study); same data as holotype; ZFMK Arg166, 167 • 1 ♀; same data as holotype; LABRE-Ar 538 • 1 ♂; El Rodeo; Jan. 1957; M.E. Galiano leg.; MACN 20015 part • 2 ♂♂, 2 ♀♀, 1 juv.; Mutquin; ~28.32° S, 66.13° W; 2000 m a.s.l.; Jan. 1966; O. de Ferrariis leg.; MACN 20050 part.

Etymology: The species epithet *guirnalda* (Spanish for a 'garland') is taken from Pablo Neruda's poem 'Sed de ti'; noun in apposition.

Description

Male (holotype). Measurements: Total body length 1.40, carapace width 0.60. Distance PME–PME 70 µm;

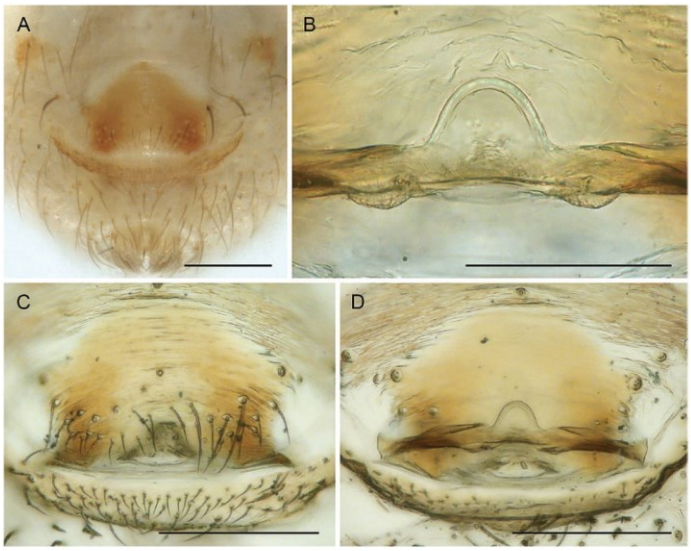

Figure 26. *Nerudia guirnalda* sp. nov.; paratype female from Argentina, Catamarca, El Rodeo (ZFMK Ar 23896). A, abdomen and epigynum, ventral view. B, median structures in internal genitalia. C, D, cleared genitalia, ventral and dorsal views. Scale lines: 0.2 mm (A, C, D), 0.1 mm (B).

diameter PME 60 µm; distance PME–ALE 20 µm; distance AME–AME 15 µm; diameter AME 45 µm. Leg 1: 4.80 (1.37 + 0.23 + 1.23 + 1.40 + 0.57), tibia 2: 1.03, tibia 3: 0.87, tibia 4: 1.27; tibia 1 L/d: 18.

Colour (in ethanol): Prosoma and legs pale ochre-yellow; with indistinct Y-mark on carapace; legs without dark rings; abdomen ochre-yellow to light grey, with indistinct internal marks.

Body: Habitus as in Figure 1F. Ocular area barely raised. Carapace with indistinct thoracic groove. Clypeus unmodified, only at rim slightly sclerotized. Sternum wider than long (0.44/0.38), with pair of low anterior processes near coxae 1. Abdomen globular.

Chelicerae: As in Figure 25G, H; with pair of short frontal apophyses pointing downward, with flattened tip, i.e. wide in frontal view, pointed in lateral view; set with strong hairs; stridulatory files on pair of low lateral protrusions.

Palps: In general, similar to *N. colina* (cf. Fig. 4); coxa unmodified; trochanter with indistinct ventral projection; femur cylindrical, slightly widened distally, proximally with indistinct retrolateral hump and prolateral stridulatory pick (modified hair), femur length/width: 1.81; patella short; tibia globular (length/width: 1.05); procursus simple (Fig. 25A–C), wide but mostly semi-transparent in lateral view, with prolateral–ventral ridge proximally; genital bulb (Fig. 25D–F) with weakly curved ventral apophysis, embolus partly membranous.

Legs: Without spines and curved hairs; with vertical hairs in two rows (prolateral, retrolateral) proximally on tibia 1 only; retrolateral trichobothrium of tibia 1 at 62%; prolateral trichobothrium absent on tibia 1; tarsus 1 with ~six pseudosegments, distally distinct.

Variation (male): Tibia 1 in six males (including holotype): 1.22–1.47 (mean 1.33).

Female: In general, similar to male but sternum without pair of anterior humps. Tibia 1 in ten females: 1.08–1.33 (mean 1.22). Epigynum (Fig. 26A) anterior plate weakly protruding, trapezoidal, medially light; posterior plate wide but short. Internal genitalia (Figs 25I, 26B–D) with posteriorly wide open receptacle.

Distribution: Known from two localities in the Cerro el Manchao region in Catamarca, Argentina (Fig. 3).

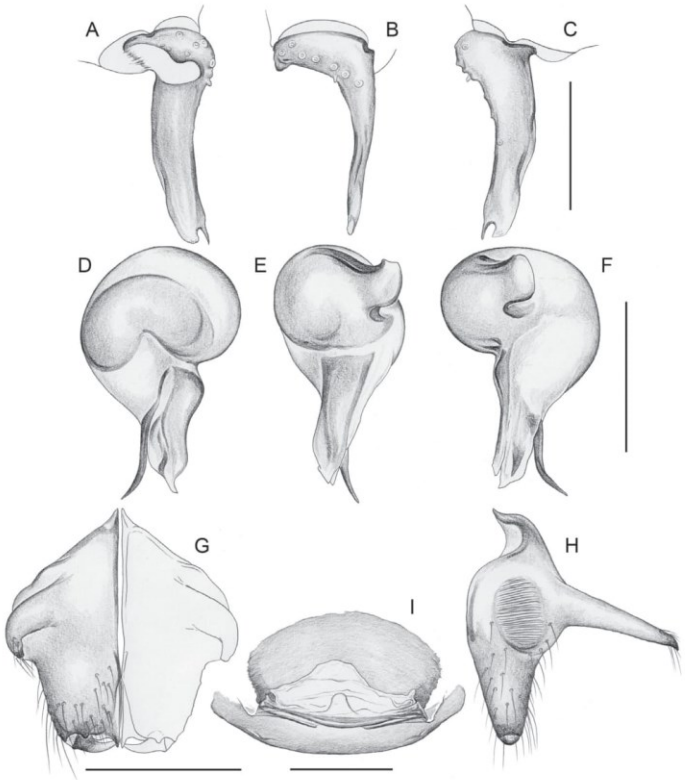

Figure 27. *Nerudia ola* sp. nov.; paratype male and paratype female from Argentina, San Juan, San Agustín de Valle Fértil (ZFMK Ar 23897). A–C, left male palpal tarsus and procursus, prolateral, dorsal, and retrolateral views. D–F, left male genital bulb, prolateral, dorsal, and retrolateral views. G, H, male chelicerae, frontal and lateral views. I, cleared female genitalia, dorsal view. Scale lines: 0.2 mm.

Natural history: At the type locality the spiders were found by turning rocks along the trail in low forest.

NERUDIA OLA HUBER SP. NOV.

(FIGS 1G, 27–30)

Zoobank registration: urn:lsid:zoobank.org:act:BF76CDC2-9B0C-4B69-8DB9-DE6925D99DD4.

Nerudia Mich20: Eberle *et al.*, 2018 (molecular data: 28S). Huber *et al.*, 2018: fig. 2.

Diagnosis: Easily distinguished from known congeners by armature of male chelicerae (Fig. 27G, H; distinctive pair of long frontal apophyses) and by shape of procursus (Fig. 27A–C; with bifid tip consisting of slender dorsal process and wider ventral membranous part); also by bulbal processes (Fig. 27D–F; ventral apophysis distally slender, curved towards ventral, same length as embolus) and by epigynum and female internal genitalia (Figs 27I, 28; epigynal plate without posterior indentation; internal genitalia simple, with barely visible transparent 'receptacle').

Type material: ARGENTINA – **San Juan**: • ♂ holotype; San Agustín de Valle Fértil; 30.6366° S, 67.4863° W; 880 m a.s.l.; under rocks near river; 5 Mar. 2019; B. A. Huber and M. A. Izquierdo leg.; *LABRE-Ar*

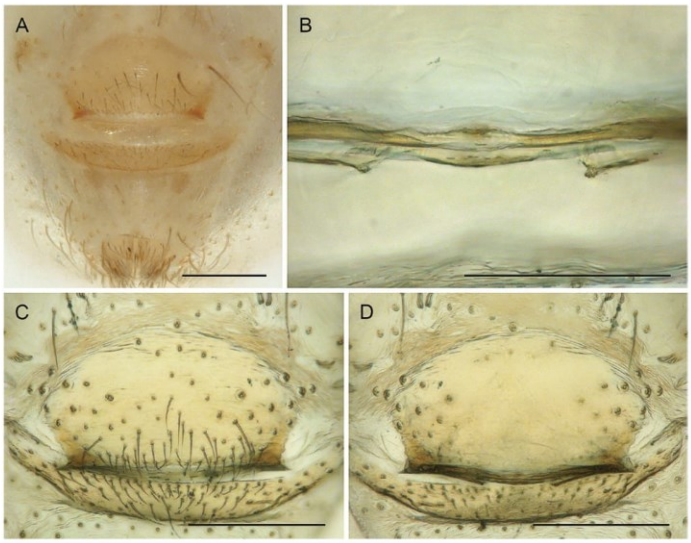

Figure 28. *Nerudia ola* sp. nov.; paratype female from Argentina, San Juan, San Agustín de Valle Fértil (ZFMK Ar 23897). A, abdomen and epigynum, ventral view. B, median structures in internal genitalia. C, D, cleared genitalia, ventral and dorsal views. Scale lines: 0.2 mm (A, C, D), 0.1 mm (B).

591 • 5 ♂♂, 2 ♀♀, paratypes; same data as holotype; ZFMK Ar 23897.

Other material examined: ARGENTINA – **San Juan**: • 12 ♂♂, 8 ♀♀, 5 juvs, in pure ethanol (two males and two females used for SEM; three female prosomata used for molecular study); same data as holotype; ZFMK Arg141 • 9 ♀♀, 3 juvs; same data as holotype; LABRE-Ar 560 • 1 ♂, in pure ethanol; same locality as holotype; 22 Jan. 2012; J. M. A. Navarro leg.; ZFMK Mich20 • 3 ♂♂, 2 ♀♀; ~7.5 km S Astica; 31.0223° S, 67.2976° W; 865 m a.s.l.; under rocks near river; 4 Mar. 2019; B. A. Huber and M. A. Izquierdo leg.; ZFMK Ar 23898 • 1 ♂, 3 ♀♀, 5 juvs, in pure ethanol; same data as preceding; ZFMK Arg135, 136 • 1 ♂, 1 ♀; same data as preceding; LABRE-Ar 528 • 5 ♂♂, 7 ♀♀, 1 juv., in pure ethanol; same data as preceding; LABRE-Ar 529, 547, 548, 552 • 1 ♂, 1 ♀; Parque Provincial Ischigualasto; 30.1839° S, 67.9026° W; 1425 m a.s.l.; under rocks; 5 Mar. 2019; B. A. Huber and M. A. Izquierdo leg.; ZFMK Ar 23899 • 2 ♀♀, in pure ethanol; same data as preceding; ZFMK Arg144 • 1 ♀, 2 juvs; same data as preceding; LABRE-Ar 531 • 1 ♀ with eggs, in pure ethanol; same data as preceding; LABRE-Ar 554 • 1 ♂; Parque Provincial Ischigualasto; 30.1821° S, 67.9010° W; 1425 m a.s.l.; in dry riverbed, hand collecting at night; 19 Dec. 2018; M. Izquierdo, F. Bollatti, A. Albin, and C. Mattoni leg.; LABRE-Ar 445 • 1 ♂; same data as preceding; LABRE-Ar 444, prep. code MAI-4709 • 1 ♀; Baldecitos; 30.2232° S, 67.6942° W; 1255 m a.s.l.; stone wall of buildings, hand collecting at night; 21 Dec. 2018; M. Izquierdo, F. Bollatti, A. Albin, and C. Mattoni leg.; LABRE-Ar 448, prep. code MAI-4710.

Assigned tentatively (see Male variation below): **La Rioja**: • 1 ♂, 1 ♀; Cuesta de Miranda, 'site 1'; 29.3511° S, 67.7924° W); 1960 m a.s.l.; under rocks; 8 Mar. 2019; B. A. Huber and M. A. Izquierdo leg.; ZFMK Ar 23900 • 2 ♀♀, in pure ethanol; same data as preceding; ZFMK Arg152 • 2 ♂♂, 1 ♀; Cuesta de Miranda, 'site 2'; 29.3468° S, 67.7205° W; 1660 m a.s.l.; under rocks; 8 Mar. 2019; B. A. Huber and M. A. Izquierdo leg.; ZFMK Ar 23901 • 2 ♀♀, in pure ethanol; same data as preceding; ZFMK Arg154 • 1 ♂, 2 ♀♀; same data as preceding; LABRE-Ar 533 • 1 ♀, in pure ethanol; same data as preceding; LABRE-Ar 553 • 1 ♀; between Chilecito and Famatina; 29.0027° S, 67.4855° W; 1300 m a.s.l.; 9 Mar. 2019; B. A. Huber and M. A. Izquierdo leg.; ZFMK Ar 23902 • 1 ♀; same data as preceding; LABRE-Ar 541 • 1 ♀ with eggs, in pure ethanol; same data as preceding; LABRE-Ar

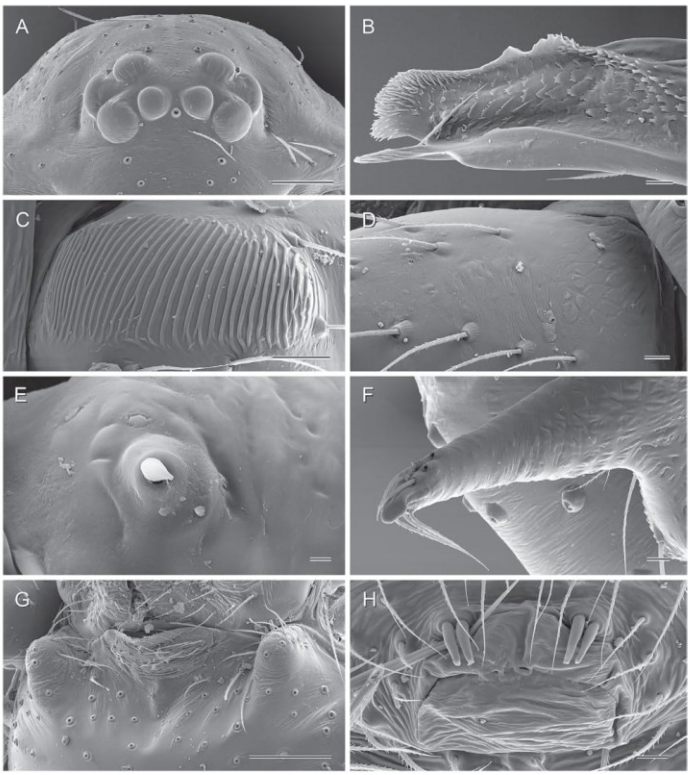

Figure 29. *Nerudia ola* sp. nov.; male and female from Argentina, San Juan, San Agustín de Valle Fértil (ZFMK Arg141). A, female prosoma, frontal view. B, left procursus tip, prolateral-dorsal view. C, stridulatory file on male chelicera. D, lateral view of female chelicera, showing absence of stridulatory file. E, stridulatory pick (modified hair) on male palpal femur. F, right male cheliceral apophysis, frontal view. G, processes on male sternum. H, male gonopore. Scale lines: 100 µm (A, G), 10 µm (B, D, F, H), 20 µm (C), 2 µm (E).

546 • 4 ♂♂, 2 ♀♀; SE Aimogasta, 'site 2'; 28.9015° S, 66.6538° W; 755 m a.s.l.; under rocks; 10 Mar. 2019; B. A. Huber and M. A. Izquierdo leg.; ZFMK Ar 23903 • 3 ♀♀, in pure ethanol; same data as preceding; ZFMK Arg162 • 1 ♂, 1 ♀, 1 juv.; same data as preceding; LABRE-Ar 532 • 1 ♀, in pure ethanol; same data as preceding; LABRE-Ar 567. **Catamarca**: • 2 ♂♂, 4 ♀♀; ~5 km NW Chumbicha, near Balneario El Caolín, 'site 2'; 28.8109° S, 66.2500° W; 640 m a.s.l.; steep rock field in forest; 28–29 Mar. 2019; B. A. Huber and M. A. Izquierdo leg.; ZFMK Ar 23904 • 7 ♀♀, 3 juvs, in pure ethanol (three female prosomata used for molecular study); same data as preceding; ZFMK Arg218 • 2 ♂♂, 6 ♀♀, 8 juvs, in pure ethanol; same data as preceding; LABRE-Ar 530, 544, 561, 563, 566 • 3 ♀♀ with eggs, in pure ethanol; same locality as preceding, 'site 1'; 28.8152° S, 66.2478° W; 605 m a.s.l.; M. A. Izquierdo and B. A. Huber leg.; LABRE-Ar 556 • 2 ♀♀, 8 juvs, in pure ethanol; same data as preceding; LABRE-Ar564 • 3 ♂♂, 2 ♀♀ (one male used for µ-CT study); ~10 km N Belén; 27.5641° S, 67.0058° W; 1380 m a.s.l.; in pile of stones; 25 Mar. 2019; B. A. Huber and M. A. Izquierdo leg.; ZFMK Ar 23905 • 5 ♀♀, 1 juv., in pure ethanol; same data as preceding; ZFMK Arg213 • 1 ♂, 7 ♀♀, 1 juv., in pure ethanol; same data as preceding; LABRE-Ar 545 • 11 ♂♂, 2 ♀♀ (three males and one female used for µ-CT

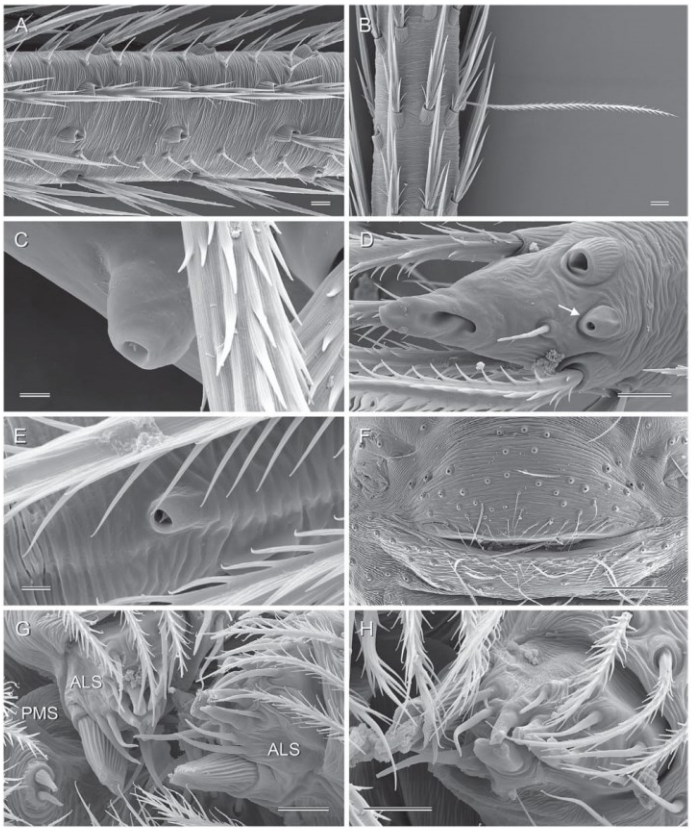

Figure 30. *Nerudia ola* sp. nov.; male and female from Argentina, San Juan, San Agustín de Valle Fértil (ZFMK Arg141). A, male right tibia 1, retrolateral view. B, male metatarsus 4 with trichobothrium. C, male palpal tarsal organ. D, tip of right female palp, dorsal view; arrow points at tarsal organ. E, tarsal organ on male tarsus 2. F, epigynum, ventral view. G, male ALS and PMS. H, female ALS. Scale lines: 10 µm (A, B, D, G, H), 2 µm (C, E), 100 µm (F).

study; two male abdomens used for karyotype study); near Nacimientos; 27.1559° S, 66.6925° W; 2120 m a.s.l.; under rocks on arid slope; 25 Mar. 2019; B. A. Huber and M. A. Izquierdo leg.; ZFMK Ar 23906 • 4 ♀♀, 3 juvs, in pure ethanol; same data as preceding; ZFMK Arg211.

Assigned tentatively (only females available): ARGENTINA – **La Rioja**: • 2 ♀♀, 1 juv.; Cuesta de Miranda; 29°21' S, 67°43' W; 1700 m a.s.l.; Aug. 1994; M. Ramírez leg.; MACN Ar 20055 • 1 ♀, in pure ethanol; SE Aimogasta, 'site 1'; 28.8069° S, 66.6635° W; 915 m a.s.l.; under rocks; 10 Mar. 2019; B. A. Huber and M. A. Izquierdo leg.; ZFMK Arg161. **Catamarca**: • 1 ♀; ~14 km W Fiambalá; 27.6590° S, 67.7607° W; 2000 m a.s.l.; under rocks; 26 Mar. 2019; B. A. Huber and M. A. Izquierdo leg.; ZFMK Ar 23907 • 2 ♀♀; Chumbicha; 28.87° S, 66.23° W; 400 m a.s.l.; Aug. 1994; M.J. Ramírez leg.; MACN Ar 20012. **San Juan**: • 1 ♀; ~35 km W Las Flores; 30.3967° S, 69.5576° W; 2910 m a.s.l.; under rocks; 6 Mar. 2019; B. A. Huber and M. A. Izquierdo leg.; ZFMK Ar 23908.

Etymology: The species epithet *ola* (Spanish for 'wave') is taken from Pablo Neruda's poem 'Poema 12'; noun in apposition.

Description

Male (holotype). Measurements: Total body length 1.55, carapace width 0.66. Distance PME–PME 70 µm; diameter PME 65 µm; distance PME–ALE 30 µm; distance AME–AME 20 µm; diameter AME 40 µm. Leg 1: 5.64 (1.48 + 0.25 + 1.45 + 1.78 + 0.68), tibia 2: 1.18, tibia 3: 1.03, tibia 4: 1.53; tibia 1 L/d: 22.

Colour (in ethanol): Prosoma and legs mostly pale ochre-yellow; carapace with light brown Y-mark behind ocular area; sternum whitish; legs without dark rings; abdomen monochromous pale grey.

Body: Habitus as in Figure 1G. Ocular area barely raised. Carapace with indistinct thoracic groove. Clypeus unmodified (only rim slightly more sclerotized than in female). Sternum wider than long (0.46/0.38), with pair of distinct anterior processes near coxae 1. Abdomen globular.

Chelicerae: As in Figure 27G, H; with distinctive pair of long frontal apophyses, tips slightly bent downwards, obtuse in frontal view, with some ventral hairs directed downwards (Fig. 29F); distance between tips of apophyses: 280 µm; stridulatory files on distinct lateral protrusions (Fig. 29C).

Palps: In general, similar to *N. colina* (cf. Fig. 4) but femur slightly slenderer (length/width 2.27) and tibia slightly thicker (length/width 0.92); procursus simple, in lateral view slightly directed towards dorsal, with bifid tip consisting of slender dorsal process and wider ventral membranous process (Fig. 27A–C); genital bulb similar to *N. colina*, with slender ventral apophysis curved towards ventral (Fig. 27D–F).

Legs: Without spines and curved hairs; with vertical hairs in higher than usual density on proximal half of tibia 1 only, in two dorsal rows (Fig. 30A); retrolateral trichobothrium of tibia 1 at 58%; prolateral trichobothrium absent on tibia 1; tarsus 1 with six to seven pseudosegments, distally distinct.

Variation (male): Tibia 1 in 36 males (including holotype): 1.04–1.60 (mean 1.33). The distance between the tips of the cheliceral apophyses varies considerably (235–340 µm), but also within localities (e.g. Nacimientos: 240–310 µm). In northern specimens (from La Rioja and Catamarca), the cheliceral apophyses are slightly straighter and longer. This difference is minimal and some males appear intermediate. In specimens from Chumbicha, the procursus is slightly shorter. Abdomen variably dark. *COI* data indicate a deep split between northern and southern specimens, and a phylogenetic analysis of the molecular data (Supporting Information, Fig. S2) even questions the monophyly of the northern + southern clade. However, deep splits also occur among southern specimens and among northern specimens (Fig. 2). As a result, a preliminary ASAP analysis (Supporting Information, Figs S3, S4) favours the existence of up to seven 'species' (lowest scores of 2.0 and 3.0). What is here interpreted as one species may thus in fact be several more or less cryptic species.

Female: In general, similar to male but sternum without pair of anterior humps and tibia 1 with usual low number of short vertical hairs. Tibia 1 in 57 females: 0.97–1.55 (mean 1.25). Epigynum (Figs 28A, 30F) anterior plate weakly protruding, without posterior indentation; posterior plate large, simple. Internal genitalia (Figs 27I, 28B–D) simple, with barely visible transparent receptacle. No difference could be seen between northern and southern specimens.

Distribution: Widely distributed in Argentina, Provinces San Juan, La Rioja and Catamarca (Fig. 3). Note that specimens from La Rioja and Catamarca are assigned tentatively.

Natural history: All specimens were found by turning rocks. The spiders started to run rapidly when disturbed but then stopped suddenly and did barely ever drop from the rock. They were found in a variety of habitats, ranging from a relatively humid block field in a low forest at 640 m a.s.l. near Chumbicha to an exposed arid hill with dry ravines at 2120 m a.s.l. near Nacimientos. At Valle Fértil, the spiders seemed to have a patchy distribution, with up to eight adult specimens on a single large rock in suitable places (with some shade and leaf litter among the rocks). They shared the microhabitat with a superficially similar species of *Metagonia* Simon, 1893 (*M.* 'MACN79'; undescribed; Valle Fértil; Chumbicha), with *Gertschiola macrostyla* (Astica; Valle Fértil; Ischigualasto; SE Aimogasta 'site 2'), with *Chibchea araona* Huber, 2000 (?) (Cuesta de Miranda, both sites) and, in at least one case, with another species of *Nerudia* (*N. poma*; Chumbicha).

NERUDIA NONO HUBER SP. NOV.

(FIGS 1H, 31, 32)

Zoobank registration: urn:lsid:zoobank.org:act:D31A81F7-8F7F-4DCA-BE7E-6EEAFFE52FBF.

Diagnosis: Distinguished from known congeners by shapes of procursus (Fig. 31A–C; wide in lateral view, narrow in dorsal view, with small prolateral flap distally) and by armature of male chelicerae (Fig. 31G, H; frontal apophyses directed towards frontal, with pointed tips), from some congeners also by bulbal processes (Fig. 31D–F; ventral apophysis

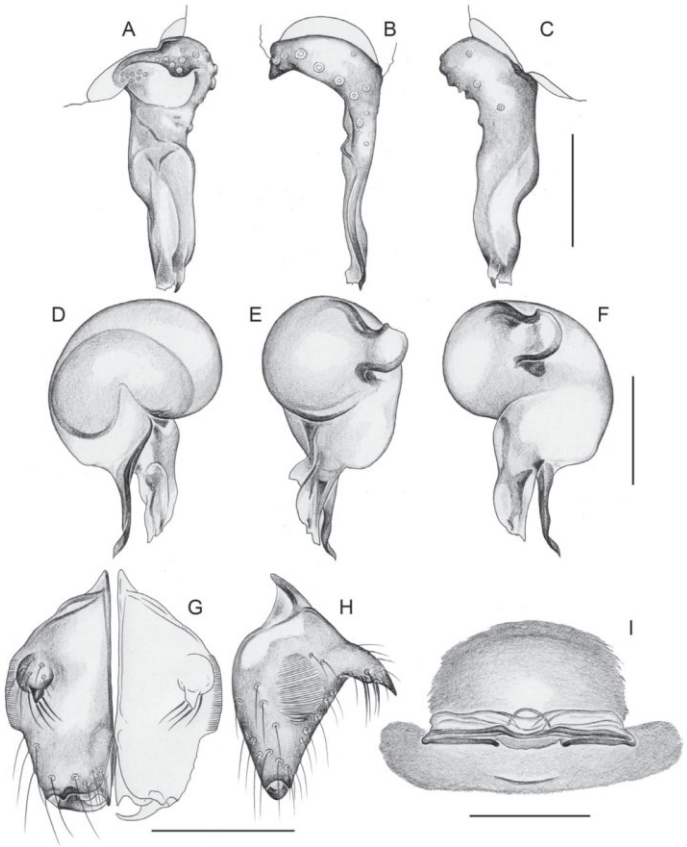

Figure 31. *Nerudia nono* sp. nov.; paratypes from Argentina, Córdoba, 5 km E Nono (♂ LABRE AR525; ♀ ZFMK Ar 23910). A–C, left male palpal tarsus and procursus, prolateral, dorsal, and retrolateral views. D–F, left male genital bulb, prolateral, dorsal, and retrolateral views. G, H, male chelicerae, frontal and lateral views. I, cleared female genitalia, dorsal view. Scale lines: 0.2 mm.

distally slender, curved towards ventral, slightly longer than embolus), and by epigynum and female internal genitalia (Figs 31I, 32; main epigynal plate semi-circular, with almost straight posterior margin; internal genitalia with indistinct semi-circular receptacle).

Type material: ARGENTINA – **Córdoba**: • ♂ holotype; ~5 km E Nono; 31.7982° S, 64.9515° W; 995 m a.s.l.; 20 Feb. 2021; M. Izquierdo, F. Cargnelutti, F. Bollatti & G. Boaglio leg.; *LABRE-Ar 592* • 3 ♂♂, paratypes; same data as holotype; LABRE AR525 • 1 ♂, paratype; same data as holotype; ZFMK Ar 23909 • 1 ♀, paratype; same data as holotype; LABRE AR534 • 3 ♀♀, paratypes; same locality as holotype; 2 Mar 2019; B.A. Huber & M.A. Izquierdo leg.; ZFMK Ar 23910.

Other material examined: ARGENTINA – **Córdoba**: • 5 ♀♀, 7 juvs, in pure ethanol; same locality as holotype; 2 Mar 2019; B.A. Huber & M.A. Izquierdo leg.; ZFMK Arg124 • 1 ♂, 1 ♀; same locality as holotype; 5 Jan. 2022; M. Izquierdo, F. Cargnelutti, G. Boaglio leg.;

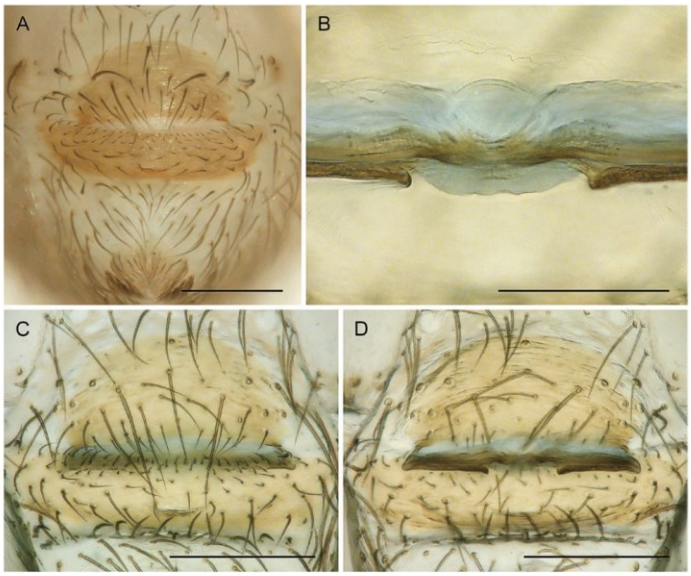

Figure 32. *Nerudia nono* sp. nov.; paratype female from Argentina, Córdoba, 5 km E Nono (ZFMK Ar 23910). A, abdomen and epigynum, ventral view. B, median structures in internal genitalia. C, D, cleared genitalia, ventral and dorsal views. Scale lines: 0.2 mm (A, C, D), 0.1 mm (B).

LABRE-Ar 593 • 6 ♀♀; same data as preceding; LABRE-Ar 595 • 2 ♂♂, 1 ♀, 1 juv.; same locality as holotype; 20 Feb. 2021; M. Izquierdo, F. Cargnelutti, F. Bollatti, G. Boaglio, leg.; LABRE-Ar 594 • 2 ♂♂, in Karnovsky (MAI-4780); same data as preceding, LABRE-Ar 568 • 1 ♂, in Karnovsky (MAI-4771); same data as preceding; LABRE-Ar 569 • 6 ♀♀, in Karnovsky (MAI-4781); same data as preceding; LABRE-Ar 570.

Etymology: The species epithet is derived from the type locality Nono in Córdoba, Argentina; noun in apposition.

Description

Male (holotype. Measurements: Total body length 1.70, carapace width 0.70. Distance PME-PME 90 µm; diameter PME 60 µm; distance PME–ALE 35 µm; distance AME–AME 20 µm; diameter AME 50 µm. Leg 1: 5.20 (1.40 + 0.25 + 1.40 + 1.55 + 0.60), tibia 2: 1.15, tibia 3: 0.95, tibia 4: 1.40; tibia 1 L/d: 20.

Colour (in ethanol): Prosoma and legs mostly pale ochre-grey; carapace with large median brown mark including ocular area, not reaching posterior margin of carapace; sternum whitish; legs without dark rings; abdomen monochromous greenish-grey.

Body: Habitus as in Figure 1H. Ocular area barely raised. Carapace with indistinct thoracic groove. Clypeus more sclerotized than in female and slightly bulging. Sternum wider than long (0.50/0.40), with pair of distinct anterior processes near coxae 1. Abdomen globular.

Chelicerae: As in Figure 31G, H; pair of frontal apophyses directed forward, with flattened tips; stridulatory files on pair of lateral protrusions, ridges barely visible in dissecting microscope.

Palps: In general, similar to *N. colina* (cf. Fig. 4); coxa unmodified; trochanter with indistinct ventral projection; femur cylindrical, only slightly widened distally, proximally with indistinct retrolateral hump and prolateral stridulatory pick (modified hair); patella short, dorsally more bulging than in *N. colina*; tibia globular; procursus wide in lateral view, narrow in dorsal view, distally with small apophysis and

prolateral flap (Fig. 31A–C); genital bulb with ventral apophysis distally slender, curved towards ventral, embolus partly membranous (Fig. 31D–F).

Legs: Without spines and curved hairs; few vertical hairs; retrolateral trichobothrium of tibia 1 at 59%; prolateral trichobothrium absent on tibia 1; tarsus 1 with seven to eight pseudosegments, mostly distinct.

Variation (male): Tibia 1 in five males (including holotype): 1.35–1.40 (mean 1.37).

Female: In general, similar to male but sternum without pair of anterior humps, chelicerae apparently without stridulatory ridges, and clypeus unmodified. Tibia 1 in nine females: 1.30–1.45 (mean 1.36). Epigynum (Fig. 32A) anterior plate weakly protruding, semi-circular, with almost straight posterior margin; posterior plate large, simple. Internal genitalia (Figs 31I, 32B–D) with indistinct semi-circular receptacle.

Distribution: Known from type locality only, near Nono in Córdoba, Argentina (Fig. 3).

Natural history: The spiders were found among the stones of a loosely built stone wall in the plain sun in a relatively arid environment (Fig. 45F). In small containers in laboratory conditions, the spiders built flimsy webs. Like other pholcids, they hang upside down in these webs. Copulation attempts were not successful. In one of them (25 Feb. 2021), the female attacked the male and started to wrap him.

NERUDIA ATACAMA HUBER, 2000

(FIGS 33, 34)

Nerudia atacama Huber, 2000: 87, figs 333–337.
Nerudia atacama – Torres *et al.*, 2015: 5, fig. 4C, D (see *N. poma*; misidentification).

Diagnosis: Distinguished from known congeners by shape of procursus (Fig. 33A–C; distal half bent towards dorsal; same width over most of its length in lateral view), by bulbal processes (Fig. 33D–F; embolus slender tubular), by armature of male chelicerae (Fig. 33G, H; frontal apophyses at half length, pointing downwards, with pointed tip in frontal view, set with regular hairs; similar to *N. flecha*), and by epigynum and female internal genitalia (Fig. 34; epigynal plate with large posterior indentation, similar to *N. flecha*; internal genitalia with large round median 'receptacle').

Type material: CHILE – **Atacama**: • ♂ holotype, re-examined; S of Domeyko, Cuesta Pajonales; 29.151° S, 70.980° W; 1200 m a.s.l.; 5 Oct. 1992; N. I. Platnick, P. Goloboff, K. Catley leg.; AMNH • 3 ♀♀ paratypes, re-examined; same data as holotype; AMNH.

Other material (not re-examined): CHILE – **Atacama**: • 1 ♀; Cuesta Pajonales, S of Domeyko; 29.146° S, 70.997° W; 1080 m a.s.l.; 5 Oct. 1992; N. I. Platnick, P. Goloboff, K. Catley leg.; AMNH.

Description (amendments; see Huber 2000*):* The distinctive male and female structures are shown (Figs 33, 34) in order to facilitate comparison with the newly described congeners.

Distribution: Known only from the type locality in Atacama, Chile (Fig. 3).

NERUDIA FLECHA HUBER **SP. NOV.**

(FIGS 35, 36)

Zoobank registration: urn:lsid:zoobank.org:act:2A718011-CA44-43E3-8053-166B6AF843DF.

Diagnosis: Easily distinguished from known congeners by shape of procursus (Fig. 35A–C; short distal element with hooked tip, without membranous part) and by bulbal processes (Fig. 35D–F; embolus much shorter than ventral apophysis); also by armature of male chelicerae (Fig. 35G, H; frontal apophyses pointing downwards, with slightly widened flat tip, set with regular hairs), and by epigynum and female internal genitalia (Figs 35I, 36; epigynal plate with large posterior indentation; internal genitalia apparently without or with small median 'receptacle').

Type material: CHILE – **Coquimbo**: • ♂ holotype, 1 ♀ paratype; road to Pascua Lama Mine; approximately 29.445° S, 70.502° W, +/– 6 km; 3000–3280 m a.s.l.; 3 Feb. 2014; A. A. Ojanguren-Affilastro, J. Pizarro-Araya, P. Agusto, R. Botero Trujillo and H. Iuri leg.; *MACN Ar 37782*.

Etymology: The species epithet *flecha* (Spanish for 'arrow') is taken from Pablo Neruda's poem 'Poema 1'; noun in apposition.

Description

Male (holotype). Measurements: Total body length 1.50, carapace width 0.62. Distance PME–PME 80 µm; diameter PME 50 µm; distance PME–ALE 20 µm; distance AME–AME 20 µm; diameter AME 35 µm. Leg 1: 4.57 (1.30 + 0.20 + 1.30 + 1.30 + 0.47), tibia 2: 1.07, tibia 3: 0.90, tibia 4: 1.27; tibia 1 L/d: 19.

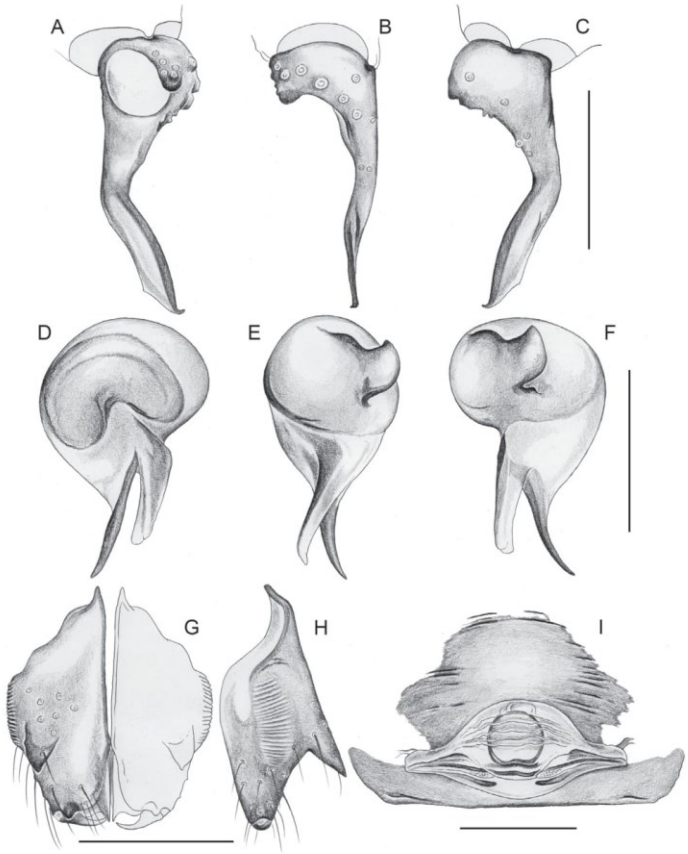

Figure 33. *Nerudia atacama*; holotype male and paratype female from Chile, Atacama, S of Domeyko (AMNH). A–C, left male palpal tarsus and procursus, prolateral, dorsal and retrolateral views. D–F, left male genital bulb, prolateral, dorsal, and retrolateral views. G, H, male chelicerae, frontal and lateral views. I, cleared female genitalia, dorsal view. Scale lines: 0.2 mm.

Colour (in ethanol): Prosoma and legs mostly pale ochre-yellow; carapace with light brown Y-mark behind ocular area; legs without dark rings; abdomen monochromous pale-grey.

Body: Habitus similar to *N. poma* (cf. Fig. 1B). Ocular area barely raised. Carapace with indistinct thoracic groove. Clypeus unmodified (only rim slightly more sclerotized than in female). Sternum wider than long (0.44/0.40), with pair of small anterior processes near coxae 1. Abdomen globular.

Chelicerae: As in Figure 35G, H; short frontal apophyses set with regular hairs, tips slightly flattened; stridulatory files on low lateral protrusions.

Palps: In general, similar to *N. colina* (cf. Fig. 4) but femur absolutely and relatively shorter (length/width 1.76) and tibia slightly less strongly enlarged (length/width 1.13); procursus simple, in lateral view slightly bent towards dorsal, distal part short, with distinctive hooked tip, without membranous element (Fig. 35A–C); genital bulb with weakly curved ventral apophysis

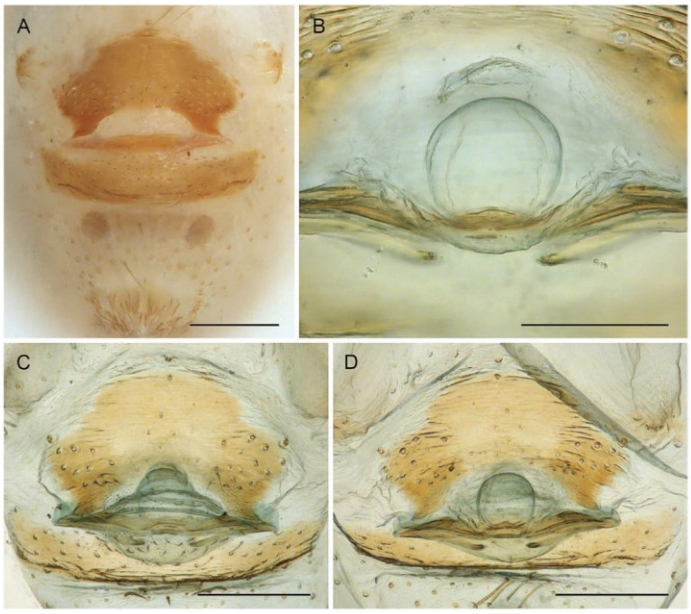

Figure 34. *Nerudia atacama*; paratype female from Chile, Atacama, S of Domeyko (AMNH). A, abdomen and epigynum, ventral view. B, median structures in internal genitalia. C, D, cleared genitalia, ventral and dorsal views. Scale lines: 0.2 mm (A, C, D), 0.1 mm (B).

distally semi-transparent, embolus much shorter than ventral apophysis (Fig. 35D–F).

Legs: Without spines and curved hairs; with vertical hairs in higher than usual density on tibia 1 only, in two dorsal rows (prolateral and retrolateral); retrolateral trichobothrium of tibia 1 at 64%; prolateral trichobothrium absent on tibia 1; tarsus 1 with ~seven pseudosegments, only distally distinct.

Female: In general, similar to male but sternum without humps and tibia 1 with usual low number of short vertical hairs. Tibia 1: 1.22; carapace width: 0.68. Epigynum (Fig. 36A) anterior plate semi-circular to trapezoidal, with large posterior indentation; posterior plate short but wide. Internal genitalia (Figs 35I, 36B–D) simple, apparently without or with small median 'receptacle'.

Distribution: Known only from type locality in Coquimbo, Chile (Fig. 3).

PUTATIVE FURTHER SPECIES

NERUDIA SP. 'ARG23A'

Three species were collected in San Juan, ~35 km W Las Flores: *N. rocio*, *N. ola* and nine females representing a third species. These females clearly differ from the two named species at this locality by the shape of the epigynum (Fig. 37A; resembles *N. flecha*); from *N. rocio* also distinguished by much shorter legs (tibia 1 length in seven females: 1.10–1.30; mean 1.21).

Material examined. ARGENTINA – **San Juan**: • 3 ♀♀; ~35 km W Las Flores; 30.3967° S, 69.5576° W; 2910 m a.s.l.; 6 Mar. 2019; B. A. Huber and M. A. Izquierdo leg.; ZFMK Ar 23911 • 5 ♀♀, in pure ethanol (two prosomata used for molecular study); same data as preceding; ZFMK Arg147; 1 ♀, with egg-sac, in pure ethanol; same data as preceding; LABRE-Ar 562.

NERUDIA SP. 'ARG163'

Two species were collected in La Rioja, SE Aimogasta: *N. ola*, and a single female specimen representing a

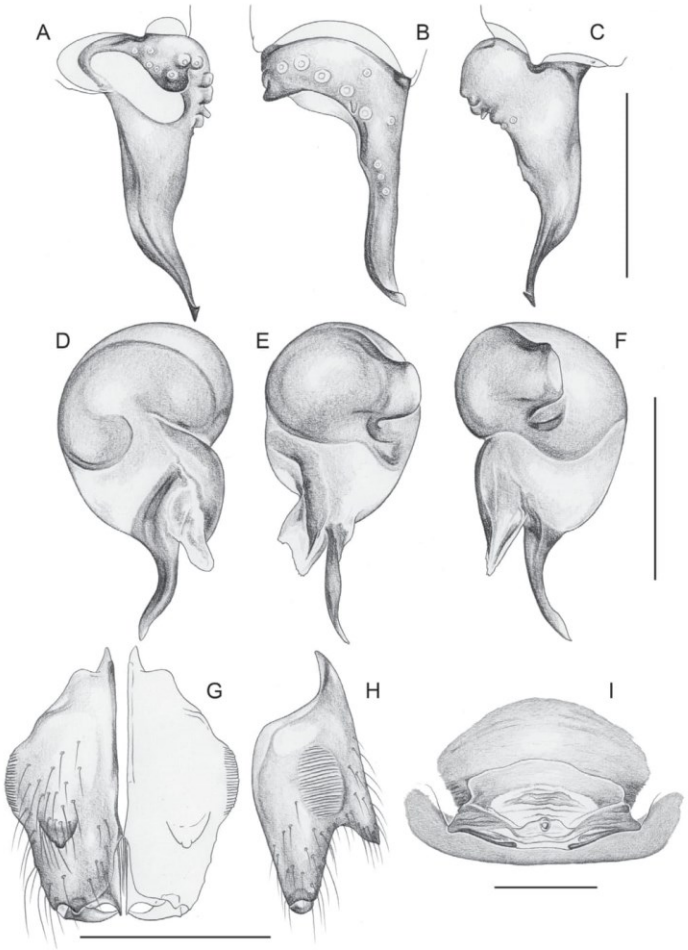

Figure 35. *Nerudia flecha* sp. nov.; holotype male and paratype female from Chile, Coquimbo, road to Pascua Lama Mine (MACN Ar 37782). A–C, left male palpal tarsus and procursus, prolateral, dorsal and retrolateral views. D–F, left male genital bulb, prolateral, dorsal and retrolateral views. G, H, male chelicerae, frontal and lateral views. I, cleared female genitalia, dorsal view. Scale lines: 0.2 mm.

different species. This female resembles *N. rocio* in having indistinct radial marks on the carapace and in having unusually long legs (tibia 1: 2.1). However, the epigynum is different (Fig. 37B) and resembles that of *N. hoguera* (and *N. flecha*). The molecular data also suggest that this specimen is closer to *N. hoguera* than to any other sequenced species (Fig. 2; Supporting Information, Fig. S4).

Material examined. ARGENTINA – **La Rioja**: • 1 ♀, in pure ethanol; SE Aimogasta, 'site 2'; 28.9015° S, 66.6538° W; 755 m a.s.l.; under rocks; 10 Mar.

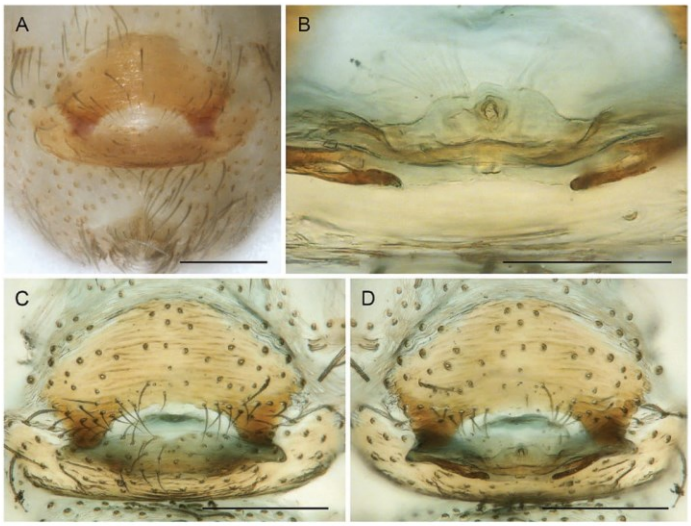

Figure 36. *Nerudia flecha* sp. nov.; paratype female from Chile, Coquimbo, road to Pascua Lama Mine (MACN Ar 37782). A, abdomen and epigynum, ventral view. B, median structures in internal genitalia. C, D, cleared genitalia, ventral and dorsal views. Scale lines: 0.2 mm (A, C, D), 0.1 mm (B).

2019; B. A. Huber and M. A. Izquierdo leg.; ZFMK Arg163.

KARYOLOGY

The male karyotype of *Nerudia ola* is composed of 24 chromosomes. It is predominated by biarmed chromosomes (Fig. 38A). The prophase of the first meiotic division includes the diffuse stage. During this period, the bivalents almost decondense. In contrast to this, sex chromosomes form a highly condensed, cross-shaped element (Fig. 38B). A diffuse stage is also found in *N. poma* and *Gertschiola macrostyla*. The metaphase of the first meiotic division (metaphase I) consists of ten bivalents and a tetravalent formed by three X chromosomes and a Y chromosome (Fig. 38C, D). Within the tetravalent, each of the X chromosomes is associated by one end with the Y chromosome (Fig. 38C). The average size of the Y chromosome (8.3 µm, $N = 3$, metaphases I) is similar to the size of the X chromosomes. There are two types of metaphases of the second meiotic division (metaphase II), one with 11 chromosomes, including the Y chromosome, and the other with 13 chromosomes, including the X chromosomes (Fig. 38E, F). It was impossible to distinguish the sex chromosomes from the other chromosomes on the basis of their morphology or behaviour during metaphase II (Fig. 38E, F). One (Fig. 39B, C) or two chromosome pairs (Fig. 39A) contain a NOR. One sex chromosome also included a NOR (Fig. 39C), at the end involved in chromosome pairing (Fig. 39B).

The male karyotype of *Nerudia poma* consists of 26 chromosomes (Fig. 40A). Metaphases I contain one bivalent more than in *N. ola* (Fig. 40B, C). The structure of the sex chromosome tetravalent is the same as in *N. ola* (Fig. 40B, C) except for the smaller size of the Y chromosome (5.1 µm, $N = 2$, metaphases I). There are two types of metaphases II, one with 12 chromosomes, including the tiny Y chromosome, and another with 14 chromosomes, including the three X chromosomes (Fig. 40D–F). It was impossible to distinguish the X chromosomes from the other chromosomes at metaphase II (Fig. 40D, F). Metaphase II with X chromosomes is formed exclusively by biarmed chromosomes (Fig. 41), which implies that all chromosome pairs and the X chromosomes are biarmed. The Y chromosome is the smallest element of metaphase II (Fig. 40E). Its morphology is unknown.

The male karyotype of *Gertschiola macrostyla* is predominated by biarmed chromosomes (Fig. 42D). Metaphases I contain 12 bivalents and a sex chromosome tetravalent $X_1X_2X_3Y$. The X chromosomes are

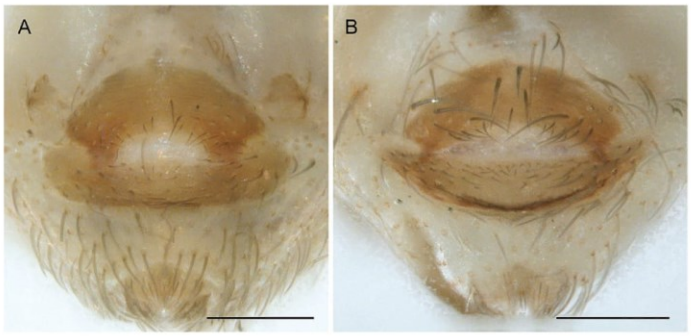

Figure 37. Epigyna of two formally undescribed putative species, ventral views. A, *Nerudia* 'Arg23a' from Argentina, San Juan, 35 km W Las Flores (ZFMK Ar 23911). B, *N.* 'Arg163' from Argentina, La Rioja, SE Aimogasta, 'site 2' (ZFMK Arg163). Scale lines: 0.2 mm.

associated by the ends of both of their arms with the tiny Y chromosome, which is much smaller than in *Nerudia* (Fig. 42A–C). The average size of the Y chromosome is only 1.6 µm (N = 2, metaphases I). One chromosome pair contains a NOR. Moreover, one X chromosome has a terminal NOR (Fig. 39D).

Sampling bias and biogeographic analyses

The areas with high densities of records of arthropods and arachnids are poorly correlated (r = 0.391, P < 0.000). In the wider area (~500 km) around the known geographic distribution of *Nerudia*, six localities stand out for their high density of records of arthropods, near the cities of Santiago, La Serena and Copiapó in Chile, and Córdoba, Cafayate and Salta in Argentina (Supporting Information, Fig. S5). For arachnids, only the cities of Santiago, Cafayate and Córdoba present a similar pattern, while an extra area with high density of records of Arachnida is observed near Tilcara, in northern Argentina (Fig. 43A). Meanwhile, the records of *Nerudia* are mostly located in poorly sampled regions (Fig. 43A), and they are not explained by the number of records of arthropods (deviance = 1.513, P = 0.2187) or by the interaction between the numbers of records of arthropods and arachnids (deviance = 2.577, P = 0.1084). However, records of *Nerudia* are significantly explained by the number of records of arachnids (deviance = 5.447, P = 0.019; Supporting Information, Fig. S6).

The species distribution modelling was based on seven principal components (PC) of the 21 predictor bioclimatic variables, which gathered 95.3% of the cumulative proportion of variance (for details, see Supporting Information, Tables S1, S2). The first PC contributed with 43% to the *Nerudia* distribution modelling (Fig. 43B; Supporting Information, Table S3), while, the second PC contributed with 33.6% (see Table S3). Most of the areas with higher relative occurrence rates for *Nerudia* (Fig. 43B) are in the northern part of the Monte biogeographic province (*sensu* Morrone, 2017) (where most *Nerudia* records are known) and in the Atacama province in Chile and the Puna province in Bolivia (where no *Nerudia* or any other Ninetinae have ever been recorded).

The second principal component analysis carried out based on the extracted values for the 21 predictor bioclimatic variables for each of the Ninetinae records (Supporting Information, Table S6), resulted in eight principal components that gather 96.0% of the cumulative proportion of variance (Supporting Information, Table S4). The first PC represented 47.7% of the proportion of variance, being positively correlated with temperature seasonality and temperature annual range, but negatively correlated with annual mean temperature, minimum temperature of coldest month and mean temperature of coldest quarter (Supporting Information, Table S5; Fig. S7). The second PC represented 19.4% of the proportion of variance, being positively correlated with the annual precipitation and the precipitation of the driest month, of the driest quarter and of the coldest quarter, but negatively correlated with precipitation seasonality (Supporting Information, Table S5). The ordination of the *Nerudia* records in the multivariate space (Fig. 44; Supporting Information, Fig. S7) indicates that this taxon is likely limited by extreme cold conditions and humid environments. Representatives of *Nerudia* occupy regions

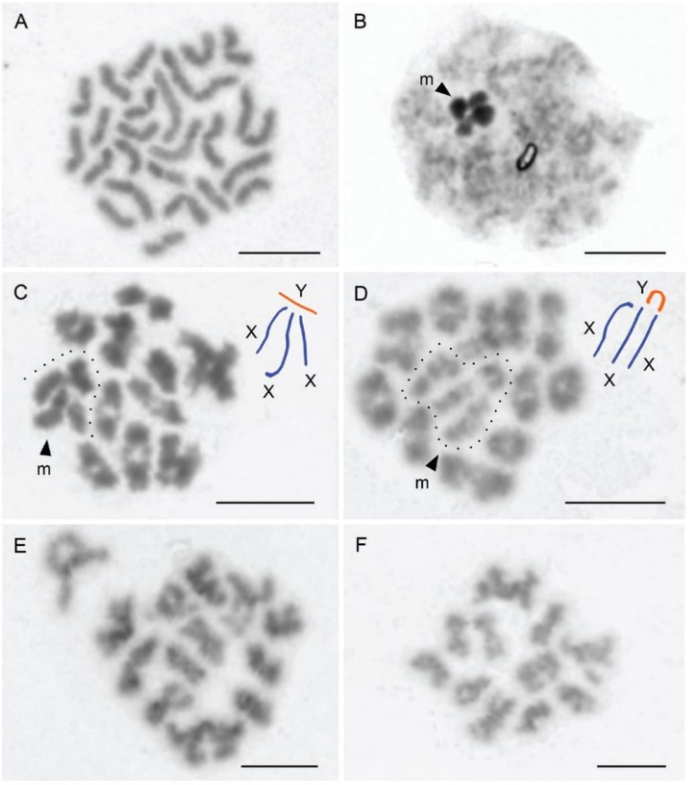

Figure 38. *Nerudia ola* sp. nov.; male chromosome plates. Panels C, D contain a scheme of the sex chromosome multivalent (blue – X chromosomes, orange – Y chromosome). A, mitotic metaphase, $2n = 24$. Note the predomination of biarmed chromosomes. B, diffuse stage. Note the cross-shaped multivalent consisting of four sex chromosomes. The multivalent exhibits positive heteropycnosis. C, D, metaphases I consisting of ten bivalents and a sex chromosome multivalent comprising three X chromosomes and a Y chromosome. Multivalent delimited by dotted line. One X chromosome is not included in the multivalent at D. E, early metaphase II containing the X chromosomes ($n = 13$). It is impossible to distinguish the X chromosomes from other chromosomes. F, early metaphase II containing the Y chromosome ($n = 11$). It is impossible to distinguish the Y chromosome from other chromosomes. Abbreviations: m, sex chromosome multivalent; X, X chromosome; Y, Y chromosome. Scale lines: 10 µm.

with lower tree density and lower tree canopy height (Supporting Information, Fig. S7), suggesting an association with open environments. However, such biotic and climatic conditions are not significantly different from those observed for most other Ninetinae; the *Nerudia* records are within the confidence interval for other taxa (Fig. 44). The environmental niche is phylogenetically conserved in the group, thus evolving as expected owing to Brownian motion (Pagel's $\lambda = 0.95$, P-value = 0.000, for the first PC axis; full results in Supporting Information, Fig. S8, Table S9).

DISCUSSION

KARYOLOGY

Only two representatives of Ninetinae have been karyotyped before, *Kambiwa neotropica* (Kraus, 1957) and *Pholcophora americana* Banks, 1896 (Ávila Herrera

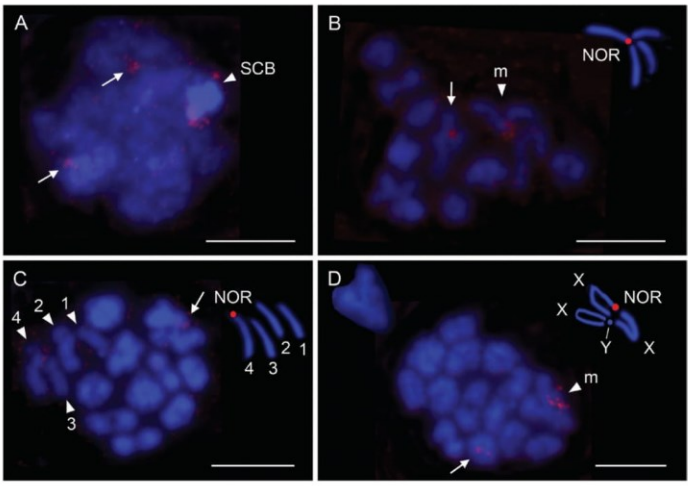

Figure 39. *Nerudia ola* sp. nov. (A–C) and *Gertschiola macrostyla* (D); male meiosis, detection of nucleolus organizer regions (NORs; red signals). Chromosomes counterstained with DAPI (blue). Panels B–D contain schemes of the sex chromosome multivalents. A, diffuse stage. Sex chromosome body and two decondensed bivalents exhibit a signal. B, metaphase I, one bivalent includes a NOR. Another NOR is at the end of a sex chromosome involved in pairing. C, metaphase I, sex chromosome multivalent collapsed. One bivalent and one end of a sex chromosome bear a NOR. D, metaphase I. One bivalent and one end of an X chromosome contains a NOR. Note the sex chromosome multivalent in the upper left corner of the panel. Symbols: arrow, NOR-bearing bivalent; arrowhead, sex chromosome body (A), sex chromosome multivalent (B, D) or particular sex chromosomes (C, numbered). Abbreviations: m, sex chromosome multivalent; SCB, sex chromosome body; X, X chromosome; Y, Y chromosome. Scale lines: 10 µm.

et al., 2021). In this study, we added three further species and two genera, namely *Nerudia poma*, *N. ola* and *Gertschiola macrostyla*. Closely related pholcids often differ in the morphology of some chromosomes (Ávila Herrera *et al.*, 2021). Unfortunately, we were only able to determine the morphology of the chromosomes for *Nerudia poma* (except for the Y chromosome). As in the vast majority of other haplogyne araneomorphs with monocentric chromosomes (Král *et al.*, 2006), karyotypes of ninetines are predominated by biarmed chromosomes (Ávila Herrera *et al.*, 2021; this study). The male prophase of the first meiotic division includes the so-called diffuse stage (Ávila Herrera *et al.*, 2021; this study), which is probably a synapomorphy of haplogyne spiders, i.e. the clade formed by Synspermiata and two cribellate families, Filistatidae and Hypochilidae (Ávila Herrera *et al.*, 2021).

Among Ninetinae, the karyotype of *P. americana* ($2n♂ = 29, X_1X_2Y$) is supposedly close to the ancestral karyotype of pholcids ($2n♂ = 33, X_1X_2Y$; Ávila Herrera *et al.*, 2021) in terms of diploid number and sex chromosome system. The X_1X_2Y system of *P. americana* includes two large metacentric X chromosomes and a metacentric Y microchromosome, which pair without chiasmata by the ends of their arms during male meiosis (Ávila Herrera *et al.*, 2021). This system has been found in seven haplogyne families (Silva, 1988; Silva *et al.*, 2002; Král *et al.*; 2006, 2019; Ávila Herrera *et al.*, 2016; Paula-Neto *et al.*, 2017; Araujo *et al.*, 2020), including some pholcid clades (Král *et al.*, 2006; Ávila Herrera *et al.*, 2021). It is probably the ancestral sex chromosome determination of araneomorph spiders, including haplogynes (Paula-Neto *et al.*, 2017; Ávila Herrera *et al.*, 2021).

In contrast to the North American *P. americana*, the karyotypes of the South American *K. neotropica* (Ávila Herrera *et al.*, 2021), *G. macrostyla* and *Nerudia* spp. (this study) contain fewer chromosome pairs. The latter three genera belong to the same clade, separate from *Pholcophora* (Huber *et al.*, 2018). Our data thus suggest that the ancestral karyotype of this South American clade was characterized by a reduction in the number of chromosome pairs. According to our data, the ancestral karyotype of the clade including

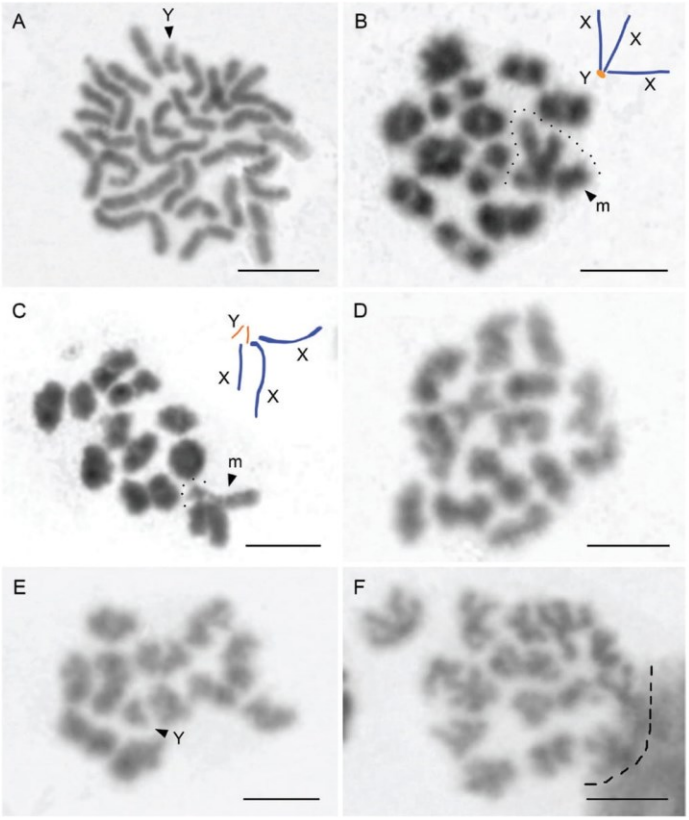

Figure 40. *Nerudia poma* sp. nov., male chromosome plates. Panels B, C contain a scheme of the sex chromosome multivalent (blue – X chromosomes, orange – Y chromosome). A, mitotic metaphase, $2n = 26$. Note the predomination of biarmed chromosomes. The Y chromosome is the smallest element of the complement. B, C, metaphases I consisting of 11 bivalents and a sex chromosome multivalent comprising three X chromosomes and a Y chromosome. Multivalent delimited by dotted line. D, metaphase II containing X chromosomes ($n = 14$). It is impossible to distinguish the X chromosomes from other chromosomes. E, early metaphase II containing the Y chromosome ($n = 12$). The Y chromosome is the smallest chromosome of the plate. F, late metaphase II containing the X chromosomes ($n = 14$). Note the predomination of biarmed chromosomes. This plate was used to construct the haploid karyotype of the species (Fig. 41). Abbreviations: m, sex chromosome multivalent; X, X chromosome; Y, Y chromosome. Scale lines: 10 µm.

Gertschiola, *Kambiwa* Huber, 2000 and *Nerudia* contained 12 chromosome pairs. This number is retained in *Gertschiola* (this study) and *Kambiwa* (Ávila Herrera *et al.*, 2021). A further reduction occurred in *Nerudia*, where this process can even be observed within the genus (this study). The reduction of chromosome numbers is a frequent phenomenon in the evolution of various spider groups (Suzuki, 1954; Kořínková & Král, 2013), including pholcids (Ávila Herrera *et al.*, 2021).

The karyotypes of *Kambiwa*, *Gertschiola* and *Nerudia* further differ from that of *Pholcophora* by the more complex sex chromosome systems (Ávila Herrera *et al.*, 2021; this study). *Gertschiola* and

Figure 41. *Nerudia poma* sp. nov., haploid karyotype (n = 14) based on metaphase II containing X chromosomes. It consists of nine metacentric (nos 1–8, 10) and five submetacentric chromosomes (nos 9, 11–14). It is impossible to distinguish X chromosomes on the basis of their morphology or behaviour. Scale line: 10 µm.

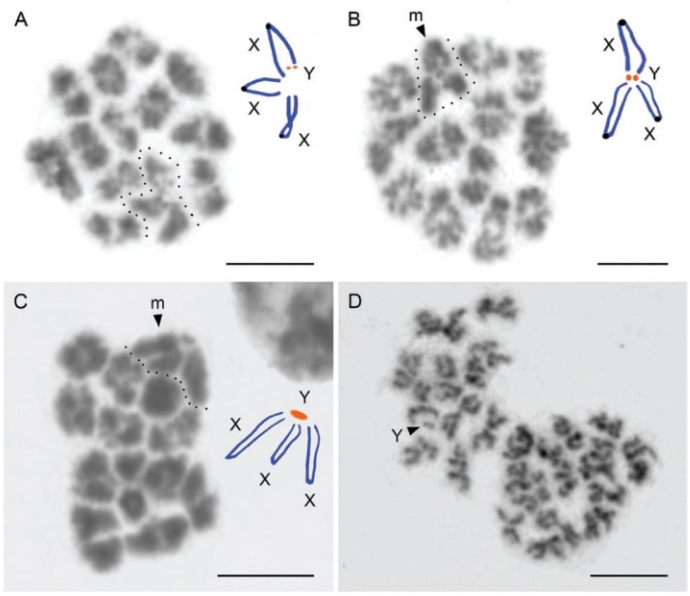

Figure 42. *Gertschiola macrostyla* sp. nov.; male chromosome plates. Panels A–C contain a scheme of the sex chromosome multivalent (blue – X chromosomes, orange – Y chromosome, black knob – supposed centromere). A–C, metaphases I consisting of 12 bivalents and a sex chromosome multivalent comprising three X chromosomes and a Y chromosome. Multivalent delimited by dotted line. D, plate composed of two sister metaphases II. Note the tiny Y chromosome. Abbreviations: m, sex chromosome multivalent; X, X chromosome; Y, Y chromosome. Scale lines: 10 µm.

Nerudia share the $X_1X_2X_3Y$ system (this study), which has not previously been reported for pholcids. We suppose that it evolved from the X_1X_2Y system, as has been hypothesized for many other sex chromosome systems previously described in pholcids (Ávila Herrera *et al.*, 2021). Chromosomes of the $X_1X_2X_3Y$ system retained achiasmatic pairing during male meiosis (this study). Furthermore, the mode of pairing of the X chromosomes in *Gertschiola* (see below) suggests that these elements retained their biarmed morphology. The third X chromosome of the $X_1X_2X_3Y$ system could arise by a nondisjunction of one of the X chromosomes, which is supposed to be the mechanism of formation of multiple X chromosomes in entelegyne araneomorphs (Postiglioni & Brum-Zorrilla, 1981; Datta & Chatterjee, 1988; Král, 2007).

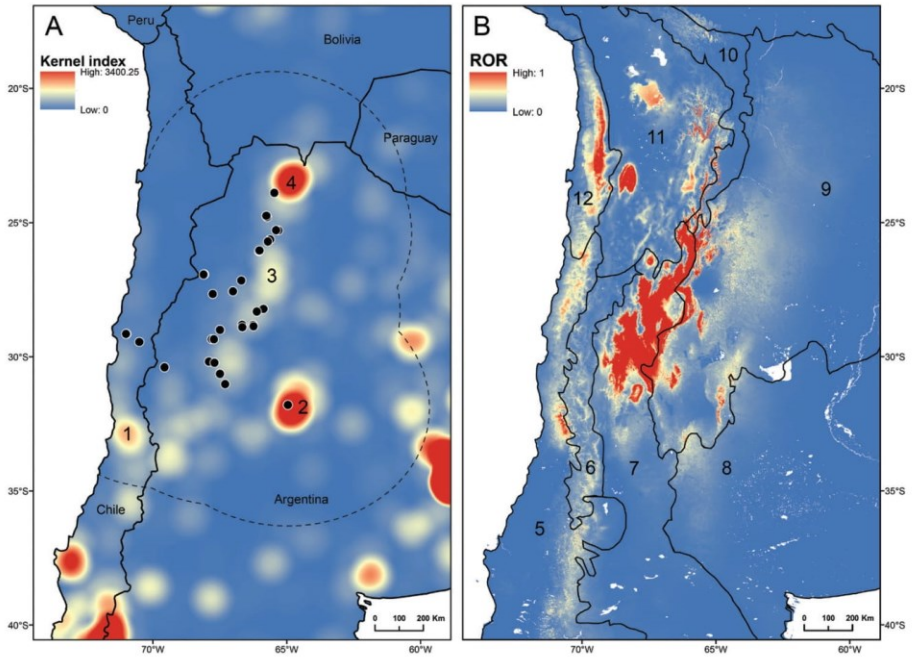

Figure 43. A, density of records of arachnids surrounding the geographic distribution of *Nerudia* representatives, with numbered high density regions (reddish areas: 1. Santiago; 2. Córdoba; 3. Cafayate; 4. Tilcara). Dotted line represents 500 km buffer around *Nerudia* records (black dots). Note that *Nerudia* records are concentrated in poorly sampled regions (bluish areas). B, relative occurrence rate (ROR) of *Nerudia* species, with numbered biogeographic regions. Polygons represent the biogeographical regionalisation (*sensu* Morrone, 2017) in the Andean (5) and Neotropical (6–12) regions. Neotropical provinces: (6) Prepuna; (7) Monte; (8) Pampean; (9) Chaco; (10) Yungas; (11) Puna; and (12) Atacama. The reddish areas denote regions where *Nerudia* is expected to occur; in some of these, no Ninetinae have ever been recorded: the Atacama province in Chile and the Puna province in Bolivia.

Alternatively, it could originate by a fission of one metacentric X chromosome of the X_1X_2Y system followed by a pericentric inversion of arising elements (to restore their biarmed morphology). The same complex rearrangement probably transformed the X_1X_20 system into $X_1X_2X_30$ in the pholcid *Smeringopus pallidus* (Blackwall, 1858) (Ávila Herrera *et al.*, 2021). Fissions have also been involved in sex chromosome evolution of some mygalomorph spiders (Král *et al.*, 2013). In *Gertschiola*, the X chromosomes still pair in meiosis by both ends and the Y chromosome retains its tiny size even after the formation of the $X_1X_2X_3Y$ system. The details of chromosome pairing in *Nerudia* remain unresolved. Each X chromosome can possibly associate by one of its ends with the Y chromosome as stated in the Results section. In another possible arrangement, each of the X chromosomes would have its arms closely aligned together and thus make the impression of pairing with the Y chromosome by one end. This is common in species with the X_1X_2Y system (Ávila Herrera *et al.*, 2021). *Nerudia* also exhibits an increase in the size of the Y chromosome. This usually results from incorporation of autosome material (e.g. Schartl *et al.*, 2016) or from expansion of heterochromatin (e.g. Kejnovský *et al.*, 2009). In *Nerudia ola*, the Y chromosome reaches the same size as the X chromosomes. The considerable extension of the Y chromosome in *Nerudia* has been

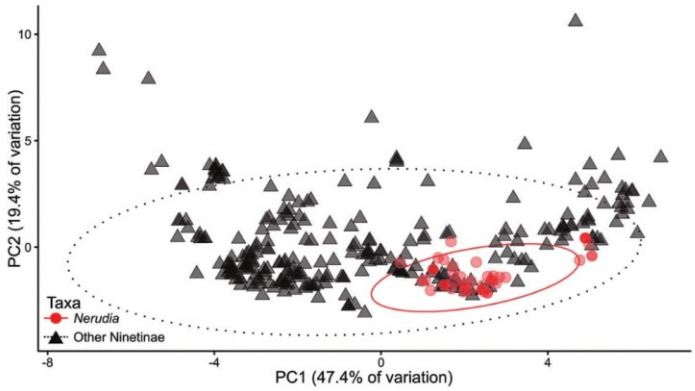

Figure 44. Principal component analysis of the environmental conditions for *Nerudia* representatives (red circles and ellipse) and other Ninetinae (black triangles and dotted line ellipse). The ellipses encompass the values within a 95% confidence interval of a multivariate t-distribution. Darker symbols result from superimposition. Note that the environmental conditions for *Nerudia* representatives are within the confidence interval for other ninetines, suggesting that the environmental niche of *Nerudia* is not significantly different from other Ninetinae taxa.

accompanied by a decrease in the number of chromosome pairs, which indicates integration of chromosome fragment(s) into the Y chromosome. Accretion of the Y chromosome has also been observed in some haplogyne spiders with the X_1X_2Y system, namely in some other pholcid lineages (Ávila Herrera *et al.*, 2021) and a representative of the family Pacullidae (Král *et al.*, 2019).

Kambiwa neotropica has an $X_1X_2X_3X_4Y$ system (Ávila Herrera *et al.*, 2021). This could originate from the X_1X_2Y system by inclusion of one chromosome pair (Ávila Herrera *et al.*, 2021). In this scenario, the $X_1X_2X_3Y$ system of *Gertschiola* and *Nerudia* arose from the $X_1X_2X_3X_4Y$ system by a centric fusion of the mono-armed chromosomes X_3 and X_4. Another plausible scenario is that the $X_1X_2X_3X_4Y$ system evolved from the $X_1X_2X_3Y$ system by a non-disjunction or fission of one biarmed X chromosome. This second scenario is favoured by the behaviour of chromosomes of the $X_1X_2X_3X_4Y$ system during male meiosis. They exhibit a similar pattern of heteropycnosis during this period. If some chromosomes of the $X_1X_2X_3X_4Y$ system had arisen from a chromosome pair, they would have retained their original meiotic behaviour and would therefore lack heteropycnosis. Therefore, the $X_1X_2X_3Y$ system is probably an ancestral character of the South American clade containing the genera *Gertschiola*, *Kambiwa* and *Nerudia*.

A further character supporting the monophyly of this clade with an $X_1X_2X_3X_4Y$ or $X_1X_2X_3Y$ system is an X chromosome-linked NOR. While the number of NORs varies considerably in pholcids (from one to nine), the position of NORs in these spiders is conservative. Almost all analysed species have terminal NORs. This pattern probably reflects the spreading of rDNA by ectopic recombinations (Ávila Herrera *et al.*, 2021). It has been suggested that ancestral ninetines had two NOR-bearing chromosome pairs (Ávila Herrera *et al.*, 2021). This pattern is preserved in *Nerudia ola*. In *G. macrostyla*, the number of NOR bearing pairs has been reduced to one. As in other haplogynes (Král *et al.*, 2006), NORs in pholcids have often spread to sex chromosomes (Ávila Herrera *et al.*, 2021). Sex chromosome-linked NORs have originated at least five times in Pholcidae (Ávila Herrera *et al.*, 2021). One of these events concerns Ninetinae. While the sex chromosomes of *Pholcophora* (X_1X_2Y) do not include NORs (Avila Herrera *et al.*, 2021), ninetines with more than two X chromosomes exhibit a sex chromosome-linked NOR. In *Gertschiola* and *Kambiwa*, this NOR is placed on an X chromosome (Ávila Herrera *et al.*, 2021; this study). For *Nerudia* we failed to determine unequivocally if a NOR is placed on an X chromosome. Its placement on the X chromosome is supported by the fact that sex chromosome-linked NORs of other studied haplogynes are located on X chromosome(s) (Král *et al.*, 2006; Oliveira *et al.*, 2007) except for the Y-linked NOR of the Pholcinae genus *Nipisa* Huber, 2018 (Ávila Herrera *et al.*, 2021). In contrast to *Kambiwa* (Ávila Herrera *et al.*, 2021), ninetines with the $X_1X_2X_3Y$ system (*Gertschiola* and *Nerudia*) have a sex chromosome-linked NOR at

Figure 45. Sample of typical *Nerudia* habitats in Argentina. A, Jujuy, between San Salvador and Purmamarca (type locality of *N. colina* sp. nov.). B, Salta, NW of Campo Quijano (type locality of *N. poma* sp. nov.). C, Catamarca, near Paso de San Francisco (type locality of *N. centaura* sp. nov.). D, San Juan, W of Las Flores (type locality of *N. rocio* sp. nov.). E, La Rioja, SE of Aimogasta (*N. ola* sp. nov.). F, Córdoba, near Nono (type locality of *N. nono* sp. nov.).

the end of the sex chromosome, which is involved in pairing (this study).

Sampling bias and biogeographic analyses

Our knowledge about the geographic distribution of the genus *Nerudia* is greatly improved in the present study. Originally the genus was known from a single record in Chile (Huber, 2000) in the Andean region *sensu* Morrone (2014, 2017). Torres *et al.* (2015) added a second record in the Western Chacoan district in the Chaco province in the Neotropical region. Our new records decrease the Wallacean shortfall in this genus (i.e. the uncertainty regarding its geographic distribution; Hortal *et al.*, 2015) by filling gaps in the Chaco, Cuyan High Andean and Monte provinces (*sensu* Morrone, 2017). However, the records in the Chaco province are mostly located at high-elevation areas that have lower precipitation levels compared to the Eastern district (Morrone, 2017), where no *Nerudia* has been recorded so far. Most of the records of *Nerudia* in the Chaco province are located close to the Monte province, supporting the affinities of these two provinces (Morrone, 2017). The distribution of *Nerudia* within the Chaco province is similar to that observed for Sicariinae spiders, which are also absent in mesic Chaco localities (Magalhaes *et al.*, 2017).

Our results suggest a strong effect of sampling bias on the Linnean (i.e. the uncertainty regarding the number of described species of a taxon; Hortal *et al.*, 2015) and Wallacean shortfalls in this group of spiders. We tested the null hypothesis that *Nerudia*

specimens were found at highly sampled areas for arthropods in general. This could result from a preference for sites visited by previous collectors. Our results do not support this hypothesis. This could, in theory, be explained by the absence of sampling with pitfalls traps in areas where *Nerudia* occurs. This explanation is poorly supported considering the sampling with pitfall traps at Rosario de Lerma (Salta, Argentina), where *Nerudia poma* occurs but was not collected by pitfall traps (Torres *et al.*, 2015). Besides, the correlation between the presence of *Nerudia* and highly sampled areas for arachnids might be due to a mere spurious correlation between these two variables, as 93% of the available specimens of *Nerudia* were directly collected by us (BAH and MAI) in a sampling expedition carried out in 2019. Most newly collected specimens were found by active searching on the undersides of rocks, directly looking for Ninetinae spiders. This exemplifies the importance of research projects focused on decreasing biodiversity shortfalls of target taxa, and the need of specific search methods adapted to those taxa.

The analysis of sampling bias was based on the use of data from the Global Biodiversity Information Facility – GBIF, which includes over 1 billion records (Hughes *et al.*, 2021). The GBIF data is not appropriate for studies that require detailed species lists (e.g. Qian *et al.*, 2022), and it provides less information regarding range filling, range extent and climatic niche of species than independent compilation efforts (e.g. Beck *et al.*, 2013). This is explained by the uneven country-based policies and institutional support for funding and dataset contributions to the platform (Yesson *et al.*, 2007; Beck *et al.*, 2013; Hughes *et al.*, 2021). However, the present study compared the density of records of arthropods and arachnids mostly inside the Argentinean territory, an associate participant country whose head of delegation is an arachnologist (see https://www.gbif.org/the-gbif-network). Therefore, GBIF data availability biases are unlikely to provide false-positive results regarding the effects of sampling bias in *Nerudia* spiders. On the contrary, the sampling bias (e.g. presence of records close to main cities) observed herein, perfectly corroborates comparative studies using large-scale biodiversity data (e.g. Oliveira *et al.*, 2016; Hughes *et al.*, 2021). An additional analytical bias accepted herein results from the decision on using the records of all *Nerudia* species to perform the species distribution modelling. As stated before, this disregards individual species environmental thresholds. However, this is unlikely to provide significant false-positives (i.e. areas with high suitability for *Nerudia* representatives), owing to the phylogenetically conserved environmental niche, which implies that *Nerudia* species share a similar niche.

Many ground-dwelling Pholcidae species, including representatives of Ninetinae, can be collected using pitfall traps. This was reported, for example, for *Ibotyporanga* Mello-Leitão, 1944 in the semiarid Brazilian Caatinga (Huber & Brescovit, 2003), for *Ninetis* Simon, 1890 in desert scrub forests in Madagascar, savannas in Namibia and dunes in Somalia (Huber & El-Hennawy, 2007) and for *Galapa* Huber, 2000 in salt marshes in the Galápagos Islands (Baert, 2014). This agrees with the observation that many ninetines (e.g. *Galapa* Huber, 2000; *Ibotyporanga* Mello-Leitão, 1944; *Kambiwa* Huber, 2000; *Magana* Huber, 2019; *Ninetis*; *Pinoquio* Carvalho & Huber, 2022; *Tolteca* Huber, 2000) run quickly when disturbed and easily drop to the ground (B. A. Huber & L. S. Carvalho, pers. obs.). By contrast, representatives of *Nerudia* live on the undersides of large rocks and seem reluctant to drop to the ground when the rock is turned. We thus hypothesize that representatives of *Nerudia* show specific behaviours related to escape reaction at disturbance that require focused and active sampling, rather than generalist traps and/or passive sampling methods. This hypothesis is corroborated by the positive correlation between the presence of *Nerudia* and records of arachnids in the region. Laboratory and/or field experiments are required to test if the anecdotal observations of behavioural differences reflect statistically significant patterns or not.

The distribution modelling suggests that *Nerudia* is not expected to occur in the low-elevation areas in the Eastern district of the Chaco biogeographic province, although the sampling effort for arachnids in that region is strikingly low (Fig. 43A). The easternmost record of *Nerudia* is located in the surroundings of Córdoba, one of the best sampled regions within the Western district. A high relative occurrence rate for *Nerudia* is predicted for the Atacama biogeographic province in northern Chile and the Puna biogeographic province in southern Bolivia (Fig. 43B). However, these are poorly sampled regions as far as the arachnid fauna is concerned (Fig. 43A), and the only known records of Ninetinae in Chile are those of *Nerudia atacama* and *N. flecha*. Based on our distribution model, we predict that the genus *Nerudia* ranges much farther north in Chile than presently known and into southern Bolivia. On the other hand, a contrasting pattern can be observed in central Chile, especially near Santiago. This region, where arachnids have been sampled extensively (Fig. 43A), coincides in our model with the southernmost region with high relative occurrence rate for *Nerudia* (Fig. 43B), but no representative of *Nerudia* has been recorded.

The geographical distribution of *Nerudia* seems to be limited by extreme cold (e.g. higher Andes and southern South America) and/or wet conditions (e.g.

mesic Chaco localities). The climatic limitations observed for *Nerudia*, along with the phylogenetically conserved environmental niche observed for ninetines in general, and the empirical natural history information available, support the hypothesis that *Nerudia* spiders have a limited dispersal ability, even under a strong sampling bias scenario. Eberle *et al.* (2018) suggested that major differences in species richness among Pholcidae clades may be due to evolutionary microhabitat shifts. Ninetinae are extremely conservative in this respect, with most species living under or among rocks and in the dry leaf litter (B. A. Huber & L. S. Carvalho, pers. obs.). This may not only explain why Ninetinae are relatively species-poor compared to other subfamilies, but it also suggests that the diversification of ninetines may be largely due to non-adaptive processes (Dimitrov *et al.*, 2013). The observed phylogenetically conserved environmental niche of ninetines and the similar microhabitat corroborates the higher importance that allopatric processes, instead of dispersal events, have had on the diversification process of Ninetinae (Dimitrov *et al.*, 2013). The phylogenetic niche conservatism shown here was also observed for *Sicarius* Walckenaer, 1847 spiders (Magalhaes *et al.*, 2019). However, these authors emphasized the effect of correlation of geography and climate with the phylogeny of *Sicarius*, hypothesizing that stochastic or deterministic (e.g. unmeasured spatially structured environmental conditions), could be more important for the evolution of that genus (Magalhaes *et al.*, 2019).

The effect of changes in the environmental niche has never been tested for pholcids before. While our results corroborate previous studies on Pholcidae diversification processes (e.g. Dimitrov *et al.*, 2013; Eberle *et al.*, 2018), we admit that they are preliminary in several ways, mainly for being based on a *COI* tree. Thus, upon the availability of more information on the phylogenetic relationships in Pholcidae, including a larger sampling among ninetines, phylogenetic comparative studies should be carried out aiming to disentangle the effect of microhabitat changes, geography and climate autocorrelations with the phylogeny of daddy long-legs spiders.

CONCLUSIONS

- Previously, the Andean genus *Nerudia* Huber, 2000 was poorly known, similar to most Ninetinae genera. It was monotypic and only seven adult specimens from two localities had been reported in the literature. We collected almost 400 adult specimens of *Nerudia* within a month and found them at 24 of the 52 visited localities in northern Argentina.
- We formally describe ten new species based on morphology and *COI* barcodes. Molecular data suggest that our samples contain at least two further species, represented by females only.
- We present the first SEM images of *Nerudia*. These data (mainly tarsal organ shape; also epiandrous spigots and spinnerets) fit the pattern of Ninetinae and thus further confirm the position of *Nerudia* in this subfamily.
- *Nerudia* was mostly found under rocks in arid habitats, at a mean elevation of 1750 m a.s.l. The highest record, at 4450 m a.s.l., represents the highest known record for Pholcidae.
- We present the first karyological data for *Nerudia* and for its putative sister-genus, *Gertschiola*. Karyotype evolution of Ninetinae has been accompanied by a reduction of the number of chromosome pairs. Available data suggest a clade including the South American genera *Gertschiola*, *Nerudia* and *Kambiwa*. The ancestral karyotype of this lineage contained 12 chromosome pairs, a $X_1X_2X_3Y$ or $X_1X_2X_3X_4Y$ system and an X chromosome-linked NOR. The $X_1X_2X_3Y$ system is either a synapomorphy linking *Nerudia* with *Gertschiola* or a more ancestral character, predating the $X_1X_2X_3X_4Y$ system of *Kambiwa*. The complex sex chromosome systems of these spiders are derived from the X_1X_2Y system, which is probably ancestral for Haplogynae spiders.
- We modelled the distribution of *Nerudia*, showing that the genus is not expected to range far beyond the area we sampled. To test this hypothesis, further sampling is needed, in particular in the Atacama and Puna biogeographic provinces, two regions without any record of *Nerudia* so far.
- Our analyses suggest that the environmental niche of *Nerudia*, and that of Ninetinae in general, is phylogenetically conserved. Niche conservatism supports the action of non-adaptive radiation in Pholcidae, in addition to mechanisms such as diversification triggered by evolutionary microhabitat shifts.
- We predict that focused collecting in arid New World regions and habitats will uncover a considerable diversity of Ninetinae, which suffer from disproportionally strong Linnean and Wallacean shortfalls compared to other daddy long-legs spiders.

ACKNOWLEDGEMENTS

We thank P. Colmenares (AMNH, New York, USA) and C. Grismado and M. Ramírez (MACN, Buenos Aires, Argentina) for sending in loan material; U. Oliveira (UFMG, Belo Horizonte, Brazil) for assistance

with biogeographic analyses; and L. Podsiadlowski (ZFMK, Bonn, Germany) for help with molecular lab work. Two anonymous reviewers provided valuable comments and suggestions. MAI was supported by the Consejo Nacional de Investigaciones Científicas y Técnicas (CONICET). IMAH and JK were supported by the Ministry of Education, Youth and Sports of the Czech Republic (project LTAUSA 19142). IMAH received further support from the Chilean National Commission for Scientific and Technological Research (ANID). Fluorescence microscopy was done in the Laboratory of Confocal and Fluorescence Microscopy, Faculty of Science, Charles University (Prague). This laboratory is co-financed by the European Regional Development Fund and the state budget of the Czech Republic, projects nos CZ.1.05/4.1.00/16.0347 and CZ.2.16/3.1.00/21515, and supported by the Czech-BioImaging large RI project LM2015062. We thank the local agencies in Argentina for providing collecting permits (N° 37-SSCyAP-2019, San Juan; N°898905053219, Córdoba; N°129/2019, Jujuy). We thank the German Research Foundation for financing field work in Argentina, lab work and the PhD position of G. Meng (DFG; project HU980/12-1).

AUTHOR CONTRIBUTIONS

BAH: initiation of the project, collecting, taxonomic descriptions, writing. IMAH and JK: karyology, writing. LSC: biogeography, distribution modelling, writing. MAI: permits, collecting, writing. GM: analysis of molecular data, writing.

DATA AVAILABILITY

The *COI* sequences generated by this study have been uploaded to GenBank and can be accessed with the accession numbers in Table 1.

REFERENCES

Araujo D, Schneider MC, Zacaro AA, de Oliveira EG, Martins R, Brescovit AD, Knysak I, Cella DM. 2020. Venomous *Loxosceles* species (Araneae, Haplogynae, Sicariidae) from Brazil: 2n♂ = 23 and X_1X_2Y sex chromosome system as shared characteristics. *Zoological Science* **37**: 128–139.

Astrin JJ, Höfer H, Spelda J, Holstein J, Bayer S, Hendrich L, Huber BA, Kielhorn K-H, Krammer H-J, Lemke M, Monje JC, Morinière J, Rulik B, Petersen M, Janssen H, Muster C. 2016. Towards a DNA barcode reference database for spiders and harvestmen of Germany. *PLoS One* **11**: e0162624.

Ávila Herrera IM, Carabajal Paladino LZ, Musilová J, Palacios Vargas JG, Forman M, Král J. 2016. Evolution of karyotype and sex chromosomes in two families of haplogyne spiders, Filistatidae and Plectreuridae. In: Martins C, Pedrosa-Harand A, Houben A, Sullivan B, Martelii L, O´Neil R, eds. 21st International Chromosome Conference, Foz do Iguaçu, Brazil. *Cytogenetic and Genome Research* **148**: 104.

Ávila Herrera IM, Král J, Pastuchová M, Forman M, Musilová J, Kořínková T, Štáhlavský F, Zrzavá M, Nguyen P, Just P, Haddad CR, Hiřman M, Koubová M, Sadílek D, Huber BA. 2021. Evolutionary pattern of karyotypes and meiosis in pholcid spiders (Araneae: Pholcidae): implications for reconstructing chromosome evolution of araneomorph spiders. *BMC Ecology and Evolution* **21**: 75.

Baert L. 2014. New spider species (Araneae) from the Galápagos Islands (Ecuador). *Bulletin de la Société Royale Belge d'Entomologie* **149**: 263–271.

Beck J, Ballesteros-Mejia L, Nagel P, Kitching IJ. 2013. Online solutions and the 'Wallacean shortfall': what does GBIF contribute to our knowledge of species' ranges? *Diversity and Distributions* **19**: 1043–1050.

Bennett R. 2014. *COSEWIC assessment and status report on the northwestern cellar spider Psilochorus hesperus in Canada*. Ottawa: Committee on the Status of Endangered Wildlife in Canada. Available at: https://publications.gc.ca/site/eng/466556/publication.html. (accessed on 12 Dec. 2022).

Bivand R, Keitt T, Rowlingson B, Pebesma E, Summer M, Hijmans R, Rouault E, Warmerdam F, Ooms J, Rundel C. 2019. *Package 'rgdal' for R: bindings for the 'geospatial' data abstraction library. R package v.1.4-6 0*. https://cran.r-project.org/web/packages/rgdal/index.html. (accessed on 1 March 2022).

Brown BV. 1993. A further chemical alternative to critical-point-drying for preparing small (or large) flies. *Fly Times* **11**: 10.

Cock PJ, Antao T, Chang JT, Chapman BA, Cox CJ, Dalke A, Friedberg I, Hamelryck T, Kauff F, Wilczynski B, de Hoon MJ. 2009. Biopython: freely available Python tools for computational molecular biology and bioinformatics. *Bioinformatics* **25**: 1422–1423.

Crowther TW, Glick HB, Covey KR, Bettigole C, Maynard DS, Thomas SM, Smith JR, Hintler G, Duguid MC, Amatulli G, Tuanmu M-N, Jetz W, Salas C, Stam C, Piotto D, Tavani R, Green S, Bruce G, Williams SJ, Wiser SK, Huber MO, Hengeveld GM, Nabuurs G-J, Tikhonova E, Borchardt P, Li CF, Powrie LW, Fischer M, Hemp A, Homeier J, Cho P, Vibrans AC, Umunay PM, Piao SL, Rowe CW, Ashton MS, Crane PR, Bradford MA. 2015. Mapping tree density at a global scale. *Nature* **525**: 201–205.

Datta SN, Chatterjee K. 1988. Chromosomes and sex determination in 13 araneid spiders of North-Eastern India. *Genetica* **76**: 91–99.

Dederichs TM, Huber BA, Michalik P. 2022. Evolutionary morphology of sperm in pholcid spiders (Pholcidae, Synspermiata). *BMC Zoology* **7**: 52.

Dimitrov D, Astrin JJ, Huber BA. 2013. Pholcid spider molecular systematics revisited, with new insights into the biogeography and the evolution of the group. *Cladistics* **29**: 132–146.

Diniz-Filho JAF, Santos T, Rangel TF, Bini LM. 2012. A comparison of metrics for estimating phylogenetic signal

under alternative evolutionary models. *Genetics and Molecular Biology* **35**: 673–679.

Dolejš P, Kořínková T, Musilová J, Opatová V, Kubcová L, Buchar J, Král J. 2011. Karyotypes of central European spiders of the genera *Arctosa*, *Tricca*, and *Xerolycosa* (Araneae: Lycosidae). *European Journal of Entomology* **108**: 1–16.

Dunlop JA, Penney D, Jekel D. 2020. A summary list of fossil spiders and their relatives. *World Spider Catalog*. Natural History Museum Bern. Available at: http://wsc.nmbe.ch, v.20.5 (accessed on 13 April 2022).

Eberle J, Dimitrov D, Valdez-Mondragón A, Huber BA. 2018. Microhabitat change drives diversification in pholcid spiders. *BMC Evolutionary Biology* **18**: 141.

Felsenstein J. 1985. Confidence limits on phylogenies: an approach using the bootstrap. *Evolution* **39**: 783–791.

Forman M, Nguyen P, Hula P, Král J. 2013. Sex chromosome pairing and extensive NOR polymorphism in *Wadicosa fidelis* (Araneae: Lycosidae). *Cytogenetic and Genome Research* **141**: 43–49.

GBIF.org. 2022. GBIF Occurrence. Available at: https://doi.org/10.15468/dl.7r7qun (acessed on 03 February 2022).

Hijmans R, Van Etten J, Cheng J, Mattiuzzi M, Sumner M, Greenberg JA, Lamigueiro O, Bevan A, Racine E, Shortridge A. 2016. *Package ' raster '. CRAN -R.2.5-8*. Available at: http://cran.r-project.org/package=raster. (accessed on 1 March 2022).

Hortal J, de Bello F, Diniz-Filho AJF, Lewinsohn TM, Lobo JM, Ladle RJ. 2015. Seven shortfalls that beset large-scale knowledge of biodiversity. *Annual Review of Ecology, Evolution and Systematics* **46**: 523–549.

Huber BA. 2000. New World pholcid spiders (Araneae: Pholcidae): a revision at generic level. *Bulletin of the American Museum of Natural History* **254**: 1–348.

Huber BA. 2011. Phylogeny and classification of Pholcidae (Araneae): an update. *Journal of Arachnology* **39**: 211–222.

Huber BA. 2021. Beyond size: sexual dimorphisms in pholcid spiders. *Arachnology* **18**: 656–677.

Huber BA. 2022. Revisions of *Holocnemus* and *Crossopriza*: the spotted-leg clade of Smeringopinae (Araneae, Pholcidae). *European Journal of Taxonomy* **795**: 1–241.

Huber BA, Brescovit AD. 2003. *Ibotyporanga* Mello-Leitão: tropical spiders in Brazilian semi-arid habitats (Araneae: Pholcidae). *Insect Systematics and Evolution* **34**: 15–20.

Huber BA, El-Hennawy HK. 2007. On Old World ninetine spiders (Araneae: Pholcidae), with a new genus and species and the first record for Madagascar. *Zootaxa* **1635**: 45–53.

Huber BA, Nuñeza OM. 2015. Evolution of genital asymmetry, exaggerated eye stalks, and extreme palpal elongation in *Panjange* spiders (Araneae: Pholcidae). *European Journal of Taxonomy* **169**: 1–46.

Huber BA, Wunderlich J. 2006. Fossil and extant species of the genus *Leptopholcus* in the Dominican Republic, with the first case of egg-parasitism in pholcid spiders (Araneae: Pholcidae). *Journal of Natural History* **40**: 2341–2360.

Huber BA, Nuñeza OM, Leh Moi Ung C. 2016. The Philippine hair wax spiders and their relatives: revision of the *Pholcus bicornutus* species group (Araneae, Pholcidae). *European Journal of Taxonomy* **225**: 1–34.

Huber BA, Eberle J, Dimitrov D. 2018. The phylogeny of pholcid spiders: a critical evaluation of relationships suggested by molecular data (Araneae, Pholcidae). *ZooKeys* **789**: 51–101.

Hughes AC, Orr MC, Ma K, Costello MJ, Waller J, Provoost P, Yang Q, Zhu C, Qiao H. 2021. Sampling biases shape our view of the natural world. *Ecography* **44**: 1259–1269.

Johnson NF, Chen H, Huber BA. 2018. New species of *Idris* Förster (Hymenoptera, Platygastroidea) from southeast Asia, parasitoids of the eggs of pholcid spiders (Araneae, Pholcidae). *ZooKeys* **811**: 65–80.

Katoh K, Standley DM 2013. MAFFT multiple sequence alignment software version 7: improvements in performance and usability. *Molecular Biology and Evolution* **30**: 772–80.

Kearse M, Moir R, Wilson A, Stones-Havas S, Cheung M, Sturrock S, Buxton S, Cooper A, Markowitz S, Duran C, Thierer T, Ashton B, Meintjes P, Drummond A. 2012. Geneious Basic: an integrated and extendable desktop software platform for the organization and analysis of sequence data. *Bioinformatics* **28**: 1647–1649.

Kejnovský E, Hobza R, Čermák T, Kubát Z, Vyskot B. 2009. The role of repetitive DNA in structure and evolution of sex chromosomes in plants. *Heredity* **102**: 533–541.

Kimura M. 1980. A simple method for estimating evolutionary rate of base substitutions through comparative studies of nucleotide sequences. *Journal of Molecular Evolution* **16**: 111–120.

Kořínková T, Král J. 2013. Karyotypes, sex chromosomes, and meiotic division in spiders. In: Nentwig W, ed. *Spider ecophysiology*. Berlin: Springer, 159–172.

Král J. 2007. Evolution of multiple sex chromosomes in the spider genus *Malthonica* (Araneae: Agelenidae) indicates unique structure of the spider sex chromosome systems. *Chromosome Research* **15**: 863–879.

Král J, Musilová J, Šťáhlavský F, Řezáč M, Akan Z, Edwards RL, Coyle FA, Ribera Almerje C. 2006. Evolution of the karyotype and sex chromosome systems in basal clades of araneomorph spiders (Araneae: Araneomorphae). *Chromosome Research* **14**: 859–880.

Král J, Kořínková T, Krkavcová L, Musilová J, Forman M, Ávila Herrera IM, Haddad CR, Vítková M, Henriques S, Palacios Vargas JG, Hedin M. 2013. Evolution of karyotype, sex chromosomes, and meiosis in mygalomorph spiders (Araneae: Mygalomorphae). *Biological Journal of the Linnean Society* **109**: 377–408.

Král J, Forman M, Kořínková T, Reyes Lerma AC, Haddad CR, Musilová J, Řezáč M, Ávila Herrera IM, Thakur S, Dippenaar-Schoeman AS, Marec F, Horová L, Bureš P. 2019. Insights into the karyotype and genome evolution of haplogyne spiders indicate a polyploid origin of lineage with holokinetic chromosomes. *Scientific Reports* **9**: 3001.

Kumar S, Stecher G, Li M, Knyaz C, Tamura K. 2018. MEGA X: molecular evolutionary genetics analysis across computing platforms. *Molecular Biology and Evolution* **35**: 1547–1549.

Leutner B, Horning N, Schwalb-Willmann J, Hijmans RJ. 2019. *Package 'RStoolbox' for R: tools for remote sensing data analysis. Package v.0.2.6*. (accessed on 1 March 2022).

Levan AK, Fredga K, Sandberg AA. 1964. Nomenclature for centromeric position on chromosomes. *Hereditas* **52**: 201–220.

Magalhaes ILF, Brescovit AD, Santos AJ. 2017. Phylogeny of Sicariidae spiders (Araneae: Haplogynae), with a monograph on Neotropical *Sicarius*. *Zoological Journal of the Linnean Society* **179**: 767–864.

Magalhaes ILF, Neves DM, Santos FR, Vidigal THDA, Brescovit AD, Santos AJ. 2019. Phylogeny of Neotropical *Sicarius* sand spiders suggests frequent transitions from deserts to dry forests despite antique, broad-scale niche conservatism. *Molecular Phylogenetics and Evolution* **140**: 106569.

Merow C, Smith MJ, Silander JA. 2013. A practical guide to MaxEnt for modeling species' distributions: what it does, and why inputs and settings matter. *Ecography* **36**: 1058–1069.

Michalik P, Ramírez MJ. 2014. Evolutionary morphology of the male reproductive system, spermatozoa and seminal fluid of spiders (Araneae, Arachnida) - current knowledge and future directions. *Arthropod Structure and Development* **43**: 291–322.

Morrone JJ. 2014. Biogeographical regionalisation of the neotropical region. *Zootaxa* **3782**: 1–110.

Morrone JJ. 2017. *Neotropical biogeography: regionalization and evolution*. Boca Raton: CRC Press. Available at: https://www.taylorfrancis.com/books/9781315390659. (accessed on 1 April 2022).

Oliveira RM, Jesus AC, Brescovit AD, Cella DM. 2007. Chromosomes of *Crossopriza lyoni* (Blackwall 1867), intraindividual numerical chromosome variation in *Physocyclus globosus* (Taczanowski 1874), and the distribution pattern of NORs (Araneomorphae, Haplogynae, Pholcidae). *Journal of Arachnology* **35**: 293–306.

Oliveira U, Paglia AP, Brescovit AD, Carvalho CJB, Silva DP, Rezente DT, Leite FDF, Batista JAN, Barbosa JPPP, Stehmann JR, Ascher JS, Vasconcelos MA, Marco P Jr, Löwenberg-Neto P, Dias PG, Ferro VG, Santos AJ. 2016. The strong influence of collection bias on biodiversity knowledge shortfalls of Brazilian terrestrial biodiversity. *Diversity and Distributions* **22**: 1232–1244.

Pagel M. 1999. Inferring the historical patterns of biological evolution. *Nature* **401**: 877–884.

Paula-Neto E, Cella DM, Araujo D, Brescovit AD, Schneider MC. 2017. Comparative cytogenetic analysis among filistatid spiders (Araneomorphae: Haplogynae). *Journal of Arachnology* **45**: 123–128.

Postiglioni A, Brum-Zorrilla N. 1981. Karyological studies on Uruguayan spiders II. Sex chromosomes in spiders of the genus *Lycosa* (Araneae-Lycosidae). *Genetica* **56**: 47–53.

Qian H, Zhang J, Jiang M-C. 2022. Global patterns of fern species diversity: an evaluation of fern data in GBIF. *Plant Diversity* **44**: 135–140.

Ratnasingham S, Hebert PDN. 2007. Bold: the barcode of life data system (http://www.barcodinglife.org). *Molecular Ecology Notes* **7**: 355–364.

Revell LJ. 2012. Phytools: an R package for phylogenetic comparative biology (and other things). *Methods in Ecology and Evolution* **3**: 217–223.

Saitou N, Nei M. 1987. The neighbor-joining method: a new method for reconstructing phylogenetic trees. *Molecular Biology and Evolution* **4**: 406–425.

Schartl M, Schmid M, Nanda I. 2016. Dynamics of vertebrate sex chromosome evolution: from equal size to giants and dwarfs. *Chromosoma* **125**: 553–571.

Silva D. 1988. Estudio cariotípico de *Loxosceles laeta* (Araneae: Loxoscelidae). *Revista Peruana de Entomología* **31**: 9–12.

Silva RW, Klisiowicz DR, Cella DM, Mangili OC, Sbalqueiro IJ. 2002. Differential distribution of constitutive heterochromatin in two species of brown spider: *Loxosceles intermedia* and *L. laeta* (Aranae, Sicariidae), from the metropolitan region of Curitiba, PR (Brazil). *Acta Biologica Paranaense Curitiba* **31**: 123–136.

Simard M, Pinto N, Fisher JB, Baccini A. 2011. Mapping forest canopy height globally with spaceborne lidar. *Journal of Geophysical Research* **116**: G04021.

Simon E. 1893. *Histoire Naturelle des Araignées, 2nd edn*. Paris: Encyclopédie Roret.

Srivathsan A, Lee L, Katoh K, Hartop E, Kutty SN, Wong J, Yeo D, Meier R. 2021. ONTbarcoder and MinION barcodes aid biodiversity discovery and identification by everyone, for everyone. *BMC Biology* **19**: 217.

Stecher G, Tamura K, Kumar S. 2020. Molecular evolutionary genetics analysis (MEGA) for macOS. *Molecular Biology and Evolution* **37**: 1237–1239.

Suyama M, Torrents D, Bork P. 2006. PAL2NAL: robust conversion of protein sequence alignments into the corresponding codon alignments. *Nucleic Acids Research* **34**: W609–W612.

Suzuki S. 1954. Cytological studies in spiders. III. Studies on the chromosomes of fifty-seven species of spiders belonging to seventeen families, with general considerations on chromosomal evolution. *Journal of Science of Hiroshima University* **2**: 23–136.

Torres VM, Pardo PL, González-Reyes AX, Rodriguez-Artigas SM, Corronca JA. 2015. New records of seven species of pholcid spiders (Araneae, Pholcidae) from the northern Argentina. *Check List* **11**: 1629.

Truett G, Heeger P, Mynatt R, Truett A, Walker J, Warman MJB. 2000. Preparation of PCR-quality mouse genomic DNA with hot sodium hydroxide and tris (HotSHOT). *Biotechniques* **29**: 52–54.

Wheeler WC, Coddington JA, Crowley LM, Dimitrov D, Goloboff PA, Griswold CE, Hormiga G, Prendini L, Ramírez MJ, Sierwald P, Almeida-Silva L, Alvarez-Padilla F, Arnedo MA, Ligia R, Benavides S, Suresh BP, Bond JE, Grismado CJ, Hasan E, Hedin M, Izquierdo MA, Labarque FM, Ledford J, Lopardo L, Maddison WP, Miller JA, Piacentini LN, Platnick NI, Polotow D, Silva-Dávila D, Scharff N, Szűts T, Ubick D, Vink CJ, Wood HM, Zhang J. 2017. The spider tree of life: phylogeny of Araneae based on target-gene analyses from an extensive taxon sampling. *Cladistics* **33**: 574–616.

World Spider Catalog. **2022**. *World Spider Catalog, v.23.0*. Natural History Museum Bern. Available at: http://wsc.nmbe.ch (accessed on 13 April 2022).

Yang C, **Zheng Y**, **Tan S**, **Meng G**, **Rao W**, **Yang C**, **Bourne DG**, **O'Brien PA**, **Xu J**, **Liao S**, **Chen A**, **Chen X**, **Jia X**, **Zhang A**, **Liu S. 2020**. Efficient COI barcoding using high throughput single-end 400 bp sequencing. *BMC Genomics* **21**: 862.

Yesson C, **Brewer PW**, **Sutton T**, **Caithness N**, **Pahwa JS**, **Burgess M**, **Gray WA**, **White RJ**, **Jones AC**, **Bisby FA**, **Culham A. 2007**. How global is the Global Biodiversity Information Facility? *PLoS One* **2**: e1124.

SUPPORTING INFORMATION

Additional supporting information may be found in the online version of this article on the publisher's website.

Figure S1. NJ-tree.
Figure S2. IQ-tree.
Figure S3. Genetic distances.
Figure S4. ASAP analysis.
Figure S5. Density of records.
Figure S6. Probability of records.
Figure S7. Ninetinae environmental niche variation.
Figure S8. Optimization of the environmental niche.
Table S1. Significant principal components used for species distribution modelling.
Table S2. Principal components and environmental predictors for the species distribution modelling.
Table S3. Contribution of the principal components to the species distribution modelling.
Table S4. Significant principal components used to compare the environmental niche.
Table S5. Eigenvectors used to compare the environmental niche.
Table S6. Records of Ninetinae used in biogeographic analyses.
Table S7. Significant principal components and phylogenetic signal.
Table S8. Eigenvectors used to compute the phylogenetic signal.
Table S9. Phylogenetic signal.

Supporting Information

High and dry: integrative taxonomy of the Andean spider genus *Nerudia* (Araneae: Pholcidae)

Supplementary Figures 211

Figure S1. NJ-tree 211

Figure S2. IQ-tree 212

Figure S3. Genetic distances 213

Figure S4. ASAP analysis 214

Figure S5. Density of records 215

Figure S6. Probability of records 216

Figure S7. Ninetinae environmental niche variation 217

Figure S8. Optimization of the environmental niche 218

Supplementary Tables 219

Table S1. Significant principal components for the environmental layers 219

Table S2. Correlations between the principal components and environmental predictors 220

Table S3. Contribution of the principal components to species distribution modelling 221

Table S4. Records of Ninetinae used in biogeographic analyses 222

Table S5. Significant principal components used for environmental niche analyses 231

Table S6. Eigenvectors of covariance factor of the principal components 232

Table S7. Significant principal components and phylogenetic signal 233

Table S8. Eigenvectors and phylogenetic signal 234

Table S9. Phylogenetic signal 235

Supplementary Figures

Figure S1. NJ-tree

Complete NJ CO1 tree, showing all analysed taxa. Accession numbers are shown for the taxa taken from GenBank. For all other terminals, see Table 1 (in main paper).

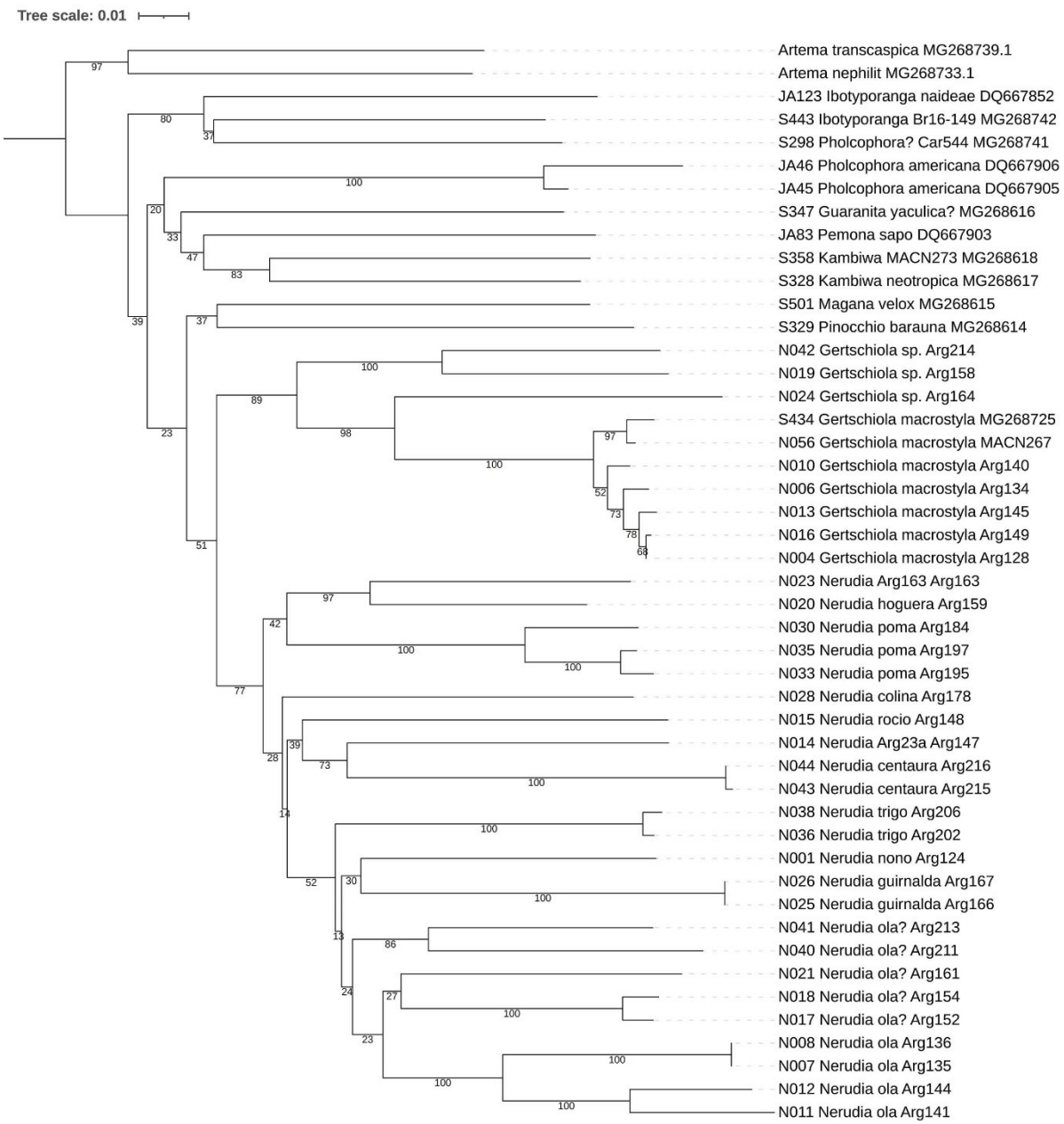

Figure S2. IQ-tree

Tree resulting from analysis with IQ-Tree (version 2.1.3) (Minh *et al.*, 2020; https://doi.org/10.1093/molbev/msaa015) based on the nucleotide alignment of CO1 barcodes of 47 specimens. Accession numbers are shown for the taxa taken from GenBank. For all other terminals, see Table 1 (in main paper). To overcome local optima during heuristics, we performed 10 independent IQ-TREE runs (--runs 10), with a smaller perturbation strength (-pers 0.2) and larger number of stop iterations (-nstop 500). Branch supports were evaluated with 2000 ultrafast bootstrap (UF-Boot) (Minh *et al.*, 2013; https://doi.org/10.1093/molbev/mst024) with the risk of potential model violations considered (-B 2000 -bnni). SH-aLRT branch test (Guindon *et al.*, 2010; https://doi.org/10.1093/sysbio/syq010) was performed using 2000 bootstrap replicates (-alrt 2000). Best-fitting substitution models were automatically determined by the ModelFinder algorithm (Kalyaanamoorthy *et al.*, 2017; https://doi.org/10.1038/nmeth.4285) in IQ-TREE. Tree visualizations were finished with the Newick utilities (version 1.6) (Junier & Zdobnov, 2010; https://doi.org/10.1093/bioinformatics/btq243) and iTOL (Letunic & Bork, 2021; https://doi.org/10.1093/nar/gkab301).

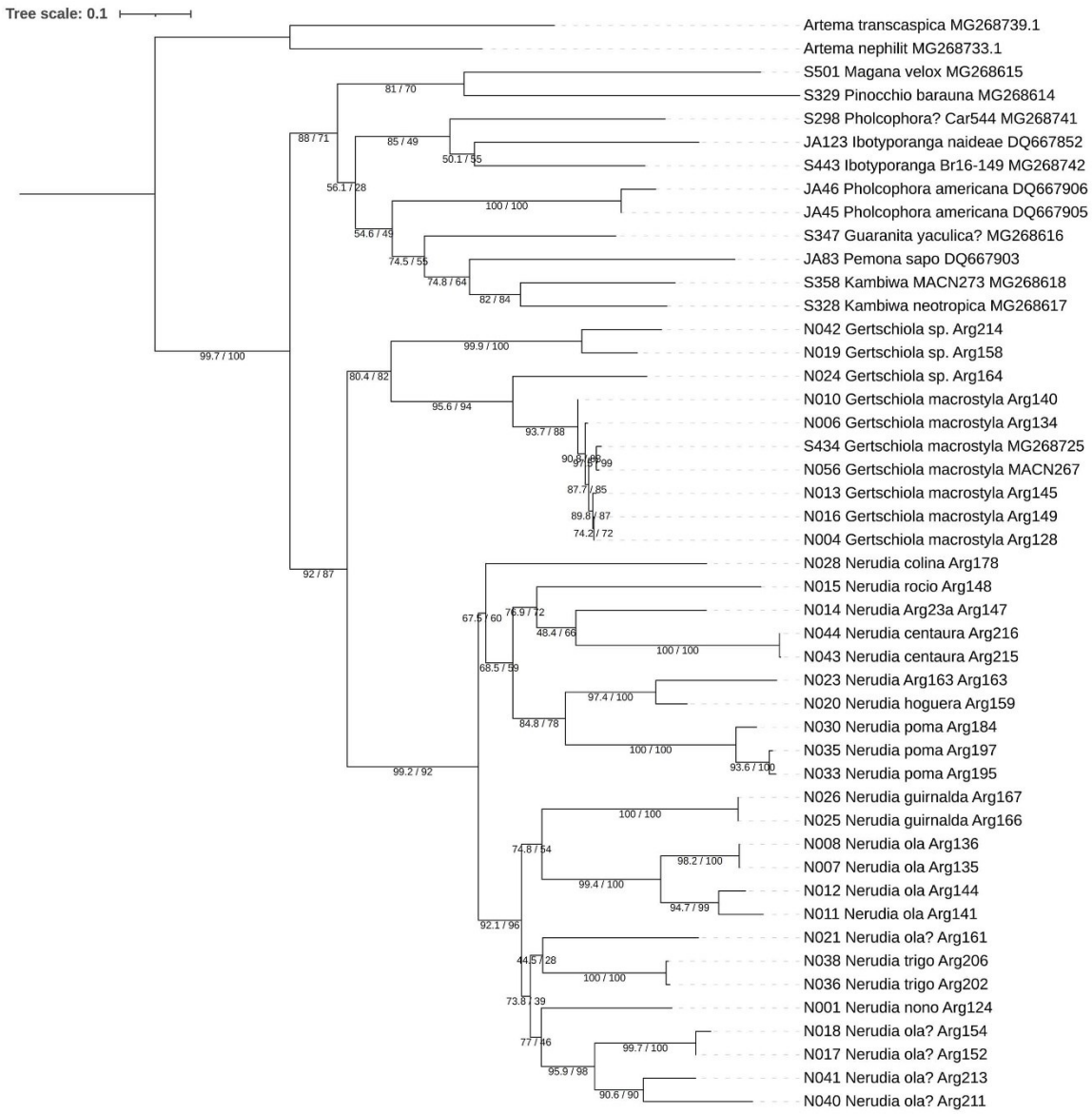

Figure S3. Genetic distances

Genetic distances among sequenced *Nerudia* specimens. The evolutionary distances were computed using the ape package (version 5.3) (Paradis & Schliep, 2019; https://doi.org/10.1093/bioinformatics/bty633) and the Kimura 2-parameter model (Kimura, 1980; https://doi.org/10.1007/bf01731581) and all ambiguous positions were removed for each sequence pair (pairwise deletion option). The visualization was done with the seaborn package (version 0.11.2) (Waskom, 2021; https://doi.org/10.21105/joss.03021).

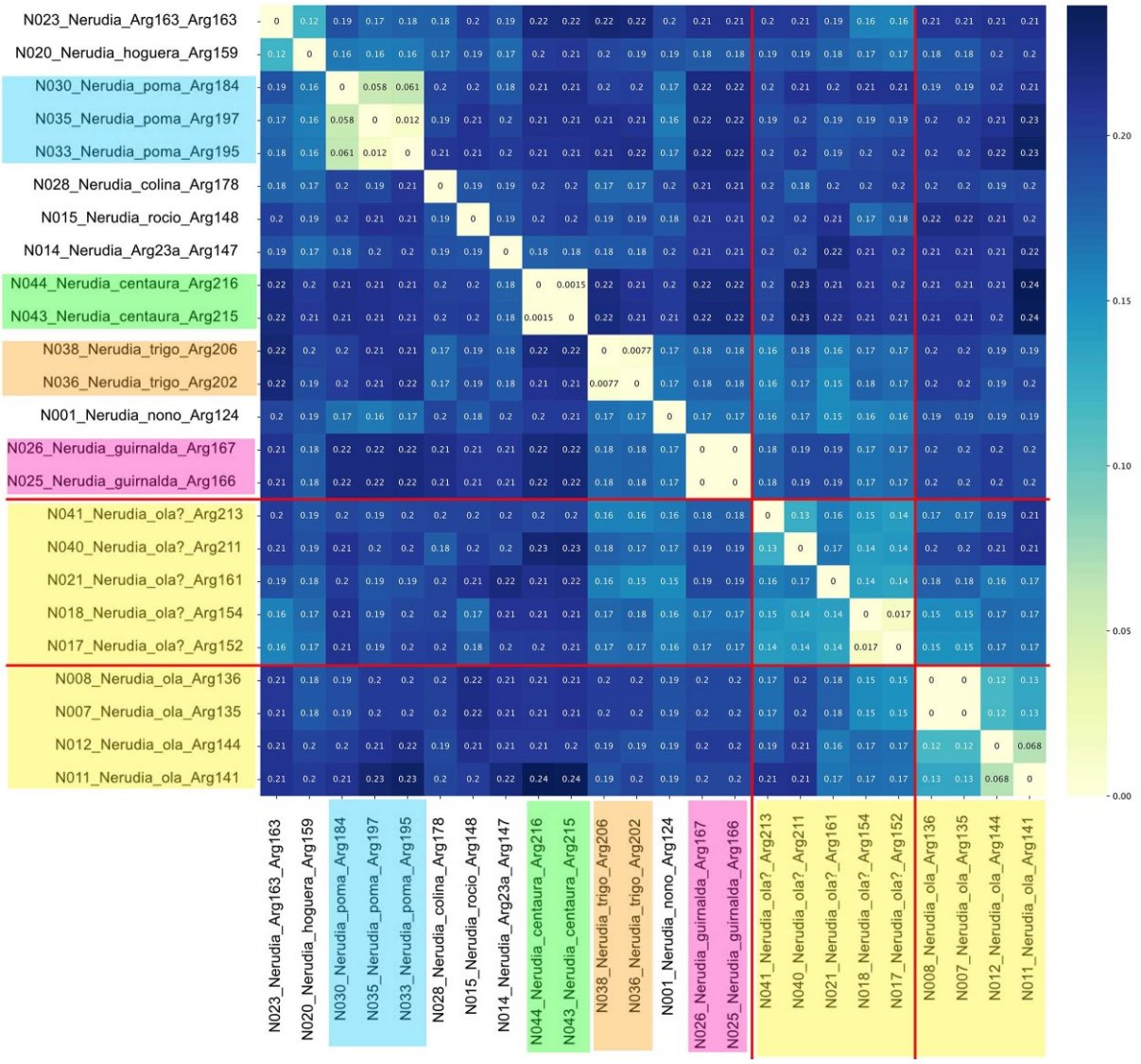

Figure S4. ASAP analysis

Results of ASAP analysis (Puillandre *et al.*, 2021; https://doi.org/10.1111/1755-0998.13281) based on the *Nerudia* sequences using the graphical web-interface version of ASAP (https://bioinfo.mnhn.fr/abi/public/asap/). Pairwise genetic distances were calculated based on the Kimura 2-parameter model (Kimura, 1980; https://doi.org/10.1007/bf01731581). Different partitions (i.e., proposed species delimitation models) are ranked based on their asap-scores, which are composed of the barcode gap width (between different partitions) and the probability of different groups of specimens of the current partition being separate species. The lower the asap-score, the better the partition. Note that the most plausible species delimitation models (scores 2.0, 3.0) support several species within '*Nerudia ola*'.

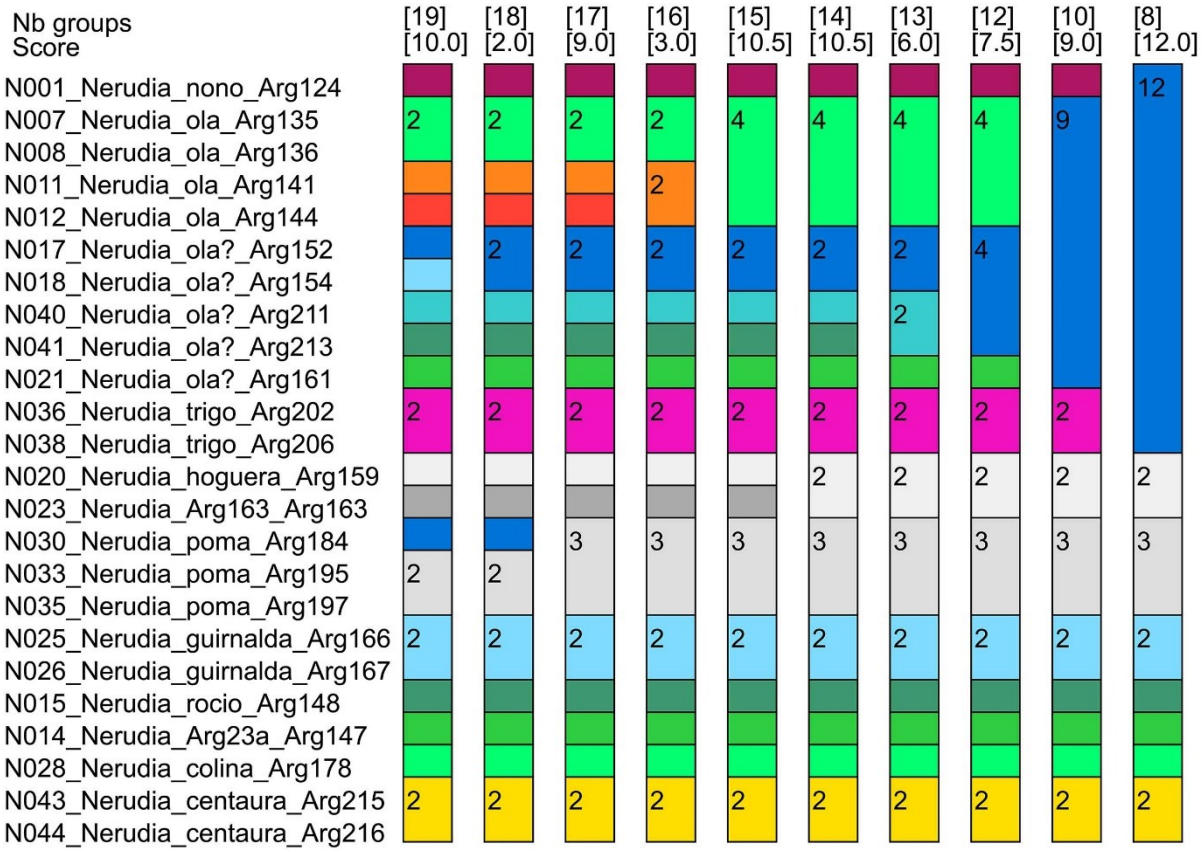

Figure S5. Density of records

Density of records of arthropods (A) and arachnids (B) surrounding the geographic distribution of *Nerudia* representatives. Dotted line represents 500 km buffer around *Nerudia* records (black dots). Correlation between maps: 0.391. Numbered cities: (1) Santiago, (2) La Serena; (3) Copiapó; (4) Córdoba; (5) Cafayate; (6) Salta; and (7) Tilcara.

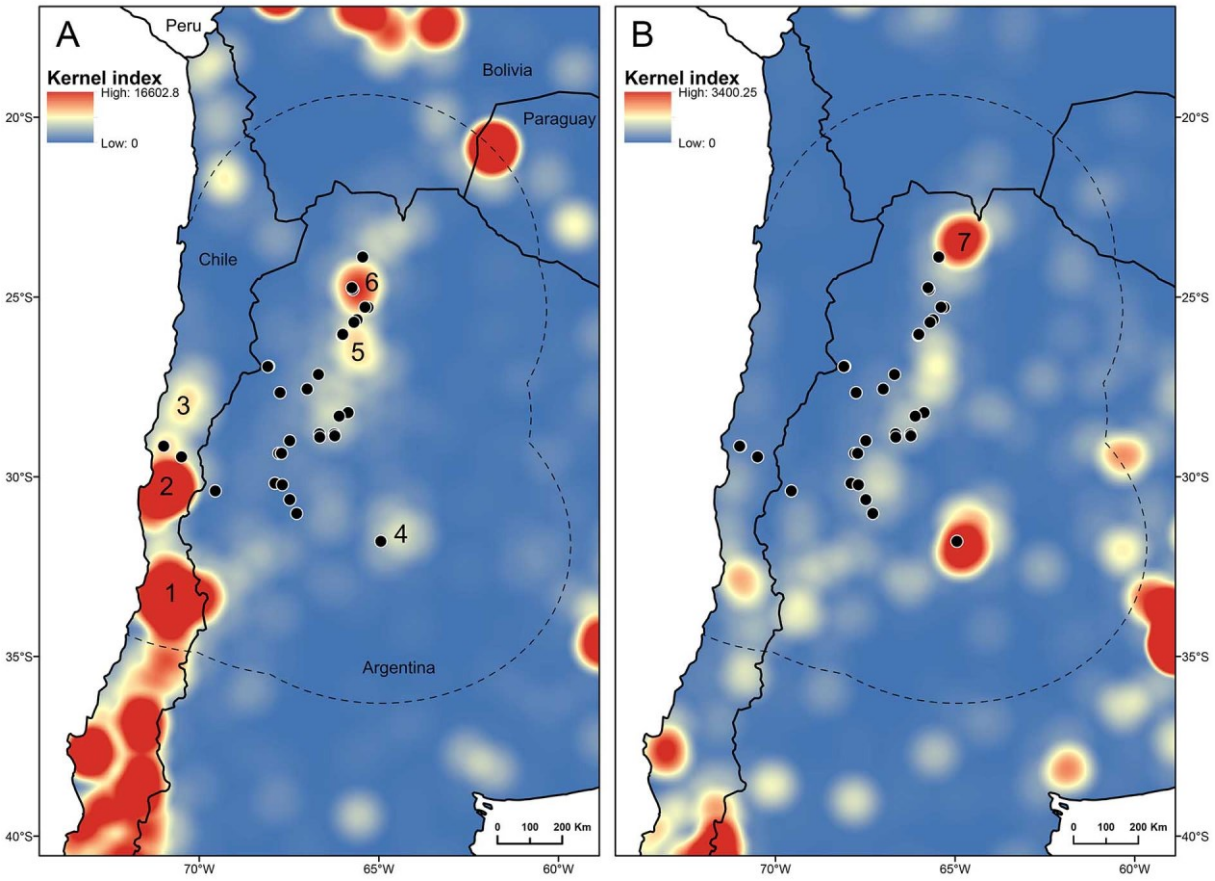

Figure S6. Probability of records

Probability of records of *Nerudia* based on the number of records of other Arachnida (left; significant) or Arthropoda (right; non-significant) taxa. Darker colours represent superimposed symbols.

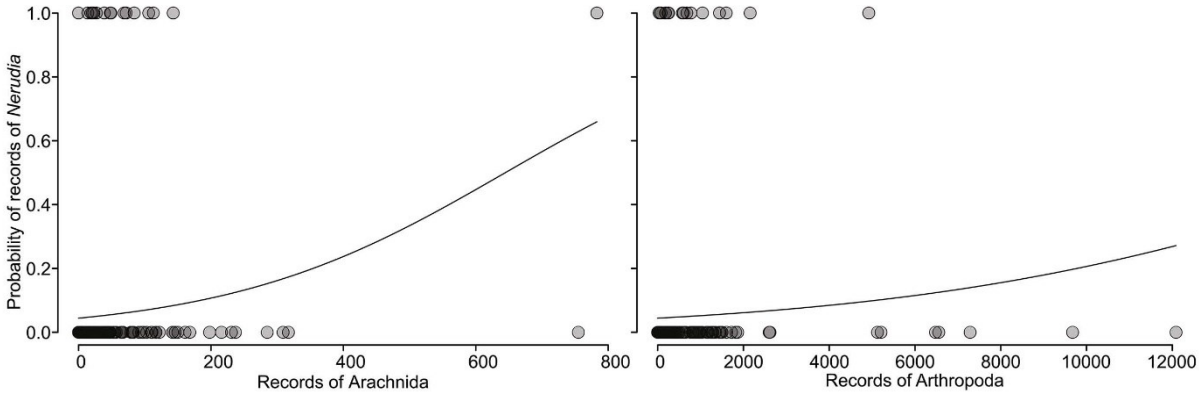

Figure S7. Ninetinae environmental niche variation

Principal component analysis of the environmental conditions for *Nerudia* representatives (red circles and ellipse) and other Ninetinae (black triangles and dotted line ellipse). The ellipses encompass the values within a multivariate t-distribution. Darker colours represent superimposed symbols. Abbreviations of climatic variables: BIO1 - Annual mean temperature; BIO2 - Mean diurnal range; BIO3 - Isothermality; BIO4 - Temperature Seasonality; BIO5 – Maximum temperature of warmest month; BIO6 - Minimum temperature of coldest month; BIO7 - Temperature annual range; BIO8 - Mean temperature of wettest quarter; BIO9 - Mean temperature of driest quarter; BIO10 - Mean temperature of warmest quarter; BIO11 - Mean temperature of coldest quarter; BIO12 - Annual precipitation; BIO13 - Precipitation of wettest month; BIO14 - Precipitation of driest month; BIO15 - Precipitation seasonality; BIO16 - Precipitation of wettest quarter; BIO17 - Precipitation of driest quarter; BIO18 - Precipitation of warmest quarter; BIO19 - Precipitation of coldest quarter.

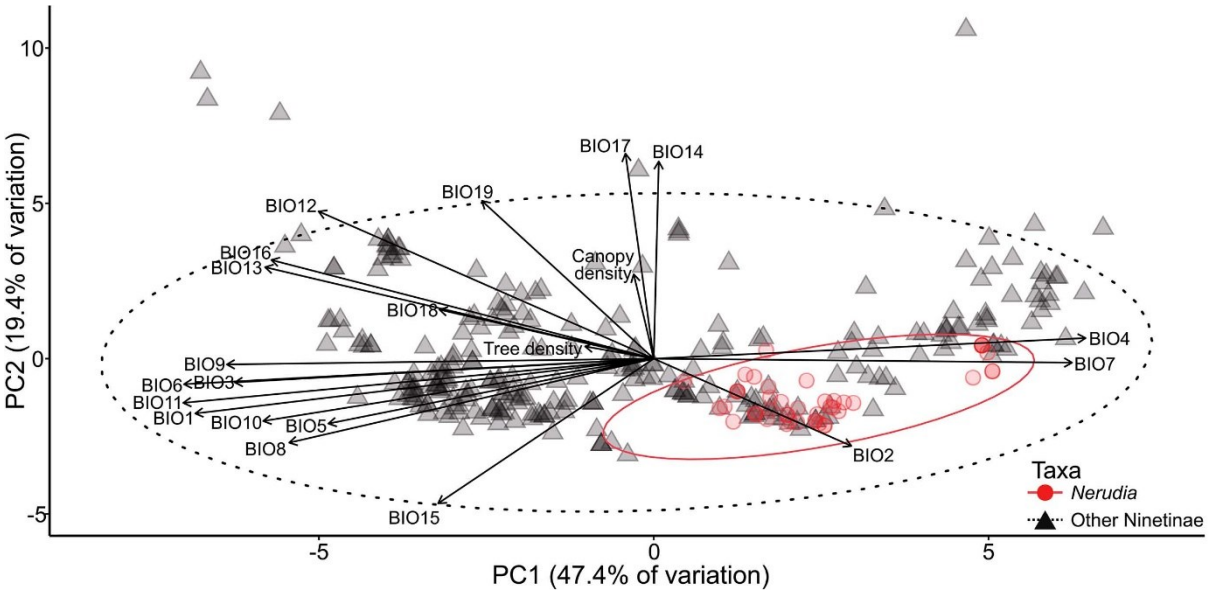

Figure S8. Optimization of the environmental niche

Optimization of the environmental niche, based on the first axis of the principal component analysis using 21 bioclimatic predictors.

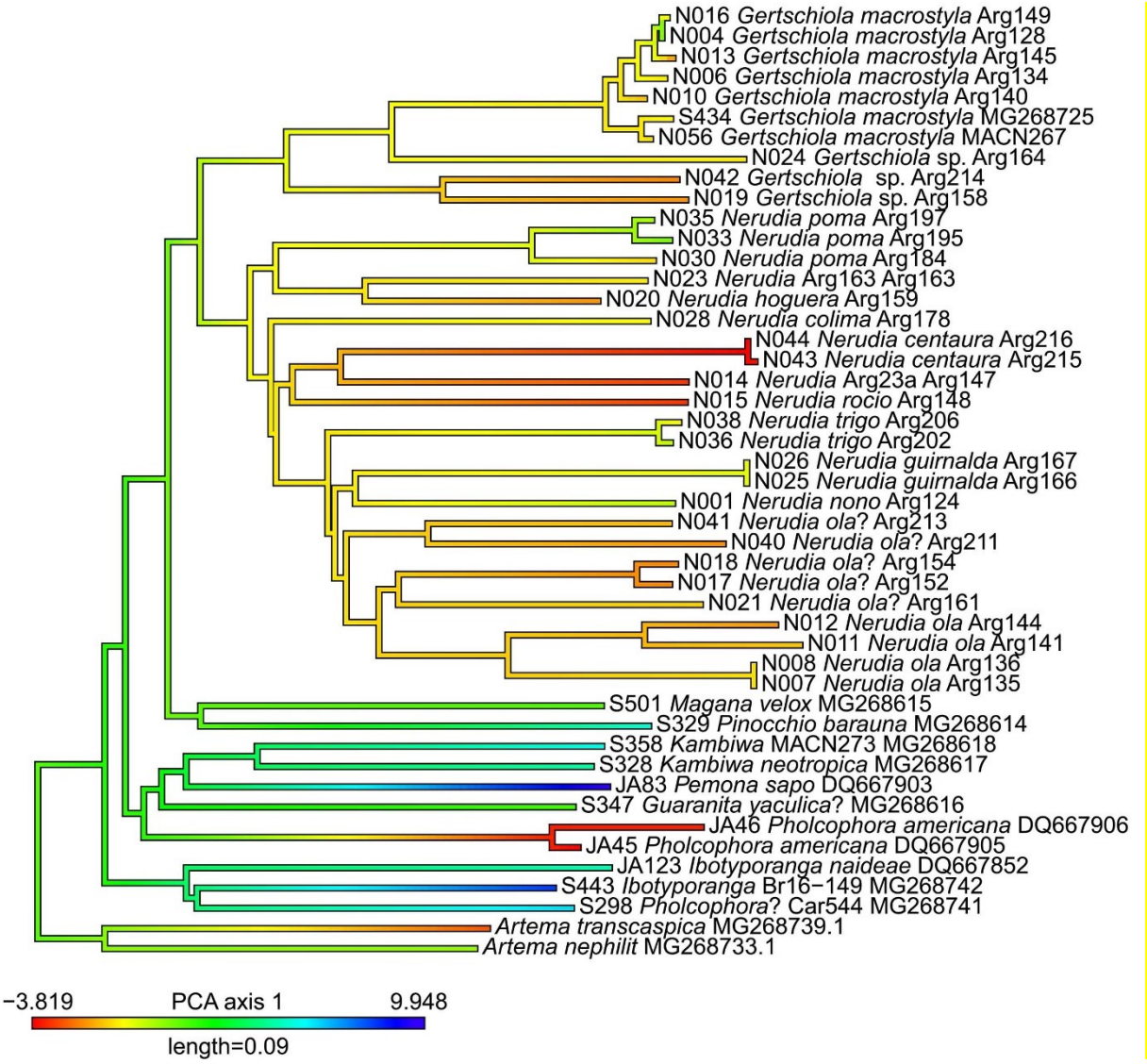

Supplementary Tables

Table S1. Significant principal components for the environmental layers

Significant principal components (PC) for the environmental layers used as predictors for the species distribution modelling (SDM) for *Nerudia* representatives. The selected PCs are those in which the total cumulative percentage of total variation sum at least 95%.

Parameter	PC1	PC2	PC3	PC4	PC5	PC6	PC7
Standard deviation	3.182	1.879	1.779	1.069	0.980	0.781	0.689
Proportion of variance	48.2%	16.8%	15.1%	5.4%	4.6%	2.9%	2.3%
Cumulative proportion	48.2%	65.0%	80.1%	85.6%	90.1%	93.0%	95.3%

Table S2. Correlations between the principal components and environmental predictors

Pearson correlation coefficients between the principal components (PC) and the environmental layers used as predictors for the species distribution modelling (SDM) for *Nerudia* representatives. The selected PCs are those in which the total cumulative percentage of total variation sum at least 95%. Variables are sorted in order of importance for the first principal component.

Variables	PC1	PC2	PC3	PC4	PC5	PC6	PC7
Min. temperature of coldest month	0.948	0.003	0.256	0.149	-0.114	-0.038	0.001
Mean temperature of coldest quarter	0.931	0.117	0.321	0.038	-0.106	0.006	0.013
Annual mean temperature	0.882	-0.079	0.458	0.016	-0.054	-0.008	0.016
Annual precipitation	0.878	-0.070	-0.361	-0.267	0.067	-0.067	-0.012
Mean temperature of driest quarter	0.878	0.038	0.164	0.240	-0.062	-0.193	-0.037
Precipitation of wettest quarter	0.843	0.189	-0.297	-0.300	0.154	-0.184	-0.005
Precipitation of wettest month	0.836	0.183	-0.303	-0.312	0.155	-0.192	0.006
Precipitation of warmest quarter	0.825	0.034	-0.121	-0.401	-0.019	0.173	0.126
Mean temperature of warmest quarter	0.734	-0.354	0.574	0.001	0.011	-0.044	-0.004
Mean temperature of wettest quarter	0.718	-0.135	0.595	-0.138	-0.057	0.128	0.062
Canopy height	0.705	0.237	-0.186	0.173	0.436	0.208	-0.609
Max. temperature of warmest month	0.642	-0.384	0.637	-0.084	0.074	-0.075	-0.054
Precipitation of driest quarter	0.476	-0.626	-0.519	-0.076	-0.096	0.238	0.057
Tree density	0.430	0.173	0.075	0.378	0.670	0.255	0.333
Precipitation of driest month	0.427	-0.647	-0.520	-0.077	-0.099	0.252	0.063
Isothermality	0.404	0.810	-0.160	-0.054	-0.194	0.214	-0.033
Precipitation of coldest quarter	0.312	-0.422	-0.661	0.090	0.209	-0.324	0.038
Precipitation seasonality	-0.211	0.801	0.099	-0.168	0.163	-0.185	0.159
Temperature seasonality	-0.602	-0.711	0.249	-0.066	0.204	-0.067	-0.021
Mean diurnal range	-0.609	0.243	0.309	-0.533	0.171	0.171	-0.048
Temperature annual range	-0.687	-0.458	0.362	-0.328	0.262	-0.030	-0.064

Table S3. Contribution of the principal components to species distribution modelling

Contribution of the principal components described in Tables S1-2 to the species distribution modelling, carried out with Maxent, without applying a threshold rule, with 500 maximum interactions, random test percentage of 25%, raw output formatted, with 15 bootstrap replicates, and by choosing to remove duplicates from the same gridcell. The average training AUC for the replicate runs is 0.971, and the standard deviation is 0.004.

Variable	Percent contribution	Permutation importance
PC1	43	61.8
PC2	33.6	29.3
PC3	18.1	6
PC4	1	0.3
PC5	1.3	0.1
PC6	1.8	1.8
PC7	1.1	0.7

Table S4. Records of Ninetinae used in biogeographic analyses

Taxa	Locality
Enetea apatellata	Bolivia, Beni, Est. Biol. Beni, El Trapiche, -14.737, -66.265
Galapa baerti	Ecuador, Galapagos Isl., Santiago, Bucanero Cove, -0.272, -90.849
Galapa baerti	Ecuador, Galapagos Isl., Santiago, Cerro Cowan, -0.21, -90.78
Galapa baerti?	Ecuador, Galapagos Isl., Santa Fé, -0.805, -90.048
Galapa baerti?	Ecuador, Galapagos Isl., Islote Venecia, -0.5178, -90.476
Galapa baerti?	Ecuador, Galapagos Isl., Pinta, littoral zone, 0.545, -90.738
Galapa bella	Ecuador, Galapagos Isl., Santa Cruz, Academy Bay, Darwin Res. St., -0.741, -90.305
Galapa bella	Ecuador, Galapagos Isl., Santa Cruz: 1 km SW Garrapatero beach, -0.7007, -90.228
Galapa bella	Ecuador, Galapagos Isl., Santa Cruz: near Canal de Itabaca, -0.4936, -90.286
Galapa floreana	Ecuador, Galapagos Isl., Floreana, La Lobería, -1.2831, -90.4907
Galapa spiniphila	Venezuela, Falcón, Peninsula de Paraguaná, near Cueva del Guano, 11.9026, -69.9456
Gertschiola macrostyla	Argentina, Catamarca, Joyango, 60 km S Andalgalá, -28.1, -66.13
Gertschiola macrostyla	Argentina, Catamarca, between Fiambalá and Tinogasta, -27.9872, -67.6306
Gertschiola macrostyla	Argentina, Catamarca, Quebrada del Cura, between Belén and Andalgalá, -27.6, -66.6
Gertschiola macrostyla	Argentina, Catamarca, Andalgalá, -27.6, -66.31
Gertschiola macrostyla	Argentina, Córdoba, between Villa Dolores and Chancani, -31.8328, -65.2647
Gertschiola macrostyla	Argentina, La Rioja, SE Aimogasta, 'site 2', -28.9015, -66.6538
Gertschiola macrostyla	Argentina, San Juan, Cuesta de Marayes, -31.4949, -67.3358
Gertschiola macrostyla	Argentina, San Juan, Valle Fértil, Chucuma, -31.0372, -67.2858
Gertschiola macrostyla	Argentina, San Juan, ~7.5 km S Astica, -31.0223, -67.2976
Gertschiola macrostyla	Argentina, San Juan, 50 km N Marayes, -31.0, -67.25
Gertschiola macrostyla	Argentina, San Juan, Astica, -30.95, -67.31
Gertschiola macrostyla	Argentina, San Juan, San Agustín de Valle Fértil, -30.6366, -67.4863
Gertschiola macrostyla	Argentina, San Juan, Parque Provincial Ischigualasto, -30.1839, -67.9026
Gertschiola macrostyla	Argentina, San Juan, between San José de Jáchal and Huaco, -30.1497, -68.6063
Gertschiola macrostyla	Argentina, San Juan, Ischigualasto, -30.0, -68.0
Gertschiola macrostyla	Argentina, San Luis, Sierra de las Quijadas N.P., -32.469, -66.961
Gertschiola macrostyla	Argentina, San Luis, Merlo, -32.33, -64.95
Gertschiola macrostyla	Argentina, Santiago del Estero, Sumampa Viejo, -29.4, -63.43
Gertschiola macrostyla	Argentina, Tucumán, Bañado, -26.45, -65.98
Gertschiola macrostyla	Argentina, San Luis, Sierra de las Quijadas N.P., -32.4937, -66.9627
Gertschiola macrostyla?	Argentina, La Rioja, between Chilecito and Famatina, -29.0027, -67.4855
Gertschiola neuquena	Argentina, Chubut, Peninsula Walden, Puerto Piramides, -42.5667, -64.2833
Gertschiola neuquena	Argentina, La Pampa, Gobernador Duval, -38.71, -66.4
Gertschiola neuquena	Argentina, Mendoza, Bardas Blancas, -35.87, -69.8
Gertschiola neuquena	Argentina, Mendoza, Nihuil, -35.01, -68.66
Gertschiola neuquena	Argentina, Neuquén, Piedra del Áquila, -40.05, -70.08
Gertschiola neuquena	Argentina, Neuquén, Ciudad de Neuquén, -38.95, -68.66

Taxa	Locality
Gertschiola neuquena	Argentina, Neuquén, Confluencia: Planicie Banderita/Loma de la Lata, -38.45, -68.68
Gertschiola neuquena	Argentina, Neuquén, Paso Huitrin, -37.66, -69.98
Gertschiola neuquena	Argentina, Rio Negro, Ñe Luan, -41.5, -68.68
Gertschiola neuquena	Argentina, Rio Negro, [Cerro] Campana Mahuida(?), -40.1, -69.5
Gertschiola sp.	Argentina, La Rioja, between Chilecito and Famatina, -29.0027, -67.4855
Gertschiola sp.	Argentina, La Rioja, SE Aimogasta, 'site 2', -28.9015, -66.6538
Gertschiola sp.	Argentina, Catamarca, ~14 km W Fiambalá, -27.659, -67.7607
Guaranita dobby	Argentina, Salta, 9 km E Cabra Corral dam, -25.2945, -65.2838
Guaranita dobby	Argentina, Salta, 1 km N Charrillos, -24.7378, -65.7545
Guaranita dobby	Argentina, Salta, ~55 km NW Campo Quijano, -24.4716, -65.9272
Guaranita goloboffi	Argentina, Salta, Chuscha, 6 km NW Cafayate, -26.0333, -66.0167
Guaranita goloboffi	Argentina, Salta, Alemanía, 7 km S, El Hongo, -25.67, -65.6
Guaranita goloboffi	Argentina, Salta, 7 km E Cabra Corral dam, -25.2944, -65.2836
Guaranita goloboffi	Argentina, Salta, nr. Cabra Corral dam, 6 km E Coronel Moldes, -25.28, -65.42
Guaranita goloboffi	Argentina, Salta, 9 km E Cabra Corral dam, -25.2861, -65.2522
Guaranita goloboffi	Argentina, Salta, 11 km E Cabra Corral dam, -25.26, -65.22
Guaranita goloboffi	Argentina, Salta, Road to Cabra Corral dam, -25.1227, -65.0622
Guaranita goloboffi	Argentina, Salta, Road to El Carmen, -24.52, -65.3508
Guaranita goloboffi	Argentina, Tucumán, Rio India Muerta, road to Ticucho, -26.55, -65.27
Guaranita goloboffi?	Argentina, Catamarca, ~5 km NW Chumbicha, near Balneario El Caolín, 'site 1', -28.8152, -66.2478
Guaranita goloboffi?	Argentina, Salta, ~1 km SW Alemanía, -25.63, -65.618
Guaranita goloboffi?	Argentina, Salta, Cabra Corral, 'site 3', ~3.5 km SE of dam, -25.2907, -65.3057
Guaranita goloboffi?	Argentina, Salta, Cabra Corral, 'site 1', ~5 km E Coronel Moldes, -25.287, -65.4238
Guaranita munda	Argentina, Catamarca, Cerro Colorado -27.0, -66.0
Guaranita munda	Argentina, Corrientes, Corrientes City, Laguna Brava, -27.49, -58.716
Guaranita munda	Argentina, Jujuy, Ledesma Dept., Caimancito oilfield, -23.6452, -64.6042
Guaranita munda	Brazil, Rio Grande do Sul, Quarái, Estancia São Roberto, -30.37, -56.42
Guaranita munda?	Argentina, Córdoba, ~2.5 km E Nono, -31.8025, -64.9762
Guaranita munda?	Argentina, Córdoba, ~1.5 km E Nono, -31.798, -64.9877
Guaranita sp.	Argentina, Jujuy, between San Salvador and Purmamarca, 'site 2', -23.8849, -65.4613
Guaranita sp.	Argentina, Entre Rios, PN El Palmar, -31.9, -58.25
Guaranita sp.	Argentina, Entre Rios, PN El Palmar, Arroyo El Palmar, -31.8931, -58.2385
Guaranita sp.	Argentina, Entre Rios, PN El Palmar, Sector Sur, -31.8877, -58.3119
Guaranita sp.	Argentina, Salta, ~5 km W Cafayate, 'site 1', -26.0641, -66.0294
Guaranita yaculica	Argentina, Corrientes, nr. Tacuarita, -28.85, -58.44
Guaranita yaculica	Argentina, Jujuy, Calilegua N.P., Seccional Aguas Negras, -23.7667, -64.8517
Guaranita yaculica	Argentina, Jujuy, Calilegua N.P., park entry area, -23.76, -64.85
Guaranita yaculica	Argentina, Jujuy, Aguas Negras, -23.7217, -64.8267
Guaranita yaculica	Argentina, Jujuy, Calilegua N.P., N Margins Zanjón Seco, -23.6868, -64.5738
Guaranita yaculica	Argentina, Jujuy, Calilegua N.P., Caimancito oilfield, -23.617, -64.6008

Taxa	Locality
Guaranita yaculica	Argentina, Salta, Aguas Blancas-Yaculica, -22.72, -64.4
Guaranita yaculica?	Argentina, Jujuy, Calilegua National Park, ~1 km NW of headquarters, -23.754, -64.8537
Guaranita yaculica?	Paraguay, Boqueron, Enciso, -21.206, -61.6574
Guaranita yaculica?	Paraguay, Boqueron, Enciso, -21.1997, -61.6607
Guaranita yaculica?	Argentina, Jujuy, Calilegua National Park, near camping area, -23.7612, -64.8517
Ibotyporanga bariro	Venezuela, Falcón, SE Bariro, 10.7304, -70.6957
Ibotyporanga diroa	Brazil, Bahia, Toca da Esperança, Jussara, -11.15, -42.11
Ibotyporanga diroa	Brazil, Bahia, near Toca da Esperança, -11.0314, -42.0672
Ibotyporanga emekori	Brazil, Bahia, Central, Abrigo de Pilões, -11.0577, -42.1044
Ibotyporanga emekori	Brazil, Bahia, Central, Toca do Indio, -11.018, -42.1558
Ibotyporanga emekori	Brazil, Bahia, Interior da Gruta dos Noivos, -12.4166, -45.0749
Ibotyporanga emekori	Brazil, Bahia, Serra do Pau D'Arco, near Toca do Índio, -11.0534, -42.1252
Ibotyporanga emekori	Brazil, Bahia, Toca de Pilões, -11.0578, -42.1044
Ibotyporanga naideae	Brazil, Amazonas, Manaus, Reserva Campina, -2.5908, -60.0308
Ibotyporanga naideae	Brazil, Maranhão, Reserva Ecológica Inhamum, -4.8917, -43.4147
Ibotyporanga naideae	Brazil, Maranhão, Campus UEMA, -4.8658, -43.355
Ibotyporanga naideae	Brazil, Mato Grosso, Poconé: Fazenda Sta. Ines, -16.26, -56.62
Ibotyporanga naideae	Brazil, Mato Grosso do Sul, Usina Hidrelétrica Sérgio Motta, -22.4781, -52.9581
Ibotyporanga naideae	Brazil, Mato Grosso do Sul, Hotel Passo do Lontra, -19.5747, -57.03778
Ibotyporanga naideae	Brazil, Mato Grosso do Sul, Morro do Azeite, -19.4833, -57.3167
Ibotyporanga naideae	Brazil, Mato Grosso do Sul, Piraputanga, Fazenda Correntes II, -20.45, -55.5
Ibotyporanga naideae	Brazil, Minas Gerais, Campus da UFMG, -19.8683, -43.9658
Ibotyporanga naideae	Brazil, Minas Gerais, trail to Cachoeira das Ostras, -20.0947, -44.0154
Ibotyporanga naideae	Brazil, Minas Gerais, Floresta Estadual Uaimii, -20.2966, -43.5747
Ibotyporanga naideae	Brazil, Minas Gerais, Fazenda Sapé, -19.5, -44.1167
Ibotyporanga naideae	Brazil, Minas Gerais, Parque Municipal das Mangabeiras, -19.9541, -43.9053
Ibotyporanga naideae	Brazil, Minas Gerais, Monumento Natural Serra da Calçada, -20.0971, -44.0279
Ibotyporanga naideae	Brazil, Pará, Aurá, -1.41, -48.39
Ibotyporanga naideae	Brazil, Pará, Bosque Rodrigues Alves, -1.4303, -48.4562
Ibotyporanga naideae	Brazil, Piauí, Fazenda Nazareth, Município de José de Freitas, -4.756, -42.5755
Ibotyporanga naideae	Brazil, Piauí, Fazenda do Colégio Técnico de Floriano, at Rio Parnaíba, -6.7592, -43.0550
Ibotyporanga naideae	Brazil, Piauí, Interior de residência, Bairro Meladão, -6.7836, -43.0399
Ibotyporanga naideae	Brazil, Piauí, Distrito de Irrigação de Tabuleiros Litorâneos do Piauí, -3.0123, -41.7968
Ibotyporanga naideae	Brazil, Piauí, Parque Municipal Pedra do Castelo, -5.2016, -41.6872
Ibotyporanga naideae	Brazil, Tocantins, Porto Nacional, -10.7, -48.4
Ibotyporanga naideae	Brazil, São Paulo, Campinas, -22.9, -47.07
Ibotyporanga ramosae	Brazil, Bahia, São Desidério, Gruta das Pedras Brilhantes, -12.609, -45.00
Ibotyporanga ramosae	Brazil, Bahia, near Gruta da Passagem, -12.4177, -45.0743
Ibotyporanga sp.	Brazil, Rondônia, Floresta Nacional do Jamari, Trilha Pedra Grande, -9.1979, -63.0810

Taxa	Locality
Ibotyporanga sp.	Brazil, Rondônia, Floresta Nacional de Jamari, Gran Piedra, -9.198, -63.082
Ibotyporanga sp.	Paraguay, Boqueron, Enciso, -21.2029, -61.6591
Ibotyporanga sp.	Brazil, Piauí, Parque Nacional da Serra das Confusões, -8.9756, -43.8181
Ibotyporanga sp.	Brazil, Piauí, Parque Nacional da Serra das Confusões, -9.2257, -43.4630
Ibotyporanga sp.	Brazil, Piauí, Parque Nacional da Serra das Confusões, -8.9380, -43.8633
Ibotyporanga sp.	Brazil, Ceará, Sítio Fundão, -7.2345, -39.4384
Ibotyporanga sp.	Brazil, Piauí, Bairro Morada do Sol, -5.0656, -42.7669
Ibotyporanga sp.	Brazil, Piauí, Fazenda Bonito, ECB Rochas Ornamentais do Brasil LTDA, -5.2266, -41.6970
Ibotyporanga sp.	Brazil, Piauí, Parque Nacional da Serra da Capivara, near Baião das Andorinhas, -8.8605, -42.6863
Ibotyporanga sp.	Brazil, Piauí, Parque Nacional da Serra da Capivara, Baixão das Andorinhas, -8.8614, -42.6867
Ibotyporanga sp.	Brazil, Piauí, Parque Nacional da Serra da Capivara, near Boqueirão do Ferreira, -8.7476, -42.4870
Ibotyporanga sp.	Brazil, Piauí, Bairro Via Azul, -6.7827, -43.0179
Ibotyporanga sp.	Brazil, Piauí, Residencial Angelim, Bairro Curtume, -6.7922, -43.0117
Ibotyporanga sp.	Brazil, Piauí, Bairro Meladão, -6.7836, -43.0399
Ibotyporanga sp.	Brazil, Piauí, Parque Municipal Pedra do Castelo, -5.2016, -41.6872
Ibotyporanga sp.	Brazil, Roraima, at road BR432, ~10km from Cantá, 2.5876, -60.641
Ibotyporanga sp.	Brazil, Minas Gerais, at road BR 367, -16.5689, -41.4838
Ibotyporanga sp.	Brazil, Minas Gerais, near Itaobim, -16.5688, -41.4809
Ibotyporanga sp.	Brazil, Minas Gerais, at road BR 111, -16.5061, -41.5089
Ibotyporanga sp.	Brazil, Bahia, Fazenda do Seu Washinton, -14.1830, -42.81280
Ibotyporanga sp.	Brazil, Bahia, near Buraco do Possidônio, -11.6473, -41.2694
Ibotyporanga sp.	Brazil, Bahia, at road BA-046, -11.793, -42.2901
Ibotyporanga sp.	Brazil, Bahia, Cachoeira da Samambaia, Rio Catolés, -13.306, -41.8544
Ibotyporanga sp.	Venezuela, Falcón, Peninsula de Paraguaná, near Cueva del Guano, 11.9026, -69.9456
Kambiwa anomala	Brazil, Paraiba, Campina Grande, -7.22, -35.89
Kambiwa neotropica	Brazil, Ceará, Zona rural, -5.9992, -38.5366
Kambiwa neotropica	Brazil, Ceará, Serra do Urucu, Santuário Nossa Senhora, -5.035, -39.0106
Kambiwa neotropica	Brazil, Pernambuco, Recife, -8.05, -34.9
Kambiwa neotropica	Brazil, Rio Grande do Norte, Lajedo do Arapuá, -5.5286, -37.614
Kambiwa neotropica	Brazil, Rio Grande do Norte, Estação Ecológica do Seridó, -6.5875, -37.2553
Kambiwa neotropica	Brazil, Rio Grande do Norte, near Portalegre, -6.0163, -37.9916
Kambiwa neotropica	Brazil, Sergipe, Usina Hidrelétrica do Xingó, -9.6244, -37.7967
Kambiwa neotropica	Brazil, Rio Grande do Norte, Lajedo do Arapuá, -5.5292, -37.6143
Kambiwa sp.	Brazil, Piauí, Parque Nacional Serra da Capivara, -8.7672, -42.56
Kambiwa sp.	Brazil, Maranhão, Reserva Ecológica Inhamum, -4.8917, -43.4147
Kambiwa sp.	Brazil, Piauí, Parque Nacional da Serra das Confusões, -9.2211, -43.4892
Kambiwa sp.	Brazil, Piauí, Fazenda Nazareth, -4.7994, -42.63
Kambiwa sp.	Brazil, Piauí, Povoado Boa Hora, -4.9060, -42.8736
Kambiwa sp.	Brazil, Piauí, Povoado Bela Vista, -4.9224, -42.8633
Kambiwa sp.	Brazil, Minas Gerais, Lavras, -21.2483, -45.00139
Kambiwa sp.	Brazil, Bahia, near Sede da Ferbasa, -13.4711, -40.4380
Kambiwa sp.	Brazil, Mato Grosso do Sul, Horto Barra do Moeda, -20.95, -51.7833

Taxa	Locality
Kambiwa sp.	Brazil, Pernambuco, near Riacho Itacuruba, -8.7874, -38.6983
Kambiwa sp.	Brazil, Minas Gerais, Parque Estadual da Mata Seca, -14.8494, -44.0078
Kambiwa sp.	Brazil, Minas Gerais, Parque Estadual da Mata Seca, -14.8483, -43.9881
Kambiwa sp.	Brazil, Minas Gerais, Fazenda Sapé, -19.4684, -44.2416
Kambiwa sp.	Brazil, Pará, FLONA de Carajás, Cave N30031 (GEM-1920), -6.0436, -50.2192
Kambiwa sp.	Brazil, Pará, FLONA de Carajás, Cave N30027 (GEM-1916), -6.0444, -50.2194
Kambiwa sp.	Brazil, Pará, FLONA de Carajás, Cave N30070, -6.0442, -50.23
Kambiwa sp.	Brazil, Pará, FLONA de Carajás, Cave N4WS0057 (GEM-1836), -6.0758, -50.1911
Kambiwa sp.	Brazil, Pará, FLONA de Carajás, Cave N4WS0060 (GEM-1839), -6.0981, -50.19
Kambiwa sp.	Brazil, Pará, FLONA de Carajás, Cave N5SM10014 (GEM-1187), -6.1069, -50.135
Kambiwa sp.	Brazil, Pará, FLONA de Carajás, Cave N5S0026 (GEM-1023), -6.0875, -50.1272
Kambiwa sp.	Brazil, Pará, FLONA de Carajás, Cave N4WS0076 (GEM-1860), -6.0744, -50.1883
Kambiwa sp.	Brazil, Pará, FLONA de Carajás, Cave N5S0005 (GEM-1047), -6.1058, -50.1336
Kambiwa sp.	Brazil, Pará, FLONA de Carajás, Cave N4E0053 (GEM-1099), -6.0342, -50.1672
Kambiwa sp.	Brazil, Pará, FLONA de Carajás, Cave N4E0048 (GEM-995), -6.0375, -50.1603
Kambiwa sp.	Brazil, Ceará, at road BR 122, -5.5735, -38.9704
Kambiwa sp.	Brazil, Pernambuco, Parque Nacional do Catimbau, Trilha da Igreja, -8.3343, -35.9609
Kambiwa sp.	Brazil, Piauí, Parque Nacional de Sete Cidades, near Cachoeira do Riachão, -4.1060, -41.6764
Kambiwa sp.	Brazil, Rio Grande do Norte, at road BR 304, -5.6755, -36.4992
Kambiwa sp.	Bolivia, Santa Cruz, Yabaré, -16.4417, -62.1725
Magana velox	Oman, Ash Sharqiyah South, between Sur and Al Kamil, 22.462, 59.388
Nerudia atacama	Chile, Atacama, Cuesta Pajonales, S Domeyko, -29.151, -70.98
Nerudia atacama	Chile, Atacama, Cuesta Pajonales, S Domeyko, -29.146, -70.997
Nerudia centaura	Argentina, Catamarca, ~20 km E Paso de San Francisco, ‘site 1’, -26.9276, -68.0709
Nerudia centaura	Argentina, Catamarca, ~20 km E Paso de San Francisco, ‘site 2’, -26.936, -68.0925
Nerudia centaura	Argentina, Catamarca, ~20 km E Paso de San Francisco, ‘site 2’, highest, -26.9369, -68.0977
Nerudia colina	Argentina, Jujuy, between San Salvador and Purmamarca, 'site 2', -23.8849, -65.4613
Nerudia colina	Argentina, Jujuy, between San Salvador and Purmamarca, 'site 1', -23.8866, -65.4588
Nerudia flecha	Chile, Coquimbo, Pascua Lama, -29.445, -70.502
Nerudia guirnalda	Argentina, Catamarca, El Rodeo, trail to Cristo Redentor, -28.2229, -65.8677
Nerudia guirnalda	Argentina, Catamarca, Mutquín, -28.3167, -66.1167
Nerudia guirnalda	Argentina, Catamarca, El Rodeo, -28.2167, -65.8667
Nerudia hoguera	Argentina, La Rioja, between Chilecito and Famatina, -29.0027, -67.4855

Taxa	Locality
Nerudia rocio	Argentina, San Juan, ~35 km W Las Flores, -30.3967, -69.5576
Nerudia nono	Argentina, Córdoba, ~5 km E Nono, -31.7982, -64.9515
Nerudia ola	Argentina, San Juan, ~7.5 km S Astica, -31.0223, -67.2976
Nerudia ola	Argentina, San Juan, San Agustín de Valle Fértil, -30.6366, -67.4863
Nerudia ola	Argentina, San Juan, Parque Provincial Ischigualasto, -30.1839, -67.9026
Nerudia ola	Argentina, San Juan, Parque Provincial Ischigualasto, -30.1821, -67.901
Nerudia ola	Argentina, San Juan, Baldecitos, -30.2232, -67.6942
Nerudia ola	Argentina, San Juan, Valle Fértil, Parque Natural Valle Fértil, -30.6378, -67.4892
Nerudia ola?	Argentina, Catamarca, ~5 km NW Chumbicha, near Balneario El Caolín, 'site 2', -28.8109, -66.25
Nerudia ola?	Argentina, Catamarca, near Nacimientos, -27.1559, -66.6925
Nerudia ola?	Argentina, Catamarca, ~10 km N Belén, -27.5641, -67.0058
Nerudia ola?	Argentina, Catamarca, ~14 km W Fiambalá, -27.659, -67.7607
Nerudia ola?	Argentina, Catamarca, ~5 km NW Chumbicha, near Balneario El Caolín, 'site 1', -28.8152, -66.2478
Nerudia ola?	Argentina, Catamarca, Chumbicha, -28.8667, -66.2333
Nerudia ola?	Argentina, La Rioja, SE Aimogasta, ‘site 2’, -28.9015, -66.6538
Nerudia ola?	Argentina, La Rioja, Cuesta de Miranda, ‘site 1’, -29.3511, -67.7924
Nerudia ola?	Argentina, La Rioja, Cuesta de Miranda, ‘site 2’, -29.3468, -67.7205
Nerudia ola?	Argentina, La Rioja, between Chilecito and Famatina, -29.0027, -67.4855
Nerudia ola?	Argentina, La Rioja, Cuesta de Miranda, -29.35, -67.72
Nerudia ola?	Argentina, San Juan, ~35 km W Las Flores, -30.3967, -69.5576
Nerudia ola?	Argentina, La Rioja, SE Aimogasta, ‘site 1’, -28.8069, -66.6635
Nerudia poma	Argentina, Catamarca, ~5 km NW Chumbicha, near Balneario El Caolín, 'site 2', -28.8109, -66.25
Nerudia poma	Argentina, La Rioja, SE Aimogasta, ‘site 2’, -28.9015, -66.6538
Nerudia poma	Argentina, Salta, ~15 km NW Campo Quijano, -24.7918, -65.7297
Nerudia poma	Argentina, Salta, Cabra Corral, ‘site 3’, ~3.5 km SE of dam, -25.2907, -65.3057
Nerudia poma	Argentina, Salta, Cabra Corral, ‘site 4’, W end of bridge, -25.2837, -65.3939
Nerudia poma	Argentina, Salta, 35 km NW Rosario de Lerma, -24.7378, -65.7544
Nerudia poma?	Argentina, Salta, ~5 km W Cafayate, ‘site 1’, -26.0641, -66.0294
Nerudia poma?	Argentina, Salta, Chuscha, 6 km NW Cafayate, -26.035, -66.017
Nerudia sp. Arg163	Argentina, La Rioja, SE Aimogasta, ‘site 2’, -28.9015, -66.6538
Nerudia sp. Arg23a	Argentina, San Juan, ~35 km W Las Flores, -30.3967, -69.5576
Nerudia trigo	Argentina, Salta, ~1 km SW Alemanía, -25.63, -65.618
Nerudia trigo	Argentina, Salta, between Alemanía and Cafayate, -25.7023, -65.7022
Ninetinae undetermined genus	Cuba, Santiago de Cuba, Siboney, no precise locality, 19.96, -75.71
Ninetinae undetermined genus	Brazil, Mato Grosso do Sul, Assentamento Canãa, Cave Gruta Córrego Azul I (Gruta 1), -20.7631, -56.7528
Ninetinae undetermined genus	Brazil, Pará, FLONA de Carajás, Cave N4WS0055 (GEM-1834), -6.0806, -50.1958
Ninetinae undetermined genus	Brazil, Piauí, Parque Nacional da Serra da Capivara, near Boqueirão do Ferreira, -8.7476, -42.4870
Ninetinae undetermined genus	Brazil, Minas Gerais, Parque Nacional Cavernas do Peruaçu, área de antenas de rádio/TV, -15.0498, -44.1819

Taxa	Locality
Ninetinae undetermined genus	Brazil, Minas Gerais, Parque Nacional Cavernas do Peruaçu, near Lapa do Rezar, -15.1430, -44.2343
Papiamenta levii	Netherlands Antilles, Curaçao, Coral [Koraal] Specht, 3 km E Willemstad, 12.0909, -68.8909
Papiamenta levii	Netherlands Antilles, Curaçao, S slope Veeris Berg, 12.1258, -68.9643
Papiamenta levii	Netherlands Antilles, Curaçao, Piscadera Baai, 12.1395, -68.9675
Papiamenta levii	Netherlands Antilles, Curaçao, SE airport, 12.1787, -68.9447
Papiamenta savonet	Netherlands Antilles, Curaçao, 3 km N Savonet, 12.37, -69.124
Papiamenta sp.	Netherlands Antilles, Curaçao, Grote Berg, 12.1909, -68.9979
Papiamenta sp.	Netherlands Antilles, Curaçao, near San Juan, Manzalina beach, 12.245, -69.105
Papiamenta sp.	Netherlands Antilles, Curaçao, Boca San Pedro [Boka San Pedro], 12.256, -69.043
Pemona sapo	Venezuela, Bolívar, Canaima, near Salto El Sapo, 6.254, -62.848
Pholcophora americana	USA, Oregon, Josephine Co., Siskiyou Nat. Forest, 42.337, -123.6095
Pholcophora americana	Canada, British Columbia, Ashcroft, 50.6907, -121.2726
Pholcophora americana	Canada, British Columbia, Ashcroft, 50.6006, -121.2961
Pholcophora americana	Canada, British Columbia, Ashcroft, 50.5389, -121.2768
Pholcophora americana	Canada, British Columbia, Ashcroft, 50.5252, -121.2787
Pholcophora americana	USA, California, Aspen Valley, Yosemite Park, 37.83, -119.77
Pholcophora americana	USA, California, Balboapark, San Diego, 32.734, -117.145
Pholcophora americana	USA, Idaho, Boise Co., Boise River above Arrowrock Dam, 43.597, -115.922
Pholcophora americana	USA, New Mexico, Cibola Co., Mt. Taylor, 35.24, -107.61
Pholcophora americana	Canada, British Columbia, Cranbrook, 49.5736, -115.5064
Pholcophora americana	USA, Montana, Flathead Co., Bigfork, 48.06, -114.07
Pholcophora americana	USA, Montana, Flathead Co., La Salle, 48.3, -114.24
Pholcophora americana	Canada, British Columbia, Flathead Valley, 49.1269, -114.4101
Pholcophora americana	USA, California, Grizzly Peak nr. Berkley, 37.883, -122.239
Pholcophora americana	Canada, British Columbia, Hedley, Old Hedley Road, 49.382, -119.160
Pholcophora americana	Canada, British Columbia, Hedley, Old Hedley Road, 49.384, -120.190
Pholcophora americana	Canada, British Columbia, Hudson's Hope, 56.0966, -121.8158
Pholcophora americana	USA, Oregon, Jackson Co., nr. Medford, 42.3, -122.87
Pholcophora americana	Canada, British Columbia, Keremeos, Ashnola River Road, 49.188, -120.002
Pholcophora americana	USA, Oregon, Klamath Co., Crater Lake NP, 42.87, -122.17
Pholcophora americana	USA, Colorado, Larimer Co., Ft. Collins, 40.55, -105.1
Pholcophora americana	Canada, British Columbia, Lillooet, Bridge River, Trehorne Dam, 50.8076, -122.1757
Pholcophora americana	Canada, British Columbia, Lillooet, Yalakom River Road, km 38, 50.8859, -122.2058
Pholcophora americana	Canada, British Columbia, Lillooet, Yalakom River Road, Yalakom River Forest Recreation Site, 50.9128, -122.2383
Pholcophora americana	Canada, British Columbia, Merritt, 49.9361, -120.9051
Pholcophora americana	USA, Colorado, Montrose Co., Black Canyon of the Gunnison, 38.58, -107.71
Pholcophora americana	Canada, British Columbia, Okanagan Falls, Allendale Road, 49.3260, -119.5447
Pholcophora americana	Canada, British Columbia, Okanagan Falls, Vaseaux Lake, 49.2999, -119.5273

Taxa	Locality
Pholcophora americana	Canada, British Columbia, Oliver, 49.1524, -119.54372
Pholcophora americana	Canada, British Columbia, Osoyoos, 49.0945, -119.5227
Pholcophora americana	Canada, British Columbia, Osoyoos, 49.0757, -119.4901
Pholcophora americana	Canada, British Columbia, Osoyoos, Grasslands Conservation Area, 49.0162, -119.5869
Pholcophora americana	Canada, British Columbia, Osoyoos, Kilpoola Lake, 49.0300, -119.5622
Pholcophora americana	USA, New Mexico, Otero Co., no precise locality, 32.9, -105.9
Pholcophora americana	Canada, British Columbia, Pavilion Lake, 50.7987, -121.6185
Pholcophora americana	Canada, British Columbia, Penticton, Max/Madeleine Lake, 49.5106, -119.6461
Pholcophora americana	Canada, British Columbia, Revelstoke, Sale Mountain, 51.1663, -118.1329
Pholcophora americana	USA, Utah, Salt Lake Co., Saltair on Great Salt Lake, 40.74, -112.17
Pholcophora americana	Canada, British Columbia, Seton Portage, 50.6502, -122.4199
Pholcophora americana	USA, Washington, Stevens Co., Cedar Lake, N Leadpoint, 48.94, -117.59
Pholcophora americana	Canada, British Columbia, Summerland, Peach Orchard Cemetary, 49.6119, -119.6574
Pholcophora americana	USA, Wyoming, Teton Co., Yellowstone NP, 44.42, -110.59
Pholcophora americana	USA, Utah, Utah Co., Lehi, 40.39, -111.85
Pholcophora americana	Canada, British Columbia, Vaseaux Creek, 49.2681, -119.5154
Pholcophora americana	Canada, British Columbia, Vaseaux Lake, Kennedy Flats, 49.2538, -119.5221
Pholcophora americana	USA, Nevada, Washoe Co., Little Valley, Whitetail Forest Reserve, 39.24, -119.88
Pholcophora americana	Canada, British Columbia, Williams Lake, Lynes Creek Road, 52.2932, -122.1562
Pholcophora americana	USA, California, Mono County, Inyo Nat. Forest, 37.8, -118.38
Pholcophora americana	USA, Montana, Missoula Co., Lolo Forest, 47.0715, -113.3843
Pholcophora bahama	Bahamas, Rum Cay, nr. Port Nelson, 23.65, -74.84
Pholcophora bahama	Turks and Caicos Islands, West Caicos, 21.67, -72.46
Pholcophora maria	Mexico, Yucatán, Cueva (Actún) Xpukil, 20.55, -89.91
Pholcophora mexcala	Mexico, Guerrero, Mexcala [=Mezcala], 17.93, -99.6
Pholcophora sp.	Puerto Rico, Isla Monito, 18.16, -67.95
Pholcophora sp.	Mexico, Puebla, ~35 km SE Tehuacan, W of Calapa bridge, 18.1619, -97.2647
Pholcophora sp.	Mexico, Puebla, ~35 km SE Tehuacan, N of Calapa bridge, 18.1652, -97.2605
Pholcophora sp.	Mexico, Guerrero, ~2 km N Mazatlán, 17.4567, -99.474
Pholcophora sp.	Mexico, Guerrero, ~5 km S Papanoa, 17.2711, -101.0328
Pholcophora sp.	Mexico, Puebla, ~35 km SE Tehuacan, N of Calapa bridge, 18.1652, -97.2605
Pholcophora texana	Mexico, Hidalgo, ~2.5 km SW Jacala, 20.9948, -99.2138
Pholcophora texana	Mexico, Hidalgo, Jacala, 2 mi SW, 21.0, -99.2
Pholcophora texana	Mexico, Nuevo León, Montemorelos, 25.18, -99.83
Pholcophora texana	Mexico, Nuevo León, Grutas de San Bartolo, 16 km S Santa Catarina, 25.5, -100.45
Pholcophora texana	Mexico, San Luis Potosí, 2 mi E Santo Domingo, 22.87, -100.25
Pholcophora texana	Mexico, Tamaulipas, Rio Guayalejo, nr. Forlón, 23.21, -98.8
Pholcophora texana	Mexico, Tamaulipas, El Tinieblo, 24.296, -98.452
Pholcophora texana	Mexico, Tamaulipas, San Fernando, 24.85, -98.15
Pholcophora texana	USA, Texas, Hidalgo Co., Edinburg, 26.3, -98.16

Taxa	Locality
Pholcophora texana	USA, Texas, 0.5 mi [Gertsch & Mulaik 1940: 5 mi] E Rio Grande City, 26.36, -98.8
Pinocchio barauna	Brazil, Rio Grande do Norte, near Baraúna, Caverna Porco do Mato II, -5.0467, -37.5398
Tolteca hesperia?	Mexico, Baja California Sur, Cabo San Lucas, 22.8897, -109.9156
Tolteca hesperia?	Mexico, Baja California Sur, nr. La Paz, 24.12, -110.3
Tolteca sp.	Mexico, Colima, ~17 km E Manzanillo, 19.0115, -104.1382
Tolteca sp.	Mexico, Colima, Manzanillo, 12 mi E, 19.02, -104.13
Tolteca sp.	Mexico, Colima, Colima, 10 mi S, 19.1, -103.7
Tolteca sp.	Mexico, Colima, ~6 km S Coquimatlán, 19.1521, -103.835
Tolteca sp.	Mexico, Michoacán, ~4 km W Huahua, 18.1972, -103.0449
Tolteca sp.	Mexico, Michoacán, ~20 km W Huahua, 18.2346, -103.202
Tolteca sp.	Mexico, Oaxaca, Tehuantepec, 3 mi W, 16.35, -95.33
Tolteca sp.	Mexico, Oaxaca, Tehuantepec, 8 mi W, 16.3667, -95.3667
Tolteca sp.	Mexico, Oaxaca, ~17 km NW Tehuantepec, 16.3919, -95.3865
Tolteca sp.	Mexico, Oaxaca, Tehuantepec, 12 mi W, 16.4, -95.41
Tolteca sp.	Mexico, Oaxaca, Tequisistlán, 5 mi W, 16.41, -95.69
Tolteca sp.	Mexico, Oaxaca, 2 mi SE Niltepec, 16.55, -94.58
Tolteca sp.	Mexico, Oaxaca, ~3 km N San Pedro Totolapa, 16.6976, -96.318
Tolteca hesperia	Mexico, Sinaloa, 3 mi E Esquinapa, 22.83, -105.73
Tolteca hesperia	Mexico, Sinaloa, Mazatlán, 35 mi S, 22.869, -106.049
Tolteca hesperia	Mexico, Sinaloa, ~3 km S Rosario, 22.9584, -105.849
Tolteca hesperia	Mexico, Sinaloa, Mazatlán, 5 mi S, 23.172, -106.34
Tolteca hesperia	Mexico, Sinaloa, Villa Union, 6 mi E, 23.2, -106.13
Tolteca hesperia	Mexico, Sinaloa, Mazatlán, 20 mi E, 23.27, -106.17
Tolteca hesperia	Mexico, Sinaloa, 5 mi E Concordia, 23.32, -105.99
Tolteca hesperia	Mexico, Sinaloa, Villa Union, 32 mi E, 23.44, -105.83
Tolteca hesperia	Mexico, Sinaloa, Culiacan, 62 mi S, El Esquintal, 24.12, -106.89
Tolteca hesperia	Mexico, Sinaloa, Culiacan, 40 mi S, 24.35, -107.09
Tolteca jalisco	Mexico, Jalisco, 29 mi N La Quemada, 21.18, -104.085
Tolteca jalisco	Mexico, Jalisco, N La Quemada, ‘site 2’, 21.1922, -104.0975

Table S5. Significant principal components used for environmental niche analyses

Significant principal components (PC) for the environmental layers used to compare the environmental niche occupied by *Nerudia* and other Ninetinae taxa. The selected PCs are those in which the total cumulative percentage of total variation sum at least 95%.

Parameter	PC1	PC2	PC3	PC4	PC5	PC6	PC7	PC8
Standard deviation	3.155	2.017	1.362	1.218	0.946	0.935	0.790	0.633
Proportion of variance	47.4%	19.4%	8.8%	7.1%	4.3%	4.2%	3.0%	1.9%
Cumulative proportion	47.4%	66.8%	75.6%	82.7%	86.9%	91.1%	94.1%	96.0%

Table S6. Eigenvectors of covariance factor of the principal components

Eigenvectors of covariance factor of the principal components (PC) for the environmental layers used to compare the environmental niche occupied by *Nerudia* and other Ninetinae taxa. The selected PCs are those in which the total cumulative percentage of total variation sum at least 95%.Variables are sorted in order of importance for the first principal component.

Variables	PC1	PC2	PC3	PC4	PC5	PC6	PC7	PC8
Temperature seasonality	0.282	0.045	0.110	-0.292	0.026	0.085	-0.097	0.264
Temperature annual range	0.273	-0.009	0.230	-0.276	0.178	0.108	-0.017	0.070
Mean diurnal range	0.129	-0.193	0.394	-0.087	0.491	0.038	0.234	-0.548
Precipitation of driest month	0.003	0.435	-0.092	-0.252	-0.072	-0.148	0.196	-0.250
Canopy height	-0.013	0.186	0.399	0.167	-0.359	0.419	-0.545	-0.385
Precipitation of driest quarter	-0.018	0.452	-0.092	-0.226	-0.061	-0.099	0.171	-0.244
Tree density	-0.045	0.027	0.491	0.128	-0.446	0.167	0.673	0.215
Precipitation of coldest quarter	-0.112	0.348	-0.088	0.075	0.354	0.357	0.159	0.139
Precipitation of warmest quarter	-0.140	0.108	0.400	-0.075	-0.115	-0.657	-0.155	0.051
Precipitation seasonality	-0.141	-0.319	0.213	0.225	0.217	-0.065	-0.009	0.131
Max. temperature of warmest month	-0.213	-0.143	0.109	-0.496	0.057	0.271	0.000	0.019
Annual precipitation	-0.219	0.325	0.134	0.019	0.188	-0.027	-0.067	0.052
Mean temperature of wettest quarter	-0.238	-0.185	0.036	-0.278	-0.046	-0.181	-0.021	-0.101
Precipitation of wettest quarter	-0.250	0.218	0.201	0.089	0.248	-0.019	-0.115	0.221
Precipitation of wettest month	-0.254	0.202	0.190	0.085	0.253	-0.008	-0.114	0.239
Mean temperature of warmest quarter	-0.255	-0.137	0.021	-0.405	-0.069	0.120	-0.060	0.092
Isothermality	-0.274	-0.052	-0.091	0.291	0.100	-0.034	0.175	-0.345
Mean temperature of driest quarter	-0.279	-0.013	-0.115	-0.022	-0.061	0.237	0.032	0.048
Annual mean temperature	-0.300	-0.121	-0.024	-0.151	-0.067	0.024	0.000	-0.057
Min. temperature of coldest month	-0.307	-0.056	-0.131	-0.004	-0.114	0.035	0.013	-0.046
Mean temperature of coldest quarter	-0.308	-0.097	-0.057	-0.011	-0.050	0.002	0.031	-0.124

Table S7. Significant principal components and phylogenetic signal

Significant principal components (PC) for the environmental layers used to compute the phylogenetic signal for the environmental niche of *Nerudia* and other taxa in the phylogenetic analyses. The selected PCs are those in which the total cumulative percentage of total variation sum at least 95%.

Parameter	PC1	PC2	PC3	PC4	PC5	PC6	PC7
Standard deviation	3.170	1.941	1.504	1.262	0.968	0.916	0.791
Proportion of variance	47.8%	17.9%	10.8%	7.6%	4.5%	4.0%	3.0%
Cumulative proportion	47.8%	65.8%	76.6%	84.1%	88.6%	92.6%	95.6%

Table S8. Eigenvectors and phylogenetic signal

Eigenvectors of covariance factor of the principal components (PC) for the environmental layers used to compute the phylogenetic signal for the environmental niche of *Nerudia* and other taxa in the phylogenetic analyses. The selected PCs are those in which the total cumulative percentage of total variation sum at least 95%. Variables are sorted in order of importance for the first principal component.

Variables	PC1	PC2	PC3	PC4	PC5	PC6	PC7
Min. temperature of coldest month	0.292	-0.142	-0.102	0.124	-0.061	0.116	-0.047
Mean temperature of coldest quarter	0.287	-0.176	-0.118	0.040	-0.016	0.130	-0.048
Precipitation of wettest month	0.286	0.045	0.010	-0.170	0.101	-0.323	-0.031
Precipitation of wettest quarter	0.285	0.057	0.029	-0.178	0.114	-0.315	-0.027
Annual precipitation	0.284	0.126	0.112	-0.128	0.130	-0.215	-0.022
Annual mean temperature	0.253	-0.298	0.017	0.046	-0.010	0.117	-0.031
Mean temperature of driest quarter	0.233	-0.123	0.141	0.332	-0.323	-0.204	-0.131
Precipitation of warmest quarter	0.212	0.059	0.130	-0.420	0.341	0.103	0.147
Isothermality	0.207	0.210	-0.340	0.029	0.069	0.017	-0.073
Precipitation of driest quarter	0.204	0.277	0.305	0.061	0.121	0.207	0.078
Precipitation of coldest quarter	0.201	0.145	0.105	0.271	0.104	-0.474	0.304
Mean temperature of wettest quarter	0.177	-0.318	-0.131	-0.180	0.274	0.348	0.051
Mean temperature of warmest quarter	0.176	-0.393	0.201	0.079	-0.011	0.062	0.006
Precipitation of driest month	0.170	0.281	0.341	0.090	0.112	0.284	0.070
Max. temperature of warmest month	0.132	-0.400	0.299	0.052	-0.006	0.002	-0.011
Tree density	0.118	0.055	0.023	-0.350	-0.627	0.123	0.648
Canopy height	0.103	0.100	0.192	-0.460	-0.399	-0.051	-0.625
Precipitation seasonality	-0.043	-0.336	-0.323	-0.252	0.049	-0.356	0.148
Temperature seasonality	-0.223	-0.177	0.395	0.023	0.015	-0.123	0.085
Temperature annual range	-0.237	-0.157	0.362	-0.104	0.067	-0.135	0.046
Mean diurnal range	-0.243	-0.049	0.117	-0.284	0.240	-0.049	0.003

Table S9. Phylogenetic signal

Phylogenetic signal (Pagel's λ) analyses using the main principal components detailed in Tables S6-7.

Principal components	Fitted λ	λ logL	λ p-value
PC 1	0.95	-102.83	0.000
PC 2	0.97	-83.22	0.000
PC 3	0.88	-76.19	0.000
PC 4	0.91	-72.00	0.000
PC 5	0.28	-65.87	0.592
PC 6	0.94	-57.16	0.000
PC 7	0.67	-54.78	0.120
PC 8	0.85	-47.18	0.013

Publication 4.5. Huber BA, Meng G, Valdez-Mondragón A, Král J, **Ávila Herrera IM**, Carvalho LS (2023). Short-legged daddy-long-leg spiders in North America: the genera *Pholcophora* and *Tolteca* (Araneae, Pholcidae). European Journal of Taxonomy. 880, 1–89. DOI.org/10.5852/ejt.2023.880.2173

IF2023: 1.398

This paper is an integrative multidisciplinary study of two genera of ninetine pholcids, *Pholcophora* and *Tolteca*, and includes the description of seven new species, scanning electron microscopy of microstructures, molecular phylogeny of analysed genera, and first cytogenetic data of *Tolteca*. Male karyotype of two analysed *Tolteca* species, *T. hesperia* and *T. oaxaca* sp. were formed by very low number of biarmed chromosomes (13-15) including the X_1X_2Y sex chromosome system. The number of chromosome pairs in *Tolteca* is one of the lowest found in araneomorph spiders with monocentric chromosomes. Karyotype contained three NOR-bearing chromosome pairs and probably a sex chromosome-linked NOR. Number of NOR-bearing chromosome pairs was close to their ancestral number in ninetine pholcids.

My contribution: Evaluation of chromosome slides, detection of NORs by FISH. Analysis and interpretation of the results. Involved into preparation of manuscript, preparation of tables and figures. Revision of the manuscript.

European Journal of Taxonomy 880: 1–89
https://doi.org/10.5852/ejt.2023.880.2173
[redacted]
ISSN 2118-9773
www.europeanjournaloftaxonomy.eu
2023 · Huber B.A. *et al.*

Monograph

urn:lsid:zoobank.org:pub:3F806FD6-2EB3-456A-AFD7-780A0FBEB2DA

Short-legged daddy-long-leg spiders in North America: the genera *Pholcophora* and *Tolteca* (Araneae, Pholcidae)

Bernhard A. HUBER [1,*], Guanliang MENG [2], Alejandro VALDEZ-MONDRAGÓN [3], Jiří KRÁL [4], Ivalú M. ÁVILA HERRERA [5] & Leonardo S. CARVALHO [6]

[1,2] Zoological Research Museum Alexander Koenig, LIB, Bonn, Germany.
[3] Laboratory of Arachnology (LATLAX), Institute of Biology, Universidad Nacional Autónoma de México-Tlaxcala, San Miguel Contla, Santa Cruz Tlaxcala, Tlaxcala, México.
[4,5] Department of Genetics and Microbiology, Faculty of Science, Charles University, Prague, Czech Republic.
[6] Campus Amílcar Ferreira Sobral, Universidade Federal do Piauí, Floriano, Piauí, Brazil.

* Corresponding author: b.huber@leibniz-lib.de
[2] Email: G.Meng@leibniz-lib.de
[3] Email: lat_mactans@yahoo.com.mx
[4] Email: spider@natur.cuni.cz
[5] Email: ivalu.a@gmail.com
[6] Email: carvalho@ufpi.edu.br

[1] urn:lsid:zoobank.org:author:33607F65-19BF-4DC9-94FD-4BB88CED455F
[2] urn:lsid:zoobank.org:author:7E8C41F8-77BB-468F-BE9A-D3F1DFCA1E4E
[3] urn:lsid:zoobank.org:author:F043A1C7-2B83-40C9-A74E-82C92F00725A
[4] urn:lsid:zoobank.org:author:E836F3B5-D704-4EEC-966A-0C4F1FAD324B
[5] urn:lsid:zoobank.org:author:E3687584-7F64-450D-9492-BE0DD4864AD6
[6] urn:lsid:zoobank.org:author:28AA7D67-3C9D-495E-8C17-33D35F1A0FAC

Abstract. The North American-Caribbean genera *Pholcophora* Banks, 1896 and *Tolteca* Huber, 2000 are representatives of Ninetinae, a group of small, cryptic, and thus poorly known pholcid spiders. We present the first comprehensive revisions of the two genera, including extensive SEM data and descriptions of seven new species from Mexico (*Pholcophora mazatlan* Huber sp. nov., *P. papanoa* Huber sp. nov., *P. tehuacan* Huber sp. nov., *Tolteca huahua* Huber sp. nov., *T. manzanillo* Huber sp. nov., *T. oaxaca* Huber sp. nov., and *T. sinnombre* Huber sp. nov.). We add new CO1 sequences of nine species to previously published molecular data and use these for a preliminary analysis of relationships. We recover a North American-Caribbean clade including 'true' (mainland) *Pholcophora*, *Tolteca* (Mexico), and a Caribbean clade consisting of the genus *Papiamenta* Huber, 2000 (Curaçao) and Caribbean '*Pholcophora*'. First karyotype data for *Tolteca* ($2n♂ = 13, X_1X_2Y$ and 15, X_1X_2Y, respectively) reveal a strong reduction of the number of chromosome pairs within the North American-Caribbean clade, and considerable karyotype differentiation among congeners. This agrees with considerable CO1 divergence among species of *Tolteca* but contrasts with very inconspicuous morphological divergence. Environmental niche analyses show that the widespread *P. americana* Banks, 1896 (western USA, SW Canada) occupies a very different niche than its Mexican congeners and other close relatives. Caribbean

taxa also have a low niche overlap with 'true' *Pholcophora* and *Tolteca*, supporting the idea that Caribbean '*Pholcophora*' are taxonomically misplaced.

Keywords. Ninetinae, Mexico, barcodes, karyotype, environmental niche.

Huber B.A., Meng, G., Valdez-Mondragón A., Král J., Ávila Herrera I. & Carvalho L.S. 2023. Short-legged daddy-long-leg spiders in North America: the genera *Pholcophora* and *Tolteca* (Araneae, Pholcidae). *European Journal of Taxonomy* 880: 1–89. https://doi.org/10.5852/ejt.2023.880.2173

Table of contents

Abstract....1
Introduction....3
Material and methods....3
Material examined....3
Taxonomy and morphology....4
Molecular data and analyses....4
Preparation of chromosome slides and their evaluation....6
Environmental niche similarity and equivalency....7
Results....8
Molecular data....8
Taxonomy....9
Pholcophora Banks, 1896....9
Pholcophora americana Banks, 1896....14
Pholcophora mazatlan Huber sp. nov.....19
Pholcophora papanoa Huber sp. nov.....24
Pholcophora texana Gertsch, 1935....29
Pholcophora tehuacan Huber sp. nov.....35
Pholcophora "Mex354"....40
Pholcophora? "Car544"....40
Pholcophora? "Cu12-325"....45
Tolteca Huber, 2000....46
Tolteca hesperia (Gertsch, 1982)....49
Tolteca jalisco (Gertsch, 1982)....55
Tolteca manzanillo Huber sp. nov.....57
Tolteca sinnombre Huber sp. nov.....62
Tolteca huahua Huber sp. nov.....65
Tolteca oaxaca Huber sp. nov.....67
Karyology....74
Biogeography....76
Discussion....78
Morphology....78
Relationships....79
Karyology....80
Biogeographic analyses....81
Acknowledgements....83
References....83
Supplementary material....89

Introduction

Pholcid spiders are commonly known as daddy-long-leg spiders, and in fact the large majority of known species are characterized by long and thin legs, reminding of harvestmen, or daddy-long-legs. However, just like harvestmen, Pholcidae C.L. Koch, 1850 includes some short-legged species as well. When Eugène Simon, the founder of modern spider systematics, discovered the first such species in Yemen, he created a separate subfamily for it, the "Ninetidinae" (now Ninetinae) (Simon 1890, 1893). Since then, a few further species have been described, mainly from the New World (Mello-Leitão 1944; Brignoli 1981; Gertsch 1982; Huber 2000; Huber & Carvalho 2019; Huber & Villarreal 2020), but with currently ~50 nominal species, the subfamily continues to be the smallest in terms of species numbers among the five pholcid subfamilies. In part, this is certainly due to their small size and cryptic lifestyle. With body lengths of ~1 mm, many species are among the smallest known Pholcidae (Huber & Eberle 2021), and most species live hidden under rocks and stones. Other aspects that probably contribute to our poor knowledge of the subfamily are the geographic restriction of most species to arid (and thus relatively poorly sampled) regions (Huber & Brescovit 2003; Huber & Carvalho 2019); their phylogenetically conserved environmental niche; and the apparent ability of representatives of certain genera to avoid pitfall traps (Huber *et al.* 2023).

In the New World, almost any tiny pholcid was originally assigned to *Pholcophora* Banks, 1896, a genus created for a species of Ninetinae from the western USA (Banks 1896). The majority of species originally described in *Pholcophora* have since been moved to other genera, partly to newly established genera of Ninetinae (*Galapa* Huber, 2000; *Tolteca* Huber, 2000; *Papiamenta* Huber, 2000; *Guaranita* Huber, 2000), partly to other subfamilies (*Anopsicus* Chamberlin & Ivie, 1938: Modisiminae Simon, 1893; *Chisosa* Huber, 2000: Arteminae Simon, 1893) (Gertsch 1982; Huber 2000; Huber *et al.* 2018). As a result, *Pholcophora* ended up including only three Dominican amber fossil species and five extant species, restricted geographically to North America and the Caribbean. The genus exemplifies well our poor general knowledge of Ninetinae: of the eight nominal species, five have been known from only a single specimen each. The situation is similar with the only other North American genus of Ninetinae: *Tolteca* Huber, 2000. This genus was created for two species originally described in *Pholcophora*; one of them has been known from a single specimen only.

Our knowledge about the phylogenetic relationships among these North American pholcids has also been rudimentary. The most comprehensive phylogeny of Pholcidae (Eberle *et al.* 2018) recognized a "North and Central American and Caribbean" clade of Ninetinae, but the species sample was small (four species, of which two could not confidently be assigned to a genus) and lacked the genus *Tolteca*. A recent comparative study of pholcid sperm ultrastructure (Dederichs *et al.* 2022) found that *Pholcophora* and *Tolteca* share cleistospermia while all other studied Ninetinae have synspermia; since synspermia are thought to be plesiomorphic for Pholcidae, this was a first indication that *Pholcophora* and *Tolteca* might be closely related.

The purpose of this study is a comprehensive revision of North American Ninetinae (*Pholcophora* and *Tolteca*). We provide taxonomic descriptions of several new species and redescriptions of most previously described species, including numerous new records and first extensive SEM data for both genera as a basis for future cladistic analyses of morphological data; we provide first molecular data and first karyotype data for the genus *Tolteca*; and we provide an analysis of niche overlap and of altitudinal ranges in North American ninetines.

Material and methods

Material examined

This study is based on the examination of ~400 adult specimens deposited in the following collections:

AMNH = American Museum of Natural History, New York, USA
LATLAX = Laboratory of Arachnology, Institute of Biology, UNAM-Tlaxcala, Mexico
USNM = National Museum of Natural History, Washington D.C., USA
ZFMK = Zoologisches Forschungsmuseum Alexander Koenig, Bonn, Germany

Further material deposited in the AMNH was examined by the first author in 1999 but not re-examined for the present study.

Taxonomy and morphology

Taxonomic descriptions follow the style of recent publications on Pholcidae (e.g., Huber *et al.* 2023; based on Huber 2000). Measurements were done on a dissecting microscope with an ocular grid and are in mm unless otherwise noted; eye measurements are ± 5 µm. Photos were made with a Nikon Coolpix 995 digital camera (2048 × 1536 pixels) mounted on a Nikon SMZ 18 stereo microscope or a Leitz Dialux 20 compound microscope. CombineZP (https://combinezp.software.informer.com/) was used for stacking photos. Drawings are partly based on photos that were traced on a light table and later improved under a dissecting microscope, or they were directly drawn with a Leitz Dialux 20 compound microscope using a drawing tube. Cleared epigyna were stained with chlorazol black. The number of decimals in coordinates gives a rough indication about the accuracy of the locality data: four decimals means that the collecting site is within about 10 m of the indicated spot; three decimals: within ~100 m; two decimals: within ~1 km; one decimal: within ~10 km. Distribution maps were generated with ArcMap ver. 10.0. For SEM photos, specimens were dried in hexamethyldisilazane (HMDS) (Brown 1993), and photographed with a Zeiss Sigma 300 VP scanning electron microscope. SEM data are presented within the descriptions but are usually not based on the specific specimen described.

Abbreviations used in figures only are explained in the figure legends. Abbreviations used in the text:

ALE = anterior lateral eye(s)
ALS = anterior lateral spinneret(s)
AME = anterior median eye(s)
a.s.l. = above sea level
L/d = length/diameter
PME = posterior median eye(s)
PMS = posterior median spinneret(s)

Molecular data and analyses

Taxon sampling

Three Arteminae outgroup taxa, two specimens of *Pholcophora americana* Banks, 1896, and seven further species of Ninetinae were taken from Eberle *et al.* (2018). To this, we added three further specimens of *P. americana*, four other species of *Pholcophora*, five species of *Tolteca*, and a second specimen of *Papiamenta levii* Huber, 2000. Table 1 lists the newly sequenced specimens. For details on previously sequenced specimens, see Eberle *et al.* (2018).

Gene sampling

For the taxa taken from Eberle *et al.* (2018) we used all available sequences (CO1 barcode, 12S, 16S, 18S, 28S, and H3). The CO1 barcode of one specimen of *Papiamenta levii* was combined with "S011 *Papiamenta MRAC639* MRAC640" from Eberle *et al.* (2018), since they actually came from the same specimen. For all newly added taxa, we sequenced the CO1 barcode only. In total, there were 69 sequences and 27 specimens.

Table 1. Geographic origins of newly sequenced specimens, sorted by code.

Code	Genus	Species	Vial	Country	Admin.	Locality	Lat.	Long.	CO1
N051	*Pholcophora*	*americana*	G090	USA	Idaho	Custer Co., Salmon-Challis Nat. Forest	44.2775	-114.4078	ON970474
N052	*Pholcophora*	*americana*	G091	USA	Oregon	Josephine Co., Siskiyou Nat. Forest	42.3370	-123.6095	ON970475
N057	*Pholcophora*	*mazatlan*	Mex209	Mexico	Guerrero	~2 km N of Mazatlán	17.4567	-99.4740	ON970476
N059	*Tolteca*	*huahua*	Mex229	Mexico	Michoacán	~4 km W of Huahua	18.1972	-103.0449	ON970481
N061	*Tolteca*	*manzanillo*	Mex232	Mexico	Colima	~17 km E of Manzanillo	19.0115	-104.1382	ON970482
N063	*Tolteca*	*jalisco*	Mex241	Mexico	Jalisco	N of La Quemada, 'site 2'	21.1922	-104.0975	ON970483
N064	*Tolteca*	*hesperia*	Mex253	Mexico	Sinaloa	~3 km S of Rosario	22.9584	-105.8490	ON970484
N065	*Pholcophora*	*texana*	Mex341	Mexico	Hidalgo	~2.5 km SW of Jacala	20.9948	-99.2138	ON970477
N066	*Pholcophora*	*tehuacan*	Mex353	Mexico	Puebla	SE of Tehuacan, N of Calapa bridge	18.1652	-97.2605	ON970478
N067	*Pholcophora*	*Mex354*	Mex354	Mexico	Puebla	SE of Tehuacan, N of Calapa bridge	18.1652	-97.2605	ON970479
N068	*Tolteca*	*oaxaca*	Mex362	Mexico	Oaxaca	~3 km N of San Pedro Totolapa	16.6976	-96.3180	ON970485
N069	*Tolteca*	*oaxaca*	Mex368	Mexico	Oaxaca	~17 km NW of Tehuantepec	16.3919	-95.3865	ON970486
N070	*Papiamenta*	*levii*	MRAC639	Curaçao		near San Juan, Manzalina beach	12.2450	-69.1050	ON970473
N071	*Papiamenta*	*levii*	MRAC640	Curaçao		near San Juan, Manzalina beach	12.2450	-69.1050	ON970487
N085	*Pholcophora*	*americana*	USA16	USA	Colorado	Lookout Mountain near Golden	39.7300	-105.2400	ON970480

DNA extraction, amplification and sequencing

One to four legs of specimens stored in non-denatured pure ethanol (~99%) at −20°C were used for DNA extraction. Extracted genomic DNA is deposited at and available from the LIB Biobank, Museum Koenig, Bonn. DNA was extracted using the HotSHOT method (Truett *et al.* 2000). CO1 primers used were LCO1490-JJ and HCO2198-JJ (Astrin *et al.* 2016; primer versions JJ2 served as backup), but with a different tag sequence (from Srivathsan *et al.* 2021) of 13 bp length at the 5'-ends of forward and reverse primers, respectively. The 20 µl reaction volume consisted of 5 µl H_2O, 1 µl DNA template, 2 µl Q-Solution, 10 µl Qiagen Multiplex-Mix, 1 µl forward primer, and 1 µl reverse primer. The PCR procedure was: (1) 95°C for 15 minutes; (2) denaturation at 94°C for 35 seconds; (3) annealing at 55°C (or 40°C) for 90 seconds; (4) elongation at 72°C for 90 seconds; (5) final elongation at 72°C for 10 minutes, followed by cooling at 10°C. Steps 2–4 were repeated for 15 cycles (or 25 cycles). The PCR products were then pooled and sequenced with the Oxford Nanopore Technologies (ONT) GridON platform.

DNA sequence alignment and editing

The newly sequenced CO1 barcodes were then assembled using the ONTbarcoder (Srivathsan *et al.* 2021) pipeline. Taxonomic assignments of the assembled sequences were checked by: (1) blasting assembled sequences against a local NT database; (2) the identification engine of the Barcode of Life Data System (BOLD) (http://www.boldsystems.org/index.php) (Ratnasingham & Hebert 2007; Yang *et al.* 2020).

Multiple sequence alignment (MSA)

For the protein-coding genes CO1 and H3, DNA sequences were translated into protein sequences using BioPython (ver. 1.78) (Cock *et al.* 2009) with invertebrate mitochondrial genetic code and standard genetic code, respectively. Next, protein-MSAs were constructed using the mafft-linsi algorithm of MAFFT (ver. 7.487) (Katoh & Standley 2013), which then assisted the construction of nucleotide level MSAs with pal2nal.pl (Suyama *et al.* 2006). This helps avoid the introduction of biologically meaningless frameshifts to the alignments (Suyama *et al.* 2006). The alignments of rRNA genes (12S, 16S, 18S, and 28S) were constructed based on secondary structure information using the mafft-xinsi algorithm in MAFFT (ver. 7.487) (Katoh & Standley 2013) and MXSCARNA (Tabei *et al.* 2008). Poorly aligned regions in the MSAs were then trimmed with Gblocks (ver. 0.91b) (Talavera & Castresana 2007) (-b5 = h), TrimAl (ver. 1.4.rev15) (Capella-Gutiérrez *et al.* 2009) (-automated 1) and ClipKIT (ver. 1.1.3) (Steenwyk *et al.* 2020), respectively. In the ClipKIT program, we used different trimming strategies (-modes gappy, kpi, kpic, kpic-gappy, kpic-smart-gap, kpi-gappy, kpi-smart-gap, smart-gap).

Phylogenetic inference

Maximum-likelihood trees were constructed based on concatenated alignments using IQ-TREE (ver. 2.1.3) (Minh *et al.* 2020). We did both an unpartitioned analysis (i.e., the whole concatenated MSA shares one evolutionary model) and a partitioned (by locus) analysis on each concatenated MSA. To overcome local optima during heuristics, we performed 10 independent IQ-TREE runs (-runs 10), with a smaller perturbation strength (-pers 0.2) and larger number of stop iterations (-nstop 500). Branch supports were evaluated with 2000 ultrafast bootstrap (UFBoot) (Minh *et al.* 2013) with the risk of potential model violations considered (-B 2000 -bnni). SH-aLRT branch test (Guindon *et al.* 2010) was performed using 2000 bootstrap replicates (-alrt 2000). Best-fitting substitution models were automatically determined by the ModelFinder algorithm (Kalyaanamoorthy *et al.* 2017) in IQ-TREE. Tree visualizations were finished with iTOL (Letunic & Bork 2021).

Preparation of chromosome slides and their evaluation

Three adult males of *Tolteca hesperia* (Gertsch, 1982) from Rosario (Mexico, Sinaloa), three adult males of *T. oaxaca* Huber sp. nov. from San Pedro Totolapa (Mexico, Oaxaca), and two adult males

of *T. oaxaca* from Tehuantepec (Mexico, Oaxaca) were used for the preparation of chromosomes (see Material examined sections of the respective species for detailed collection data). Voucher specimens are deposited at the Zoological Research Museum Alexander Koenig (Bonn, Germany). Chromosome preparations were obtained from testes. These organs contained meiotic cells except for a few mitotic cells and premeiotic interphases in *T. oaxaca* sp. nov.

Chromosome slides were produced by the spreading technique described in Ávila Herrera *et al.* (2021). Slides were analysed with an Olympus BX 50 microscope equipped with a DP 71 CCD camera. Several metaphases II were used to determine the relative chromosome length (RCL) and chromosome morphology. In *T. hesperia*, plates containing both sister metaphases II were available for evaluation. In *T. oaxaca* sp. nov., only single metaphase II cells were found. Relative chromosome length was estimated as the percentage of the total chromosome length (TCL) of the haploid set. This set also included the sex chromosomes X_1, X_2, and Y. Chromosome morphology was based on the position of the centromere (Levan *et al.* 1964), which was calculated as the ratio of the longer and shorter chromosome arms.

Following the analysis with a light microscope, and after the removal of immersion oil and Giemsa stain, preparations were used for the detection of nucleolus organizer regions (NORs) with a biotin labelled 18S rDNA probe from the haplogyne spider *Dysdera erythrina* (Walckenaer, 1802) using fluorescence in situ hybridization (FISH). The technique used is described in detail in Forman *et al.* (2013); the probe is specified in Ávila Herrera *et al.* (2021). The probe was detected by streptavidin-Cy3, with amplification of the signal (biotinylated antistreptavidin, streptavidin-Cy3). Chromosomes were counterstained by DAPI. Selected chromosome plates were photographed with an Olympus IX81 microscope equipped with an ORCA-AG CCD camera (Hamamatsu). Images were pseudocoloured (red for Cy3, blue for DAPI) and superimposed with Cell^R software (Olympus Soft Imaging Solutions).

Environmental niche similarity and equivalency

The results of the phylogenetic analyses allowed the proposition of biogeographic hypotheses concerning the environmental niches occupied by representatives of the North American-Caribbean clade. We aimed to describe and compare the environmental niches occupied by six different clades or groups of species: (1) *Pholcophora americana* only; (2) Caribbean clade (i.e., *Papiamenta* and Caribbean species of '*Pholcophora*'); (3) Mexican *Pholcophora* (includes species known mainly from Mexico, with one species ranging into southern Texas); (4) Non-Caribbean ('true') *Pholcophora* (i.e., groups 1 + 3); (5) *Papiamenta*; and (6) *Tolteca*. The analyses were based on the null expectation of a high similarity and equivalency among them, corroborating the niche conservatism previously shown for Ninetinae in general (Huber *et al.* 2023). We performed tests for niche overlap (Schoener's overlap 'D' metric; Schoener 1970), similarity, and equivalency (both described in detail in Warren *et al.* 2008) by making pairwise comparisons among the groups. These analyses were implemented using functions available in the R package 'ecospat' (Di Cola *et al.* 2017). The analyses did not consider using Caribbean '*Pholcophora*' as an independent group, as the used functions require a minimum of five sites where the taxa occur (only four are known in this group). Three pairwise comparisons (Caribbean clade vs *Papiamenta*; non-Caribbean *Pholcophora* vs Mexican *Pholcophora*; non-Caribbean *Pholcophora* vs *P. americana*) include several duplicate occurrences (i.e., same occurrence used in both compared groups). In these comparisons, a high niche overlap is expected, and, if observed, potentially artificial. However, the use of pairwise comparisons seems to be the only way to allow the assessment of niche variation within the Caribbean (owing to the low number of occurrences in this region) and between the Caribbean taxa and other compared groups.

To run these analyses, we defined a background area as a 500 km radius buffer around the sampling points of each of the six analysed groups. This buffer is subjective, but compared to other studies, it seems neither too conservative (cf. 800 km in Cuervo *et al.* 2021) nor exaggerated (cf. 33 km in

Herrando-Moraira *et al.* 2019; 111 km in Silva *et al.* 2016). The buffer was filled by a 0.5 side-by-side degree hexagon grid, and further clipped to country borders. At each hexagon, up to ten random points were created, with a distance of at least 1 km from each other. This procedure aimed to provide a more homogeneous distribution of random points through the area to estimate the available environmental niche for each group of taxa. For each of these points, we extracted the values for 21 predictive variables, including the 19 climatic layers of the WorldClim 2 database (Fick & Hijmans 2017), the mean tree density (Crowther *et al.* 2015) and the mean canopy height (Simard *et al.* 2011), the latter two at a 1 km_2 scale.

The 21 predictive variables were used in a principal component analysis calibrated on the entire environmental space of the study area, including species occurrences. This analysis, the so-called PCA-env (as described by Broennimann *et al.* 2012), was carried out to provide a kernel density of the environmental niche occupied by each taxon, based on their sites of occurrences. Then, the niche overlap, equivalency, and similarity tests were performed, each with 100 replicates. The D metric for niche overlap ranges from 0 (no overlap) to 1 (complete overlap) (Broennimann *et al.* 2012). Equivalency and similarity analyses compare the observed environmental niche overlap against null models simulated by randomly reallocating the occurrence records between distribution ranges (for the equivalency tests); or by randomly shifting the niches within the available conditions of the study area (for the similarity tests) (Broennimann *et al.* 2012; Di Cola *et al.* 2017; Hazzi & Hormiga 2021). As we aimed to test for niche conservatism between sister taxa, the parameter 'overlap.alternative' was set to 'higher' (i.e., the niche overlap is more equivalent/similar than random), and 'rand.type' was set to '1' (i.e., there is no assumption about a reference niche, and the niches of both groups can be simultaneously shifted), following recommendations from Di Cola *et al.* (2017).

Building on the results of the previous analyses, we further explored the microhabitat occupied by each taxon by comparing the altitudes of the records of *P. americana*, Mexican *Pholcophora*, *Tolteca*, and the Caribbean clade. The altitude was not used as a predictor in the previous approaches as it would result in a tautological variable, owing to its direct effect on temperature and precipitation (see Hof *et al.* 2012), detailed in the climatic variables taken from WorldClim. To compare the altitude occupied by each taxon, we performed a generalized linear model with quasi-poisson distribution of errors, using base R functions. This analysis was preferred over a poisson distribution owing to overdispersion issues, checked using the function 'rdiagnostic' from the R package 'RT4Bio' (Reis *et al.* 2015). Post hoc contrast analyses (see Crawley 2012) were performed using the 'coms' function from the R package 'RT4Bio' (Reis *et al.* 2015). The elevation data was taken from the WorldClim 2 database (Fick & Hijmans 2017) and the values were extracted using the R package 'raster' (Hijmans 2022).

Results

Molecular data

All unpartitioned analyses using the ClipKIT trimming strategies consistently recovered a clade consisting of 'true' (North American) *Pholcophora*, *Tolteca*, two undescribed Caribbean species tentatively assigned to *Pholcophora*, and the Caribbean (Curaçao) genus *Papiamenta* (Fig. 1; Supp. file 1: Fig. S76). The support for this clade varied widely (SH-aLRT supports: 25–90). Since this clade is also strongly supported by preliminary analyses of UCE data (G. Meng, L. Podsiadlowski, B.A. Huber, unpubl. data), we chose a ClipKIT tree for Figure 1 and did not further consider the TrimAI and Gblocks trees (in which this clade was not recovered). For the same reason we also rejected the trees resulting from partitioned analyses: in all of them (except when using untrimmed sequences), this North American-Caribbean clade was not recovered. In addition, unpartitioned analyses recovered the same interspecific relationships within *Tolteca* as the analysis of UCE data (see below) while the partitioned analysis did not. A summary tree showing these alternative topologies is shown in Supporting Information (Supp. file 1: Fig. S77).

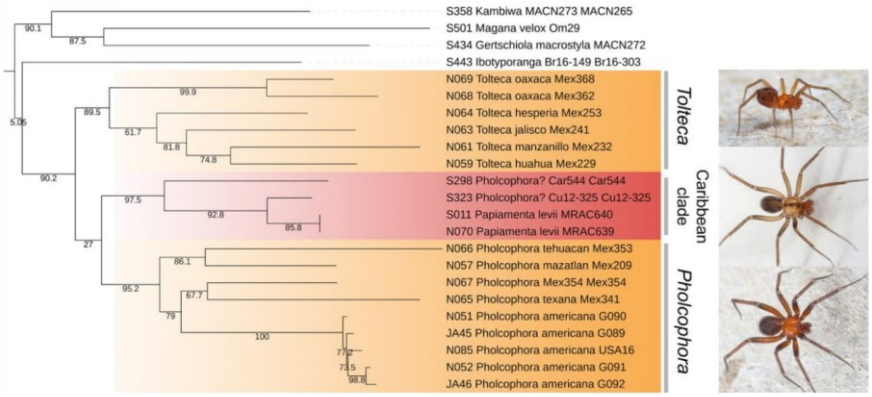

Fig. 1. Relationships of *Pholcophora* Banks, 1896 and *Tolteca* Huber, 2000 derived from analysis of molecular data using IQ-Tree and the ClipKIT gappy trimming strategy. Newly generated CO1 sequences (codes starting with N) were combined with data from Eberle *et al.* (2018) (all other codes). Numbers on the branches are SH-aLRT supports (%). The tree shows only the ingroups and the Ninetinae outgroups. Clade colours are as in Figs 2 and 35. For the complete tree, and for clade support using different alignment strategies, see Supp. file 1: Fig. S76. Photos on the right from top to bottom: *Tolteca manzanillo* Huber sp. nov.; *Papiamenta savonet* Huber, 2000; *Pholcophora papanoa* Huber sp. nov.

Within this North American-Caribbean clade, there was consistently reasonable to high support for *Tolteca* (unpartitioned analysis: 84–90; partitioned analysis: 78–81), for 'true' *Pholcophora* (unpartitioned analysis: 91–95; partitioned analysis: 76–81), and for a Caribbean clade consisting of *Papiamenta* and Caribbean '*Pholcophora*' (unpartitioned analysis: 97–98; partitioned analysis: 90–92). All analyses recovered a sister group relationship between 'true' *Pholcophora* and the Caribbean clade, but partly with low support (unpartitioned analysis: 27–80; partitioned analysis: 86–90). For further details, see Relationships sections in the genus descriptions below.

Taxonomy

Class Arachnida Cuvier, 1812
Order Araneae Clerck, 1757
Family Pholcidae C.L. Koch, 1850
Subfamily Ninetinae Simon, 1890

Genus ***Pholcophora*** Banks, 1896

Pholcophora Banks, 1896: 57. Type species: *P. americana* Banks, 1896.

Pholcophora – Gertsch 1971: 76; 1977: 112; 1982: 96. — Huber 2000: 113.

Diagnosis

Easily distinguished from only other North American Ninetinae genus *Tolteca* by strong male cheliceral apophyses originating proximally (Figs 5A–B, 10A–B; in *Tolteca* small and originating distally); also by presence of stridulatory ridges on male chelicerae; most species (except *P. tehuacan* Huber sp. nov.) also

by larger size (body length ~1.7–3.1; in *Tolteca* ~1.1–1.4) and longer legs (tibia 1 > 1.0, in *Tolteca* < 0.7); from most species of *Tolteca* also by absence of knob-shaped structure between epigynum and pedicel (also absent in *Tolteca sinnombre* Huber sp. nov.). From other geographically close genera (*Papiamenta*, *Galapa*) also by simple rod-shaped procursus (Figs 5C–E, 10C–E; much shorter in *Papiamenta*; with dorsal process in *Galapa*); by presence of humps on male sternum (absent in *Papiamenta*); and by unmodified male cheliceral fangs (with processes in *Galapa*).

Description

Male

Measurements . Total body length 1.2–3.1, carapace width 0.55–1.40. Legs relatively short, tibia 1: 0.65–1.85, i.e., 1.2–2.0 × carapace width; tibia 1 L/d 8–16; tibia 2 much shorter than tibia 4 (tibia 2 / tibia 4: 0.75–0.85).

Colour. Live specimens (Fig. 3) ochre to brown, prosoma sometimes reddish (which is lost in ethanol); carapace monochromous, sometimes with indistinct darker median Y-mark; abdomen colour slightly variable, usually monochromous, sometimes with indistinct dorsal marks (bluish in ethanol); legs without dark or light bands, femora sometimes distally darkened.

Body. Ocular area barely raised (cf. Fig. 8A), eight eyes, AME relatively large, diameter 20–60 µm, 45–75% of PME diameter; carapace with low and indistinct thoracic groove (cf. Figs 8A, 13A). Clypeus unmodified but sometimes slightly more protruding than in female. Sternum wider than long, with pair of distinct anterior processes near leg coxae 1. Abdomen globular; gonopore with four epiandrous spigots arranged in two pairs (Fig. 29C; examined: *P. americana* Banks, 1896; *P. tehuacan* sp. nov.); ALS with seven spigots each (cf. Figs 8C, 29G): one strongly widened spigot, one long pointed spigot, and five cylindrical spigots (one of which is unusually large); PMS with two short, pointed spigots; PLS without spigots.

Chelicerae . With one pair of large frontal apophyses (Figs 5A–B, 10A–B); with stridulatory files (Fig. 29A), distances between ridges ~2.0–3.8 µm, distances proximally often smaller than distally.

Palps. Coxa unmodified; trochanter barely modified (with indistinct or without ventral projection); femur proximally with retrolateral-ventral process and prolateral stridulatory pick (modified hair), distally widened but simple, slightly curved towards dorsal, in *P. texana* Gertsch, 1935 with distinctive brush of feathered hairs ventrally (Fig. 19A, C); femur-patella joints slightly shifted toward prolateral side; tibia globular, with two trichobothria; tibia-tarsus joints not shifted to one side; palpal tarsal organ raised, capsulate with small opening (Fig. 29E; diameter of opening ~1.5 µm – measured in *P. tehuacan* sp. nov. only); procursus simple and straight, without dorsal flap, not strongly elongated, often with semi-transparent distal element; genital bulb distally cone-shaped, with species-specific sclerotized and membranous elements.

Legs. Without spines and curved hairs; in some species with very short vertical hairs in higher than usual density on tibiae (only anterior tibiae or all tibiae) (length of hairs ~30 µm). Trichobothria in usual arrangement: three on each tibia (except tibia 1: prolateral trichobothrium absent), one on each metatarsus; slightly feathered (Figs 18F, 24E); length of dorsal trichobothrium on tibia 1: ~90 µm; retrolateral trichobothrium of tibia 1 in very distal position (at 50–65% of tibia length). Tarsus 1 with 5–8 pseudosegments, sometimes only distally fairly distinct; tarsus 4 distally with one comb-hair on prolateral side (cf. Figs 13H, 24H); leg tarsal organs very small, capsulate with small opening (cf. Fig. 8F–H; diameter of opening ~1.3–1.8 µm); three claws (cf. Figs 13G, 24G, 29H).

Female

In general (size, colour) similar to male but sternum without pair of anterior humps, leg tibia 1 with usual low number of short vertical hairs, and chelicerae without stridulatory ridges; legs either slightly shorter than in males or of same length (only *P. americana* with reasonable sample size: male/female tibia 1 length: 1.12). Spinnerets, comb-hairs, and leg tarsal organs as in male; palpal tarsal organ slightly less strongly raised (Figs 18E, 23H). Epigynum main (anterior) plate large, rectangular to oval, sometimes posteriorly excavated, weakly protruding in lateral view; posterior plate also large, short but wide, median part sometimes separated from lateral parts by whitish band. Without knob-shaped structure between epigynum and pedicel. Internal genitalia variable: either without sacs (Fig. 33A–H; *P. americana* Banks, 1896; *P. mazatlan* Huber sp. nov.; *P. papanoa* Huber sp. nov.; *P.* "Mex354") or with pair of distinct membranous sacs (Fig. 33I–L; *P. texana* Gertsch, 1935; *P. tehuacan* sp. nov.); in Caribbean '*Pholcophora*' with single median tube-like sac (Fig. 33M–N; *P. bahama* Gertsch, 1982; *P.* "Car544"; *P.* "Cu12-325"); with pair of distinct transversal sclerites; apparently without pore plates (possibly with very indistinct pair of pore plates near median line, indicated in Fig. 33E–F, J–L).

Relationships

In the molecular analysis of Eberle *et al.* (2018), the type species *Pholcophora americana* was part of a North American-Caribbean clade of Ninetinae, together with "*Pholcophora*? Car544", an unidentified Cuban species ("Gen. Cu12-325"; treated below as "*Pholcophora*? Cu12-325"), and the genus *Papiamenta*. The genus *Tolteca* was not included.

Our new molecular analyses mostly support this North American-Caribbean clade (Fig. 1; see also general results of molecular analyses above), and they also support the idea that Caribbean '*Pholcophora*' are not true *Pholcophora* but more closely related with the Caribbean genus *Papiamenta*. Our analyses suggest a sister group relationship between true *Pholcophora* and the Caribbean clade (*Papiamenta* + Caribbean '*Pholcophora*'). By contrast, preliminary analyses of UCE data (G. Meng, L. Podsiadlowski, B.A. Huber, unpubl. data) suggest a sister-group relationship between true *Pholcophora* and *Tolteca*. Since we consider these UCE results more reliable, we will not further discuss relationships here, except for two species not yet included in any molecular dataset: *Pholcophora maria* Gertsch, 1977 from Yucatán, and *Pholcophora bahama* Gertsch, 1982 from the Bahamas. Judging from the female internal genitalia (compare Huber 2000: fig. 1357 with Fig. 28B), we hypothesize that *Pholcophora maria* is closely related with the newly described *P. tehuacan* sp. nov. It is thus probably a true *Pholcophora*. *Pholcophora bahama* resembles "*Pholcophora*? Car544" in having a median tube-like sac in the female internal genitalia (compare Huber 2000: fig. 1356 with Fig. 31G). It is thus probably not a true *Pholcophora* but part of the Caribbean clade.

Distribution

The genus appears limited to North America (Fig. 2); Caribbean species (including Dominican amber fossils) currently placed in *Pholcophora* are probably misplaced (see Relationships above). Of the seven North American named species, six are largely or entirely restricted to Mexico.

Natural history

Gertsch (1982) briefly characterized *Pholcophora* spiders as living "reclusive lives under ground objects, in leaf and plant detritus, and in soil openings and caves", and mentioned that they "spin web tangles in dark spaces and remain there in close contact with such webs as permanent residents, often in informal colonies". Our newly collected species and specimens fit this description. Most were collected by turning rocks or sifting litter in shady spots of low and dry forests (Fig. 34). They usually shared the microhabitat with one or more other pholcids. In only one case we found two species of *Pholcophora* at a single locality; we never found *Pholcophora* to share a locality with *Tolteca*. Females carried their

flattened egg-sacs slightly under the prosoma (Fig. 3); eggs sacs contained ~6–30 eggs, each with a diameter of ~0.40–0.60 mm (Huber & Eberle 2021). Some females had a genital plug (cf. Fig. 16C).

Composition

The genus now includes 11 nominal species. Of these, seven occur in North America and are here considered to represent 'true' *Pholcophora*: *Pholcophora americana* Banks, 1896; *P. maria* Gertsch, 1977; *P. mazatlan* sp. nov.; *P. mexcala* Gertsch, 1982; *P. papanoa* sp. nov.; *P. tehuacan* sp. nov.; *P. texana* Gertsch, 1935. The Caribbean *P. bahama* Gertsch, 1982 is here considered to be misplaced (see Relationships above). All extant species are treated below except *P. bahama* and *P. mexcala* for which we have no new data [in 2019 we searched at four localities close to Mezcala (= "Mexcala") but could not find *P. mexcala*].

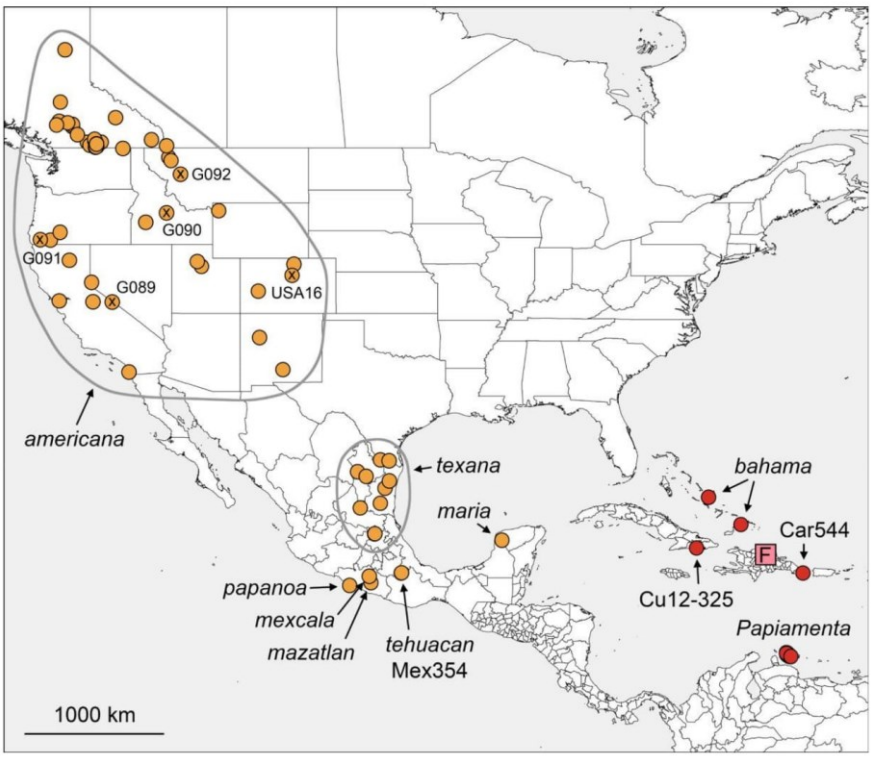

Fig. 2. Known distributions of 'true' *Pholcophora* Banks, 1896 (orange marks) and of presumably misplaced Caribbean '*Pholcophora*' and of *Papiamenta* Huber, 2000 (red marks). Dominican amber species currently placed in *Pholcophora* are represented by an "F" in a pink square. Our molecular data suggest that Caribbean '*Pholcophora*' are more closely related with the genus *Papiamenta* than with true *Pholcophora*. Barcoded specimens of *Pholcophora americana* Banks, 1896 are marked with an "x" and accompanied by the vial code (see Table 1 for details).

Three nominal species are only known from amber fossils originating from Hispaniola (Wunderlich 1988): *P. brevipes* Wunderlich, 1988; *P. gracilis* Wunderlich, 1988; and *P. longicornis* Wunderlich, 1988. We did not re-examine the amber specimens but judging from their geographic origin we speculate that the three species are part of the clade including Caribbean '*Pholcophora*' and *Papiamenta*. However, the three amber species fit the diagnosis above with respect to the strong male cheliceral apophyses originating proximally and the simple rod-shaped procursus. They are unusually small (but in this respect similar to the exceptionally small extant *P. tehuacan* sp. nov. and *P. maria*), and the original

Fig. 3. *Pholcophora* Banks, 1896, live specimens. **A**. *P. americana* Banks, 1896, male from USA, Colorado, near Golden. **B–E**. *P. mazatlan* Huber sp. nov., males and females with egg-sacs from Mexico, Guerrero, N of Mazatlán. **F–G**. *P. papanoa* Huber sp. nov., male and female from Mexico, Guerrero, S of Papanoa. **H–I**. *P. texana* Gertsch, 1935, male and female with egg-sac from Mexico, Hidalgo, SW of Jacala. **J–K**. *P. tehuacan* Huber sp. nov., male and female with egg-sac from Mexico, Puebla, SE of Tehuacan. **L**. *P.* "Mex354", female with egg-sac from Mexico, Puebla, SE of Tehuacan.

descriptions remain silent about male cheliceral stridulation and male sternal humps. The females of the three fossil species remain unknown.

Pholcophora americana Banks, 1896
Figs 3A, 4–8, 33A–B

Remark

For synonymy, type material, and redescription, see Huber (2000).

Diagnosis

Easily distinguished geographically by being the only representative of *Pholcophora* (and of Ninetinae) in the western USA and Canada (Fig. 2); morphologically distinguished from similar congeners (*P. mexcala*; *P. mazatlan* sp. nov.; *P. papanoa* sp. nov.) by shape of male cheliceral apophyses (Fig. 5A– B; directed towards frontal rather than upwards, without proximal humps, relatively short), by tip of procursus (Fig. 5C–E; semi-transparent process widening distally), and by epigynum (main epigynal plate posteriorly strongly indented, Fig. 6A, C).

Material examined (new records)

USA – **Colorado** • 3 ♀♀, in pure ethanol; Lookout Mountain near Golden, 'sites 1 & 2'; 39.73° N, 105.24° W; 2220–2230 m a.s.l.; 6 Jul. 2016; B.A. Huber leg.; one female used for SEM, two prosomata used for molecular work; ZFMK USA16 • 2 ♂♂, in pure ethanol; same collection data as for preceding; vouchers of Ávila Herrera *et al.* (2021); ZFMK Kra55–56. – **California** • 2 ♂♂, 5 ♀♀, 1 juv., in pure ethanol; Mono County, Inyo Nat. Forest; 37.80° N, 118.38° W; 15 Jun. 2003; P. Paquin and N. Dupérré leg.; under wood debris in pine forest; ZFMK G089 • 1 ♂, 1 ♀; Plumas County, Lassen National Forest, Warner Creek Campground; 40.3625° N, 121.3081° W; 1540 m a.s.l.; 18 May 2015; K. Schneider leg.; beaten from fallen pine cones; ZFMK Ar 23944. – **Idaho** • 1 ♀, in pure ethanol; Custer County,

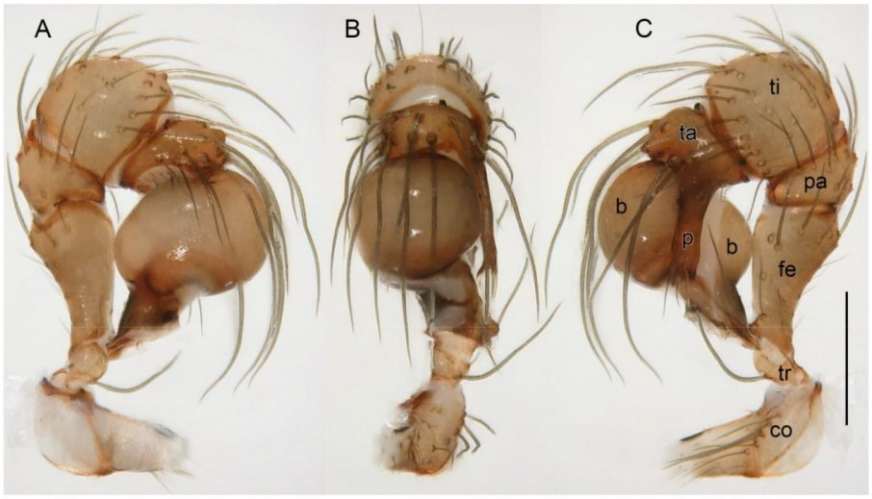

Fig. 4. *Pholcophora americana* Banks, 1896, male from USA, Colorado, near Golden (ZFMK Kra55). Left palp, prolateral, dorsal, and retrolateral views. Abbreviations: b = genital bulb; co = coxa; fe = femur; p = procursus; pa = patella; ta = tarsus; ti = tibia; tr = trochanter. Scale bar = 0.3 mm.

Salmon-Challis Nat. Forest, Kinnikinic Creek Road; 44.278° N, 114.408° W; 19 Sep. 2003; P. Paquin and D. Wytrykush leg.; scree under *Picea glauca* forest; ZFMK G090. – **Montana** • 1 ♂, 2 ♀♀, 1 juv., in pure ethanol; Missoula County, Lolo Nat. Forest, near Salmon Lake; 47.072° N, 113.384° W; 18 Sep. 2003; P. Paquin and D. Wytrykush leg.; under rocks, scree; ZFMK G092. – **Oregon** • 2 ♂♂, 2 ♀♀, 1 juv., in pure ethanol; Josephine County, Siskiyou Nat. Forest, Briggs Valley Road; 42.337° N, 123.610° W; 23 Sep. 2003; P. Paquin and D. Wytrykush leg.; ZFMK G091.

Description (amendments; see Huber 2000)

Male

Measurements of a male from Hat Creek, California: carapace width 0.95; tibia 1 length: 1.75; distance PME-PME 75 µm; diameter PME 80 µm; distance PME-ALE 30 µm; distance AME-AME 20 µm; diameter AME 60 µm; diameters of leg femora 0.20–0.23, of leg tibiae 0.11–0.12. Clypeus unmodified, clypeus rim to ALE 0.30. Chelicerae as in Fig. 5A–B; distances between cheliceral stridulatory ridges 2.5–2.7 µm. Procursus as in Fig. 5C–E, with distinctive transparent element distally; genital bulb as in

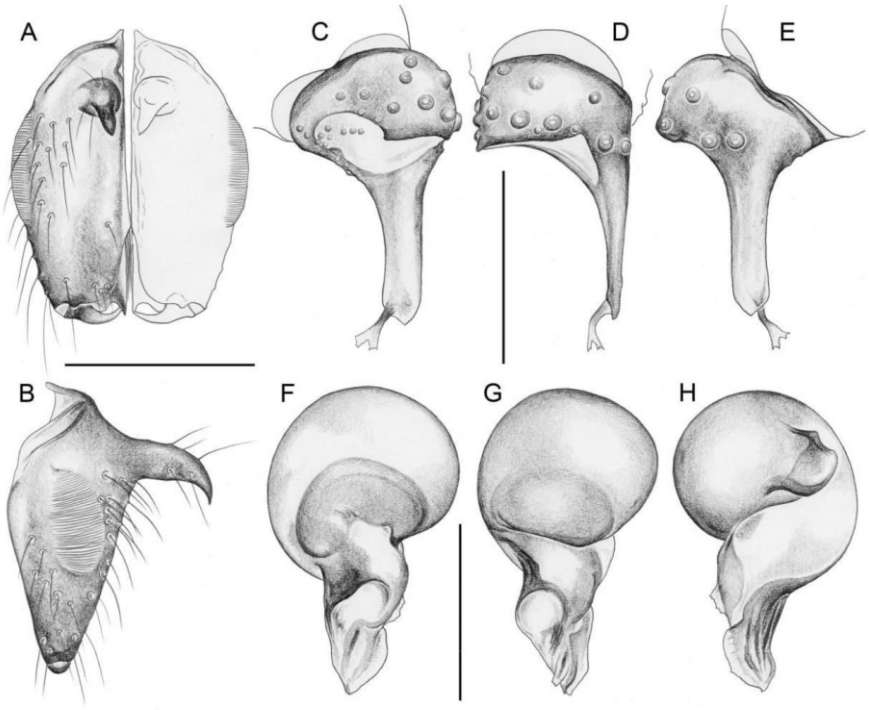

Fig. 5. *Pholcophora americana* Banks, 1896, males. **A–E**. From USA, Montana, Lolo Nat. Forest (ZFMK G092). **F–H**. From California, Inyo Nat. Forest (ZFMK G089). **A–B**. Chelicerae, frontal and lateral views. **C–E**. Left palpal tarsus and procursus, prolateral, dorsal, and retrolateral views. **F–H**. Left genital bulb, prolateral, dorsal, and retrolateral views. Scale bars = 0.3 mm.

Fig. 5F–H. Legs with few vertical hairs; prolateral trichobothrium absent on tibia 1. Tibia 1 length in 14 males (incl. specimens measured in Huber 2000): 1.50–1.75 (mean 1.62).

Female

In general similar to male but sternum without pair of anterior humps, and chelicerae without stridulatory files. Tibia 1 in 15 females (incl. specimens measured in Huber 2000): 1.25–1.70 (mean 1.48). Epigynum and internal female genitalia as in Figs 6–7, apparently without median receptacle, without or with very small pore plates.

Distribution

Widely distributed in the western USA, ranging into SW Canada (British Columbia) (Fig. 2). The map in Fig. 2 includes many records from British Columbia that were first shown in a map in Bennett (2014: fig. 5). A list of locality names was later published online in the Checklist of the Spiders (Araneae)

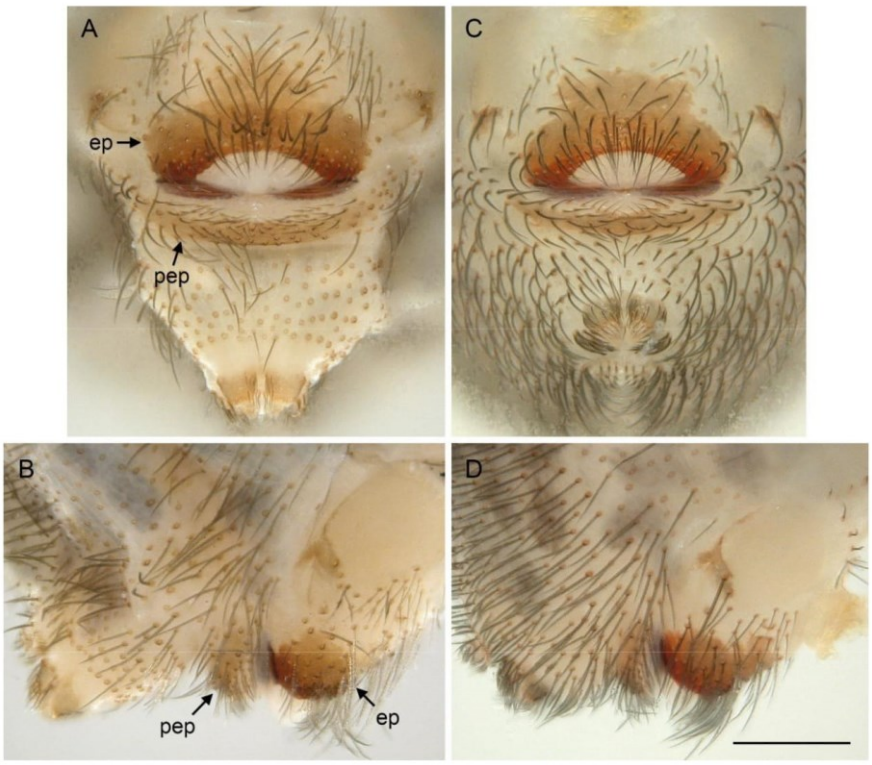

Fig. 6. *Pholcophora americana* Banks, 1896, females. **A–B**. From USA, California, Inyo Nat. Forest (ZFMK G089). **C–D**. From Colorado, near Golden (ZFMK USA16). Epigyna, ventral and lateral views. Abbreviations: ep = epigynum (main epigynal plate); pep = posterior epigynal plate. Scale bar = 0.3 mm (all at same scale).

of British Columbia (http://staff.royalbcmuseum.bc.ca/). The Canadian dots in Fig. 2 are based on coordinates of specimens digitized at the Royal British Columbia Museum that were kindly provided by C. Copley (pers. com. Feb. 2017).

Natural history

Surprisingly, nothing is known about the biology of this widespread spider beyond some basic habitat data taken from labels. It has usually been found under rocks, wood debris, and other objects on the ground, often in pine forests. The most northern records (British Columbia) suggest that this species tolerates very cold winters, with occasional temperatures below -10°C.

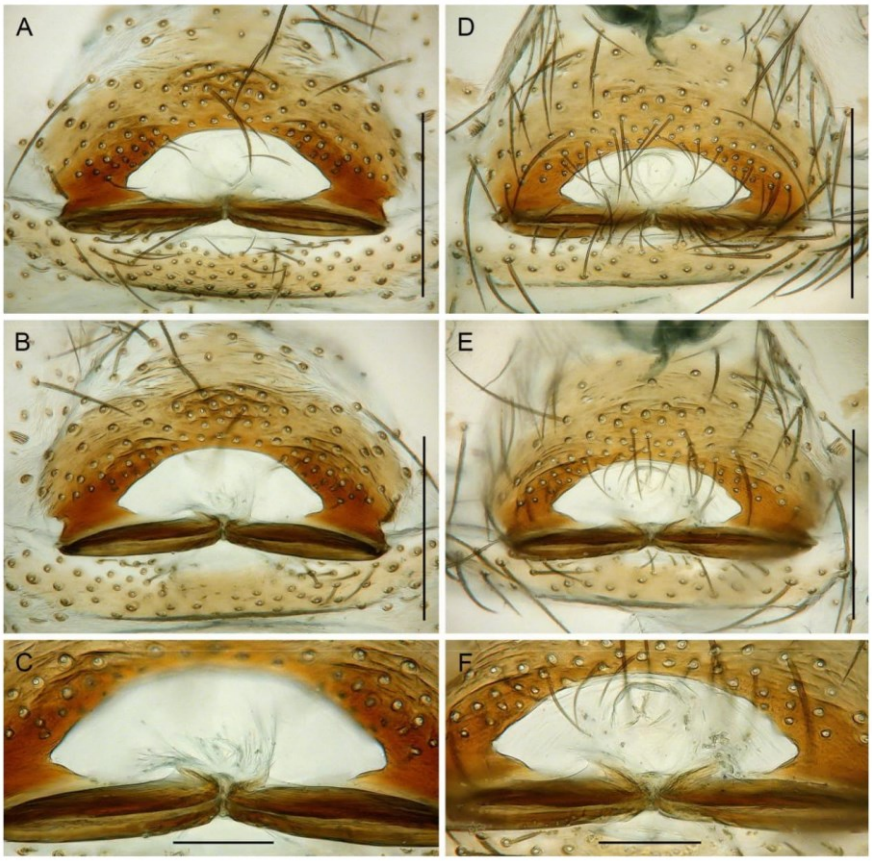

Fig. 7. *Pholcophora americana* Banks, 1896, cleared female genitalia. **A–C**. From USA, California, Inyo Nat. Forest (ZFMK G089). **D–F**. From Colorado, near Golden (ZFMK USA16). **A, D**. Ventral views. **B, E**. Dorsal views. **C, F**. Detail of median internal structures. Scale bars: A–B, D–E = 0.3 mm; C, F = 0.1 mm.

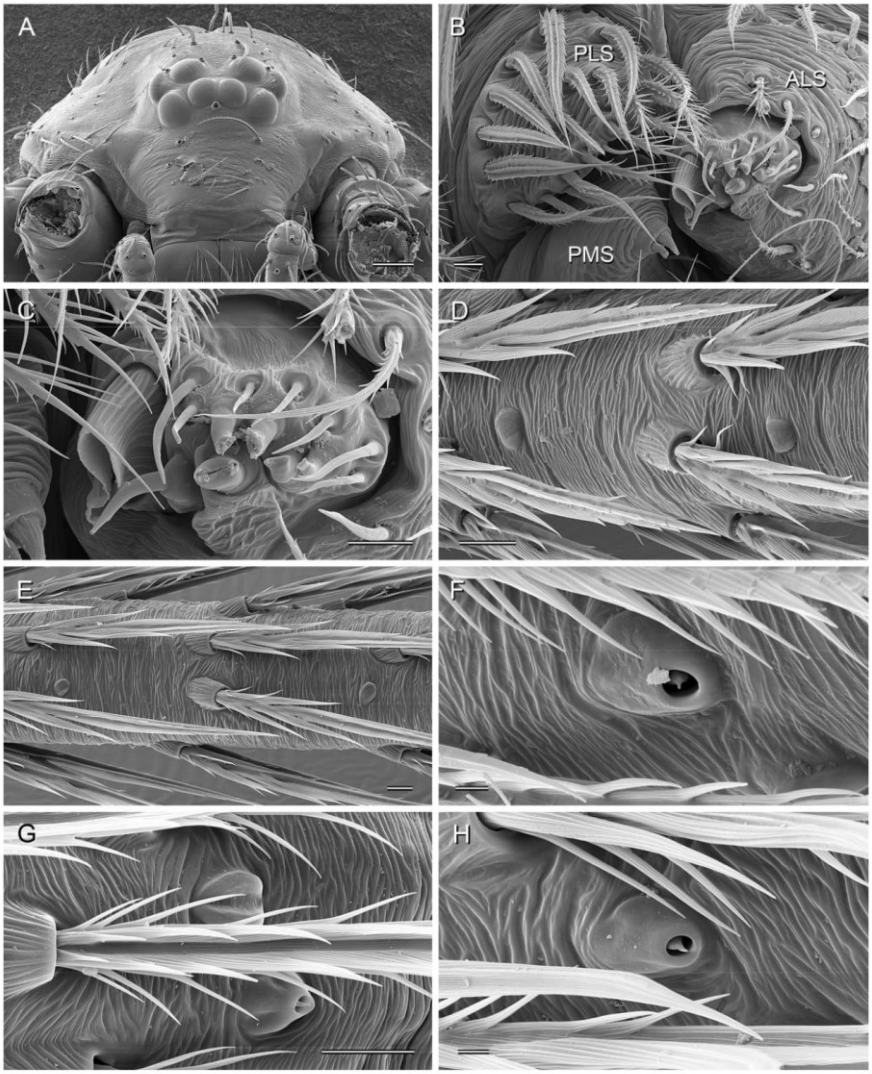

Fig. 8. *Pholcophora americana* Banks, 1896, female from USA, Colorado, near Golden (ZFMK USA16). **A**. Prosoma, frontal view. **B**. Right spinnerets. **C**. Anterior lateral spinneret. **D**. Detail of tibia 1. **E**. Detail of metatarsus 4. **F**. Tarsal organ on tarsus 1. **G**. Tarsal organ and slit sensillum on tarsus 3. **H**. Tarsal organ on tarsus 4. Scale bars: A = 100 µm; B–E, G = 10 µm; F, H = 2 µm.

Ninetinae ***Pholcophora mazatlan*** Huber sp. nov.

urn:lsid:zoobank.org:act:C787210E-FE17-42BD-AF00-7C5364558495
Figs 3B–E, 9–13, 33C–D

Diagnosis

Distinguished from similar congeners (*P. papanoa* sp. nov., *P. mexcala*, *P. americana*) by shape of male cheliceral apophyses (Fig. 10A–B; very long, directed upwards, without proximal humps) and by shape of male bulbal process (Fig. 10F–H; small dorsal process in very distal position; distinctive semi-transparent ventral flap). From very similar *P. papanoa* also by main element of procursus more gradually narrowing distally (Fig. 10E), by male cheliceral apophyses more strongly directed upwards, and by thinner male leg femora (0.18–0.20 vs 0.28–0.30). From *P. americana* also by tip of procursus (semi-transparent process not widening distally) and by shape of epigynum (Fig. 11A, C; main epigynal plate posteriorly straight).

Etymology

The species name is derived from the type locality; noun in apposition.

Type material

Holotype

MEXICO – **Guerrero** • ♂; ~2 km N of Mazatlán; 17.4567° N, 99.4740° W; 1300 m a.s.l.; 3 Oct. 2019; B.A. Huber and A. Valdez-Mondragón leg.; LATLAX.

Paratypes

MEXICO – **Guerrero** • 1 ♀; same collection data as for holotype; ZFMK Ar 23943 • 1 ♂, 11 ♀♀; same collection data as for holotype; LATLAX.

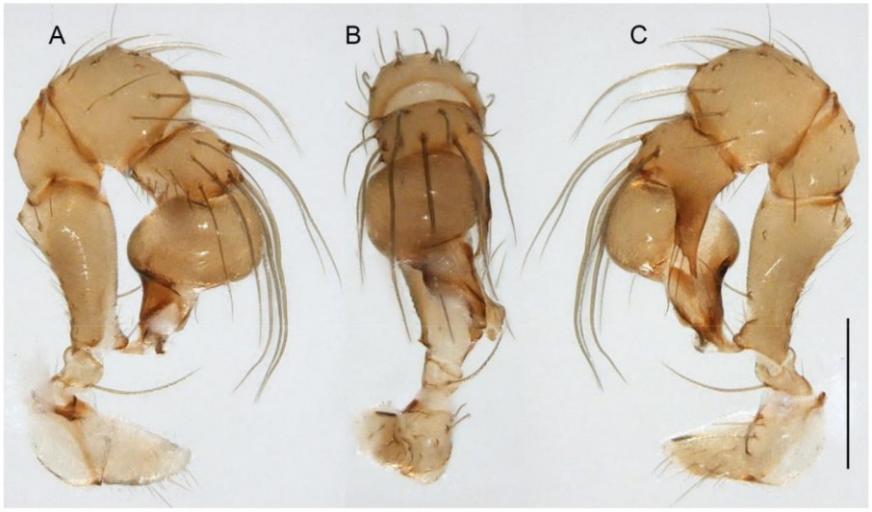

Fig. 9. *Pholcophora mazatlan* Huber sp. nov., male holotype from Mexico, Guerrero, N of Mazatlán (LATLAX). Left palp, prolateral, dorsal, and retrolateral views. Scale bar = 0.3 mm.

Other material examined

MEXICO – **Guerrero** • 3 ♀♀, in pure ethanol; same collection data as for holotype; one female used for SEM; ZFMK Mex209 • 3 ♀♀ abdomens, together with female paratype; same collection data as for holotype; prosomata used for molecular work; ZFMK Ar 23943.

Description

Male (holotype)

Measurements. Total body length 1.90, carapace width 0.80. Distance PME-PME 70 µm; diameter PME 60 µm; distance PME-ALE 30 µm; distance AME-AME 20 µm; diameter AME 30 µm. Leg 1: 4.55 (1.30 + 0.30 + 1.15 + 1.30 + 0.50), tibia 2: 1.00, tibia 3: 0.85, tibia 4: 1.25; tibia 1 L/d: 12; diameters of leg femora 0.18–0.20, of leg tibiae 0.10.

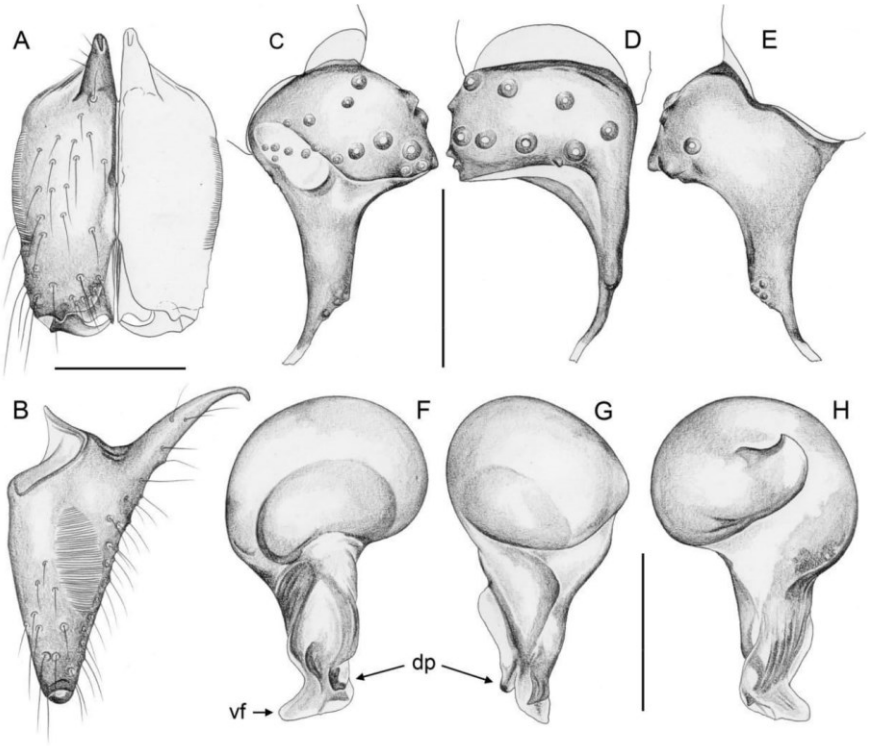

Fig. 10. *Pholcophora mazatlan* Huber sp. nov.; male holotype from Mexico, Guerrero, N of Mazatlán (LATLAX). **A–B**. Chelicerae, frontal and lateral views. **C–E**. Left palpal tarsus and procursus, prolateral, dorsal, and retrolateral views. **F–H**. Left genital bulb, prolateral, dorsal, and retrolateral views. Abbreviations: dp = dorsal process; vf = ventral flap. Scale bars = 0.2 mm.

Colour (in ethanol). Prosoma and legs ochre-yellow, carapace with indistinct Y-mark, legs without darker rings; abdomen grey with dark bluish internal marks; ventrally with ochre plate in front of gonopore.

Body (Fig . 3B–C). Ocular area barely raised. Carapace with distinct but shallow thoracic groove (cf. Fig. 13A). Clypeus unmodified, very short (clypeus rim to ALE: 0.22). Sternum slightly wider than long (0.56/0.46), oval (not narrow posteriorly), with pair of distinct anterior processes (~0.1 long) near coxae 1. Abdomen globular.

Chelicerae (Fig. 10A–B). With pair of long frontal apophyses; stridulatory files very fine, poorly visible in dissecting microscope; distances between cheliceral stridulatory ridges proximally 2.4 µm, distally 3.5 µm.

Palps (Fig. 9). Coxa unmodified; trochanter without process; femur proximally with retrolateral-ventral process and prolateral stridulatory pick, distally widened but simple, slightly curved towards dorsal; femur-patella joints slightly shifted toward prolateral side; tibia globular, with two trichobothria; tibia-

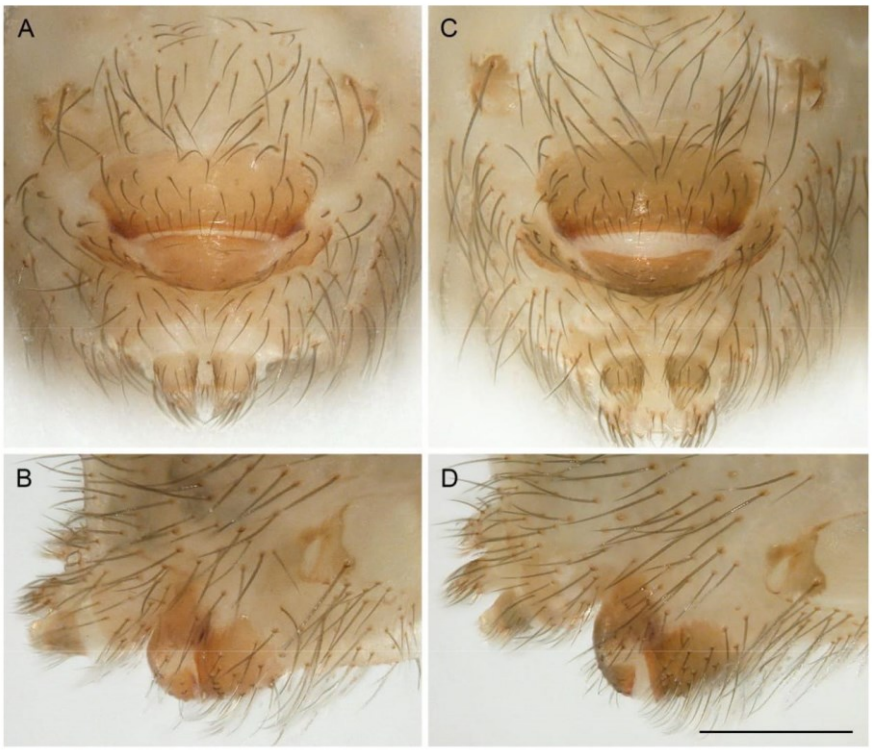

Fig. 11. *Pholcophora mazatlan* Huber sp. nov., females from Mexico, Guerrero, N of Mazatlán (ZFMK Ar 23943). Epigyna, ventral and lateral views. Scale bar = 0.3 mm (all at same scale).

tarsus joints not shifted to one side; procursus very simple (Fig. 10C–E), narrow distal part slightly bent towards prolateral, with semi-transparent tip; genital bulb with small dorsal process in very distal position, distally with distinctive semi-transparent ventral flap (Fig. 10F–H).

L $_{egs}$. Without spines and curved hairs; with vertical hairs in two narrow dorsal bands proximally on tibiae 1 and 2 (length ~30 µm; length of dorsal trichobothrium on tibia 1: ~90 µm); retrolateral trichobothrium of tibia 1 at 64%; prolateral trichobothrium absent on tibia 1; tarsus 1 with ~7 pseudosegments, only distally 2–3 distinct.

Variation (male)
Tibia 1 in second male: 1.30.

Female
In general, similar to male (Fig. 3D–E) but sternum without pair of anterior humps, tibiae without higher than usual density of short vertical hairs, and chelicerae without stridulatory files. Tibia 1 in

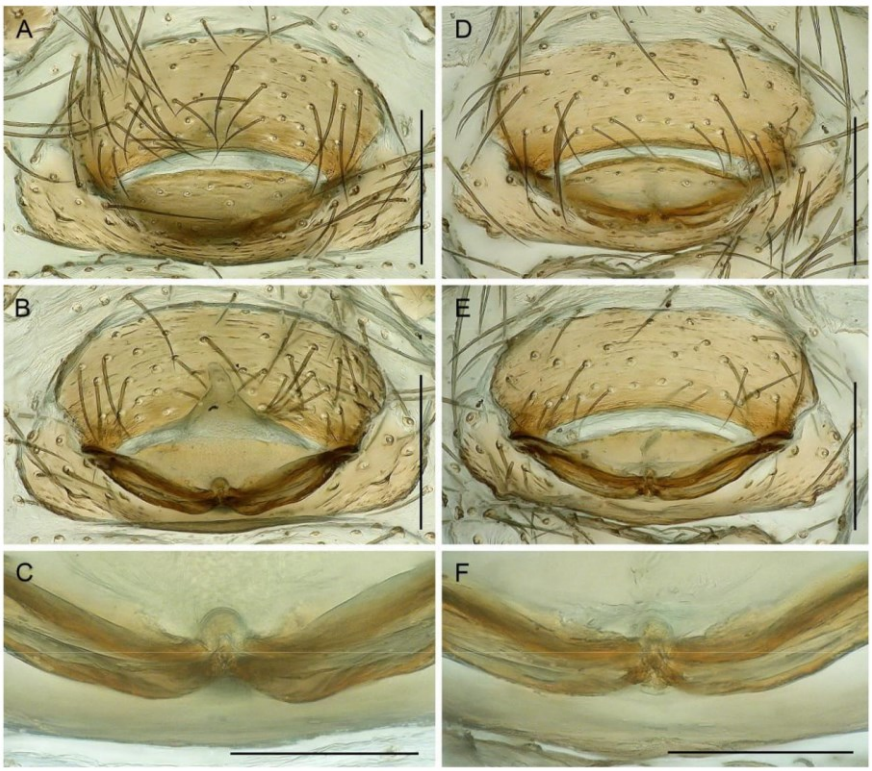

Fig. 12. *Pholcophora mazatlan* Huber sp. nov., females from Mexico, Guerrero, N of Mazatlán (ZFMK Ar 23943), cleared female genitalia. **A, D**. Ventral views. **B, E**. Dorsal views. **C, F**. Detail of median internal structures. Scale bars: A–B, D–E = 0.2 mm; C, F = 0.1 mm.

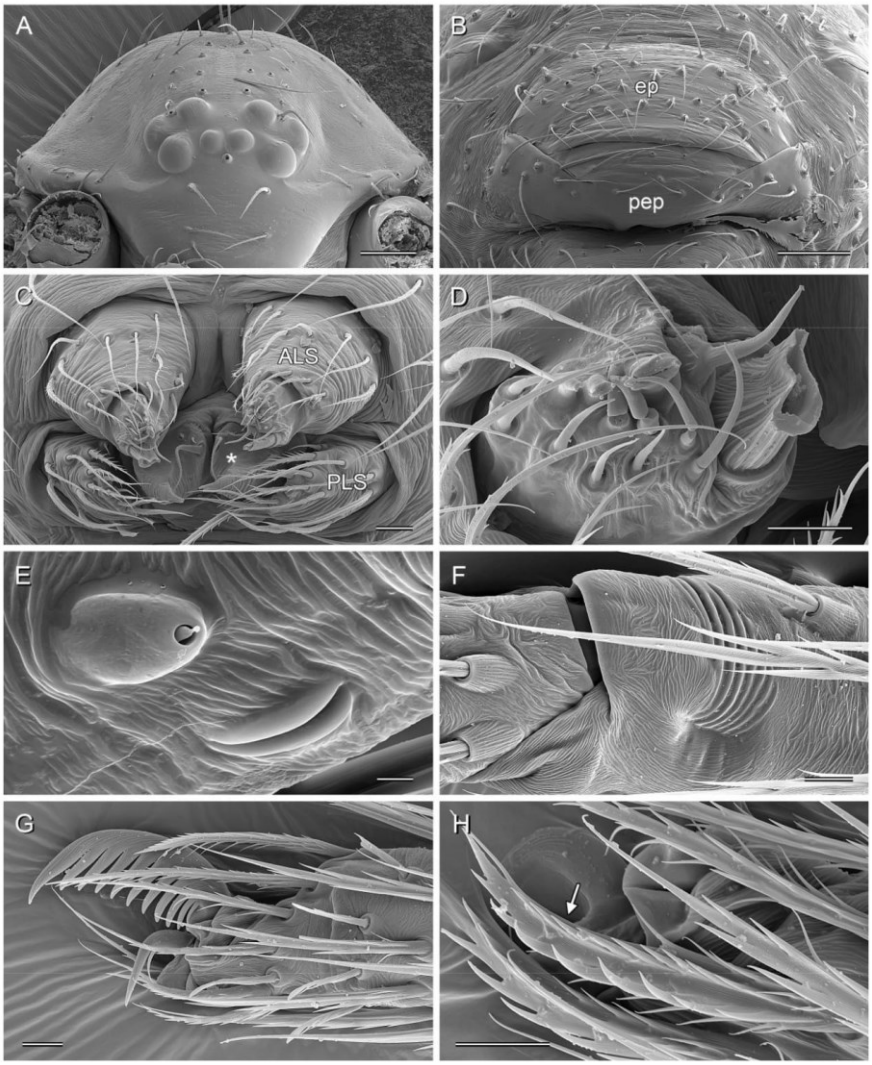

Fig. 13. *Pholcophora mazatlan* Huber sp. nov., female from Mexico, Guerrero, 2 km N of Mazatlán (ZFMK Mex209). **A**. Prosoma, frontal view. **B**. Epigynum, ventral view. **C**. Spinnerets; asterisk: PMS. **D**. Anterior lateral spinneret. **E**. Tarsal organ and slit sensillum on tarsus 3. **F**. Metatarsus-tarsus 1 joint with lyriform organ, dorsal view. **G**. Tip of right tarsus 3, prolateral view. **H**. Comb hair (arrow) on tarsus 4, prolateral view. Abbreviations: ep = epigynum (main epigynal plate); pep = posterior epigynal plate. Scale bars: A–B = 100 µm; C = 20 µm; D, F–H = 10 µm; E = 2 µm.

11 females: 1.00–1.20 (mean 1.08). Epigynum (Figs 11, 13B) with simple anterior plate protruding in lateral view; posterior plate wide, median part separated anteriorly from lateral parts by pair of whitish areas. Internal genitalia (Fig. 12) very simple, apparently without or with small and indistinct median receptacle, without or with very small pore plates.

Distribution

Known from type locality only, in Mexico, Guerrero (Fig. 2).

Natural history

The spiders were found by turning rocks in a forested valley (Fig. 34A). They shared the microhabitat with at least four further species of Pholcidae (Modisiminae): two representatives of *Modisimus* Simon, 1893, one *Psilochorus* Simon, 1893, and one species of uncertain generic position.

Pholcophora papanoa Huber sp. nov.
urn:lsid:zoobank.org:act:C2E5858B-2822-4630-BCEC-D34864087C0A
Figs 3F–G, 14–18, 33E–F

Diagnosis

Distinguished from similar congeners (*P. mazatlan* sp. nov., *P. mexcala*, *P. americana*) by shape of male bulbal process (Fig. 15F–H; distinctive dorsal process, without ventral flap) and by shape of male cheliceral apophyses (Fig. 15A–B; long, directed upwards, without or with barely visible proximal humps); from very similar *P. mazatlan* also by main element of procursus more truncated (Fig. 15E), by male cheliceral apophyses less strongly directed upwards, and by thicker male leg femora (0.28–0.30 vs 0.18–0.20). From *P. americana* also by tip of procursus (semi-transparent process not widening distally) and by shape of epigynum (Fig. 16; main epigynal plate posteriorly straight).

Fig. 14. *Pholcophora papanoa* Huber sp. nov., male paratype from Mexico, Guerrero, S of Papanoa (ZFMK Ar 23945). Left palp, prolateral, dorsal, and retrolateral views. Scale bar = 0.3 mm.

Etymology

The species name is derived from the type locality; noun in apposition.

Type material

Holotype

MEXICO – **Guerrero** • ♂; ~5 km S of Papanoa; 17.2711° N, 101.0328° W; 75 m a.s.l.; 4 Oct. 2019; B.A. Huber and A. Valdez-Mondragón leg.; low forest, leaf litter; LATLAX.

Paratypes

MEXICO – **Guerrero** • 1 ♂, 1 ♀; same collection data as for holotype; ZFMK Ar 23945.

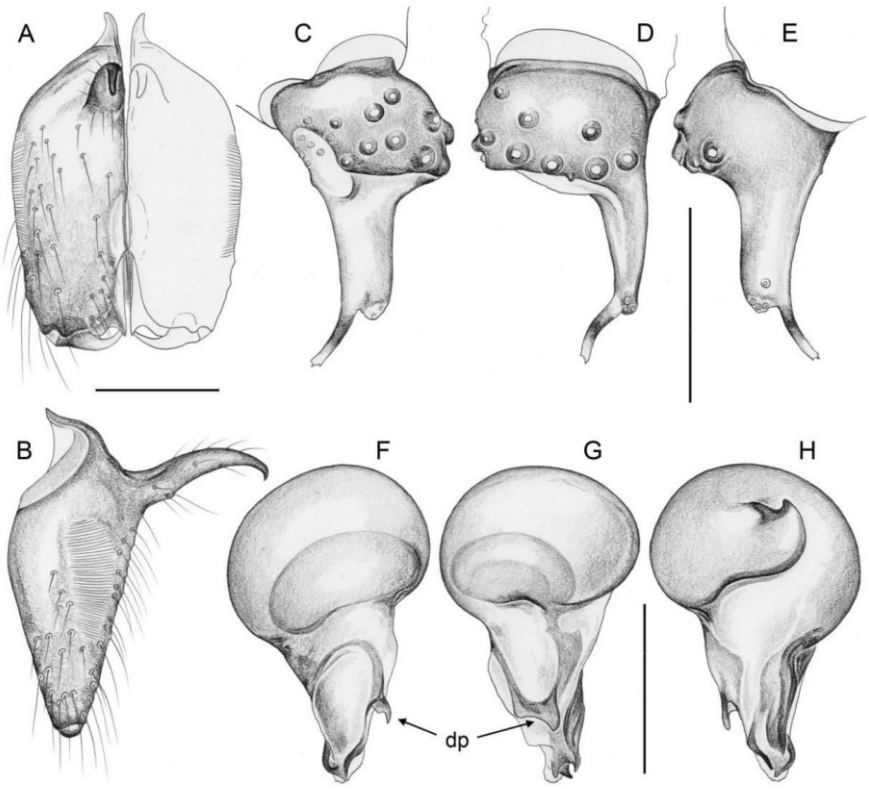

Fig. 15. *Pholcophora papanoa* Huber sp. nov., male paratype from Mexico, Guerrero, S of Papanoa (ZFMK Ar 23945). **A–B**. Chelicerae, frontal and lateral views. **C–E**. Left palpal tarsus and procursus, prolateral, dorsal, and retrolateral views. **F–H**. Left genital bulb, prolateral, dorsal, and retrolateral views. Abbreviation: dp, dorsal process. Scale bars = 0.2 mm.

Other material examined

MEXICO – **Guerrero** • 3 ♀♀, 1 juv., in pure ethanol (one female used for SEM); same collection data as for holotype; ZFMK Mex216 • 3 ♀♀ abdomens, together with paratypes (prosomata used for molecular work); same collection data as for holotype; ZFMK Ar 23945 • 2 ♂♂ (partly used for µ-CT study); same collection data as for holotype; ZFMK Ar 23947 • 1 ♂ (partly used for karyotype analysis); same collection data as for holotype; ZFMK Ar 23948.

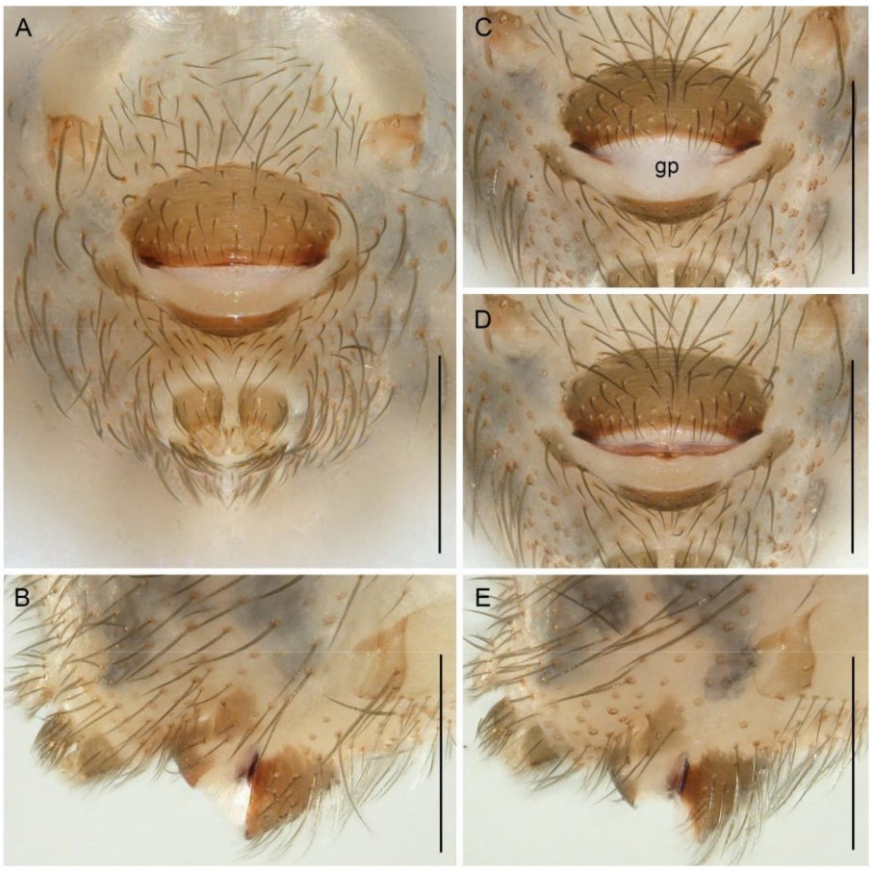

Fig. 16. *Pholcophora papanoa* Huber sp. nov., females from Mexico, Guerrero, S of Papanoa (ZFMK Ar 23945), epigyna. **A, C–D**. Ventral views. **B, E**. Lateral views. Figs C and D show the same specimen, with genital plug (gp) and without plug. Scale bars = 0.3 mm.

Description

Male (holotype)

Measurements. Total body length 2.4, carapace width 1.05. Distance PME-PME 60 µm; diameter PME 70 µm; distance PME-ALE 30 µm; distance AME-AME 20 µm; diameter AME 40 µm. Leg 1: 5.30 (1.50 + 0.40 + 1.30 + 1.55 + 0.55), tibia 2: 1.15, tibia 3: 1.05, tibia 4: 1.50; tibia 1 L/d: 9; diameters of leg femora 0.28–0.30, of leg tibiae 0.14–0.15.

Colour (in ethanol) . Prosoma and legs ochre-orange, no dark marks on carapace, leg femora distally darkened; abdomen grey with dark bluish internal marks; ventrally with light brown plate in front of gonopore.

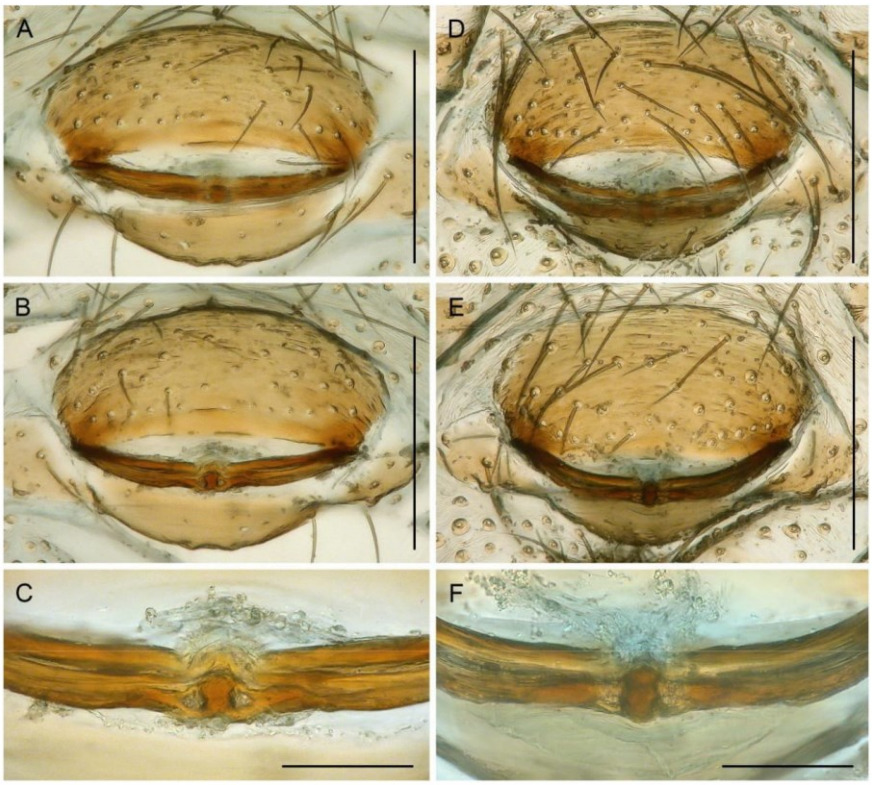

Fig. 17. *Pholcophora papanoa* Huber sp. nov., females from Mexico, Guerrero, S of Papanoa (ZFMK Ar 23945), cleared female genitalia. **A, D**. Ventral views. **B, E**. Dorsal views. **C, F**. Detail of median internal structures. Scale bars: A–B, D–E = 0.2 mm; C, F = 0.05 mm.

Body (Fig. 3F). Ocular area barely raised. Carapace with distinct but shallow thoracic groove. Clypeus unmodified, very short (clypeus rim to ALE: 0.24). Sternum slightly wider than long (0.68/0.58), heart-shaped (i.e., narrow posteriorly), with pair of distinct anterior processes near coxae 1. Abdomen globular.

Chelicerae (Fig. 15A–B). With pair of long frontal apophyses; stridulatory files fine but clearly visible in dissecting microscope; distances between cheliceral stridulatory ridges proximally 3.0 µm, distally 3.8 µm.

Palps (Fig. 14). Coxa unmodified; trochanter without process; femur proximally with retrolateral-ventral process and prolateral stridulatory pick, distally widened but simple, slightly curved towards

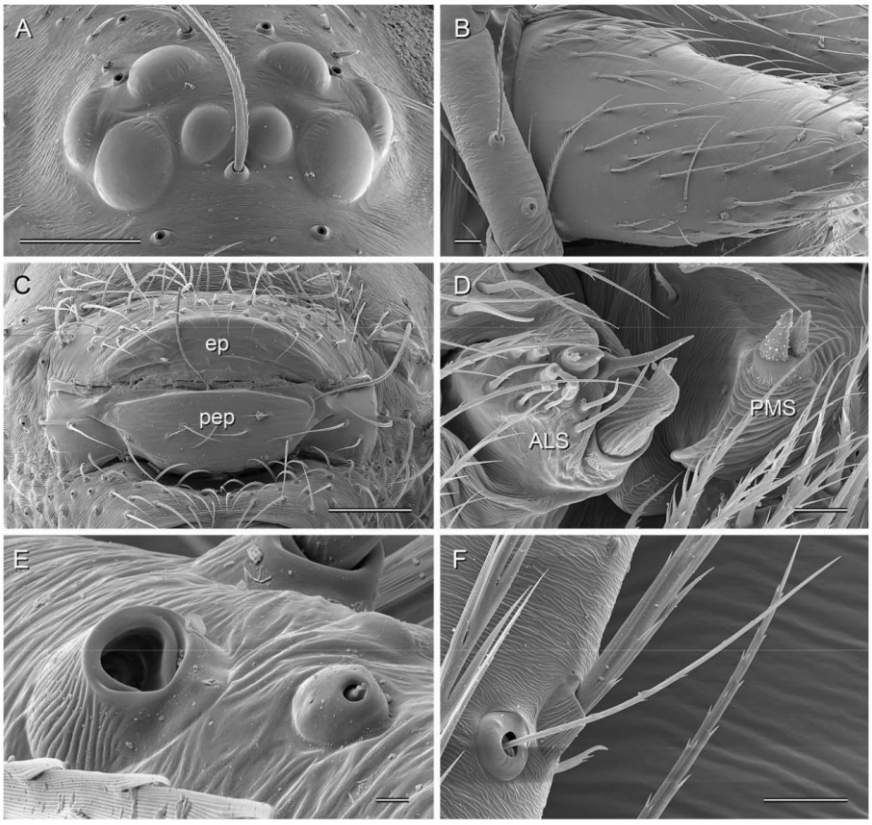

Fig. 18. *Pholcophora papanoa* Huber sp. nov., female from Mexico, Guerrero, S of Papanoa (ZFMK Mex216). **A**. Ocular area, frontal view. **B**. Right chelicera, lateral view, showing absence of stridulatory file. **C**. Epigynum, posterior view. **D**. Spinnerets. **E**. Palpal tarsal organ (and base of 'regular' hair). **F**. Prolateral trichobothrium on tibia 2. Abbreviations: ep = epigynum (main epigynal plate); pep = posterior epigynal plate. Scale bars: A, C = 100 µm; B, F = 20 µm; D = 10 µm; E = 2 µm.

dorsal; femur-patella joints slightly shifted toward prolateral side; tibia globular, with two trichobothria; procursus very simple (Fig. 15C–E), narrow distal part directed towards prolateral, with semi-transparent tip; genital bulb with distinctive dorsal process and sclerotized and membranous distal elements (Fig. 15F–H).

Legs. Without spines and curved hairs; with vertical hairs in two narrow dorsal bands on all tibiae (length ~20 µm); length of dorsal trichobothrium on tibia 1: ~100 µm; retrolateral trichobothrium of tibia 1 at 57%; prolateral trichobothrium absent on tibia 1; tarsus 1 with ~7 pseudosegments, only distally 2–3 distinct.

Variation (male)
Tibia 1 in other male: 1.35.

Female
In general, similar to male (Fig. 3G) but sternum without pair of anterior humps, tibiae without higher than usual density of short vertical hairs, and chelicerae without stridulatory files. Tibia 1 in four females: 0.90, 0.90, 1.00, 1.05. Epigynum (Figs 16, 18C) with simple anterior plate protruding posteriorly; posterior plate wide, median part separated anteriorly from lateral parts by pair of whitish areas. Internal genitalia (Fig. 17) very simple, apparently without or with small and indistinct median receptacle, without or with very small pore plates.

Distribution

Known from type locality only, in Mexico, Guerrero (Fig. 2).

Natural history

The spiders were found in dry leaf litter in a low hillside forest (Fig. 34C). They shared the microhabitat with at least three further species of Pholcidae (Modisiminae): one representative of *Modisimus* Simon, 1893, one *Anopsicus* Chamberlin & Ivie, 1938, and one species of uncertain generic position.

Pholcophora texana Gertsch, 1935
Figs 3H–I, 19–24, 33I–J

Remark

For synonymy, type material, and redescription, see Huber (2000).

Diagnosis

Easily distinguished from known congeners by unique brush of modified hairs on male palpal femur (Fig. 19A, C) and by pair of round sacs in female internal genitalia (Fig. 22B–D); also by shape of procursus (Fig. 20C–E; tip in lateral view with wide transparent flap), by shape of distal bulbal process (Fig. 20F–H), and by indistinct plate in front of main epigynal plate (Fig. 21A, C).

Material examined (new record)

MEXICO – **Hidalgo** • 1 ♂, 1 ♀, 3 female abdomens; ~2.5 km SW of Jacala; 20.9948° N, 99.2138° W; 1430 m a.s.l.; 21 Oct. 2019; B.A. Huber and A. Valdez-Mondragón leg.; ZFMK Ar 23952 • 7 ♀♀, 2 juvs, in pure ethanol (three female prosomata used for molecular work, abdomens transferred to ZFMK Ar 23952); same collection data as for preceding; ZFMK Mex341 • 6 ♀♀, 2 juvs (subadult ♂♂); same collection data as for preceding; LATLAX.

Description (amendments; see Huber 2000)

Male

Measurements of male from SW of Jacala, Hidalgo (ZFMK Ar 23952): body length 1.75, carapace width 0.70; tibia 1 length 1.25, metatarsus 1 length 1.30, tibia 2 length 0.95, tibia 4 length 1.25. Distance PME-PME 70 µm; diameter PME 50 µm; distance PME-ALE 25 µm; distance AME-AME 15 µm; diameter AME 30 µm. Diameters of leg femora 0.14–0.16, of leg tibiae 0.08–0.09. Clypeus unmodified, but slightly more protruding than in female; clypeus rim to ALE 0.21. Distances between cheliceral stridulatory ridges proximally 2.0 µm, distally 3.2 µm. Sternum humps very distinct, ~0.08 long. Procursus as in Fig. 20C–E, with distinctive transparent element distally (barely visible in dissecting microscope); genital bulb as in Fig. 20F–H. Leg tibiae with slightly higher number of vertical hairs than in female (proximally on tibiae 1 and 2); prolateral trichobothrium absent on tibia 1. Tibia 1 in previously measured specimens: 0.72 (Gertsch 1982); 0.96, 0.97, 1.39 (Huber 2000).

Female

In general, similar to male but sternum without pair of anterior humps, and chelicerae without stridulatory files. Tibia 1 in 11 females from SW of Jacala: 0.90–1.18 (mean 1.03). Epigynum and internal female genitalia as in Figs 21, 22, 23C, with pair of receptacles (shape varies slightly with angle of view), without (or with very small?) pore plates.

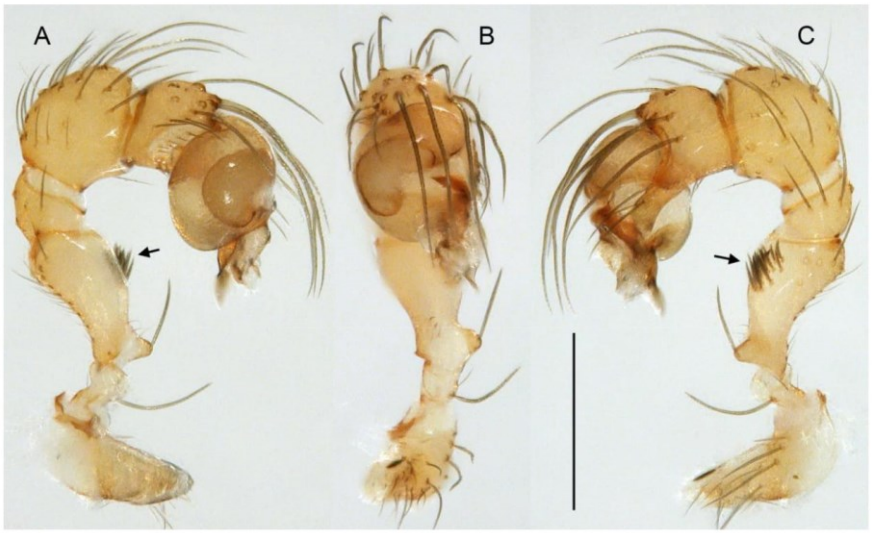

Fig. 19. *Pholcophora texana* Gertsch, 1935, male from Mexico, Hidalgo, SW of Jacala (ZFMK Ar 23952). Left palp, prolateral, dorsal, and retrolateral views; arrows point at unique brush of modified hairs. Scale bar = 0.3 mm.

Distribution

Apparently widely distributed in north-eastern Mexico, ranging into southern Texas (Fig. 2). However, the map in Fig. 2 includes four records that are based exclusively on females, i.e., the identifications should be verified (e.g., by collecting males or by sequencing specimens from these localities).

Natural history

The newly collected specimens were found under rocks on an arid hillside set with low thorn scrub (Fig. 34B).

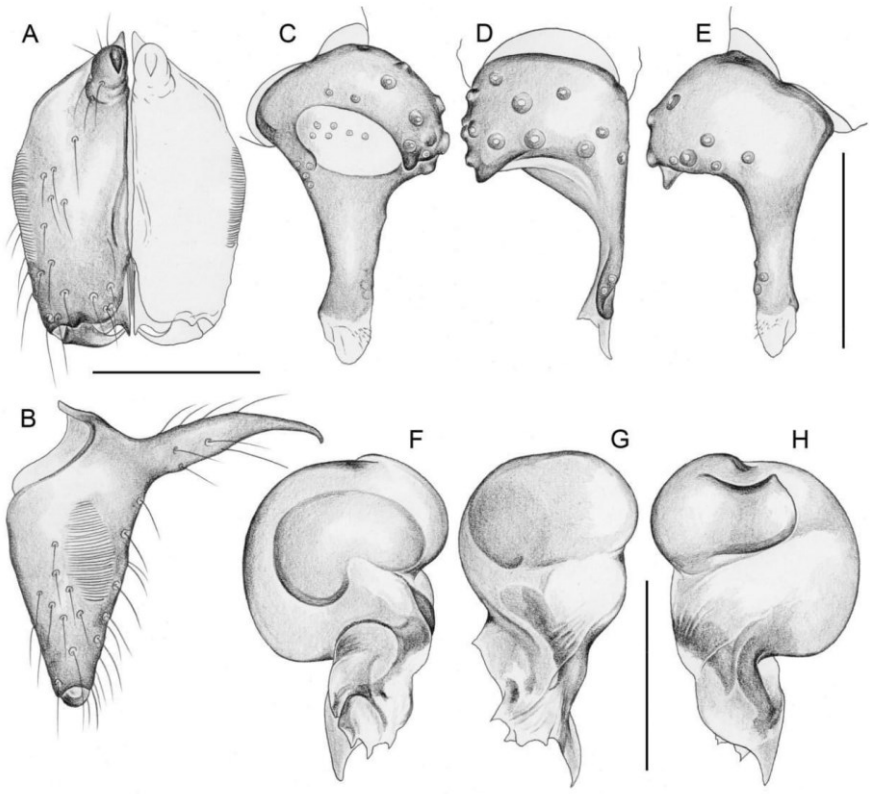

Fig. 20. *Pholcophora texana* Gertsch, 1935, male from Mexico, Hidalgo, SW of Jacala (ZFMK Ar 23952). **A–B**. Chelicerae, frontal and lateral views. **C–E**. Left palpal tarsus and procursus, prolateral, dorsal, and retrolateral views. **F–H**. Left genital bulb, prolateral, dorsal, and retrolateral views. Scale bars = 0.2 mm.

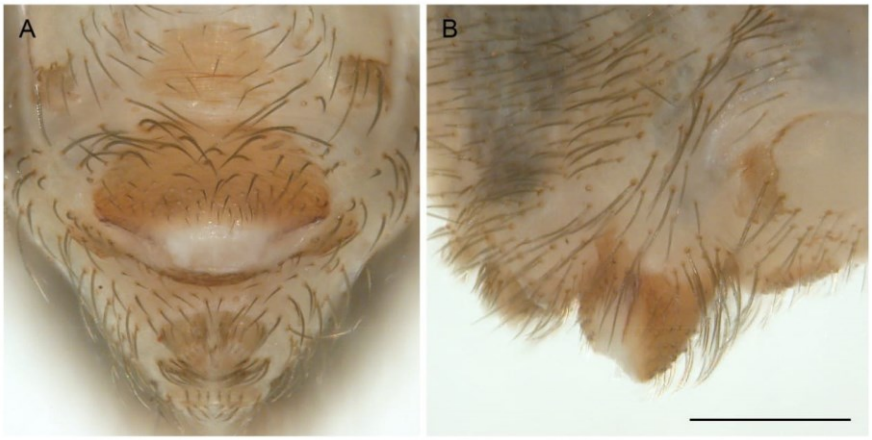

Fig. 21. *Pholcophora texana* Gertsch, 1935, female from Mexico, Hidalgo, SW of Jacala (ZFMK Ar 23952), epigynum. **A**. Ventral view. **B**. Lateral view. Scale bar = 0.3 mm (both at same scale).

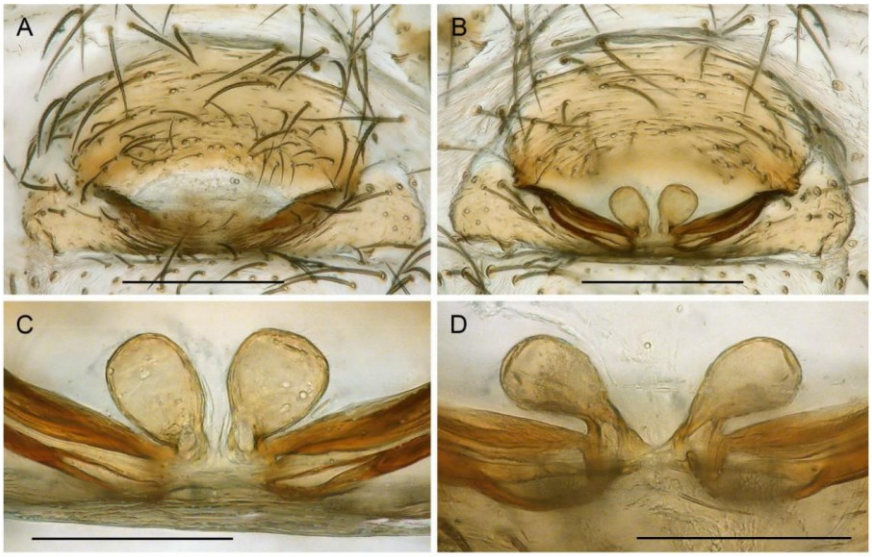

Fig. 22. *Pholcophora texana* Gertsch, 1935, females from Mexico, Hidalgo, SW of Jacala (ZFMK Ar 23952). **A–B**. Cleared female genitalia, ventral and dorsal views. **C–D**. Detail of median internal structures in two different specimens (slightly different angles of view). Scale bars: A–B = 0.2 mm; C–D = 0.1 mm.

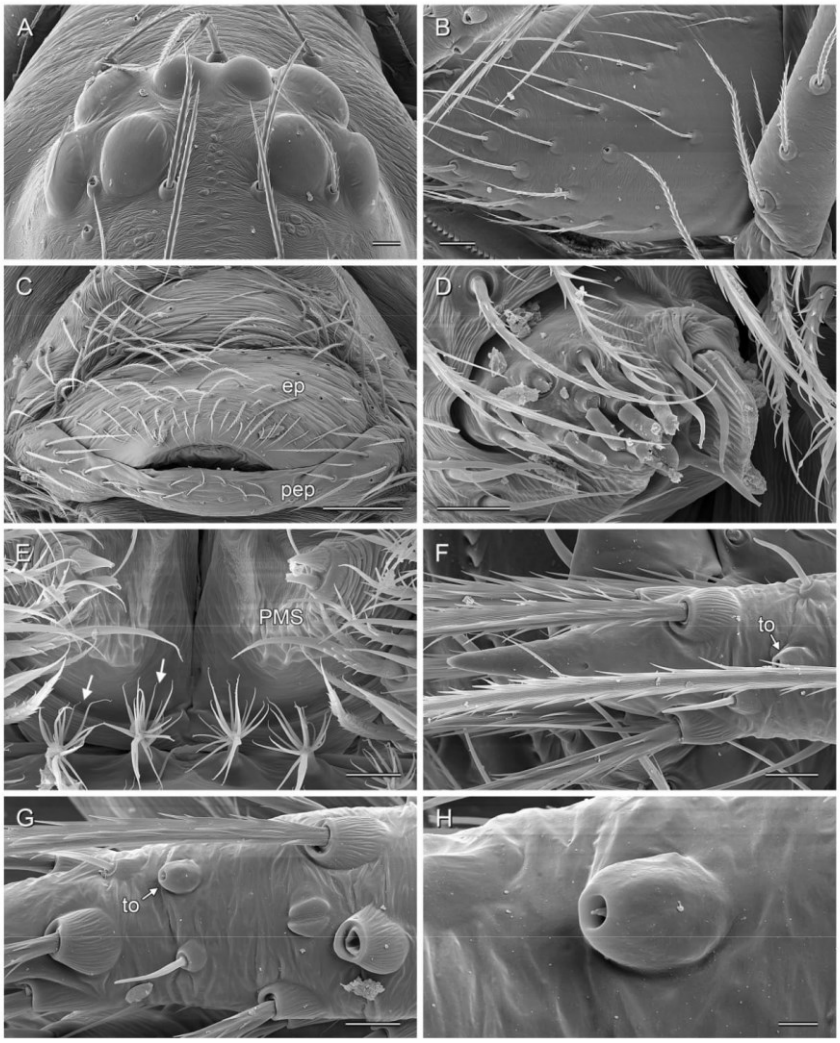

Fig. 23. *Pholcophora texana* Gertsch, 1935, female from Mexico, Hidalgo, 2.5 km SW of Jacala (ZFMK Mex341). **A**. Ocular area, dorsal view. **B**. Lateral face of chelicera, showing absence of stridulatory file. **C**. Epigynum, ventral (slightly posterior) view. **D**. ALS. **E**. PMS and anal hairs (arrows). **F**. Tip of left palpal tarsus, dorsal view. **G**. Detail of right palpal tarsus, dorsal view. **H**. Palpal tarsal organ. Abbreviations: ep = epigynum (main epigynal plate); pep = posterior epigynal plate; to = tarsal organ. Scale bars: A–B = 20 µm; C = 100 µm; D–G = 10 µm; H = 2 µm.

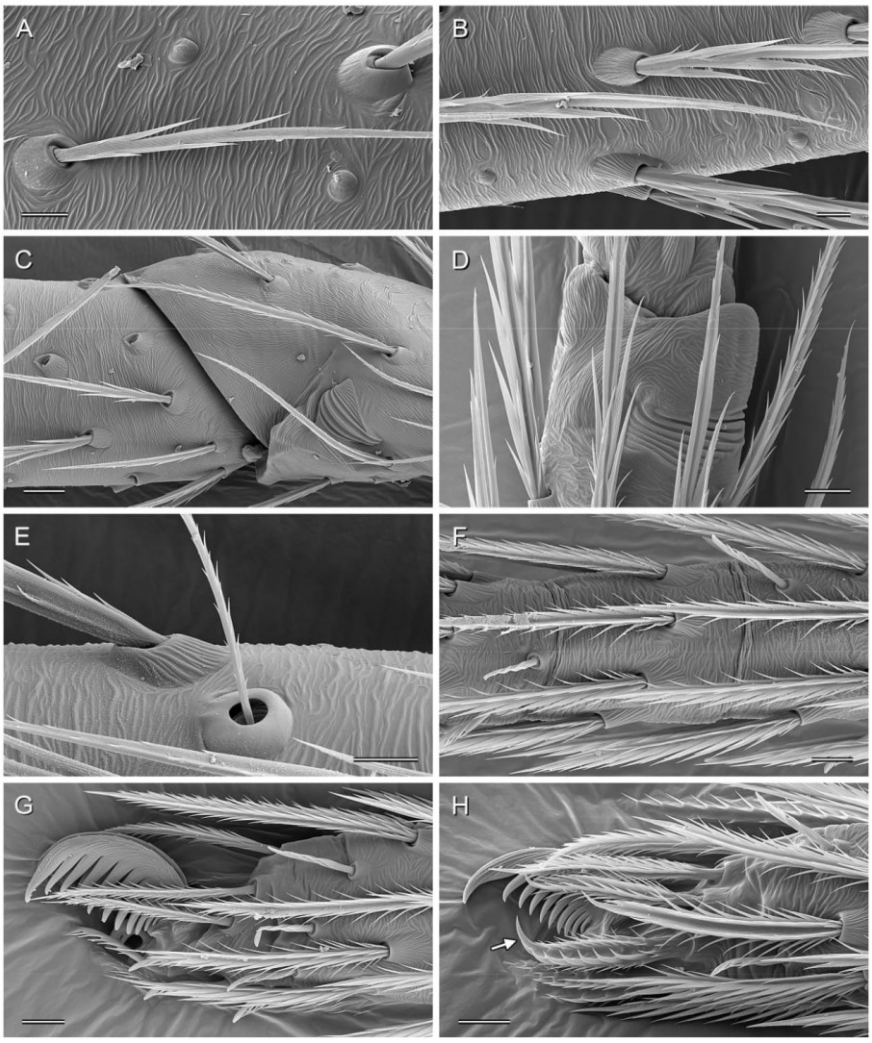

Fig. 24. *Pholcophora texana* Gertsch, 1935, female from Mexico, Hidalgo, 2.5 km SW of Jacala (ZFMK Mex341). **A**. Detail of femur 2, retrolateral view. **B**. Detail of tibia 4, retrolateral view. **C**. Patella-tibia 1 joint, retrolateral view. **D**. Metatarsus-tarsus 2 joint, retrolateral view. **E**. Retrolateral trichobothrium of tibia 1. **F**. Detail of tarsus 1, showing pseudosegmentation. **G**. Tip of tarsus 2, retrolateral view. **H**. Tip of tarsus 4, prolateral view, showing comb-hair (arrow). Scale bars: A–B, D–H = 10 µm; C = 20 µm.

Ninetinae ***Pholcophora tehuacan*** Huber sp. nov.

urn:lsid:zoobank.org:act:D7F69EC5-F4AB-4425-AABF-3257B146EA8A
Figs 3J–K, 25–29, 33K–L

Diagnosis

Easily distinguished from most known congeners (except *P. maria* Gertsch, 1977) by small size (carapace width < 0.70; tibia 1 length < 1.0) and by pair of tube-like sacs in female internal genitalia (Fig. 28B). From *P. maria* by shorter female internal sacs (60 µm vs 110 µm), smaller body (total body length 1.2 vs 1.65; carapace width 0.55 vs 0.65) and shorter legs (female tibia 1: 0.60–0.65 vs 0.93). Male of *P. maria* unknown.

Remark

Judging from the female internal genitalia (compare Fig. 28B with Huber 2000: fig. 1357), this species may be closely related to *P. maria* Gertsch, 1977 which is known from a single female specimen originating from Yucatan, Cueva (Gruta, Actún) Xpukil (20.551° N, 89.912° W, 80 m a.s.l.). This implies that *P. maria* is probably correctly placed in *Pholcophora* (it was considered incertae sedis in Huber 2000).

Etymology

The species name is derived from the type locality; noun in apposition.

Type material

Holotype

MEXICO – **Puebla** • ♂; ~35 km SE of Tehuacan, Calapa bridge, N side; 18.1652° N, 97.2605° W; 1020 m a.s.l.; 24 Oct. 2019; B.A. Huber and A. Valdez-Mondragón leg.; LATLAX.

Paratypes

MEXICO – **Puebla** • 2 ♂♂, 1 ♀, and 1 female abdomen; same collection data as for holotype; ZFMK Ar 23949 • 4 ♂♂, 22 ♀♀; same collection data as for holotype; LATLAX • 1 ♂, 1 ♀; same collection

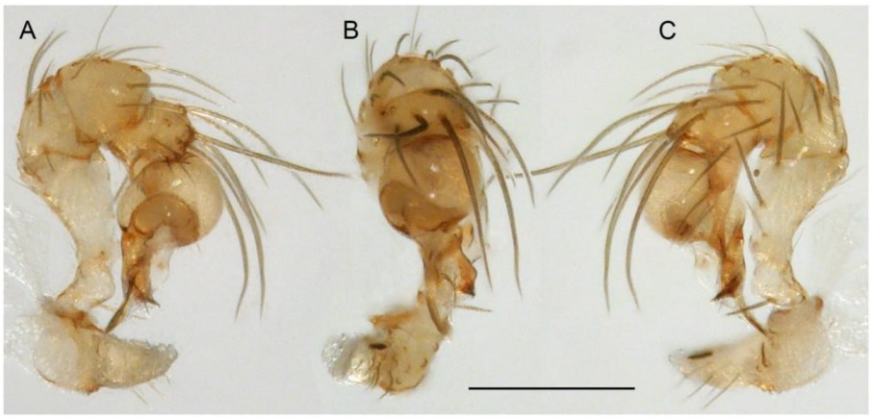

Fig. 25. *Pholcophora tehuacan* Huber sp. nov., male paratype from Mexico, Puebla, SE of Tehuacan (ZFMK Ar 23949). Left palp, prolateral, dorsal, and retrolateral views. Scale bar = 0.2 mm.

data as for holotype but W side of Calapa bridge; 18.1619° N, 97.2647° W; 1010 m a.s.l.; 23 Oct. 2019; ZFMK Ar 23950.

Other material examined

MEXICO – **Puebla** • 2 ♂♂, 6 ♀♀, 5 juvs, in pure ethanol; same collection data as for holotype; four female prosomata used for molecular work, 1 ♂ 1 ♀ used for SEM, 1 female abdomen transferred to ZFMK Ar 23949; ZFMK Mex353 • 1 ♂, 1 ♀; same collection data as for holotype; partly used for µ-CT study; ZFMK • 1 ♂; same collection data as for holotype; partly used for karyotype analysis; ZFMK 23951 • 1 juv., in pure ethanol; same collection data as for holotype but W side of Calapa bridge; ZFMK Mex350.

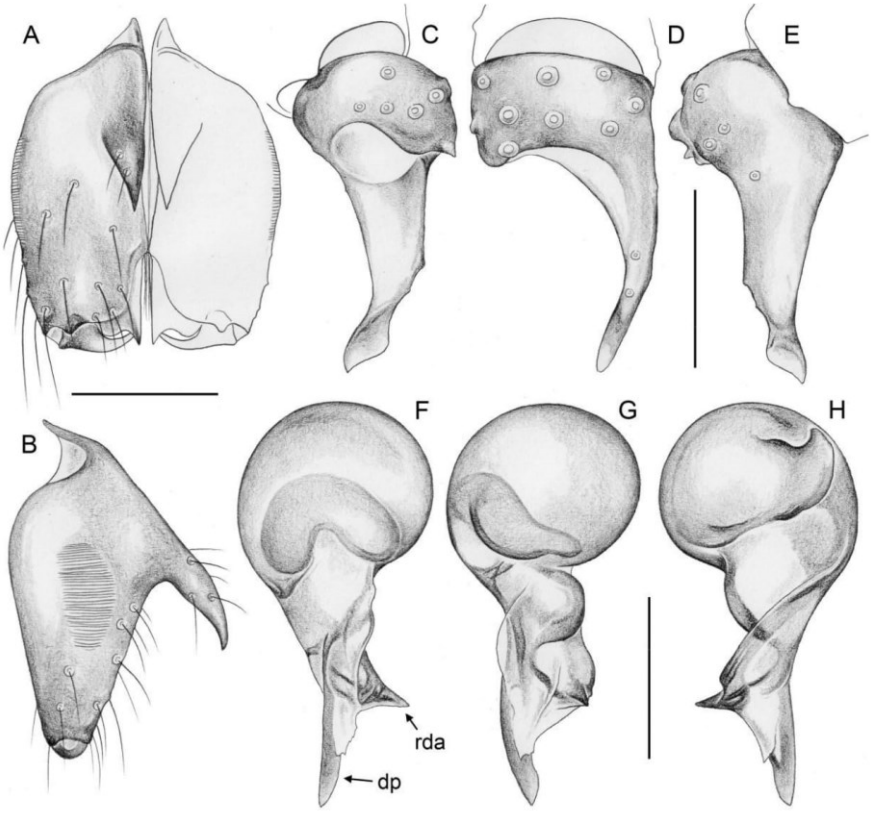

Fig. 26. *Pholcophora tehuacan* Huber sp. nov., male paratype from Mexico, Puebla, SE of Tehuacan (ZFMK Ar 23949). **A–B**. Chelicerae, frontal and lateral views. **C–E**. Left palpal tarsus and procursus, prolateral, dorsal, and retrolateral views. **F–G**. Left genital bulb, prolateral, dorsal, and retrolateral views. Abbreviations: dp = distal process; rda = retrolateral-dorsal apophysis. Scale bars = 0.1 mm.

Description

Male (holotype)

Measurements. Total body length 1.20, carapace width 0.55. Distance PME-PME 40 µm; diameter PME 45 µm; distance PME-ALE 20 µm; distance AME-AME 15 µm; diameter AME 20 µm. Leg 1: 2.55 (0.75 + 0.20 + 0.65 + 0.60 + 0.35), tibia 2: 0.55, tibia 3: 0.50, tibia 4: 0.75; tibia 1 L/d: 8; diameters of leg femora 0.11–0.12, of leg tibiae 0.08.

Colour (in ethanol). Prosoma and legs monochromous pale ochre-yellow; abdomen slightly darker, also monochromous.

Body. Habitus as in Fig. 3J. Ocular area barely raised. Carapace with low thoracic groove. Clypeus unmodified, very short (clypeus rim to ALE 0.12). Sternum slightly wider than long (0.34/0.32), almost round (i.e., not heart-shaped), with pair of small but distinct anterior processes (~30 µm long) near coxae 1. Abdomen globular; gonopore with four epiandrous spigots (Fig. 29C); ALS with seven spigots, PMS with two spigots (Fig. 29G).

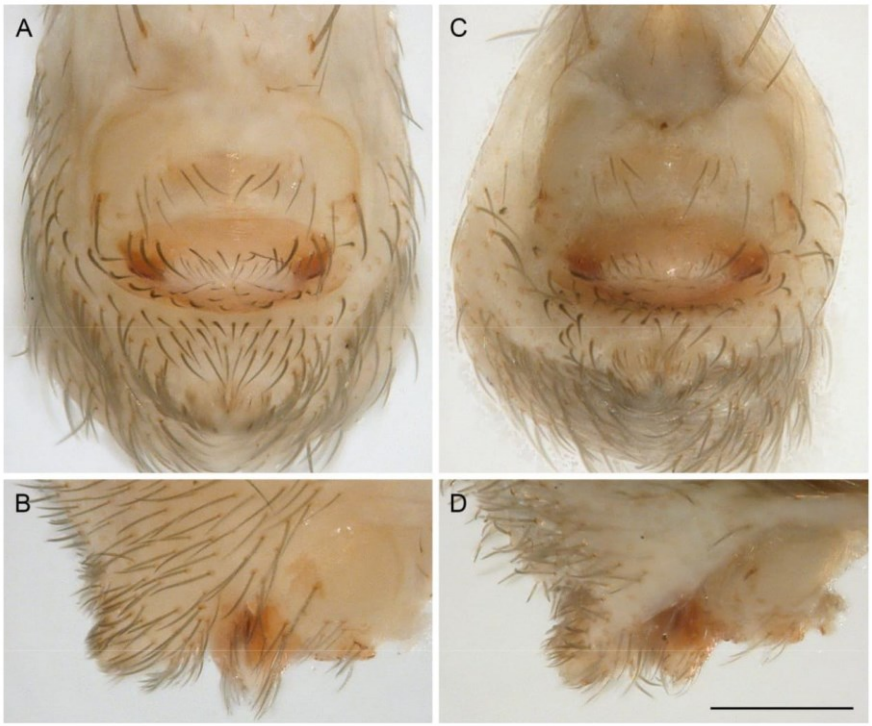

Fig. 27. *Pholcophora tehuacan* Huber sp. nov., females from Mexico, Puebla, SE of Tehuacan (ZFMK Ar 23949), epigyna. **A, C**. Ventral views. **B, D**. Lateral views. Scale bar = 0.2 mm (all at same scale).

Chelicerae (Fig. 26A–B). With pair of frontal apophyses directed downwards; stridulatory ridges very fine (Fig. 29A; distances between ridges 2.0–2.2 µm), not visible in dissecting microscope.

Palps (Fig. 25). Coxa unmodified; trochanter without process; femur proximally with retrolateral-ventral process and prolateral stridulatory pick, distally widened but simple, slightly curved towards dorsal; femur-patella joints slightly shifted toward prolateral side; tibia very short, with two trichobothria; tibia-tarsus joints not shifted to one side; tarsal organ raised, with small opening (Fig. 29E); procursus very simple (Fig. 26C–E), with subdistal constriction and semi-transparent tip; genital bulb complex (Fig. 26F–H), with distinctive retrolateral-dorsal apophysis and long distal process.

Legs. Without spines and curved hairs; with usual low number of short vertical hairs; retrolateral trichobothrium of tibia 1 at 60%; prolateral trichobothrium absent on tibia 1; tarsus 1 with 6 pseudosegments, all fairly distinct.

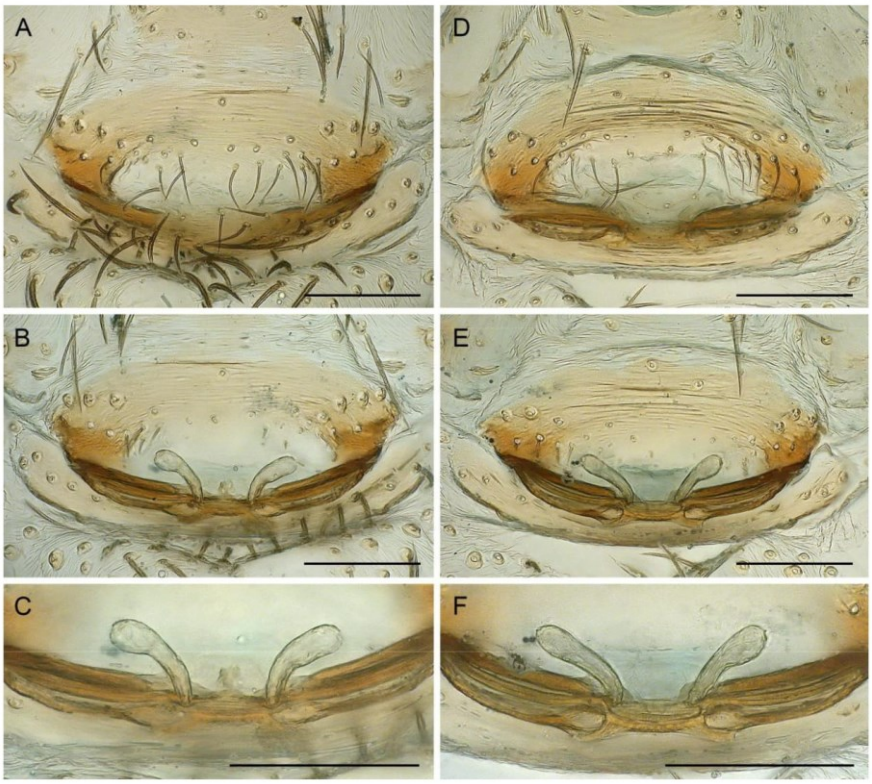

Fig. 28. *Pholcophora tehuacan* Huber sp. nov., females from Mexico, Puebla, SE of Tehuacan (ZFMK Ar 23949), cleared female genitalia. **A, D**. Ventral views. **B, E**. Dorsal views. **C, F**. Detail of median internal structures. Scale bars = 0.1 mm.

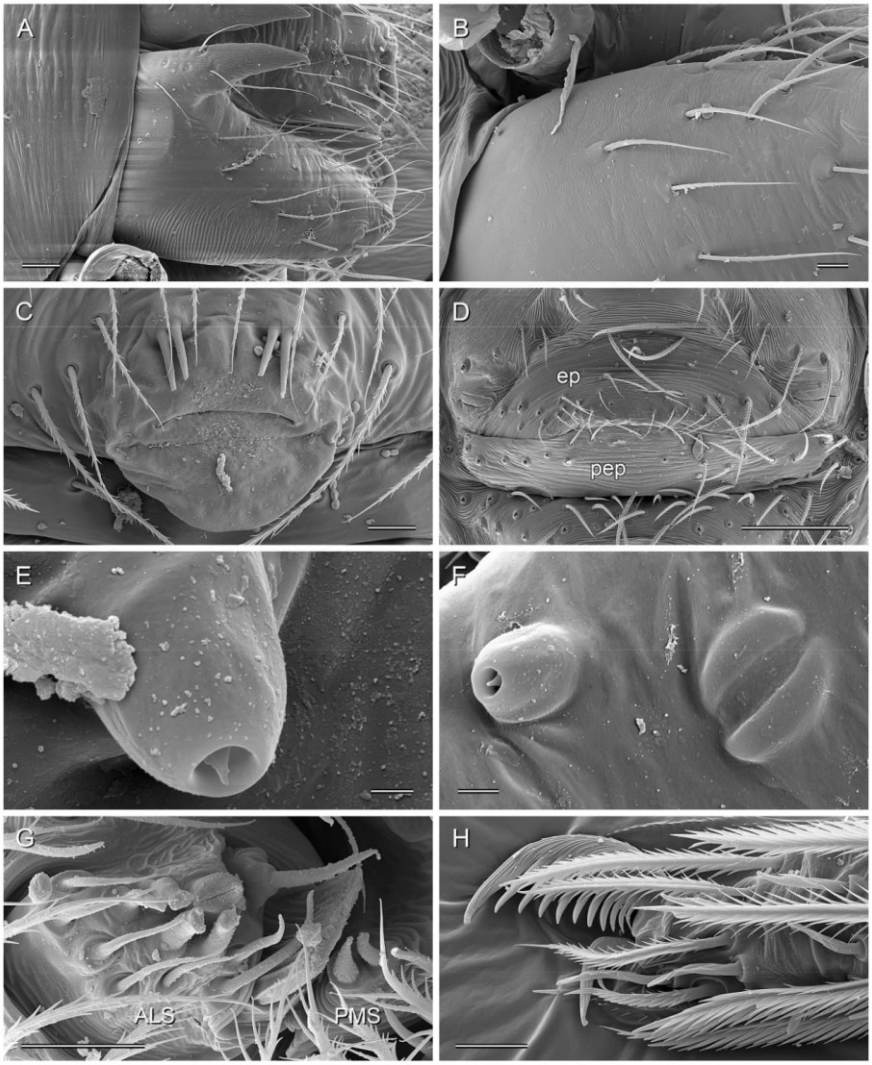

Fig. 29. *Pholcophora tehuacan* Huber sp. nov., male and female from Mexico, Puebla, 35 km SE of Tehuacan (ZFMK Mex353). **A**. Male chelicerae, oblique frontal view. **B**. Lateral face of female chelicera, showing absence of stridulatory file. **C**. Male gonopore with epiandrous spigots. **D**. Epigynum, ventral view. **E**. Male palpal tarsal organ. **F**. Female palpal tarsal organ and slit sensillum. **G**. Male ALS and PMS. **H**. Tip of right male tarsus 2, prolateral view. Abbreviations: ep = epigynum (main epigynal plate); pep = posterior epigynal plate. Scale bars: A = 20 µm; B–C, G–H = 10 µm; D = 100 µm; E = 1 µm; F = 2 µm.

Variation (male)
Tibia 1 in ten males (incl. holotype): 0.60–0.65 (mean 0.62).

Female
In general, similar to male (Fig. 3K) but sternum without pair of anterior humps, and chelicerae without stridulatory files (Fig. 29B). Total body length ~1.20–1.40; tibia 1 in 14 females 0.60–0.65 (mean 0.62). Epigynum (Fig. 27) with short and simple anterior plate slightly protruding in lateral view; posterior plate wide, median part not separated from lateral parts by pair of whitish anterior areas. Internal genitalia (Fig. 28) with pair of distinct sacs (receptacles?) 60 μm long, without (or with very small?) pore plates.

Distribution

Known from type locality only, in Mexico, Puebla (Fig. 2).

Natural history

The spiders were found by turning rocks in a very dry area (Fig. 34D). They shared the microhabitat and sometimes the individual rock with a small undescribed species of *Physocyclus* Simon, 1893, and were difficult to distinguish from juveniles of that species. At disturbance they started to run rapidly and dropped from the rock to the ground (where they could no longer be found). The area was shared by a second representative of *Pholcophora* ("Mex354", see below), which also shared the microhabitat but was never found on the same rock as *Pholcophora tehuacan* sp. nov.

Putative further species

Pholcophora "Mex354"
Figs 3L, 30, 33G–H

This species is not formally described because no male is available. The morphology of the epigynum (Fig. 30A–B) reminds of geographically close congeners (*P. mazatlan* sp. nov.; *P. papanoa* sp. nov.) but the main epigynal plate is not straight posteriorly but has a pair of lateral indentations, and the legs tend to be longer (tibia 1 in 10 females 1.12–1.40, mean 1.28). The female of *P. mexcala* is unknown, but *P. mexcala* seems to be a much bigger species (male tibia 1 length > 4.0). The specimens were collected in a dry area, together with a second representative of *Pholcophora* (*P. tehuacan* sp. nov.), and five further species of Pholcidae (*Physocyclus modestus* Gertsch, 1971; *Physocyclus* sp.; *Modisimus* sp.; *Psilochorus* spp.). The spiders were usually found on the undersides of rocks, apparently in tiny webs; they did not run unless the web was damaged by turning the rock.

Material examined

MEXICO – **Puebla** • 5 ♀♀, in pure ethanol; ~35 km SE of Tehuacan, N of Calapa bridge; 18.1652° N, 97.2605° W; 1020 m a.s.l.; 24 Oct. 2019; B.A. Huber and Valdez-Mondragón leg.; thorn scrub, under rocks; two prosomata used for molecular work; ZFMK Mex354 • 8 ♀♀; same collection data as for preceding; LATLAX.

Pholcophora? "Car544"
Figs 31, 33M

S298 *Pholcophora*? *Car544* Car544 – Eberle *et al.* 2018 (molecular data). — Huber *et al.* 2018:

55. **Remarks**

The two adult females available of this species resemble *P. bahama* Gertsch, 1982 that is known from a single adult female specimen (from Bahamas, West Caicos Island). The two species are distinguished by the strong rectangular sclerite between pedicel and epigynum in the present species (Fig. 31C). Habitus

and size of the two species appear identical, and the female internal genitalia share a median tube-like sac (compare Fig. 31G with Huber 2000: fig. 1356). The distinctive pair of internal posterior structures appears more widely separated in the present species (only one female cleared). Our molecular data

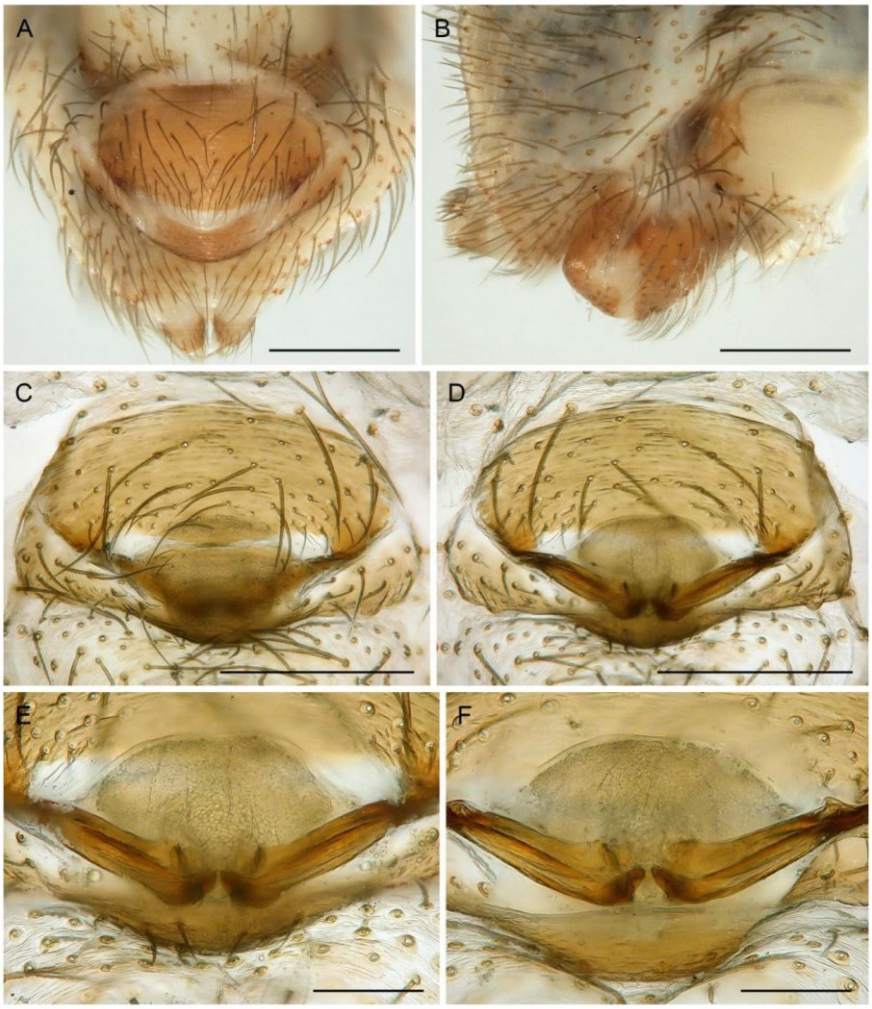

Fig. 30. *Pholcophora* "Mex354", females from Mexico, Puebla, SE of Tehuacan (ZFMK Mex354). **A–B**. Epigynum, ventral and lateral views. **C–D**. Cleared female genitalia, ventral and dorsal views. **E–F**. Detail of median internal structures in two different specimens. Scale bars: A–D = 0.3 mm; E–F = 0.1 mm.

suggest that the present species (together with *Pholcophora bahama* if the similarity above indeed reflects close relationship) is more closely related with an undescribed Cuban species (see below) and

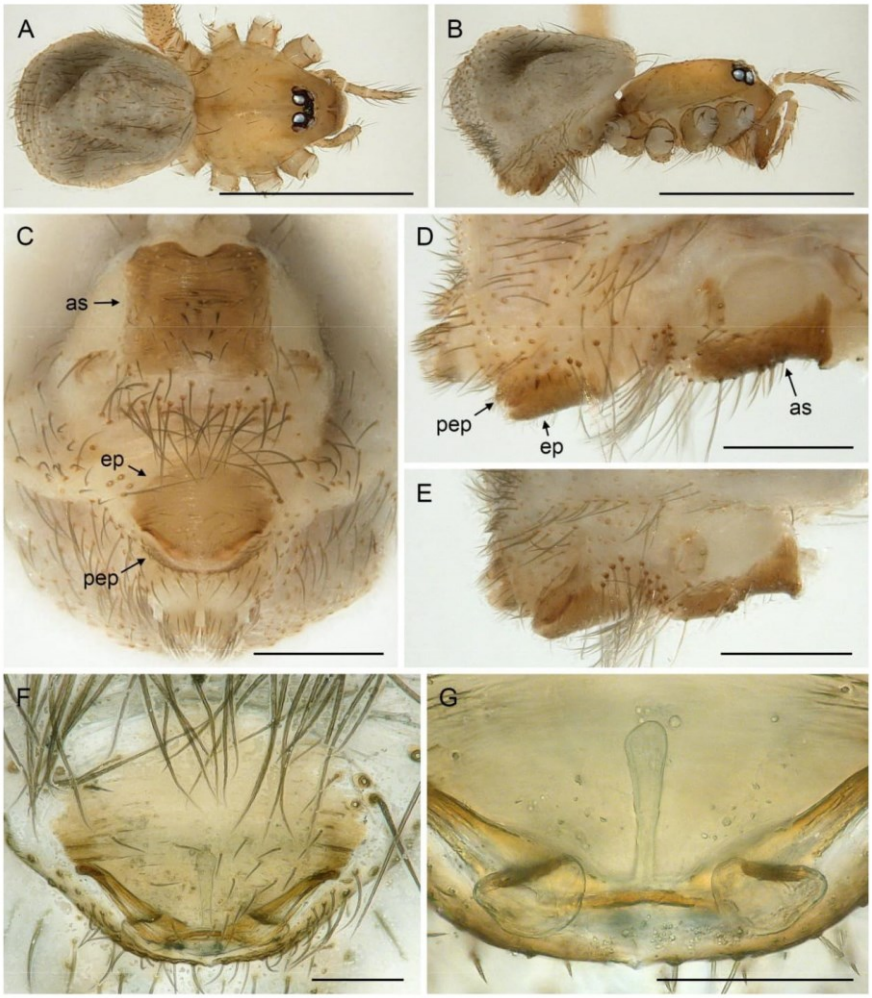

Fig. 31. *Pholcophora*? "Car544", females from Puerto Rico, Isla Mono (USNM ENT 783464, 783466). **A–B**. Habitus, dorsal and lateral views. **C**. Abdomen, ventral view. **D–E**. Abdomens of two specimens, lateral views (at same scale). **F**. Cleared female genitalia, ventral view. **G**. Detail of median internal structures, dorsal view. Abbreviations: as = anterior sclerite; ep = epigynum (main epigynal plate); pep = posterior epigynal plate. Scale bars: A–B = 1 mm; C–E = 0.3 mm; F–G =0.1 mm.

with the Caribbean (Curaçao) genus *Papiamenta* Huber, 2000 than with true *Pholcophora*. Our UCE dataset (G. Meng, L. Podsiadlowski, B.A. Huber, unpubl. data) does not include the present species.

Material examined

PUERTO RICO – **Isla Monito** • 2 ♀♀, 1 juv., in pure ethanol; precise locality not specified; 18.16° N, 67.95° W; 14 Aug. 2012; I. Agnarsson *et al.* leg.; USNM ENT 783463, 783464, 783466.

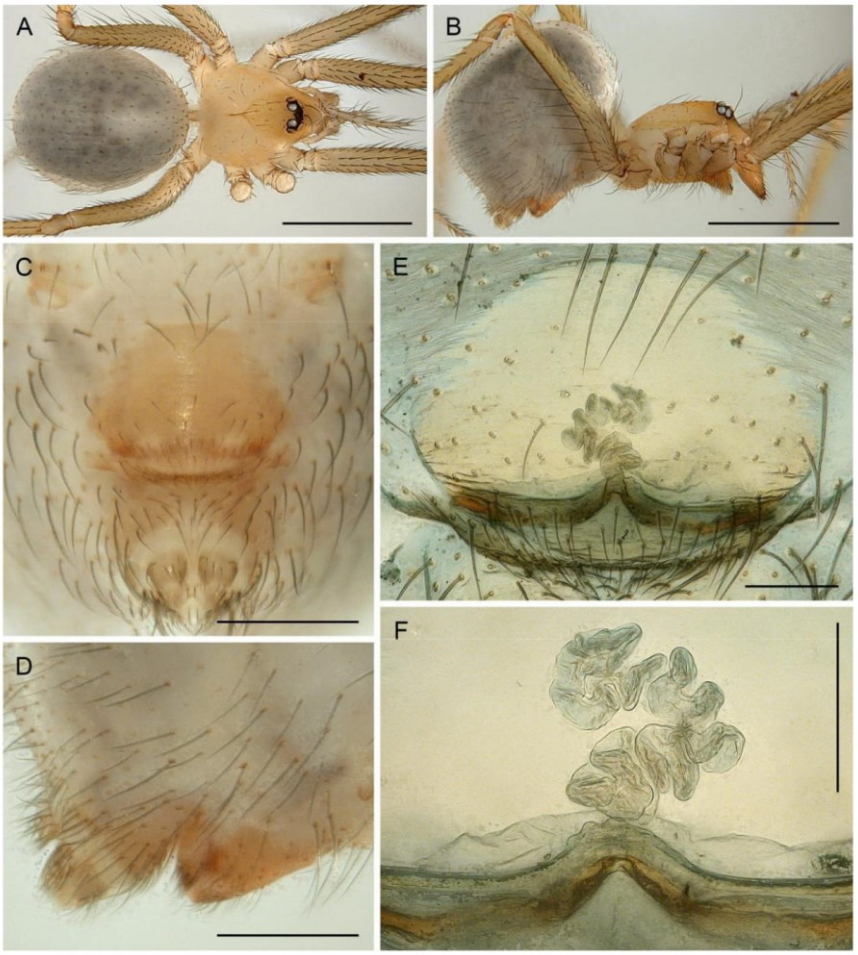

Fig. 32. *Pholcophora*? "Cu12-325", female from Cuba, Santiago de Cuba, Siboney (ZFMK Cu12-325). **A–B**. Habitus, dorsal and lateral views. **C–D**. Abdomen, ventral and lateral views. **E**. Cleared female genitalia, ventral view. **F**. Detail of median internal structures, dorsal view. Scale bars: A–B = 1 mm; C–D = 0.3 mm; E–F = 0.1 mm.

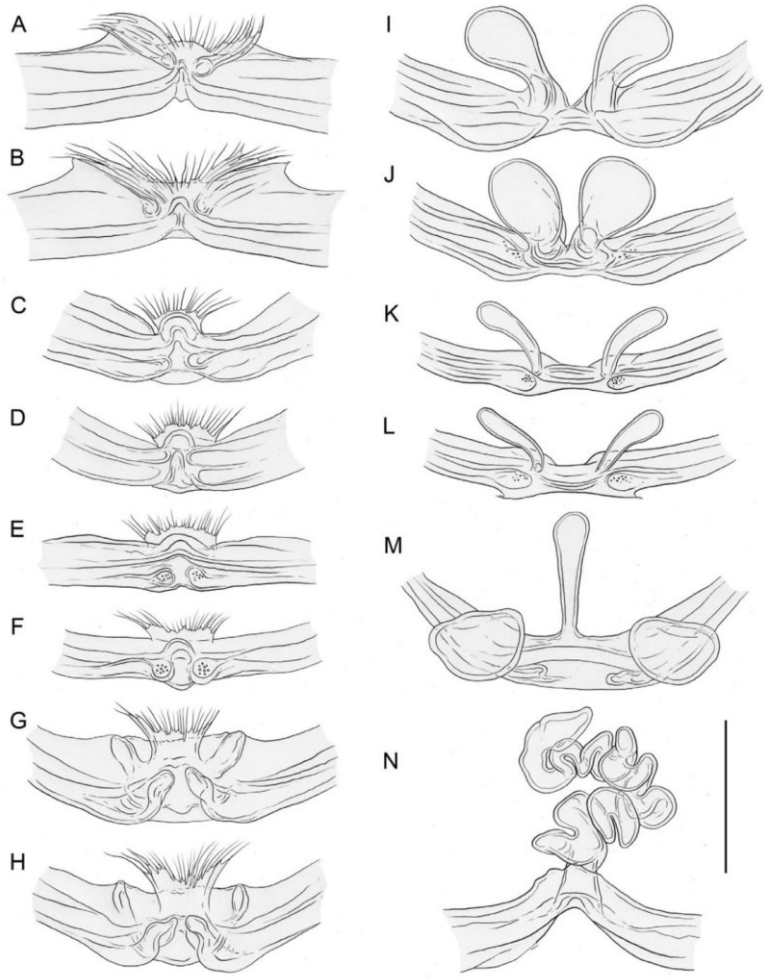

Fig. 33. *Pholcophora* internal female genitalia, median sections of main transversal internal sclerite. **A–B**. *P. americana* Banks, 1896, females from USA, California, Inyo Nat. Forest (ZFMK G089) and Colorado, near Golden (ZFMK USA16). **C–D**. *P. mazatlan* Huber sp. nov., females from Mexico, Guerrero, N of Mazatlán (ZFMK Ar 23943). **E–F**. *P. papanoa* Huber sp. nov., females from Mexico, Guerrero, S of Papanoa (ZFMK Ar 23945). **G–H**. *P.* "Mex354", females from Mexico, Puebla, SE of Tehuacan (ZFMK Mex354). **I–J**. *P. texana* Gertsch, 1935, females from Mexico, Hidalgo, SW of Jacala (ZFMK Ar 23952). **K–L**. *P. tehuacan* Huber sp. nov., females from Mexico, Puebla, SE of Tehuacan (ZFMK Ar 23949). **M**. *Pholcophora*? "Car544", female from Puerto Rico, Isla Mono (USNM ENT 783464). **N** . *Pholcophora*? "Cu12-325", female from Cuba, Santiago de Cuba, Siboney (ZFMK Cu12-325). Scale bar = 0.1 mm.

***Pholcophora*? "Cu12-325"**
Figs 32, 33N

S323 Gen. *Cu12-325* Cu12-325 – Eberle *et al.* 2018 (molecular data). — Huber *et al.* 2018: 55.

Remarks

The two adult females available of this species resemble other large representatives of the genus (Fig. 32A–B); body length 2.4; tibia 1 length 1.28, 1.36. Epigynum (Fig. 32C–D) consisting of trapezoidal anterior plate and short but wide posterior plate; internal genitalia (Fig. 32E–F) with distinctive median tube, curled up and ~600 µm long (reminding of the putatively distantly related *Gertschiola neuquena* Huber, 2000; see Huber 2000: fig. 354).

Our molecular data suggest that the present species is more closely related with other Caribbean taxa (*Pholcophora bahama*, the undescribed *Pholcophora*? "Car544", and the genus *Papiamenta*) than with true *Pholcophora*.

Material examined

CUBA – **Santiago de Cuba** • 2 ♀♀, in pure ethanol; Siboney, Cueva de los Majases; 19.9623° N, 75.7171° W; ~90 m a.s.l.; Apr. 2012; F. Cala Riquelme leg.; ZFMK Cu12-325.

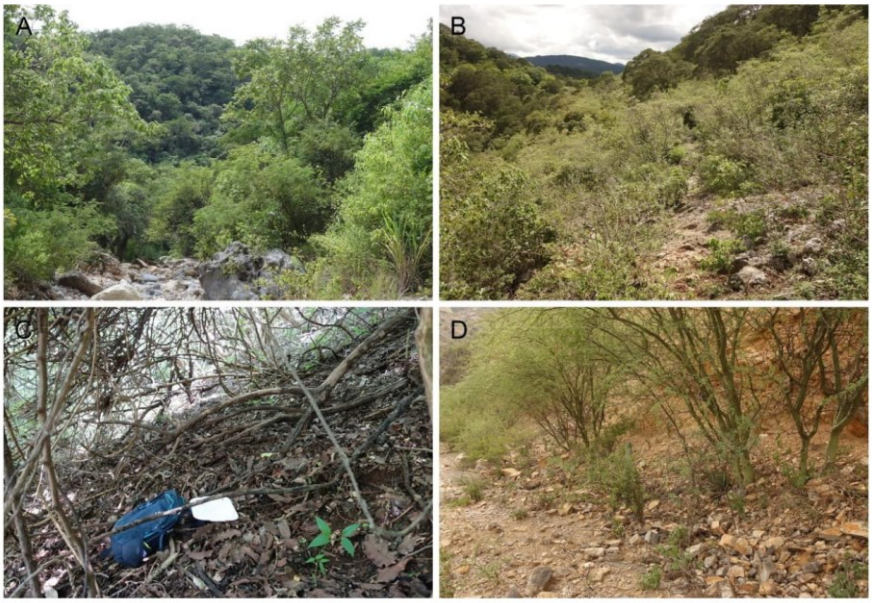

Fig. 34. Representative sample of habitats of *Pholcophora* Banks, 1896 in Mexico. **A**. Guerrero, 2 km N of Mazatlán (type locality of *P. mazatlan* Huber sp. nov.). **B**. Hidalgo, 2.5 km SW of Jacala (*P. texana* Gertsch, 1935). **C**. Guerrero, 5 km S of Papanoa (type locality of *P. papanoa* Huber sp. nov.; with collecting tray). **D**. Puebla, 35 km SE of Tehuacan (type locality of *P. tehuacan* Huber sp. nov.).

Genus ***Tolteca*** Huber, 2000

Tolteca Huber, 2000: 117. Type species: *Pholcophora hesperia* Gertsch, 1982.

Diagnosis

Easily distinguished from only other North American Ninetinae genus *Pholcophora* by small male cheliceral apophyses originating distally (Figs 38A–B, 44; in *Pholcophora* large and originating proximally); also by absence of stridulatory ridges on male chelicerae (Figs 41A, 46F); most species (except *T. sinnombre* sp. nov.) also by knob-shaped structure between epigynum and pedicel (Figs 43A, 45A, 49A); from most species (except *P. tehuacan* sp. nov.) also by smaller size (body length ~1.1–1.4; in *Pholcophora* ~1.7–3.1) and shorter legs (tibia 1 < 0.7, in *Pholcophora* > 1.0). From other geographically close genera (*Papiamenta*, *Galapa*) also by simple rod-shaped procursus (Figs 38C, 51C; much shorter in *Papiamenta*; with dorsal process in *Galapa*), by presence of humps on male sternum (absent in *Papiamenta*), and by unmodified male cheliceral fangs (with processes in *Galapa*).

Description

Male

Measurements. Total body length 1.1–1.4, carapace width 0.45–0.55. Legs very short, tibia 1 ~0.45– 0.60; tibia 1 ~1.0–1.1 x carapace width; tibia 1 L/d 7–9; tibia 2 much shorter than tibia 4 (tibia 2 / tibia 4: 0.6–0.7).

Colour. Live specimens reddish brown (Fig. 36); carapace usually monochromous, sometimes with very indistinct darker median line widening anteriorly behind ocular area; abdomen colour slightly variable, usually monochromous, sometimes with indistinct dorsal marks; legs without dark or light bands. Colour in ethanol similar but paler, rather yellowish.

Body. Ocular area barely raised, eight eyes, AME relatively large, diameter ~25–30 µm, ~60–80% of PME diameter; Carapace without thoracic groove or with very indistinct low median indentation (visible in frontal view only). Clypeus unmodified or with rim slightly more sclerotized than in female. Sternum wider than long, with pair of distinct anterior processes near leg coxae 1. Abdomen globular; presence of epiandrous spigots unclear (reported as present in Huber 2000: fig. 126; not seen in two newly examined males of *T. hesperia* and *T. manzanillo* Huber sp. nov.; Fig. 46G); ALS with seven spigots each (Fig. 54C): one strongly widened spigot, one long pointed spigot, and five cylindrical spigots (one of which is unusually large); PMS with two short, pointed spigots (Fig. 54C); PLS without spigots.

Chelicerae. With one pair of simple frontal apophyses (Figs 38A–B, 41A–B); without stridulatory files (Figs 41A, 46F).

Palps. Coxa unmodified; trochanter barely modified (indistinct ventral projection); femur cylindrical, slightly widened distally, proximally without retrolateral hump; patella short; tibia globular, with two trichobothria; palpal tarsal organ raised, capsulate with small opening (Figs 41E–F, 46C–D; diameter of opening ~1.1–1.3 µm); procursus simple and straight (Figs 38C, 46A–B), without dorsal flap, not strongly elongated; genital bulb large (compared to palp size), with complex distal system of sclerites and folds, partly only visible in SEM (Figs 41C–D, 46A–B).

Legs. Without spines and curved hairs; with very short vertical hairs in higher density on tibia 1 (Fig. 42A–B; length of hairs ~20 µm). Trichobothria in usual arrangement: three on each tibia (except tibia 1: prolateral trichobothrium absent), one on each metatarsus; slightly feathered (Fig. 54D); length of dorsal trichobothrium on tibia 1: ~100 µm; retrolateral trichobothrium of tibia 1 in very distal

position (at 59–65%). Tarsus 1 with 4–6 distinct pseudosegments; tarsus 4 distally with one comb-hair on prolateral side (cf. Fig. 54H); leg tarsal organs very small, capsulate with small opening (Fig. 46E; diameter of opening ~1.0–1.4 µm); three claws (Fig. 42H).

Female

In general (size, colour) similar to male (Fig. 36) but sternum without pair of anterior humps, palpal tarsal organ less strongly raised (Figs 41G, 54E), and leg tibia 1 with usual low number of short vertical hairs; legs either slightly shorter than in males or of same length (only *T. oaxaca* sp. nov. with reasonable sample size: male/female tibia 1 length: 1.06). Spinnerets and comb-hairs as in male. Epigynum main (anterior) plate transversal band-shaped to crescent-shaped, weakly protruding in lateral view; posterior plate often indistinct, short but wide, usually with median anterior projection. Usually with distinct knob-shaped structure between epigynum and pedicel (Figs 43A, 45A, 49A, 54A–B; absent in *T. sinnombre* sp. nov.). Internal genitalia very simple, with pair of distinct transversal sclerites and pair of membranous sacs originating medially (Fig. 55), sacs very short in *T. oaxaca* (9–13 µm) and in *T. jalisco* (Gertsch, 1982) (18 µm), very long in *T. sinnombre* (85 µm); in other species ~42–48 µm; apparently without pore plates (possibly with very indistinct tiny groups of pores near median line).

Relationships

The genus *Tolteca* was not included in the molecular analysis of Eberle *et al.* (2018). Our new molecular data mostly suggest that *Tolteca* is sister to a clade consisting of true *Pholcophora* and a Caribbean clade (*Papiamenta* Huber, 2000 + Caribbean '*Pholcophora*'). This supports a monophyletic North American-Caribbean clade of Ninetinae (Fig. 1; see also general results of molecular analyses above). The latter clade is also strongly supported in our preliminary analyses of UCE data (G. Meng, L. Podsiadlowski, B.A. Huber, unpubl. data), but in that case with *Papiamenta* as sister to *Tolteca* + true *Pholcophora* (no Caribbean '*Pholcophora*' is included in the UCE dataset).

Within *Tolteca*, our unpartitioned analysis suggests that the most southern species (*T. oaxaca* sp. nov.) is sister to all other species; among those, *T. hesperia* is sister to *T. jalisco* + (*T. manzanillo* sp. nov. + *T. huahua* Huber sp. nov.). Our unpublished UCE dataset does not include *T. huahua* but otherwise it supports the same intrageneric relationships.

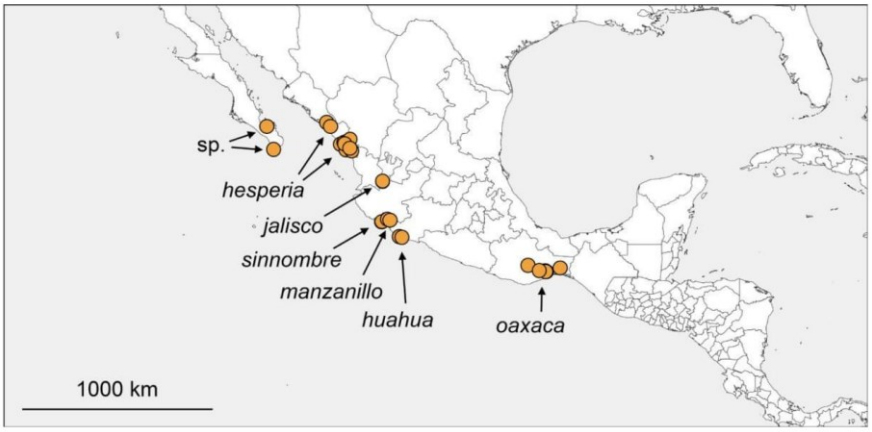

Fig. 35. Known distribution of *Tolteca* Huber, 2000.

Distribution

The genus appears restricted to the Pacific Lowlands and Baja Californian biogeographic provinces of Mexico, as delimited in Morrone *et al.* (2017) (Fig. 35). The female specimens originating from San Luis Potosí and Puebla provinces tentatively identified as *Tolteca* and briefly mentioned in Huber (2000: 120) are possibly not *Tolteca*.

Natural history

Most newly collected specimens were found in low, relatively dry forests (Fig. 56). Here they occupied the thin layers of leaf litter and sometimes the spaces under small stones and pebbles. They often shared

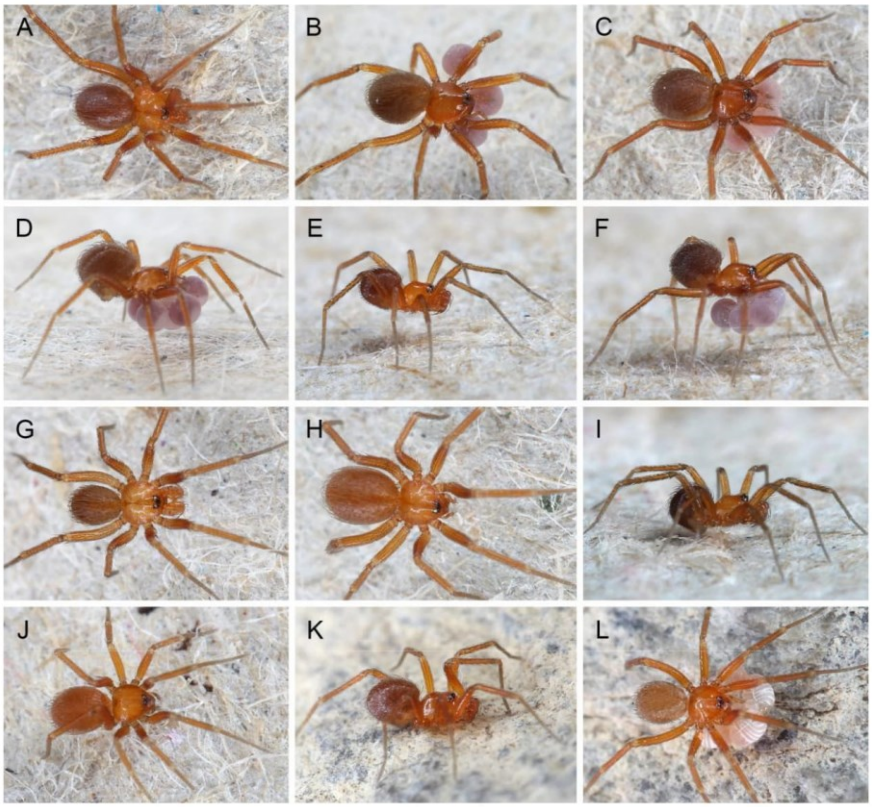

Fig. 36. *Tolteca* Huber, 2000 live specimens. **A–B**. *T. hesperia* (Gertsch, 1982), male and female with egg-sac from Mexico, Sinaloa, S of Rosario. **C–D**. *T. jalisco* (Gertsch, 1982), females with egg-sacs from Mexico, Jalisco, N of La Quemada. **E–F**. *T. manzanillo* Huber sp. nov., male and female with egg-sac from Mexico, Colima, E of Manzanillo. **G–H**. *T. sinnombre* Huber sp. nov., male and female from Mexico, Colima, S of Coquimatlán. **I–J**. *T. huahua* Huber sp. nov., male and female from Mexico, Michoacán, W of Huahua. **K–L**. *T. oaxaca* Huber sp. nov., male and female with egg-sac from Mexico, Oaxaca, NW of Tehuantepec.

the microhabitat with other species of Pholcidae, but *Tolteca* appeared largely restricted to the dryer areas while other genera (mostly *Modisimus*) seemed to prefer slightly more humid leaf litter. No webs were observed in the field, but the spiders built tiny silk mats in the glass vials. When disturbed, they ran rapidly and barely slowed down for several minutes. Females carried their disc-shaped egg-sacs under the prosoma (Fig. 36); egg-sacs usually contained 5 or 6 eggs, each with a diameter of ~0.35–0.45 mm (Huber & Eberle 2021). Some females had a genital plug (cf. Fig. 49A–B).

Composition

The genus now includes six nominal species, all of which are treated below.

Tolteca hesperia (Gertsch, 1982)
Figs 36A–B, 37–42

Pholcophora hesperia Gertsch, 1982: 102 (part; see Remarks below), figs 34–36, 45–47 (♂♀).

Tolteca hesperia – Huber 2000: 118 (part, see Remarks below), fig. 454 (other figures refer to *T. oaxaca* sp. nov.; see Remarks below).

Remarks

Gertsch (1982) designated a male specimen from Sinaloa as holotype, and in the text description he explicitly refers to that specimen. However, it is not clear if the figures of the male (Gertsch 1982: figs 34–36) are from the holotype or not. The procursus (narrowing gradually) and chelicerae (apophyses weakly protruding) suggest he drew another specimen of what is now considered a different species (maybe *T. huahua* sp. nov. or *T. manzanillo* sp. nov.). Gertsch's (1982) figures from the female (Gertsch

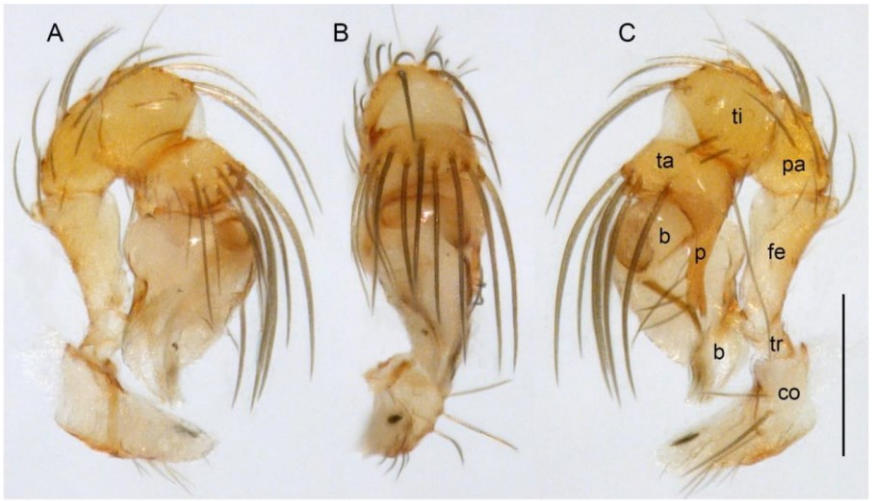

Fig. 37. *Tolteca hesperia* (Gertsch, 1982), male from Mexico, Sinaloa, S of Rosario (ZFMK Ar 23953). Left palp, prolateral, dorsal, and retrolateral views. Abbreviations: b = genital bulb; co = coxa; fe = femur; p = procursus; pa = patella; ta = tarsus; ti = tibia; tr = trochanter. Scale bar = 0.2 mm.

1982: figs 45–47) are certainly not from a topotypical female as no such female was available to him. It is not possible to tell from Gertsch's figures which species he illustrated.

The redescription of *T. hesperia* in Huber (2000) is mainly based on specimens from Oaxaca (2 mi SE of Niltepec) that are here considered a different species (*T. oaxaca* sp. nov.). Only the illustration of the procursus (Huber 2000: fig. 454) is from the holotype.

We have not restudied Gertsch's (1982) *T. hesperia* specimens but consider all specimens except for those from Sinaloa to represent other species. Judging from the geographic closeness to newly collected specimens, Gertsch's specimens from Colima probably represent *T. sinnombre* sp. nov. (10 mi S of Colima) and *T. manzanillo* sp. nov. (12 mi E of Manzanillo); those from Oaxaca probably represent *T. oaxaca* sp. nov. We cannot comment on the specimens from Baja California Sur listed in Gertsch (1982) and Huber (2000).

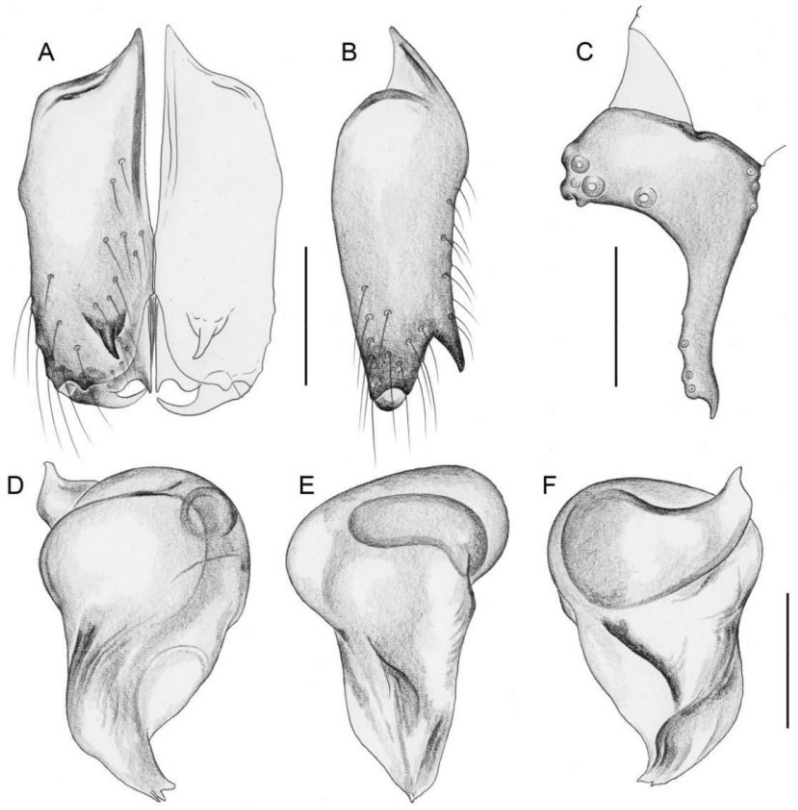

Fig. 38. *Tolteca hesperia* (Gertsch, 1982), male from Mexico, Sinaloa, S of Rosario (ZFMK Ar 23953). **A–B**. Chelicerae, frontal and lateral views. **C**. Left palpal tarsus and procursus, retrolateral view. **D–F**. Left genital bulb, prolateral, dorsal, and retrolateral views. Scale bars = 0.1 mm.

Diagnosis

Distinguished from known congeners by the combination of: male genital bulb without dorsal ridge (Fig. 38F; unlike *T. jalisco*); procursus tip abruptly narrowing (Fig. 38C; similar to *T. sinnombre* sp. nov., unlike other species); male cheliceral apophyses in lateral view with large angle against distal-frontal face of chelicera (Fig. 38B; ~60° versus 25–35° in other species; not checked in *T. jalisco*); main epigynal plate band-like (Fig. 39A, C; rather than crescent-shaped as in *T. manzanillo* sp. nov., *T. huahua* sp. nov., and *T. oaxaca* sp. nov.); sacs in female internal genitalia ~40–50 µm long (Fig. 40C, F; i.e., longer than in *T. jalisco* and *T. oaxaca*, shorter than in *T. sinnombre*).

Material examined

Holotype

MEXICO – **Sinaloa** • ♂; 5 mi S of Mazatlán; ~23.20° N, 106.36° W; ~10–20 m a.s.l.; 23 Jul. 1954; W.J. Gertsch leg.; AMNH; examined (Huber 2000).

New record

MEXICO – **Sinaloa** • 4 ♂♂, 1 ♀, and 2 cleared epigyna; ~3 km S of Rosario; 22.9584° N, 105.8490° W; 65 m a.s.l.; 9 Oct. 2019; B.A. Huber and A. Valdez-Mondragón leg.; one male used for SEM; ZFMK Ar 23953 • 12 ♀♀, 5 juvs, in pure ethanol; same collection data as for preceding; one female used for SEM,

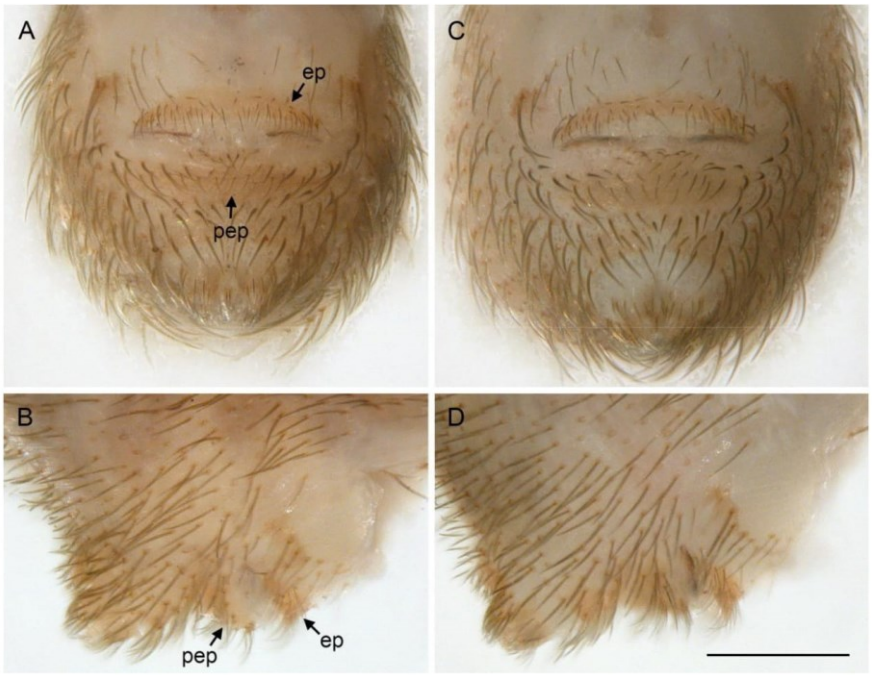

Fig. 39. *Tolteca hesperia* (Gertsch, 1982), females from Mexico, Sinaloa, S of Rosario (ZFMK Mex253), epigyna. **A, C**. Ventral views. **B, D**. Lateral views. Abbreviations: ep = epigynum (main epigynal plate); pep = posterior epigynal plate. Scale bar = 0.2 mm (all at same scale).

four female prosomata used for molecular work, two abdomens cleared and transferred to ZFMK Ar 23953; ZFMK Mex253 • 2 ♂♂; same collection data as for preceding; partly used for karyotype analyses; ZFMK Ar 23954 • 3 ♂♂, 2 ♀♀; same collection data as for preceding; partly used for µ-CT study; ZFMK Ar 23955 • 1 ♂, 4 ♀♀, 1 juv. (subadult male); same collection data as for preceding; LATLAX.

Description (amendments; see Gertsch 1982; Huber 2000)

Male (ZFMK Ar 23953)

Measurements. Total body length 1.40, carapace width 0.52. Distance PME-PME 40 µm; diameter PME 40 µm; distance PME-ALE 15 µm; distance AME-AME 10 µm; diameter AME 30 µm. Leg 1: 2.32 (0.65 + 0.17 + 0.57 + 0.60 + 0.33), tibia 2: 0.47, tibia 3: 0.43, tibia 4: 0.73; tibia 1 L/d: 7; diameters of leg femora 0.135, of leg tibiae 0.08.

Colour (in ethanol). Prosoma and legs monochromous ochre-yellow; abdomen ochre-grey, also monochromous.

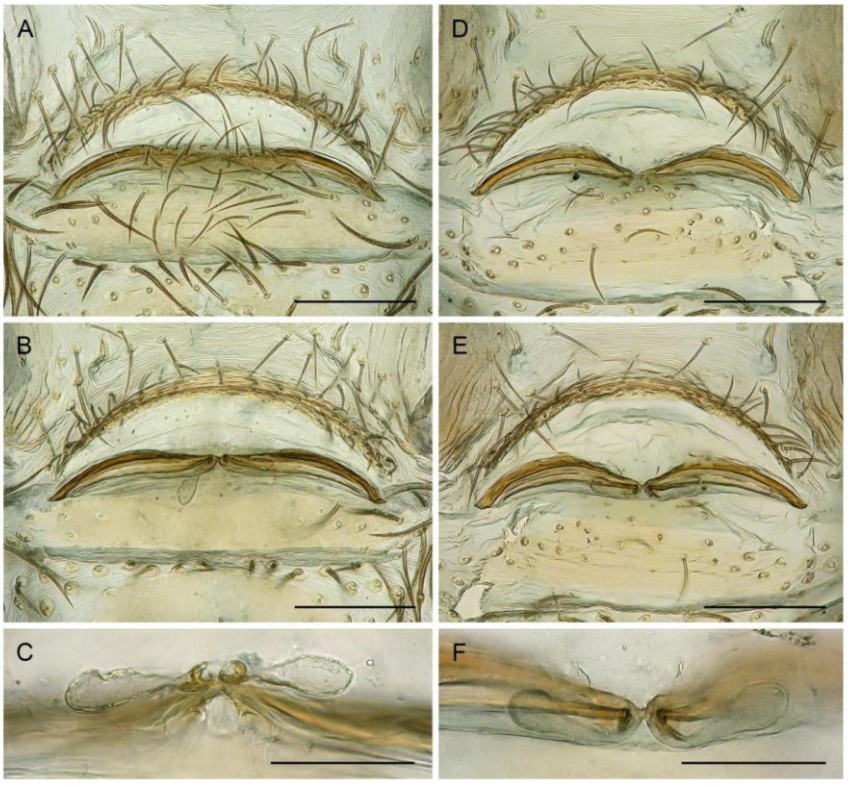

Fig. 40. *Tolteca hesperia* (Gertsch, 1982), females from Mexico, Sinaloa, S of Rosario (ZFMK Ar 23953), cleared female genitalia, **A, D**. Ventral views. **B, E**. Dorsal views. **C, F**. Detail of median internal structures. Scale bars: A–B, D–E = 0.1 mm; C, F = 0.05 mm.

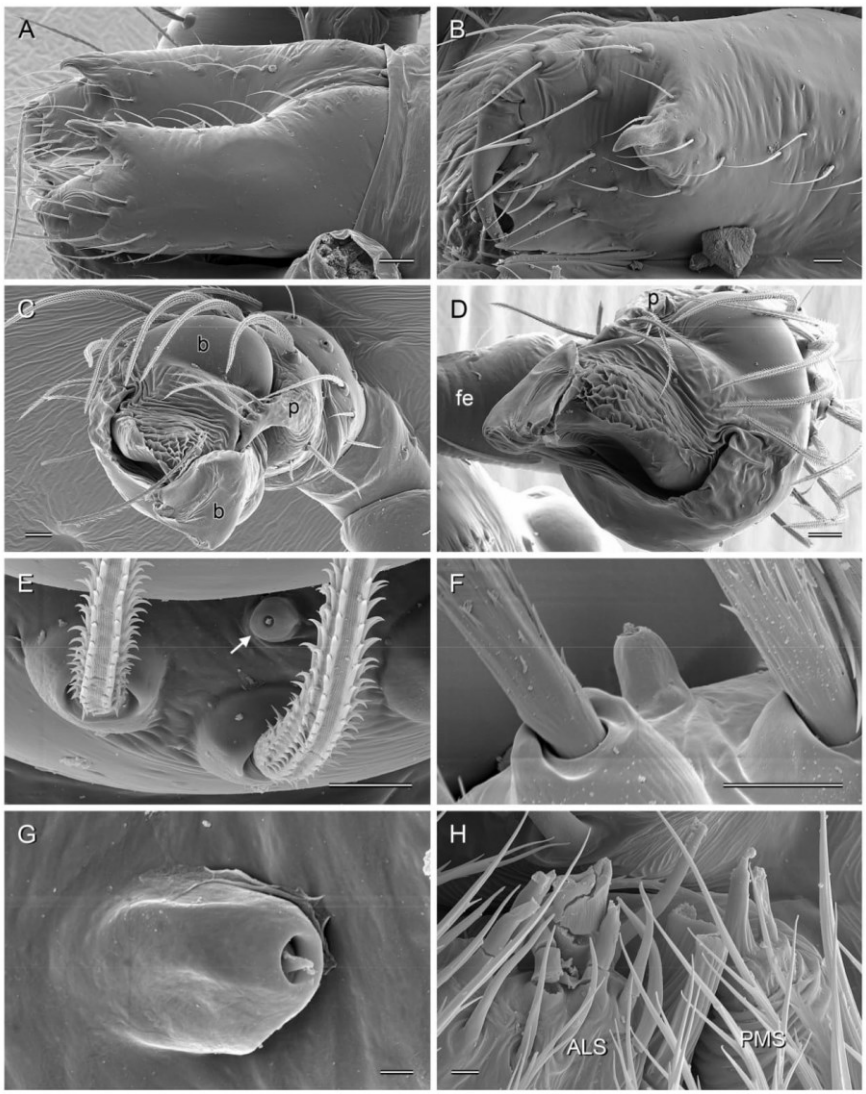

Fig. 41. *Tolteca hesperia* (Gertsch, 1982), male and female from Mexico, Sinaloa, 3 km S of Rosario (ZFMK Ar23953 and Mex253). **A**. Male chelicerae, lateral view. **B**. Male right chelicera, frontal view. **C**. Left male palp, distal view. **D**. Right genital bulb (and procursus), dorso-distal view. **E**. Detail of male palpal tarsus showing position of tarsal organ (arrow). **F**. Male palpal tarsal organ. **G**. Female palpal tarsal organ. **H**. Male ALS and PMS. Abbreviations: b = genital bulb; fe = femur; p = procursus. Scale bars: A, C–D = 20 µm; B, E–F = 10 µm; G = 1 µm; H = 2 µm.

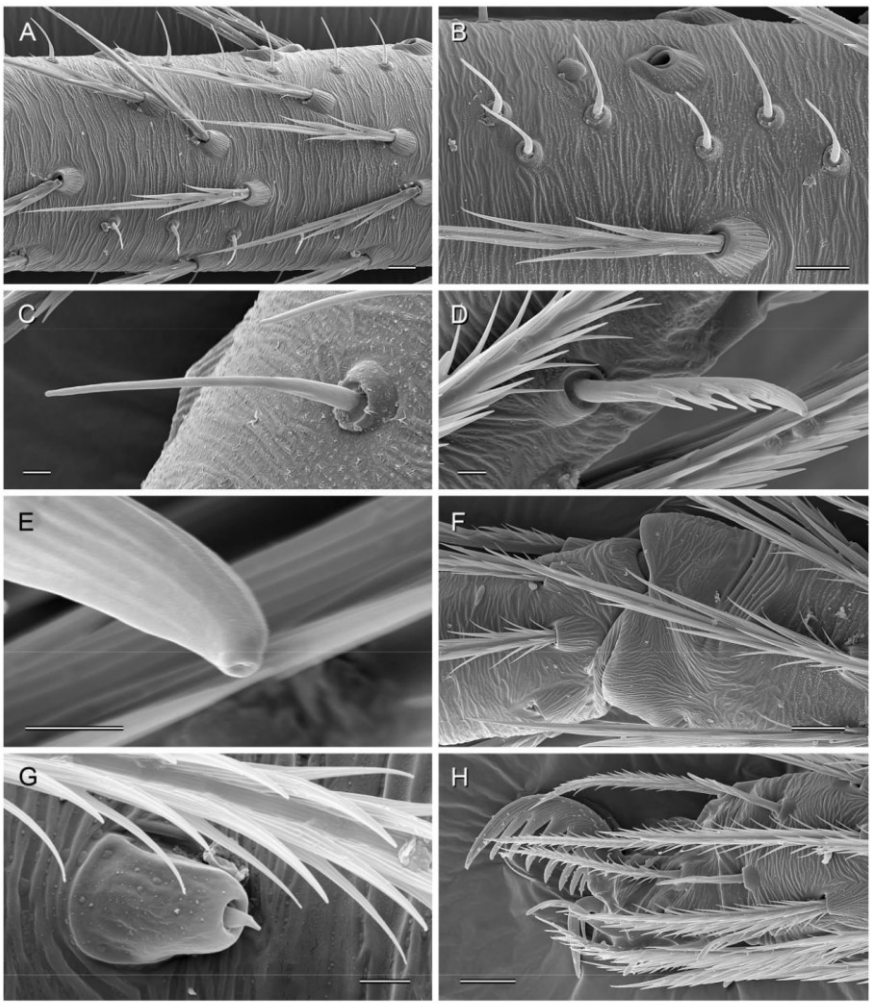

Fig. 42. *Tolteca hesperia* (Gertsch, 1982), male and female from Mexico, Sinaloa, 3 km S of Rosario (ZFMK Ar23953 and Mex253). **A**. Male tibia 1, prolateral view. **B**. Male tibia 1, retrolateral view. **C**. Sexually dimorphic short vertical hair on male tibia 1. **D** . 'Regular' short vertical hair on male metatarsus 1. **E**. Tip of 'regular' short vertical hair, detail of preceding image. **F**. Male metatarsus-tarsus 1 joint, retrolateral-dorsal view. **G**. Tarsal organ on female tarsus 1. **H**. Tip of left male tarsus 2, retrolateral view. Scale bars: A–B, F, H = 10 µm; C–D, G = 2 µm; E = 1 µm.

Body (Fig. 36A). Ocular area barely raised. Carapace without thoracic groove. Clypeus unmodified, only rim slightly more sclerotized, short (clypeus rim to ALE: 160 µm). Sternum wider than long (0.40/0.37), with pair of small but distinct anterior processes (~60 µm diameter at basis, ~60 µm long) near coxae 1. Abdomen globular.

Chelicerae (Figs 38A–B, 41A–B). With pair of frontal apophyses pointing downwards, distance between tips of apophyses: 60 µm; without stridulatory files.

Palps (Fig. 37). Coxa unmodified; trochanter without process; femur proximally without process, distally widened but simple, slightly curved towards dorsal; femur-patella joints minimally shifted toward prolateral side; tibia very short, with two trichobothria; tibia-tarsus joints not shifted to one side; procursus very simple (Figs 38C, 41C), with distal ventral process; genital bulb (Figs 38D–F, 41C–D) large, complex, possibly indistinguishable from congeners.

Legs. Without spines and curved hairs; with slightly increased density of short vertical hairs on tibia 1 (Fig. 42A–C; barely visible in dissecting microscope); retrolateral trichobothrium of tibia 1 at 64%; prolateral trichobothrium absent on tibia 1; tarsus 1 with five pseudosegments, all fairly distinct.

Variation (male)
Tibia 1 in three other newly collected males: 0.55, 0.57, 0.60.

Female
In general, similar to male (Fig. 36B) but sternum without pair of anterior humps and tibia 1 without increased density of short vertical hairs. Total body length: ~1.20–1.40; tibia 1 in 12 newly collected females: 0.47–0.62 (mean 0.52). Epigynum (Fig. 39) very short band-shaped anterior plate slightly protruding in lateral view; posterior plate wide, median part slightly protruding anteriorly. With distinct knob between epigynum and pedicel (accidentally missing in specimens shown in Figs 39 and 40 – the knob sometimes stays attached to the prosoma when the abdomen is detached from it). Internal genitalia (Fig. 40) with pair of strong transversal sclerites, pair of distinct sacs (receptacles?), without (or with very small?) pore plates.

Distribution

Apparently widely distributed in southern and central Sinaloa, Mexico (Fig. 35). All specimens from outside of Sinaloa listed in Gertsch (1982) and Huber (2000) are here either considered to represent different (new) species (specimens from Colima and Oaxaca) or dubious (specimens from Baja California Sur – not re-examined).

Natural history

The newly collected spiders were found in the thin leaf litter layer and under stones in a low and quite dry roadside forest (Fig. 56A). They shared the locality with up to four unidentified species of *Modisimus*, one of them apparently in much the same microhabitat.

Tolteca jalisco (Gertsch, 1982)
Figs 36C–D, 43, 55C

Pholcophora jalisco Gertsch, 1982: 102, figs 40–41 (♂).

Tolteca jalisco – Huber 2000: 120, figs 458–459 (♂).

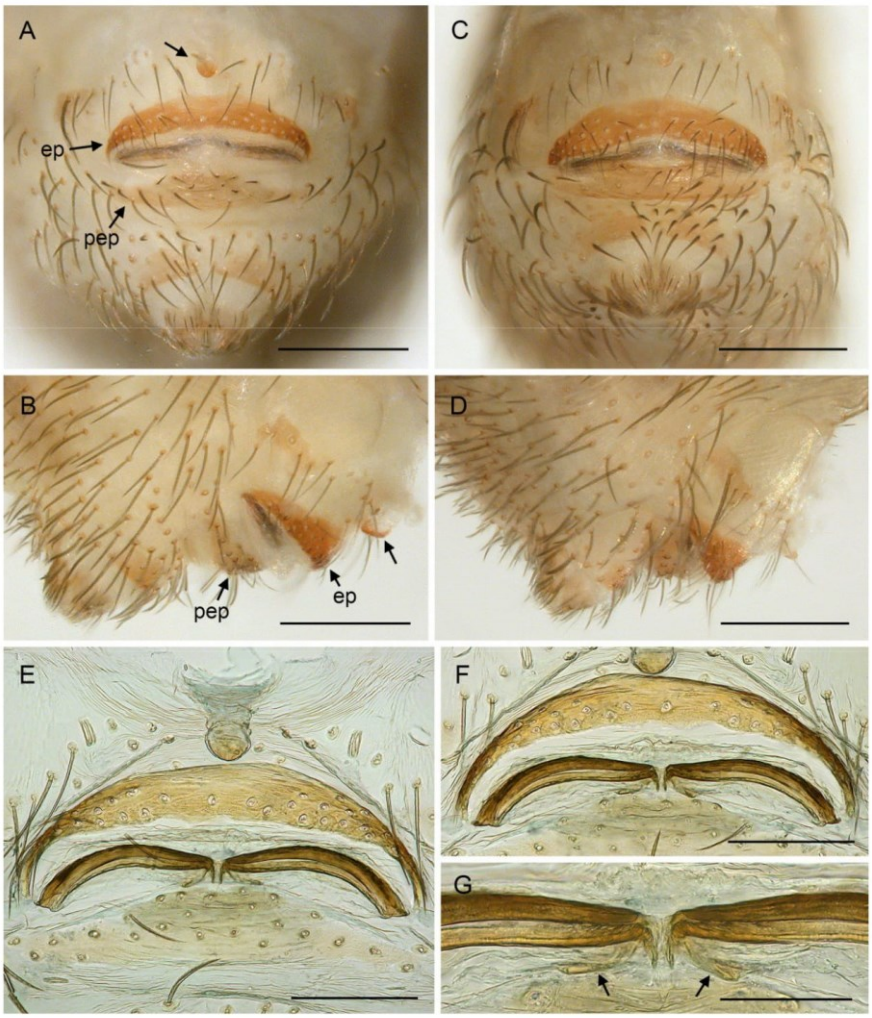

Fig. 43. *Tolteca jalisco* (Gertsch, 1982), females from Mexico, Jalisco, N of La Quemada (ZFMK Ar 23956). **A–D**. Epigyna, ventral (A, C) and lateral (B, D) views; arrows point at anterior knob-shaped structure. **E–G**. Cleared female genitalia, ventral (E) and dorsal (F) views, and detail of median internal structures (G); arrows point at membranous sacs (cf. Fig. 55C). Abbreviations: ep = epigynum (main epigynal plate); pep = posterior epigynal plate. Scale bars: A–D = 0.2 mm; E–F = 0.1 mm; G = 0.05 mm.

Diagnosis

Distinguished from known congeners by dorsal ridge on male genital bulb (Gertsch 1982: fig. 40; Huber 2000: fig. 458); also by the combination of: procursus tip gradually narrowing (Gertsch 1982: fig. 40; Huber 2000: fig. 459; unlike *T. hesperia* and *T. sinnombre* sp. nov.); main epigynal plate band-like (Fig. 43A, C; rather than crescent-shaped as in *T. manzanillo* sp. nov., *T. huahua* sp. nov., and *T. oaxaca* sp. nov.); sacs in female internal genitalia ~18–25 µm long (Fig. 55C; i.e., longer than in *T. oaxaca*, shorter than in all other species).

Material examined

Holotype

MEXICO – **Jalisco** • ♂; 20 mi N of La Quemada; ~21.18° N, 104.085° W; 28 Jul. 1954; W.J. Gertsch leg.; AMNH; examined (Huber 2000).

Remark

The information on the label accompanying the holotype deviates slightly from the data published by Gertsch (1982). This affects not only the date (28 or 24 Jul. 1954) but also the exact type locality, which is either 20 mi N of La Quemada (i.e., ~21.18° N, 104.085° W) or 29 mi N of La Quemada (i.e., ~21.23° N, 104.06° W).

New record

MEXICO – **Jalisco** • 2 ♀♀ abdomens; N of La Quemada, 'site 2'; 21.1922° N, 104.0975° W; 630 m a.s.l.; 7 Oct. 2019; B.A. Huber and A. Valdez-Mondragón leg.; ZFMK Ar 23956 • 6 ♀♀ in pure ethanol; same collection data as for preceding; two abdomens transferred to ZFMK Ar 23956, three prosomata used for molecular work; ZFMK Mex241.

Description

Female

In general, very similar to congeners (Fig. 36C–D); total body length 1.25; tibia 1 in three females: 0.50, 0.50, 0.53. Epigynum (Fig. 43A–D) very distinct short band-shaped anterior plate slightly protruding in lateral view; posterior plate wide, median part slightly protruding anteriorly. With distinct knob between epigynum and pedicel. Internal genitalia (Fig. 43E–G) with pair of strong transversal sclerites, pair of very small sacs (receptacles?), without (or with very small?) pore plates.

Distribution

Known from type locality and one neighbouring site only, in Mexico, Jalisco (Fig. 35). The exact coordinates of the type locality are unknown, but the type locality is either within ~2 km from the new locality or ~6 km NE of the new locality (see Remark above).

Natural history

The newly collected specimens were found in a small forest remnant at the roadside. Few specimens were found despite of intensive search (> 2 hrs); no other pholcid species shared the leaf litter with *Tolteca*. The locality was shared with *Physocyclus brevicornus* Valdez-Mondragón, 2010.

Tolteca manzanillo Huber sp. nov.
urn:lsid:zoobank.org:act:97805AAF-C4EE-4A3E-A1F7-4B980E70005E
Figs 36E–F, 44A–C, 45–46, 55E

Pholcophora hesperia Gertsch, 1982: 102 (only specimens from 12 mi E of Manzanillo; see Remarks under *T. hesperia*).

Diagnosis

Distinguished from known congeners by the combination of: male genital bulb without dorsal ridge (unlike *T. jalisco*); procursus tip gradually narrowing (Fig. 44C; unlike *T. hesperia* and *T. sinnombre* sp. nov.); male cheliceral apophyses wide apart (Fig. 44A; distance between tips ~65 µm, i.e., much wider apart than in *T. huahua* sp. nov. and *T. oaxaca* sp. nov.), in lateral view with small angle against distal-frontal face of chelicera (Fig. 44B; unlike *T. hesperia*; not checked in *T. jalisco*); main epigynal plate crescent-shaped (Fig. 45A, C; rather than band-like as in *T. hesperia* and *T. jalisco*); sacs in female internal genitalia ~40–50 µm long (Fig. 55E; i.e., longer than in *T. jalisco* and *T. oaxaca*, shorter than in *T. sinnombre*).

Etymology

The species name is derived from the type locality; noun in apposition.

Type material

Holotype

MEXICO – **Colima** • ♂; ~17 km E of Manzanillo; 19.0115° N, 104.1382° W; 35 m a.s.l.; 6 Oct. 2019; B.A. Huber and A. Valdez-Mondragón leg.; LATLAX.

Paratypes

MEXICO – **Colima** • 7 ♂♂; same collection data as for holotype; one male used for SEM; ZFMK Ar 23958 • 4 ♂♂, 8 ♀♀, 4 juvs; same collection data as for holotype; LATLAX.

Other material examined

MEXICO – **Colima** • 4 ♀♀, 9 juvs, in pure ethanol; same collection data as for holotype; two prosomata used for molecular work, two abdomens transferred to ZFMK Ar 23958; ZFMK Mex232 • 1 ♂; same collection data as for holotype; partly used for karyotype analyses; ZFMK 23959.

Description

Male (holotype)

Measurements. Total body length 1.10, carapace width 0.45. Distance PME-PME 40 µm; diameter PME 30 µm; distance PME-ALE 20 µm; distance AME-AME 10 µm; diameter AME 25 µm. Leg 1: 2.01 (0.55 + 0.15 + 0.50 + 0.48 + 0.33), tibia 2: 0.40, tibia 3: 0.37, tibia 4: 0.60; tibia 1 L/d: 7; diameters of leg femora 0.10, of leg tibiae 0.07.

Colour (in ethanol). Prosoma and legs monochromous ochre-yellow; abdomen slightly darker ochre-grey, also monochromous.

Body (Fig. 36E). Ocular area barely raised. Carapace without thoracic groove. Clypeus unmodified, short (clypeus rim to ALE: 120 µm). Sternum wider than long (0.36/0.30), almost round (i.e., not heart-shaped), with pair of small but distinct anterior processes (~40 µm diameter at basis, ~40 µm long) near coxae 1. Abdomen globular; gonopore apparently without epiandrous spigots (Fig. 46G); ALS with seven spigots each (Fig. 46H).

Chelicerae (Fig. 44A–B). With pair of frontal apophyses pointing downwards; distance between tips of apophyses 65 µm; without stridulatory files (Fig. 46F).

Palps. In general possibly indistinguishable from congeners (cf. Figs 37, 50); coxa unmodified; trochanter without process; femur proximally without process, distally widened but simple, slightly curved towards dorsal; femur-patella joints not shifted to one side; tibia very short, with two trichobothria; tibia-tarsus joints not shifted to one side; procursus very simple (Figs 44C, 46A–B), with distal ventral process;

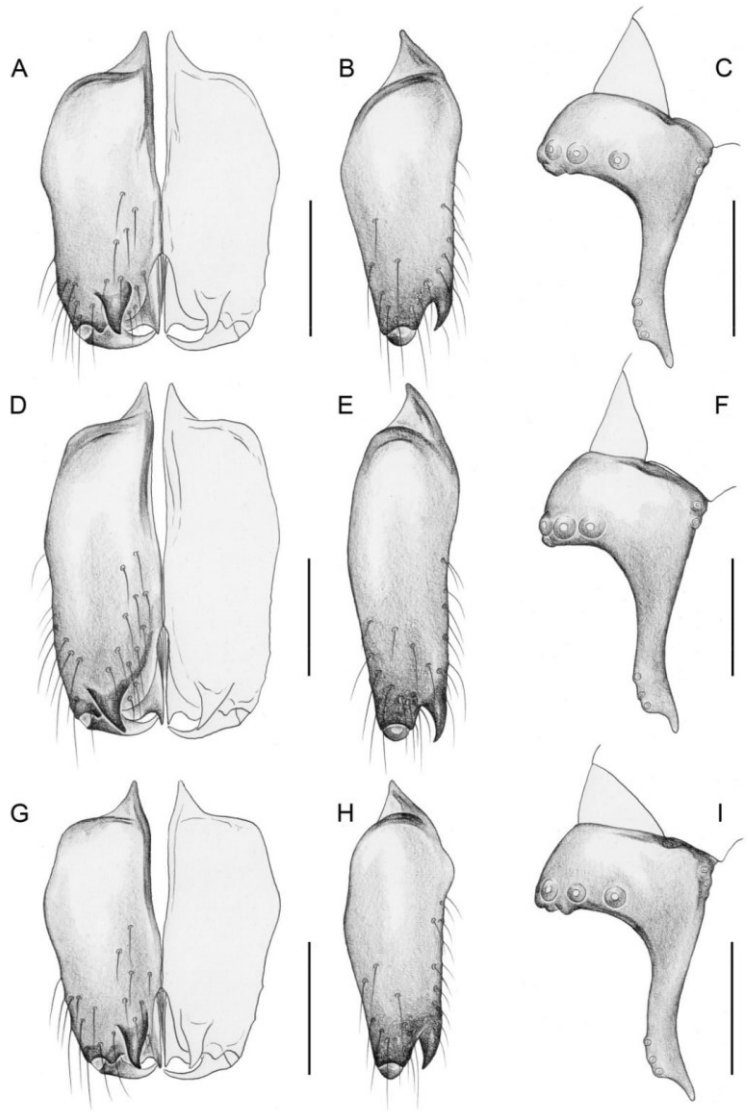

Fig. 44. *Tolteca* spp., male chelicerae, frontal and lateral views, and left male palpal tarsi and procursi, retrolateral views. **A–C**. *T. manzanillo* Huber sp. nov., paratype from Mexico, Colima, E of Manzanillo (ZFMK Ar 23958). **D–F**. *T. sinnombre* Huber sp. nov., holotype from Mexico, Colima, S of Coquimatlán (LATLAX). **G–I**. *T. huahua* Huber sp. nov., paratype from Mexico, Michoacán, W of Huahua (ZFMK Ar 23957). Scale bars = 0.1 mm.

genital bulb large, complex (Fig. 46A–B), in light microscope possibly indistinguishable from congeners (cf. Figs 38D–F, 51D–F).

Legs. Without spines and curved hairs; with slightly increased density of short vertical hairs on tibia 1 (barely visible in dissecting microscope); retrolateral trichobothrium of tibia 1 at 61%; prolateral trichobothrium absent on tibia 1; tarsus 1 with four pseudosegments, all fairly distinct.

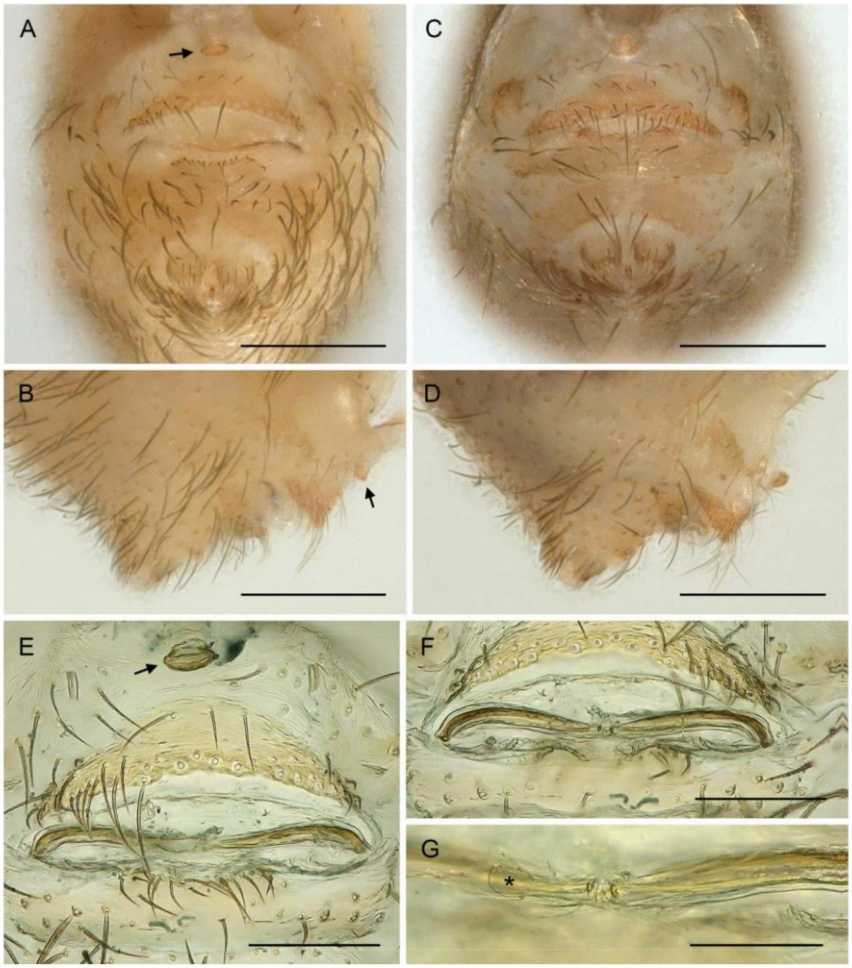

Fig. 45. *Tolteca manzanillo* Huber sp. nov., females from Mexico, Colima, E of Manzanillo (ZFMK Ar 23958). **A–D**. Epigyna, ventral (A, C) and lateral (B, D) views. **E–G**. Cleared female genitalia, ventral (E) and dorsal (F) views, and detail of median internal structures (G). Arrows point at anterior epigynal knob. Asterisk: membranous sac (cf. Fig. 55E). Scale bars: A–D = 0.2 mm; E, F = 0.1 mm; G = 0.05 mm.

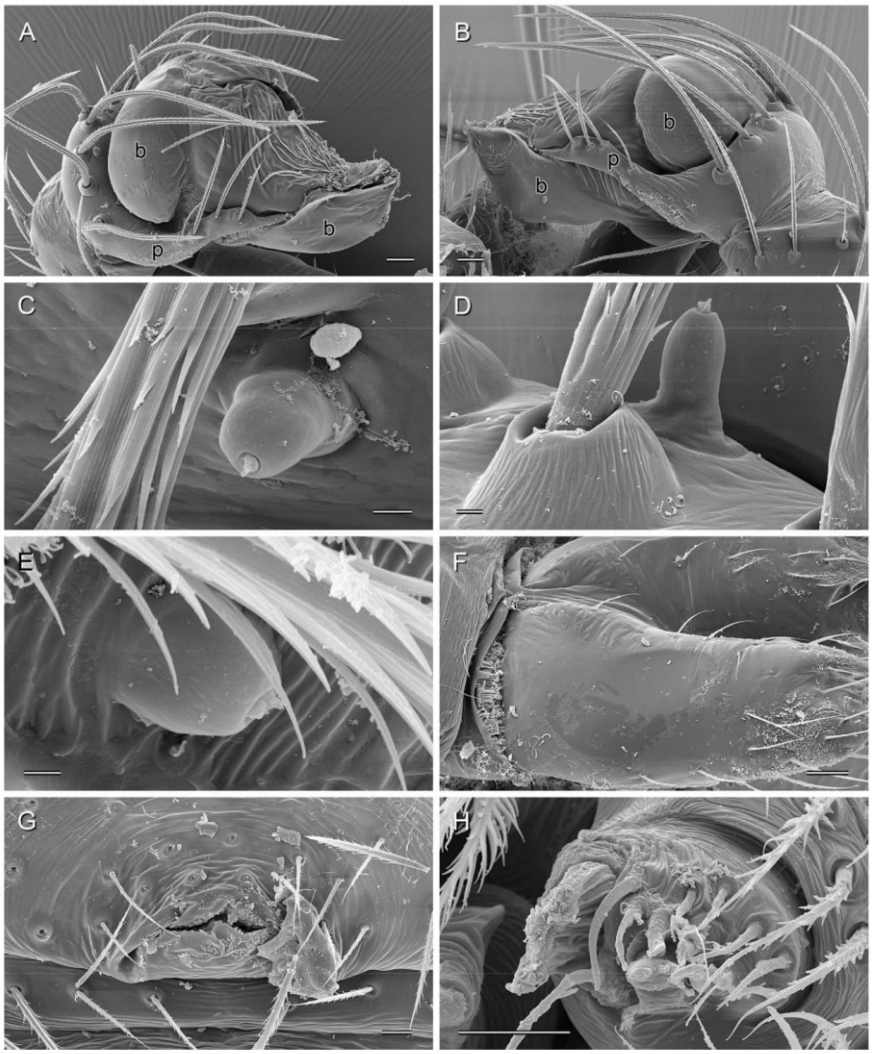

Fig. 46. *Tolteca manzanillo* Huber sp. nov.; male from Mexico, Colima, 17 km E of Manzanillo (ZFMK Ar 23958). **A**. Right palp, retrolateral-distal view. **B**. Left palp, retrolateral-dorsal view. **C–D**. Palpal tarsal organ. **E**. Tarsal organ on tarsus 2. **F**. Lateral face of right chelicera, showing absence of stridulatory file. **G**. Gonopore. **H**. ALS. Abbreviations: b = genital bulb; p = procursus. Scale bars: A–B, F = 20 µm; C–D = 2 µm; E = 1 µm; G–H = 10 µm.

Variation (male)
Tibia 1 in six males (incl. holotype): 0.45–0.52 (mean 0.48).

Female
In general, similar to male (Fig. 36F) but sternum without pair of anterior humps. Total body length: ~1.20–1.30; tibia 1 in eight females: 0.43–0.47 (mean 0.45). Epigynum (Fig. 45A–D) short crescent-shaped anterior plate slightly protruding in lateral view; posterior plate wide, median part slightly protruding anteriorly. With distinct knob between epigynum and pedicel. Internal genitalia (Fig. 45E–G) with pair of strong transversal sclerites, pair of distinct sacs (receptacles?), without (or with very small?) pore plates.

Distribution

Known from type locality and one poorly specified neighbouring locality in Mexico, Colima (Fig. 35). We do not have exact coordinates for Gertsch's (1982) specimens from "12 mi. E Manzanillo", but that locality is probably within a few km from the type locality.

Natural history

The spiders were very abundant in the dry leaf litter of a low thorn forest covering a hill near the Laguna of Cuyutlán (Fig. 56B).

Tolteca sinnombre Huber sp. nov.
urn:lsid:zoobank.org:act:51577DD3-55BD-4916-B9C2-E8A52181090C
Figs 36G–H, 44D–F, 47–48

Pholcophora hesperia Gertsch, 1982: 102 (only specimens from 10 mi S of Colima; see Remarks under *T. hesperia*).

Diagnosis

Distinguished from known congeners by the combination of: male genital bulb without dorsal ridge (unlike *T. jalisco*); procursus tip abruptly narrowing (Fig. 44F; similar to *T. hesperia*, unlike other species); male cheliceral apophyses wide apart (distance between tips ~75 µm, i.e., much wider apart than in *T. huahua* sp. nov. and *T. oaxaca* sp. nov.), in lateral view with small angle against distal-frontal face of chelicera (Fig. 44E; unlike *T. hesperia*; not checked in *T. jalisco*); main epigynal plate very short, band-shaped, densely set with short hairs (Fig. 48A–B); without knob between epigynum and pedicel (Fig 47A, C); female internal genitalia with pair of very long sacs (85 µm) (Figs 48D, 55F).

Etymology

The species name is derived from the type locality; noun in apposition.

Type material

Holotype
MEXICO – **Colima** • ♂; ~6 km S of Coquimatlán, near 'Cueva sin Nombre'; 19.1521° N, 103.8350° W; 280 m a.s.l., 6 Oct. 2019; B.A. Huber and A. Valdez-Mondragón leg.; LATLAX.

Other material examined

MEXICO – **Colima** • 2 ♀♀ abdomens; same collection data as for holotype; ZFMK Ar 23960 • 2 ♀♀ and 2 female prosomata (abdomens transferred to ZFMK Ar 23960), in pure ethanol; same collection data as for holotype; ZFMK Mex237.

Description

Male (holotype)
Measurements. Total body length 1.25, carapace width 0.56. Distance PME-PME 45 µm; diameter PME 45 µm; distance PME-ALE 20 µm; distance AME-AME 15 µm; diameter AME 30 µm. Leg 1:

2.26 (0.63 + 0.17 + 0.58 + 0.55 + 0.33), tibia 2: 0.47, tibia 3: 0.43, tibia 4: 0.72; tibia 1 L/d: 7; diameters of leg femora 0.130–0.135, of leg tibiae 0.08.

Colour (in ethanol). Prosoma and legs monochromous ochre-yellow, only carapace with slightly darker median line widening anteriorly; abdomen slightly darker ochre-grey, with some indistinct darker marks dorsally.

Body (Fig. 36G). Ocular area barely raised. Carapace without thoracic groove. Clypeus unmodified but with sclerotized rim, short (clypeus rim to ALE: 170 µm). Sternum wider than long (0.40/0.36), almost round (i.e., not heart-shaped), with pair of small but distinct anterior processes (~80 µm diameter at basis, ~80 µm long) near coxae 1. Abdomen globular.

Chelicerae (Fig. 44D–E). With pair of frontal apophyses pointing downwards; distance between tips of apophyses 75 µm; without stridulatory files.

Palps. In general possibly indistinguishable from congeners (cf. Figs 37, 50) but patella ventrally apparently longer than in other species; coxa unmodified; trochanter without process; femur proximally without process, distally widened but simple, slightly curved towards dorsal; femur-patella joints very

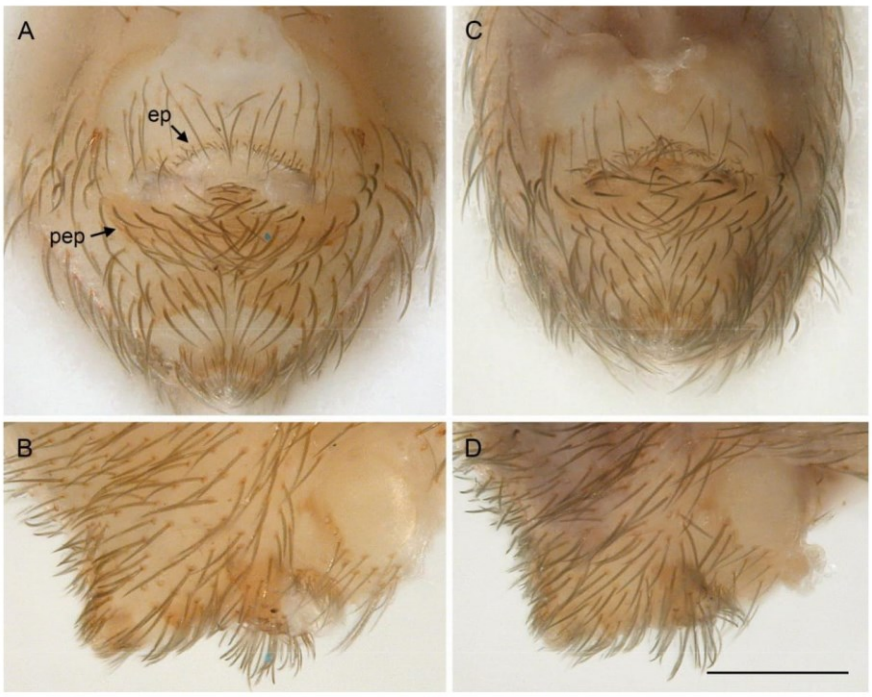

Fig. 47. *Tolteca sinnombre* Huber sp. nov., females from Mexico, Colima, S of Coquimatlán (ZFMK Ar 23940), epigyna. **A, C**. Ventral views. **B, D**. Lateral views. Abbreviations: ep = epigynum (main epigynal plate); pep = posterior epigynal plate. Scale bar = 0.2 mm (all at same scale).

slightly shifted toward prolateral side; tibia very short, with two trichobothria; tibia-tarsus joints not shifted to one side; procursus very simple (Fig. 44F), with distal ventral process; genital bulb large, complex, in light microscope possibly indistinguishable from congeners (cf. Figs 38D–F, 51D–F).

Legs. Without spines and curved hairs; with slightly increased density of short vertical hairs on tibia 1 (barely visible in dissecting microscope); retrolateral trichobothrium of tibia 1 at 63%; prolateral trichobothrium absent on tibia 1; tarsus 1 with five pseudosegments, all fairly distinct.

Female

In general, similar to male (Fig. 36H) but sternum without pair of anterior humps. Total body length: ~1.20–1.30; tibia 1 in four females: 0.48, 0.50, 0.53, 0.58. Epigynum (Fig. 47) with very short band-shaped anterior plate densely set with short hairs; posterior plate wide, median part distinctly protruding anteriorly. Without knob between epigynum and pedicel. Internal genitalia (Fig. 48) with pair of strong transversal sclerites, pair of distinct sacs (receptacles?), without (or with very small?) pore plates.

Distribution

Known from type locality and one poorly specified neighbouring locality in Mexico, Colima (Fig. 35). We do not have exact coordinates for Gertsch's (1982) specimens from "10 mi. S Colima", but that locality is probably within 10 km from the type locality.

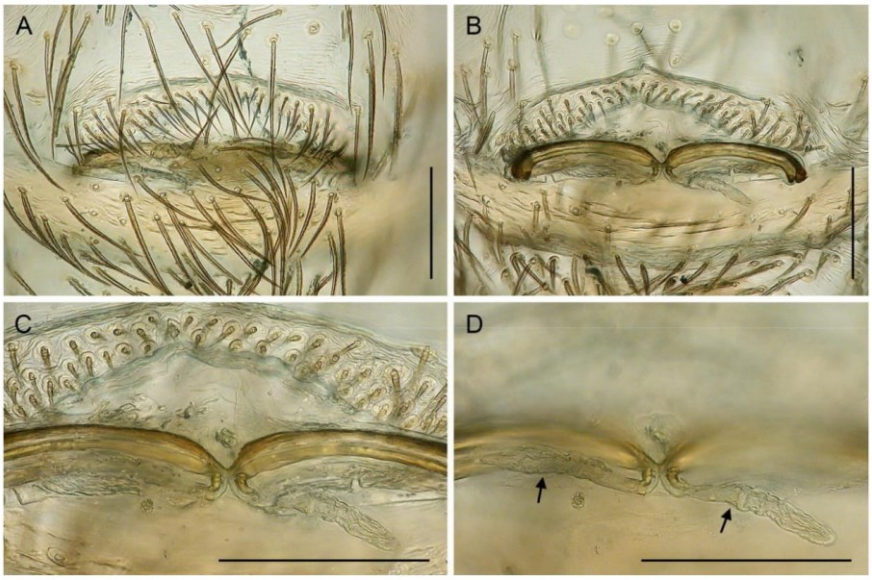

Fig. 48. *Tolteca sinnombre* Huber sp. nov., female from Mexico, Colima, S of Coquimatlán (ZFMK Ar 23960), cleared female genitalia. **A**. Ventral view. **B**. Dorsal view. **C–D** . Detail of median internal structures. Arrows point at membranous sacs (cf. Fig. 55F). Scale bars = 0.1 mm.

Natural history

The specimens were collected in a low forest in a sink below the 'Cueva sin Nombre' cave. The leaf litter was partly humid and was shared with two other small pholcids (*Anopsicus* sp., *Modisimus* sp.).

Tolteca huahua Huber sp. nov.
urn:lsid:zoobank.org:act:DE7A2222-3EA8-49E2-8BA1-FEBC61571376
Figs 36I–J, 44G–I, 49, 55D

Diagnosis

Distinguished from known congeners by the combination of: male genital bulb without dorsal ridge (unlike *T. jalisco*); procursus tip gradually narrowing (Fig. 44I; unlike *T. hesperia* and *T. sinnombre* sp. nov.); male cheliceral apophyses close together (Fig. 44G; distance between tips ~40 µm, similar to *T. oaxaca* sp. nov.), in lateral view with small angle against distal-frontal face of chelicera (Fig. 44H; unlike *T. hesperia*; not checked in *T. jalisco*); main epigynal plate crescent-shaped (Fig. 49A, C; rather than band-like as in *T. hesperia* and *T. jalisco*); sacs in female internal genitalia ~40–50 µm long (Figs 49G, 55D; i.e., longer than in *T. jalisco* and *T. oaxaca*, shorter than in *T. sinnombre*).

Etymology

The species name is derived from the type locality; noun in apposition.

Type material

Holotype

MEXICO – **Michoacán** • ♂; ~20 km W of Huahua; 18.2346° N, 103.2020°W; 205 m a.s.l.; 5 Oct. 2019; B.A. Huber and A. Valdez-Mondragón leg.; LATLAX.

Paratypes

MEXICO – **Michoacán** • 1 ♂; same collection data as for holotype; ZFMK Ar 23957 • 3 ♂♂, 9 ♀♀, 2 juvs; same collection data as for holotype; LATLAX.

Other material examined

MEXICO – **Michoacán** • 3 ♀♀, 2 ♀♀ prosomata (abdomens transferred to ZFMK Ar 23957), 5 juvs, in pure ethanol; same collection data as for holotype; ZFMK Mex231 • 1 ♀, 2 juvs, in pure ethanol; ~4 km W of Huahua; 18.1972° N, 103.0449° W; 40 m a.s.l.; 5 Oct. 2019; B.A. Huber and A. Valdez-Mondragón leg.; ZFMK Mex229.

Description

Male (holotype)

Measurements. Total body length 1.10, carapace width 0.46. Distance PME-PME 40 µm; diameter PME 40 µm; distance PME-ALE 20 µm; distance AME-AME 10 µm; diameter AME 25 µm. Leg 1: 1.89 (0.50 + 0.17 + 0.47 + 0.47 + 0.28), tibia 2: 0.37, tibia 3: 0.35, tibia 4: 0.60; tibia 1 L/d: 7; diameters of leg femora 0.10, of leg tibiae 0.07.

Colour (in ethanol). Prosoma and legs monochromous ochre-yellow; abdomen slightly darker ochre-grey, with very indistinct large dorsal marks.

Body (Fig. 36I). Ocular area barely raised. Carapace without thoracic groove (very low indentation visible in frontal view only). Clypeus unmodified, short (clypeus rim to ALE 150 µm). Sternum wider than long (0.34/0.26), with pair of small but distinct anterior processes (~50 µm diameter at basis, ~50 µm long) near coxae 1. Abdomen globular.

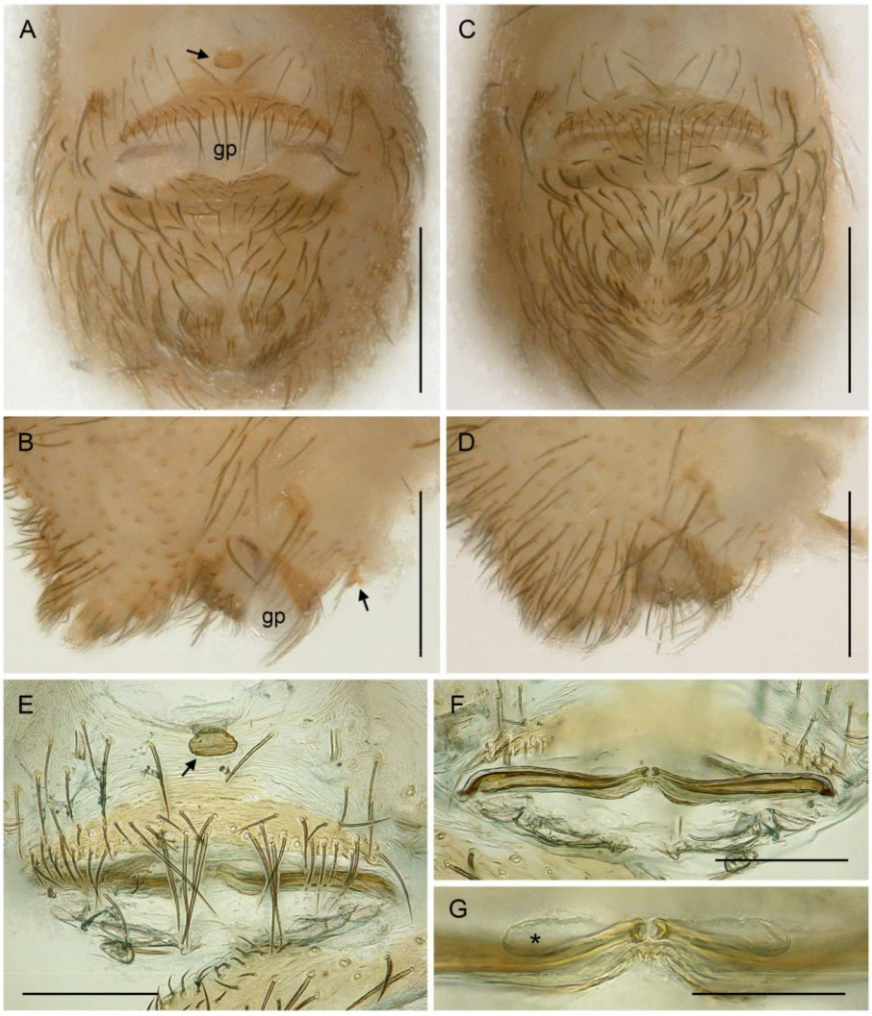

Fig. 49. *Tolteca huahua* Huber sp. nov., females from Mexico, Michoacán, W of Huahua (ZFMK Ar 23957). **A–D**. Epigyna, ventral (A, C) and lateral (B, D) views. **E–G**. Cleared female genitalia, ventral (E) and dorsal (F) views, and detail of median internal structures (G). Arrows point at knob-shaped structure. Asterisk: membranous sac (cf. Fig. 55D). Abbreviation: gp = genital plug. Scale bars: A–D = 0.2 mm; E–F = 0.1 mm; G = 0.05 mm.

Chelicerae (Fig. 44G–H). With pair of frontal apophyses pointing downwards, distance between tips: 50 µm; without stridulatory files.

Palps. In general possibly indistinguishable from congeners (cf. Figs 37, 50); coxa unmodified; trochanter without process; femur proximally without process, distally widened but simple, slightly curved towards dorsal; femur-patella joints very slightly shifted toward prolateral side; tibia very short, with two trichobothria; tibia-tarsus joints not shifted to one side; procursus very simple (Fig. 44I), with distal ventral process; genital bulb large, complex, in light microscope possibly indistinguishable from congeners (cf. Figs 38D–F, 51D–F).

Legs. Without spines and curved hairs; with slightly increased density of short vertical hairs on tibia 1 (barely visible in dissecting microscope); retrolateral trichobothrium of tibia 1 at 63%; prolateral trichobothrium absent on tibia 1; tarsus 1 with four pseudosegments, all fairly distinct.

Variation (male)
Tibia 1 in five males (incl. holotype): 0.47–0.55 (mean 0.50).

Female
In general, similar to male (Fig. 36J) but sternum without pair of anterior humps; tibia 1 not with increased density of short vertical hairs. Total body length: ~1.20; tibia 1 in 12 females: 0.43–0.51 (mean 0.47). Epigynum (Fig. 49A–D) with short crescent-shaped anterior plate slightly protruding in lateral view; posterior plate wide, median part slightly protruding anteriorly. With distinct knob between epigynum and pedicel. Internal genitalia (Fig. 49E–G) with pair of strong transversal sclerites, pair of distinct sacs (receptacles?), without (or with very small?) pore plates.

Distribution

Known from two neighbouring localities in Mexico, Michoacán (Fig. 35).

Natural history

At the type locality, a low roadside forest, *Tolteca* was only found in rather dry leaf litter, while more humid litter contained different species of Pholcidae (*Modisimus* sp.; *Anopsicus* sp.; *Physocyclus lautus* Gertsch, 1971). At the second locality, *Tolteca* was only found in the dry leaf litter of a sun-exposed part of the forest. In the leaf litter of the neighbouring, more humid part of the forest, four other species of Pholcidae were found (*Anopsicus* sp.; *Modisimus* spp.).

Tolteca oaxaca Huber sp. nov.
urn:lsid:zoobank.org:act:85F8D1C1-9EC5-407C-A507-90D0270F18A9
Figs 36K–L, 50–54, 55G–H

Pholcophora hesperia Gertsch, 1982: 102 (specimens from Oaxaca only; see Remarks under *T. hesperia*).

Tolteca hesperia – Huber 2000: 118 (part; see Remarks under *T. hesperia*), figs 75, 126, 448–453, 455–457 (not fig. 454).

Diagnosis

Distinguished from known congeners by the combination of: male genital bulb without dorsal ridge (unlike *T. jalisco*); procursus tip gradually narrowing (Fig. 51C; unlike *T. hesperia* and *T. sinnombre* sp. nov.); male cheliceral apophyses close together (Fig. 51A; distance between tips ~40 µm, i.e., closer together than in *T. manzanillo* sp. nov. and *T. sinnombre*), in lateral view very small and with small angle against distal-frontal face of chelicera (Fig. 51B; unlike *T. hesperia*; not checked in *T. jalisco*); main

epigynal plate crescent-shaped (Fig. 52A, C; rather than band-like as in *T. hesperia* and *T. jalisco*); sacs in female internal genitalia tiny, only ~9–13 µm long (Fig. 55G–H; smaller than in all known congeners).

Etymology

The species name is derived from the type locality; noun in apposition.

Type material

Holotype

MEXICO – **Oaxaca** • ♂; ~3 km N of San Pedro Totolapa; 16.6976° N, 96.3180° W; 1100 m a.s.l.; 26 Oct. 2019; B.A. Huber and A. Valdez-Mondragón leg.; LATLAX.

Paratypes

MEXICO – **Oaxaca** • 4 ♂♂; same collection data as for holotype; ZFMK Ar 23961.

Other material examined

MEXICO – **Oaxaca** • 19 ♀♀, in pure ethanol; same collection data as for holotype; four prosomata used for molecular work, two females used for SEM, two cleared abdomens transferred to ZFMK Ar 23961; ZFMK Mex362 • 3 ♂♂; same collection data as for holotype; partly used for karyotype analyses; ZFMK 23962 • 3 ♂♂, 3 ♀♀; same collection data as for holotype; partly used for µ-CT study; ZFMK 23963 • 2 ♂♂, 2 ♀♀ abdomens; ~17 km NW of Tehuantepec; 16.3919° N, 95.3865° W; 165 m a.s.l.; 27 Oct. 2019; B.A. Huber and A. Valdez-Mondragón leg.; ZFMK Ar 23964 • 4 ♀♀, 4 juvs, in pure ethanol; same collection data as for preceding; two female abdomens transferred to ZFMK Ar 23964; ZFMK Mex368 • 2 ♂♂; same collection data as for preceding; partly used for karyotype analyses; ZFMK 23965 • 2 ♂♂, 3 ♀♀; same collection data as for preceding; partly used for µ-CT study; ZFMK 23966 • 2 ♂♂, 11 ♀♀, 2 juvs (subadult males); same collection data as for preceding; LATLAX.

Fig. 50. *Tolteca oaxaca* Huber sp. nov., male paratype from Mexico, Oaxaca, N of San Pedro Totolapa (ZFMK Ar 23961). Left palp, prolateral, dorsal, and retrolateral views. Scale bar = 0.2 mm.

Description

Male (holotype)

Measurements. Total body length 1.13, carapace width 0.47. Distance PME-PME 45 µm; diameter PME 45 µm; distance PME-ALE 15 µm; distance AME-AME 10 µm; diameter AME 30 µm. Leg 1: 2.07 (0.55 + 0.17 + 0.52 + 0.53 + 0.30), tibia 2: 0.42, tibia 3: 0.38, tibia 4: 0.65; tibia 1 L/d: 9; diameters of leg femora 0.11, of leg tibiae 0.06.

Colour (in ethanol). Prosoma and legs monochromous ochre-yellow; abdomen slightly darker ochre-grey, also monochromous.

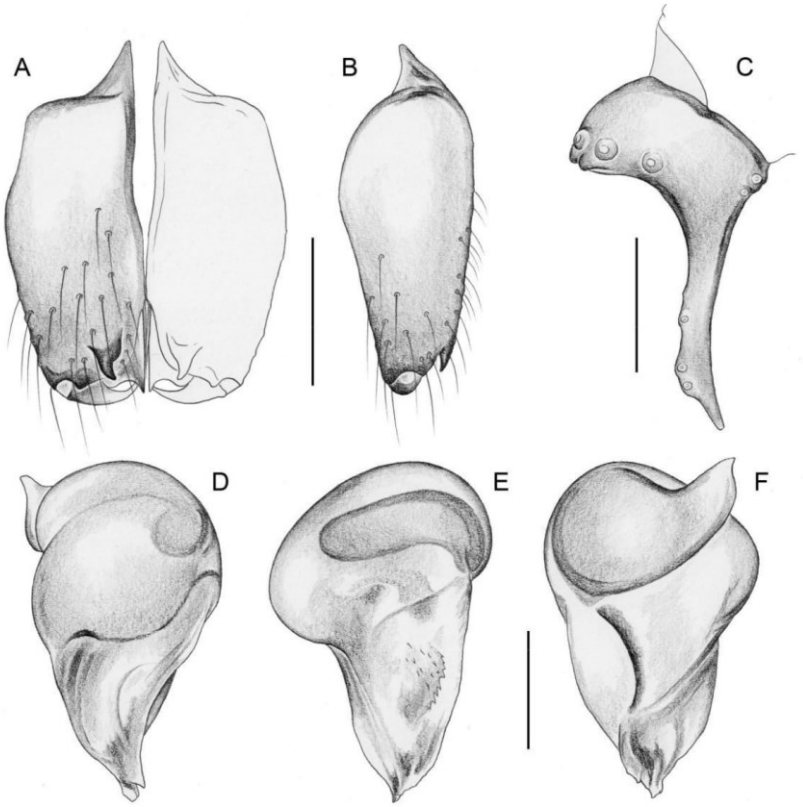

Fig. 51. *Tolteca oaxaca* Huber sp. nov., male paratype from Mexico, Oaxaca, N of San Pedro Totolapa (ZFMK Ar 23961). **A–B**. Chelicerae, frontal and lateral views. **C**. Left palpal tarsus and procursus, retrolateral view. **D–F**. Left genital bulb, prolateral, dorsal, and retrolateral views. Scale bars = 0.1 mm.

Body (Fig. 36K). Ocular area barely raised. Carapace without thoracic groove. Clypeus unmodified, short (clypeus rim to ALE: 130 µm). Sternum wider than long (0.35/0.30), almost round (i.e., not heart-shaped), with pair of small but distinct anterior processes (~50 µm diameter at basis, ~50 µm long) near coxae 1. Abdomen globular.

Chelicerae (Fig. 51A–B). With pair of frontal apophyses pointing downwards, distance between tips of apophyses: 50 µm; without stridulatory files.

Palps (Fig. 50). Coxa unmodified; trochanter without process; femur proximally without process, distally widened but simple, slightly curved towards dorsal; femur-patella joints not (or barely) shifted to one side; tibia very short, with two trichobothria; tibia-tarsus joints not shifted to one side; procursus very simple (Fig. 51C), with distal ventral process; genital bulb as in Fig. 51D–F, in light microscope possibly indistinguishable from congeners.

Legs. Without spines and curved hairs; with slightly increased density of short vertical hairs on tibia 1 (barely visible in dissecting microscope); retrolateral trichobothrium of tibia 1 at 59%; prolateral trichobothrium absent on tibia 1; tarsus 1 with six pseudosegments, all fairly distinct.

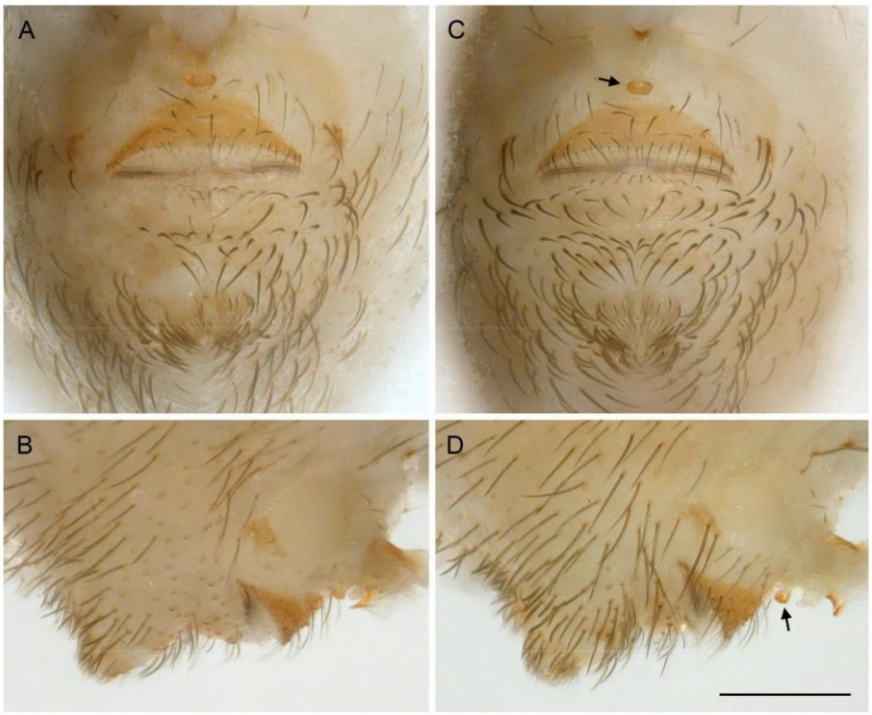

Fig. 52. *Tolteca oaxaca* Huber sp. nov., females from Mexico, Oaxaca, N of San Pedro Totolapa (ZFMK Ar 23961), epigyna. **A, C**. Ventral views. **B, D**. Lateral views. Arrows: knob-shaped structure. Scale bar = 0.2 mm (all at same scale).

Variation (male)
Tibia 1 in seven newly collected males (incl. holotype): 0.48–0.58 (mean 0.53).

Female
In general, similar to male (Fig. 36L) but sternum without pair of anterior humps, tibia 1 without increased density of short vertical hairs. Total body length: ~1.20; tibia 1 in 21 newly collected females: 0.47–0.56 (mean 0.51). Epigynum (Figs 52, 54A) short crescent-shaped anterior plate slightly protruding in lateral view; posterior plate short and wide, very indistinct, barely visible. With distinct knob between epigynum and pedicel (Fig. 54B). Internal genitalia (Fig. 53) with pair of strong transversal sclerites, with very short sacs (Fig. 55G–H), without (or with very small?) pore plates.

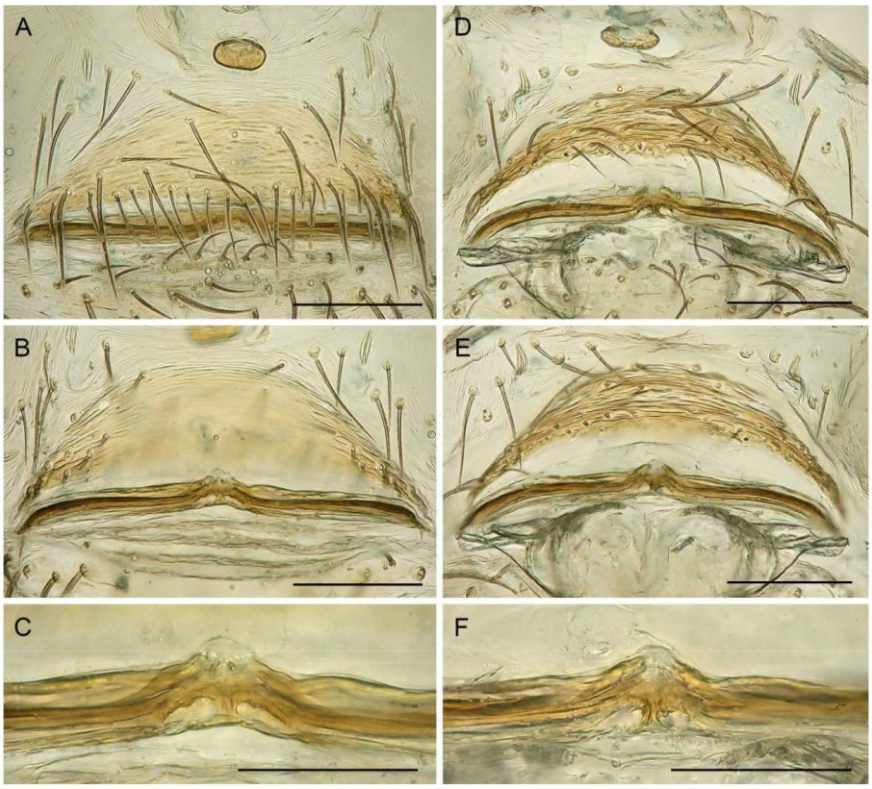

Fig. 53. *Tolteca oaxaca* Huber sp. nov., females from Mexico, Oaxaca, N of San Pedro Totolapa (ZFMK Ar 23961). **A–B, D–E**. Cleared female genitalia, ventral (A, D) and dorsal (B, E) views. **C, F**. Detail of median internal structures. Scale bars: A–B, D–E = 0.1 mm; C, F = 0.05 mm.

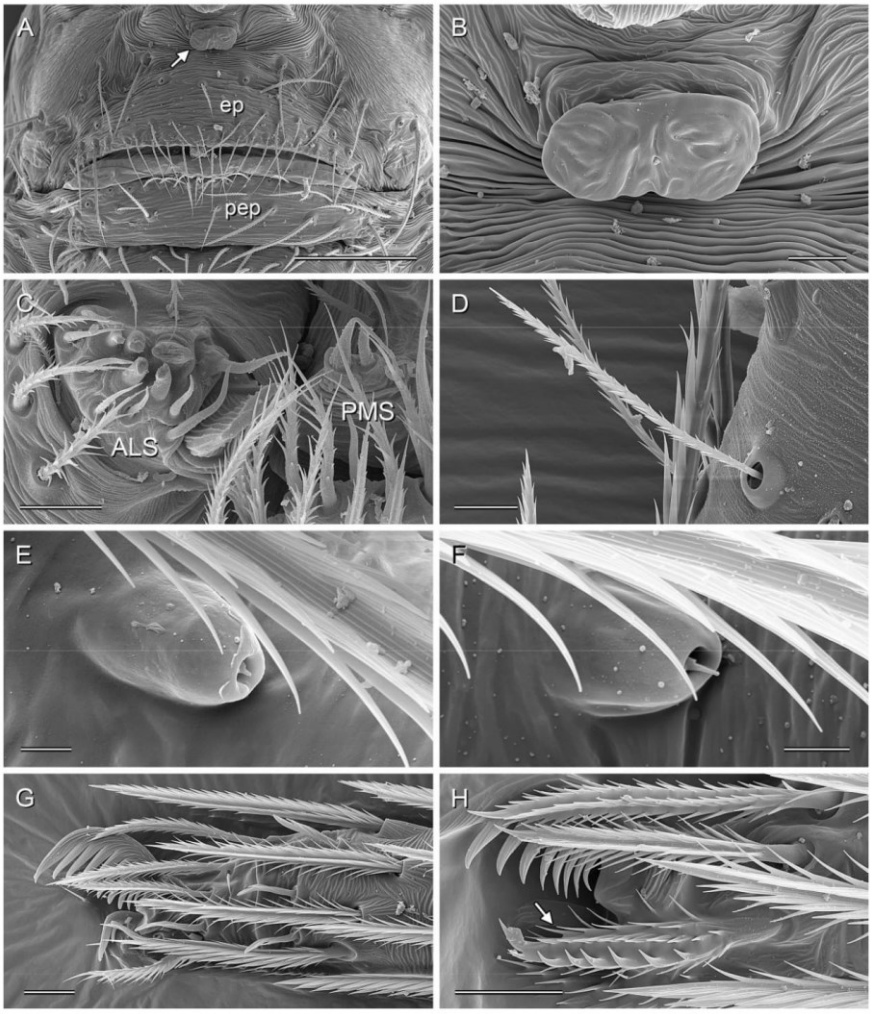

Fig. 54. *Tolteca oaxaca* Huber sp. nov., female from Mexico, Oaxaca, 3 km N of San Pedro Totolapa (ZFMK Mex362). **A**. Epigynum, ventral view (arrow: knob-shaped structure). **B**. Knob-shaped structure between epigynum and pedicel. **C**. ALS and PMS. **D**. Prolateral trichobothrium on tibia 3. **E**. Palpal tarsal organ. **F**. Tarsal organ on tarsus 2. **G**. Tip of left tarsus 2, retrolateral view. **H**. Tip of right tarsus 4, prolateral view, showing comb hair (arrow). Abbreviations: ep = epigynum (main epigynal plate); pep = posterior epigynal plate. Scale bars: A = 100 µm; B–D, G–H = 10 µm; E–F = 2 µm.

Distribution

Apparently widely distributed in the state of Oaxaca, Mexico (Fig. 35). We have not restudied Gertsch's (1982) and Huber's (2000) specimens but consider all their records of *Pholcophora/Tolteca hesperia* from Oaxaca to represent this species.

Natural history

At the type locality, a dry hill with a sparse and low tree cover (Fig. 56C), the spiders were found in high densities in the thin layer of leaf litter and among small pebbles on the ground (Fig. 56D). Within ~1.5 h, ~30 individuals were seen within an area of ~4 m_2. In slightly more humid (shaded) areas on the same hill, two other species of Pholcidae were found (*Modisimus* sp.; *Physocyclus paredesi* Valdez-Mondragón, 2010). At the second locality, a slightly higher and denser roadside forest, *Tolteca* was also collected at a rather dry spot with a thin layer of leaf litter, while more humid areas contained other Pholcidae genera (*Modisimus* sp.; *Physocyclus paredesi*; *Anopsicus* sp.; *Psilochorus* sp.).

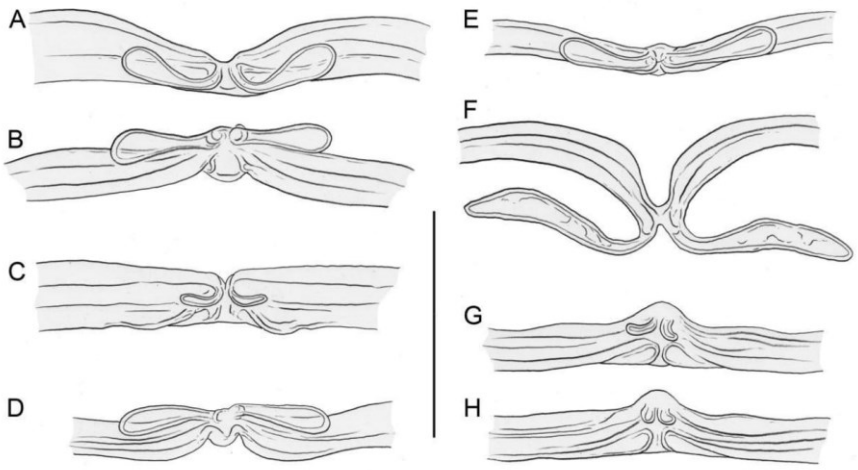

Fig. 55. *Tolteca* Huber, 2000 internal female genitalia, median section of main transversal internal sclerite. **A–B**. *T. hesperia* (Gertsch, 1982); females from Mexico, Sinaloa, S of Rosario (ZFMK Ar 23953). **C**. *T. jalisco* (Gertsch, 1982), female from Mexico, Jalisco, N of La Quemada (ZFMK Ar 23956). **D**. *T. huahua* Huber sp. nov., female from Mexico, Michoacán, W of Huahua (ZFMK Ar 23957). **E**. *T. manzanillo* Huber sp. nov., female from Mexico, Colima, E of Manzanillo (ZFMK Ar 23958). **F**. *T. sinnombre* Huber sp. nov., female from Mexico, Colima, S of Coquimatlán (ZFMK Ar 23960). **G–H**. *T. oaxaca* Huber sp. nov., females from Mexico, Oaxaca, N of San Pedro Totolapa (ZFMK Ar 23961). Scale bar = 0.1 mm.

Fig. 56. Representative sample of habitats of *Tolteca* Huber, 2000 in Mexico. **A**. Sinaloa, 3 km S of Rosario (*T. hesperia* (Gertsch, 1982)). **B**. Colima, 17 km E of Manzanillo (type locality of *T. manzanillo* Huber sp. nov.; showing collection method). **C–D**. Oaxaca, 3 km N of San Pedro Totolapa (type locality of *P. oaxaca* Huber sp. nov.; overview and spot with high abundance of specimens).

Karyology

The male karyotype of *T. hesperia* consisted of 15 chromosomes including a X_1X_2Y system. Chromosome pairs were metacentric. The last two chromosome pairs were much shorter than the first four pairs. X chromosomes were probably metacentric. The Y chromosome was a tiny element (3.35% of TCL); its morphology was not resolved (Fig. 57A). The male set of *T. oaxaca* sp. nov. comprised five chromosome pairs and a X_1X_2Y system, i.e., 13 chromosomes. The haploid karyotype consisted of five chromosomes (each representing a particular chromosome pair), which decreased gradually in size, and the sex chromosomes X_1, X_2, and Y. All chromosomes were metacentric except for the chromosome representing the third pair, which was submetacentric. The Y chromosome was a tiny element (4.33% of TCL) (Fig. 57B). Three chromosome pairs contained a NOR (Fig. 58). In some plates, the sex chromosome body also included a signal, which suggests the presence of a sex chromosome-linked NOR (Fig. 58B). However, we were not able to determine which sex chromosome carried a NOR.

Sex chromosomes did not differ by behaviour or intensity of staining from the other chromosomes at spermatogonial prometaphase (Fig. 57C). They formed an overcondensed body on the periphery of the premeiotic nucleus, which exhibited positive heteropycnosis (i.e., more intensive staining than the other chromosomes) (Fig. 57D). Bivalents were considerably decondensed during the diffuse stage.

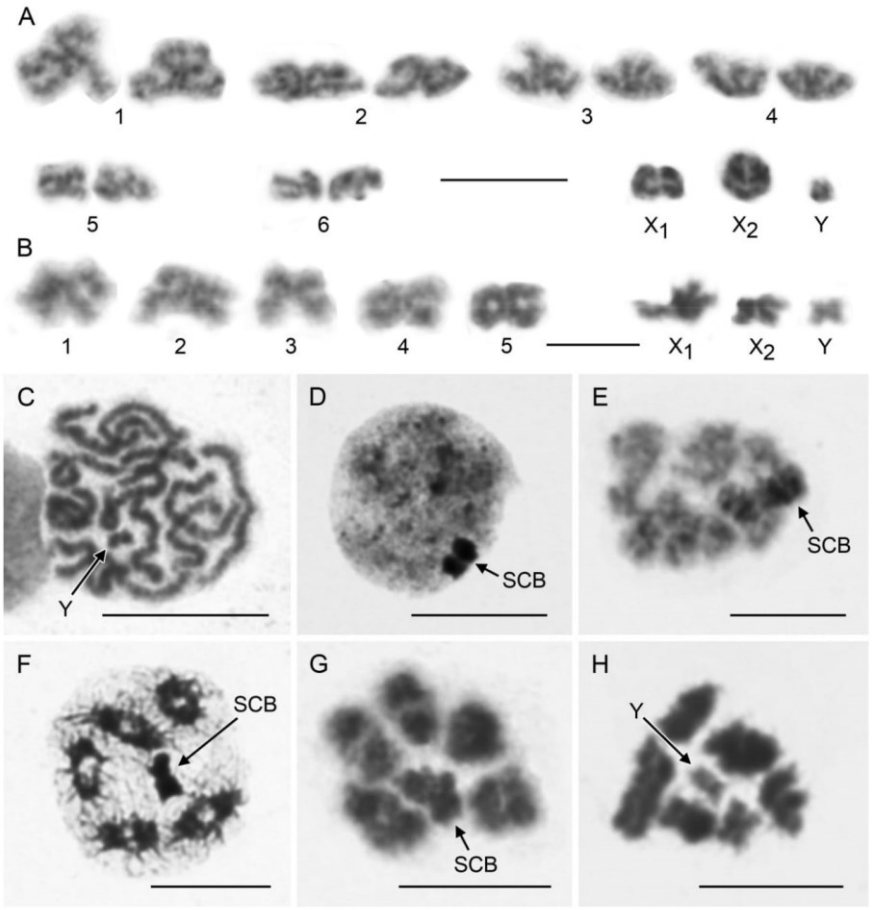

Fig. 57. *Tolteca* Huber, 2000, karyotypes and sex chromosome behaviour in male germline; stained by Giemsa. **A**. *T. hesperia* (Gertsch, 1982), diploid karyotype (2n♂ = 15, X_1X_2Y), based on two fused sister prometaphases II. X chromosomes are probably metacentric, morphology of Y chromosome is unresolved. Note positive heteropycnosis of X chromosomes. **B–G**. *T. oaxaca* Huber sp. nov. **B**. Haploid karyotype (n♂ = 8, X_1X_2Y), based on metaphase II. Note positive heteropycnosis of X chromosomes. **C**. Spermatogonial prometaphase. Note metacentric morphology of tiny Y chromosome. **D**. Premeiotic interphase. Sex chromosomes form an overcondensed body on the periphery of the nucleus. **E**. Late diffuse stage. Sex chromosomes are positively heteropycnotic; bivalents are considerably decondensed. **F**. Diplotene. Note five bivalents and sex chromosome body exhibiting a positive heteropycnosis. **G**. Metaphase I containing five bivalents and sex chromosome body. **H**. *T. hesperia*, metaphase II consisting of seven chromosomes. Note tiny Y chromosome. Abbreviations: SCB = sex chromosome body; X_1 = X_1 chromosome; X_2 = X_2 chromosome; Y = Y chromosome. Scale bars= 10 µm.

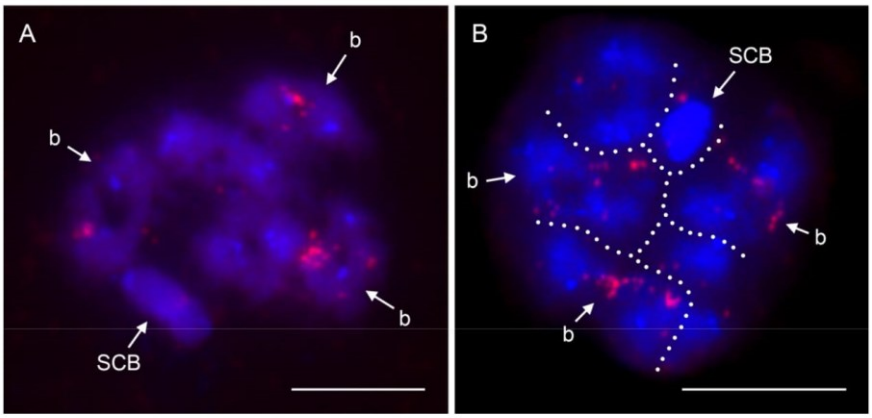

Fig. 58. *Tolteca oaxaca* Huber sp. nov., male meiosis, detection of NORs (FISH). Metaphase I comprising five bivalents and sex chromosome body; three bivalents contain NORs. **A**. Sex chromosome body without visible signal. **B**. Sex chromosome body includes signal. Individual elements separated by dashed line. Abbreviations: b = NOR bearing bivalent; SCB = sex chromosome body. Scale bars = 10 µm.

In contrast to this, sex chromosomes formed a highly condensed body during this stage (Fig. 57E). This body persisted until metaphase I (Fig. 57G), which impeded the determination of the mode of sex chromosome pairing during late prophase I (i.e., diplotene and diakinesis) and metaphase I. Bivalents contained a single chiasma only (Fig. 57F). X chromosomes were associated at metaphase II being positively heteropycnotic (Fig. 57A–B).

Biogeography

The environmental niche occupied by non-Caribbean ('true') *Pholcophora* is more similar to the niche occupied by *Tolteca* than to randomly generated niches (p = 0.010; Table 2; Fig. 59A; Supp. file 1: Fig. S54), and vice-versa (p = 0.010; Table 2; Supp. file 1: Fig. S69). The equivalency tests between the niches occupied by non-Caribbean *Pholcophora* and *Tolteca* revealed that their niche overlap is constant when randomly reallocating the occurrences of both groups between their ranges (p = 0.015; Table 2; Fig. 59B). These groups also exhibited a relatively high niche overlap (D = 0.40; Table 2; Fig. 59D).

The niche similarity tests were also significant between non-Caribbean *Pholcophora* and (1) the Caribbean clade (p = 0.010; Table 2; Supp. file 1: Figs S51, S63), (2) Mexican *Pholcophora* (p = 0.049; Table 2; Supp. file 1: Figs S52, S67), and (3) *Papiamenta* (p = 0.010; Table 2; Supp. file 1: Figs S53, S63). Besides, the niches occupied by the Caribbean clade and *Papiamenta* were significantly more similar than expected by chance (p = 0.010; Table 2; Supp. file 1: Figs S46, S61).

The niche overlap between *Pholcophora americana* and any other group was extremely low (Table 2), even when compared with congeneric but disjunct taxa, such as "Mexican *Pholcophora*" (i.e., Mexican species of *Pholcophora* incl. *P. texana*; D = 0.00). As expected (see Material and methods), the niche of the Caribbean clade (i.e., *Papiamenta* spp. and Caribbean '*Pholcophora*') showed a large overlap with the niche of *Papiamenta* (D = 0.59; Supp. file 1: Fig. S16). The niche overlap between the Caribbean

clade and both the non-Caribbean *Pholcophora* (D = 0.21; Supp. file 1: Fig. S21) and Mexican *Pholcophora* (D = 0.11; Supp. file 1: Fig. S18) is higher than the overlap between the Caribbean clade and *P. americana* (D = 0.00; Supp. file 1: Fig. S25) and *Tolteca* (D = 0.06; Supp. file 1: Fig. S17).

The altitudinal range differed among the compared groups (d.f. = 131, resid. def. = 46268, p = 0.000; Fig. 61). Taxa from the Caribbean clade were recorded from sea level up to ~70 m a.s.l., presenting the lowest altitudinal range (mean 25 m a.s.l.). They were followed by *Tolteca* (sea level to 1540 m a.s.l.; mean 286 m a.s.l.). The highest altitudinal range was observed for *Pholcophora* (30 to > 3000 m a.s.l.; mean 970 m a.s.l.), without statistically significant differences between *P. americana* and Mexican *Pholcophora* (Fig. 61).

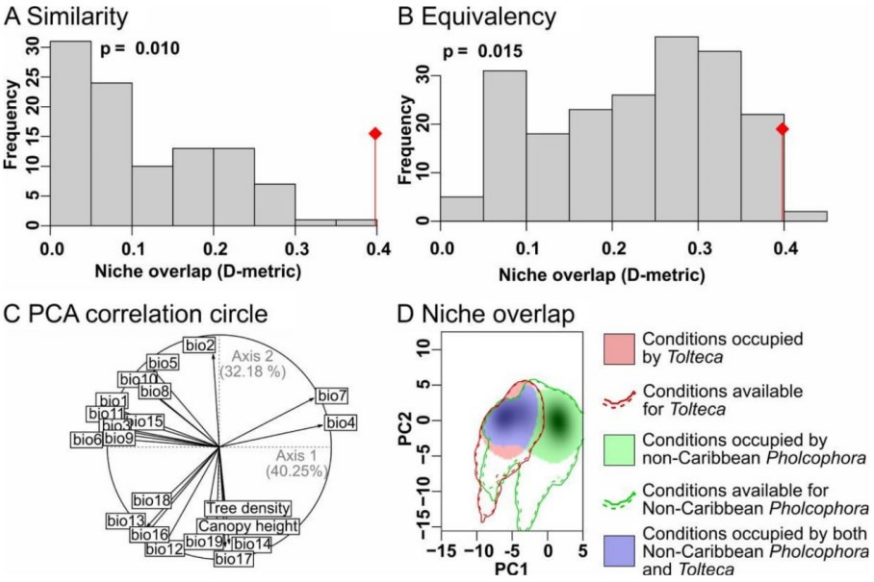

Fig. 59. Environmental niche comparisons between non-Caribbean ('true') *Pholcophora* Banks, 1896 and *Tolteca* Huber, 2000. Red lines in similarity and equivalency graphs indicate the observed niche overlap (D-metric), while grey bars show the distribution of the D-metric for 100 simulated comparisons. Note that the similarity and equivalency of the environmental niche between non-Caribbean *Pholcophora* and *Tolteca* was higher than randomly expected. The distribution of *Pholcophora* includes areas with high temperature annual range (bio7 in C) and seasonality (bio4 in C) not occupied by *Tolteca*. The two taxa exhibit a relatively high niche overlap (D = 0.40; bluish area in D). Climatic variables in the PCA: bio1 = annual mean temperature; bio2 = mean diurnal range; bio3 = isothermality; bio4 = temperature seasonality; bio5 = max temperature of warmest month; bio6 = min temperature of coldest month; bio7 = temperature annual range; bio8 = mean temperature of wettest quarter; bio9 = mean temperature of driest quarter; bio10 = mean temperature of warmest quarter; bio11 = mean temperature of coldest quarter; bio12 = annual precipitation; bio13 = precipitation of wettest month; bio14 = precipitation of driest month; bio15 = precipitation seasonality; bio16 = precipitation of wettest quarter; bio17 = precipitation of driest quarter; bio18 = precipitation of warmest quarter; bio19 = precipitation of coldest quarter.

Discussion

Morphology

Both in *Pholcophora* and in *Tolteca*, males but not females have short vertical hairs in higher than usual density on some or all of their leg tibiae (e.g., Fig. 42A–B). Our SEM data show that these hairs are structurally very different from the 'usual' short vertical hairs found on the legs (mainly the distal segments) of males and females of all pholcid spiders: they are simple without branches and apparently without an opening at the tip (Fig. 42C), while the 'usual' short vertical hairs have several short side branches and an opening at the tip (Fig. 42D–E). These latter hairs are very likely chemoreceptors (Foelix & Chu-Wang 1973). In the recent taxonomic literature on Pholcidae, numerous descriptions refer to "short vertical hairs" without discriminating between the 'usual' hairs found in males and females and the sexually dimorphic hairs found in males only (e.g., Lee *et al.* 2021; Yao *et al.* 2021; Zhu & Li 2021). In at least some of the treated taxa (e.g., *Pholcus* Walckenaer, 1805) sexually dimorphic vertical hairs are not known to exist, and the descriptions thus probably refer to the trivial presence of the ubiquitous chemoreceptors.

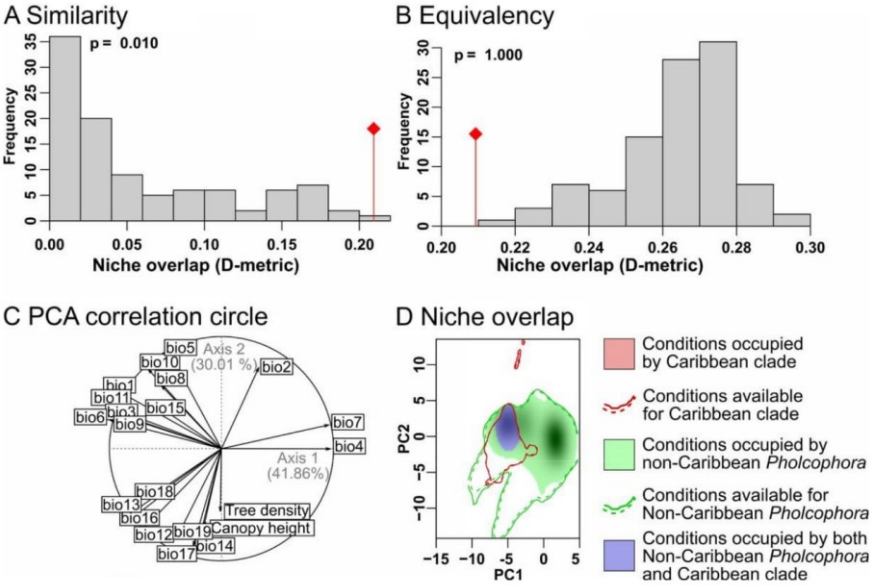

Fig. 60. Environmental niche comparisons between non-Caribbean ('true') *Pholcophora* Banks, 1896 and the Caribbean clade. Red lines in equivalency and similarity graphs indicate the observed niche overlap (D-metric), while grey bars show the distribution of the D-metric for 100 simulated comparisons. Note that the similarity of the environmental niche between non-Caribbean *Pholcophora* and the Caribbean clade was higher than randomly expected, while the equivalency was not (i.e., the niche is similar, but not identical). The distribution of the Caribbean clade is related to warmer conditions (bio5, bio8, and bio10 in C), while the distribution of non-Caribbean *Pholcophora* is more related to temperature annual range (bio7 in C) and seasonality (bio4 in C). A relatively low niche overlap is observed (D = 0.209; bluish area in D). Climatic variables in the PCA as in Fig. 59.

The function of the sexually dimorphic hairs remains a mystery. In Pholcidae, such hairs have apparently evolved several times convergently, in at least three subfamilies (Huber 2021). In Ninetinae, they have been reported for *Ibotyporanga* Mello-Leitão, 1944; *Papiamenta* Huber, 2000; and *Nerudia* Huber, 2000 (Huber 2000; Huber & Villarreal 2020; Huber *et al.* 2023), and they also occur in *Guaranita* Huber, 2000 and in *Galapa* Huber, 2000 (B.A. Huber unpubl. data). In other Ninetinae genera they may have been overlooked due to their size (~2 µm diameter at the basis, ~20–30 µm long).

Relationships

Our molecular data support the idea that a northern clade of Ninetinae (North America and Caribbean taxa) is nested within South American Ninetinae (cf. Huber *et al.* 2018). The monophyly of this northern clade suggests that cleistospermia have evolved at least twice in Pholcidae: once in the ancestor of *Pholcophora* and *Tolteca* (Dederichs *et al.* 2022), and once in all Pholcidae except Ninetinae. The sperm transfer form of *Papiamenta* is unknown but our results generate the prediction that *Papiamenta* males also transfer cleistospermia.

Within the northern clade, we found high support for the Mexican genus *Tolteca*, for a core-group of non-Caribbean (true) *Pholcophora*, and for a Caribbean clade consisting of *Papiamenta*, '*Pholcophora*' *bahama*, and some undescribed species tentatively placed in *Pholcophora*. All these extant Caribbean '*Pholcophora*' are known from females only. We thus prefer to keep them as "*Pholcophora*?" until males become available. We expect that the study of males will facilitate a decision as to whether they should be (1) described in one or more new genera, (2) assigned to *Papiamenta*, or (3) if *Papiamenta* should be synonymized with *Pholcophora*. In this context, the three Dominican amber fossil species currently placed in *Pholcophora* should also be restudied. They are known from males only, and the original drawings suggest that they partly resemble *Pholcophora* (long procursus), and partly *Papiamenta* (genital

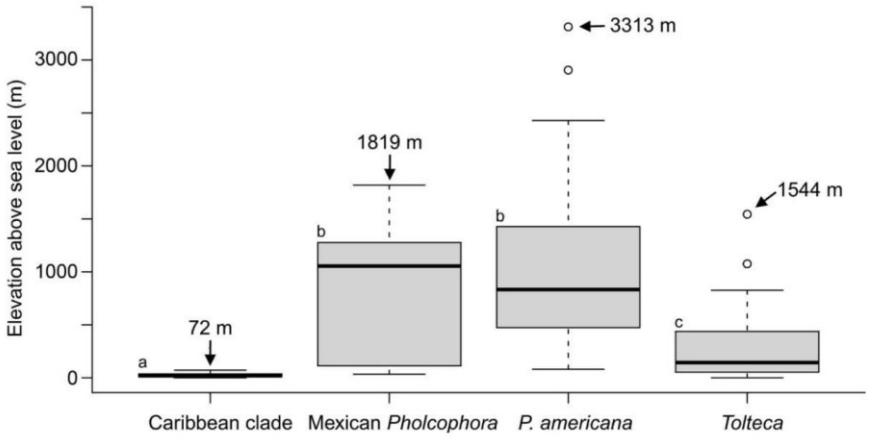

Fig. 61. Known altitudinal variation for records of the Caribbean clade, Mexican *Pholcophora* Banks, 1896, *P. americana* Banks, 1896, and *Tolteca* Huber, 2000. Highest altitudinal record for each group is detailed. Letters indicate statistically significant groups (p = 0.000). Note that the altitudinal range is significantly lower for the Caribbean clade, intermediate for *Tolteca*, and higher for both *Pholcophora* groups. Note that the two outliers for *P. americana* result from rough estimates of the coordinates; the actual collecting sites may have been lower.

bulb with distinct sclerite). We predict that extant Caribbean (Greater Antilles, Bahamas) '*Pholcophora*' males will most closely resemble these Dominican amber fossil species.

Karyology

The karyotypes of *Pholcophora* (Avila-Herrera *et al.* 2021) and *Tolteca* (this study) are formed by biarmed (i.e., metacentric and submetacentric) chromosomes. The prophase of the first meiotic division of males contains the so-called diffuse division, which is characterized by considerable decondensation of chromosome pairs (Ávila Herrera *et al.* 2021; this study). These features are probably ancestral for haplogyne spiders, i.e., for a clade formed by Synspermiata Michalik & Ramírez, 2014 and two cribellate families, Filistatidae Ausserer, 1867 and Hypochilidae Marx, 1888 (Ávila Herrera *et al.* 2021). The behaviour of sex chromosomes during male meiosis is similar to other pholcids examined except for the persistence of the sex chromosome body until metaphase I in *Tolteca*. In other pholcids studied, this behaviour was found only in the distantly related *Cantikus sabah* (Huber, 2011) (Ávila Herrera *et al.* 2021). The number of NOR bearing chromosome pairs in *T. oaxaca* sp. nov. (three) is close to the supposed ancestral pattern of ninetines (two NOR bearing chromosome pairs) (Ávila Herrera *et al.* 2021). Furthermore, this species probably displays a sex chromosome-linked NOR. Nucleolus organizer regions often spread to sex chromosomes during the evolution of haplogynes, including pholcids (Král *et al.* 2006; Ávila Herrera *et al.* 2021).

The karyotype of *Pholcophora americana* ($2n♂ = 29$, X_1X_2Y) is close to the supposed ancestral karyotype of pholcid spiders (Ávila Herrera *et al.* 2021). Like in many other spider groups (e.g., Suzuki 1954; Kořínková & Král 2013; Král *et al.* 2013), the number of chromosome pairs decreased during the evolution of many pholcid lineages (Ávila Herrera *et al.* 2021) including ninetines (Huber *et al.* 2023; this study). In *Tolteca*, the number of chromosome pairs has been reduced considerably, namely to six (*T. hesperia*) or even five (*T. oaxaca* sp. nov.) (this study). There are only a few other araneomorph spiders with standard chromosome structure that exhibit lower numbers of chromosome pairs than *T. oaxaca*, namely representatives of the genus *Micropholcus* Deeleman-Reinhold & Prinsen, 1987 (Pholcinae) (Lomazi *et al.* 2018; Ávila Herrera *et al.* 2021) and *Uloborus danolius* Tikader, 1969 (Uloboridae) (Parida & Sharma 1987).

Closely related genera of pholcids do usually not differ considerably in the number of chromosome pairs. A notable exception is a clade in Pholcinae including the genera *Cantikus* Huber, 2018; *Leptopholcus* Simon, 1893; *Micropholcus* Deeleman-Reinhold & Prinsen, 1987; *Pehrforsskalia* Deeleman-Reinhold & van Harten, 2001; and *Pholcus* Walckenaer, 1805; in this clade, the number of pairs decreased from eleven (*Pholcus*) to four (*Micropholcus*) (Ávila Herrera *et al.* 2021). The clade formed by the genera *Pholcophora* (13) and *Tolteca* (5–6) seems to be another case of considerable reduction of the number of chromosome pairs among closely related pholcids. Despite the molecular support for the close relationship between *Pholcophora* and *Tolteca*, the considerable difference in the number of chromosome pairs in the two genera motivates us to speculate about a possible alternative. Such an alternative phylogenetic placement of *Tolteca* is suggested by the presence of a sex chromosome-linked NOR in *Tolteca* but not in *Pholcophora*. Among ninetines, this marker was also found in the genera *Gertschiola* Brignoli, 1981, *Kambiwa* Huber, 2000, and *Nerudia* Huber, 2000, which may form

a separate clade being characterised by complex sex chromosome systems ($X_1X_2X_3Y$ and $X_1X_2X_3X_4Y$) and sex chromosome-linked NOR (Huber *et al.* 2023). These systems arose from X_1X_2Y, which is most probably the ancestral sex chromosome system of haplogynes (Paula-Neto *et al.* 2017; Ávila Herrera *et al.* 2021). Provided that the sex chromosome-linked NOR has originated already in the X_1X_2Y system of ninetines, *Tolteca* could be a basal member of the clade containing *Gertschiola*, *Kambiwa*, and *Nerudia.*

The two analysed species of *Tolteca* differ in several karyotype features, which indicates a considerable karyotype differentiation within the genus despite very little morphological differentiation. First, the karyotype of *T. hesperia* contains one chromosome pair more than the karyotype of *T. oaxaca* sp. nov., which suggests a reduction of the number of chromosome pairs by fusion in the latter species. While the chromosome pairs of *T. oaxaca* decrease gradually in length, the last two pairs of *T. hesperia* are much smaller than the other pairs. Moreover, one pair of *T. oaxaca* has a submetacentric morphology. These differences suggest operation of additional rearrangements, namely inversions and translocations. Such changes frequently took part in the karyotype evolution of pholcids (Ávila Herrera *et al.* 2021; Král *et al.* 2022). They might be involved in the formation of interspecific reproductive barriers (e.g., Rieseberg 2001; Ayala & Coluzzi 2005).

Biogeographic analyses

The niche overlap, similarity, and equivalence used in the present study are frequently applied to describe these parameters for native and invaded localities of introduced species (e.g., Broennimann *et al.* 2007). For spiders, these analyses were recently used to show that the non-native American populations of the orb-weaver spider *Cyrtophora citricola* (Forsskål, 1775) occupy climatic conditions with a higher similarity to those in southern Africa than to those in the Mediterranean (Segura-Hernández *et al.* 2022). These analyses thus favoured the hypothesis of an African origin of the American populations of *C. citricola* (Segura-Hernández *et al.* 2022). To date, there is no evidence for human-mediated dispersal in any species of *Pholcophora*, *Tolteca*, and *Papiamenta*. However, the wide geographic distribution of *P. americana*, covering much of the western USA and ranging into Canada (Fig. 2), raises questions about the dispersal strategies of this species. *Pholcophora americana* is likely to be the most widespread Ninetinae species in the World (Huber *et al.* 2023: Table S4). The results shown in the present study suggest that *P. americana* occupies a very distinct environmental niche compared to related taxa (see Table 2 and Supp. file 1). Further studies should address the phylogeography and genetic diversity of *P. americana* to provide further details on its population structure and the colonization history of such a different niche.

The environmental niche analyses carried out in the present study were first used to compare the niches between closely related taxa by Broennimann *et al.* (2014). These authors showed that the niche overlap between polymorphic local populations of two European snake species was higher than that of polymorphic and monomorphic populations of each species individually. This conclusion allowed the authors to suggest that polymorphism may enable the exploitation of different resources (Broennimann *et al.* 2014). Similar analyses showed that two phylogenetically related wandering spiders (*Phoneutria* Perty, 1833) exhibited a higher-than-expected niche conservatism and equivalency, corroborating the hypothesis of allopatric speciation for these species (Hazzi & Hormiga 2021).

The highest niche overlap we found in this study was between the Caribbean clade and *Papiamenta*. However, this is a somewhat tautological result, owing to the low number of Caribbean species currently assigned to *Pholcophora*, yielding a background dominated by the occurrence records of *Papiamenta*. Upon the discovery of further records of '*Pholcophora*' taxa in the Caribbean region, these analyses should be carried out independently between the Caribbean '*Pholcophora*' and *Papiamenta* species. No major niche overlap (i.e., $D > 0.5$) was observed for any other pairwise comparisons (see Table 2). It is important to highlight that, apart from the tautological comparison above, the D-metric for niche overlap was not higher than 0.21 for any other comparison with the Caribbean clade (Table 2). This suggests that the Caribbean taxa occupy a very distinct environmental niche compared to other taxa in the North American-Caribbean clade of Ninetinae.

Some Mexican species of *Pholcophora* and *Tolteca* (ca are known from relatively close localities 250 km straight-line), but never in sympatry. The niche overlap among these taxa is relatively

Table 2. Niche overlap metrics (Schoener's D-index), equivalency and similarity tests in environmental space among six compared groups. The 'Caribbean clade' includes *Papiamenta* and Caribbean '*Pholcophora*'. 'Mexican *Pholcophora*' refers to all Mexican species of *Pholcophora* including *P. texana*. Bold underlined values are significant p-values. Similarity is shown by the two-way (1 vs 2 / 2 vs 1) comparison between groups. Graphs corresponding to all pairwise comparisons are shown in Supp. file 1: Figs S1–75.

Group 1	Group 2	Schoener's D-index	Equivalency p-value	Similarity (1 vs 2) p-value	Similarity (2 vs 1) p-value
Caribbean clade	*Papiamenta*	0.592	0.198	**0.010**	**0.020**
Caribbean clade	*Tolteca*	0.065	0.980	0.119	0.129
Mexican *Pholcophora*	Caribbean clade	0.114	1.000	0.198	0.188
Mexican *Pholcophora*	*Papiamenta*	0.109	1.000	0.188	0.188
Mexican *Pholcophora*	*Tolteca*	0.187	0.762	0.267	0.307
Non-Caribbean *Pholcophora*	Caribbean clade	0.209	1.000	**0.010**	**0.020**
Non-Caribbean *Pholcophora*	Mexican *Pholcophora*	0.239	1.000	**0.049**	**0.049**
Non-Caribbean *Pholcophora*	*Papiamenta*	0.183	1.000	**0.010**	**0.030**
Non-Caribbean *Pholcophora*	*Tolteca*	0.398	**0.015**	**0.009**	**0.020**
P. americana	Caribbean clade	0.000	1.000	1.000	1.000
P. americana	Mexican *Pholcophora*	0.002	1.000	0.574	0.554
P. americana	Non-Caribbean *Pholcophora*	0.096	1.000	0.277	0.267
P. americana	*Papiamenta*	0.000	1.000	1.000	1.000
P. americana	*Tolteca*	0.004	1.000	0.525	0.564
Papiamenta	*Tolteca*	0.054	0.980	0.099	0.099

low (D = 0.19; see Table 2). However, upon comparing the niche overlap between *Tolteca* and 'true' (non-Caribbean) *Pholcophora*, a significantly higher index was observed (D = 0.40). This pair also included taxa with similar and identical niches (hence the significant equivalency test; see Warren *et al.* 2008) (Table 2). This result might be biased by methodological constraints, as the background for both groups encompasses most of Mexico and the southwestern USA, which includes a huge variation in environmental conditions. Additionally, the significantly different altitudinal ranges occupied by *Tolteca* and non-Caribbean *Pholcophora* species suggests that additional environmental variables not used in the present study constrain the geographic distribution of these taxa.

The low number of statistically significant similarity and equivalency tests, associated with the low niche overlap, corroborates the environmental niche conservatism reported for ninetines in general (Huber *et al.* 2023). The niche in ninetines has been shown to evolve following the expectations of Brownian motion evolution (Huber *et al.* 2023), i.e., this trait changes randomly and continuously through time (Revell 2021). As such, the compared groups occupy environments that are as similar and equivalent as expected, not identical. The decrease in biodiversity shortfalls (see Hortal *et al.* 2015) related to ninetines (e.g., Huber & Villarreal 2020; Huber *et al.* 2023) has revealed taxa with island and continental representatives, which suggests that the diversification of these spiders is likely to be as complex as observed for other arachnids (e.g., McHugh *et al.* 2014; Chamberland *et al.* 2018; Esposito & Prendini 2019; Cala-Riquelme *et al.* 2022). Therefore, upon availability of a comprehensive phylogeny of Ninetinae, the effects of dispersal, vicariance, and allopatric speciation processes should be re-evaluated under a niche conservatism scenario for the diversification of these pholcids.

Acknowledgements

We thank Claudia Copley for providing coordinate data of *Pholcophora americana* records in British Columbia. We thank Pierre Paquin and Ken Schneider for contributing specimens from the USA, and Rudy Jocqué for donating specimens from Curaçao. The specimens from Mexico were collected under Scientific Collector Permit FAUT-0309 from the Secretaría de Medio Ambiente y Recursos Naturales (SEMARNAT) to AVM. LSC thanks Olivier Broennimann for assisting with the interpretation of the results of the niche equivalency analyses. The cytogenetic work was supported by the Ministry of Education, Youth, and Sports of the Czech Republic (projects LTAUSA 19142 and SVV 260568: IMAH, JK) and by the Chilean National Commission for Scientific and Technological Research (ANID) (IMAH). AVM thanks the program Cátedras CONACyT, Consejo Nacional de Ciencia y Tecnología (CONACyT), Mexico, for financial support of the project No. 59: "Laboratorio Regional de Biodiversidad y Cultivo de Tejidos Vegetales (LBCTV) del Instituto de Biología, Universidad Nacional Autónoma de México (IBUNAM), sede Tlaxcala". AVM also thanks SEP-CONACyT for financial support of the project Basic Science (Ciencia Básica) 2016, No. 282834, supporting field work in Mexico. Further financial support was received from the German Research Foundation (DFG; project HU980/12-1). We thank two anonymous reviewers for helpful comments on the manuscript.

Author contributions

BAH: initiation of project, collecting, taxonomy, writing
GM: analysis of molecular data, writing
AVM: permits, collecting, writing
IMAH and JK: karyology, writing
LSC: biogeography, writing

References

Astrin J.J., Höfer H., Spelda J., Holstein J., Bayer S., Hendrich L., Huber B.A., Kielhorn K.-H., Krammer H.-J., Lemke M., Monje J.C., Morinière J., Rulik B., Petersen M., Janssen H. & Muster C. 2016. Towards

a DNA barcode reference database for spiders and harvestmen of Germany. *PLoS One* 11 (9): e0162624. https://doi.org/10.1371/journal.pone.0162624

Ávila Herrera I.M., Král J., Pastuchová M., Forman M., Musilová J., Kořínková T., Šťáhlavský F., Zrzavá M., Nguyen P., Just P., Haddad C.R., Hiřman M., Koubová M., Sadílek D. & Huber B.A. 2021. Evolutionary pattern of karyotypes and meiosis in pholcid spiders (Araneae: Pholcidae): implications for reconstructing chromosome evolution of araneomorph spiders. *BMC Ecology and Evolution* 21: 75. https://doi.org/10.1186/s12862-021-01750-8

Ayala F. & Coluzzi M. 2005. Chromosome speciation: humans, *Drosophila*, and mosquitoes. *Proceedings of the National Academy of Sciences of the USA* 102: 6535–6542. https://doi.org/10.1073/pnas.0501847102

Banks N. 1896. New North American spiders and mites. *Transactions of the American Entomological Society* 23: 57–77. Available from https://www.biodiversitylibrary.org/page/7508724 [accessed 26 May 2023].

Bennett R. 2014. COSEWIC assessment and status report on the northwestern cellar spider *Psilochorus hesperus* in Canada. Committee on the Status of Endagered Wildlife in Canada, Ottawa. Available from https://wildlife-species.canada.ca/species-risk-registry/default.asp?lang=En&n=092035C0-1 [accessed 26 May 2023].

Brignoli P.M. 1981. Studies on the Pholcidae, I. Notes on the genera *Artema* and *Physocyclus* (Araneae). *Bulletin of the American Museum of Natural History* 170: 90–100.

Broennimann O., Treier U.A., Müller-Schärer H., Thuiller W., Peterson A.T. & Guisan A. 2007. Evidence of climatic niche shift during biological invasion. *Ecology Letters* 10: 701–709. https://doi.org/10.1111/j.1461-0248.2007.01060.x

Broennimann O., Fitzpatrick M.C., Pearman P.B., Petitpierre B., Pellissier L., Yoccoz N.G., Thuiller W., Fortin M.J., Randin C., Zimmermann N.E., Graham C.H. & Guisan A. 2012. Measuring ecological niche overlap from occurrence and spatial environmental data. *Global Ecology and Biogeography* 21: 481–497. https://doi.org/10.1111/j.1466-8238.2011.00698.x

Broennimann O., Ursenbacher S., Meyer A., Golay P., Monney J.-C., Schmocker H., Guisan A. & Dubey S. 2014. Influence of climate on the presence of colour polymorphism in two montane reptile species. *Biology Letters* 10 (11): 20140638. https://doi.org/10.1098/rsbl.2014.0638

Brown B.V. 1993. A further chemical alternative to critical-point-drying for preparing small (or large) flies. *Fly Times* 11: 10.

Cala-Riquelme F., Wiencek P., Florez-Daza E., Binford G.J. & Agnarsson I. 2022. Island-to-island vicariance, founder-events and within-area speciation: the biogeographic history of the *Antillattus* clade (Salticidae: Euophryini). *Diversity* 14: 224. https://doi.org/10.3390/d14030224

Capella-Gutiérrez S., Silla-Martínez J.M. & Gabaldón T. 2009. trimAl: a tool for automated alignment trimming in large-scale phylogenetic analyses. *Bioinformatics* 25: 1972–1973. https://doi.org/10.1093/bioinformatics/btp348

Chamberland L., McHugh A., Kechejian S., Binford G.J., Bond J.E., Coddington J., Dolman G., Hamilton C.A., Harvey M.S., Kuntner M. & Agnarsson I. 2018. From Gondwana to GAARlandia: evolutionary history and biogeography of ogre-faced spiders (*Deinopis*). *Journal of Biogeography* 45: 2442–2457. https://doi.org/10.1111/jbi.13431

Cock P.J., Antao T., Chang J.T., Chapman B.A., Cox C.J., Dalke A., Friedberg I., Hamelryck T., Kauff F., Wilczynski B. & de Hoon M.J. 2009. Biopython: freely available Python tools for computational molecular biology and bioinformatics. *Bioinformatics* 25: 1422–1423. https://doi.org/10.1093/bioinformatics/btp163

Crawley M.J. 2012. *The R Book*. Wiley, UK.
Available from http://www.bio.ic.ac.uk/research/mjcraw/therbook/index.htm [accessed 26 May 2023].

Crowther T.W., Glick H.B., Covey K.R., Bettigole C., Maynard D.S., Thomas S.M., Smith J.R., Hintler G., Duguid M.C., Amatulli G., Tuanmu M.-N., Jetz W., Salas C., Stam C., Piotto D., Tavani R., Green S., Bruce G., Williams S.J., Wiser S.K., Huber M.O., Hengeveld G.M., Nabuurs G.-J., Tikhonova E., Borchardt P., Li, C.-F., Powrie L.W., Fischer M., Hemp A., Homeier J., Cho P., Vibrans A.C., Umunay P.M., Piao S.L., Rowe C.W., Ashton M.S., Crane P.R. & Bradford M.A. 2015. Mapping tree density at a global scale. *Nature* 525: 201–205. https://doi.org/10.1038/nature14967

Cuervo P.F., Flores F.S., Venzal J.M. & Nava S. 2021. Niche divergence among closely related taxa provides insight on evolutionary patterns of ticks. *Journal of Biogeography* 48: 2865–2876. https://doi.org/10.1111/jbi.14245

Dederichs T.M., Huber B.A. & Michalik P. 2022. Evolutionary morphology of sperm in pholcid spiders (Pholcidae, Synspermiata). *BMC Zoology* 7: 52. https://doi.org/10.1186/s40850-022-00148-3

Di Cola V., Broennimann O., Petitpierre B., Breiner F.T., D'Amen M., Randin C., Engler R., Pottier J., Pio D., Dubuis A., Pillissier L., Mateo R.G., Hordijk W., Salamin N. & Guisan A. 2017. ecospat: an R package to support spatial analyses and modeling of species niches and distributions. *Ecography* 40: 774–787. https://doi.org/10.1111/ecog.02671

Eberle J., Dimitrov D., Valdez-Mondragón A. & Huber B.A. 2018. Microhabitat change drives diversification in pholcid spiders. *BMC Evolutionary Biology* 18: 141. https://doi.org/10.1186/s12862-018-1244-8

Esposito L.A. & Prendini L. 2019. Island ancestors and new world biogeography: a case study from the scorpions (Buthidae: Centruroidinae). *Scientific Reports* 9 (1): 3500. https://doi.org/10.1038/s41598-018-33754-8

Fick S.E. & Hijmans R.J. 2017. WorldClim 2: new 1-km spatial resolution climate surfaces for global land areas. *International Journal of Climatology* 37: 4302–4315. https://doi.org/10.1002/joc.5086

Foelix R.F. & Chu-Wang I.-W. 1973. The morphology of spider sensilla. II. Chemoreceptors. *Tissue and Cell* 5: 461–478. https://doi.org/10.1016/S0040-8166(73)80038-2

Forman M., Nguyen P., Hula P. & Král J. 2013. Sex chromosome pairing and extensive NOR polymorphism in *Wadicosa fidelis* (Araneae: Lycosidae). *Cytogenetic and Genome Research* 141: 43–49. https://doi.org/10.1159/000351041

Gertsch W.J. 1971. A report on some Mexican cave spiders. *Association of Mexican Cave Studies, Bulletin* 4: 47–111.

Gertsch W.J. 1977. Report on cavernicole and epigean spiders from the Yucatan Peninsula. *Association of Mexican Cave Studies, Bulletin* 6: 103–131.

Gertsch W.J. 1982. The spider genera *Pholcophora* and *Anopsicus* (Araneae, Pholcidae) in North America, Central America and the West Indies. *Association of Mexican Cave Studies, Bulletin* 8: 95–144 / *Texas Memorial Museum, Bulletin* 28: 95–144.

Guindon S., Dufayard J.-F., Lefort V., Anisimova M., Hordijk W. & Gascuel O. 2010. New algorithms and methods to estimate maximum-likelihood phylogenies: assessing the performance of PhyML 3.0. *Systematic Biology* 59: 307–321. https://doi.org/10.1093/sysbio/syq010

Hazzi N.A. & Hormiga G. 2021. Morphological and molecular evidence support the taxonomic separation of the medically important Neotropical spiders *Phoneutria depilata* (Strand, 1909) and *P. boliviensis* (F.O. Pickard-Cambridge, 1897) (Araneae, Ctenidae). *ZooKeys* 1022: 13–50. https://doi.org/10.3897/zookeys.1022.60571

Herrando-Moraira S., Nualart N., Herrando-Moraira A., Chung M.Y., Chung M.G. & López-Pujol J. 2019. Climatic niche characteristics of native and invasive *Lilium lancifolium*. *Scientific Reports* 9 (1): 14334. https://doi.org/10.1038/s41598-019-50762-4

Hijmans R.J. 2022. raster: geographic data analysis and modeling. R package version 3.6-3. Available from https://CRAN.R-project.org/package=raster [accessed 26 May 2023].

Hof A.R., Jansson R. & Nilsson C. 2012. The usefulness of elevation as a predictor variable in species distribution modelling. *Ecological Modelling* 246: 86–90. https://doi.org/10.1016/j.ecolmodel.2012.07.028

Hortal J., de Bello F., Diniz-Filho J.A.F., Lewinsohn T.M., Lobo J.M. & Ladle R.J. 2015. Seven shortfalls that beset large-scale knowledge of biodiversity. *Annual Review of Ecology, Evolution, and Systematics* 46: 523–549. https://doi.org/10.1146/annurev-ecolsys-112414-054400

Huber B.A. 2000. New World pholcid spiders (Araneae: Pholcidae): a revision at generic level. *Bulletin of the American Museum of Natural History* 254: 1–348. https://doi.org/brh26h

Huber B.A. 2021. Beyond size: sexual dimorphisms in pholcid spiders. *Arachnology* 18: 656–677. https://doi.org/10.13156/arac.2020.18.7.656

Huber B.A. & Brescovit A.D. 2003. *Ibotyporanga* Mello-Leitão: tropical spiders in Brazilian semi-arid habitats (Araneae: Pholcidae). *Insect Systematics and Evolution* 34: 15–20. https://doi.org/10.1163/187631203788964926

Huber B.A. & Carvalho L.S. 2019. Filling the gaps: descriptions of unnamed species included in the latest molecular phylogeny of Pholcidae (Araneae). *Zootaxa* 4546: 1–96. https://doi.org/10.11646/zootaxa.4546.1.1

Huber B.A. & Eberle J. 2021. Mining a photo library: eggs and egg sacs in a major spider family. *Invertebrate Biology* 140: e12349. https://doi.org/10.1111/ivb.12349

Huber B.A. & Villarreal O. 2020. On Venezuelan pholcid spiders (Araneae, Pholcidae). *European Journal of Taxonomy* 718: 1–317. https://doi.org/10.5852/ejt.2020.718.1101

Huber B.A., Eberle J. & Dimitrov D. 2018. The phylogeny of pholcid spiders: a critical evaluation of relationships suggested by molecular data (Araneae, Pholcidae). *ZooKeys* 789: 51–101. https://doi.org/10.3897/zookeys.789.22781

Huber B.A., Meng G., Král J., Ávila Herrera I.M., Izquierdo M.A. & Carvalho L.S. 2023. High and dry: integrative taxonomy of the Andean spider genus *Nerudia* (Araneae: Pholcidae). *Zoological Journal of the Linnean Society* 198 (2): 534–591. https://doi.org/10.1093/zoolinnean/zlac100

Kalyaanamoorthy S., Minh B.Q., Wong T.K.F., von Haeseler A. & Jermiin L.S. 2017. ModelFinder: fast model selection for accurate phylogenetic estimates. *Nature Methods* 14: 587–589. https://doi.org/10.1038/nmeth.4285

Katoh K. & Standley D.M. 2013. MAFFT multiple sequence alignment software version 7: improvements in performance and usability. *Molecular Biology and Evolution* 30: 772–780. https://doi.org/10.1093/molbev/mst010

Kořínková T. & Král J. 2013. Karyotypes, sex chromosomes, and meiotic division in spiders. *In*: Nentwig W. (ed.) *Spider Ecophysiology*: 159–172. Springer, Berlin.

Král J., Musilová J., Šťáhlavský F., Řezáč M., Akan Z., Edwards R.L., Coyle F.A. & Ribera Almerje C. 2006. Evolution of the karyotype and sex chromosome systems in basal clades of araneomorph spiders (Araneae: Araneomorphae). *Chromosome Research* 14: 859–880. https://doi.org/10.1007/s10577-006-1095-9

Král J., Kořínková T., Krkavcová L., Musilová J., Forman M., Ávila Herrera I.M., Haddad C.R., Vítková M., Henriques S., Palacios Vargas J.G. & Hedin M. 2013. Evolution of karyotype, sex chromosomes, and meiosis in mygalomorph spiders (Araneae: Mygalomorphae). *Biological Journal of the Linnean Society* 109: 377–408. https://doi.org/10.1111/bij.12056

Král J., Ávila Herrera I.M., Šťáhlavský F., Sadílek D., Pavelka J., Chatzaki M. & Huber B.A. 2022. Karyotype differentiation and male meiosis in European clades of the spider genus *Pholcus* (Araneae, Pholcidae). *Comparative Cytogenetics* 16 (4): 185–209. https://doi.org/10.3897/CompCytogen.v16i4.85059

Lee J.G., Lee J.H., Choi D.Y., Park S.J., Kim A.Y. & Kim S.K. 2021. Five new species of the genus *Pholcus* Walckenaer (Araneae, Pholcidae) from South Korea. *Zootaxa* 5052: 61–77. https://doi.org/10.11646/zootaxa.5052.1.3

Letunic I. & Bork P. 2021. Interactive Tree Of Life (iTOL) v5: an online tool for phylogenetic tree display and annotation. *Nucleic Acids Research* 49: W293–W296. https://doi.org/10.1093/nar/gkab301

Levan A.K., Fredga K. & Sandberg A.A. 1964. Nomenclature for centromeric position on chromosomes. *Hereditas* 52: 201–220. https://doi.org/10.1111/j.1601-5223.1964.tb01953.x

Lomazi R.L., Araujo D., Carvalho L.S. & Schneider M.C. 2018. Small pholcids (Araneae: Synspermiata) with big surprises: the lowest diploid number in spiders with monocentric chromosomes. *Journal of Arachnology* 46: 45–49. https://doi.org/10.1636/JoA-S-17-033R2.1

McHugh A., Yablonsky C., Binford G. & Agnarsson I. 2014. Molecular phylogenetics of Caribbean *Micrathena* (Araneae: Araneidae) suggests multiple colonization events and single island endemism. *Invertebrate Systematics* 28: 337–349. https://doi.org/10.1071/IS13051

Mello-Leitão C. de. 1944. Aranhas da região Amazônica. *Boletim do Museu Nacional, Rio de Janeiro (Nova Série, Zoologia)* 25: 1–12.

Minh B.Q., Nguyen M.A.T. & von Haeseler A. 2013. Ultrafast approximation for phylogenetic bootstrap. *Molecular Biology and Evolution* 30: 1188–1195. https://doi.org/10.1093/molbev/mst024

Minh B.Q., Schmidt H.A., Chernomor O., Schrempf D., Woodhams M.D., von Haeseler A. & Lanfear R. 2020. IQ-TREE 2: New models and efficient methods for phylogenetic inference in the genomic era. *Molecular Biology and Evolution* 37: 1530–1534. https://doi.org/10.1093/molbev/msaa015

Morrone J.J., Escalante T. & Rodríguez-Tapia G. 2017. Mexican biogeographic provinces: map and shapefiles. *Zootaxa* 4277: 277–279. https://doi.org/10.11646/zootaxa.4277.2.8

Parida B.B. & Sharma N.N. 1987. Chromosome number, sex mechanism and genome size in 27 species of Indian spiders. *Chromosome Information Service* 43: 11–13.

Paula-Neto E., Cella D.M., Araujo D., Brescovit A.D. & Schneider M.C. 2017. Comparative cytogenetic analysis among filistatid spiders (Araneomorphae: Haplogynae). *Journal of Arachnology* 45: 123–128. https://doi.org/10.1636/M14-69.1

Ratnasingham S. & Hebert P.D.N. 2007. bold: The Barcode of Life Data System (http://www.barcodinglife.org). *Molecular Ecology Notes* 7: 355–364. https://doi.org/10.1111/j.1471-8286.2007.01678.x

Reis R. Jr, Oliveira M.L. & Borges G.R.A. 2015. RT4Bio: R Tools for Biologists. Available from https://sourceforge.net/projects/rt4bio/ [accessed 1 Jun. 2022].

Revell L. 2021. A variable-rate quantitative trait evolution model using penalized-likelihood Brownian motion. *PeerJ* 9:e11997. https://doi.org/10.7717/peerj.11997

Rieseberg L.H. 2001. Chromosomal rearrangements and speciation. *Trends in Ecology and Evolution* 7: 351–358. https://doi.org/10.1016/S0169-5347(01)02187-5

Schoener T.W. 1970. Nonsynchronous spatial overlap of lizards in patchy habitats. *Ecology* 51: 408–418. https://doi.org/10.2307/1935376

Segura-Hernández L., Barrantes G., Chacón-Madrigal E. & García-Rodríguez A. 2022. Species distribution models and climatic niche comparisons provide clues on the geographic origin of a spider invasion in the Americas. *Biological Invasions* 25: 251–265. https://doi.org/10.1007/s10530-022-02904-5

Silva D.P., Vilela B., Buzatto B.A., Moczek A.P. & Hortal J. 2016. Contextualized niche shifts upon independent invasions by the dung beetle *Onthophagus taurus*. *Biological Invasions* 18: 3137–3148. https://doi.org/10.1007/s10530-016-1204-4

Simard M., Pinto N., Fisher J.B. & Baccini A. 2011. Mapping forest canopy height globally with spaceborne lidar. *Journal of Geophysical Research* 116: G04021. https://doi.org/10.1029/2011JG001708

Simon E. 1890. Étude sur les arachnides de l'Yemen. *Annales de la Société entomologique de France* 6: 77–124.

Simon E. 1893. *Histoire Naturelle des Araignées*. 2nd Ed. Encyclopédie Roret, Paris. https://doi.org/10.5962/bhl.title.51973

Srivathsan A., Lee L., Katoh K., Hartop E., Kutty S.N., Wong J., Yeo D. & Meier R. 2021. ONTbarcoder and MinION barcodes aid biodiversity discovery and identification by everyone, for everyone. *BMC Biology* 19: 217. https://doi.org/10.1186/s12915-021-01141-x

Steenwyk J.L., Buida III T.J., Li Y., Shen X.-X. & Rokas A. 2020. ClipKIT: A multiple sequence alignment trimming software for accurate phylogenomic inference. *PLoS Biology* 18: e3001007. https://doi.org/10.1371/journal.pbio.3001007

Suyama M., Torrents D. & Bork P. 2006. PAL2NAL: robust conversion of protein sequence alignments into the corresponding codon alignments. *Nucleic Acids Research* 34: W609–W612. https://doi.org/10.1093/nar/gkl315

Suzuki S. 1954. Cytological studies in spiders. III. Studies on the chromosomes of fifty-seven species of spiders belonging to seventeen families, with general considerations on chromosomal evolution. *Journal of Science of Hiroshima University* 2: 23–136.

Tabei Y., Kiryu H., Kin T. & Asai K. 2008. A fast structural multiple alignment method for long RNA sequences. *BMC Bioinformatics* 9: 33. https://doi.org/10.1186/1471-2105-9-33

Talavera G. & Castresana J. 2007. Improvement of phylogenies after removing divergent and ambiguously aligned blocks from protein sequence alignments. *Systematic Biology* 56: 564–577. https://doi.org/10.1080/10635150701472164

Truett G., Heeger P., Mynatt R., Truett A., Walker J. & Warman M.J.B. 2000. Preparation of PCR-quality mouse genomic DNA with hot sodium hydroxide and tris (HotSHOT). *Biotechniques* 29: 52–54. https://doi.org/10.2144/00291bm09

Warren D.L., Glor R.E. & Turelli M. 2008. Environmental niche equivalency versus conservatism: quantitative approaches to niche evolution. *Evolution* 62: 2868–2883. https://doi.org/10.1111/j.1558-5646.2008.00482.x

Wunderlich J. 1988. Die fossilen Spinnen im Dominikanischen Bernstein. *Beiträge zur Araneologie* 2: 1–378.

Yang C., Zheng Y., Tan S., Meng G., Rao W., Yang C., Bourne D.G,. O'Brien P.A., Xu J., Liao S., Chen A., Chen X., Jia X., Zhang A. & Liu S. 2020. Efficient COI barcoding using high throughput single-end 400 bp sequencing. *BMC Genomics* 21: 862. https://doi.org/10.1186/s12864-020-07255-w

Yao Z., Luo Y. & Li S. 2021. *Tangguoa* gen. nov., one new genus of daddy-long-leg spiders (Araneae: Pholcidae) from southern China. *Zootaxa* 4938: 131–140. https://doi.org/10.11646/zootaxa.4938.1.7

Zhu W. & Li S. 2021. Six new species of the spider genus *Belisana* (Araneae: Pholcidae) from Southeast Asia. *Zootaxa* 4963: 115–137. https://doi.org/10.11646/zootaxa.4963.1.5

Manuscript received: 2 November 2022
Manuscript accepted: 21 February 2023
Published on: 17 July 2023
Topic editor: Tony Robillard
Section editor: Rudy Jocqué
Desk editor: Pepe Fernández

Printed versions of all papers are also deposited in the libraries of the institutes that are members of the *EJT* consortium: Muséum national d'histoire naturelle, Paris, France; Meise Botanic Garden, Belgium; Royal Museum for Central Africa, Tervuren, Belgium; Royal Belgian Institute of Natural Sciences, Brussels, Belgium; Natural History Museum of Denmark, Copenhagen, Denmark; Naturalis Biodiversity Center, Leiden, the Netherlands; Museo Nacional de Ciencias Naturales-CSIC, Madrid, Spain; Leibniz Institute for the Analysis of Biodiversity Change, Bonn – Hamburg, Germany; National Museum of the Czech Republic, Prague, Czech Republic.

Supplementary material

Supp. file 1. Supplementary figures. https://doi.org/10.5852/ejt.2023.880.2173.9287

Figs S1–S15. Equivalency among the compared groups.
Figs S16–S30. Niche overlap among the compared groups.
Figs S31–S45. PCA correlation circles for the compared groups.
Figs S46–S75. Similarity among the compared groups.
Fig. S76. Summary tree of all trees using unpartitioned analysis.
Fig. S77. Summary tree of all trees using partitioned analysis.

Supp. file 1. Supplementary figures. https://doi.org/10.5852/ejt.2023.880.2173.9287

Supplementary figures

Figure S1. Equivalency between all Caribbean clade vs *Papiamenta*.
Figure S2. Equivalency between all Caribbean clade vs *Tolteca*.
Figure S3. Equivalency between all Mexican *Pholcophora* vs Caribbean clade.
Figure S4. Equivalency between all Mexican *Pholcophora* vs *Papiamenta*.
Figure S5. Equivalency between all Mexican *Pholcophora* vs *Tolteca*.
Figure S6. Equivalency between all Non-Caribbean *Pholcophora* vs Caribbean clade.
Figure S7. Equivalency between all Non-Caribbean *Pholcophora* vs Mexican *Pholcophora*.
Figure S8. Equivalency between all Non-Caribbean *Pholcophora* vs *Papiamenta*.
Figure S9. Equivalency between all Non-Caribbean *Pholcophora* vs *Tolteca*.
Figure S10. Equivalency between all *P. americana* vs Caribbean clade.
Figure S11. Equivalency between all *P. americana* vs Mexican *Pholcophora*.
Figure S12. Equivalency between all *P. americana* vs Non-Caribbean *Pholcophora*.
Figure S13. Equivalency between all *P. americana* vs *Papiamenta*.
Figure S14. Equivalency between all *P. americana* vs *Tolteca*.
Figure S15. Equivalency between all *Papiamenta* vs *Tolteca*.
Figure S16. Niche Overlap between Caribbean clade vs *Papiamenta*.
Figure S17. Niche Overlap between Caribbean clade vs *Tolteca*.
Figure S18. Niche Overlap between Mexican *Pholcophora* vs Caribbean clade.
Figure S19. Niche Overlap between Mexican *Pholcophora* vs *Papiamenta*.
Figure S20. Niche Overlap between Mexican *Pholcophora* vs *Tolteca*.
Figure S21. Niche Overlap between Non-Caribbean *Pholcophora* vs Caribbean clade.
Figure S22. Niche Overlap between Non-Caribbean *Pholcophora* vs Mexican *Pholcophora*.
Figure S23. Niche Overlap between Non-Caribbean *Pholcophora* vs *Papiamenta*.
Figure S24. Niche Overlap between Non-Caribbean *Pholcophora* vs *Tolteca*.
Figure S25. Niche Overlap between *P. americana* vs Caribbean clade.
Figure S26. Niche Overlap between *P. americana* vs Mexican *Pholcophora*.
Figure S27. Niche Overlap between *P. americana* vs Non-Caribbean *Pholcophora*.
Figure S28. Niche Overlap between *P. americana* vs *Papiamenta*.
Figure S29. Niche Overlap between *P. americana* vs *Tolteca*.
Figure S30. Niche Overlap between *Papiamenta* vs *Tolteca*.
Figure S31. PCA correlation circle for Caribbean clade vs *Papiamenta*.
Figure S32. PCA correlation circle for Caribbean clade vs *Tolteca*.
Figure S33. PCA correlation circle for Mexican *Pholcophora* vs Caribbean clade.
Figure S34. PCA correlation circle for Mexican *Pholcophora* vs *Papiamenta*.
Figure S35. PCA correlation circle for Mexican *Pholcophora* vs *Tolteca*.
Figure S36. PCA correlation circle for Non-Caribbean *Pholcophora* vs Caribbean clade.
Figure S37. PCA correlation circle for Non-Caribbean *Pholcophora* vs Mexican *Pholcophora*.
Figure S38. PCA correlation circle for Non-Caribbean *Pholcophora* vs *Papiamenta*.
Figure S39. PCA correlation circle for Non-Caribbean *Pholcophora* vs *Tolteca*.
Figure S40. PCA correlation circle for *P. americana* vs Caribbean clade.
Figure S41. PCA correlation circle for *P. americana* vs Mexican *Pholcophora*.
Figure S42. PCA correlation circle for *P. americana* vs Non-Caribbean *Pholcophora*.
Figure S43. PCA correlation circle for *P. americana* vs *Papiamenta*.
Figure S44. PCA correlation circle for *P. americana* vs *Tolteca*.
Figure S45. PCA correlation circle for *Papiamenta* vs *Tolteca*.

Figure S46. Similarity between Caribbean clade vs *Papiamenta*.
Figure S47. Similarity between Caribbean clade vs *Tolteca*.
Figure S48. Similarity between Mexican *Pholcophora* vs Caribbean clade.
Figure S49. Similarity between Mexican *Pholcophora* vs *Papiamenta*.
Figure S50. Similarity between Mexican *Pholcophora* vs *Tolteca*.
Figure S51. Similarity between Non-Caribbean *Pholcophora* vs Caribbean clade.
Figure S52. Similarity between Non-Caribbean *Pholcophora* vs Mexican *Pholcophora*.
Figure S53. Similarity between Non-Caribbean *Pholcophora* vs *Papiamenta*.
Figure S54. Similarity between Non-Caribbean *Pholcophora* vs *Tolteca*.
Figure S55. Similarity between *P. americana* vs Caribbean clade.
Figure S56. Similarity between *P. americana* vs Mexican *Pholcophora*.
Figure S57. Similarity between *P. americana* vs Non-Caribbean *Pholcophora*.
Figure S58. Similarity between *P. americana* vs *Papiamenta*.
Figure S59. Similarity between *P. americana* vs *Tolteca*.
Figure S60. Similarity between *Papiamenta* vs *Tolteca*.
Figure S61. Similarity between *Papiamenta* vs Caribbean clade.
Figure S62. Similarity between *Tolteca* vs Caribbean clade.
Figure S63. Similarity between Caribbean clade vs Mexican *Pholcophora*.
Figure S64. Similarity between *Papiamenta* vs Mexican *Pholcophora*.
Figure S65. Similarity between *Tolteca* vs Mexican *Pholcophora*.
Figure S66. Similarity between Caribbean clade vs Non-Caribbean *Pholcophora*.
Figure S67. Similarity between Mexican *Pholcophora* vs Non-Caribbean *Pholcophora*.
Figure S68. Similarity between *Papiamenta* vs Non-Caribbean *Pholcophora*.
Figure S69. Similarity between *Tolteca* vs Non-Caribbean *Pholcophora*.
Figure S70. Similarity between Caribbean clade vs *P. americana*.
Figure S71. Similarity between Mexican *Pholcophora* vs *P. americana*.
Figure S72. Similarity between Non-Caribbean *Pholcophora* vs *P. americana*.
Figure S73. Similarity between *Papiamenta* vs *P. americana*.
Figure S74. Similarity between *Tolteca* vs *P. americana*.
Figure S75. Similarity between *Tolteca* vs *Papiamenta*.
Figure S76. Summary tree of all trees using unpartitioned analysis.
Figure S77. Summary tree of all trees using partitioned analysis.

Figure S1

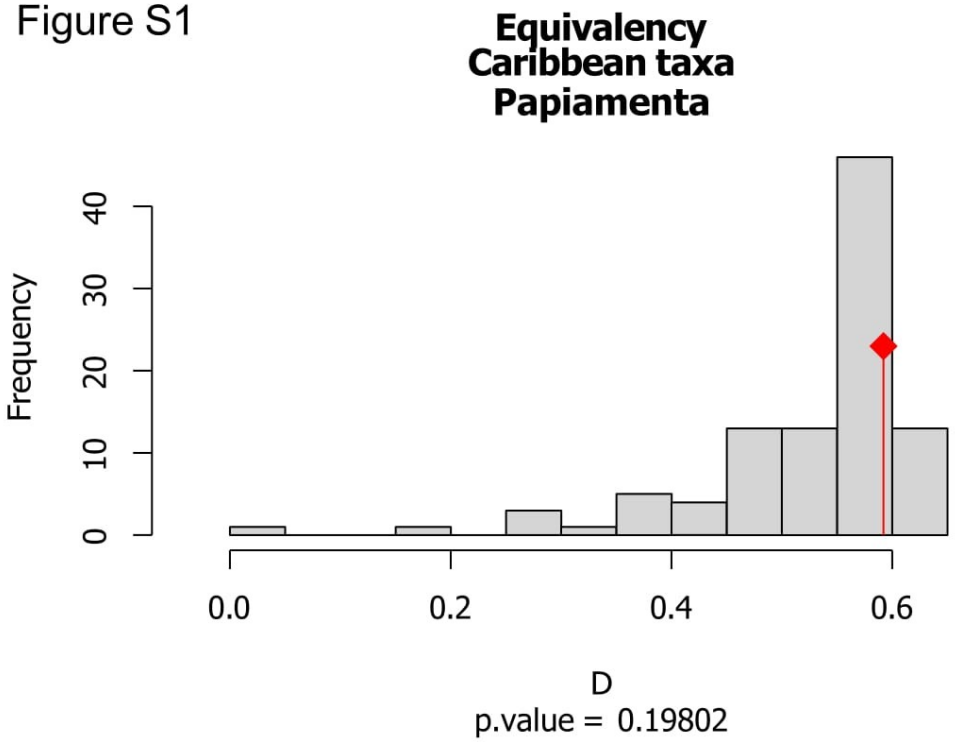

Figure S2

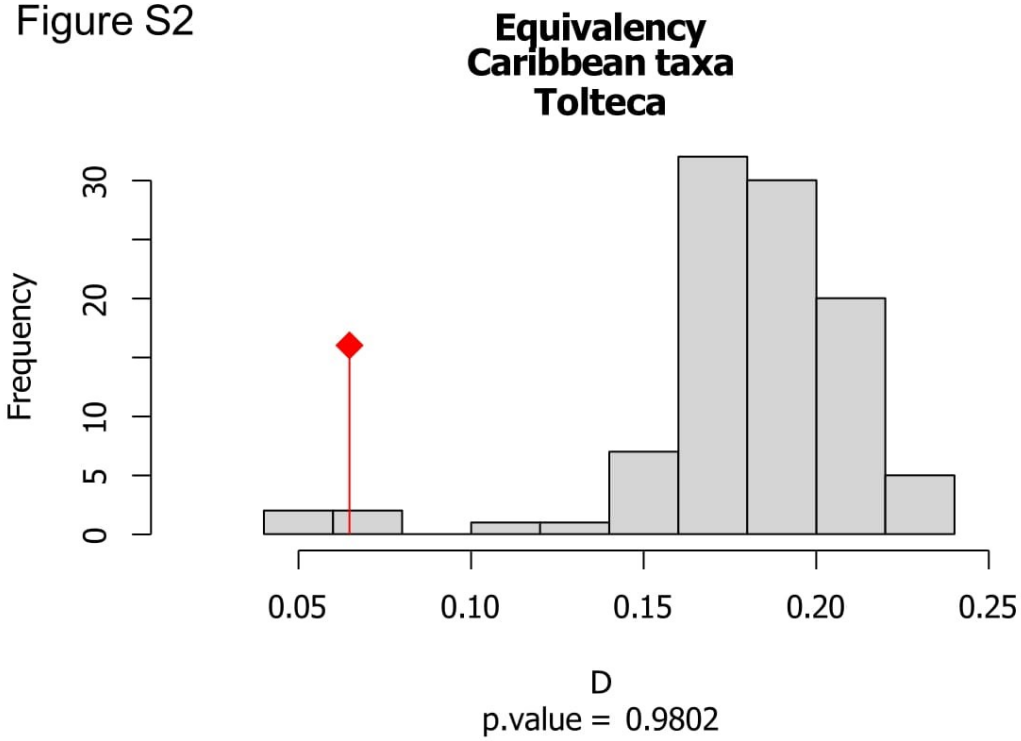

Figure S3

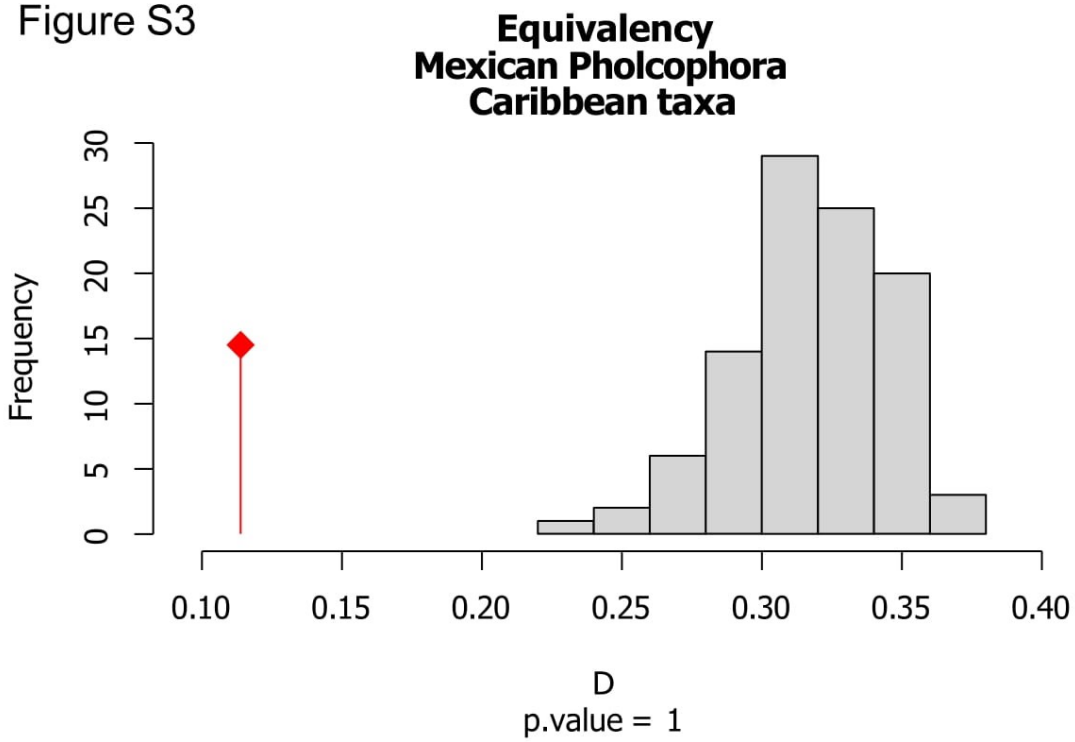

Figure S4

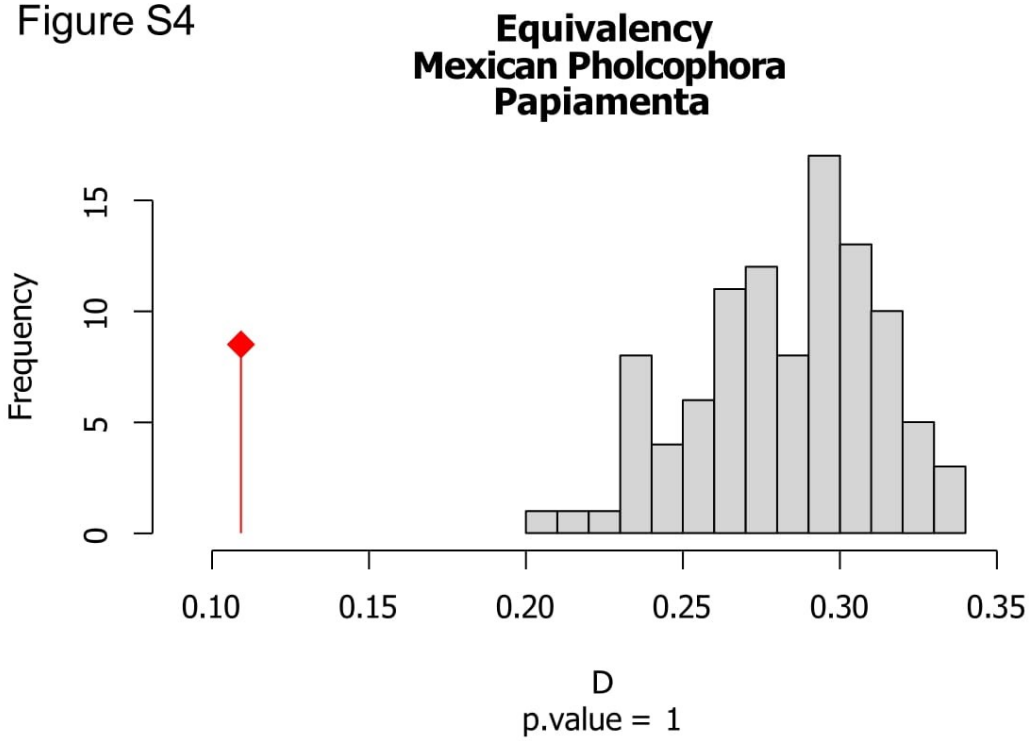

Figure S5

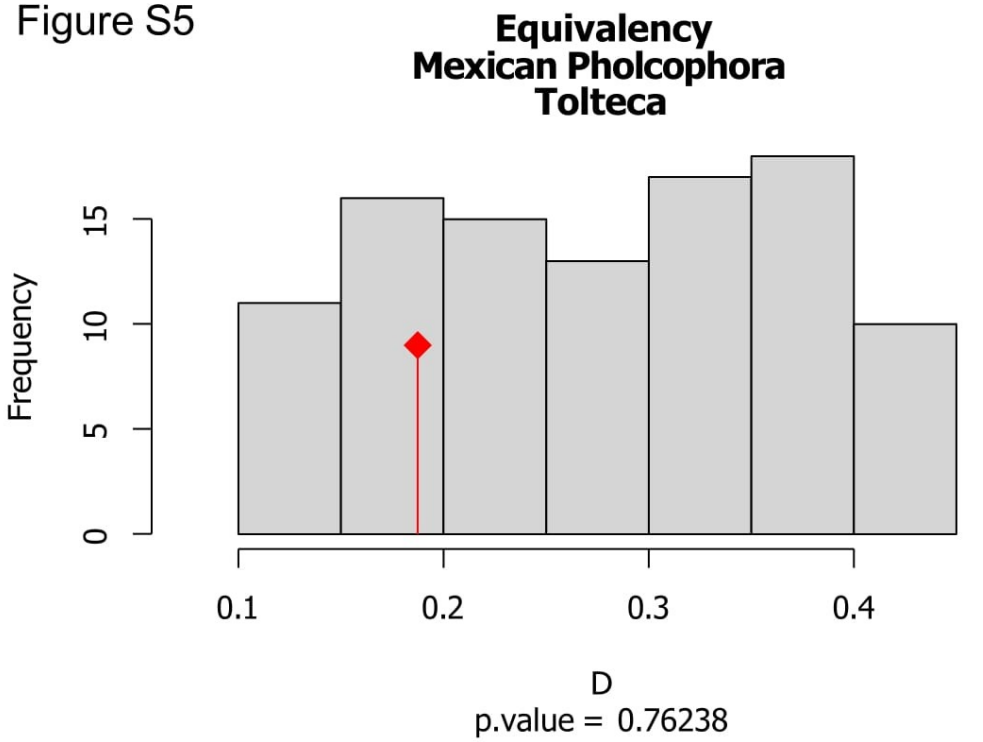

Figure S6

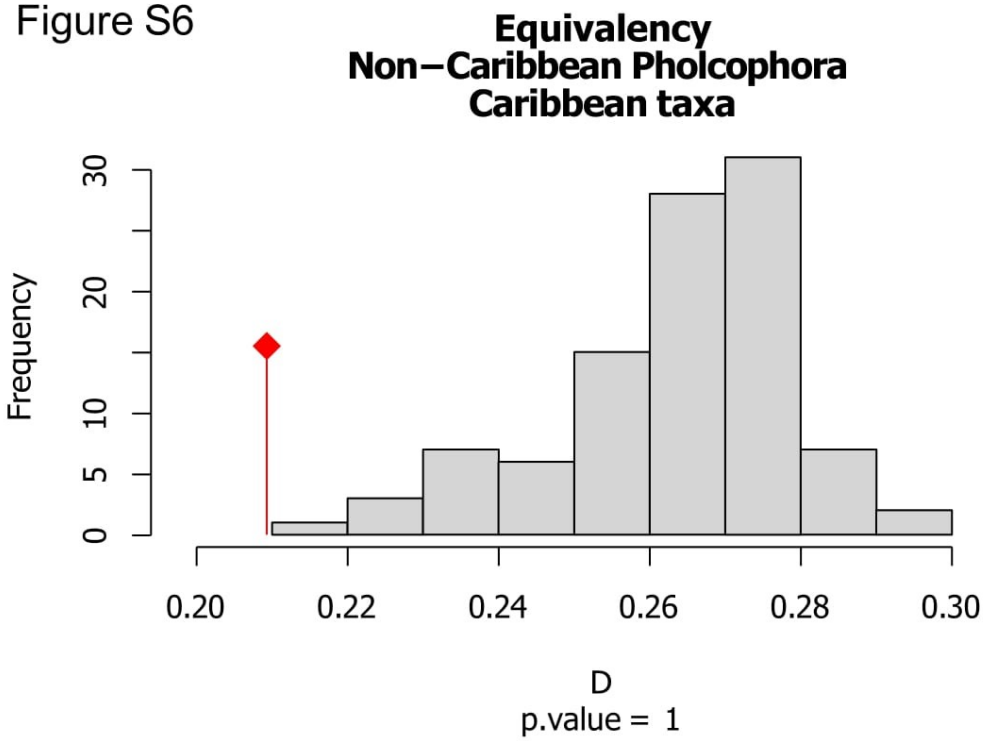

Figure S7

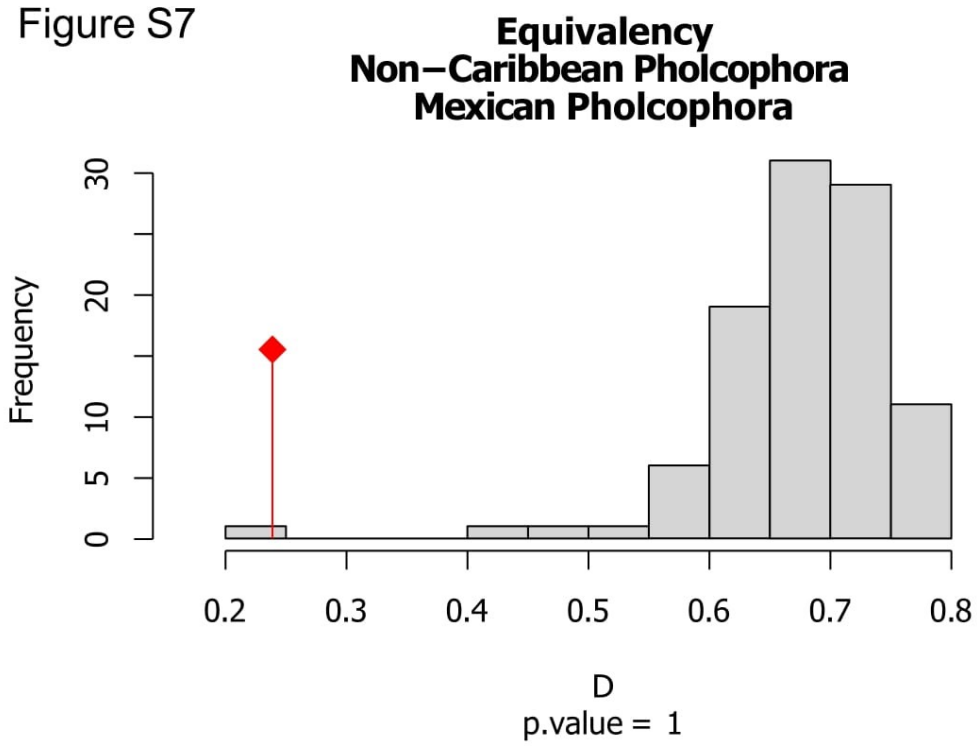

Figure S8

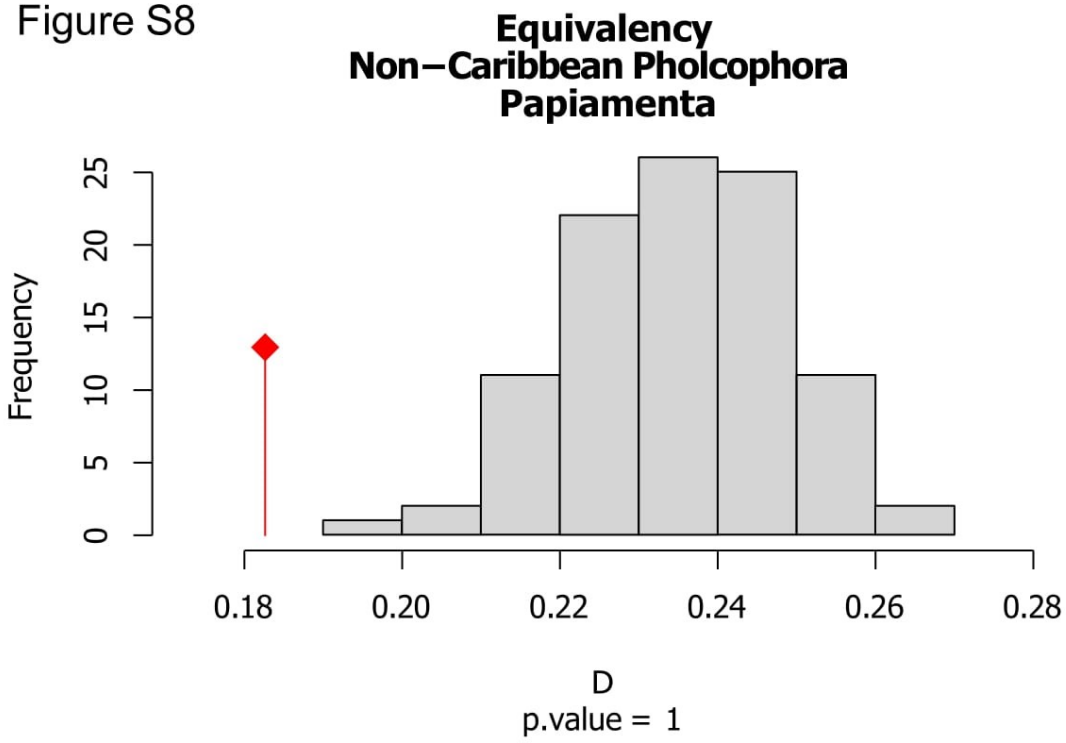

Figure S9

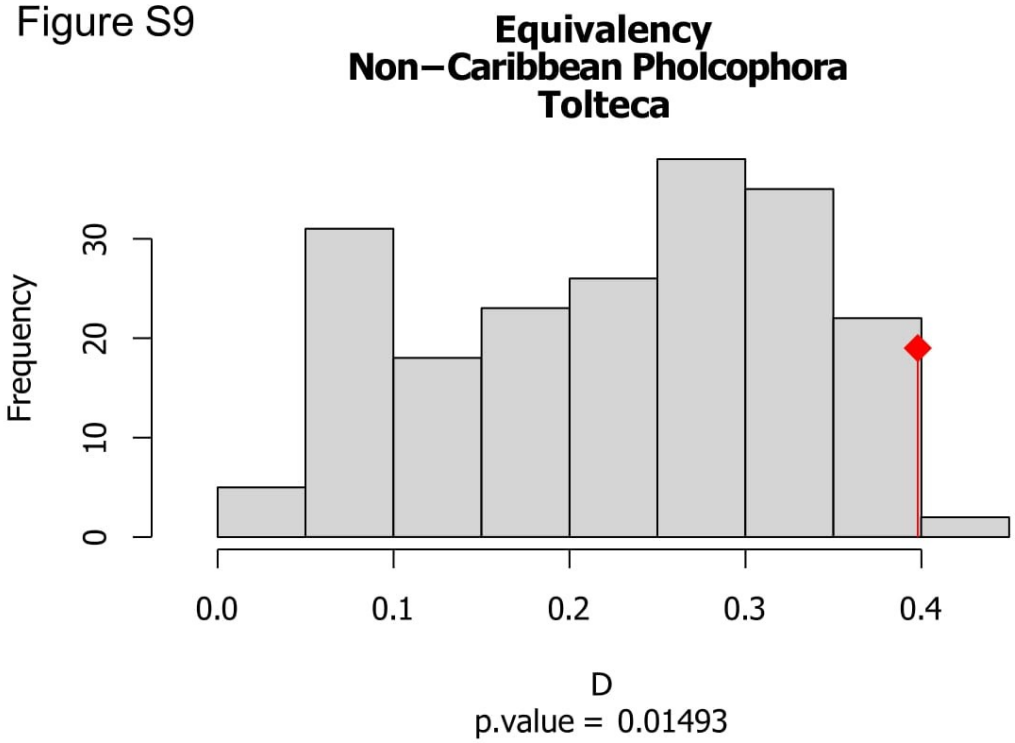

Figure S10

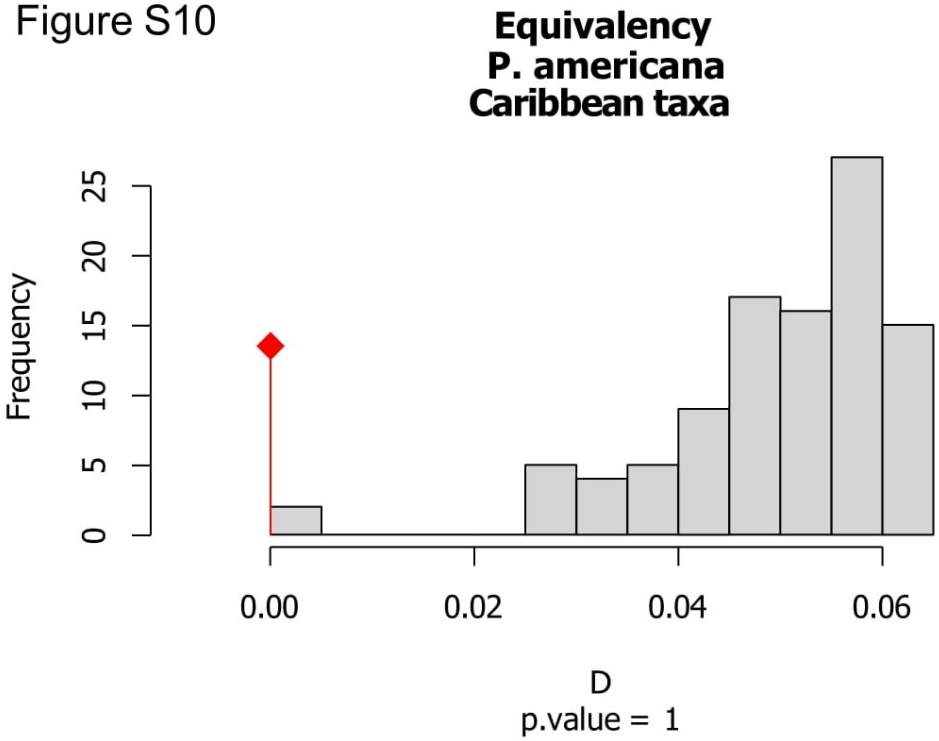

Figure S11

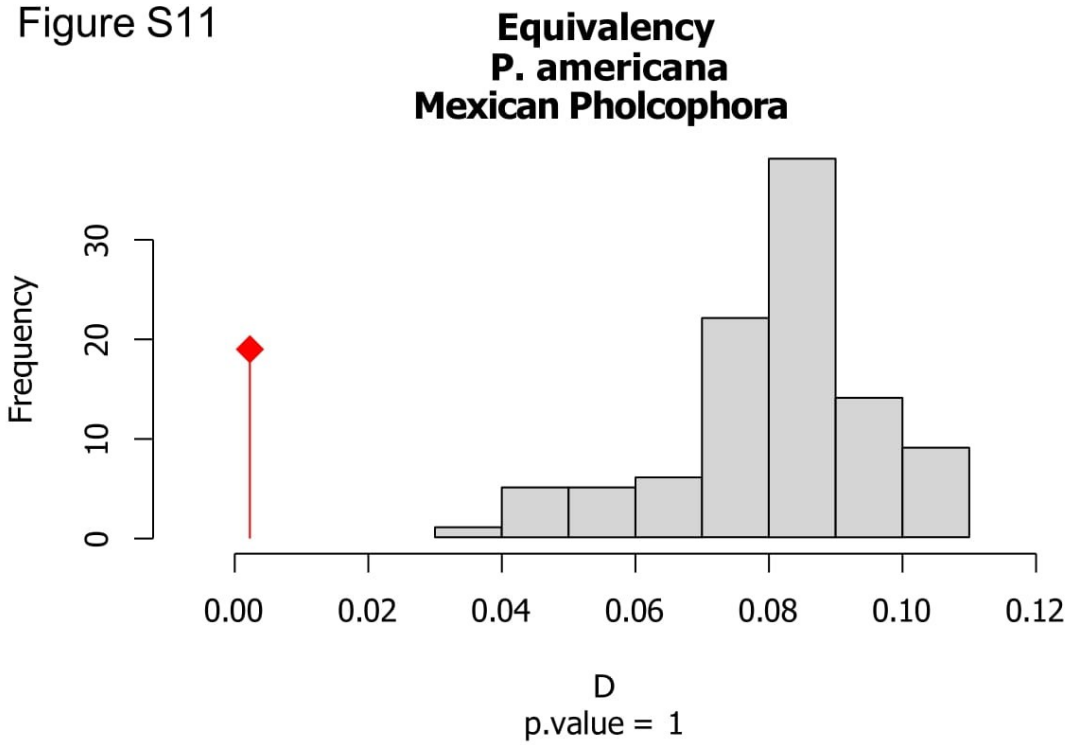

Figure S12

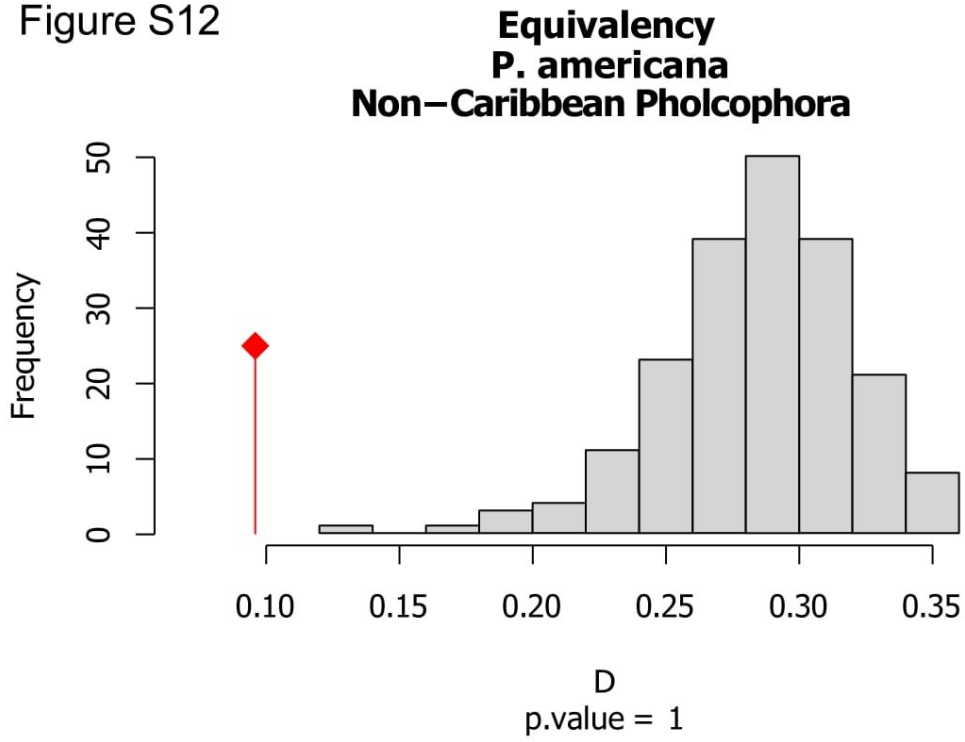

Figure S13

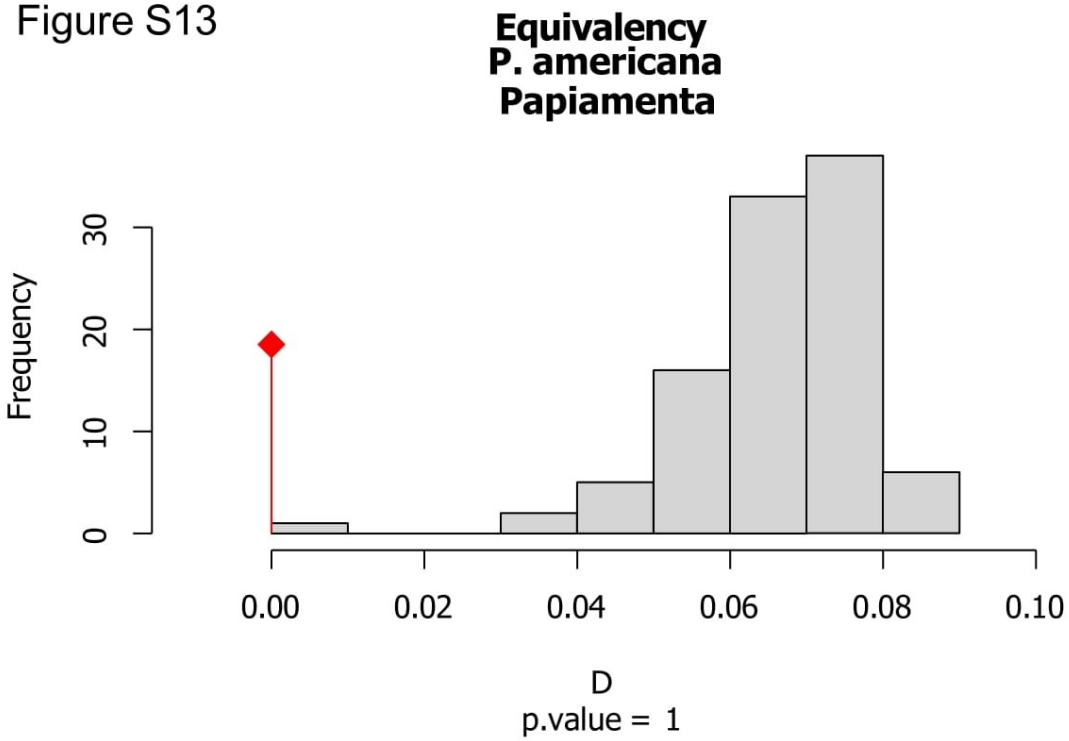

Figure S14

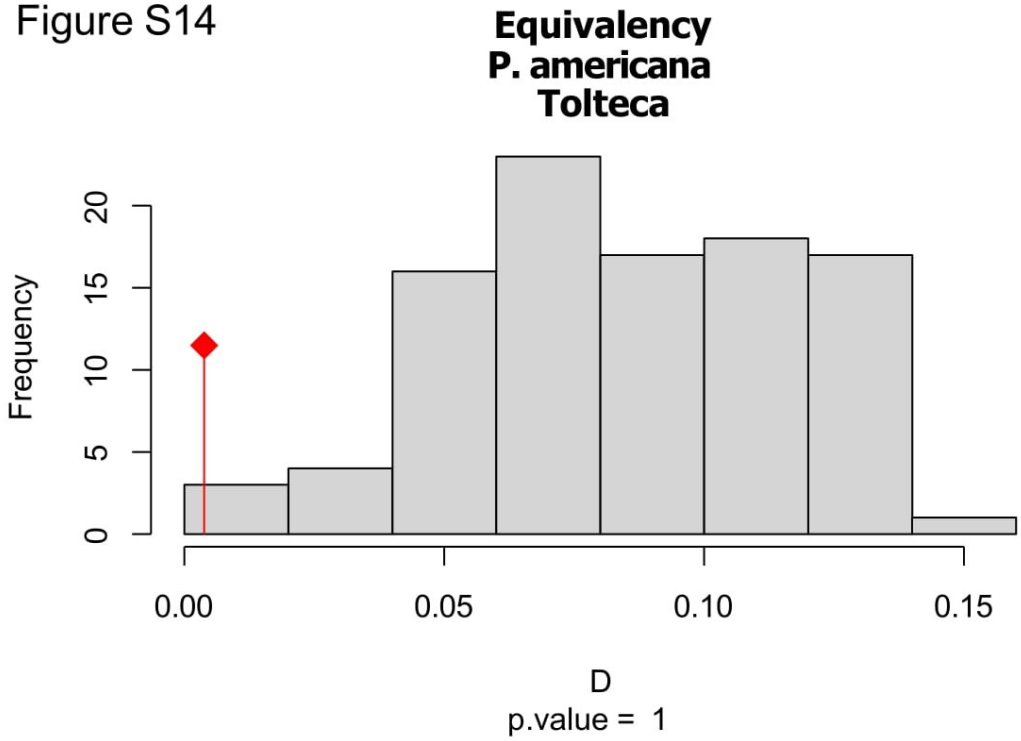

Figure S15

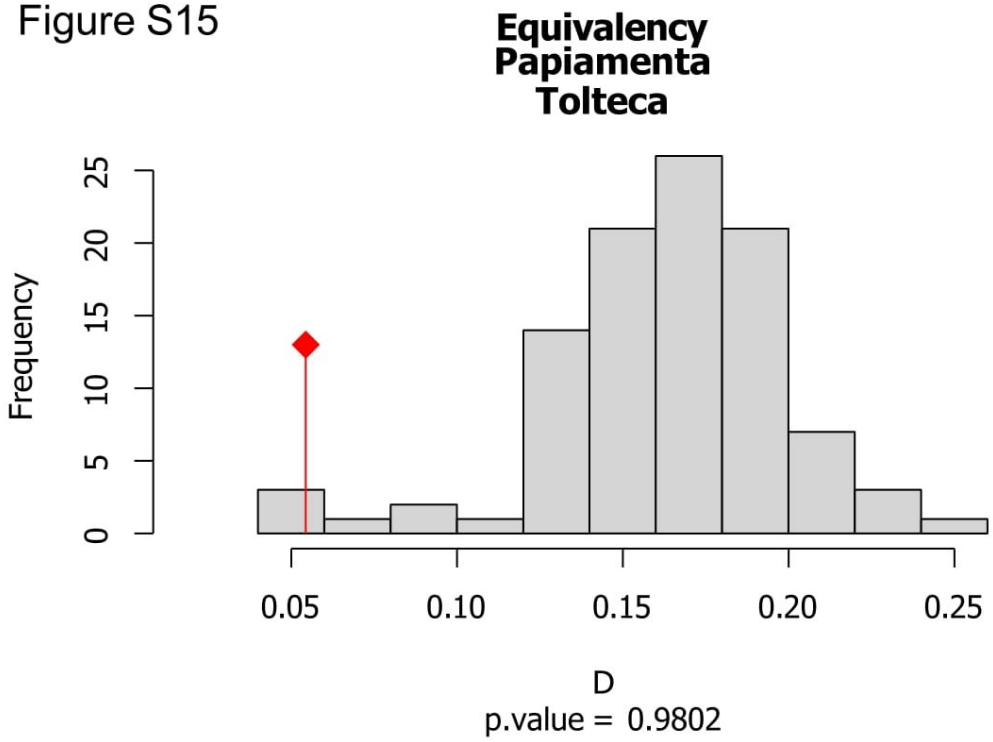

Figure S16

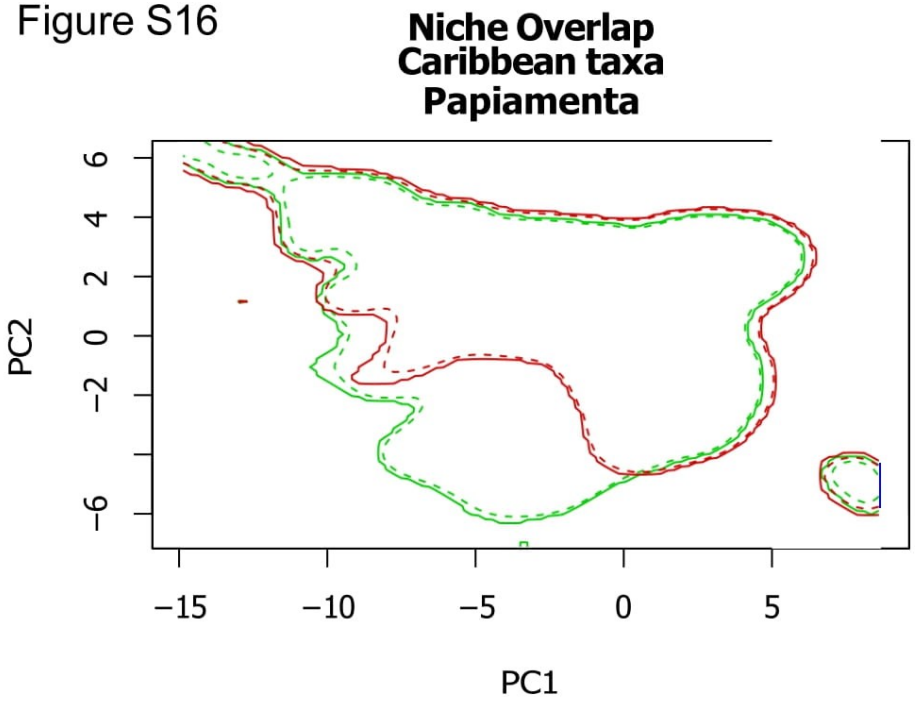

Figure S17

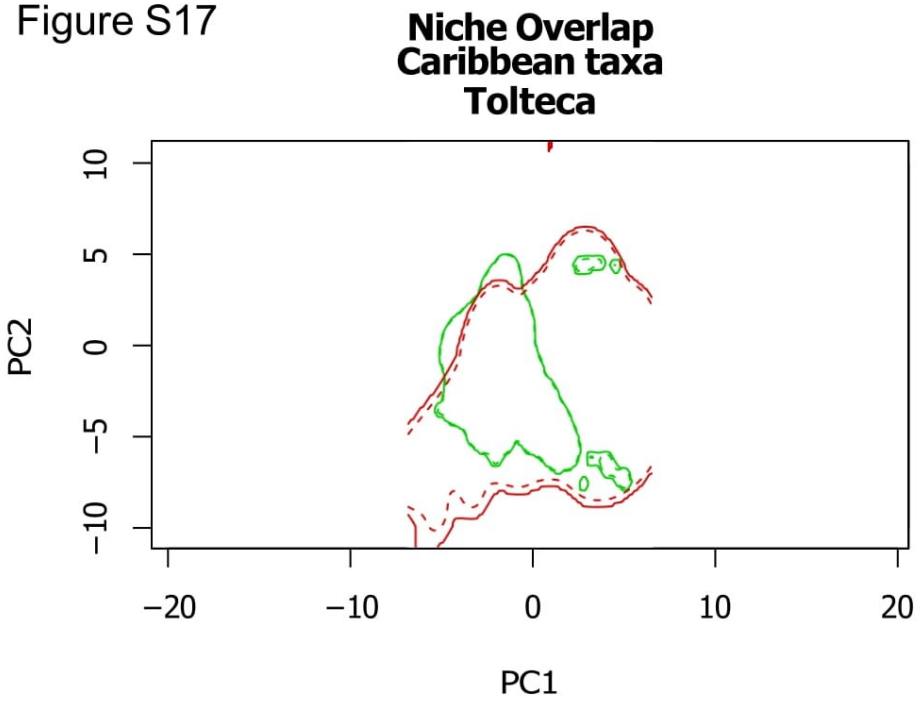

Figure S18

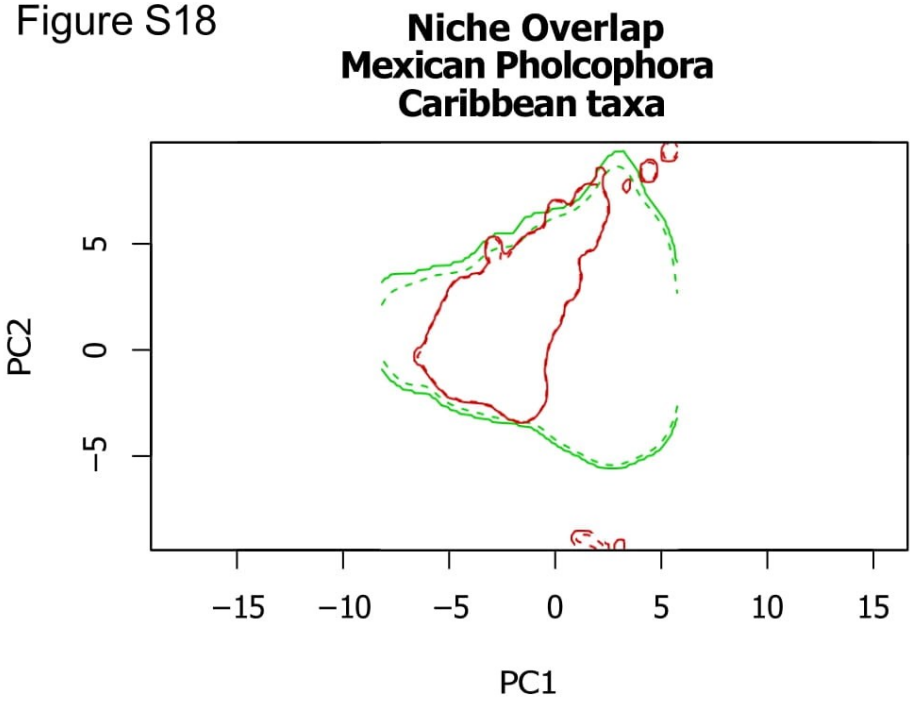

Figure S19

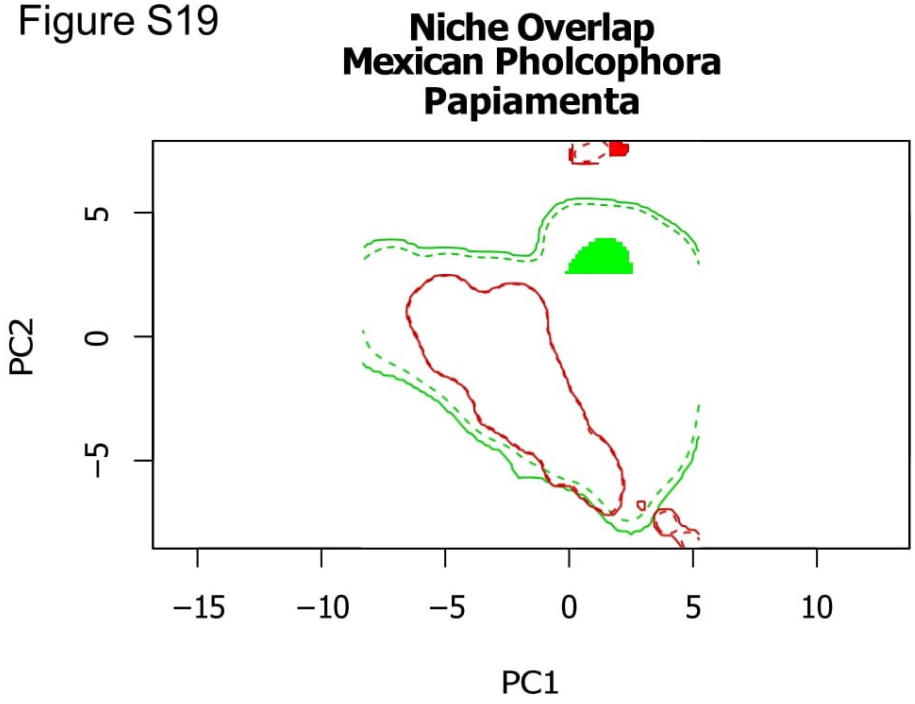

Figure S20

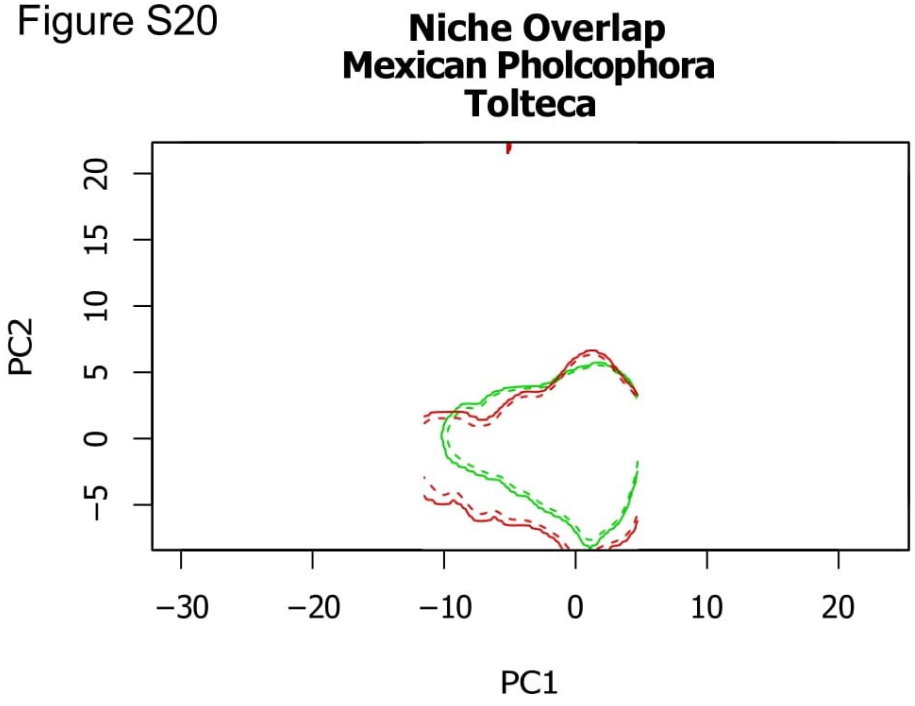

Figure S21

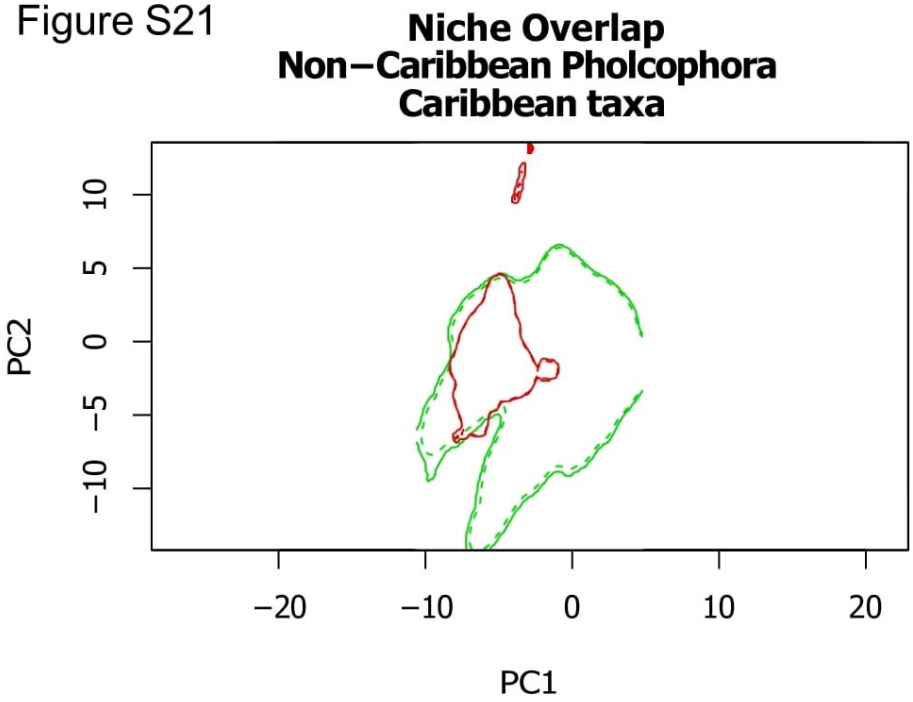

Figure S22

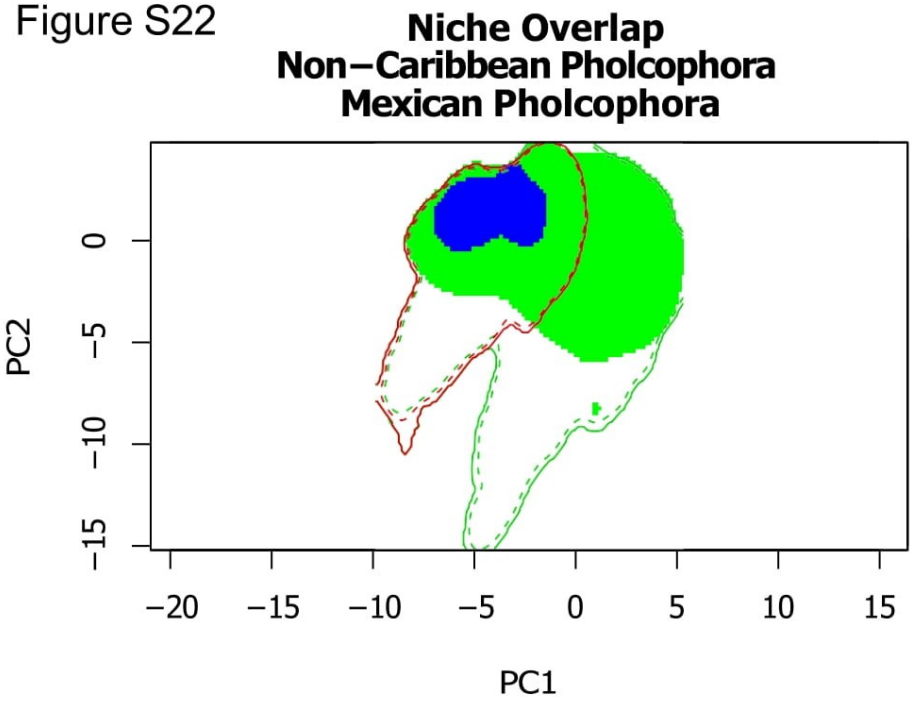

Figure S23

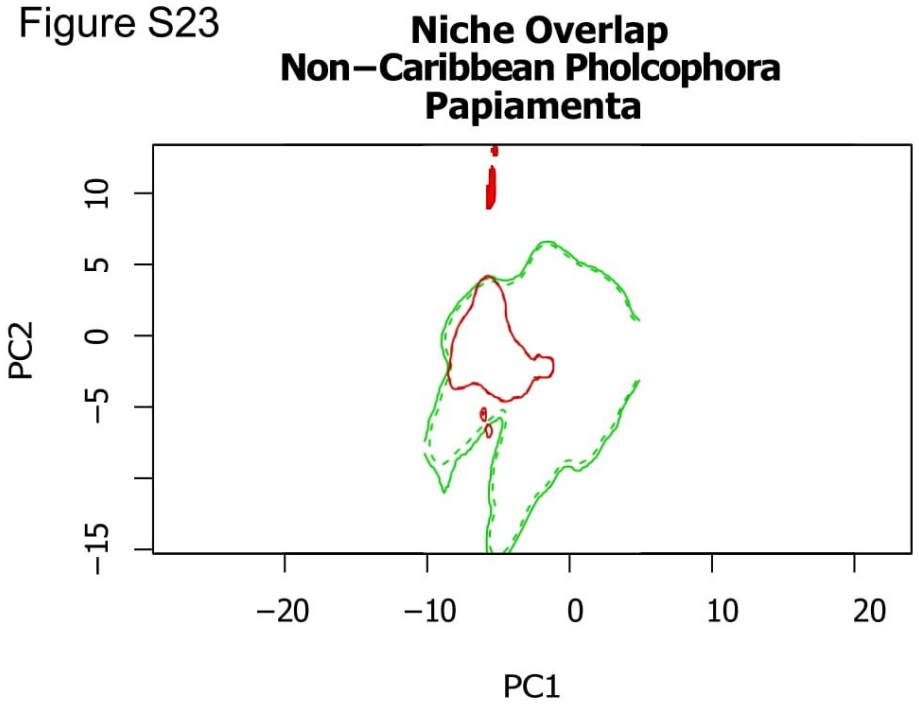

Figure S24

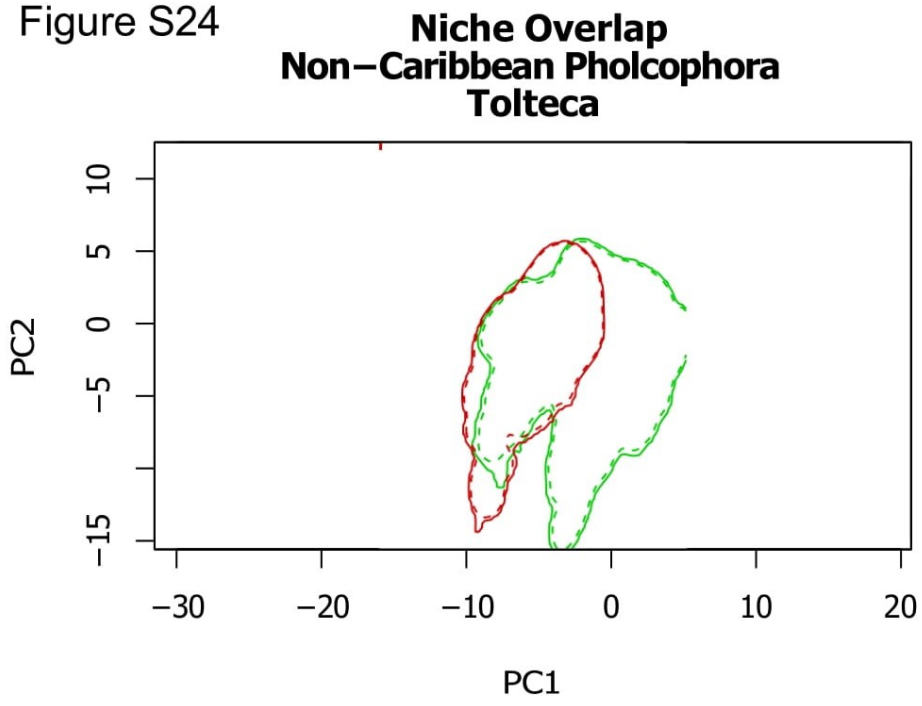

Figure S25

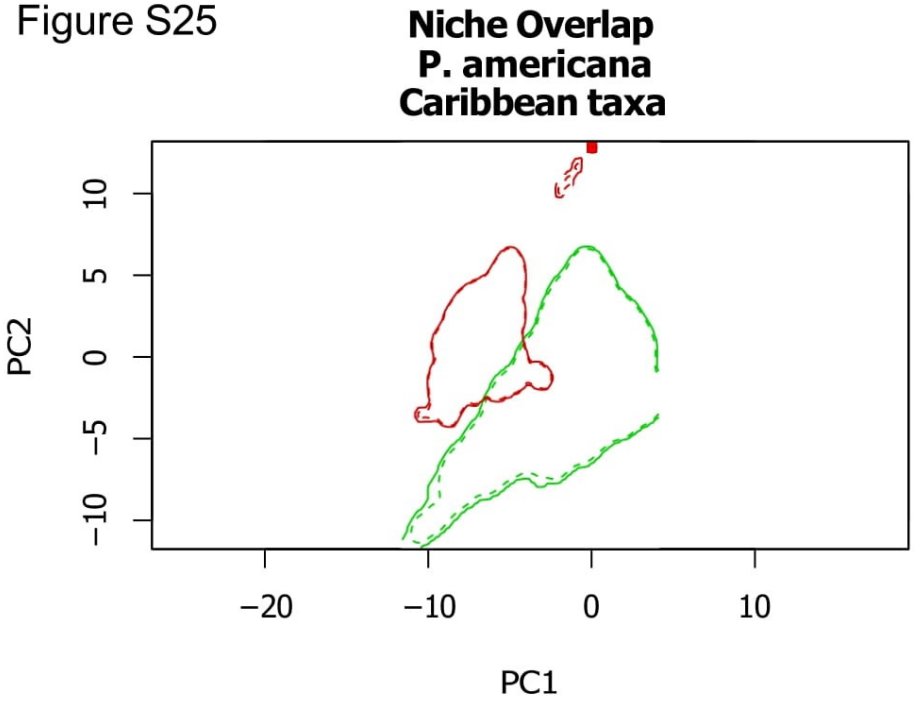

Figure S26

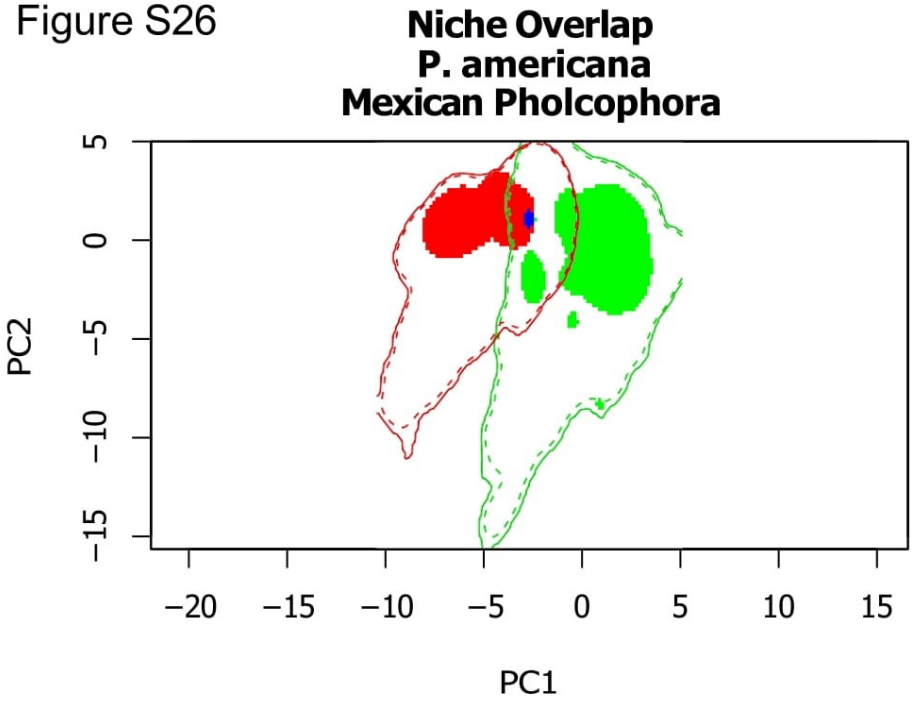

Figure S27

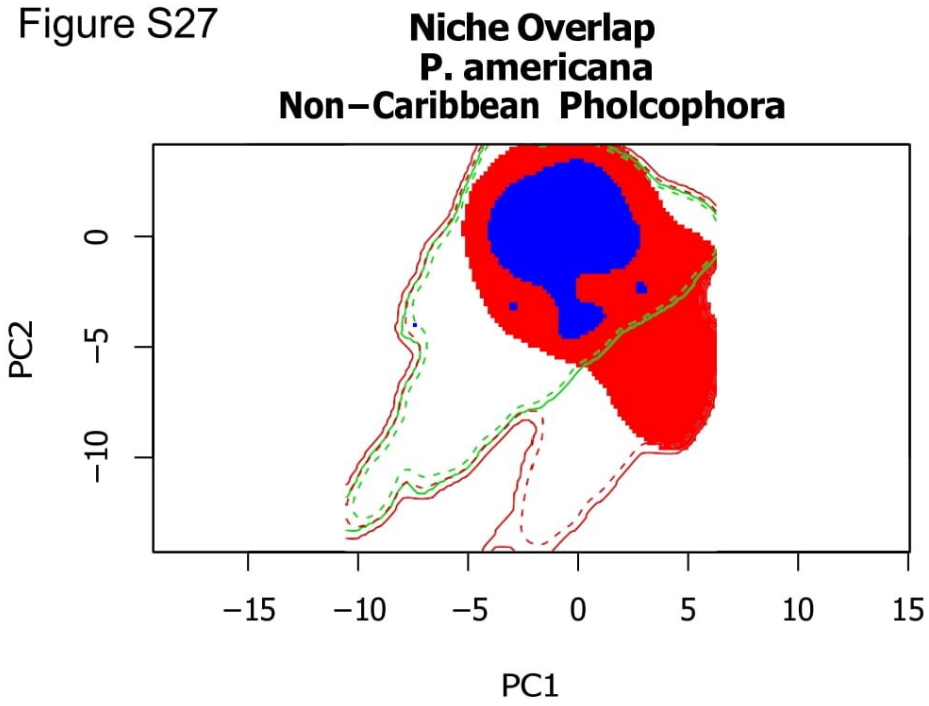

Figure S28

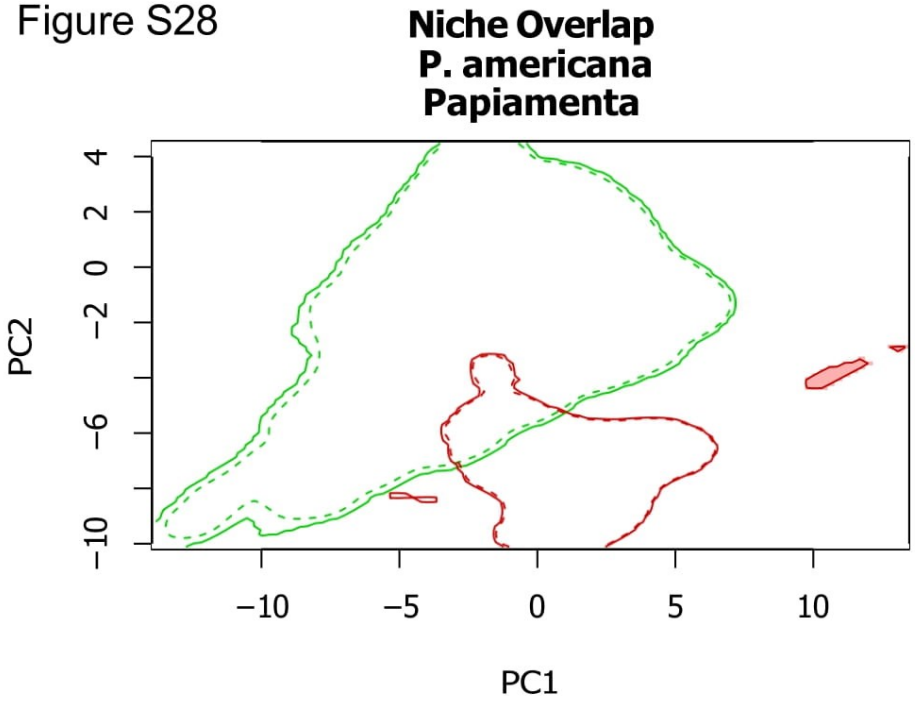

Figure S29

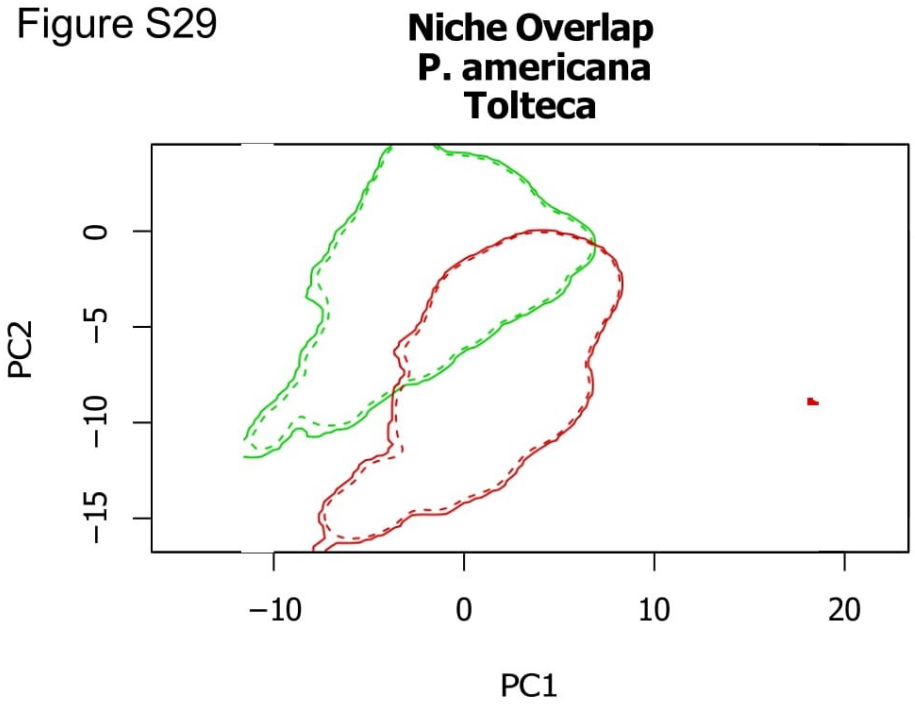

Figure S30

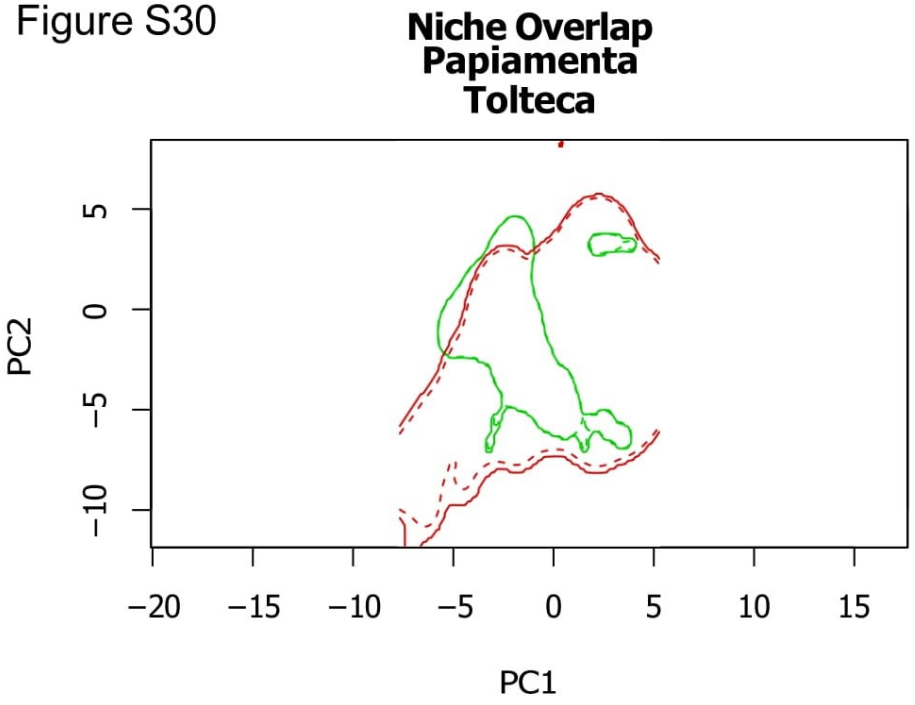

Figure S31

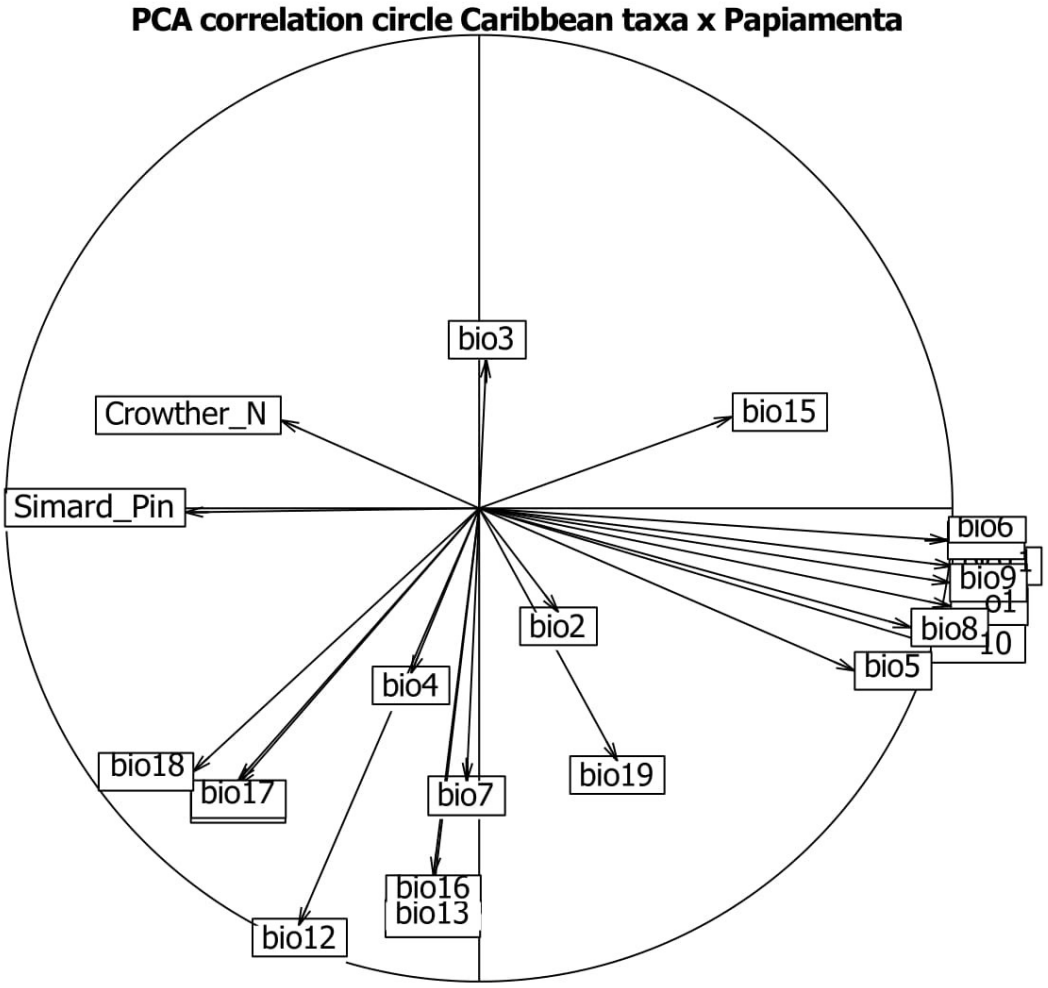
PCA correlation circle Caribbean taxa x Papiamenta
bio3
Crowther_N
bio15
Simard_Pin
bio6
bio9
bio8
bio2
bio5
bio4
bio18
bio17
bio7
bio19
bio16
bio13
bio12
Axis 1 = 35.5 % Axis 2 = 18.47 %

Figure S32

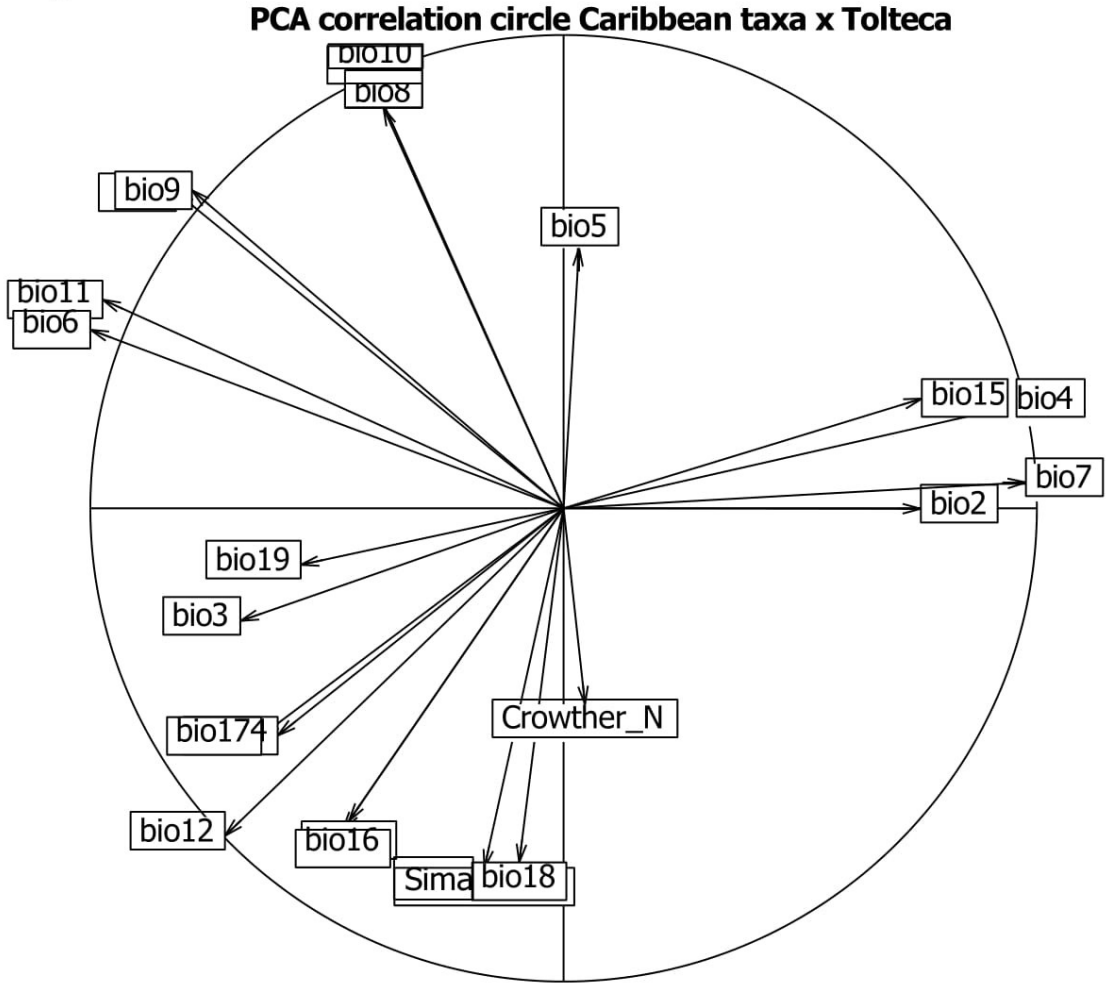
PCA correlation circle Caribbean taxa x Tolteca
bio10
bio8
bio9
bio5
bio11
bio6
bio15
bio4
bio7
bio2
bio19
bio3
bio174
Crowther_N
bio12
bio16
Sima
bio18
Axis 1 = 36.33 % Axis 2 = 25.63 %

Figure S33

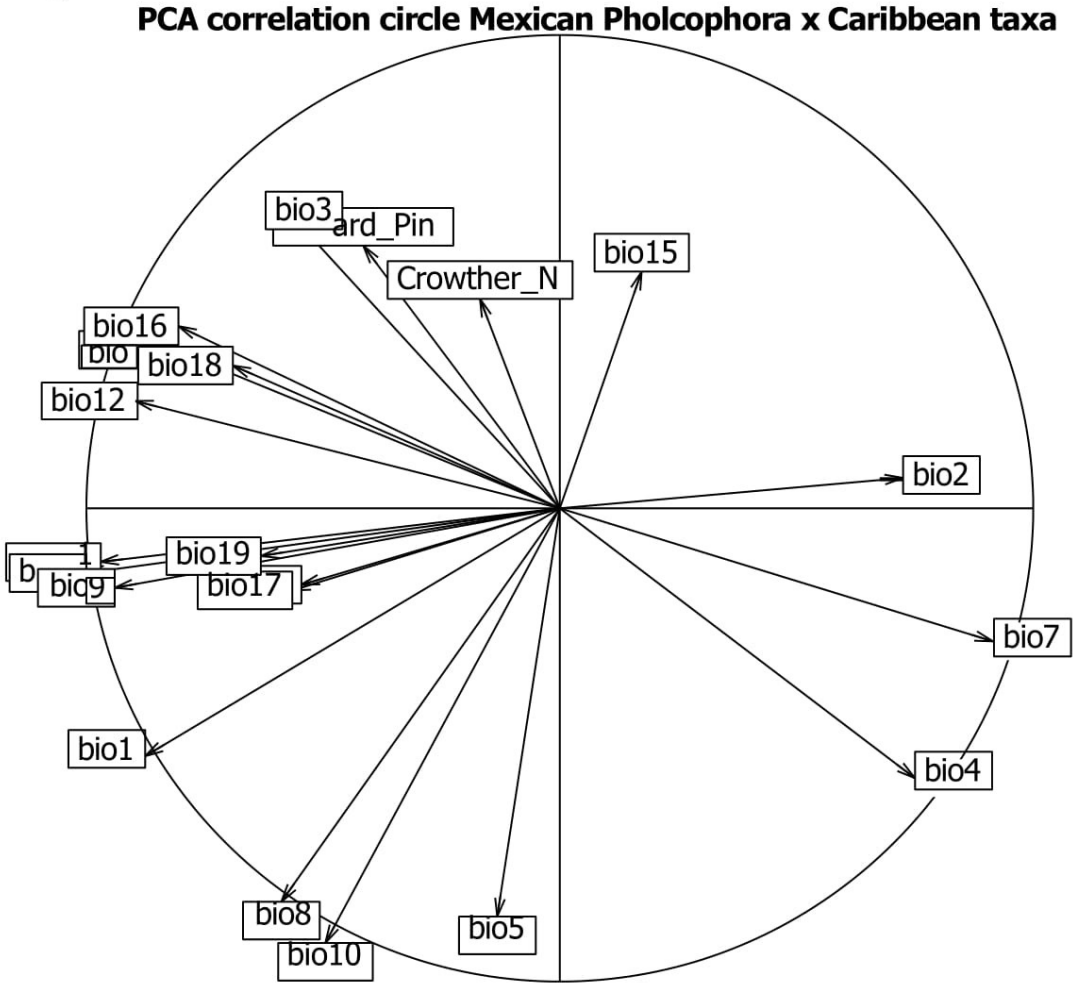
PCA correlation circle Mexican Pholcophora x Caribbean taxa
bio3
ard_Pin
bio15
Crowther_N
bio16
bio18
bio12
bio2
bio19
bio17
bio7
bio1
bio4
bio8
bio10
bio5
Axis 1 = 41.93 % Axis 2 = 18.75 %

Figure S34

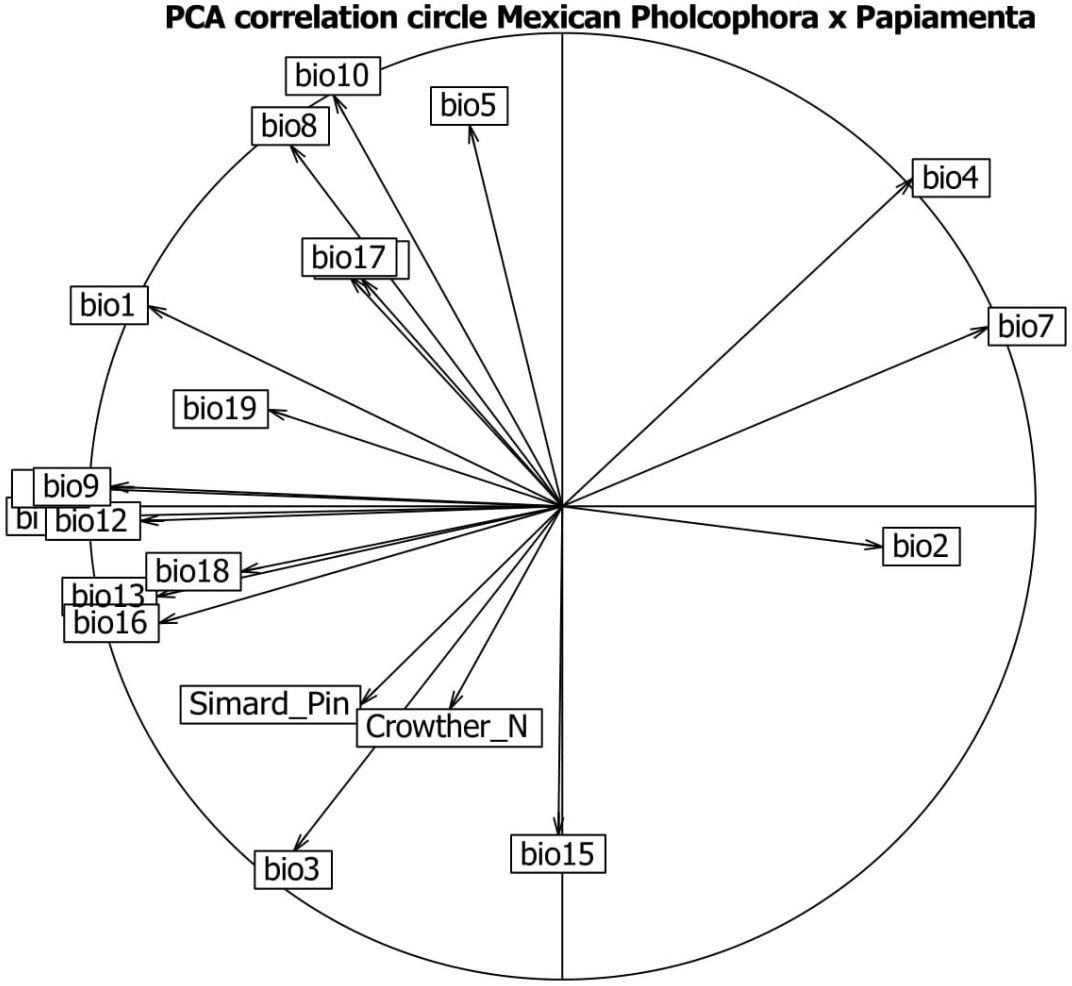
PCA correlation circle Mexican Pholcophora x Papiamenta
bio10
bio5
bio8
bio4
bio17
bio1
bio7
bio19
bio9
bio12
bio2
bio18
bio13
bio16
Simard_Pin
Crowther_N
bio15
bio3
Axis 1 = 41.38 % Axis 2 = 19.68 %

Figure S35

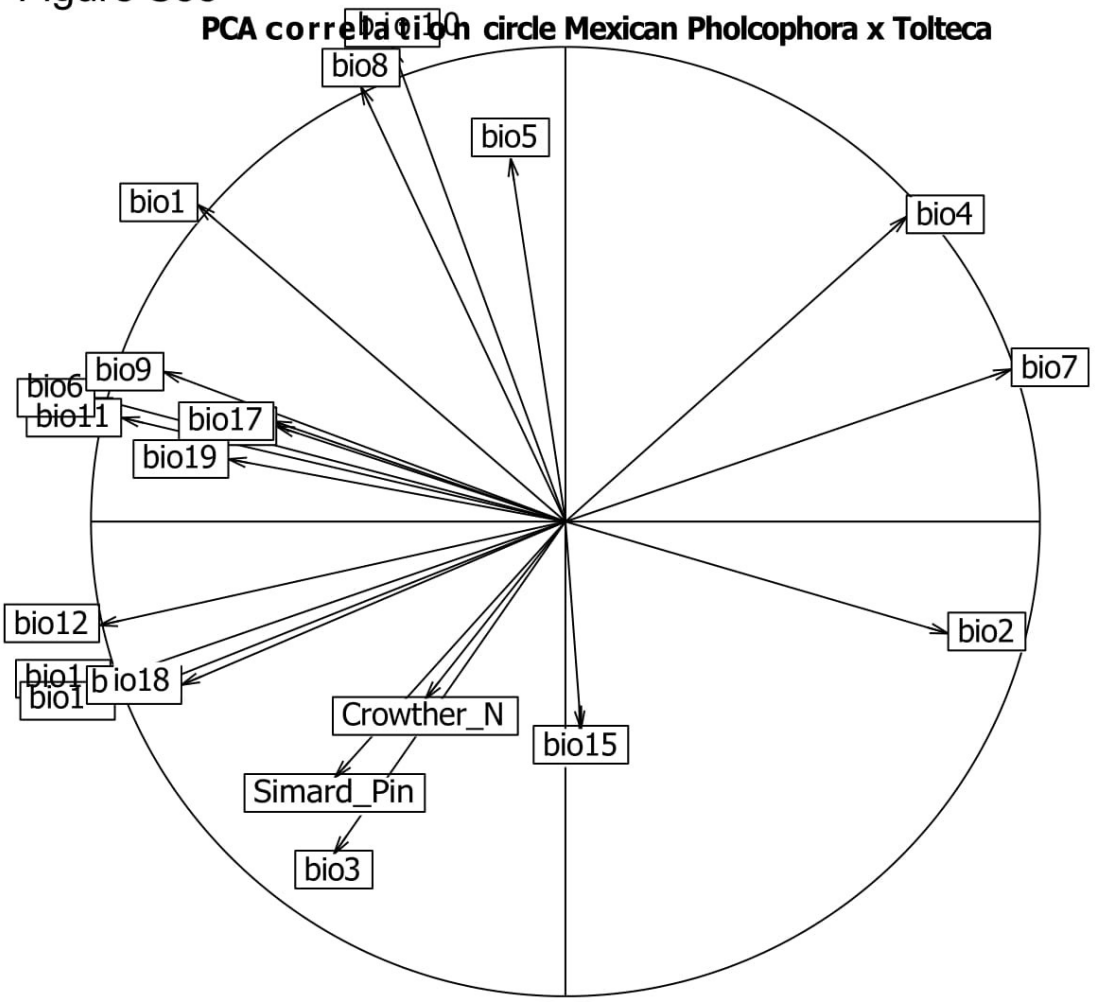

Axis 1 = 41.69 % Axis 2 = 20.4 %

Figure S36

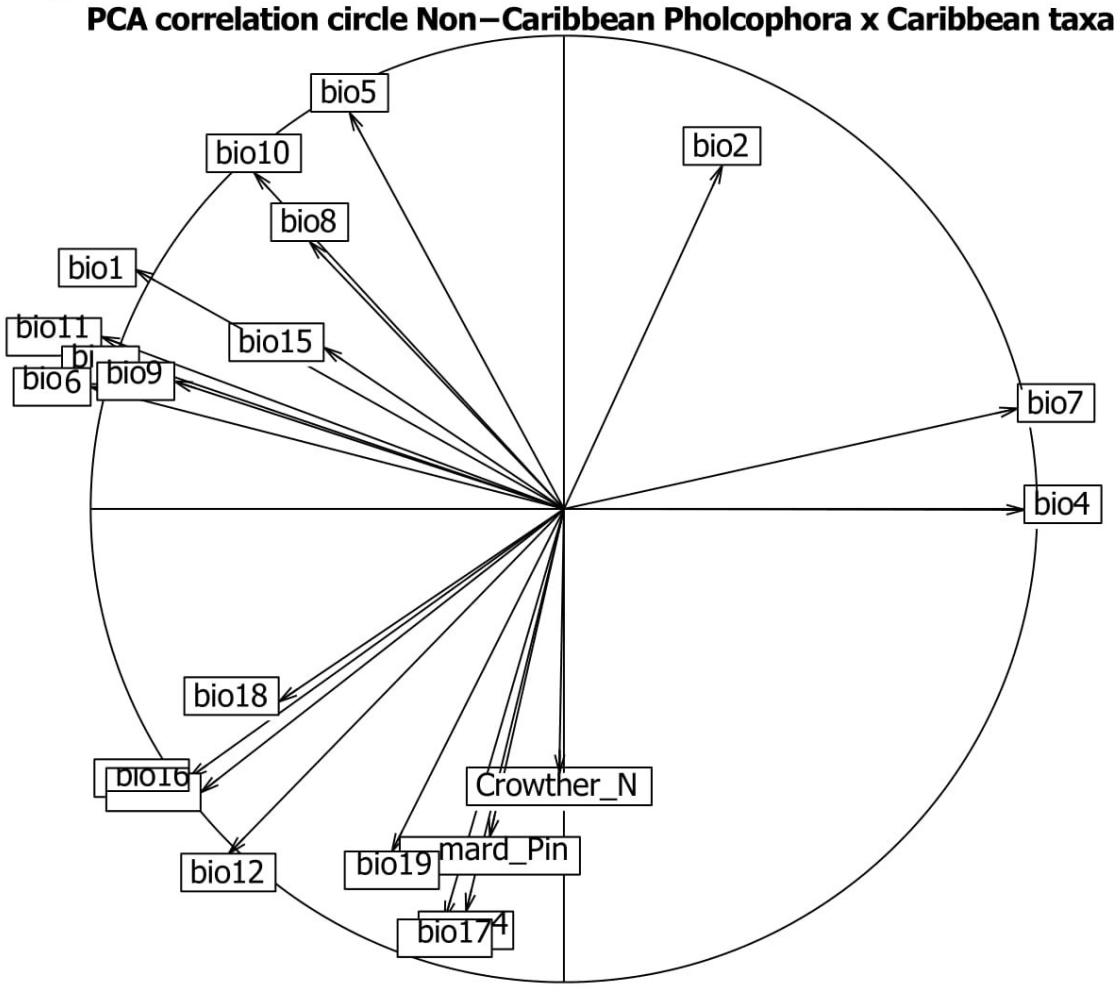
PCA correlation circle Non−Caribbean Pholcophora x Caribbean taxa
bio5
bio10
bio8
bio1
bio11
bio15
bio6
bio9
bio2
bio7
bio4
bio18
bio16
Crowther_N
mard_Pin
bio19
bio12
bio17
Axis 1 = 41.86 % Axis 2 = 30.01 %

Figure S37

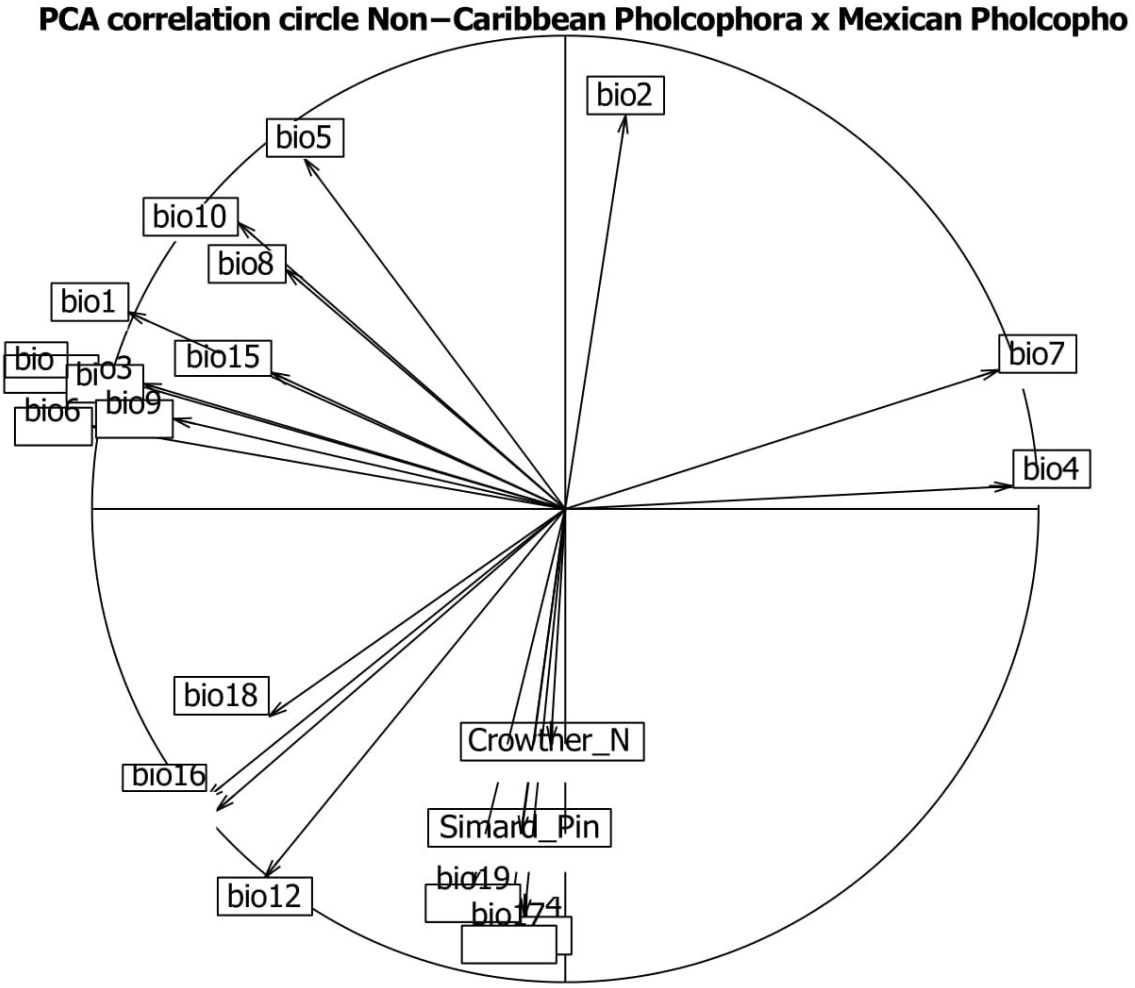
PCA correlation circle Non−Caribbean Pholcophora x Mexican Pholcopho
bio2
bio5
bio10
bio8
bio1
bio
bio15
bio3
bio6
bio9
bio7
bio4
bio18
Crowther_N
bio16
Simard_Pin
bio19
bio12
bio17
bio4
Axis 1 = 42.24 % Axis 2 = 30.37 %

Figure S38

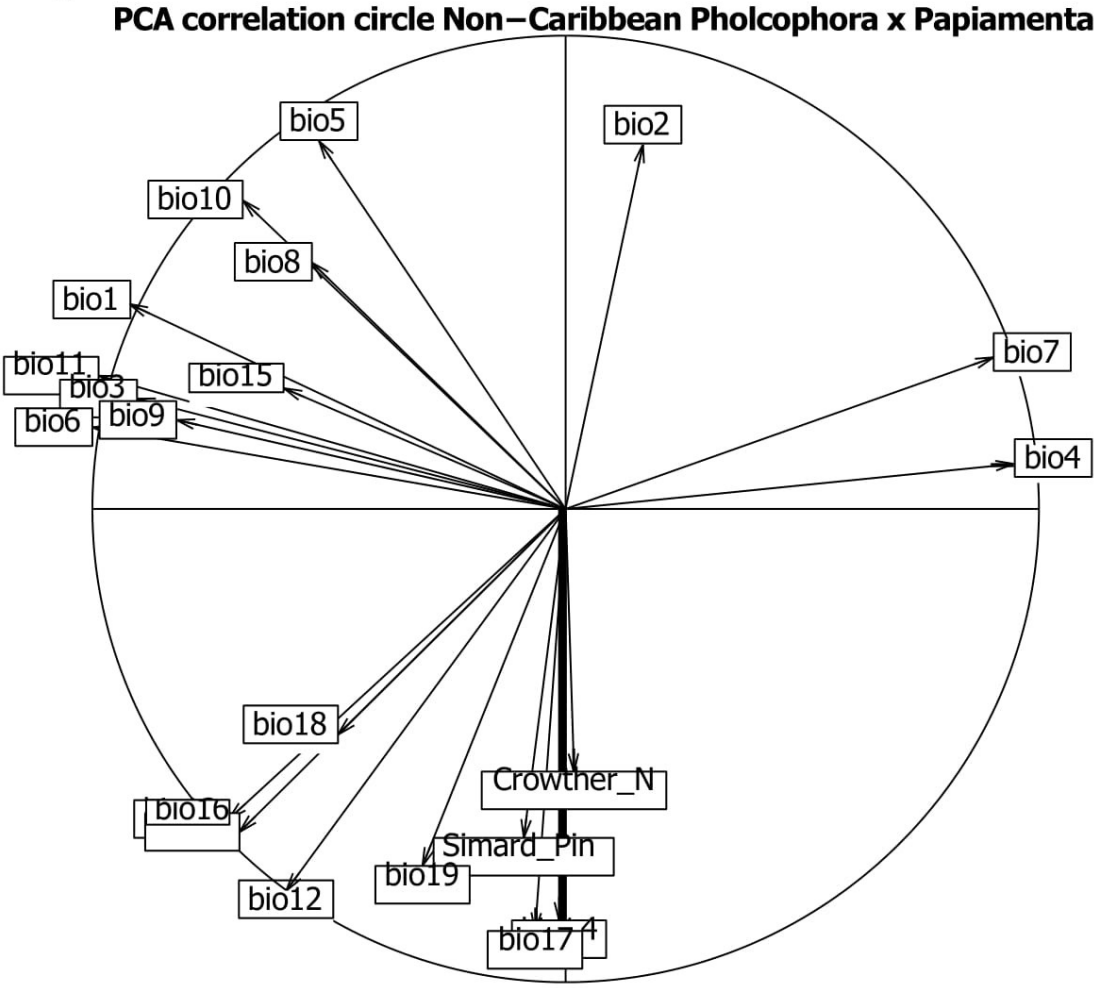
PCA correlation circle Non−Caribbean Pholcophora x Papiamenta
bio5
bio2
bio10
bio8
bio1
bio7
bio11
bio15
bio3
bio9
bio6
bio4
bio18
Crowther_N
bio16
Simard_Pin
bio19
bio12
bio17
Axis 1 = 40.28 % Axis 2 = 31.59 %

Figure S39

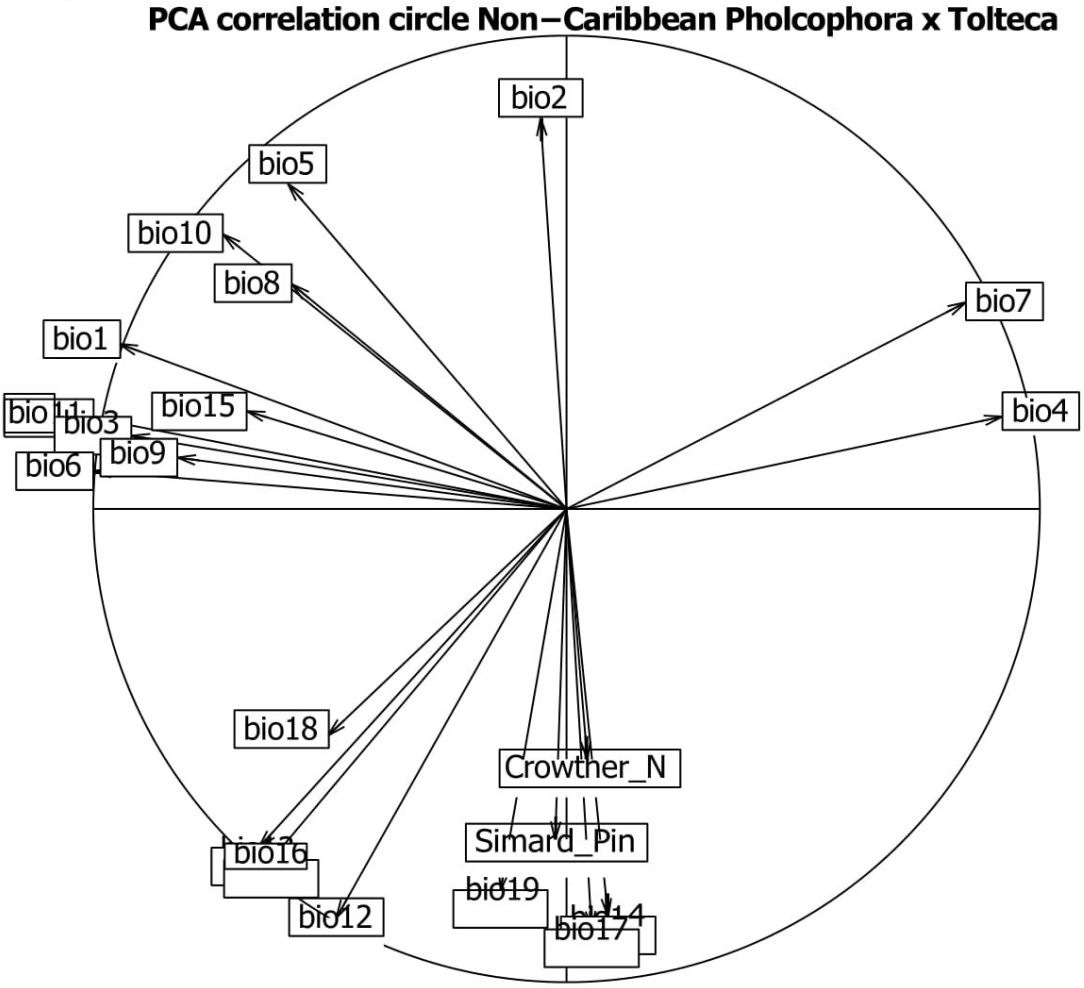
PCA correlation circle Non−Caribbean Pholcophora x Tolteca
bio2
bio5
bio10
bio8
bio7
bio1
bio15
bio4
bio3
bio9
bio6
bio18
Crowther_N
Simard_Pin
bio16
bio19
bio12
bio17
Axis 1 = 40.25 % Axis 2 = 32.18 %

Figure S40

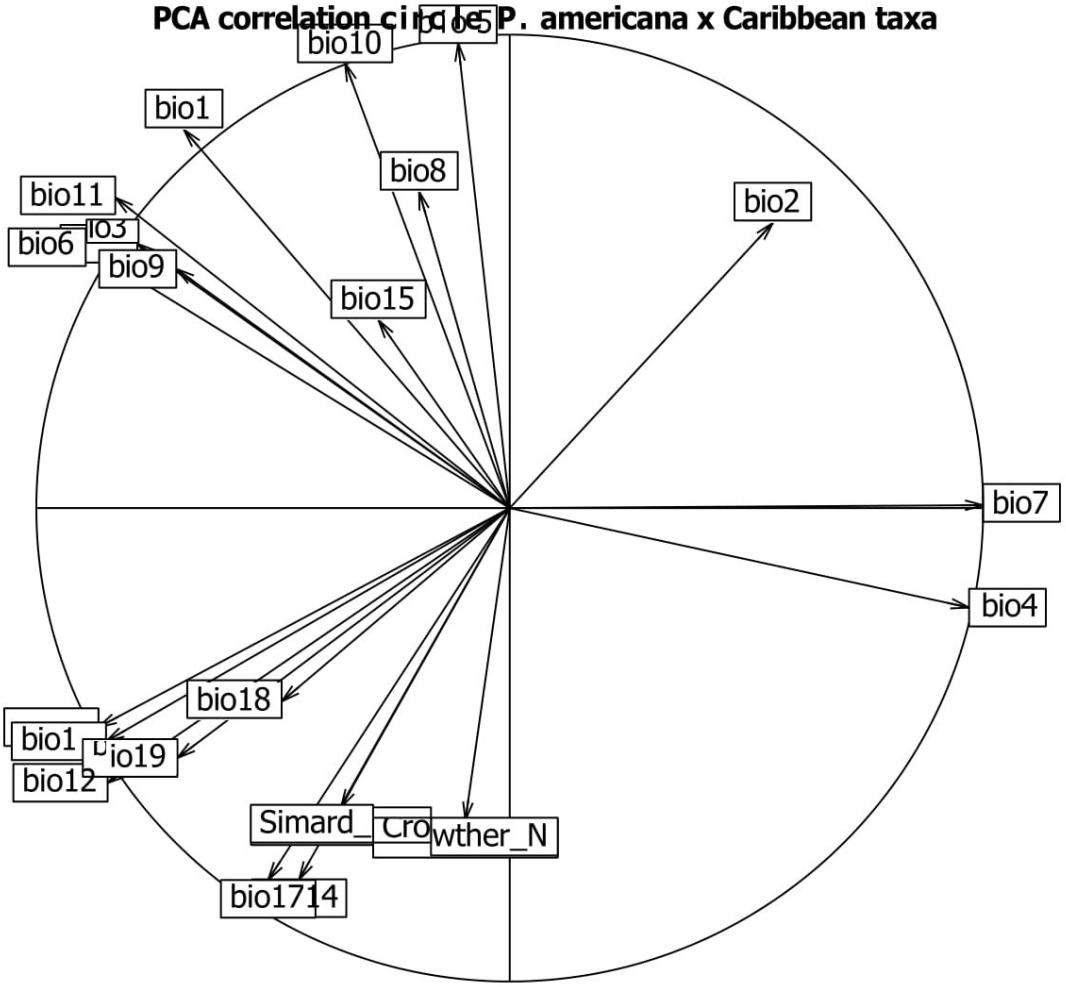

Axis 1 = 37.95 % Axis 2 = 33.78 %

Figure S41

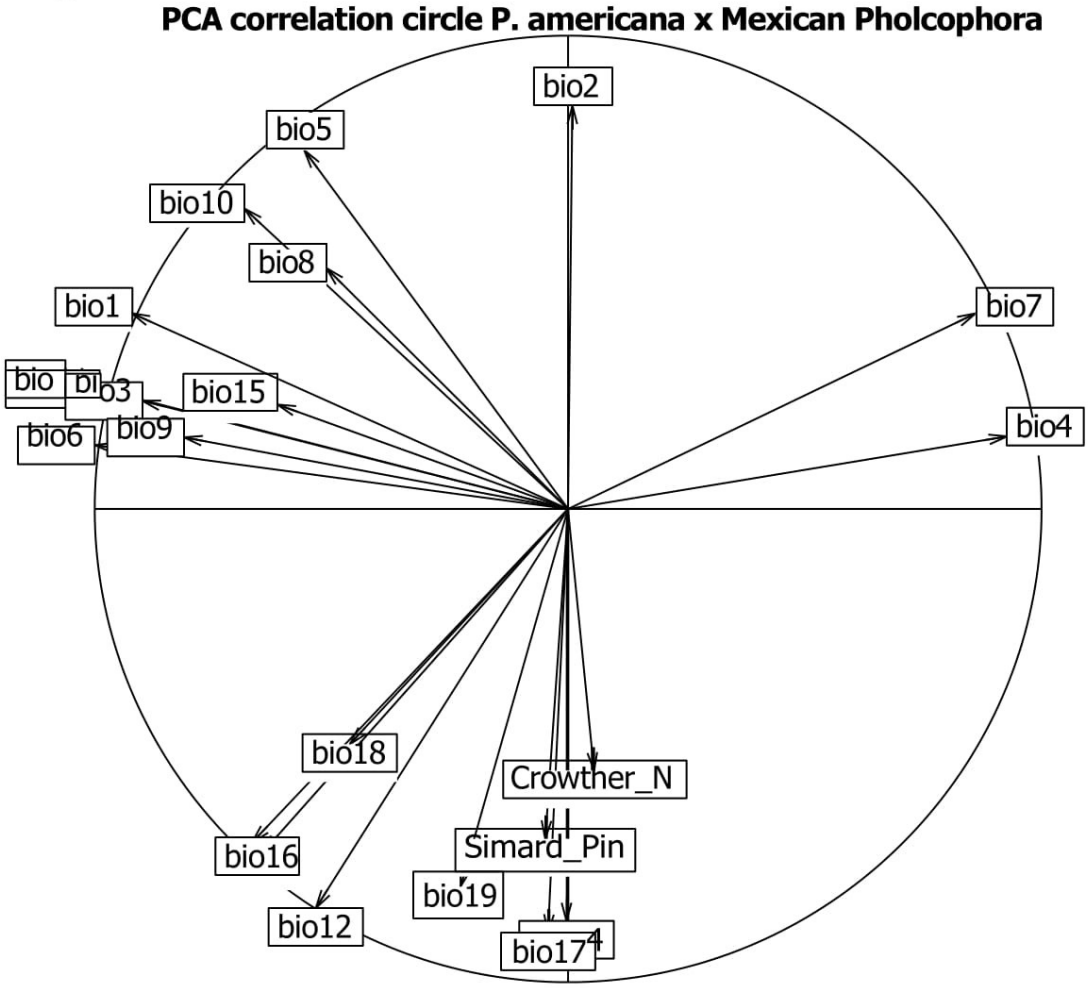
PCA correlation circle P. americana x Mexican Pholcophora
bio2
bio5
bio10
bio8
bio1
bio7
bio
bi
03
bio15
bio6
bio9
bio4
bio18
Crowther_N
Simard_Pin
bio16
bio19
bio12
bio17
4
Axis 1 = 38.94 % Axis 2 = 33.45 %

Figure S42

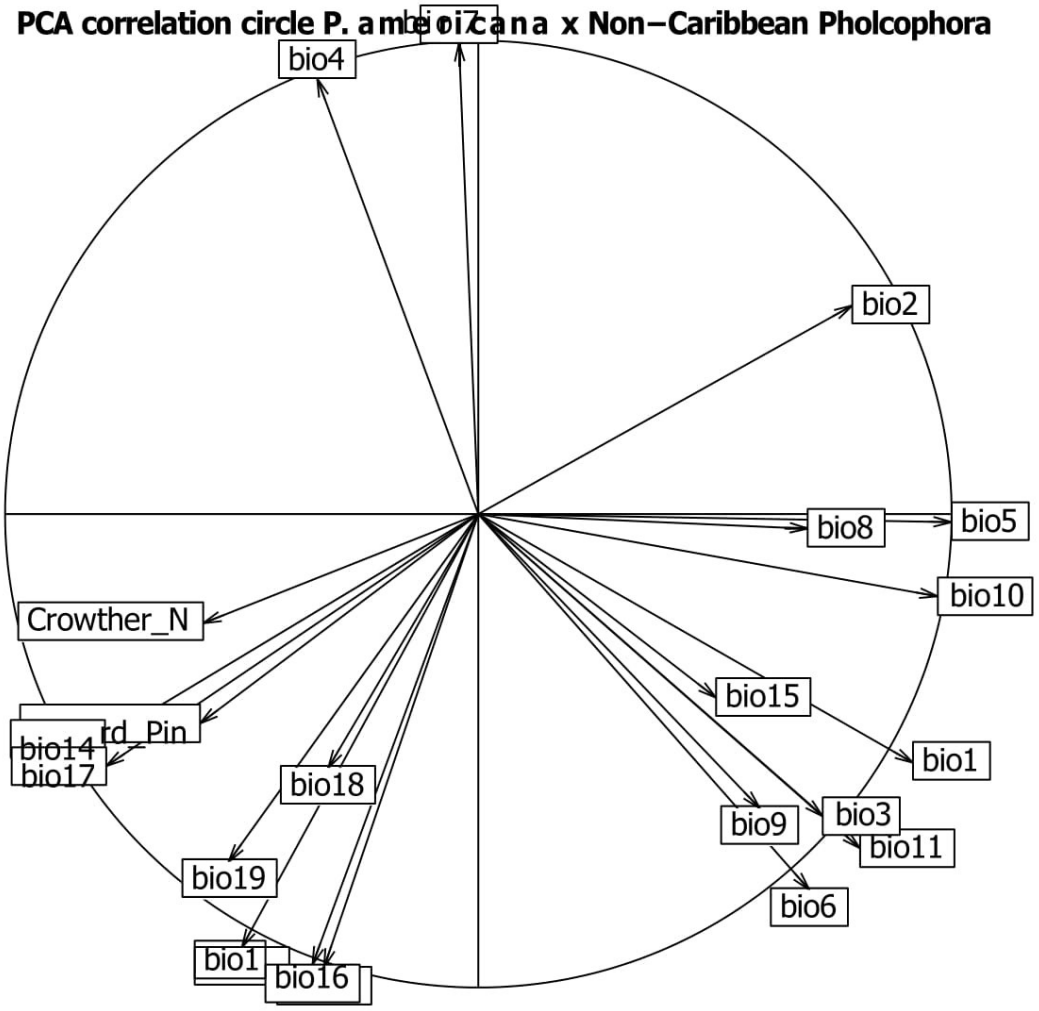
PCA correlation circle P. americana x Non−Caribbean Pholcophora
bio4
bio2
bio8
bio5
bio10
Crowther_N
bio15
bio1
bio14
bio17
bio18
bio9
bio3
bio11
bio19
bio6
bio1
bio16
Axis 1 = 36.84 % Axis 2 = 35.15 %

Figure S43

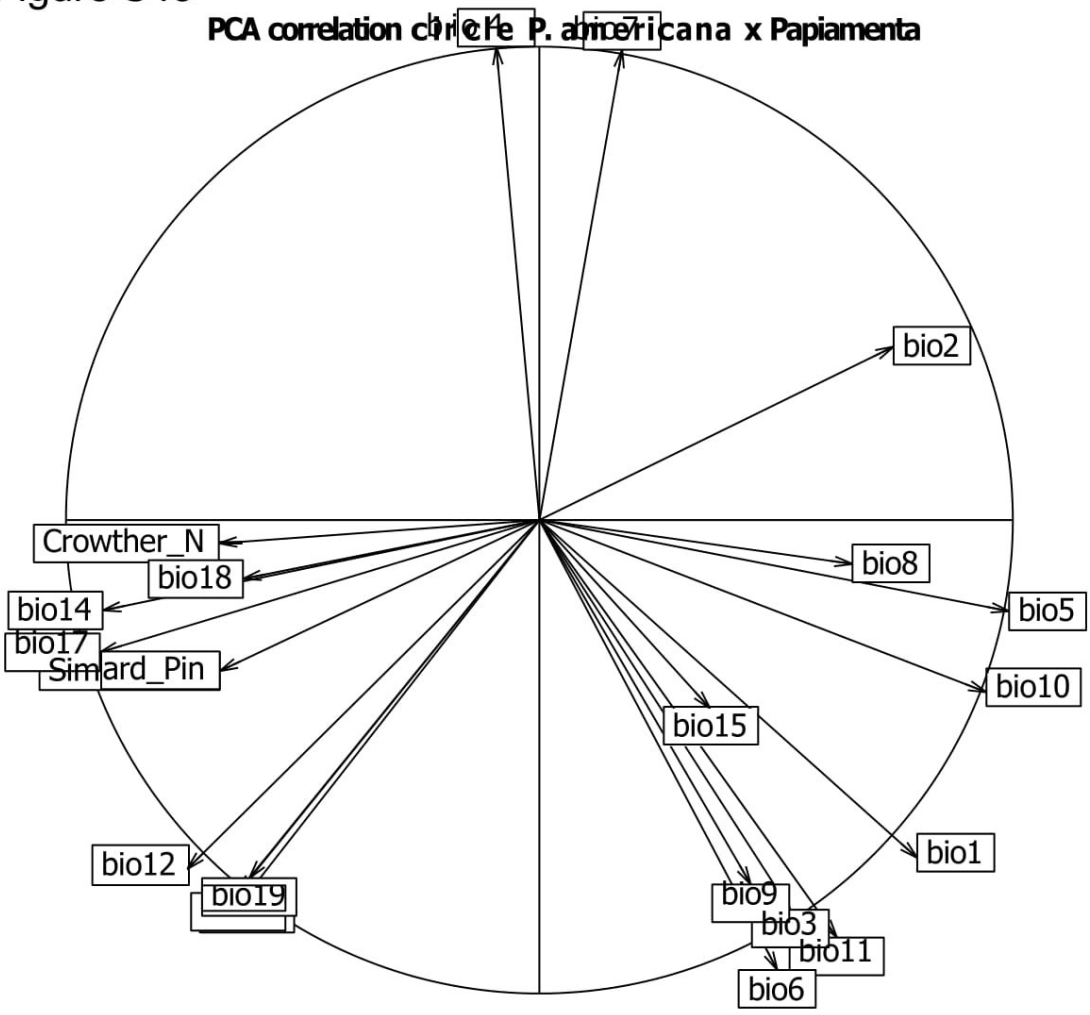
PCA correlation circle P. americana x Papiamenta
bio4
bio7
bio2
Crowther_N
bio18
bio14
bio17
Simard_Pin
bio8
bio5
bio10
bio15
bio1
bio12
bio19
bio9
bio3
bio11
bio6
Axis 1 = 38.01 % Axis 2 = 33.92 %

Figure S44

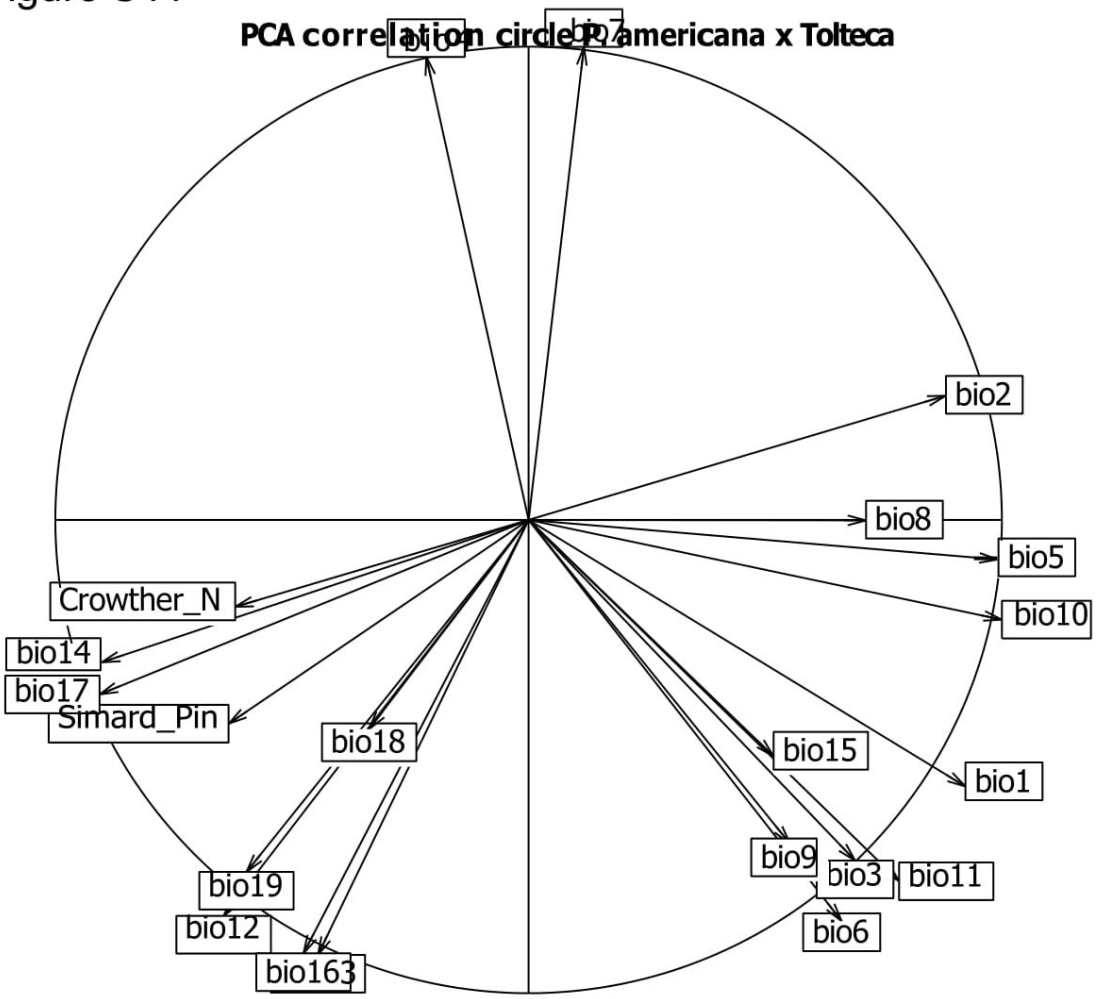
PCA correlation circle P. americana x Tolteca
bio4
bio7
bio2
bio8
bio5
bio10
bio1
bio9
bio3
bio11
bio6
bio15
bio18
Crowther_N
bio14
bio17
Simard_Pin
bio19
bio12
bio163
Axis 1 = 38.92 % Axis 2 = 33.09 %

Figure S45

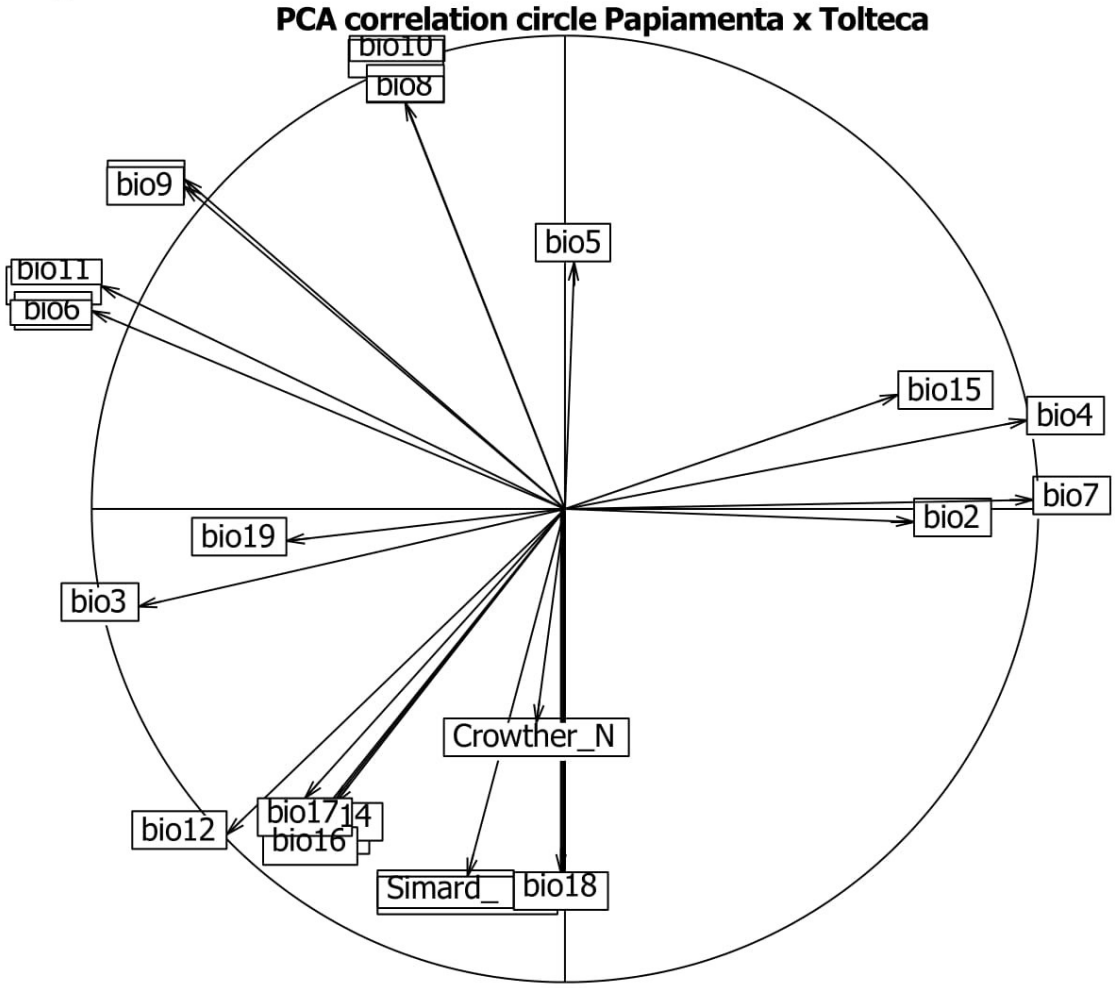
PCA correlation circle Papiamenta x Tolteca
bio10
bio8
bio9
bio5
bio11
bio6
bio15
bio4
bio7
bio2
bio19
bio3
Crowther_N
bio12
bio17
bio14
bio16
Simard_
bio18
Axis 1 = 36.44 % Axis 2 = 26.85 %

Figure S46

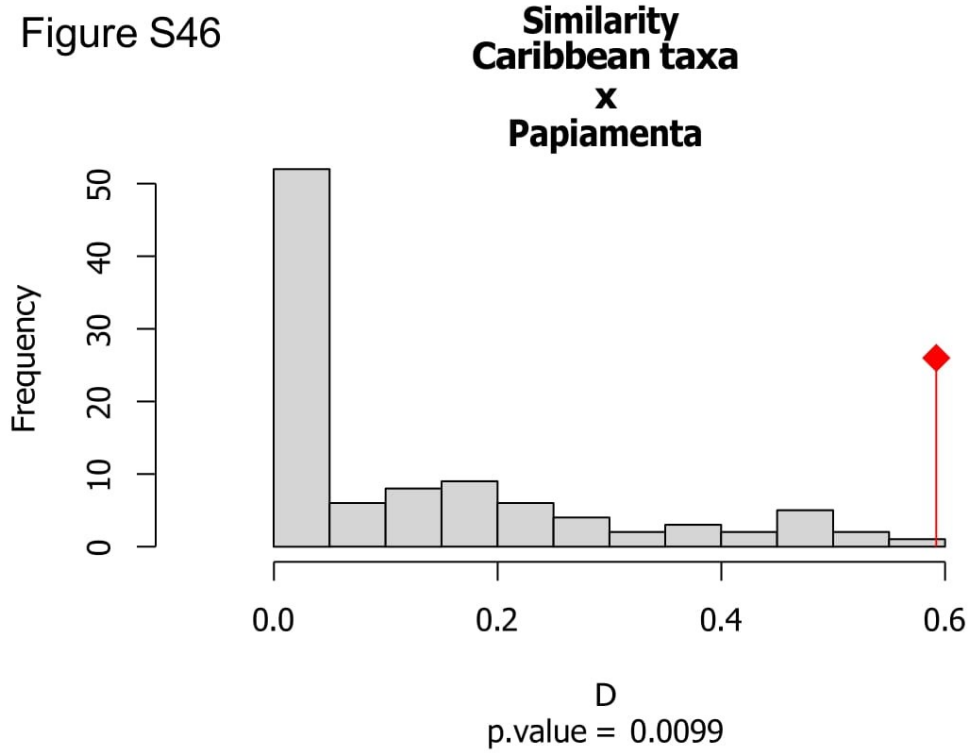

Figure S47

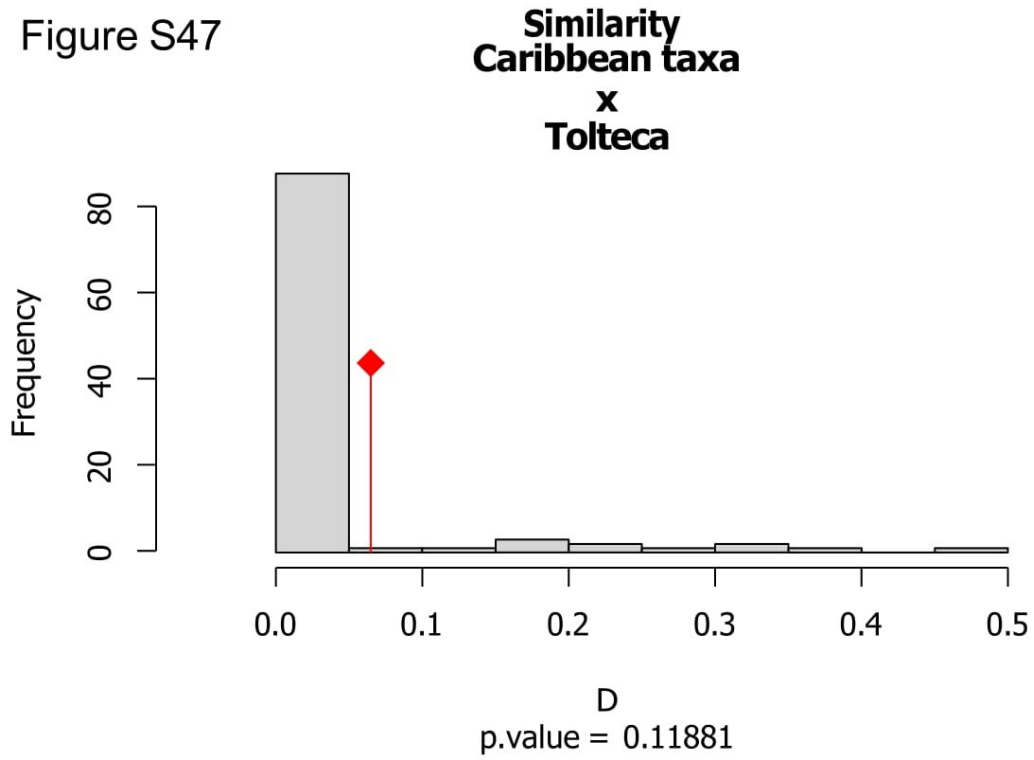

Figure S48

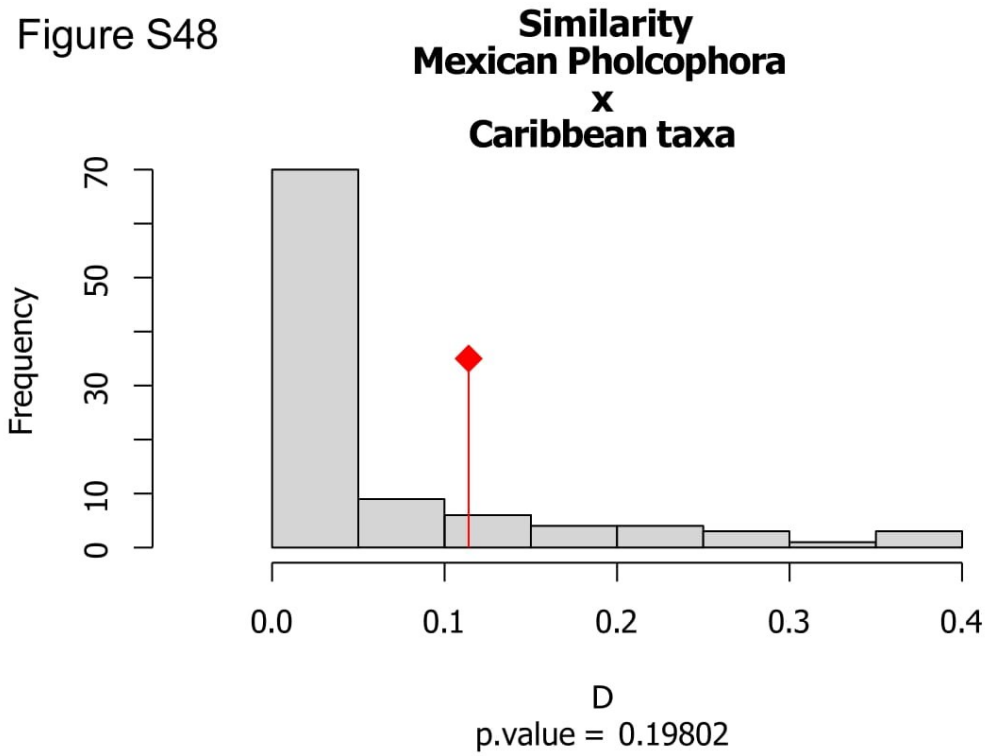

p.value = 0.19802

Figure S49

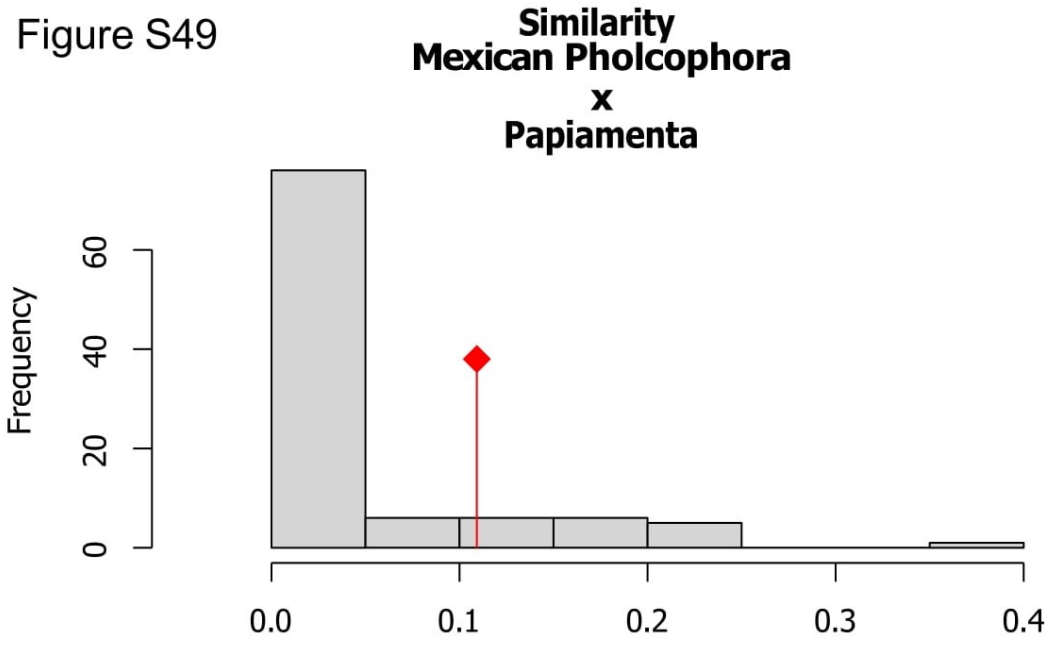

p.value = 0.18812

Figure S50

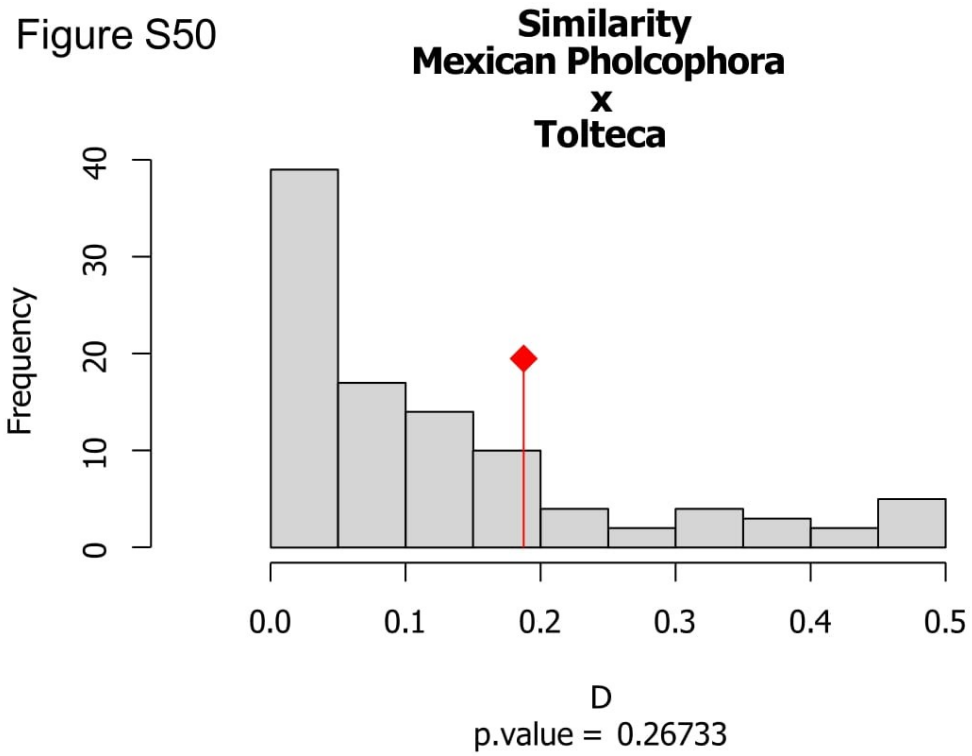

Figure S51

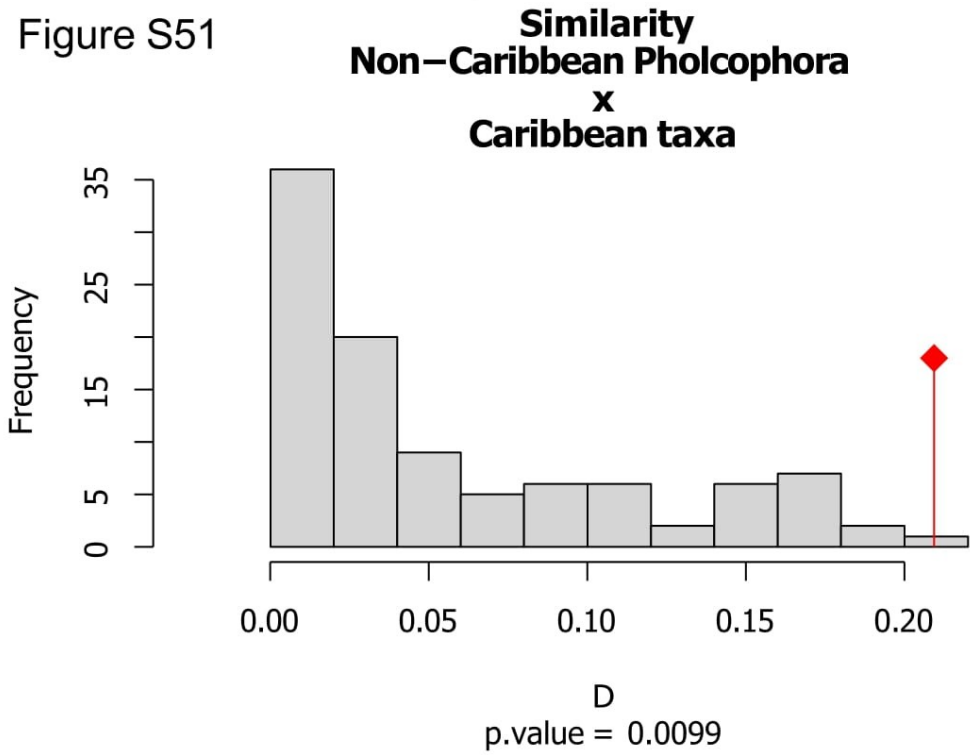

Figure S52

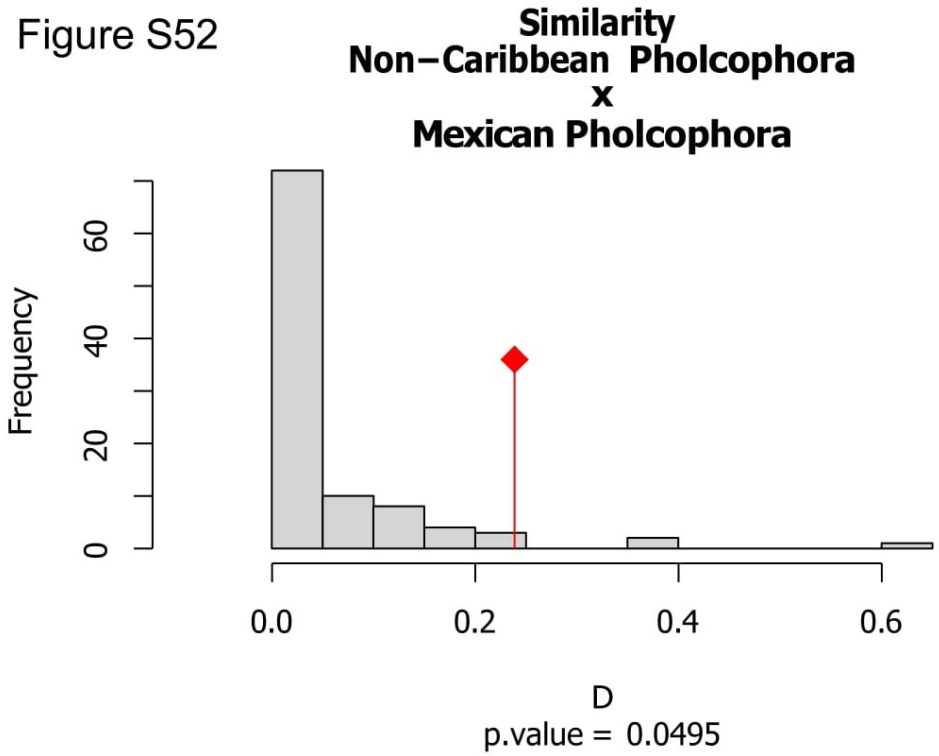

Figure S53

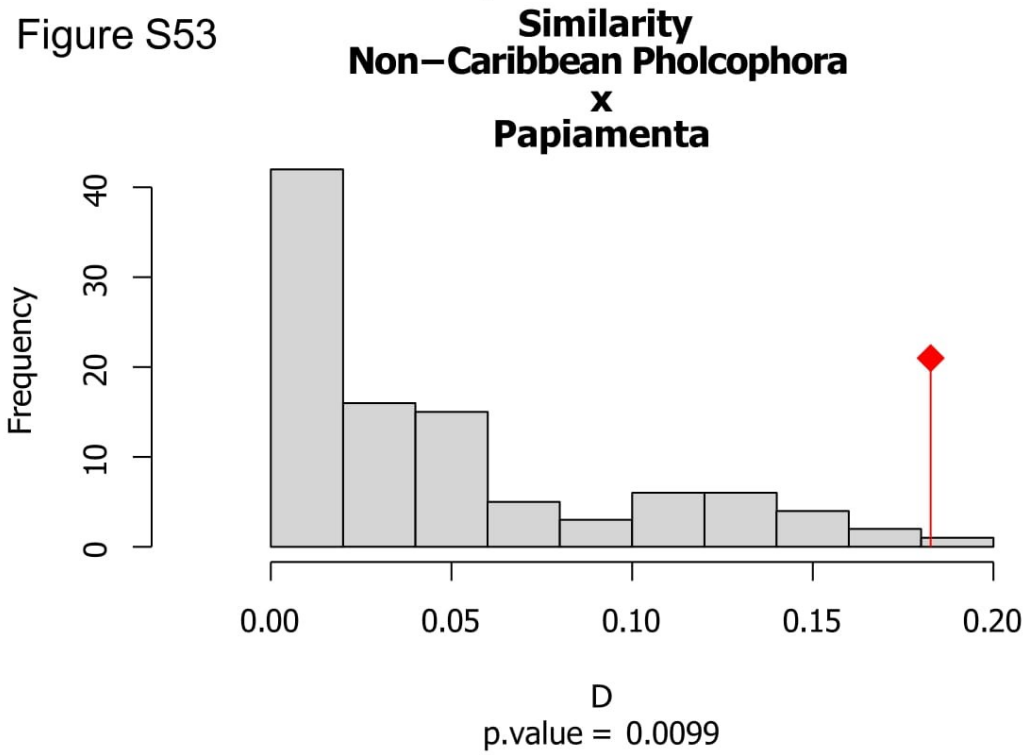

Figure S54

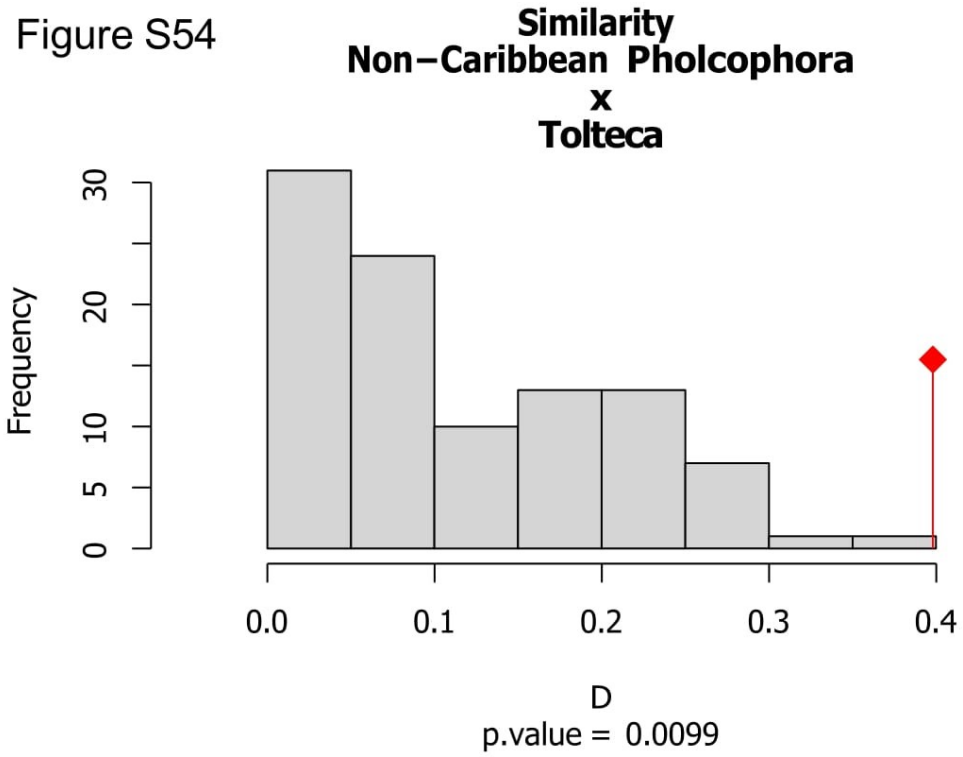

Figure S55

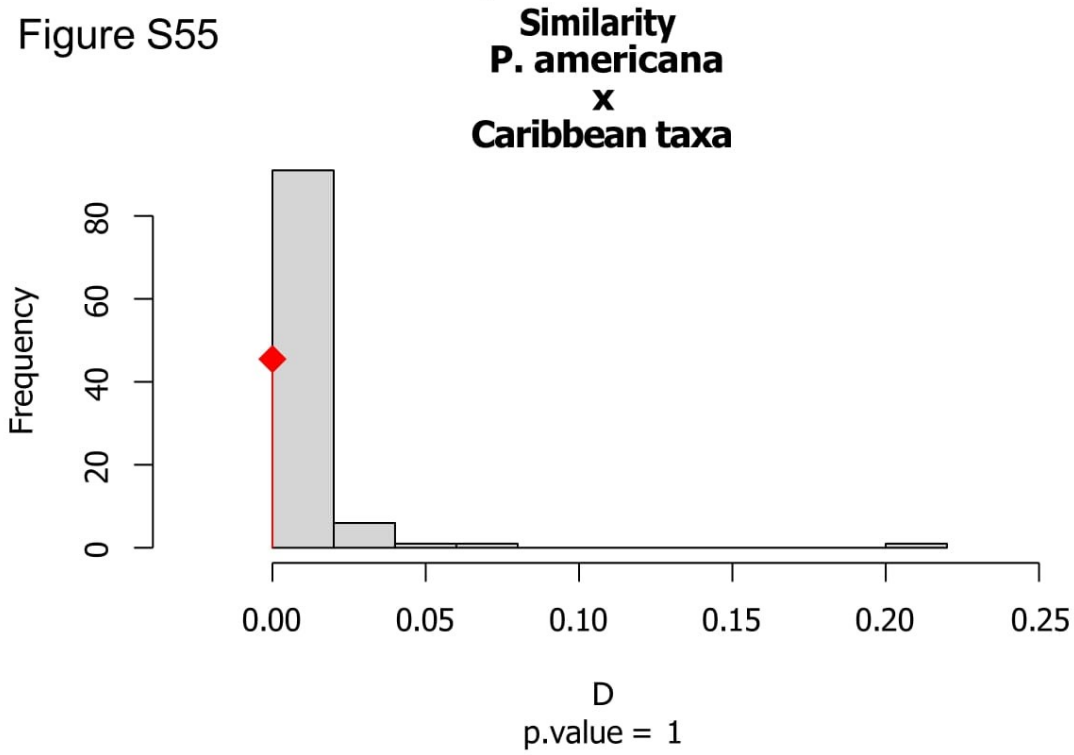

Figure S56

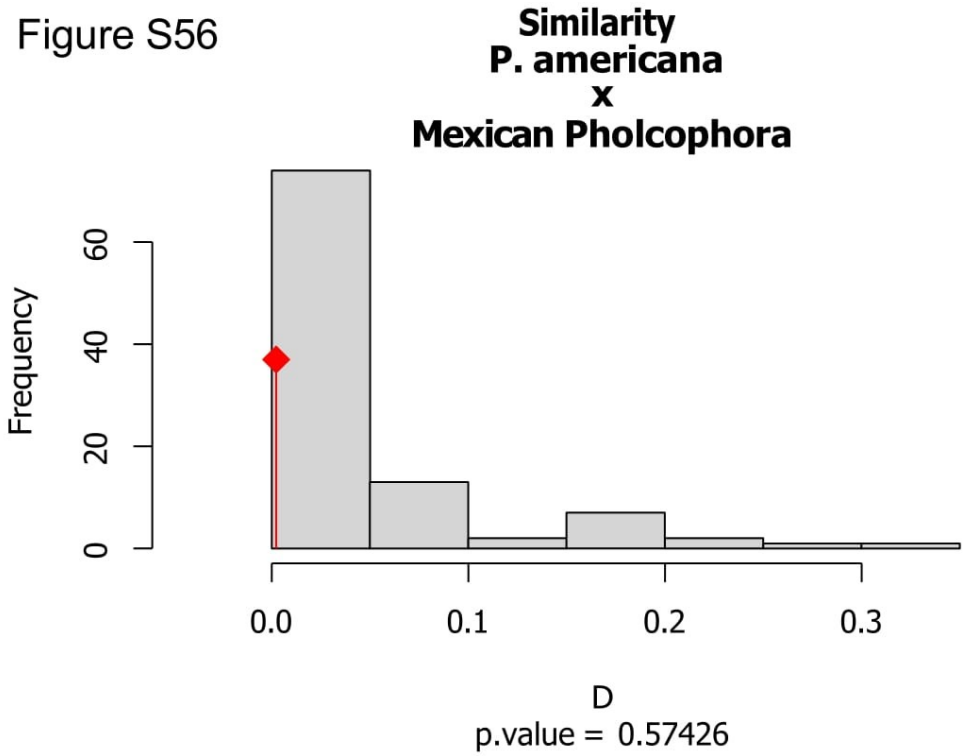

Figure S57

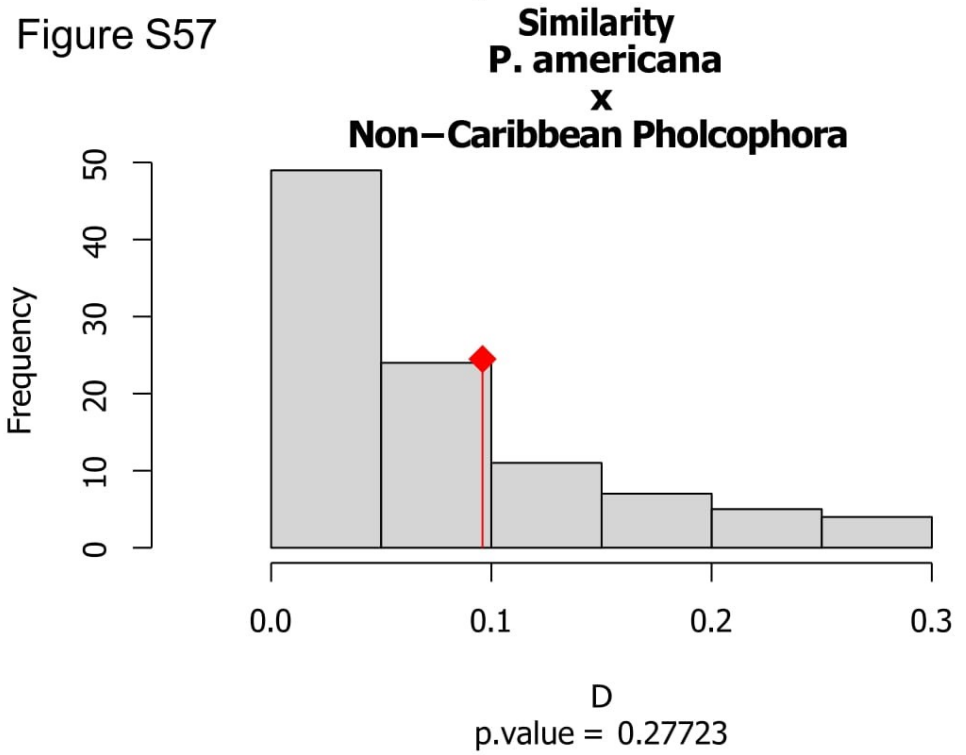

Figure S58

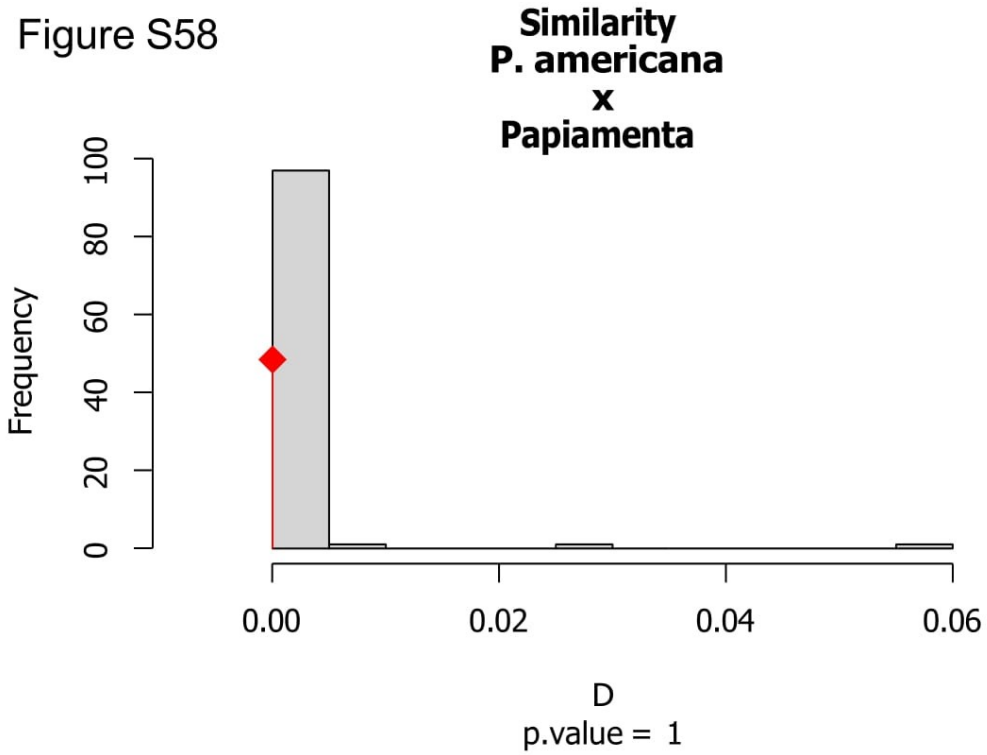

Figure S59

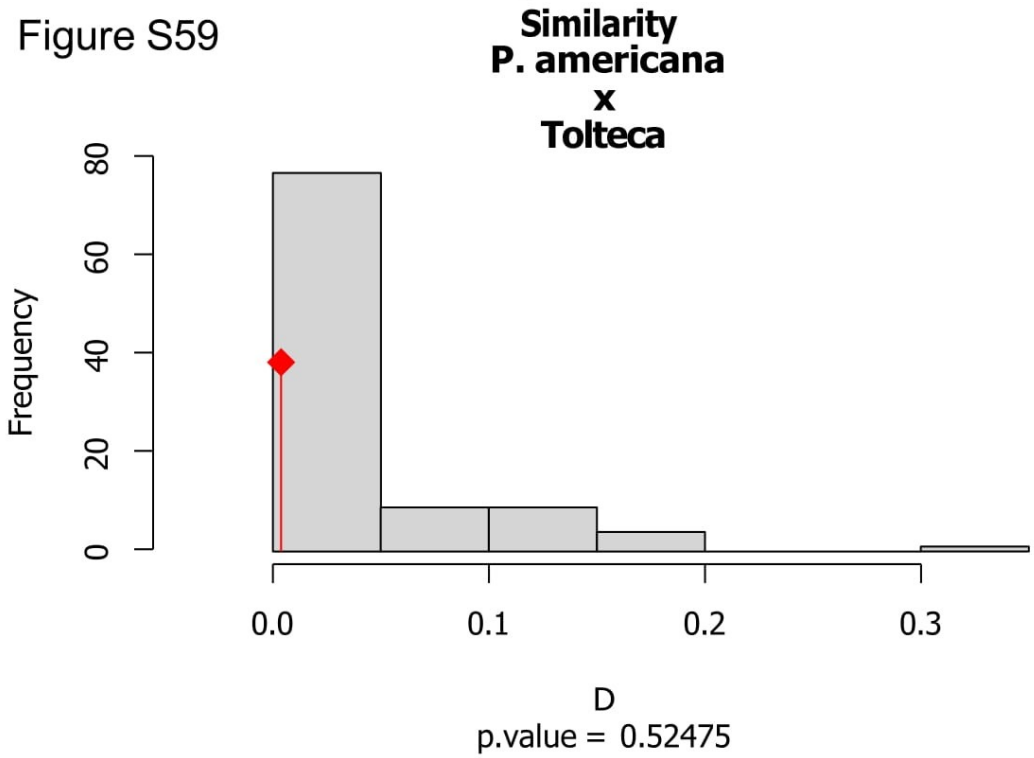

Figure S60

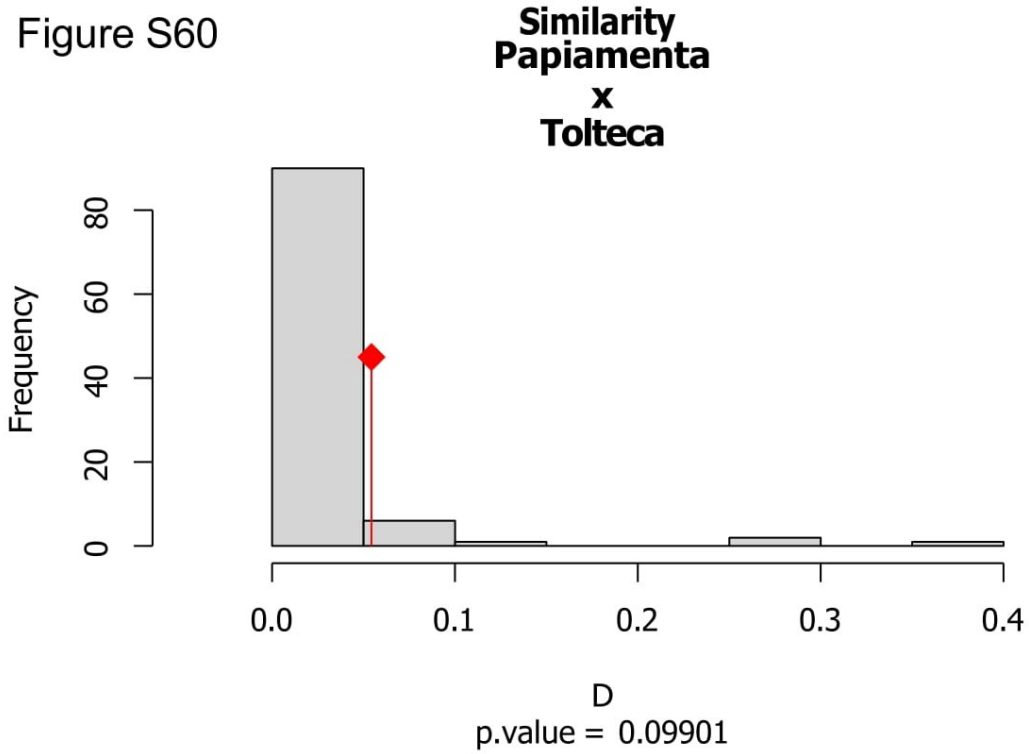

Figure S61

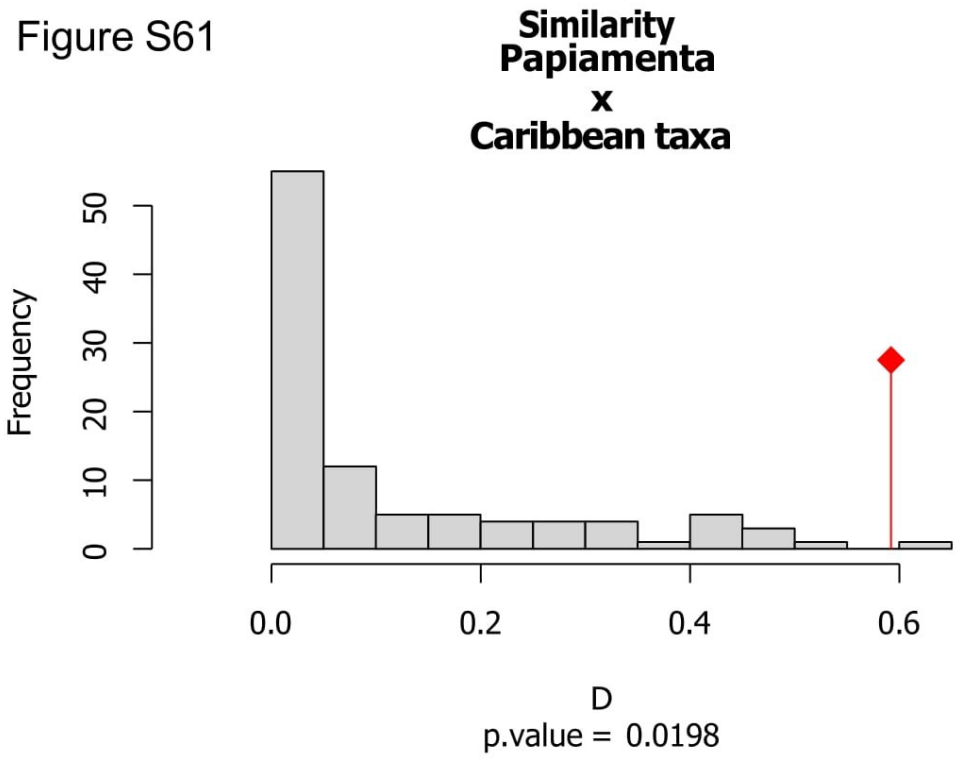

Figure S62

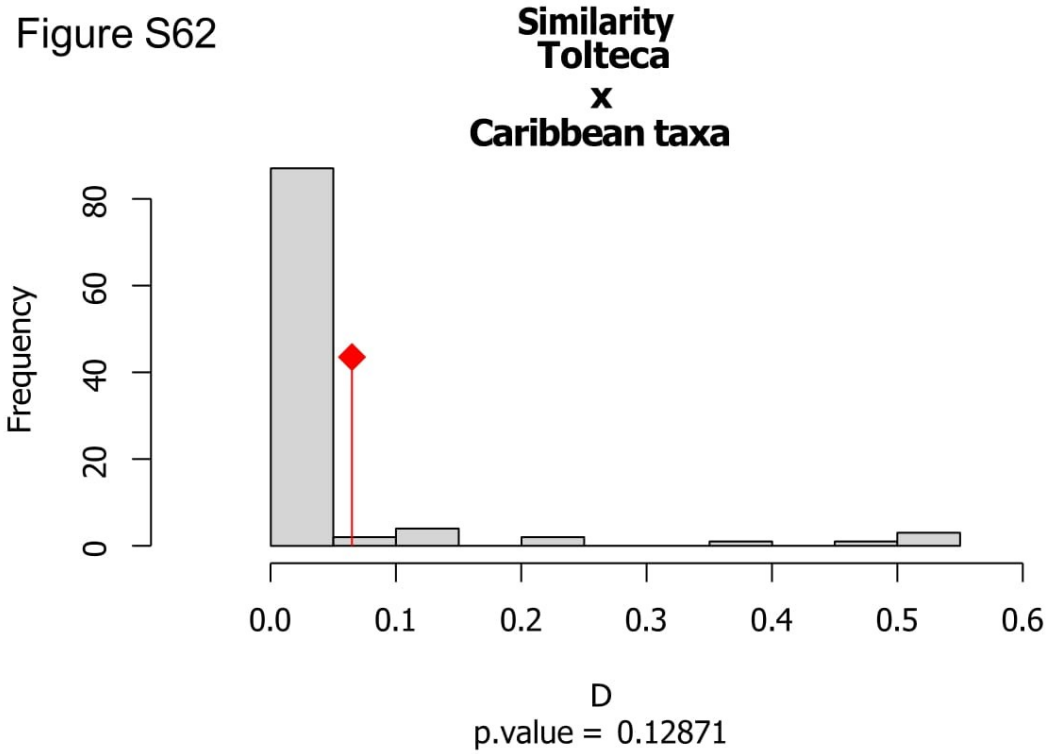

Figure S63

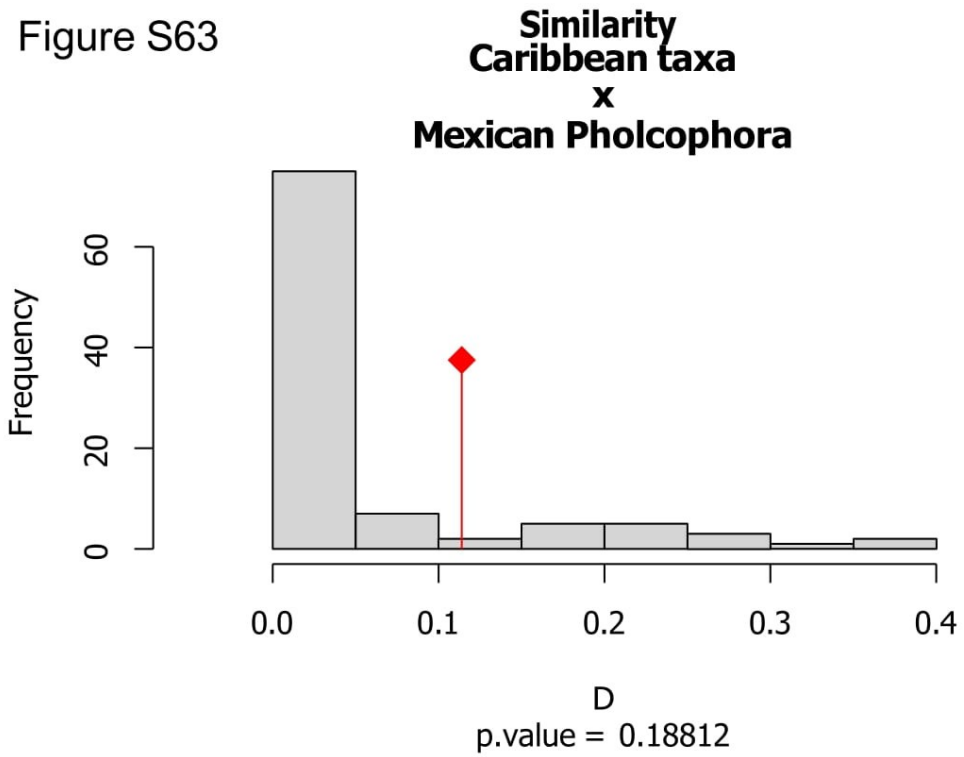

Figure S64

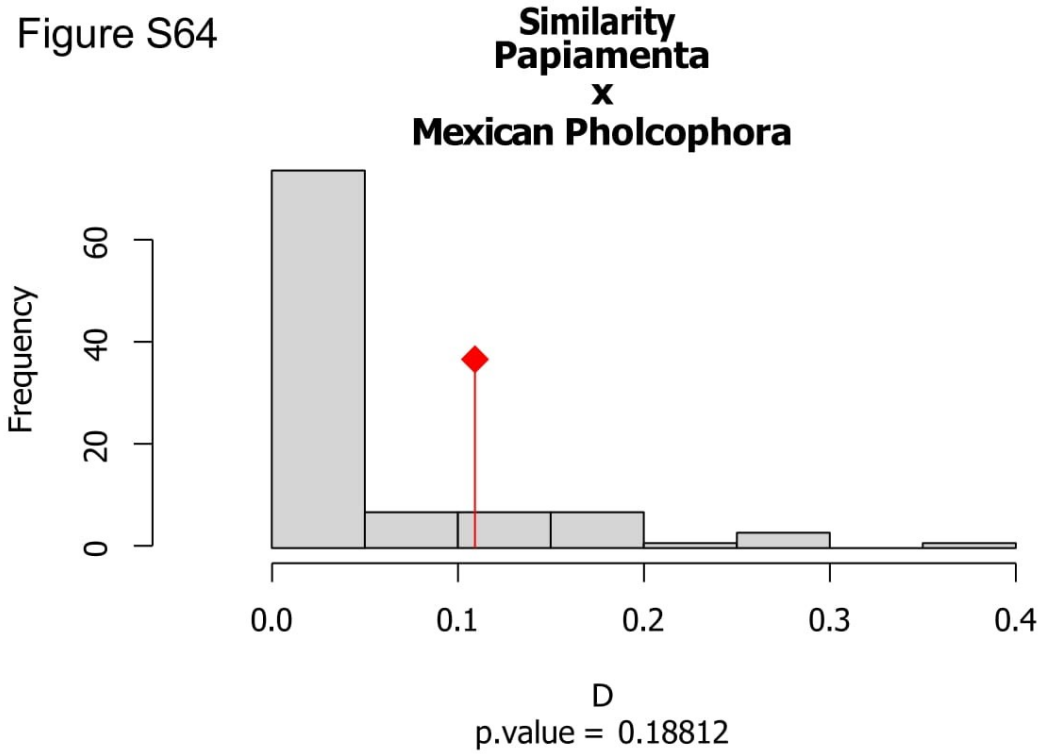

Figure S65

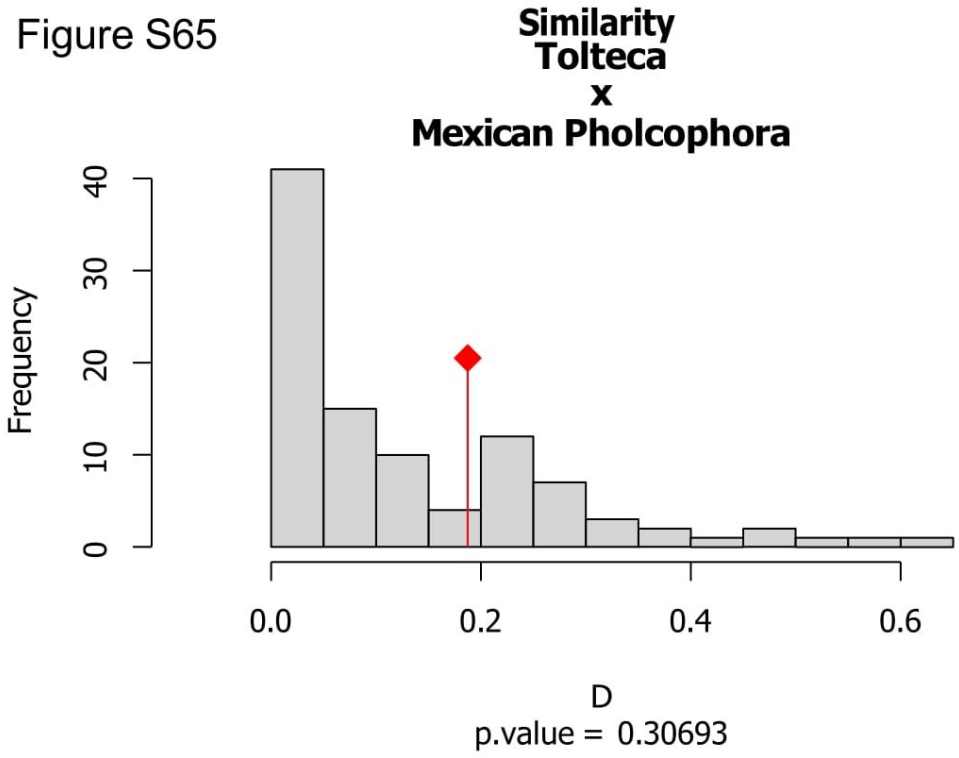

Figure S66

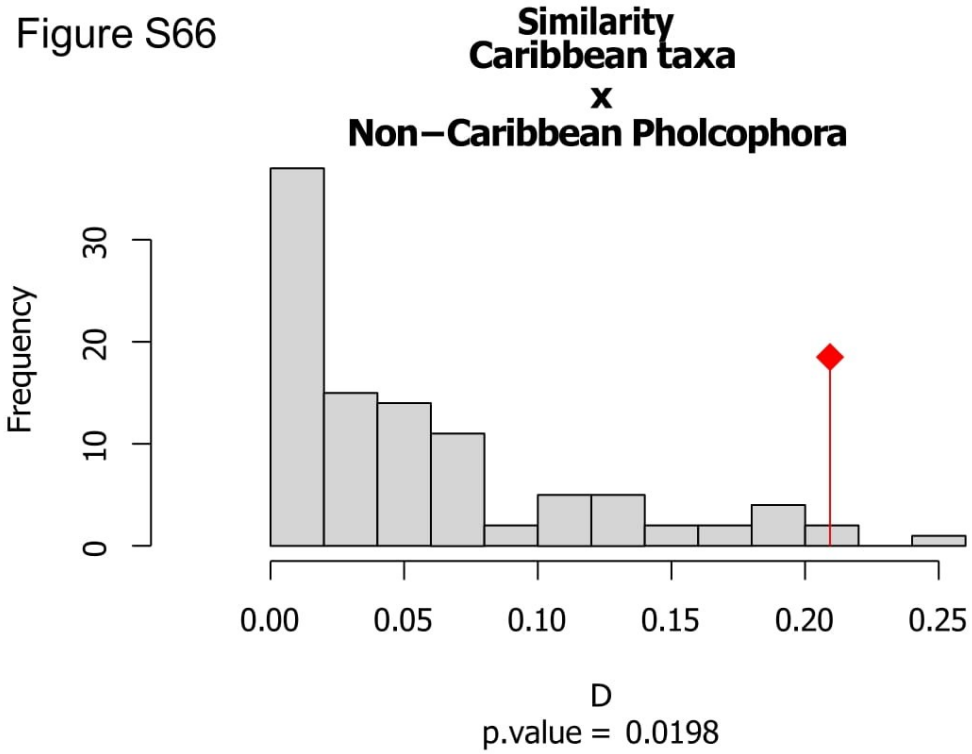

Figure S67

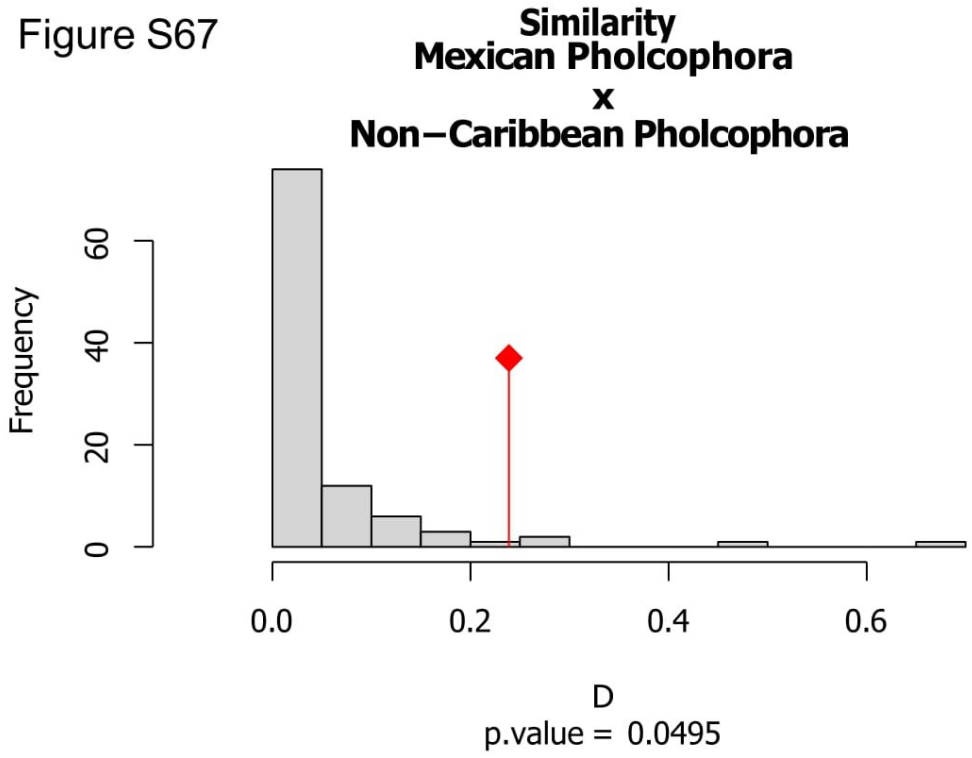

Figure S68

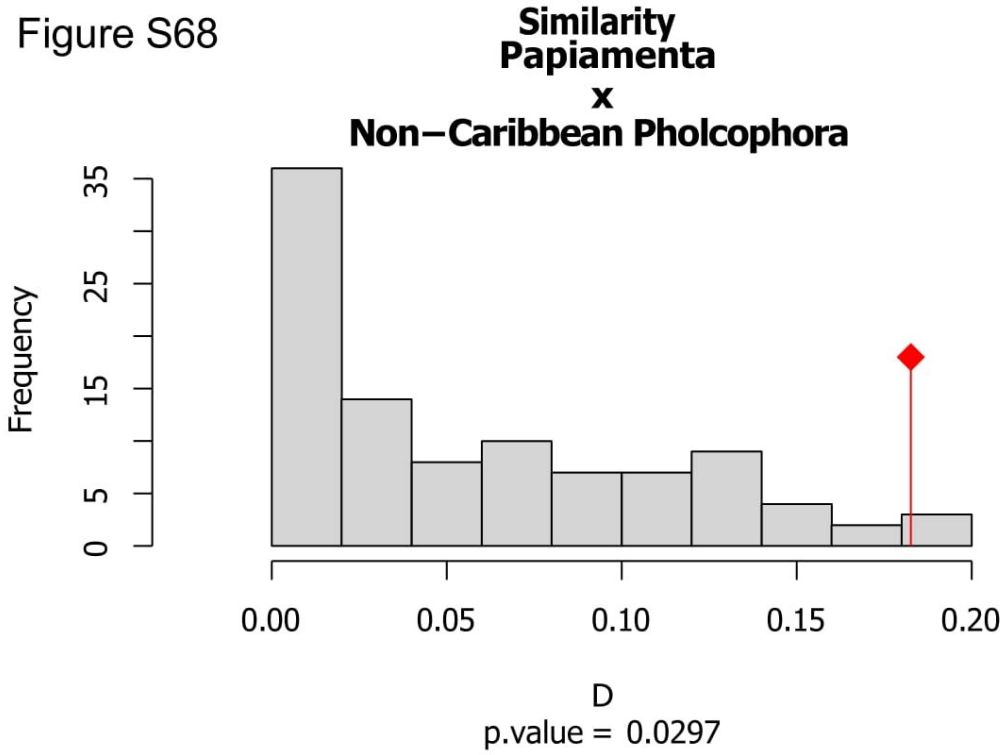

Figure S69

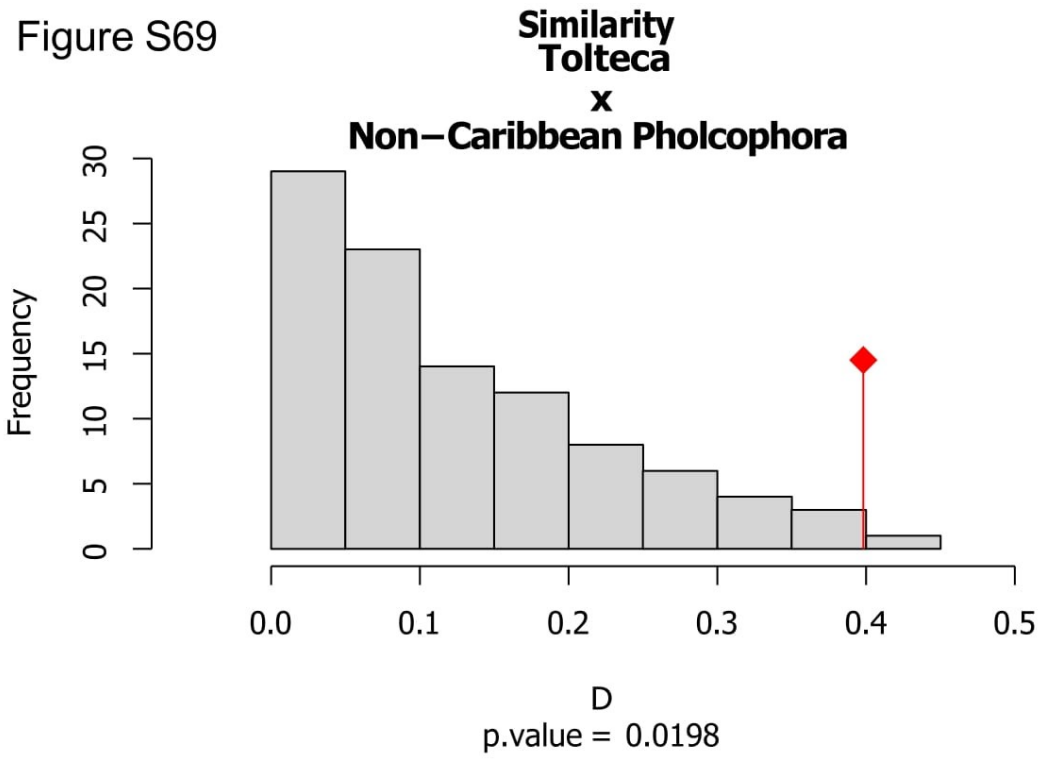

Figure S70

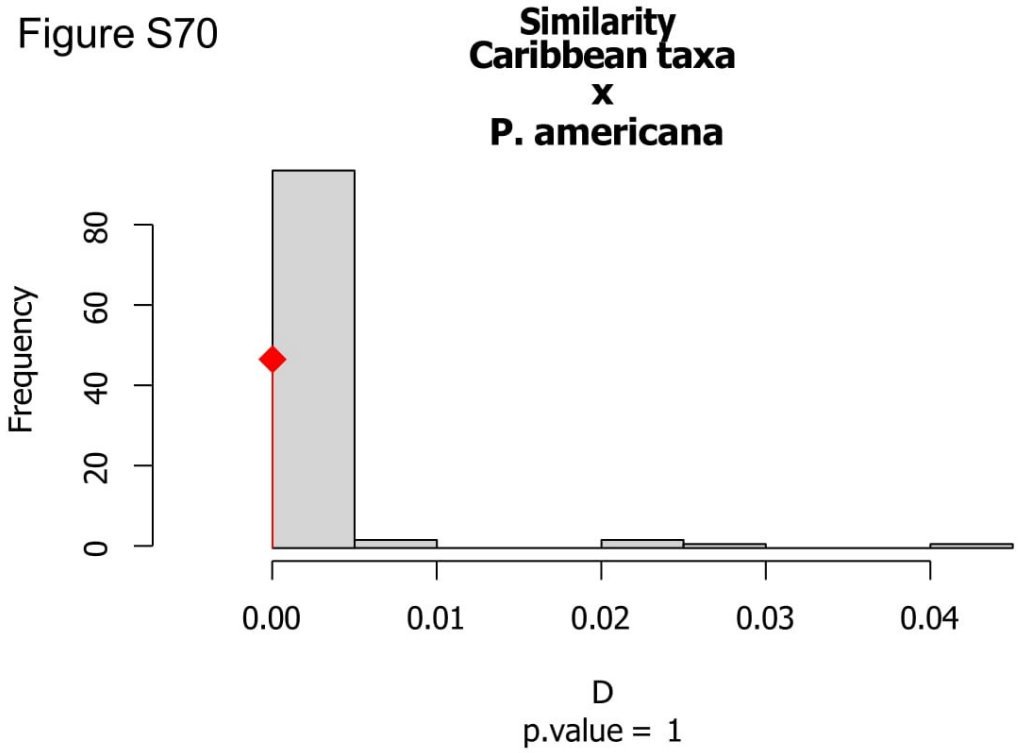

Figure S71

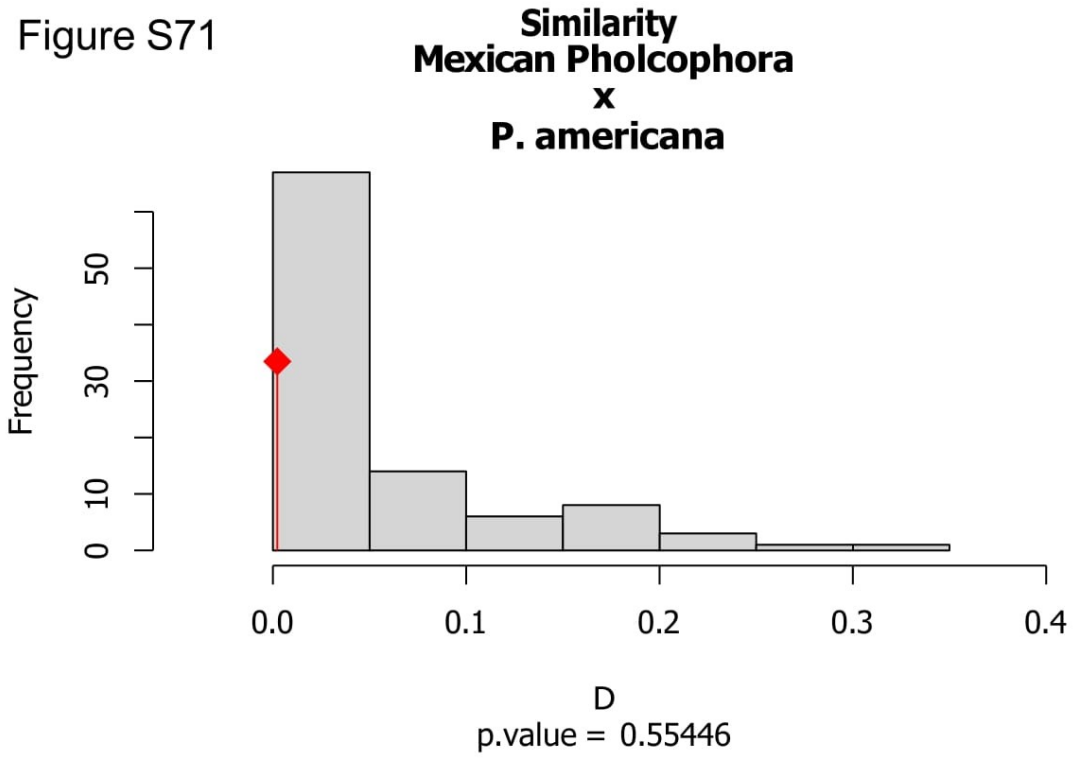

Figure S72

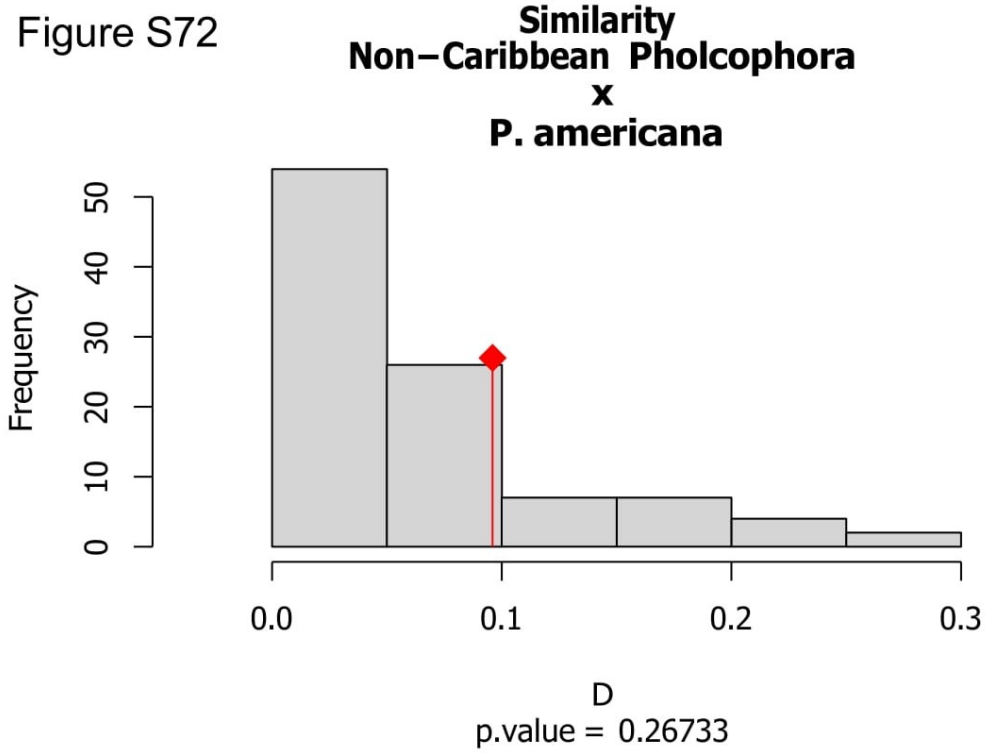

Figure S73

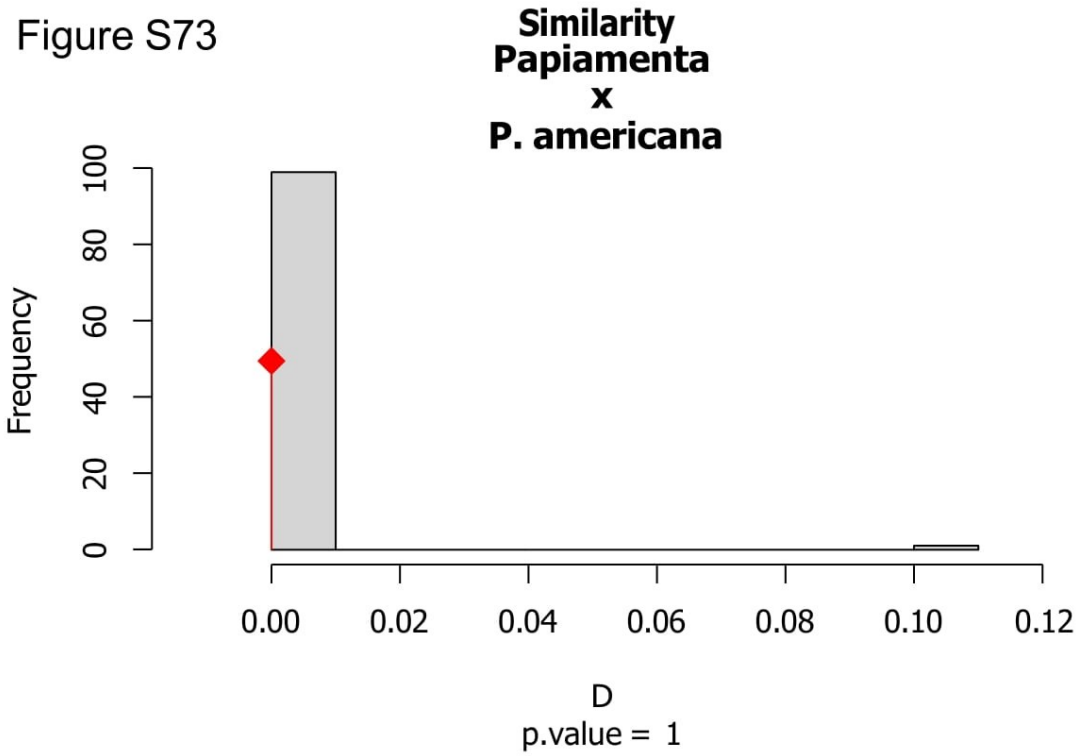

Figure S74

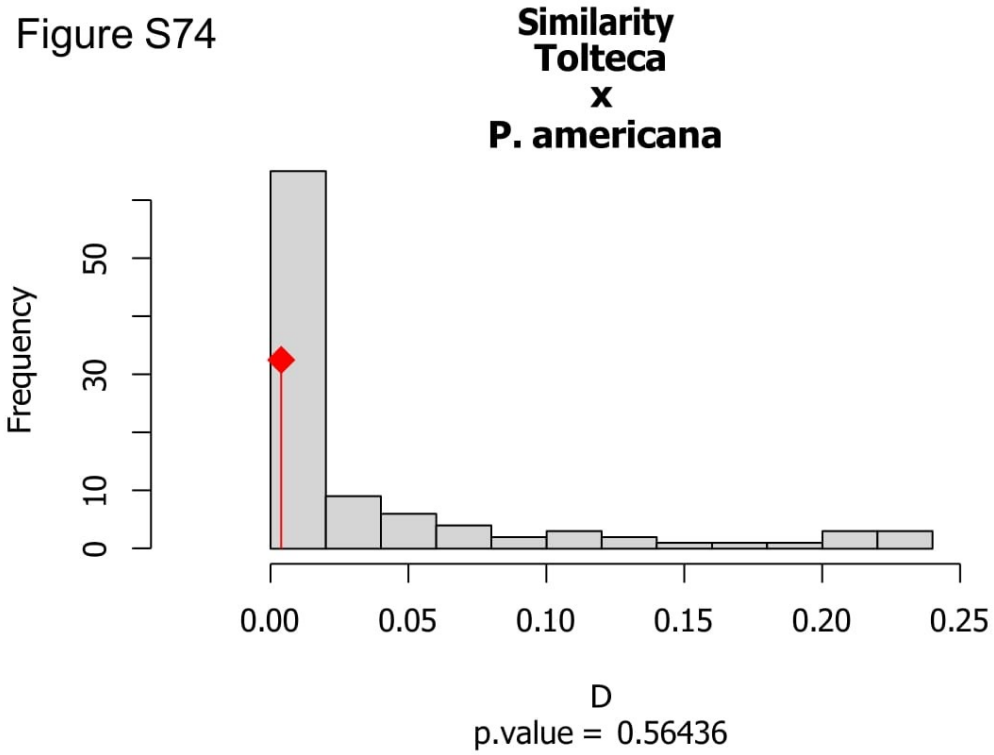

Figure S75

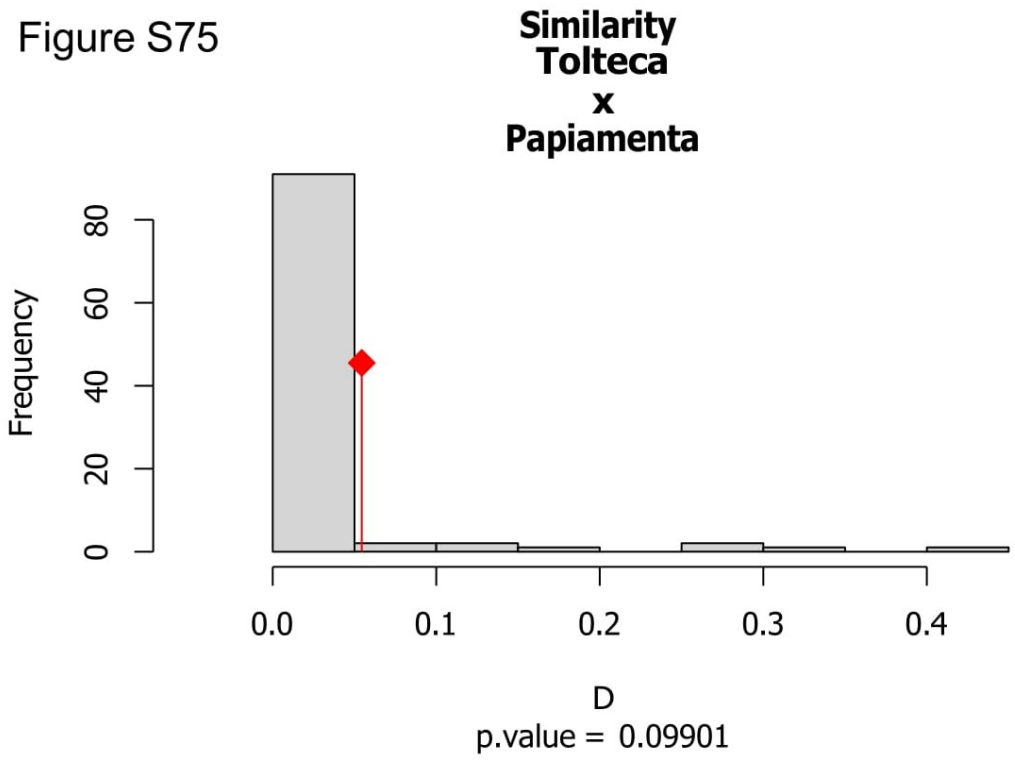

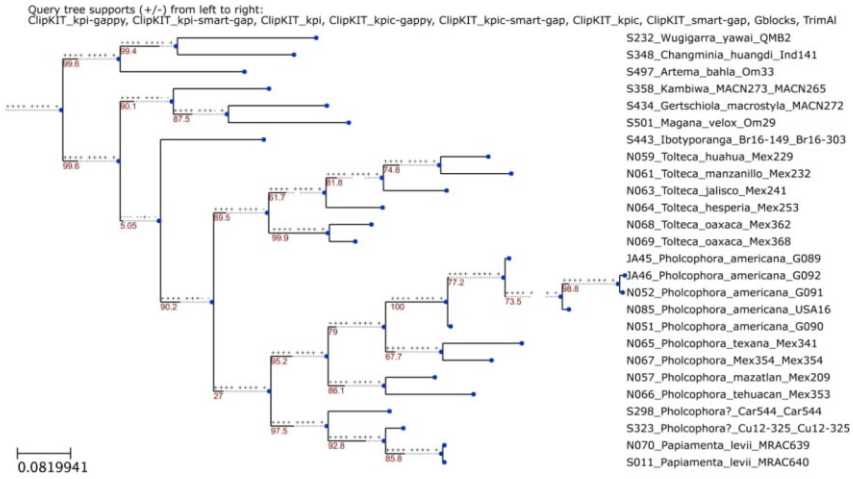

Figure S76. Summary tree of all trees using unpartitioned analysis. All the trees were constructed from the same gene set but with different multiple-sequence-alignment (MSA) trimming strategies. The ClipKIT_gappy tree was used as the reference tree, the trees (query trees) from other MSA-trimming strategies were compared to the reference tree, with '+' or '-' indicating that the query trees agree or disagree with the branching events, respectively. Numbers on the branches are SH-aLRT support (%). Best-fit model according to BIC for the reference tree: SYM+I+G4.

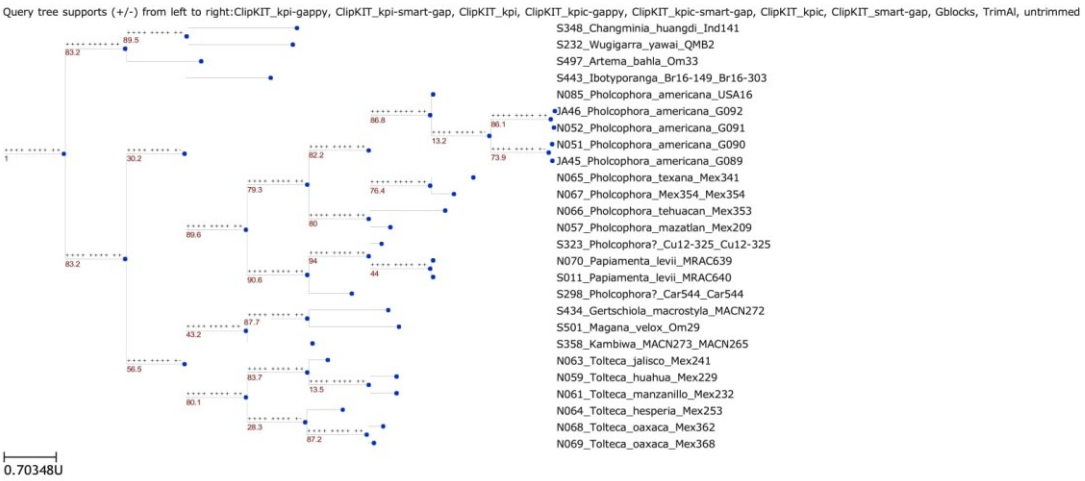

Figure S77. Summary tree of all trees using partitioned analysis. All the trees were constructed from the same gene set but with different multiple-sequence-alignment (MSA) trimming strategies or the untrimmed MSA. The ClipKIT_gappy tree was used as the reference tree, the trees (query trees) from other MSA-trimming strategies were compared to the reference tree, with '+' or '-' indicating that the query trees agree or disagree with the branching events, respectively. Numbers on the branches are SH-aLRT support (%).

5. Discussion

5.1 Evolution of karyotype in mygalomorphs of the superfamily Atypoidea

Concerning mygalomorphs, I focused on the superfamily Atypoidea. This clade is composed by the families Atypidae, Antrodiaetidae, Mecicobothriidae, Hexurellidae, and Megahexuridae (Hedin et al. 2019). Diploid numbers in this superfamily are lowest than in most species of the superfamily Avicularioidea. The male diploid numbers within Atypoidea range from 14 (*Atypus affinis*) (Řezáč et al. 2006) to 47 (*Atypoides riversi*) (Král et al. 2013). The morphology of the chromosomes is predominantly biarmed (Řezáč et al. 2006, Král et al. 2011, 2013). The three sex chromosome systems have been reported, namely X0, X_1X_20, and XY (Suzuki, 1949, 1950a, 1954, Řezáč et al. 2006, Král et al. 2011, 2013). The X_1X_20 system is described for only one species of the family Atypidae (Suzuki 1954). In this case, it is very likely a confusion with the X0 system, as our revision shows, see below.

With the aim to contribute to understanding the karyotype evolution of Atypoidea, I revised the karyotype of *Atypus karschi* from East Asia, which has been introduced into USA. Available karyotype data on this species differ from our information. While Suzuki (1954) reported in male of this species 44 chromosomes, all acrocentric, my data show the karyotype composed by 41 chromosomes, all biarmed, which is supposed to be ancestral for European species of *Atypus* (Řezáč et al. 2006). Considering that this karyotype occurs also in analyzed Asian species, it could be ancestral for the genus *Atypus*. As far as chromosome morphology is concerned, it is extremely unlikely that the population studied by Suzuki and our populations will differ fundamentally in the morphology of all chromosomes. The report of acrocentric karyotype in spiders studied by Suzuki could be due to the poor chromosome spreading because during this period hypotonic solution was not yet used. In addition, the *Atypus* has small chromosomes, it is difficult to determine their morphology. The absence of hypotonisation may also have led to the different diploid count reported by Suzuki. Concerning *Atypus*, a derived karyotype was found in *A. affinis* 2n♂= 14, XY (all chromosomes biarmed) from the Czech Republic (Řezáč et al. 2006). This karyotype arose from the set 41, X0 via multiple fusions, which took also part in formation of neo-sex chromosome system XY in this species (Řezáč et al. 2006). Suzuki (1954) reports an X_1X_20 system for *A. karschi*, but our revision did not confirm this system. In the male meiosis of entelegyne spiders, on which Suzuki otherwise mainly focused, two acrocentric X chromosomes are paired by their ends,

which closely resembles the metacentric X chromosome in the X0 system with a primary constriction in the middle of the chromosome, which we found in *A. karschi*. The X0 system, which is probably ancestral to the superfamily Atypoidea, may have arisen from the fusion of the X_1 and X_2 chromosomes in the X_1X_20 system, which is supposed to be ancestral in mygalomorphs (Král et al. 2013). Our findings in *A. karschi* support idea that X_1X_20 system is however not present in recent representatives of the superfamily.

Our study on *A. karschi* also includes detection of constitutive heterochromatin and NORs. In Mygalomorphae, the constitutive heterochromatin has been detected in several species only. These species do not belong to the family Atypidae. The pattern of the constitutive heterochromatin detected in *A. karschi* is similar to the distribution described in other spiders (Kořínková and Král 2013). The blocks of heterochromatin were found in the centromeric and telomeric regions (Řezáč et al. 2022). Nucleolus organizer regions of mygalomorphs were detected by silver staining or FISH (Král et al. 2013, Cabral-de-Mello and Marec 2021). Nucleolus organizer regions have been studied in a low number of mygalomorphs so far including four species of Atypoidea subfamily (Král et al. 2013). Thus, it is not yet possible to determine the basic traits of NOR evolution in mygalomorphs. The NORs of Atypoidea are placed on autosomes and their number range from one to four (Kořínková and Král 2013, Řezáč et al. 2022). In Atypoidea, they are localized in the ends of autosome pairs, which is probably an ancestral feature of the spiders (Kořínková and Král 2013). A single NOR was found in *A. karschi*. The low number of NORs is probably also an ancestral feature of spiders (Král et al. 2013). According to our data, the NOR of *A. karschi* is associated with the large block of heterochromatin. The comparison of location of heterochromatin and NOR revealed that NOR-associated heterochromatin is composed by inactive rDNA, which is common in eukaryotes (Fujiwara et al. 1998, Guetg and Santoro 2012).

5.2 Karyotype evolution in Pholcidae spiders

Current phylogenetic analyses have resulted in many taxonomic changes in haplogyne araneomorphs, which are now composed of Synspermiata and the clade formed by the families Hypochilidae and Filistatidae (Wheeler et al. 2017, Fernandez et al. 2018, Kulkarni et al. 2021, 2023). While chromosomes of most haplogynes have standard structure, chromosomes of members of the superfamily Dysderoidea are holokinetic (Král et al. 2019).

I selected the family Pholcidae as a model group of haplogynes with standard chromosome structure for the analysis of karyotype evolution at the family level. This family is very suitable for these purposes. It is the most diverse family of haplogyne spiders (World Spider Catalog 2024), and it has a worldwide distribution, especially in the tropics and subtropics (Huber 2011). Some species are synanthropic (Huber 2005a). Finally, pholcid molecular phylogeny was studied in detail (Huber et al. 2018).

Although pholcids are the most studied group of haplogynes from the cytogenetic point of view, the reconstruction of their karyotype evolution was only made possible after inclusion of information contained in the papers included in my thesis, which provide data on a further 63 species. These species represent an extensive cross-section through all major pholcids clades (Ávila et al. 2021, Král et al. 2022, Huber et al. 2022, 2023a,b,c). Moreover, we determined NOR pattern of 41 species. Large dataset on pholcid NORs allowed us to reconstruct the evolution of this key chromosome structure at the family level for the first time in spiders (Ávila et al. 2021, Král et al. 2022, Huber et al. 2022, 2023a,b,c).

Analyzed species show karyotype dominated by biarmed chromosomes. While predomination of biarmed chromosomes seem to be symplesiomorphy of opisthothele spiders (Král et al. 2013), the male diffuse stage is probably synapomorphy of Haplogynae clade (Král *et al.* 2006; Kořínková & Král 2013, Ávila et al. 2021, Král et al. 2022). Predomination of acrocentric chromosomes was reported only in the species *Pholcus manueli* (Xiuzhen et al. 1997a). However, this conclusion is based on the pattern of heterochromatin on mitotic chromosomes only. According to our experience, it could be difficult to determine unequivocally whether the blocks of heterochromatin are located in the centromeric region of mitotic chromosomes in pholcids; they may be also intercalary ones. This is consistent with our unpublished findings in this species, which show that its karyotype is dominated by biarmed chromosomes as in other pholcids.

The most basal clade of pholcids is the subfamily Arteminae. Our karyotype data indicate that this subfamily is paraphyletic (Ávila et al. 2021). Except for *Artema*, all other genera nest karyotypically with the subfamily Modisiminae. The same pattern was revealed by molecular phylogeny (Huber et al. 2018). Furthermore, some authors report X_1X_20 system in *Artema atlanta* (Sharma & Parida, 1987, Parida & Sharma, 1987a, Arunkumar & Jayaprakash 2015). Our results showed system X_1X_2Y including tiny Y chromosome, which was probably overlooked by previous authors. Several Syspermiata spiders display

the same karyotype as *A. atlanta* (2n♂=33, X_1X_2Y), namely *Filistata insidiatrix* (Filistatidade) and *Paculla* sp. (Pacullidae) (Král et al. 2019). Therefore, the ancestral pholcid karyotype could be the same as found in these spiders. Phylogenetic distribution of 2n♂=33, X_1X_2Y karyotype indicates that it could be also ancestral for haplogynes (Ávila et al. 2021). Alternatively, it could be karyotype 39, X_1X_2Y found in the haplogyne family Drymusidae. Very similar karyotype has been found in austrochilids 2n♂=38, XY (Král et al. 2006), which are the most basal members of the lineage formed by protoentelegynes and entelegynes, sister clade of haplogynes. At present, cytogenetic information is not sufficient to decide which of these hypothesis on ancestral haplogyne karyotype is correct.

In some pholcids, several different diploid numbers have been reported. According to our results, the populations of *Micropholcus fauroti* from Brazil and Cabo Verde islands, and South Africa display the lowest diploid number found in Pholcidae, 2n♂=9 (Ávila et al. 2021). In another Brazilian population, male karyotype 17, X0 has been reported (Araujo et al. 2005b). This result is most likely wrong. Presumably the two fused figures were scored as a single, so the number of chromosomes was approximately double compared to our karyotype. Our conclusion is supported by data of the other species of the genus, which possess also karyotype 2n♂=9 (Lomazi et al. 2018). Likewise, different karyotypes has been reported in the synanthropic species *Crossopriza lyoni*, the diploid number of Indian populations range from 23 to 27 (Bole-Gowda 1958, Srivastava & Shukla 1986, Parida & Sharma, 1987a, Sharma & Parida, 1987). In contrast to this, the populations from Brazil (Oliveira et al. 2007) and Vietnam (Ávila et al. 2021) exhibit the same karyotype 23, X0, which we also found in other *Crossopriza* species (Ávila et al. 2021). The increase of the diploid number in the Indian populations can be explained on the basis of fissions of autosomes, however this rearrangement is improbable as it was not found in other pholcids. Therefore, the most probable cause of karyotype diversity is the misidentifications of the specimens by some authors. This idea is supported by distribution of diploid numbers in the subfamily Smeringopinae. Karyotypes with higher number of chromosomes reported for *C. lyoni* were also found in the some other clades of the subfamily Smeringopinae but in the clade containing *Crossopriza* only karyotype with 23 chromosomes has been reported (Ávila et al. 2021).

During the evolution of spiders, the number of chromosomes was reduced in multiple clades by chromosome fusions (Suzuki 1954, Král et al. 2006, Kořínková and Král 2013).

This process also occurred during the karyotype evolution of many pholcid clades (Ávila et al. 2021, Huber et al. 2023a,b). In some species there were one or two monoarmed pairs, produced by pericentric inversion or translocation (Ávila Herrera et al. 2021), as for example a monoarmed pair in most representatives of the genus *Pholcus* (Král et al. 2022). It is probably a synapomorphy of Euroean clades of *Pholcus* or all this genus (Král et al. 2022). My data show that in this genus the monoarmed pair was formed by pericentric inversion, and in some species the same rearrangement changed it back to a biarmed pair (Král et al. 2022). The centric fusion of two monoarmed pairs may then have reduced the number of chromosomes (Ávila Herrera et al. 2021).

According to our results, Pholcidae show very diverse SCS, namely X0, X_1X_20, $X_1X_2X_30$, XY, X_1X_2Y, $X_1X_2X_3Y$, and $X_1X_2X_3X_4Y$ (Ávila et al. 2021, Král et al. 2022, Huber et al. 2023a,b). The X_1X_2Y system, which is considered to be ancestral for araneomorphs (Paula-Neto et al. 2017), has been reported in 7 families of haplogynes, namely Filistatidae (Král et al. 2006, 2019, Paula-Neto et al. 2017), Drymusidae (Král el at. 2006), Hypochilidae (Král el at. 2006), Pacullidae (Král et al. 2019), Pholcidae (Král et al. 2006, 2022, Ávila et al. 2021, Huber et al. 2023a,bc, 2024), Plectreuridae (Ávila et al. 2016), and Sicariidae (Silva et al. 1988, 2002, Král et al. 2006, Kumbiçak, 2014, Araujo et al. 2020, Sember et al. 2020). Placement of available karyotype data into the recent spider phylogenetic trees suggest that X_1X_2Y system could arise even in common ancestor of mygalomorphs and araneomorph spiders (Ávila et al. 2021). Supposed ancestral SCS of entelegynes and mygalomorphs, X_1X_20, could evolve from X_1X_2Y system via the deletion of Y chromosome (Paula-Neto et al. 2017, Ávila et al. 2021). Origin of the X_1X_2Y system remains unresolved. Silva et al. (2002) proposed the origin of X_1X_2Y system by the rearrangements between autosomes and sex chromosomes. According to another hypothesis, these chromosomes evolved from CSCP chromosomes via nondisjunctions (Ávila et al. 2021). The chromosomes composing the X_1X_2Y system are dynamic elements, they were modified frequently by rearrangements during the Pholcidae evolution. The common rearrangements were the pericentric inversions and translocations between sex chromosomes and between sex chromosomes and autosomes, which do not change the sex chromosome number (Král et al. 2022). Rearrangements of sex chromosomes often result in reproductive isolation (Rieseberg 2001, Ayala et al. 2005).

Some rearrangements led to changes in the number of sex chromosomes and change of the sex chromosome system. In haplogynes the diverse sex chromosomes systems evolved from the ancestral X_1X_2Ysystem. According our results from pholcids, in some clades the Y chromosomes has been lost, giving rise to the X_1X_20 system (Ávila et al. 2021). In other pholcid clades, XY system has evolved by the X chromosome fusion (Ávila et al. 2021). X0 system found in some pholcids arose from X_1X_20 system. In other clades it has evolved from XY system (Ávila et al. 2021). Entelegyne and mygalomorph spiders display frequently the $X_1X_2X_30$ system (Král et al. 2013, Araujo et al. 2014). Nevertheless, in haplogynes it was only described in one species, namely *Smeringopus pallidus* (Pholcidae). Origin of the $X_1X_2X_30$ system in *Smeringopus* is unresolved. It could arise from X_1X_20 system by nondisjunction as supposed in many entelegynes (Šťáhlavský et al. 2020), or by fission of biarmed chromosomes followed by pericentric inversion of resulting products (Ávila et al. 2021). The unique systems with more sex chromosomes have been detected in the subfamily Ninetinae, namely $X_1X_2X_3Y$ and $X_1X_2X_3X_4Y$ (Huber et al. 2023 a,b, 2024). According Huber et al. (2023 a,b), these systems arose from the X_1X_2Y system by fissions of biarmed X chromosomes and/or by non-disjunctions (Huber et al. 2024).

Nucleolus organizer regions have been detected in spiders mostly by silver staining so far (Oliveira et al. 2007, Dolejš et al. 2011, Král et al. 2006, 2013). This approach detects only NORs, which were transcriptionally active during preceding interphase (Miller et al. 1976). In my studies, I detected NORs by FISH (Ávila et al. 2021, Král et al. 2022). This approach allow to detect all NORs including inactive ones. The most NORs of pholcids show terminal location. This position suggests that NORs have expanded to other location usually by ectopic recombination. These events are more frequent in telomeric areas (Goldman and Lichten 1996). The ectopic recombinations have been found in many organisms, for example yeast, tobacco, and *Drosophila* (Ayala et al. 2005, Roy et al. 2005).

According to our results, Pholcidae display very diverse NORs numbers, from one to nine loci (Ávila et al. 2021, Král et al. 2022). Some pholcids exhibited the sex-chromosome-linked NORs. Our results show that this location arose independently several times in pholcids (Ávila et al. 2021). Sex chromosome-linked NORs are also frequent in other haplogynes (e.g., Král et al. 2006, Ávila et al. 2016). This feature is a synapomorphy of

some haplogyne clades (Král et al. 2006, Ávila et al. 2021). By contrast, this location is rare in mygalomorphs and entelegynes (Král et al. 2011, 2013, Araujo et al. 2015).

The sex chromosome-linked NORs of pholcids are almost always located on the X chromosomes (Ávila et al. 2021). Y chromosome exhibit frequently a high condensation, which probably reduces spreading of NORs on this element. Placement of sex-chromosome linked NORs at the ends of sex chromosomes involved into achiasmatic sex chromosome pairing during male meiosis suggest that NORs could be involved into this pairing (Ávila et al. 2021, Král et al. 2022). Sember et al. (2020) revealed by CGH that some sequences of the Y chromosomes spreaded to the terminal part of the X_2 chromosome. These sequences could also take part in the paring of the sex chromosomes. Some species of the genus *Pholcus* have lost sex-linked NORs (Ávila Herrera et al. 2021, Král et al. 2022). However, rDNA sequences responsible for pairing may persist on the sex chromosomes, as in some species of *Drosophila* (Roy et al. 2005, Presgraves 2008)

6. Conclusions and future directions

The aim of the thesis was to analyze the karyotype evolution of selected clades of haplogyne and mygalomorph spiders by conventional and molecular cytogenetic methods.

In mygalomorphs I focused on the revision of the karyotype of the atypid *Atypus karschi*. The original description of its karyotype was highly inaccurate neither the diploid number, chromosome morphology nor the sex chromosome determination system was correctly determined. Revised data show that the karyotype of this East Asian species is very similar to European representatives of the genus. The first data on heterochromatin distribution and nucleolar organizers in the family Atypidae have been obtained. Furthermore, the probable ancestral karyotype of the genus *Atypus* was determined. Although the data obtained are of great importance for understanding the evolution of karyotype in the mygalomorphs of the superfamily Atypoidea, many more species, representatives of all families of Atypoidea, will have to be investigated. To understand karyotype evolution in the mygalomorphs, the superfamily Avicularioidea should also be more thoroughly analyzed. Attention should be focused in particular on phylogenetically basal families, which are mostly understudied, and on families not yet karyotyped.

Concerning haplogynes, I focused on Pholcidae, the most diverse haplogyne family with monocentric structure of chromosomes. This is the first analysis of karyotype evolution at the family level in monocentric haplogynes. Diploid numbers ranged widely in these spiders, and sex chromosome systems and patterns of nucleolar organizers were also diverse. Diploid numbers found in the genus *Micropholcus* were lowest in araneomorph spiders with standard chromosome structure. On the basis of my findings, hypotheses about the ancestral karyotype of haplogyne spiders were made. In the course of pholcid evolution, the diploid chromosome number decreased in different branches as in most other spider groups. As in most other monocentric haplogynes, karyotypes of pholcids were dominated by biarmed chromosomes. This pattern is probably ancestral for opisthothele spiders. The ancestral sex chromosome system in pholcids is the X_1X_2Y system, available data suggests that it is probably also ancestral to araneomorph spiders. This system has been further changed by rearrangements involving inversions, translocations, chromosome fissions and fusions. In various clades, the number of X chromosomes increased or decreased, while in some branches the Y chromosome was

lost or increased in size. In some lineages, autosome fragments have been probably integrated into sex chromosomes. Complicated sex chromosomes systems $X_1X_2X_3Y$ and $X_1X_2X_3X_4Y$ have been found in the subfamily Ninetinae. Their origin could involve nondisjunctions. Pholcids, as other haplogynes, exhibited a specific meiotic modification in male prophase I, which is called diffuse stage. This period is distinguished by an extreme decondensation of bivalents.

My data allowed to analyse NOR evolution on family level, for the first time in spiders. The ancestral feature is probably a single autosomal terminal NOR. During following evolution, number of NORs increased. Furthermore, NORs often spreaded to sex chromosomes via ectopic recombination. Sex-chromosome linked NORs were probably involved in the achiasmatic pairing. Finally, number of autosome and sex chromosome linked NORs was reduced in some clades. In some species of *Pholcus*, sex-chromosome linked NORs have disappeared completely. Nevertheless, sequences of rRNA clusters that play a role in chromosome pairing may persist, as has been shown in *Drosophila*. It would be interesting to test this hypothesis.

Data from other haplogyne families show that many of the processes of karyotype differentiation found in pholcids may also apply to other groups, such as a similar pattern of sex chromosome evolution or a reduction in diploid number. In addition, there are trends that are largely absent or missing in pholcids, such as chromosome fissions or polyploidization. The evolution of haplogyne spiders with holokinetic chromosomes is very specific and distinct. In order to describe the global karyotype evolution of haplogyne spiders, the karyotypes of a much larger number of species need to be analyzed, which is especially true for rDNA clusters in nucleolar organizers. The pattern of evolution of other gene clusters and other genes at karyotype of haplogynes remains unexplored. Our results suggest a low intraspecific diversity of pholcid karyotypes. In *P. phalangioides*, two cytotypes were revealed, which differ by several karyotype features. These cytotypes could be separate species. This shows that cytogenetic data can also be important for taxonomy and phylogeny of spiders.

7. References

Abbott JK, Nordén AK, Hansson B (2017). Sex chromosome evolution: historical insights and future perspectives. Proc. Biol. Sci. 284, 20162806.

Akan Z, Varol I, Özaslan MA (2005). Cytotaxonomical investigation on spiders (Arachnida: Araneae). Environ. Biotechnol. 19, 101–104.

Almeida BRR, Noronha RCR, Costa MRJ, Nagamachi CY, Pieczarka JC (2019). Meiosis in scorpion *Tityus silvestris*: new insigths into achiasmatic chromosome. Biol. Open. 8: bio040352.

Araujo D, Rheims CA, Brescovit AD, Cella DM (2008). Extreme degree of chromosome number variability in species of the spider genus *Scytodes* (Araneae, Haplogynae, Scytodidae). J. zool. syst. evol. res. 46, 89–95.

Araujo D, Schneider MC, Paula-Neto E, Cella DM (2012). Sex chromosomes and meiosis in spiders: a review. In Meiosis—Molecular mechanisms and cytogenetic diversity. Swan A, Ed. In Tech Open: Rieka, Croatia. pp. 87–108.

Araujo D, Oliveira EG, Giroti AM, Mattos VF, Paula-Neto E, Brescovit AD, Schneider MC, Cella DM (2014). Comparative cytogenetics of seven Ctenidae species (Araneae). Zool. Sci. 31, 83–88.

Araujo D, Paula-Neto E, Brescovit AD, Cella DM, Schneider MC (2015). Chromosomal similarities between *Nephilidae* and Tetragnathidae indicate unique evolutionary traits among Araneoidea. Ital. J. Zool. 82, 513–520.

Araujo D, Schneider MC, Zacaro AA, de Oliveira EG, Martins R, Brescovit AD (2020). Venomous *Loxosceles* species (Araneae, Haplogynae, Sicariidae) from Brazil: $2n♂= 23$ and X_1X_2Y sex chromosome system as shared characteristics. Zool. Sci. 37, 128–39.

Araujo D, Schneider MC, Paula-Neto E, Cella DM (2024). The spider cytogenetic database. Available in www.arthropodacytogenetics.bio.br/spiderdatabase (Accessed on June 17th, 2024).

Arunkumar S, Jayaprakash (2015). Chromosomal studies of two spider species of Pholcidae (Aranae: Haplogynae). Int. J. Curr Res. 2, 2650–3.

Alvarez L, Perafán C, Pérez-Milles (2016). At what time, for what distance, and for how long does the tarantula *Eupalaestrus weijenberghi* (Aranae, Theraphosidae) leave its burrow during the mating season. Arachnology. 17, 152–154.

Ávila Herrera IM, Carabajal Paladino LZ, Musilová J, Palacios Vargas JG, Forman M, Král J (2016). Evolution of karyotype and sex chromosomes in two families of haplogyne spiders, Filistatidae and Plectreuridae. In: Martins C, Pedrosa-Harand A, Houben A, Sullivan B, Martelli L, O´Neil R, Eds. 21st international chromosome conference. Foz do Iguaçu, Brazil. Cytogenet. Genome. Res. 148,104.

Ávila Herrera IM, Král J, Pastuchová M, Forman M, Musilová J, Kořínková T, Šťáhlavský F, Zrzavá M, Nguyen P, Just P, et al (2021). Evolutionary pattern of karyotypes and meiosis in pholcid spiders (Araneae: Pholcidae): Implications for reconstructing chromosome evolution of araneomorph spiders. BMC. Ecol. Evol. 21, 75.

Ayala F, Coluzzi M (2005). Chromosome speciation: humans, *Drosophila*, and mosquitoes. Proc. Natl. Acad. Sci. USA. 1, 6535–42.

Bachtrog D, Kirkpatrick M, Mank JE, McDaniel SF, Pires JC, Rice W, Valenzuela N. (2011) Are all sex chromosomes created equal? Trends. Genet. 27, 350–7.

Bachtrog D (2013). Y-chromosome evolution: emerging insights into processes of Y-chromosome degeneration. Nat. Rev. Genet. 14, 113–24.

Benavente R, Wettstein R (1977). An ultrastructural cytogenetic study on the evolution of sex chromosomes during the spermatogenesis of *Lycosa malitiosa* (Arachnida). Chromosoma. 64, 255–277.

Benavente R, Wettstein R (1980). Ultrastructural characterization of the sex chromosomes during spermatogenesis of spiders having holocentric chromosomes and a long diffuse stage. Chromosoma. 77, 69–81.

Benavente R, Wettstein R, Papa M (1982). Ultrastructural analysis of the $X_1X_2X_30$ sex chromosome system during the spermatogenesis of *Tegenaria domestica* (Arachnida). J. Cell. Sci. 58, 411–422.

Bole-Gowda BN (1950). The chromosome study in the spermatogenesis of two lynx-spiders (Oxyopidae). Proc. Zool. Soc. 3, 95–107.

Bole-Gowda BN (1952). Studies on the chromosomes and the sex-determining mechanism in four hunting spiders (Sparassidae). Proc. Zool. Soc. 5, 51–70.

Bole-Gowda BN (1958). A study of the chromosomes during meiosis in twenty-two species of Indian spiders. Proc. Zool. Soc. 11, 69–108.

Bond JE, Hendrixson BE, Hamilton CA, Hedin M (2012). A reconsideration of the classification of the spider infraorder Mygalomorphae (Arachnida: Araneae) based on three nuclear genes and morphology. PLoS ONE. 7, e38753.

Beukeboom LW (1995). Sex determination in Hymenoptera: a need for genetic and molecular studies. BioEssays. 17, 813–817.

Beukeboom LW and Perrin N (2014). The evolution of sex determination. In: Oxford, UK: Oxford University Press.

Blackmon H, Ross L, Bachtrog D (2017). Sex determination, sex chromosomes, and karyotype evolution in insects. J. Hered. 108, 594.

Butlin RK (2005). Recombination and speciation. Mol. Ecol. 14, 2621–2635.

Bureš P, Zedek F, Marková M (2013). Holocentric cromosomes. In: Greilhuber J, Dolezel J, Wendel J, Eds. J. Plant. Genome. Sci. Springer, Vienna.

Bureš P, Zedek F (2014). Holokinetic drive: Centromere drive in chromosomes without centromeres. Evolution. 68, 2412–20.

Bureš P. (2018) Holocentric chromosomes: From tolerance to fragmentation to colonization of the land. Ann. Bot. 121, 9–16.

Cabral G, Marques A, Schubert V, Pedrosa-Harand A, Schlogelhofer P (2014). Chiasmatic and achiasmatic inverted meiosis of plants with holocentric chromosomes. Nat. Commun. 5, 5070.

Cabral-de-Mello D, Martins C (2010). Breaking down the genome organization and karyotype differentiation through the epifluorescence microscope lens: insects and fish as models. In: Méndez-Vilas A, Díaz J, Eds. Formatex, Research Center, Badajoz, Spain. 658–669.

Cabral-de-Mello DC, Marec F (2021). Universal fluorescence in situ hybridization (FISH) protocol for mapping repetitive DNAs in insects and other arthropods. Mol. Genet. Genom. 296, 513-526.

Cavenagh AF, Rincão MP, Dias FC, Brescovit AD, Dias AL (2022). Chromosomal diversity in three species of *Lycosa Latreille*, 1804 (Araneae, Lycosidae): inferences on diversification of diploid number and sexual chromosome systems in Lycosinae. Genet. Mol. Biol. 45,1e20200440.

Charlesworth B (1978). Model for evolution of Y chromosomes and dosage compensation. Proc. Natl. Acad. Sci. USA. 75, 5618-5622.

Charlesworth D (2021).When and how do sex-linked regions become sex chromosomes? Evolution. 75, 569–581.

Coddington JA (2005). Phylogeny and classification of spiders. In: Spiders of North America: An Identification Manual; Ubick D, Paquin P, Cushing PE, Roth V, Eds. American Arachnology Society: San Francisco, CA, USA. 18–24.

Coddington JA, Levi HW (1991). Systematics and evolution of spiders (Araneae). Annu. Rev. Ecol. Syst. 22, 565–592.

Cokendolpher JC and Brown JD (1985). Air-dry method for studying chromosomes of insects and arachnids. Entomol. News. 96, 114–118.

Cokendolpher JC (1989). Karyotypes of three spider species (Araneae: Pholcidae: *Physocyclus*). J.N.Y. Entomol. Soc. 97, 475–478.

Cordellier M, Schneider JM, Uhl G, Posnien N (2020). Sex differences in spiders: from phenotype to genomics. Dev. Genes. Evol. 230, 155–172.

Costa FG, Pérez-Miles F (2002). Reproductive biology of Uruguayan Theraphosids (Araneae, Mygalomorphae). J. Arachnol. 30, 571–587.

Cuacos MH, Franklin FC, Heckmann S. (2015). Atypical centromeres in plants what they can tell us. Front. Plant. Sci. 6, 1247.

da Costa Pinto Neto JP, Pinto Neto L, Gusso Goll L, Gross C, Gross MC, Feldsberg E, Schneide CH (2020). Cytogenetic analysis of three Ctenidae species (Araneae) from the Amazon. Genet. Mol. Biol. 16, 43(4), e20200069.

Dapper AL, Slater GP, Shores K, Harpur BA (2022). Population Genetics of Reproductive Genes in Haplodiploid Species. Genome. Biolo. Evol. 14, evac070.

Datta SN and Chtterjee K (1988). Chromosomes and sex determination in 13 araneid spiders of North-Eastern India. Genetica. 76, 91–99.

Dedukh D, da Cruz I, Kneitz S, Anatolie M, Ormanns J, Tichopád T, Lu Y, Alsheimer M, Janko K, Schartl M (2022). Achiasmatic meiosis in the unisexual Amazon molly, *Poecilia formosa*. Chromosome. Res 30, 443–457.

de Vos JM, Augustijnen H, Bätscher L, Lucek K (2020). Speciation through chromosomal fusion and fission in Lepidoptera: Chromosomal fusion & fission. Philos. Trans. R. Soc. B. Biol. Sci. 375, 20190539.

Dernburg AF (2001). Here, there, and everywhere: kinetochore function on holocentric chromosomes. J. Cell. Biol. 153, F33–8.

Diaz MO and Saez FA (1966). Karyotypes of South-American Araneida. Mem. Inst. Butantan. 33, 153–154.

Diaz MO, Maynard R, Brum-Zorrilla N (2010). Diffuse centromere and chromosome polymorphism in haplogyne spiders of the families Dysderidae and Segestriidae. Cytogenet. Genome. Res. 128, 131–138.

Drinnenberg IA, deYoung D, Henikoff S, Malik HS (2014). Recurrent loss of CenH3 is associated with independent transitions to holocentricity in insects. Elife. 3, e03676.

Dolejš P, Kořínková T, Musilová J, Opatová V, Kubcová L, Buchar J, Král J *(2011).* Karyotypes of central European spiders of the genera *Arctosa*, *Tricca* and *Xerolycosa* (Araneae: Lycosidae). Eur. J. Entomol. 108, 1–16.

Duarte Dutra D, Brescovit AD, Araujo D (2023). Chromosomal study on selected small araneomorph spiders from Brazil, including the first records in Palpimanidae and Theridiosomatidae (Araneae, Araneomorphae). Zool. Stud. 62, e42.

Eroğlu HE, Sedat P (2016). Karyotype analysis of *Zygoribatula cognata* (Oudemans) (Acari: Oribatida: Oribatulidae). Türk. entomol. derg. 40, 1.

Escudero M, Hahn M, Brown BH, Lueders K, Hipp AL (2016). Chromosomal rearrangements in holocentric organisms lead to reproductive isolation by hybrid dysfunction: The correlation between karyotype rearrangements and germination rates in sedges. Am. J. Bot. 103, 1529–36.

Escuer P, Pisarenco VA, Fernández-Ruiz AA, Vizueta J, Sánchez-Herrero JF, Arnedo MA, Sánchez-Gracia A, Rozas J (2021). The chromosome-scale assembly of the Canary Islands endemic spider *Dysdera silvatica* (Arachnida, Araneae) sheds light on the origin and genome structure of chemoreceptor gene families in chelicerates. Mol. Ecol. Resour. 22, 375–390.

Escoubas P, Diochot S, Corzo G (2000). Structure and pharmacology of spider venom neurotoxins. Biochimie. 82, 893–907.

Fernández R, Kallal RJ, Dimitrov D, Ballesteros JA, Arnedo MA, Giribet G, Hormiga G (2018). Phylogenomics, diversification dynamics, and comparative transcriptomics across the spider tree of life. Curr. Biol. 28, 1489–1497.

Foelix RF (2011). Biology of Spiders. Second Edition. Oxford University Press. Thieme Verlag G, Edit. New York, Oxford.

Forman M, Nguyen P, Hula V, Král J (2013). Sex chromosome pairing and extensive NOR polymorphism in *Wadicosa fidelis* (Araneae: Lycosidae). Cytogenet. Genome. Res. 141, 43–9.

Franco JF and Andía JM (2013). El cariótipo de *Sicarius* sp. (Araneae: Haplogynae: Sicariidae), y sus relaciones citotaxonómicas. Bioma. 4–9.

Garb J, Sharma PP, Ayoub NA (2018). Recent progress and prospects for advancing arachnid genomics. Curr. Opin. Insect. Sci. 25, 51–57.

Garrison NL, Rodriguez J, Agnarsson I, Coddington JA, Griswold CE, Hamilton CA, et al (2016). Spider phylogenomics: untangling the spider tree of life. PeerJ**.** 4, e1719.

Gregory TR (2024). Animal Genome Size Database. http://www.genomesize.com. (Accessed on June 24th, 2024).

Golding AE, Paliulis LV (2011). Karyotype, sex determination, and meiotic chromosome behavior of two pholcid (Araneomorphae, Pholcidae) spiders: implications for karyotype evolution. PLoS. ONE. 9, e24748.

Griswold C, Ramirez M, Coddington J, Platnick N (2005). Atlas of phylogenetic data for entelegyne spiders (Araneae: Araneomorphae: Entelegynae) with comments on their phylogeny. Griswold C, Ramirez ME, Coddington JA, Platnick, Eds. 56, 1–324.

Galián, J. Serrano J, de la Rúa P (1995). Localization and activity of rDNA genes in tiger beetles (Coleoptera: Cicindelinae). J. Hered. 74, 524–530.

Gimenez- Pinheiro T, Carvalho LS, Brescovit AD, Magalhaes ILF, Schneider MC (2022). Cytogenetic study in sand spiders (Sicariidae) from the Brazilian Caatinga: Sex chromosome system diversity in closely related species. J. Basic. Appl. Genet. 33, 1–10.

Guetg C, Santoro R (2012). Formation of nuclear heterochromatin: The nucleolar point of view. Epigenetics. 7, 811–814.

Godwin RL, Opatova V, Garrison NL, Hamilton CA, Bond JE (2018). Phylogeny of a cosmopolitan family of morphologically conserved trapdoor spiders (Mygalomorphae, Ctenizidae) using Anchored Hybrid Enrichment, with a description of the family, Halonoproctidae (Pocock 1901). Mol. Phylogenetics. Evol. 126, 303–313.

Goldman AS, Lichten M (1996). The efficiency of meiotic recombination between dispersed sequences in *Saccharomyces cerevisiae* depends upon their chromosomal location. Genetics. 144, 43–55.

Hedin M, Derkarabetian S, Ramírez MJ, Vink C, Bond JE (2018). Phylogenomic reclassification of the world's most venomous spiders (Mygalomorphae, Atracinae), with implications for venom evolution. Sci. Rep. 8, 1636.

Hedin M, Derkarabetian S, Alfaro A, Ramírez MJ, Bond JE (2019). Phylogenomic analysis and revised classification of atypoid mygalomorph spiders (Araneae, Mygalomorphae), with notes on arachnid ultraconserved element loci. PeerJ. 7(e6864), 1–24.

Heethoff M, Bergmann P, Norton RA (2006). Karyology and sex determination of oribatid mites. Acaralogia. 46, 127–131.

Herberstein ME, Wignall AE (2011). Introduction: spider biology. In: Herberstein ME, Ed. Spider behaviour: flexibility and diversity. Cambridge, New York: Cambridge University Press.

Hetzler S (1979). Some studies of spider chromosomes. JoA. 20:20.

Hill C, Guerrero F, Zee J, Geraci N, Walling J, Stuart J (2009). The position of repetitive DNA sequence in the southern cattle tick genome permits chromosome identification. Chromosome Res. 17, 77–89.

Howell WM, Black DA (1980). Controlled silver-staining of nucleolus organizer regions with a protective colloidal developer: a 1-step method. Experientia. 36, 1014.

Hu X, Vasanthavada K, Kohler K, McNary S, More AMF, Vierra CA (2006). Molecular mechanisms of spider silk. Cell. Mol. Life Sci. 63, 1986–1999.

Huber BA (2005). Pholcidae. In: Ubick, D, Paquin P, Cushing, PE, Roth V, Eds. Spiders of North America: an identification manual. 194-196.

Huber BA (2011). Revision and cladistic analysis of *Pholcus* and closely related taxa (Araneae, Pholcidae). Bonn. Zool. Monogr. 58, 1–509.

Huber BA, Eberle J, Dimitrov D (2018). The phylogeny of pholcid spiders: a critical evaluation of relationships suggested by molecular data (Araneae, Pholcidae). ZooKeys. 789, 51–101.

Huber BA, Meng G, Král J, Ávila Herrera IM, Izquierdo MA, Carvalho LS (2023a). High and dry: integrative taxonomy of the Andean spider genus *Nerudia* (Araneae: Pholcidae). Zool. J. Linn. Soc. 198, 534–591.

Huber BA Meng G, Valdez-Mondragón A, Král J, Ávila Herrera IM, Carvalho, LS (2023b). Short-ledgged daddy-long-leg spiders in North America: the genera *Pholcophora* and *Tolteca* (Araneae, Pholcidae). Eur. J. Taxon. 880, 1–89.

Huber BA, Meng G, Král J, Ávila Herrera IM, Izquierd MA (2023c). Revision of the South American *Ninetinae* genus *Guaranita* (Araneae, Pholcidae). Eur. J. Taxon. 900, 32–80.

Huber BA, Meng G, Dederichs TM, Michalik P, Forman M and Král J (2024). Castaways: The Leeward Antilles endemic spider genus *Papiamenta* (Araneae: Pholcidae). Invertebr. Syst. 38, IS23052.

Jankowska M, Fuchs J, Klocke E, Fojtová M, Polanská P, Fajkus J, Schubert V, Houben A (2015). Holokinetic centromeres and efficient telomere healing enable rapid karyotype evolution. Chromosoma.124, 519–28.

Janssen A, Colmenares SU, Karpen GH (2018). Heterochromatin: Guardian of the genome. Annu. Rev. Cell Dev. Biol. 34, 265–288.

Kaiser VB, Bachtrog D (2010). Evolution of sex chromosomes in insects. Annu. Rev. Genet. 44, 91–112.

Kallal RJ, Kulkarni S, Dimitrov D, Benavides LR, Arnedo MA, Giribet G, Hormiga G (2020). Converging on the orb: denser taxon sampling elucidates spider phylogeny and new analytical methods support repeated evolution of the orb web. Cladistics. 37, 298–316.

Klášterská I (1977): The concept of the prophase of meiosis. Hereditas. 86, 205 –210.

Kořínková T, Král J (2013). Karyotype, sex chromosomes, and meiotic division in spiders. In: Netwing W, Ed. Spider Ecophisiology. Springer Verlag, Berlin. 159–172.

Král J (1994a). Holokinetic (holocentric) chromosomes. Biol. Listy. 59: 191–217. [In Czech, with English summary].

Král J, Musilová J, Šťáhlavský F, Řezáč M, Akan Z, Edwards R, Coyle F, Ribera C (2006). Evolution of the karyotype and sex chromosome systems in basal clades of araneomorph spiders (Araneae: Araneomorphae). Chromosome Res. 14, 859–880.

Král J (2007). Evolution of multiple sex chromosomes in the spider genus *Malthonica* (Araneae: Agelenidae) indicates unique structure of the spider sex chromosome systems. Chromosome. Res. 15, 863–79.

Král J, Kováč L, Šťáhlavský F, Lonský P, Ľuptáčik P (2008): The first karyotype study in palpigrades, a primitive order of arachnids (Arachnida: Palpigradi). Genetica. 134, 79–87.

Král J, Kořínková T, Forman M, Krkavcová L (2011). Insights into the meiosis behavior and evolution of multiple sex chromosome systems in spiders. Cytogenet. Genome. Res. 133, 43–66.

Král J, Kořínková T, Krkavcová L, Musilová J, Forman M, Ávila Herrera IM, Haddad C R, Vítková M, Henriques S, Vargas JGP, Hedin M (2013). Evolution of karyotype, sex chromosomes, and meiosis in mygalomorph spiders (Araneae: Mygalomorphae). Biol. J. Linn. Soc. 109, 377–408.

Král J, Forman M, Kořínková T, Reyes Lerma AC, Haddad CR, Musilová J, Řezáč M, Ávila Herrera IM, Thakur S, Dippenaar-Schoeman AS, Marec F, Horová L, Bureš P (2019). Insights into the karyotype and genome evolution of haplogyne spiders indicate a polyploid origin of lineage with holokinetic chromosomes. Sci. Rep. 9: 3001.

Král J, Ávila Herrera IM, Šťáhlavský F, Sadílek D, Pavelka J, Chatzaki M, Huber BA (2022). Karyotype differentiation and male meiosis in European clades of the spider genus *Pholcus* (Araneae, Pholcidae). Comp. Cytogenet. 16, 185–209.

Kuznetsova V, Grozeva S, Gokhman V (2019). Telomere structure in insects: A review. J. Zool. Syst. Evol. Res. 58, 127–158.

Kurdzo EL, Dawson DS (2015). Centromere pairing – tethering partner chromosomes in meiosis I. FEBS J. 282, 2458-70.

Kurdzo EL, Chuong HH, Evatt JM, Dawson DS (2018). A ZIP1 separation-of-function allele reveals that centromere pairing drives meiotic segregation of achiasmate chromosomes in budding yeast. PLoS. Genet. 14, e1007513.

Kulkarni S, Hormiga (2021). Hooroo mates! Phylogenomic data suggest that the closest relatives of the iconic Tasmanian cave spider *Hickmania troglodytes* are in Australia and New Zealand, not in South America. Invertebr. Syst. 35, 850–856.

Kulkarni S, Wood HM, Hormiga G (2023). Advances in the reconstruction of the spider tree of life: A roadmap for spider systematics and comparative studies. Cladistics. 39, 479–532.

Kumbiçak Z (2014). Cytogenetic characterization of ten araneomorph spiders (Araneae): karyotypes and meiotic features. J. Biol. 69, 644–650.

Kumar SA, Venu G, Jayaprakash G, Venkatachalaiah G (2017). Studies on chromosomal characteristics of *Ctenus indicus* (Gravely 1931) (Araneae: Ctenidae). Nucleus 60, 1.

Lanzone C, de Souza MJ (2006). Chromosome complement and meiosis in three species of the Neotropical bug genus *Antiteuchus* (Heteroptera, Pentatomidae, Discocephalinae). Genet. Mol. Biol. 29, 49–55.

Lomazi RL, Araujo D, Carvalho LS, Schneider MC. (2018). Small pholcids (Araneae: Synspermiata) with big surprises: the lowest diploid number in spiders with monocentric chromosomes. J. Arachnol. 46, 45–49.

Lucas S, Da silva Jr, I and Bertani R (1993). *Vitalius* a new genus of the subfamily Theraphosinae (Thorell, 1870) (Araneae: Theraphosidae) from Brazil. Spixiana. 16, 241–245.

Maddison WP (1982). XXXY sex chromosomes in males of the jumping spider genus *Pellenes* (Araneae: Salticidae). Chromosoma. 5, 23–37.

Maddison WP, Leduc-Robert G (2013). Multiple origins of sex chromosome fusions correlated with chiasma localization in *Habronattus* jumping spiders (Araneae: Salticidae). Evolution. 67, 2258–2272.

Maddison WP, Maddison DR, Derkarabetian S, Hedin M (2020). Sitticine jumping spiders: phylogeny, classification, and chromosomes (Araneae, Salticidae, Sitticini). ZooKeys. 925, 1–54.

McDaniel SF, Perroud PF (2012). Invited perspective: Bryophytes as models for understanding the evolution of sexual systems. Bryologist. 115, 1–11.

McStay B. (2016). Nucleolar organizer regions: Genomic ‘dark matter’ requiring illumination. Genes. Dev. 30, 1598–1610.

Mandrioli M, Manicardi GC (2012). Unlocking holocentric chromosomes: New perspectives from comparative and funcional genomics? Curr. Genomics. 13, 343–349.

Mandrioli M, Manicardi GC (2020). Holocentric chromosomes. PLoS. Genet. 16, e1008918.

Melters DP, Paliulis LV, Korf IFS, Chan SWL (2012). Holocentric chromosomes: convergent evolution, meiotic adaptations, and genomic analysis. Chromosome. Res. 20, 579–593.

Michalik P, Ramírez MJ (2014). Evolutionary morphology of the male reproductive system, spermatozoa and seminal fluid of spiders (Araneae, Arachnida) – Current knowledge and future directions. Arthropod. Struct. Dev. 43, 291–322.

Miller O, Miller D, Dev V, Tantravahi R, Croce C (1977). Expression of human and suppression of mouse nucleolus organizer activity in mouse – human somatic cell hybrids. Proc. Natl. Acad. Sci. USA. 73, 4531–5.

Millot J, Tuzet, O (1934). La spermatogenèse chez les Pédipalpes. Bull. Biol. Fr. Belg. 68, 77–83.

Mola LM, Papeschi AG (2006). Holokinetic chromosomes at a glance. J. Appl.Genet. 17, 17–33.

Mola LM, Rebagliati PJ, Rodríguez-Gil SG, Adilardi RS (2011). Variaciones meióticas y evolución cromosómica en insectos y arácnidos con cromosomas holocinéticos. J. Appl.Genet. 22, 1.

Nagaki K, Kashihara K, Murata M (2005). Visualization of diffuse centromeres with centromere-pecific histone H3 in the holocentric plant *Luzula nivea*. Plant. Cell. 17, 1886–1893.

Neumann P, Oliveira L, Jang T-S, Novák P, Koblížková A, Schubert V, Houben A, Macas J (2023). Disruption of the standard kinetochore in holocentric *Cuscuta* species. Proc Natl Acad Sci USA. 120, e2300877120.

Norton RA, Kethley J, Johnston DE, O'Connor BM (1993). Phylogenetic perspectives on genetic systems and reproductive modes of mites. In: Wrensch

D.L. & Ebbert MA, Eds. Evolution and diversity of sex ratio in insects and mites. Chapman & Hall, New York. 8–99

Oliveira RM, Jesus AC, Brescovit AD, Cella DM (2007). Chromosomes of *Crossopriza lyoni* (Blackwall 1867), intraindividual numerical chromosome variation in *Physocyclus globosus* (Taczanowski 1874), and the distribution pattern of NORs (Araneomorphae, Haplogynae, Pholcidae). J. Arachnol. 35, 293–306.

Oliver J H Jr (1977). Cytogenetics of mites and ticks. Annu. Rev. Entomol. 22, 407–429.

Oliver JH. Jr (1983). Chromosomes, genetic variance and reproductive strategies among mites and ticks. Bull. Entomol. Soc. Amer. 29, 8–17.

Opatova V, Halmilton CA, Hedin M, Montes de Oca L, Král J, Bond JE (2020). Phylogenetic systematics and evolution of the spider infraorder Mygalomorphae using genomic scale data. Syst. Biol. 69, 671–707.

Painter TS. (1914). Spermatogenesis in spiders. Zool. Jahrb. Abt. Anat. Ontog. Tiere. 38, 509–576.

Palazzo AF, Lee ES (2015). Non-coding RNA: what is functional and what is junk? Front. Genet. 6, 2.

Parida BB, Sharma NN (1987a). Chromosome number, sex mechanism and genome size in 27 species of Indian spiders. Chromosome. Inf. Serv. 43, 11–13.

Parida BB, Sharma NN (1987b). Cytological studies on Indian spiders I. Meiosis in three species of wolf spiders (Lycosidae: Arachnida). Caryologia. 40, 89–97.

Patau K (1948). X-segregation and heterochromasy in the spider *Aranea reaumuri*. J. Hered. 2, 77–100.

Paula-Neto E, Cella D, Araujo D, Brescovit A, Schneider M. (2017). Comparative cytogenetic analysis among filistatid spiders (Araneomorphae: Haplogynae). J. Arachnol. 45, 123–128.

Prakash A, Prakash S (2014a). Short term somatic cell culture approach for cytogenetic analysis of *Crossopriza lyoni* spider: Pholcidae. Int. J. Eng. Res. 8, 29–32.

Penney D, Selden PA (2011). Fossil Spiders: the evolutionary history of a mega-diverse order. ZooKeys. 119, 73–76.

Pérez-Miles F, Perafán C (2020). Theraphosinae. In: Pérez-Miles, F, Ed. New World Tarantulas. Zoological Monographs, Springer, Cham.

Poneke S, Sigeman H, Abbott JK, Hansson B (2018) Why do sex chromosomes stop recombining? Trends. Genet. 34, 492–503.

Postiglioni A, Brum-Zorrilla M (1981). Karyological studies on Uruguayan spiders II. Sex chromosomes in spiders of the genus *Lycosa* (Araneae-Lycosidae). Genetica 56, 47–53.

Presgraves DC (2008). Sex chromosomes and speciation in *Drosophila*. Trends. Genet. 24, 336–43.

Ramalho MO, Araujo D, Schneider MC, Brescovi AD, Doralice MC (2008). *Mesabolivar hvasiliensis* (Moenkhaus 1898) and *Mesabolivar cyaneotaeniatiis* (Keyserling 1891) (Araneomorphae, Pholcidae): dose relationship reinforced by cytogenetic analyses. J. Arachnol. 36, 453–456.

Reyes Lerma AC, Forman M, Kořínková T, Pekár S, Bird T, Brookhart J, Král J (2015). First data on karyotypes and nucleolar organizer regions of solipugids (Solifugae). 29th European Congress of Arachnology. August 24th to 28th Brno, Czech Republic.

Řezáč M, Král J, Musilová J, Pekár S (2006). Unusual karyotype diversity in the European spiders of the genus *Atypus* (Araneae: Atypidae). Hereditas 143, 123–129.

Řezáč M, Král J, Pekár S (2007). The spider genus *Dysdera* (Araneae, Dysderidae) in Central Europe: revision and natural history. J. Arachnol. 35, 432–462.

Řezáč M, Gasparo F, Král J, Heneberg P (2014). Integrative taxonomy and evolutionary history of a newly revealed spider *Dysdera ninii* complex (Araneae: Dysderidae). Zool. J. Linn. Soc. 172, 451–474.

Řezáč M, Arnedo MA, Opatova V, Musilová J, Řezáčová V, Král J (2018). Taxonomic revision and insights into the speciation mode of the spider *Dysdera*

erythrina species complex (Araneae: Dysderidae): sibling species with sympatric distributions. Invertebr. Syst. 32, 10–54.

Řezáč M, Tessler S, Heneberg P, Ávila Herrera IM, Gloríková N, Forman M, Řezáčová V, Král J (2022). *Atypus karschi* Dönitz, 1887 (Araneae: Atypidae): An Asian purse-web spider established in Pennsylvania, USA. PLoS. ONE. 7, e0261695.

Řezáč M, Arnedo MA, Opatova V, Musilová J, Řezáčová V, Král J (2018). Taxonomic revision and insights into the speciation mode of the spider *Dysdera erythrina* species-complex (Araneae: Dysderidae): sibling species with sympatric distributions. Invertebr. Syst. 32, 10–54.

Rieseberg LH (2001). Chromosomal rearrangements and speciation. Trends. Ecol. Evol. 1, 351–358.

Rincão MP, Brescovit AD, Dias AL (2020). Insights on repetitive DNA behavior in two species of *Ctenus* Walckenaer, 1805 and *Guasuctenus* (Polotow and Brescovit, 2019) (Araneae, Ctenidae): Evolutionary profile of H3 histone, 18S rRNA genes and heterochromatin distribution. PLoS. ONE 15, 1–13.

Rincão M, Chavari J, Brescovit A, Dias A (2017). Cytogenetic analysis of five Ctenidae species (Araneae): Detection of heterochromatin and 18S rDNA sites. Comp. Cytogenet. 11, 627–639.

Rodríguez Gil SG, Mola LM, Papeschi AG, Scioscia CL (2002). Cytogenetic heterogeneity in common haplogyne spiders from Argentina (Arachnida: Araneae). J. Arachnol. 30, 47–56

Rodríguez Gil S, Merani M, Scioscia C, Mola L (2007). Cytogenetics in three species of *Polybetes* (Simon 1897) from Argentina (Araneae: Sparassidae) I. Karyotype and chromosome banding pattern. J. Arachnol. 35, 227–237.

Roy V, Monti-Dedieu L, Chaminade N, Siljak-Yakovlev S, Aulard S, Lemeunier F, Montchamp-Moreau C (2005). Evolution of the chromosomal location of rDNA genes in two *Drosophila* species subgroups: a*nanassae* and *melanogaster*. Heredity 94, 388–395.

Sadílek D, Nguyen P, Koç H, Kovařík F, Yağmur EA, Šťáhlavský F (2015). Molecular cytogenetics of *Androctonus* scorpions: an oasis of calm in the

turbulent karyotype evolution of the diverse family Buthidae. Biol. J. Linn. Soc. 115, 69–76.

Sahara K, Marec F, Traut W (1999). TTAGG telomeric repeats in chromosomes of some insects and other arthropods. Chromosome. Res. 7, 449–460.

Shanahan CM, Hayman DL (1990). Synaptonemal complex formation in male scorpions exhibiting achiasmate meiosis and structural heterozygosity. Genome. 33, 914–926.

Sharma S, Ramakrishna S (2019). Cytological studies on three species of Indian spiders. IJSRM. 4, 1–6.

Sánchez-Herrero JF, Frías-López C, Escuer P, Hinojosa-Alvarez S, Arnedo MA, Sánchez-Gracia A, Rozas J (2019). The draft genome sequence of the spider *Dysdera silvatica* (Araneae, Dysderidae). A valuable resource for functional and evolutionary genomic studies in chelicerates. GigaScience. 8, giz099.

Satomura K, Osada N, Endo T (2019). Achiasmy and sex chromosome evolution. Ecol. Genet. Genom. 13, 100046.

Selden PA, Da Costa Casado, Vianna Mesquita M (2006). Mygalomorph spiders (Araneae: Dipluridae) from the Lower Cretaceous Crato lagerstätte, Araripe Basin, north-east Brazil. J. Paleontol. 49, 817 – 826.

Selden PA, Penney D (2009). Fossil spiders. Biol. Rev. Camb. Philos. Soc. 85, 171–206.

Sember A, Pappová M, Forman M, Nguyen P, Marec F, Dalíková M, Divišová K, Doležálková-Kaštánková M, Zrzavá M, Sadílek D, Hrubá B, Král J (2020). Pattern of sex chromosomes differentiation in spiders: Insights from comparative genomic hybridisation. Genes. 11, 1–28.

Sheffer MM, Cordellier M, Forman M, Grewoldt M, Hoffmann K, Jensen C, Kotz M, Král J, Kuss AW, Líznarová E, Uhl G (2022). Identification of sex chromosomes using genomic and cytogenetic methods in a range-expanding spider, *Argiope bruennichi* (Araneae: Araneidae). Biol. J. Linn. Soc. 136, 405–416.

Silva D. (1988). Estudio cariotípico de *Loxosceles laeta* (Araneae: Loxoscelidae). Rev. Peru. Ent. 1, 9–12.

Silva RW, Klisiowicz DR, Cella DM, Mangili OC, Sbalqueiro IJ (2002). Differential distribution of constitutive heterochromatin in two species of brown spider: *Loxosceles intermedia* and *L. laeta* (Araneae, Sicariidae), from the metropolitan region of Curitiba, PR (Brazil). Acta Biol. Par. Curitiba. 31, 123–36.

Silva BC, Souza LHB, Chamorro-Rengifo J, Araujo D (2019). Karyotypes of three species of *Hyperophora*, (Brunner von Wattenwyl, 1878) (Tettigoniidae, Phaneropterinae) enable morphologically similar species to be distinguished. Comp. Cytogenet. 13, 87–93.

Sochorová J, García S, Gálvez F, Symonová R, Kovařík A (2018). Evolutionary trends in animal ribosomal DNA loci: introduction to a new online database. Chromosoma. 127, 141–150.

Sochorová J, Gálvez F, Matyášek R, Garcia S, Kovařík A (2021). Analyses of the Updated "Animal rDNA Loci Database" with an Emphasis on Its New Features. Int. J. Mol. Sci. 22, 11403.

Souza LHB, Costa CC, Silva BC, Dutra DD, Montanholi AS, Oliveira B, Roghanian A, Lemos LC, Pontes HRC, Pádua AA, Dias RRSS, Brescovit AD, Araujo D (2022). Unveiled chromosomal diversity in the Araneidae (Araneomorphae): the highest diploid number among entelegynes and the first record of the $X_1X_2X_3X_4$ sex chromosome system in the family. J. Arachnol. 50, 13–22.

O'Sullivan RJ, Karlseder J (2010). Telomeres: protecting chromosomes against genome instability. Nat. Rev. Mol. Cell. Biol. 1, 171–181.

Sumner AT (2003). Chromosomes Organization and Function. Blackwell Publishing Company. John Wiley & Sons, USA.

Šťáhlavský F, Král J (2004). Karyotype analysis and achiasmatic meiosis in pseudoscorpions of the family Chthoniidae (Arachnida: Pseudoscorpiones). Hereditas. 140, 49–60.

Šťáhlavský F, Forman M, Just P, Denič F, Haddad CR, Opatova V (2020). Cytogenetics of entelegyne spiders (Arachnida, Araneae) from southern Africa. Comp. Cytogenet. 14, 107–138.

Suzuki S (1949). Cytological studies of some spiders. Zool. Mag. 58, 89–90.

Suzuki S (1950a). Sex determination and karyotypes in spiders. Zool. Mag. 59, 31–32.

Suzuki S (1954). Cytological studies in spiders. III. Studies in the chromosomes of fifty-seven species of spiders belonging to seventeen families, with general considerations on chromosomal evolution. J. Sci. Hiroshima Univ. Ser. B, Div.1, Zool. 15, 23–136.

Schneider MC, Mattos VF, Cella DM (2024). The scorpion cytogenetic database. Available in www.arthropodacytogenetics.bio.br/scorpiondatabase. (Accessed on June 11th, 2024).

Srivastava M, Shukla S (1986). Chromosome number and sex-determining mechanism in forty-seven species of Indian spiders. Chromos. Inf. Serv. 1, 23–6.
Šťáhlavský F, Forman M, Just P, Denič F, Haddad CR, Opatova V (2020). Cytogenetics of entelegyne spiders (Arachnida, Araneae) from southern Africa. Comp. Cytogenet. 14, 107–138.
Stahlavsky F (2024). The pseudoscorpion cytogenetic database. Available in www.arthropodacytogenetics.bio.br/pseudoscorpiondatabase.

Traut W, Marec F (1996). Sex chromatin in lepidoptera. Q. Rev. Biol. 71, 239-56.

Tsurusaki N, Svojanovská H, Schöenhofer A, Šťáhlavský F (2024). The harvestmen cytogenetic database. Available in www.arthropodacytogenetics.bio.br/index.html

Tugmon CR, Brown JD, Horner NV (1990). Karyotypes of seventeen USA spiders species (Araneae, Araneidae, Gnaphosidae, Loxoscelidae, Lycosidae, Oxyopidae, Philodromidae, Salticidae and Theridiidae). J. Arachnol. 18, 41–48.

Ubinski CV, Carvalho LS, Schneider MC (2018). Mechanisms of karyotype evolution in the Brazilian scorpions of the subfamily Centruroidinae (Buthidae). Genetica. 146, 475–486.

Vázquez MM, Ávila Herrera IM, Just P, Reyes Lerma AC, Chatzakid M, Hellere TL (2021). A new opilioacarid species (Parasitiformes: Opilioacarida) from Crete (Greece) with notes on its karyotype. Acarologia. 61, 548–563.

Vítková M, Král J, Traut W, Zrzavý J, Marec F (2005). The evolutionary origin of insect telomeric repeats, (TTAGG)n. Chromosome Res. 13, 145–156.

Wheeler WC, Coddington JA, Crowley LM, Dimitrov D, Goloboff PA, Griswold CE, et al (2017). The spider tree of life: phylogeny of Araneae based on target-gene analyses from an extensive taxon sampling. Cladistics. 33, 574–616.

White MJD (1968). Karyotypes and nuclear size in the spermatogenesis of Grasshoppers belonging to the subfamilies Gomphomastacinae, Chininae and Biroellinae (Orthoptera, Eumastacidae). Caryologia. 21, 167–179.

Viera A, Page J, Rufas JS (2009). Inverted meiosis: the true bugs as a model to study. Genome. Dyn. 5, 137-156

World Arachnida Catalog (2024). Natural History Museum Bern. Available online: https://wac.nmbe.ch (Accessed on June 14th, 2024).

Zedek F, Šmerda J, Veselý P, Horová L, Kocmanová J, Bureš P (2021) Elevation-dependent endopolyploid response suggests that plants with holocentric chromosomes are less stressed by UV. B. Bot. J. Linn. Soc. 195, 106–113.

Zedek F, Bureš P (2018). Holocentric chromosomes: from tolerance to fragmentation to colonization of the land. Ann. Bot.121, 9–16.

Zedek F, Bureš P (2019). Pest arthropods with holocentric chromosomes are more resistant to sterilizing ionizing radiation. Radiat. Res. 191, 255–261.

8. Publications not related to the doctoral thesis

Orellana O, **Ávila IM**, Estrada P (2012). Diversity of spiders in an almond *Prunus dulcis* (Mill.) D.A. Webb orchard in the Metropolitan Region of Chile (Central Chile). Idesia (Chile). 30, 17–24.

Král J, Kořínková T, Krkavcová L, Musilová J, **Avila Herrera IM**, Forman M, Vítková M, Haddad C.R, Hedin M, Henriques S, Vargas JP (2013). Evolution of the karyotype, Sex chromosome systems, and meiosis in mygalomorph spiders (Araneae: Mygalomorphae). Biology Journal of the Linnean Society. 109, 377– 408.

Ávila Herrera IM, Carabajal Paladino LZ, Musilová J, Palacios Vargas JG, Forman M, Král J (2016). Evolution of karyotype and sex chromosomes in two families of haplogyne spiders, Filistatidae and Plectreuridae. 21st International Chromosome Conference (ICC). Cytogenetic Genome Research. 148,104.

Král J, Forman M, Kořínková T, Reyes Lerma AC, **Ávila Herrera IM**, Musilová J, et al. (2019). Insights into the karyotype and genome evolution of haplogyne spiders indicate a polyploidy origin of lineage with holokinetic chromosomes. Scientific Reports. 9, 3001. DOI: https://doi.org/10.1038/s41598-019-39034–3.

Vázquez, MM, **Ávila Herrera IM**, Just P, Reyes Lerma AC, Chatzaki M, Heller TL, Král J (2021). A new opilioacarid species (Parasitiformes: Opilioacarida) from Crete (Greece) with notes on its karyotype. Acarologia. 3, 548–563.
DOI.org/10.24349/acarologia/20214449.

Huber BA, Meng G, Král J, **Ávila Herrera IM**, Izquierdo MA (2023). Revision of the South American Ninetinae genus *Guaranita* (Araneae, Pholcidae). European Journal of Taxonomy. 900, 32–80.
DOI: https://doi.org/10.5852/ejt.2023.900.2301

Huber BA, Meng G, Král J, **Ávila Herrera IM**, Carvalhi LS. Diamonds in the rough: Ibotyporanga (Araneae, Pholcidae) spiders in semi-arid Neotropical environments. (Accepted).

Král J, Sember A, Divišová K, Kořínková T, Reyes Lerma AC, **Ávila Herrera IM**, Forman M, et al. Insights into the karyotype evolution of Tetrapulmonata and two other arachnid groups, Ricinulei and Solifugae (submitted).